Investigating the Interaction of Soluble Host Proteins (SP-D, C1q and Fibronectin) with *Mycobacteria*

A Thesis Submitted in Partial Fulfilment of the Requirement for the Degree of Doctor of Philosophy

By

Suha Nadim Shwayat

October 2017

Division of Biosciences

Department of Life Sciences

College of Health and Life Sciences

Brunel University London

Abstract

Mycobacterium tuberculosis (*Mtb*), one of the major pathogens of mankind, kills approximately 2 million people each year. *Mtb* induces inflammation at the site of infection, leading to leakage of serum proteins, which in turn, are likely to come in contact with the pathogen, thus modulate the pathogenesis of tuberculosis. We studied some of these proteins such as surfactant protein D (SP-D), complement protein C1q and fibronectin, which are either produced locally or they leak-out from serum during inflammation, for their interaction with *M.smegmatis* and BCG. These non-pathogenic mycobacteria were used as model for *Mtb*.

In this study, the recombinant form of truncated human surfactant protein D (rhSP-D) and three globular heads of human C1q (ghA, ghB, and ghC) were expressed in *E.coli*. The interaction of each of these proteins with mycobacteria and human monocytic cell line THP-1, was examined via ELISA. We demonstrated that rhSP-D, C1q, three globular heads of C1q and fibronectin bind with both mycobacteria and THP-1 cells. Moreover, using rhSP-D and globular heads of C1q, the binding of SP-D and C1q was localised to C-terminal globular regions. The direct effect for each of these proteins on mycobacterial growth, their effect on the uptake and intracellular fate of mycobacteria inside THP-1 cells were also investigated.

Direct interaction of rhSP-D and C1q inhibited mycobacterial growth, whereas fibronectin interaction with the mycobacteria increased their growth. RhSP-D inhibited the uptake and growth of mycobacteria inside THP-1 cells, whereas C1q and each individual globular heads of C1q enhanced the uptake of mycobacteria by THP-1 cells. However, C1q protein inhibited BCG growth but enhanced *M.smegmatis* growth inside these cells and the later activity was localised to ghA. Fibronectin increased the uptake and growth of mycobacteria inside THP-1 cells. Examining the gene expression of inducible nitric oxide synthase, pro-inflammatory and anti-inflammatory cytokines produced by THP-1 cells infected with the proteins treated and untreated mycobacteria, along with cytokine neutralization experiments, suggest that the nitric oxide components and cytokines could be responsible for mycobacterial growth control inside THP-1 cells.

These novel and interesting functions of SP-D, C1q, and fibronectin on mycobacteria provide an insight into the modulatory function of these proteins on *Mtb* infection, and, therefore, in the pathogenesis of tuberculosis.

Table of contents

List of Figures

Chapter 1

Chapter 2

Chapter 3

Chapter 4

Chapter 6

List of Tables

Chapter 1

Chapter 2

Chapter 3

Chapter 5

Acknowledgments

I would like to thank the following people who helped me during this research.

My husband, Yousif, the most amazing and wonderful person in my life, without his cooperation, none of this would have been possible. Thanks also go to my sweet sons Yaphet and Yaman for bearing with me throughout my PhD study period.

Dr Ansar Pathan, my main supervisor, for his endless guidance, inspiration, and encouragement. I benefitted enormously from his knowledge through our discussions and his attention to detail in preparation of this thesis.

My second supervisor Dr Antony Tsolaki for his support.

Dr Uday Kishore for his help with protein purification and for valuable suggestions.

I am extremely indebted to Lina for her amazing help during writing this thesis. Also, Eswari for her valuable help and support in the lab.

My friend Sahar Al-Barari for her incredible support.

Professor George Meegan who gave his valuable time in reading my thesis.

Colleagues: Suhair, Asif, Naj, Abhi, Agnes, Lubna, Basu, Anu, Iman and Suleman for their valuable help. I thank you all.

List of Abbreviations

ADC	Albumin dextrose catalase
Ag	Antigen
AIDS	Acquired immune deficiency syndrome
BAL	Bronchoalveolar lavage
BCG	Bacillus Calmette–Guérin
BSA	Bovine serum albumin
CNS	Central nervous system
cDNA	Complementary DNA
CHO	Chinese Hamster Ovary
CLIP	Class II-associated invariant chain peptide
CLR	Collagen like region
CR	Complement receptor
CR3	Complement receptor 3
CR4	Complement receptor 4
CRD	Carbohydrate recognition domain
cRPMI	Complete RPMI
CR	Complement receptor
DAB	3’3-Diaminobenzidine
DAPI	Diamidino-phenylindole
DALYs	Disability- adjusted life years
DC’s	dendritic cells
DC-SIGN	Dendritic Cell-Specific Intercellular adhesion molecule-3-Grabbing Non-integrin
DMSO	Dimethyl sulfoxide
DNA	Deoxyribonucleic acid
DNase	Deoxyribonuclease
EDTA	Ethylenediaminetetraacetic acid
ELISA	Enzyme Linked Immunosorbent Assay
FAP	Fibronectin attachment protein
FH	Factor H
FITC	Fluorescein isothiocyanate
FN	Fibronectin
FWD	Forward
G-CSF	Granulocyte-colony stimulating factor
gh	globular head
GRO	Growth-related oncogene
γ/δ	Gamma/delta
HEK	Human Embryonic kidney
HIV	Human Immune suppressive virus

HLA	Human Leukocyte antigen
HRP	Horseradish peroxidase
IFN-ϒ	Interferon gamma
Ig	Immunoglobulin
iNOS	inducible nitric oxide synthase
IL	Interleukin
IFN-γ	Interferon- γ
IPTG	isopropyl-beta-D-thiogalactopyranoside
KDa	Kilo Dalton
LAL	Lumulus Amebocyte Lysate
LB	Lauria Broth media
L-NMMA	N^G-Methyl-L-arginine acetate
LAM	Lipoarabinomannan
LPS	Lipopolyscaccharides.
MAC	Membrane attack complex
ManLAM	Mannose capped Lipoarabinomanann
MBP	Maltose binding protein
MBL	Mannose binding lectin
MCP	Monocyte chemo-attractant protein
MDC	Macrophage derived chemokine
µg	Microgram
MGCs	Multinucleated giant cells
MIP	Macrophage inflammatory protein
MHC	Major Histocompatibility complex
MP	Macrophage
MR	Mannose receptor
mRNA	Messenger Ribonucleic acid
Mtb	*Mycobacterium tuberculosis*
Mwt	Molecular weight
NF $_K$B	Nuclear factor k B
NK cells	Natural killer cells.
NO	Nitric Oxide.
O.D	Optical density
OPD	O-Phenylenediamine dihydrochloride
PAMP	Pathogen associated molecular pattern.
PAP	Pulmonary alveolar proteinosis
PBMC	Peripheral blood mononuclear cell
PBS	Phosphate buffered saline
Pen/Strep	Penicillin/Streptomycin
PFA	Paraformaldehyde
PIM	Phosphatidylinositol mannoside
PMA	phorbol-12-myristate-13-acetate
PMSF	Phenylmethanesulfonylfluoride or phenylmethylsulfonyl fluoride

PRRs	Pattern recognition receptors
q PCR	quantitative polymerase chain reaction.
RNA	Ribonucleic acid
RNase	Ribonuclease
rfhSP-D	Recombinant human surfactant protein –D.
RNA	Ribonucleic acid
RNIs	Reactive nitrogen intermediates.
ROIs	Reactive oxygen intermediates.
Rpm	round per minute
RPMI	Roswell Park Memorial Institute medium
RQ	Relative quantification
SD	Standard deviation
SDS	Sodium dodecyl sulphate
SDS-PAGE	Sodium dodecyl sulphate polyacrylamide gel electrophoresis.
SP	Surfactant Protein
SP-D	Surfactant Protein – D
SIRP-α	Signal-inhibitory regulatory protein α
SLE	Systemic lupus erythematosus
SR	Scavenger receptor
TDM	Trehalose-6,6′-dimycolate
TB	Tuberculosis
TGF-β	Transforming growth factor-β
Th	T helper
Th1	T helper 1
Th2	T helper 2
TMB	3,3',5,5'-tetramethylbenzidine
TLR	Toll-like receptor
TNF-α	Tumor Necrosis Factor alpha
WHO	World Health Organization

Chapter 1 - Introduction

1.1 Tuberculosis

Tuberculosis is primarily a disease of the respiratory system. It is the second leading cause of death after HIV/AIDS in the world, killing around 2 million people every year (WHO, 1999), making it one of the major killers of mankind. One third of the world population is latently infected with *Mtb,* providing a huge reservoir for reactivation of this latent infection into an active disease (Sundaramurthy and Pieters, 2007). The majority of infected people develop long-lived protective immunity. According to the World Health Organization (WHO, 2016), 10.4 million new TB incidents were estimated in 2015, and of that 6.1 million cases were reported. In 2004, 8-9 million new cases were estimated, and 3.9 million cases were sputum-smear positive (Dye, 2006). Most cases occurred in people aged between 15 and 49. The highest incident rate was recorded in Sub-Saharan Africa. Asia has the largest numbers of cases: India, China, Indonesia, Bangladesh, and Pakistan together account for more than half of the world's cases (Frieden *et al*., 2003). 80% of new cases occur in 22 high-burden countries (Figure 1.1). More than 80% of tuberculosis cases lost DALYs (disability- adjusted life years), this being due to the premature death of young people rather than illness itself (Dye, 2006).

The WHO target for eliminating TB by 2050 is falling, especially since the introduction of HIV, which targets CD4+ T cells, the main fighting force against *Mtb* infection. New and effective drugs for preventing TB would improve TB control (Lönnroth, 2008). Although, drug treatment is available, both the high cost and prolonged (6 months) duration of treatment is an issue. This has resulted in multi-drug resistant tuberculosis. This is one of the major hurdles in the control of tuberculosis in developing countries. BCG which is the only vaccine available to control the *Mtb* infection is not effective in adult populations. Where the world's major burden of tuberculosis occurs. Adults are responsible for the major spread of this infection. It is therefore vital that new interventions are created to control *Mtb* infection.

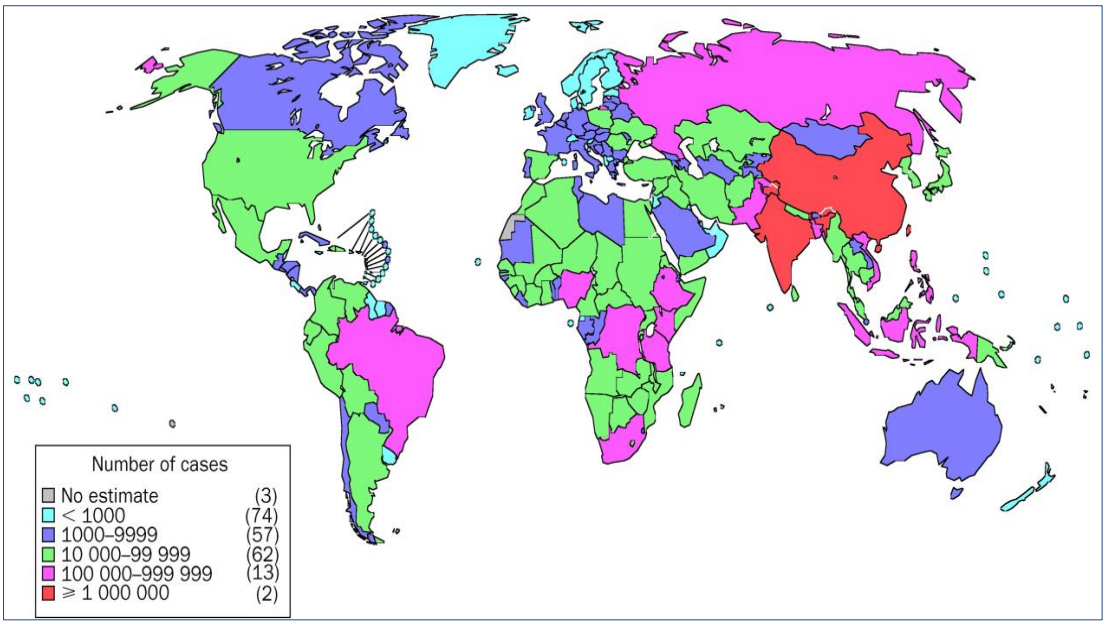

Figure 1.1: Distribution of Tuberculosis in the world. The top 10 countries with TB patients are India, China, Indonesia, Nigeria, South Africa, Banqladish, Ethiopia, Pakistan, Philippines and Congo. Drug resistant TB occurs in more than 80 countries (WHO, 2008).

1.2 Mycobacteria

The genus *Mycobacteria* belongs to the family *Mycobacteriacae.* They are non-motile, obligate aerobic and gram-positive bacilli. The majority members of this genus are soil saprophytes. Mycobacteria include more than 120 different species, but only a few species are pathogenic, thus causing serious diseases in humans and animals. Tuberculosis is caused by members of the *M.tuberculosis* complex. *M.tuberculosis* is the causative agent for tuberculosis in humans. *M.africanum* causes tuberculosis in Africa, *M.bovis* causes tuberculosis in cattle and human, *M.lepra* causes leprosy in human, *M.marinum* causes infection in frogs, fish and skin lesions in human, *M.ulcerans* causes Buruli ulcers, *M.avium* complex causes infection in immune-compromised patients, *M.microti* causes infection in voles but is a virulent in human. *M.canettii* and *M.smegmatis* rarely cause any infection in humans (Cosma *et al*., 2003).

1.2.1 *Mycobacterium tuberculosis*

Mycobacterium tuberculosis (*Mtb*) the causative agent of tuberculosis is a slow growing, facultative intracellular pathogen that prefers to live inside phagocytic

cells especially macrophages. Using light microscopy, *Mtb* appears as straight or slightly curved rods, 1-4 µm in length and 0.3-0.6µm in width (Sakamoto, 2012).

1.2.2 *Mycobacterium smegmatis (M.smegmatis)*

M.smegmatis is a non-pathogenic saprophytic bacterium which was used in this study as a model for *Mtb*. This organism is fast growing and can be grown in LB culture within 72 hours (Young *et al*., 2004). It is 3.0 to 5.0 µm long. This bacteria shares 95% gene homology and the same cell wall structure as *Mtb* (King, 2003, Garnier *et al*., 2003).

1.2.3 *Mycobacterium bovis* (BCG)

Bacillus Calmette–Guérin (BCG) is an attenuated form of *Mycobacterium Bovis* (*M. Bovis*) that is in current use as a preventive vaccine against tuberculosis. BCG shares 99.95% gene homology with *Mtb* and has been used as a model for *Mtb* infection in this study (Brosch, 2002). This organism is slow growing and can be grown in the same cultures as used for *M.tuberculosis* within 2-4 weeks.

1.3 Cell wall structure of *Mycobacterium tuberculosis*

The members of genus mycobacteria share the same unique cell wall structure. 50% of the cell wall's dry weight consists of mycolic acids. Mycolic acids are complex hydroxylated branched-chain fatty acids with higher numbers of carbon (60-90). In *Mtb*, mycolic acids form a thick hydrophobic external layer which slows down nutrient entry and slows its growth (*Mtb* divides every 12-24 hour). This characteristic feature makes the pathogen more resistant to cellular lysosomal enzymes, drying, acidity/ alkalinity and is resistant to many antibiotics (Strohmeier & Fenton, 1999). The outer membrane also contains glycolipids including mannose-capped lipomannan and manno-glycoproteins (Daffe and Etienne, 1999). The inner layer is composed of peptidoglycan which is linked to arabinogalactan layer (Kleinnijenhuis *et al*., 2011). The various components of the cell wall structure are shown in Figure 1.2. Some of the important components of *Mtb* cell wall are discussed below.

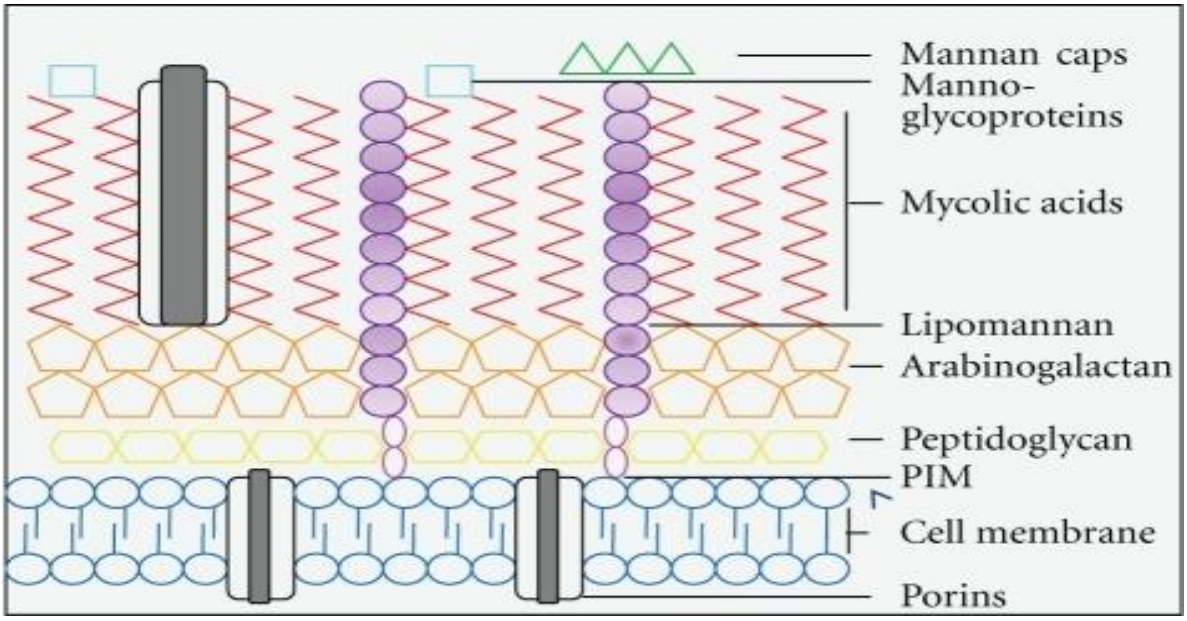

Figure 1.2: Cell wall structure of *Mycobacterium tuberculosis*. The cell surface consists of a peptidoglycan layer that covers the lipid bilayer. Arabinogalactan, lipomannan, and mycolic acids are attached covalently to the peptidoglycan layer. In addition, the outer layer consists of proteins, polysaccharides and lipids.

Lipoarabinomannan (LAM): When LAM capped with short mannose oligosaccharide is involved in phagocytosis of *M. tuberculosis* through binding with mannose receptor on macrophages. DC-SIGN receptor on Dendritic cells (DCs) has been identified as the key receptor for *M. tuberculosis* through its interaction with LAM (Tailleux *et al*., 2003) and ManLAM. The interaction of DCs with ManLAM leads to loss of their phagocytic activity and priming of naive T-cells (Dulphy *et al*., 2007). Lipomannan is similar in structure to LAM. Lipomannan from *M.bovis* (BCG) activate TLR2 signalling in infected mice and induce pro-inflammatory response by enhancing nitric oxide, tumour necrosis factor-α (TNF-α) and lL-12 synthesis (Quesniaux *et al*., 2004).

Cord factor or trehalose dimycolate: It is a glycolipid found in the *Mycobacterium tuberculosis* cell wall. Ryll *et al*., 2001 revealed that mycolic acid-containing trehalose-6,6′-dimycolate (TDM), is able to stimulate immune response against tuberculosis with the production of IL-12, INF-γ, TNF-α, lL-4, IL-6, and IL-10 by immune cells. TDM has been shown to stimulate IL-12 production that stimulates nitric oxide production by macrophages in mice (Oswald *et al*., 1997). TDM can also stimulate alveolar macrophages to produce TNF-α and enhance

granuloma formation. It has been shown that granuloma formation was decreased by administration of anti-TNF-α antibody into TDM injected mice (Takimoto *et al*., 2006).

19 kDa lipoprotein: It is located in the cell wall of *Mycobacterium tuberculosis* and BCG. It induces macrophage apoptosis (Sánchez *et al*., 2012, Noss *et al*., 2000). It also increases the uptake of the bacilli by binding to mannose receptors on THP-1 cells (Diaz-Silvestre *et al*., 2005). The 19 kDa antigen is required by the bacilli to initiate macrophage phagocytosis in order to live and replicate. It has been demonstrated that mycobacteria lacking the 19 kDa antigen can be cleared more rapidly in mice than mycobacteria present with the 19 kDa antigen (Lathigra *et al*., 1996). This lipoprotein inhibits MHC-II antigen processing and presentation by the macrophages (Noss *et al*., 2000). It also blocks INF-γ signalling through a Toll-like receptor 2 (TLR-2) (Pennini *et al*., 2006). This indicates that the19 kDa antigen is one of *Mtb* virulence factors. Therefore, it should not be included in any vaccine formulation against tuberculosis.

1.4 Pathogenesis of *Mycobacterium tuberculosis*

Most humans are resistant to tuberculosis and only a small percentage of infected people develop the disease. In fact, only 10-30% of exposed people become infected, 90% of those infected do not develop the disease and resolve the infection to a level that cannot cause active tuberculosis and this infection remains latent. Of the remaining 10% of infected people, half develop active TB within one year. Although only 10% of *Mtb* infected people actually develop tuberculosis, this disease is still a major public health problem and several million people die every year from this disease.

Tuberculosis is a chronic disease that begins with the inhalation of aerosol droplets containing tubercle bacilli from infected people. These droplets can stay in the air for a prolong period of time (McNerney *et al*., 2012). Inhalation of a droplet containing 1-10 bacteria is sufficient to initiate the infection (Sundaramurthy & Pieters, 2007). The inhaled bacilli reach the lung alveoli and are taken away by alveolar macrophages and dendritic cells. These bacilli can be

cleared by the immune system in most people. Or they can escape host defence mechanisms, and they can survive within the alveolar macrophages. If the host immune system fails to clear *Mtb*, the immune responses form the granulomas, and within each granuloma, the bacilli can live and survive (latent). Understanding the processes involved in mycobacterial pathogenesis at the cellular levels will be beneficial in developing effective methods to control this lethal disease.

1.4.1 Granuloma structure and function

Granulomas form in the lung as an outcome of mycobacterial infection. Granulomas begin by accumulating macrophages at sites of infection, which is a hallmark of *Mtb* infection (Figure 1.3). This is a major step in *Mtb* pathogenesis and determines the outcome of disease. Granulomas are fundamental in containing bacilli so dissemination from the lungs is limited and bacterial growth reduced inside macrophages. Granulomas are composed of a variety of cells that play different roles in granuloma function such as tissue macrophages (derived from blood monocytes), natural killer cells (NK) cells, neutrophils and lymphocytes (CD4+, CD8+, and γ/δ T- cells). Infected macrophages initiate T- cell response by recruiting $CD4^+$ T- cells, which in turn recruit fibroblasts, CD8+ T- cells, and B-cells. Eventually, these granulomas can show central necrosis and cavities and fibroses develops within the granuloma and in the surrounding parenchyma, which form nodules (tubercles). The disease can advance in adults involving bronchioles and spread of infection to other areas of the lungs. Granulomas are formed as a response to adaptive immunity against *Mtb* infection to prevent bacilli dissemination to other organs. Alongside this, granulomas represent the delicate balance that does not harm the host and doesn't kill mycobacteria (Sundaramurthy & Pieters, 2007). If the infected individual has a compromised immune system, including people with HIV, or aging individuals, they will be unable to efficiently form granulomas (Segovia-juarez *et al*., 2004). Recent studies on non-human primates have shown that latent *Mtb* is metabolically active and replicates in host tissues without any clinical signs of disease (Gideon and Flynn, 2011). Disease reactivation occurs when the host immunity becomes weak due to HIV infection, old age, or immune suppressant drugs. Different stages of granuloma formation are shown in Figure 1.3.

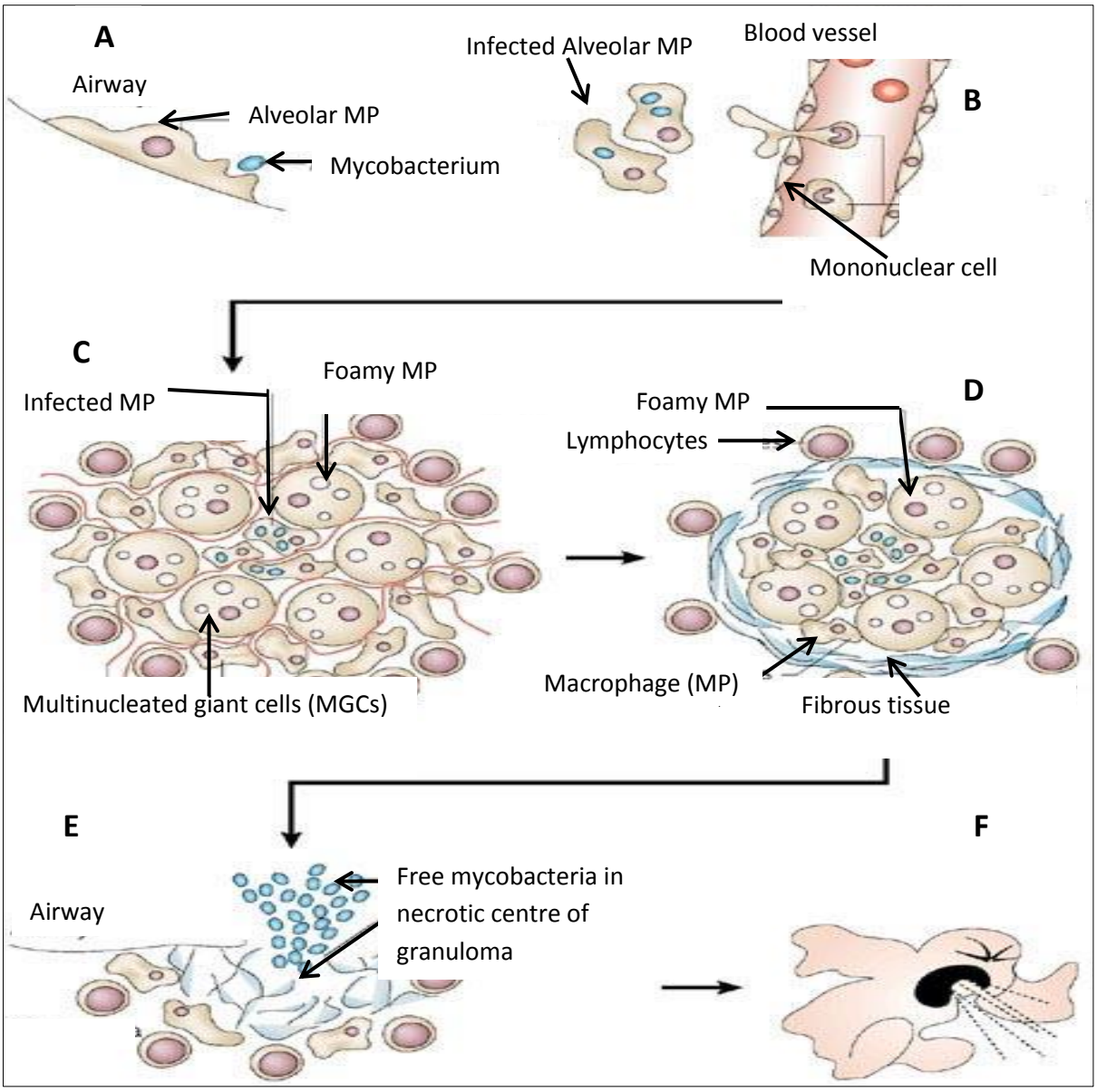

Figure 1.3: Granuloma formation and maturation in the lungs. Following inhalation of *Mtb* it moves down to the lung alveoli where it is recognized by alveolar macrophages (A). This promotes recruitment of more macrophages, dendritic cells and lymphocytes to the infection site (B). The recruited cells arrange in a spherical structure with infected macrophages in the middle surrounded by lymphocytes (C & D). Macrophages (MP) can fuse to form multinucleated giant cells (MGCs) or differentiate into lipid-rich foamy cells (FM) (Silva Miranda *et al*., 2012). B lymphocytes aggregate in follicular-type structures next to the granuloma. *Mtb* can survive for decades inside granuloma but can be reactivated according to specific conditions such as HIV infection and malnutrition. A necrotic zone (called caseum) will develop in the centre of the granuloma (E). When the granuloma structure disintegrates this allows the bacilli to exit and spread infection to other individuals (E and F).

1.4.2 The role of innate immunity in tuberculosis

The Innate immune system can distinguish between host cells (self) and pathogens (non-self) by various receptors found on innate immune cells called pattern recognition receptors (PRRs) (Figure 1.4). These PRRs recognize pathogen associated molecular patterns (PAMPs) of pathogens; such as bacterial lipopolysaccharides (LPS), peptidoglycan, lipoprotein, nucleic acid (DNA and RNA), mycobacterial lipoarabinomannan (LAM) and mannose capped lipoarabinomannan (ManLAM).

Innate immune system consists of cellular and humoral components. Humoral component include the complement activation through classical, lectin and alternative pathways. These pathways lead to deposition of C3b and iC3b on the surface of pathogens, which help in the uptake of bacteria by complement receptors on phagocytic cells. The membrane attack complex C5-C9 is not effective on *Mtb* due to high lipid content in mycobacterial cell wall. The main components of cellular part of innate immune system are discussed below.

1.4.2.1 Macrophages

Alveolar macrophages are the first line of defence against mycobacterial infection. In the early stages of infection, mycobacterial survival inside macrophages depends on the activation status of these cells. If macrophages are not activated by protective cytokines such as INF-γ or TNF-α, then they allow phagocytosed mycobacteria to grow inside and provide a safe haven for them. If the macrophages are activated by the cytokines, they then can control and prevent the infection into developing into an active disease. Alveolar macrophages can kill mycobacteria by expressing nitrogen free radicals (Chensue, 1994). It is known that *Mycobacterium tuberculosis* can avoid killing within macrophages by blocking the fusion between the phagosomes, those containing the bacilli and the lysosomes (Houben *et al*., 2006). Pathogens contained within the phagolysosome are usually killed by lysosome hydrolytic enzymes and by free radicals.

1.4.2.2 Dendritic cells (DCs)

Dendritic cells play a key role in the initiation and direction of the immune response against mycobacteria. This is achieved by antigen presentation to T cells after phagocytosis and by the production of several cytokines and chemokines (Mueller and Pieters, 2006). DC-SIGN is the main receptor for *Mtb* on DCs, and the LAM from mycobacteria was identified as a main ligand of DC-SIGN (Tailleux *et al*., 2003).

1.4.2.3 Neutrophils

The role of neutrophils in mycobacterial infection is still not clear. Neutrophils are the first leukocytes to respond in host defence against invading pathogens; killing by both oxidative/non-oxidative mechanisms. The infected macrophages recruit neutrophils by chemokines such IL-8, MIP-1 alpha, MIP-1 beta, and GRO. However, despite neutrophils present at infection sites in tuberculosis, their role in defence against mycobacteria is still not clear. They play a role in tuberculosis by recruiting macrophages and granuloma formation (Karthik, 2013). On the other hand, Neutrophils can also carry mycobacteria to different organs and spread the infection (Karthik, 2013). Neutrophil behaviour was studied on zebrafish during infection with *Mycobacterium marinum* and it was found that neutrophils do not interact with mycobacteria at the initial infection site; Neutrophils are recruited to the emerging granuloma in response to signals from the dying infected macrophages (Yang *et al.,* 2012). It seems IL-17, IL-23 produced by Th17 cells and IL-18 produced by macrophages are important cytokines in neutrophils recruitment (Cruz *et al.,* 2010, Lyons *et al.,* 2002). A new killing mechanism used by neutrophils has been described recently, neutrophils can kill Gram positive, Gram negative bacteria and fungi by extra cellular trap nets consisting of chromatin studded with granule proteins that bind and kill bacteria (Brinkmann & Zychlinsky, 2012, Ramos-Kichik *et al.,* 2009). *Mtb* binds to neutrophil nets but it can evade their killing (Ramos-Kichik *et al.,* 2009).

1.4.2.4 Natural Killer (NK) cells

NK cells are large granular lymphocytes found in the blood; they recognise and kill infected cells. NK cells have been shown to enhance IL-12, IL-15, IL-18, and IFN-γ production by macrophages *in vitro* (Abbas and Lichtman, 2006, Vankayalapati and Barnes 2009). IL-22 produced by NK cells was shown to inhibit *Mtb* growth by enhancing fusion between phagosomes containing *Mtb* and lysosomes (Dhiman *et al*., 2009). One study demonstrates that NK cells can lyse and kill macrophages infected with *Mtb in vitro* (Vankayalapati and Barnes 2009). The role of NK cells *in vivo* is still not clear. They can be activated early due to *Mtb* infection. It has been shown that NK cells increased in the lungs of *Mtb* infected mice in the first 21 days of infection (Junqueira-Kipnis *et al*., 2003). In addition, NK cells isolated from infected lungs were able to produce IFN-γ, however NK depleted mice had no influence on bacterial load within the lungs (Junqueira-Kipnis *et al*., 2003). It is just possible that NK cells could play a role in early resistance against *Mtb*, however their presence is not essential, as the removal of NK cells does not markedly change the expression of host resistance (Junqueira-Kipnis *et al*., 2003).

1.4.3 The role of adaptive immune response in tuberculosis

The adaptive immune response can effectively remove a wide range of pathogens. It consists of cell mediated immunity (T lymphocytes consisting of $CD4^+$ T-cells and $CD8^+$ T-cells) and humoral immunity (B lymphocytes or B- cells), that are responsible for antibody production. Adaptive immune response for both cell mediated immunity and humoral immunity are activated in the peripheral lymphoid organs. Naïve T cells and B cells circulate regularly in the blood searching for specific antigens. B cells can directly interact with antigens whereas T cells interact with antigens presented by MHC peptide complex on the surface of professional antigen presenting cells (Gupta *et al*., 2012). The adaptive immune response to *M.tuberculosis* is delayed when compared to the adaptive response of the other pathogens; this delay allows more bacterial growth inside the lungs before it can be detected by adaptive immunity. A study on mice showed that the adaptive immune response to *M.tuberculosis* in lung-draining lymph nodes is delayed until 10-12 days after infection (Wolf *et al*., 2008). The same study found

that the activation of Ag85B-specific $CD4^+$ T- cells depends on the number of bacteria in the lymph node but not in the lungs. During early stages of infection by *M.tuberculosis*, the bacteria stay inside the phagosomes and prevent dendritic cells and macrophages from antigen presentation to T cells, which allow an increase in bacterial growth inside the lungs. This increased bacterial population resist the effector mechanisms of the adaptive immune response (Wolf *et al*., 2008). Humans with tuberculosis can generate a Th1 response to *Mtb* with higher levels of $CD4^+$ and $CD8^+$ T-cells in the lungs and blood of infected people (Feng *et al.*, 1999). Human T cell response to *Mtb* involves $CD4^+$ T-cells, $CD8^+$ T-cells, and γ/δ T- cells. These cells can recognize different peptides on mycobacteria presented with MHC Class I and II molecules. T cells also interact with CD1 on antigen presenting cells which display lipid antigens such as mycolic acids. γ/δ T cells recognize antigens containing phosphate without any need for antigen presenting molecules.

1.4.3.1 $CD4^+$ T- cells (Helper T- Cells)

Tuberculosis mainly induces *Mtb* specific $CD4^+$ T- cell response of the Th1 type. Th1 $CD4^+$ T- cells produce INFγ, TNF-α and IL-2 cytokines. The main function of Th-1 $CD4^+$ T - cells is to recruit monocytes to the infection site, and to stimulate the anti-microbial activities inside macrophages and help CD8 T- cells (Geginat *et al*., 2001).

$CD4^+$ T- cells recognise antigens presented on MHC Class II molecules. These MHC class II molecules can access phagosomes containing bacilli and present *Mtb* antigens to the $CD4^+$ T- cells. T cell response to *Mtb* is activated in the local lung lymph node (Gupta *et al*., 2012). Activated T- cells undergo clonal expansion and differentiate into $CD4^+$ T- cells and migrate from the lymph node to the infection site with the help of chemokines. In the infection site $CD4^+$ T- cells produce INF-γ to activate *Mtb* killing within the infected macrophages (Gupta *et al*., 2012).

$CD4^+$ T- cells are important in granuloma formation. It has been shown that $CD4^+$ T-cells deficient mice are unable to recruit cells to form granulomas at an efficient rate (Saunders *et al*., 2002). Both human and mice have been shown to become highly susceptible to *Mtb* if they become deficient in $CD4^+$ T-cells (Gallegos *et al*., 2011). In addition, depletion of *Mtb* specific $CD4^+$ T- cells from the circulation of HIV patients increased their susceptibility to develop active TB (Geldmacher *et al*., 2012).

The balance between Th1 and Th2 subsets of $CD4^+$ T-cells is an important factor that determines the outcome of *Mtb* infection. Th1 secrete INF-γ to activate infected macrophages, whilst Th2 play a role in limiting tissue damage by excessive immune response by the production of IL-4, IL-10, and IL-13 (Abbas and Lichtman, 2006). A previous study has suggested that *Mtb* inhibits Th1 response and induce Th2 response in order to evade their killing by macrophages (Zhang *et al*., 1995).

1.4.3.2 $CD8^+$ T- cells (Cytotoxic T- cells)

Although $CD8^+$ T- cells are present in smaller amounts in the outer borders of granulomas, they still play an important function within the granuloma during late infection. $CD8^+$ T- cells recognize antigen peptides produced in cytosolic compartment and then loaded on MHC class I molecule in the endoplasmic reticulum (Dorhoi *et al.*, 2012). This loading can occur due to *Mtb* proteins diversifying from phagosome to cytosol (Dorhoi *et al.,* 2012). In addition, apoptotic vesicles from infected macrophages and dendritic cells can be up taken again by immature dendritic cells, and processed to be recognized by MHC class I (Schaible *et al*., 2003). $CD8^+$ T- cells can also produce INF-γ during *Mtb* infection, but they cannot substitute for the lack of $CD4^+$ T- cells (Prezzemolo *et al*., 2014). Upon activation, $CD8^+$ T- cells release cytokines or cytotoxic molecules that cause apoptosis. The role of $CD8^+$ T- cells is still unclear in TB. $CD8^+$ T - cells may not be necessary for granuloma formation as $CD8^+$ T- cells deficient mice have been shown to still have the ability to form normal granuloma structure and function (Prezzemolo *et al.,* 2014). Murine model studies indicate that $CD8^+$ T- cells are

primed within 2 weeks in the lymph nodes after infection, and can be detected in the infection site after 2 weeks of infection. Moreover, granulomas in non- human primates contains equal amounts of $CD4^+$ T-cells and $CD8^+$ T-cells (Chen *et al*., 2009) and people with latent TB have shown to contain $CD8^+$ T-cells specific to *Mtb* (Tufariello *et al*., 2003).

1.4.3.3 Th17 cells

Th17 cells are a type of pro-inflammatory T-cells. They produce IL-17, IL-21 and IL-22 cytokines which induce protective immunity against tuberculosis (Korn *et al.,* 2007). IL-17 plays a role in pathogen clearance in mucosal surfaces. Several studies using respiratory infection model, established a central role for IL-17 in protective immune response against fast growing extracellular bacteria, mediated by efficient neutrophil recruitment and tissue repair (Happel *et al.,* 2005). In intracellular bacterial infection, the role of IL-17 is still not well understood. Recent studies suggested that IL-17 enhances immunity against intracellular pathogens; however the effect is not dramatic as in case of extracellular bacteria (Torrado and Cooper, 2010). IL-17 induces the expression of chemokines that initiate neutrophil recruitment and granuloma formation, but absence of IL-17 doesn't significantly influence the ability of mice to control *Mtb.* It has been suggested that a balance between Th17 and Th1 responses is needed during the chronic phase of *Mtb* infection in order to control bacterial growth; and excessive IL-17 production could sustain neutrophil recruitment (Torrado and Cooper, 2010).

1.4.3.4 B cells and antibodies

B cells and humoral immunity (antibodies) can modulate the immune response to *M. tuberculosis*. It has been shown that B cells can regulate the reactions within the granuloma, cytokine production, and the T cell response (Kozakiewicz *et al*., 2013). B cells deficient *Mtb* infected mice have shown an increase in neutrophils recruitment, higher levels of IL-10, and higher levels of mortality in comparison to

wild type *Mtb* infected control mice (Maglione *et al*., 2009). It has been reported that the antibodies against *Mtb* helps in the uptake of *Mtb* by macrophages, and these antibodies play some role in protection (Chan *et al.,* 2014). Moreover monoclonal anti-bodies (HBHA, MPB83, and 16kDa acrystallin) against *Mtb* antigens enhanced granuloma formation, reduced mycobacterial concentration, inhibited bacterial growth in the lung and enhanced mice survival (Chambers *et al*., 2004). However the mechanisms of mycobacterial growth inhibition by these antibodies are still unknown.

1.4.4 Receptors for Mycobacteria on phagocytic cells

Mtb is recognized during the early stages of infection by pattern recognition receptors (PRRs) such as toll-like receptors, complement receptors, Dendritic Cell-Specific Intercellular adhesion molecule-3-Grabbing Non-integrin (DC-SIGN), mannose receptors, CD14 receptors and scavenger receptors (Figure 1.4 & Table 1.1). Some of these receptors such as Toll-like receptors (TLR2 & TLR4) stimulate host immune cells (macrophages and the dendritic cells) to produce cytokines such as TNF-α and lL-12, which are important in mycobacterial growth regulation, granuloma formation, initiation of the adaptive immune response and host protection against *M.tuberculosis* (Hossain and Norazmi, 2013). Figure 1.4 shows some pattern recognition receptors that have been identified on phagocytic cells, these receptors can recognize and bind to pathogen associated molecular patterns (PAMPs) on *mycobacterium tuberculosis*.

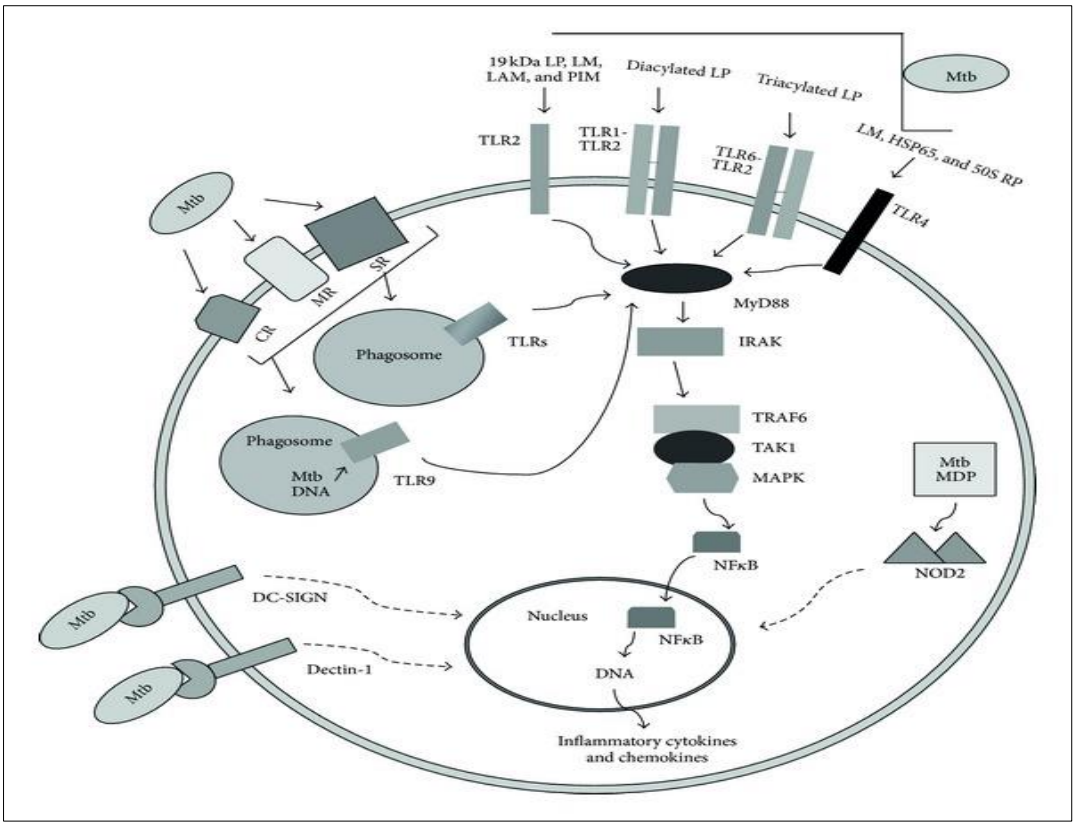

Figure 1.4: *Mycobacterium tuberculosis* receptors on/in phagocytic cells. This diagram shows the different pattern recognition receptors on/in macrophages that are responsible for detection and uptake of *mycobacterium tuberculosis (Mtb).* CR: complement receptor, MR: Mannose receptor, SR: Scavenger receptor. TLR: Toll-like receptor (Hossain and Norazmi, 2013).

1.4.4.1 Toll-like receptors: TLR2 can recognize the 19kDa lipoprotein, lipomannan, and lipoarabinonmannan on mycobacteria. TLR1:TLR2 and TLR6:TLR2 heterodimers bind to lipopolysaccharides (LPS), whereas TLR4 binds lipomannan, and 50S ribosomal protein. Phagosomal TLR9 recognize mycobacterial DNA, while TLR2 and TLR4 activate NF-kB which leads to the synthesis of nitric oxide synthase (iNOS) (Krutzik & Modlin, 2004). Macrophages from TLR2 deficient mice have shown to respond to *Mtb*, while macrophages from TLR4 deficient mice have not shown any response (Bulut *et al.,* 2005).

1.4.4.2 Complement receptors (CR1 and CR3): These receptors are responsible for the uptake of opsonized mycobacteria by macrophages (Hossain and Norazmi, 2013, Schlesinger *et al*., 1990). The complement receptor 3 (CR3) can mediate phagocytosis of C3b and iC3b opsonised mycobacteria by macrophages (Velasco-Velázquez *et al*., 2003). A study indicates that phagocytosis of

mycobacteria via complement receptors are more favourable by *Mtb* as this triggers less superoxide production (Russell, 2005).

1.4.4.3 Mannose receptors: These receptors are involved in non-opsonin-mediated phagocytosis of mycobacteria. Mannose receptors mediate *Mtb* phagocytosis through recognition of terminal mannose residues on LAM (Schlesinger *et al*., 1996) and through binding to 19kDa lipoprotein on *Mtb* (Diaz-Silvestre *et al.,* 2005). Mycobacterial phagocytosis mediated with mannose receptors (MR) direct the bacilli into phagosome compartments that have less ability to fuse with lysosomes (Kang *et al*., 2005). Also it is believed that phagocytosis of mycobacteria by MR is the first step for mycobacterial infection of the cells.

1.4.4.4 Scavenger receptors: These receptors can be used by mycobacteria to be engulfed by macrophages (Schäfer *et al.,* 2009).

1.4.4.5 CD14 receptors: These receptors have been involved in the phagocytosis of mycobacteria. *M.bovis* has been shown specifically to infect alveolar macrophages subpopulations with the higher expression of CD14 receptors (Khanna *et al*., 1996).

1.4.4.6 DC-SIGN receptor: This receptor facilitates *M. tuberculosis* uptake by DCs. *M. tuberculosis* targets DC-SIGN to infect DCs and also to down-regulate DC-mediated immune responses (Geijtenbeek *et al*., 2003). *Mtb* infection reduces the expression of MHC Class II on DC's surface. Moreover, *Mtb* infection prevents antigen presentation to T cells and it interferes with loading of MHC class II in the endosomal compartment and blocks CLIP removal (Hmama et al., 1998).

Table 1.1: Receptors for mycobacteria on/in host cells

Receptor on/in host cells	Ligand implicated on mycobacteria	Function	Reference
Mannose receptor	19kDa lipoprotein. MAN LAM	Increase mycobacterial phagocytosis, promotes inhibition in phagosome-lysosome fusion	Diaz-Silvestre *et al*., 2005; Kang *et al*., 2005
Scavenger receptor	Lipoproteins	Mycobacterial recognition	Schäfer *et al.,* 2009, Pai et al., 2004
Complement receptors (CR1, CR3)	Opsonised mycobacteria	Phagocytosis	Hossain and Norazmi, 2013
DC-SIGN receptor on DC's	MANLAM Lipomannans	Phagocytosis, induce IL-10 production	Dulphy *et al*., 2007, Geijtenbeek *et al*., 2003
TLR2/TLR1 heterodimer	Recognize LAM, (araLAM 19kDa mycobacterial glycoprotein, and phosphatidylinositol mannoside (PIM)	Required for cytokine secretion	Sandor *et al*., 2003
TLR2	LAM, 19kDa lipoprotein	Induce pro-inflammatory response TNF-α and nitric oxide production	Queniaux *et al.,* 2004
TLR2/TLR6 heterodimer	Diacylated lipoproteins	Stimulation of IL-1β production	Kleinnijenhuis *et al.*, 2009
TLR3	BCG RNA	Induce IL-10	Bai *et al*., 2014
TLR4	Lipomannan	Protection against TB	Krutzik & Modlin, 2004
TLR9	*Mtb* DNA	Activates macrophages and induces proinflammatory cytokine synthesis	Hemmi *et al*., 2000
FCγ	IgG opsonized *Mtb*	Phagocytosis, induce ROI_s and formation of phago-lysosomes to kill mycobacteria	Armstrong and D'Arcy Hart, 1975
CD14	Carbohydrates moiety of CD14	*Mtb* phagocytosis, TNF-α & IL-1β release.	Shams *et al.,* 2003; Zhang et al., 1993
Dectin-1	Recognize α-glucan on the surface of some *Mtb* species	Induce Th1 & Th17 responses, and secretion of pro-inflammatory cytokines	van de Veerdonk *et al*., 2010

1.4.5 Role of pro-inflammatory cytokines in tuberculosis

The interaction of mycobacterial ligands with PRRs enables macrophages and dendritic cells to secrete various cytokines. Cytokines are small proteins (5-20kDa) that serve as messengers between cells in order to regulate the body's response to infection. Cytokines include chemokines, interferons, interleukins, lymphokines, and tumour necrosis factors. Pro-inflammatory cytokines (protective cytokines) are produced by activated macrophages and are involved in enhancing inflammation (Table 1.2).

1.4.5.1 Tumor Necrosis Factor-α (TNF-α)

TNF-α is a pro-inflammatory cytokine that regulates mycobacterial growth, granuloma formation, initiation of adaptive immunity and host protection. Activated macrophages and *Mtb* activated $CD4^+$ T- cells produce TNF-α. Previous studies have shown that TNF-α deficient mice are more susceptible to *Mtb* infection (Kaneko *et al*., 1999). Also TNF-α secretion by mycobacterial infected macrophages stimulates reactive nitrogen intermediates (Chan *et al*., 1992). Neutralization of TNF-α in latent TB induce the reactivation of the disease in mice (Mohan *et al*., 2001). In human, it has been shown that TB was reactivated in rheumatoid arthritis patients who received anti-TNF-α antibody treatment (Gardam *et al*., 2003).

1.4.5.2 Interleukin-1β (IL-1β)

IL-1β is a pro—inflammatory cytokine that is produced by monocytes, macrophages, and dendritic cells (Kleinnijenhuis *et al*., 2011). It is involved in the host immune response against *Mtb*. It is expressed at the infected site of TB patients. It has been shown that IL-1β receptor deficient mice are more susceptible to *Mtb* infection and showed impaired granuloma formation (Juffermans *et al*., 2000, Yamada *et al*., 2000).

1.4.5.3 IL-6

IL-6 is a pro-inflammatory cytokine that is produced by phagocytic cells early in *Mtb* infection. It plays opposing roles in the immune system. IL-6 deficient mice have shown to be more susceptible to *Mtb* infection (Saunders *et al.,* 2000). On the other hand, IL-6 has shown to inhibit TNF-α and IL-1β production and to facilitate *M.avium* growth in vitro (Schindler *et al.,* 1990).

1.4.5.4 Interferon- γ (INF-γ)

IFN-γ is a pro-inflammatory cytokine that is critical for adaptive immunity against infections. It is produced by NK cells, $CD4^+$ and $CD8^+$ T- cells. Its production is mediated by IL-12 and IL-18 (Munder *et al*., 2001). IFN-γ is an important activator of macrophages and an inducer of Class II major histocompatibility complex (MHC) molecule expression on immune cells. INF-γ facilitates polarization of $CD4^+$ T- cells towards Th1 type of immunity. INF-γ is also important for antigen presentation; it inhibits *Mtb* growth in mice macrophages (Flesch *et al*., 1987). It has been shown that mice deficient in the INF-γ gene were able to form granuloma but they failed to produce reactive nitrogen species and to inhibit *Mtb* growth (Flynn *et al.,* 1993). Furthermore, tissue necrosis was enhanced in the absence of the INF-γ gene and mice died early due to tuberculosis compared to normal mice infected with *Mtb* (Flynn *et al.,* 1993). Moreover, INF- γ receptor deficient people are more susceptible to mycobacterial infection (Dorman & Holland, 2000).

1.4.5.5 IL-12

IL-12 cytokine is composed of P40 and P70 chains. It is a pro- inflammatory cytokine produced by *Mtb* infected macrophages. IL-12 has a role in INF-γ production and initiation of Th1 immunity. IL-12 deficient mice are at high risk of *Mtb* infection, and giving IL-12 supplements leads to *Mtb* killing at the early stages of infection (Flyyn *et al*., 1995). The expression of IL-12 is detected in granulomas of patients with active TB, (Zhang *et al*., 1994). IL-12 receptor deficient mice are more susceptible to mycobacterial infection (Hossain and Norazmi, 2013).

1.4.5.6 IL-18

IL-18 is a pro inflammatory cytokine that induces INF-γ production. It is produced mainly by macrophages and dendritic cells, and it has a protective role against tuberculosis (Schneider *et al*., 2010). IL-18 knockout mice are more susceptible to *Mtb* and BCG infections (Sugawara *et al*., 1999). Proliferation of mycobacteria in IL-18 knockout mice was responsible for premature death (Schneider *et al*., 2010).

1.4.5.7 IL-23

IL-23 is a pro-inflammatory cytokine composed of IL-12 p40 and IL-23 p19 subunits. It is secreted by monocytes, macrophages, and dendritic cells (Wiekowski *et al.*, 2001). IL-23 activates $CD4^+$ T- cells in lymph nodes (Cooper *et al*., 1995). Mice lacking both IL-12 and IL-23 are more susceptible to *Mtb* infection. On the other hand, mice deficient in IL-12 only exhibit partial protective immunity against *Mtb,* which suggests a protective role of IL-23 against *Mtb* (Cooper *et al.*, 2002).

1.4.6 The role of anti- inflammatory cytokines in tuberculosis

The anti-inflammatory (suppressive) cytokines inhibit cell activation by inhibiting the production of pro-inflammatory cytokines or by opposing their biological effect. The major anti-inflammatory cytokines are IL-4, IL-10, and TGF-β (Table 1.2).

1.4.6.1 IL-4

IL-4 plays a role in macrophage deactivation and polarizing of CD4 T- cells toward Th2 type of immunity (Powrie *et al.,* 1993). Over expression of IL-4 in mice induces progressive disease and reactivation of latent *Mtb* infection (Hernandez-Pando *et al.,* 1996).

1.4.6.2 IL-10

IL-10 is an anti-inflammatory cytokine that deactivates macrophages by down regulating IL-12 and TNF-α expression, which reduce the production of INF-γ by $CD4^+$ T- cells; this will lead to decreased reactive oxygen intermediates (ROIs)

and reactive nitrogen intermediates (RNIs) and increased *Mtb* survival (Gazzinelli *et al*., 1992, Moore *et al.*, 2001). IL-10 also inhibits $CD4^+$ T- cell responses, it impairs macrophage function in mice, inhibits phagosome maturation and *Mtb* antigen presentation in the infected cells (Rojas, R.E. *et al*., 1999, O'Leary *et al*., 2011, Murray *et al.,* 1997).

1.4.6.3 Transforming Growth Factor-β (TGF-β)

TGF-β is an anti-inflammatory cytokine that opposes the protective immunity in tuberculosis. It is secreted by human monocytes and dendritic cells in granuloma lesions and it inhibits the production of ROI and RNI by macrophages (Ding *et al*., 1990). TGF-β also suppresses T cells proliferation (Rojas, R.E. *et al*., 1999), and it causes down regulation of pro-inflammatory cytokine release (Ruscetti *et al.*, 1993). It also inhibits phagocytosis and accelerates mycobacterial growth (Toossi *et al.,* 1995). Table 1.2 below shows the role of pro-inflammatory and anti-inflammatory cytokines in tuberculosis.

Table 1.2: Role of pro-inflammatory and anti-inflammatory cytokines in TB

Cytokine	Pro or anti-inflammatory	Function	Reference
TNF-α	Pro-inflammatory	Regulates granuloma formation, initiate adaptive immune response and stimulate reactive nitrogen intermediates	Kaneko et al., 1999, Chan et al., 1992
Il-1β	Pro-inflammatory	Regulates granuloma formation	Juffermans et al., 2000, Yamada et al., 2000
IL-6	Pro-inflammatory	It has opposing roles. It protect against *Mtb* and it inhibit TNF-α and Il-1β production	Saunders et al., 2000, Schindler et al., 1990
INF-Ɣ	Pro-inflammatory	Activate Mtb killing by macrophages by RNI, and by facilitating polarization of $CD4^+$ T-cells towards Th1 immunity	Flesch et al., 1987, Flynn et al., 1993
IL-12	Pro-inflammatory	Initiate Th1 immunity and INF-Ɣ production	Flyyn et al., 1995

IL-18	Pro-inflammatory	Induce INF-Ɣ production	Schneider et al., 2010
IL-2	Pro-inflammatory	Activates $CD4^+$ T-cells	Cooper et al., 1995
IL-4	Anti-inflammatory	Deactivates the function of macrophages, polarizes CD4 T-cells towards Th2 immunity	Powire et al., 1993
IL-10	Anti-inflammatory	Deactivates macrophages by down regulating IL-12 and TNF-α expression, decrease ROS and RNI, inhibits phagosome maturation, antigen presentation, T cells responses and INF-Ɣ production,	Gazzinelli et al., 1992, Moore et al 2001, Rojas, R E et al., 1999, O' Leary et al., 2011, Murray et al., 1997
TGF-β	Anti-i flammatory	Inhibits phagocytosis, ROS and RNI by macrophages, suppresses T- cells proliferation and increases mycobacterial growth	Toossi et al., 1995, Ding et al., 1990, Rojas R E et al., 1999

1.4.7 Role of chemokines

Chemokines are small chemo-attractant proteins. They are similar in structure, and can be distinguished by the number of amino acids between conserved cysteine residues. There are four chemokine families; CC, CXC, CX3C, and C (Johnston & Butcher, 2002), and these families were based on the position of four cysteine residues that form two disulfide bonds. Chemokine receptors are expressed on human blood monocytes, these receptors include; CXCR1, CXCR2, CXCR4, CCR1, CCR2, CCR4, and CCR7 (Geissmann *et al*., 2003). The interactions between these receptors and their specific chemokines induce monocyte arrest on endothelium, transmigration through the endothelium, and other functions (Haribabu *et al*., 1999).

1.4.7.1 IL-8: It is a chemokine that can be produced by a variety of cells including; macrophages, epithelial cells, smooth muscle cells and endothelial cells. It attracts neutrophils to the site of infection. Phagocytosis of pathogens by neutrophils is

usually accompanied by the release of granule enzymes and superoxide (Baggiolini *et al*., 1989). Neutrophil attraction causes inflammation and tissue damage.

1.4.7.2 Macrophage inflammatory proteins (MIP-1α and MIP-1β)

These proteins belong to the CC chemokine family and are involved in acute inflammation. They are produced by activated macrophages. Their main function is to attract monocytes, natural killer cells and neutrophils to the site of infection. MIP-1α induces interleukin 1 (IL-1), IL-6 and TNF-α synthesis and their release. Both MIP-1 alpha (CCL3) and MIP-1 beta (CCL4) attract T-cells to the site of infection. 100pg/ml of MIP-1 alpha was shown to attract B cells and cytotoxic T cells to the infection site (Schall *et al.,* 1993). These chemokines can produce relatively more fever than produced by TNF-α and IL-1β.

1.4.7.3 Monocyte chemo-attractant protein-1 (MCP-1 or CCL2): This protein belongs to the CC chemokine family. It is produced by a variety of cells including; endothelial, fibroblasts, epithelial, and smooth muscle (Deshmane *et al*., 2009). This small cytokine recruits monocytes, memory T cells, and dendritic cells to the sites of infection. It also enhances Th2 polarization (Rose *et al.,* 2003)

1.4.7.4 Monocyte chemo-attractant protein-3 (MCP-3 or CCL7): It belongs to the CC chemokine family. It is produced by macrophages (Ruhwald *et al*., 2009). This chemokine attracts monocytes and macrophages to the site of infection. Bronchoalveolar lavage fluid from *Mtb* patients has shown to contain higher expression level of MCP-3 when compared to controls (Ruhwald *et al*., 2009).

1.4.7.5 Growth-related oncogene1 (GRO1) GRO-α (CXCL1): It is expressed by macrophages, epithelial cells and neutrophils. It supports monocyte arrest in inflammation (Smith *et al*., 2005). It also attracts neutrophils and monocytes to the site of infection (Nakagawa *et al*., 1994).

1.4.7.6 Granulocyte-colony stimulating factor (G-CSF) is produced by monocytes, fibroblasts, and endothelial cells (Schneider *et al*., 2005). It stimulates the survival, proliferation, differentiation, and function of neutrophil precursors and

mature neutrophils. G-CSF remarkably regulates neutrophils survival by inhibition of apoptosis (Hu & Yasui, 1997)

1.4.7.7 Macrophage derived chemokine (MDC) belongs to the CC chemokine family. MDC is produced by macrophages and dendritic cells. It attracts the monocytes, monocyte-derived dendritic cells and IL-2–activated natural killer cells (Godiska *et al.,* 1997). MDC is a strong attractant for CCR4 expressing polarized Th2 cells (Mantovani *et al*., 2000).

1.4.8 Mechanisms used by *Mycobacterium tuberculosis* to survive inside host cells

1.4.8.1 Blocking phagosome-lysosome fusion

Mtb uses unique strategies to survive inside macrophages. One of the mechanisms of intracellular killing by macrophages is phagosome-lysosome fusion. *Mtb* prevent phagosome maturation and lysosome fusion after uptake by host macrophages. By blocking phagosome fusion with lysosome, *Mtb* avoids acidic proteases within lysosomes and avoids the exposure to this bactericidal mechanism.

1.4.8.2 Interference with MHC Class II antigen presentation

Mtb prevents its own antigen processing and presentation to the immune system (Pieters, 2001). It can delay the early induction of T- cell responses and modulation of antigen presentation to $CD4^{+}$T- cells (Urdahl *et al*., 2011, Shaler *et al*., 2012). A study has shown that *Mtb* infection in mice reduced the expression of MHC Class II molecules on antigen presenting cells. *Mtb* can interfere with peptide loading to MHC Class II in the endosomal compartment by either blocking removal of CLIP or loading of peptide to MHC Class II (Hmama *et al.,* 1998). It has been shown that *M.bovis* BCG down-regulated the mRNA expression of CIITA regulatory protein which down-regulated the expression of MHC Class II in murine macrophages (Wojciechowski *et al.,* 1999) and human macrophages (Pai *et al*.,

2003). It has been shown that 19kDa lipoprotein from *M. bovis BCG* and *Mtb* inhibited antigen processing and presentation by MHC-II (Noss *et al*., 2000, 2001).

1.4.8.3 Other mechanisms

Mtb inhibits phagosomal proton pump into phagosome, which increase the PH of this compartment, and inhibiting the proteolytic activity of lysosomal enzymes (Wong *et al*., 2011). It also inhibits Th1 response and induces Th2 response to evade their killing by macrophages (Zhang *et al.,* 1995). *Mtb* can also detoxify reactive oxygen and nitrogen species inside host cells (Shaler *et al*., 2012). Virulent *Mtb* strains can inhibit apoptosis by interfering with TNF-α signalling and by expression of anti-apoptotic Mc1-1 (Spira *et al*., 2003).

1.4.9 Mechanisms used by host cells for killing *Mycobacterium tuberculosis*

1.4.9.1 Reactive nitric oxide intermediates (RNI)

One of the most powerful and necessary antibacterial defence mechanisms against *Mtb* is the production of nitric oxide as reactive nitric oxide intermediates (RNI). These RNI are very toxic and it can kill mycobacteria inside phagosomes by damaging bacterial DNA, lipids and proteins. RNI are generated as intermediate products through the conversion of L-arginine to citrulline by nitric oxide synthase. The produced nitric oxide is quickly oxidized to nitrite (NO2) and nitrate (NO3). Nitric oxide intermediates have been detected previously in infected macrophages (Nicholson *et al*., 1996). Also, mice deficient in the nitric oxide synthase gene are more susceptible to *Mtb* infection than control mice (Flesch & Kaufmann, 1991, Yang *et al*., 2009). Moreover, *Mtb* infected mice treated with iNOS inhibitors were more susceptible to tuberculosis. And, Inhibition of iNOS expression in human leads to latent *Mtb* reactivation (Gardam *et al*., 2003).

1.4.9.2 Apoptosis (programmed cell death)

Apoptosis is a distinct form of cell death that is important for regulation of the immune system (Oddo, 1998). It is a non-inflammatory removal process of dying

cells. Caspases are serine proteases, expressed as proenzymes that function to initiate and complete apoptosis. In apoptosis, the cytoplasmic contents of dying cells are confined within apoptotic bodies (membrane bound vesicles) that express signals to be taken by another phagocytic cell to be destroyed. There are three distinct pathways for apoptosis. The extrinsic apoptosis pathway is induced by TNF-α and Fas ligand and procaspase-8 is activated in this pathway (Chen and Wang, 2002). The intrinsic apoptosis pathway is induced by intracellular stress factors such as DNA damage, less nutrients and oxidative stress. Procaspase-9 is activated in the intrinsic pathway. The third pathway way is initiated by granzyme B released from cytotoxic T-cells and NK cells (Lee et al., 2009). All these pathways finally activate procaspase 3, 6 and 7 to their active forms, which induce apoptosis.

TNF-α apoptosis reduces the viability of intracellular mycobacteria (Oddo, 1998, Lee *et al*., 2009). Mycobacteria induce apoptosis in macrophages, which release apoptotic vesicles that carry mycobacterial antigens to uninfected antigen presenting cells. These antigens can be presented by MHC-I molecule to T cells (Schaible *et al*., 2003). It is known that virulent *Mtb* strains inhibit apoptosis by interfering with TNF-α signalling and by expression of anti-apoptotic Mc1-1 (Spira *et al*., 2003, Balcewicz-Sablinska et al., 1998, Sly *et al*., 2003). Also, it has been shown that IFN-Ɣ induces apoptosis in mycobacteria-infected macrophages (Herbst *et al.,* 2011). NO-mediated apoptosis is a new defence mechanism against *M. tuberculosis* by activated macrophages.

1.4.9.3 Role of Interferon-γ (IFN-γ): INF-γ produced by $CD4^+$ T- cells enables macrophages to kill mycobacteria by disabling phagosome maturation block and by exposure of phagocytosed mycobacteria to nitric oxide (NO). Also, IFN-γ helps mycobacterial killing by recruiting $CD4^+$ T-cells and $CD8^+$ T- cells (Munder *et al*., 2001).

1.4.9.4 Role of vitamin D3

African individuals with Low vitamin D3 serum levels are more susceptible for tuberculosis (Liu *et al.,* 2006). Moreover, it has been shown that mycobacteria

were killed effectively using African serum supplemented with vitamin D3 *in vitro* as compared to un- supplemented African serum (Liu *et al*., 2006).

1.5 TB diagnosis

Tuberculosis is diagnosed by the following methods.

1.5.1 Light microscopy

Sputum smear containing *Mycobacterium tuberculosis* can be observed directly by light microscopy after staining with Acid-fast or Ziel-Neelsen staining. Microscopy is a simple, inexpensive method and the results are available within one hour. However, one disadvantage is that the sensitivity of this method is only 50-60% in adult population. Sputum stained with Acid fast is positive in up to 75% of adults with pulmonary TB whilst less than 20% of children with pulmonary TB have a positive Acid fast stain smear from sputum or gastric aspirate (Khan and Starke, 1995). In addition, people with HIV and TB together usually have less levels of *Mtb* in their sputum, which gives a false negative result.

1.5.2 Culture

Sputum sample or other samples obtained from the infected site can be grown on solid media. Culture results usually take up to 8 weeks (Alastair Innes, 2016). Around 10-100 viable bacilli are required for sputum to be culture positive.

BACTEC is a liquid culture medium that accelerates bacterial growth and tests for rifampicin drug resistant gene (Alastair Innes, 2016). The test result usually takes 7-21 days. The new generation, BACTEC MGIT 960 system is testing of *Mycobacterium tuberculosis* susceptibility to isoniazid, rifampin, and ethambutol plus streptomycin. The sensitivity of this method is 100% for all four TB first line drugs, and specificity is 89.8% for streptomycin and 100% for rifampin (Bemer *et al*., 2002).

1.5.3 Tuberculin (skin test)

Tuberculin used to test whether an individual has immunological reactivity to *Mtb* antigens. This test could be false positive in BCG vaccinated individuals and those

exposed to other mycobacteria (Alastair Innes, 2016). False negative skin test could result with children, older people and people with HIV infection.

1.5.4 Interferon γ -release assay

Interferon-γ (IFN-γ) release assay (IGRA) is blood test used in diagnosis of tuberculosis. This assay depends on IFN-γ released by T-lymphocytes when exposed to *Mtb* antigens. The advantage of this test is that it requires only one patient visit, and results can be available within 24 hours. IGRAs are more specific than Tuberculin (skin test) and not affected by BCG vaccination. IGRA is recommended to diagnose latent TB (Gudjónsdóttir *et al*., 2016). Disadvantages include that they does not differentiate between active and latent TB infection, blood sample must be processed quickly, and test requires laboratory facilities. There are two IFN-γ based release assays used for TB diagnosis:

1.5.4.1 QuantiFERON-TB Gold test (QFT-G): It is a T cell based assay for detecting active and latent *Mtb* infection. In this assay, blood samples are mixed with *Mtb* antigens (ESAT-6 and CFP-10). Then, the amount of interferon-gamma (IFN-gamma) is measured after 16 to 24 hours of incubation by ELISA. *Mtb* infected people will produce higher amount of IFN-γ. Its sensitivity is approximately 80% for active TB patients.

1.5.4.2 T-SPOT.TB: It is a type of ELISPOT assay and is also based on T cell response to the *Mtb* antigens (ESAT-6 and CFP-10). In this assay interferon-gamma is produced by T cells on nitrocellulose paper in the ELISA plate (Agarwal *et al*., 2016). This assay is 10% more sensitive than QFT-GIT in detecting latent TB infection (Van Zyl-Smit *et al*., 2016).

1.5.5 Genexpert Test

The Genexpert test is based on *Mtb* nucleic acid amplification (Marlowe *et al*., 2011). It is an automated test that can detect DNA from *Mtb.* It also tests for rifampicin resistance by nucleic acid amplification. It uses a sputum sample and results can be available within 2 hours.

1.5.6 Chest X-ray

Acute pulmonary TB can be easily seen on an X-ray. Nodules, cavities and lesions may appear in the lungs. Normal chest X-ray cannot exclude an extra pulmonary TB.

1.6 TB treatment

Drugs currently used for TB treatment are divided into first line TB drugs and second line TB drugs (Table 1.3).

1.6.1 First line TB drugs

These drugs are used for treatment of pulmonary and extra pulmonary TB, which refers to new infection in previously uninfected individuals. This treatment is effective on drug-susceptible *Mtb* strains only. The basic TB treatment includes an oral administration of isoniazid, rifampicin, pyrazinamide and ethambutol for the first 2 months. These are followed by isoniazid and rifampicin for the next 4 months. Six months of treatment should be given for pulmonary TB and extra pulmonary TB individuals. However, 12 months of treatment is recommended for meningeal TB, and ethambutol can be replaced by streptomycin. In case of pregnant women and malnourished patients, Pyridoxine (vitamin B6) should be used to reduce the risk of peripheral neuropathy which may be caused by isoniazid. After treatment course, there is a small (less than 5%) risk of relapse. Without treatment, TB patients will remain infectious, and around 25% of untreated patients will die in their first year (Alastair Innes, 2016).

1.6.1.1 Isoniazid (isonicotinic acid hydrazide, INH)

Isoniazid is an antibiotic commonly used in the treatment of TB since 1952 (Robitzek and Selikoff, 1952). It is bactericidal by diffusing across the *Mtb* membrane (Raynaud *et al.,* 1999). Isoniazid is a prodrug whose activation in the bacteria requires an enzyme KatG. The active metabolites of this drug inhibit mycolic acid synthesis in *Mtb* cell wall (Takayama *et al.,* 1975). These active metabolites also inhibit the synthesis of nucleic acids (Gangadharam *et al.,* 1963), phospholipids (Brennan, Rooney *et al.,* 1970) and NAD metabolism in mycobacteria (Bekiekunst, 1966). Isoniazid is used as a first line drug of

tuberculosis treatment. Although, *Mtb* resistant strains to this drug have been reported (Kolyva and Karakousis, 2012).

1.6.1.2 Rifampin

Rifampin is a wide spectrum antibiotic, and is used in the first line of TB treatment. It was first isolated from Streptomyces in 1957. This antibiotic is lipophilic and diffuses easily across the *Mtb* cell wall. It is bactericidal, and it inhibits *Mtb* DNA transcription by binding with bacterial RNA polymerase. It has been reported that more than 90% of rifampin resistant isolates are also resistant to isoniazid (Telenti *et al.,* 1993).

1.6.1.3 Pyrazinamide

Pyrazinamide is an antibiotic which was discovered in 1952 (Yeager *et al*., 1952). It is bactericidal but it is poorer to that of INH and rifampin (Jindani *et al.,* 1980). It targets semi-dormant *Mtb* residing in the acidic environment (Mitchison, 1985).

1.6.1.4 Ethambutol

Ethambutol is an antibiotic that inhibit *Mtb* growth. It was discovered in 1961. It is bactericidal and it kills *Mtb* by inhibiting polymerization of arabinan in *Mtb's* cell wall (Mikusova *et al*., 1995).

1.6.2 Second line TB drugs

These drugs are used for treatment of drug resistant TB. Drug–resistant *Mtb* strains have been increased in the poorest countries, which is associated with in accurate and insufficient treatment (Alastair Innes, 2016). This treatment can take around 2 years. These drugs are more expensive, toxic and have serious side effects. The following TB drugs are recommended for treatment of rifampicin resistant and multi drug resistant TB (WHO, 2016).

1.6.2.1 Group A: Fluoroquinolones include Levofloxacin, Moxifloxacin and Gatifloxacin.

Fluoroquinolones are currently used as second-line drugs in TB treatment. Fluoroquinolones are bactericidal; they kill mycobacteria by blocking DNA

replication and transcription. *Mtb* resistance to fluoroquinolones is also common (Kolyva and Karakousis, 2012).

1.6.2.2 Group B: Aminoglycoside drugs (Amikacin, Capreomycin, Kanamycin and Streptomycin).

Aminoglycosides kill mycobacteria by binding to the 30S ribosomal subunit, which affects protein synthesis (Kolyva and Karakousis, 2012). Streptomycin was discovered in 1940. It was used in TB treatment, and currently not commonly used as an anti-tuberculosis drug. This is due to the toxicity of aminoglycosides. Other aminoglycosides, such as Kanamycin, Capreomycin and Amikacin are used as a second line drugs, but side effects are major problem.

1.6.2.3 Group C: Other core second line agents.

These drugs include Ethionamide/Prothionamide, Cycloserine/Terizidone, Linezolid and Clofazimine.

Ethionamide is a synthetic compound which is similar to Isoniazid in structure. It inhibits the synthesis of mycolic acid. Around three-quarters of *Mtb* isolates are resistance to Ethionamide (Morlock *et al*., 2003).

Cycloserine or Terizidone is a bacteriostatic antibiotic which interferes with the synthesis of peptidoglycan in the *Mtb* cell wall (Caceres, Harris *et al*., 1997). Terizidone is used currently for the treatment of multidrug resistant TB (Weyer, 2005).

Linezolid belongs to the Oxazolidinone class, and is the first antibiotic approved for clinical use in this group. It can enter macrophages and kills intracellular bacilli. Linezolid inhibits protein synthesis by binding to 50S ribosomal subunit (Zhang, 2005). Linezolid is used to treat drug resistant TB, but has serious side effects, such as leukopenia and irreversible peripheral neuropathy.

Clofazimine was discovered in 1954. Clofazimine has shown activity against multidrug resistant-TB (MDR-TB). Clofazimine can release reactive oxygen species (ROS) during its spontaneous oxidation (Yano *et al.,* 2011). As there is no specific target for ROS, resistance to clofazimine is rare.

1.6.2.4 Group D: Add-on agents (not part of the core MDR-TB regimen) include Pyrazinamide, Ethambutol, High-dose isoniazid, Bedaquiline, Delamanid, p-aminosalicylic acid, Imipenem-cilastatin, Meropenem, Amoxicillin-clavulanate and Thioacetazone.

Bedaquiline is specifically used for MDR-TB treatment, and when other treatment cannot be used. It should be used along with at least three other drugs for tuberculosis. It is bactericidal; it blocks the proton pump for ATP synthase of mycobacteria which leads to mycobacterial killing (Worley *et al.,* 2014).

Delamanid, (OPC-67683) a nitro-dihydro-imidazooxazole derivative, is a new antituberculosis medication that inhibits mycolic acid synthesis and has shown strong activity against both susceptible and drug-resistant strains of *Mtb* (Gler *et al.,* 2012, Matsumoto *et al.*, 2006).

Paraaminosalicylic acid is thought to inhibit the biosynthesis of folic acid and iron uptake by *Mtb* (Wade and Zhang, 2004).
Imipenem is broad spectrum antibiotic which was developed in 1980. It has been shown to be effective against *Mtb*. Imipenem is always administered intravenously as a combination of equal quantities of imipenem and cilastatin. Cilastatin (MK0791) helps in preventing the imipenem breakdown inside the kidneys (Kahan *et al*., 1983).

Meropenem- clavulanate

Meropenem together with β-lactamase inhibitor clavulanate results in rapid cell lysis, releasing cytoplasmic contents of *Mtb*. Meropenem targets the transpeptidases that introduce interpeptide cross-links into bacterial peptidoglycan (Kumer *et al.,* 2012; Hugonnet *et al*., 2009). In addition, Meropenem has been shown to inhibit anaerobically grown cultures of *Mtb*, and to inhibit the growth of 13 extensively drug-resistant strains of *Mtb* (Hugonnet *et al.,* 2009)

Amoxicillin- clavulanate

Amoxicillin is an antibiotic that has β-lactam activity. It has been shown that the combination of (<4μg/ml) of amoxicillin with (<2μg/ml) clavulanic acid was

bactericidal for 14 of 15 *Mtb* isolates (Cynamon and Palmer, 1983). Clavulanate reacts with bacterial β-lactamase quickly to form inactive forms of the enzyme. Clavulanate can be used in combination with approved β-lactam antibiotics such as amoxicillin and Meropenem to treat multi-drug resistant (MDR) and extremely drug resistant (XDR) strains of *M. tuberculosis* (Hugonnet and Blanchard, 2007).

Thioacetazone is used in TB treatment but it has weak activity against *Mtb*. It is only useful in preventing resistance to isoniazid and rifampicin (The main effective drugs against TB). It is never used alone for TB treatment; it is used in a similar way to ethambutol. It can be used instead of ethambutol in TB treatment. Thioacetazone is still used by many countries in sub-Saharan Africa because it is extremely cheap. On the other hand, the use of thioacetazone can cause severe (sometimes fatal) skin reactions in HIV positive patients (Rieder *et al.,* 2001).

Table 1.3: Drugs used for TB treatment

First line drugs: These are used to treat new *Mtb* infection in previously uninfected individuals

Drug	Effect on *Mtb*	Mechanism of action	Reference
Isoniazid (INH)	bactericidal	Inhibit mycolic acid synthesis in *Mtb* cell wall. Inhibit nucleic acids and phospholipids synthesis and NAD metabolism in mycobacteria	Takayama et al., 1975, Gangadharam et al., 1963, Brennan, Rooney et al., 1970, Bekiekunst, 1966).
Rifampin	bactericidal	Inhibits *Mtb* DNA transcription by binding with bacterial RNA polymerase	Telenti et al., 1993
Pyrazinamide	bactericidal	Targets semi-dormant *Mtb* residing in the acidic environment	Mitchison, 1985
Ethambutol	bactericidal	Kills by inhibiting polymerization of arabinan in *Mtb*'s cell wall	Mikusova et al., 1995

Second line drugs: These are used for treatment of drug resistant TB

Drug	Effect on *Mtb*	Mechanism of action	Reference
Group A: Fluoroquinolones include Levofloxacin, Moxifloxacin and Gatifloxacin.	bactericidal	Blocking DNA replication and transcription in mycobacteria	Kolyva and Karakousis, 2012
Group B: Aminoglycoside drugs (Amikacin, Capreomycin, Kanamycin and Streptomycin	bactericidal	Inhibits by binding to 30S ribosomal subunit, which affects protein synthesis	Kolyva and Karakousis, 2012
Group C: Ethionamide/Prothionamide, Cycloserine/Terizidone, Linezolid and Clofazimine.	bacteriostatic	Inhibits the synthesis of mycolic acid, peptidoglycan, and protein synthesis by binding to 50S ribosomal subunit	Morlock et al., 2003, Caceres, Harris et al., 1997, Zhang, 2005

Group D: Add-on agents

Bedaquiline	bactericidal	blocks the proton pump for ATP synthase	Worley et al., 2014
Delamanid	bacteriostatic	Inhibits mycolic acid synthesis	Gler et al., 2012, Matsumoto et al., 2006
Paraaminosalicylic acid	bacteriostatic	Inhibits folic acid biosynthesis and iron uptake by Mtb	Wade and Zhang, 2004
Amoxicillin-clavulanate	bactericidal	Inactivates bacterial β-lactamase	Hugonnet and Blanchard, 2007)
Meropenem- clavulanate	bactericidal	causes rapid cell lysis	Kumer et al., 2012; Hugonnet et al., 2009
Thioacetazone	bactericidal	Preventing resistance to isoniazid and rifampicin	Rieder et al., 2001

1.7 Anti TB vaccines

1.7.1 Bacillus Calmette-Guerin (BCG) vaccine: BCG is most commonly used vaccine against TB in the world. BCG is an attenuated strain of *M.bovis*. This strain is a virulent to human due to deletion of RD1 locus that encodes 10kDa filtered protein and secreted proteins CFP-10, ESAT-6 (6kDa) (Ganguly *et al*., 2008). These secreted proteins are considered crucial virulence factors to the pathogenesis of *Mtb* (Stanley *et al*., 2003). They help *Mtb* to evade their killing by host immune cells. The lack of these genes from BCG prevents mycobacteria to counteract its destruction that allows *Mtb* killing by host cells (Ritz *et al.,* 2008). Both INF-γ and interleukin 17 pathways were strongly induced in BCG vaccinated adults. Also, *Mtb* growth was reduced in previously BCG-vaccinated adults as compared to BCG-unvaccinated adults in the United Kingdom (Matsumiya *et al.,* 2015). BCG vaccination prevents disseminated meningeal and miliary TB in children (O'Shea and McShane, 2016).

Although BCG is safe in human but it can cause disease in immunocompromised individuals such as people live with HIV. For this reason, BCG vaccine is not recommended for infants infected with HIV. Moreover, BCG has variable efficacy. This could be due to several reasons. Firstly, the original BCG strain used for vaccinations several decades ago was sent to different laboratories in order to produce BCG vaccine. Hundreds of BCG passages and different growth protocols could be responsible for genetic variability between different BCG strains, and that might lead to variable efficacy of BCG vaccine (Behr and Small, 1999). Secondly,

the previous exposure to non-tuberclous mycobacteria in some populations could masks the effect of BCG (Black *et al*., 2002). Thirdly, Immunity induced by non-tuberclous mycobacteria might inhibit BCG replication, which is essential for this vaccine to work (Brandt *et al*., 2002).

1.7.2 Anti TB vaccines under clinical trials

Currently, there are several vaccine candidates being evaluated in clinical trials (Table 1.4). These TB vaccine candidates can be classified as:

1.7.2.1 Preventive pre-exposure vaccines (Priming vaccines): They are administrated to individuals before exposure to *Mtb*. Typically given to neonates (Kaufmann *et al.,* 2017). Examples of such vaccine in clinical trials are MTBVAC (Attenuated *Mtb*) and VPM1002 (recombinant Live BCG expressing listeriolysin).

1.7.2.2: Prime- boost vaccines. Here BCG (priming vaccine) vaccinated children are given another vaccine which act as a booster vaccine. Examples are BCG-MVA85A, BCG-M72/AS01, BCG-Crucell Ad35 expressing *Mtb* antigens 85A, 85B and 85C.

1.7.2.3 Preventive post-exposure vaccines (posting vaccines): They are targeted adolescents and adult with latent TB infection (Kaufmann et al., 2017). Examples of such vaccine in clinical trials are Modified Vaccinia virus Ankara (MVA85A) and M72/AS01$_E$. Modified Vaccinia virus Ankara (MVA85A) was one of the most advanced vaccines for TB. MVA85A was developed to be administrated following BCG vaccination. This vaccine showed to be safe and increases the frequency of IFN-γ secreting T cells (Pathan *et al*., 2012), but recently MVA85A failed as preventive in pre-exposure phase IIB clinical trials in South African infants (Tameris *et al*., 2013). Another phase IIB trial, with GSK candidate M72/AS01$_E$, is started in Africa by GlaxoSmithKline (Penn-Nicholson *et al*., 2015). This vaccine is composed of antigen M72, which is a recombinant fusion protein derived from the *Mtb* proteins Mtb32A and Mtb39A, and the AS01 Adjuvant System (Montoya *et al*., 2013). This vaccine has been shown to be safe, and

induces humoral and cell-mediated immunity in healthy, HIV-infected, *Mtb*-infected individuals, and in BCG-vaccinated babies (Gillard *et al*., 2016, Montoya *et al.,* 2013, Leroux-Roels *et al*., 2013, Cohen *et al.,* 2013, Penn-Nicholson *et al*., 2015, Thacher *et al*., 2014, Idoko *et al.,* 2014).

1.7.2.4 Therapeutic vaccines such as Heat-killed *Mycobacterium vaccae* and DNA vaccines: To be administrated in adjunct with TB drugs (Kaufmann *et al*., 2017). Heat-killed *Mycobacterium vaccae* showed activity as an adjunct to anti-TB chemotherapy. In China, administration of *Mycobacterium vaccae* to MDR TB every 3-4 weeks for 6 months showed better sputum conversion and cavity closure (Luo *et al.*, 2000). DNA vaccines expressing specific *M. tuberculosis* genes such as Hsp65, ESAT-6, and Ag85A, has shown 1-3 log improvement in *Mtb* clearance in mice (Lowrie and Silva, 2000).

Table 1.4: Summary of TB vaccines currently under clinical trials (Frick, 2015).

Strategy	Vaccine candidate	Vaccine type	Phase	Sponsor
Prime	MTBVAC	Live genetically attenuated *M. tb*	IIa	University of Zaragoza; Biofabri; Tuberculosis Vaccine Initiative (TBVI)
	VPM1002	Live recombinant BCG	IIa	Serum Institute of India; Vakzine Projekt Management; TBVI; Max Planck Institute for Infection Biology
Prime-boost	M72/AS01	Protein/adjuvant	IIb	GlaxoSmithKline; Aeras
	Hybrid 4 + IC31	Protein/adjuvant	IIa	Statens Serum Institut (SSI); Sanofi Pasteur; Valneva; Aeras
	Hybrid 56 + IC31	Protein/adjuvant	IIa	SSI; Valneva; Aeras
	Hybrid 1 + IC31	Protein/adjuvant	IIa	SSI; Valneva
	Ad5Ag85A	Viral vector	I	McMaster University; CanSino
	Crucell Ad35 + MVA85A	Viral vector	I	Crucell; Oxford University; Aeras
	ChAdOx1.85A + MVA85A	Viral vector	I	Oxford University
	Dar-901	Whole-cell *M. obuense*	I	Dartmouth University; Aeras
	MVA85A (aerosol)	Viral vector	I	Oxford University
	MVA85A-IMX313	Viral vector	I	Oxford University; Imaxio
	ID93 + GLA-SE	Protein/adjuvant	I	Infectious Disease Research Institute; Aeras
	TB/FLU-04L	Viral vector	I	Research Institute for Biological Safety Problems
Immunotherapeutic	*M. vaccae*	Whole-cell *M. vaccae*	III	AnHui Longcom
	RUTI	Fragmented *M. tb*	IIa	Archivel Farma

1.8 Pulmonary surfactants

Pulmonary surfactant is a mixture of proteins and lipids produced by the lungs and secreted into the alveolar space. Surfactant decreases the fluid surface tension in the lungs and prevents lung alveoli from collapsing during exhalation. There are four surfactant proteins of which two are hydrophilic (SP-A & SP-D), and two are hydrophobic (SP-B & SP-C). Hydrophobic surfactants play an important role in the reduction of surface tension in the lungs, whereas, hydrophilic surfactants play an important role in host defense against pathogens. Pulmonary surfactant protein-D (SP-D) is produced mainly by alveolar type II cells of the lungs. It is a member of the C-type lectin (also known as collectin) family (Souji *et al*., 1997). This family is characterized by a carbohydrates recognition domain (CRD), neck, collagen-like domain, and an N-terminal domain rich with cysteine. This family includes surfactant protein A (SP-A), and other serum proteins produced by the liver such as mannose- binding lectin (MBL) (Worthley *et al*., 2009), collectin 43 (CL-43) and bovine conglutinin (Hansen & Holmskov, 1998).

1.8.1 Surfactant Protein-D (SP-D)

SP-D is a large hydrophilic glycoprotein protein (520kDa), which under physiological conditions forms a cruciform structure made of 12 chains (each chain has a molecular mass of 43 kDa under reducing conditions) arranged in 4 trimeric sub-units. The primary structure of each polypeptide chain consists of a cysteine-rich N-terminal region (25 amino acids), a triple – helical collagen like region (177amino acids) consisting of repeat Gly-x-y triplets, an α-helical coiled coil neck region and a carbohydrate recognition domain (CRD) (153 amino acids) (Figure 1.5). The CRD can recognize carbohydrate on microbes, whilst the collagen region can interact with the receptors of the immune cells (Kishore *et al.,* 2006). SP-D purified from some patients with alveolar proteinosis was shown to contain pre-dominantly higher order SP-D multimers, which can contain 32 or more trimeric subunits (Crouch, 2000).

SP-D binds to a variety of receptors like TLR2 and TLR4 through the CRD region (Ohya *et al*., 2006). Moreover, SP-D binds SIRPα and inhibits the expression of pro-inflammatory cytokines. The CLR of SP-D binds to calreticulin–CD91 complex

and this binding drives the ingestion of apoptotic cells by phagocytes (Vandivier et al., 2002), scavenger, and mannose receptors on the macrophages (Ferguson, 2006, Kuroki *et al.,* 2007). Table 1.5 shows different receptors on host cells that bind to SP-D. In human, SP-D gene is located on the long arm of chromosome 10 at 10q22.2-23.1. SP-D has eight exons (seven coding) (Kishore *et al*., 2006).

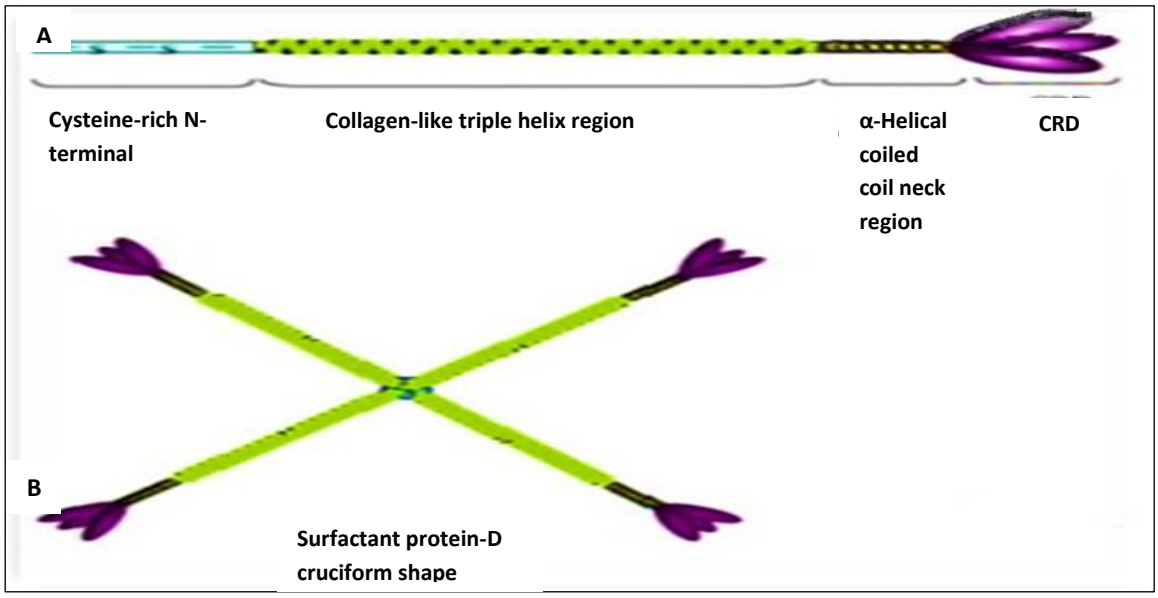

Figure 1.5: Surfactant protein-D (SP-D) structure: Three polypeptide chains together form a trimeric structure which consists of CRD, α-Helical coiled coil neck, Collagen like region, and N-terminal region (A). Four trimmers join together to form the SP-D cruciform shape (B). (Qaseem *et al*., 2013).

Table 1.5: Receptors for SP-D on host cells

Receptor on host cell	Part implicated of SP-D	Function	Reference
Mannose receptor	CRD	Phagocytosis	Kuroki *et al.,* 2007 and Ferguson et al., 1999)
Scavenger receptor	CRD	Phagocytosis	Kuroki et al., 2007
TLR2 & TLR4	CRD	Signaling	Ohya *et al.,* 2006
SIRP-α (CD172) on macrophages and DCs	CRD	Inhibit phagocytosis and Inhibit pro-inflammatory release in resting, non-inflammed lungs	Janssen *et al*., 2008
CD14 on alveolar macrophages	CRD	Release pro-inflammatory cytokines	Sano *et al.,* 2000;
Calreticulin (CD91)	Collagen domain	Enhance phagocytosis of apoptotic cells and induce pro-inflammatory response	Forbes and Haczku, 2010, Vandivier *et al*., 2002

1.8.2 Structure of recombinant human surfactant protein-D (rfhSP-D)

The recombinant human SP-D (rfhSP-D) (20kDa) used in this study is trimeric; each chain consists of a carbohydrates recognition domain (CRD) region, an α-helical neck and 8 Gly-x-y repeats from the collagen like region (Mahajan *et al*., 2008). The recombinant fragment of SP-D is expressed and purified using *E.coli* BL21 (λDE3) pLysS expression system (Singh *et al*., 2003), and this has been used previously in functional studies (Ferguson, 2002). The *E. coli* strain BL21 can express any gene under the control of T7 promoter. This strain is deficient in two proteases (lon and ompT). These proteases are responsible for lysis and damaging any expressed foreign proteins. The phage DE3 expresses the T7 RNA polymerase gene under the control of the lacUV5 promoter. The pLysS strain expresses the T7 lysozyme gene, which suppresses the expression of T7 RNA polymerase prior to induction with IPTG.

1.8.3 Expression and binding of Surfactant Protein–D (SP-D)

Lung is the main site for synthesis and secretion SP-D in to the airspaces. SP-D has been detected in extra pulmonary regions such as; in the umbilical cord blood in new born infants, amniotic fluid and placenta (Dahl *et al*., 2005, Leth-Larsen *et al*., 2004). Also it was detected in female genital tract including (vagina, cervics, uterus, fallopian tubes, and ovaries) (Leth-Larsen *et al.,* 2004). SP-D is also synthesised in trachea, brain, salivary gland, heart, testis, prostate gland, pancreas, kidney, small intestine, mammary glands, and stomach (Madsen *et al*., 2000).

Previous literatures showed that SP-D can bind to bacteria including *Klebsiella pneumonia, Pseudomonas aeruginosa, Haemophilus influenzae, Streptococcus pneumonia, Staphylococcus aureus, Escherichia coli, Mycobacterium tuberculosis, and Mycobacterium avium* (Crouch et al., 2000). SP-D interacts directly with *Histoplasma capsulatum* and *Mycoplasma pneumonia* (Kuroki *et al*., 2007 and Wu *et al*., 2003), influenza A virus (IAV) (Hartshorn *et al*., 2000) and Chlamydia trachomatis (Oberley *et al.,* 2004).

1.8.4 Functions of Surfactant Protein–D (SP-D)

SP-D plays an important role in reducing the growth of some pathogens in the lungs (Kuroki *et al*., 2007). It is involved in the clearance of bacteria, fungi, apoptotic cells, necrotic cells, determination of inflammation (Kishore *et al*., 2006) and inhibiting the activity of influenza A virus (Hartshorn *et al*., 2000). Previous studies showed different effects of SP-D on phagocytosis of pathogens (Table 1.6). It can decrease or increase the phagocytosis of different mycobacterial species. Ferguson *et al.,* 1999 showed that recombinant rat SP-D can reduce phagocytosis of *Mycobacterium tuberculosis* by macrophages. There is also evidence to show that SP-D can increase the uptake of some fungi and bacteria by macrophages (Geunes- Boyer *et al.,* 2012, Giannoni *et al*., 2006). It increases the phagocytosis of *Streptococcus pneumonia*, *Mycobacterium avium and E.coli* (Kuroki *et al*., 2007, Ariki *et al*., 2011, Brinker *et al.,* 2001). Previous studies showed that SP-D decreases the growth of *Histoplasma capsulatum*, *Mycoplasma pneumonia, Escherichia coli (*Wu *et al*., 2003) and inhibits *Chlamydia trackmatis* infection of cervical epithelial cells (Oberley *et al*., 2004). SP-D facilitates uptake of *E.coli* by dendritic cells, and increases antigen presentation of *E.coli* to T cells (Brinker *et al*., 2001). SP-D deficiency is associated with chronic lung inflammation and fibrosis in SP-D knockout mice (Wert *et al.,* 2000).

Presence of SP-D in blood and in a wide range of tissues suggests an important role for SP-D in general innate immunity outside the lungs (Kishore *et al*., 2006). SP-D has role in asthma and allergy. With asthmatic patients SP-D binds to apoptotic eosinophil's to enhance their uptake by alveolar macrophages (Mahajan *et al*., 2008). It also binds and enhances the uptake of pollen derived starch granules by alveolar macrophages and suppresses allergen-induced inflammation (Winkler *et al*., 2010). SP-D inhibits histamine release, suppress the activation of sensitized basophils, mast cells or eosinophil's, and it suppress the proliferation of B cells, it inhibits IL-2 secretion and T cells polarization, modulation of dendritic cells and macrophages, (Kishore *et al.,* 2002-A). Presence of SP-D in placenta, umbilical cord and amniotic fluid could be helpful in preventing the infections during implantation of the embryo and during pregnancy (Malhotra *et al.,* 1994).

Table 1.6: Binding ligands for SP-D on pathogens

Ligand implicated on microorganisms	Part of SP-D implicated	Function	Reference
MAN LAM of *Mtb*	CRD	Decrease the *Mtb* uptake. Enhance phagolysosomal fusion and intracellular killing	Chroneos, 2009 and Ferguson *et al*., 1999
Lipoarabinomannan of *M.avium*	CRD	Agglutination. Stimulates cell surface localization of mannose receptor and increase the phagocytosis	Ariki *et al*., 2011 and Kudo *et al.,* 2004
LPS of Gr-negative bacteria	Neck domain and CRD	aggregation	Lim *et al.,* 1994
Lipoteichoic acid and peptidoglycan of Gr-positive bacteria	CRD	Increase phagocytosis of *S. aureus*	Van de Wetering *et al*., 2001
Membrane lipids of mycoplasma	CRD	Growth inhibition	Chiba *et al*., 2002
Glycoproteins of fungi and yeast	CRD	Agglutination of yeast, fungi, increasing cell membrane permeability, and decrease hypha formation	Schelenz *et al*., 1995, Madan et al., 1997
Mannosylated, N linked carbohydrates of IAV virus	CRD	Inhibit IAV virus activity	Hartshorn *et al*., 2000 and 1994
Nucleic acids (DNA, RNA)	CRD	Phagocytosis of DNA in apoptotic cells to enhance their clearance	Palaniyar *et al*., 2003

1.8.5 SP-D as a biomarker

The normal SP-D concentration in broncho alveolar lavage (BAL) fluid is around 51µg/ml. This SP-D level can decrease to 12-19 µg/ml in cigarette smokers. Cigarette smoking increases alveolar permeability which results in SP-D leakage into blood capillaries (Winkler *et al*., 2011). Smoking also lead to an imbalance in host defence and a higher incident rate for infections such as tuberculosis (Moré *et al*., 2010). On the other hand the SP-D level in BAL fluid can increase in pulmonary alveolar proteinosis (PAP) patients (Honda *et al.,* 1995, Crouch *et al*., 1993).

The mean serum SP-D level in healthy individuals is between 48.7-109ng/ml (Kuroki *et al.,* 1998). SP-D serum concentration can also increase in pulmonary fibrosis and idiopathic interstitial pneumonia due to leakage of SP-D from injured

alveolar capillaries and basement membranes to blood vessels. Also, SP-D serum levels increased 7.0 folds in PAP patients when compared to healthy volunteers. Moreover, circulating SP-D levels are extremely high in post-mortem subjects (Eisner *et al*., 2003). Radiation therapy for lung, breasts, and lymphoma cancers increased SP-D production by 21-26% (Nayak *et al*., 2012-A). Measurement of serum SP-D levels could be a good marker for the integrity of lung alveoli and disease severity (Honda *et al*., 1995).

1.9 Complement system

Complement is a collection of more than 30 different soluble proteins that are present in blood and other cell surfaces (Dunkelberger and Song, 2010). The complement system plays a critical role in the innate defence against pathogens. It serves as a bridge between innate and adaptive immunity. Innate immune responses are composed of immunological effectors that provide immediate and nonspecific immune responses. Complement responses target its accumulative activation towards pathogens. In the presence of pathogens, complement proteins become activated and interact with each other to form several pathways of complement activation. The final outcome is facilitating the phagocytosis of pathogens to be killed by macrophages or directly by lysis. There are three complement activation pathways, the classical pathway, the alternative pathway and the lectin pathway (Figure 1.7).

The classical pathway: This pathway is initiated by C1q binding to antibodies bound to the pathogens. C1q binding activates C1s to cleave C4 and C2 to C4a, C4b, C2a, and C2b which generate C3 convertase (C4b2a).

The lectin pathway: This pathway is initiated by mannose binding lectin (MBL) and L-ficolin. These proteins bind to short carbohydrate structures such as Mannose sugar on the surface of pathogens, which leads to cleavage of C4 and C2 by MASP-1 & MASP-2 and generating C3 convertase (C4b2a).

The alternative pathway: This pathway is initiated by spontaneous hydrolysis of C3 and binding of C3b directly by covalent attachment to the pathogen surface (Murphy, 2012). Factor D then cleaves protein B into Ba and Bb. C3b with Bb bind together to form C3 convertase (C3bBb).

All the three C3 convertase will bind to C3b to form C5 convertase (C4b2aC3b & C3bBbC3b) (Figure 1.6). This C5 convertase will breakdown C5 into C5a and C5b. C5b then bind to several complement proteins C6, C7, C8 and multiple units of C9 protein to form a membrane attack complex (MAC), which form pores in the cell membrane (Janeway *et al.,* 2012).

M.bovis BCG has been shown to activate the three complement pathways. BCG activates the classical pathway via binding to C1q, and it can activate lectin pathway by binding to mannose binding lectin (MBL). The alternative pathway is activated by deposition of C3b on the cell surface of BCG (Carroll *et al.,* 2009). Complement activation through C3b binding enhance the mycobacterial uptake by alveolar macrophages (Ferguson *et al.,* 2004). On the other hand it has been shown that *M.bovis* BCG bind to factor H, which is the negative regulatory factor of the complement system (Carroll *et al*., 2009). This suggests that mycobacteria can up-regulate the complement system by binding to C1q or MBL and enhance its uptake by macrophages. It also can down-regulates the effector functions of the complement system, such as the membrane attack complex formation by binding to factor H.

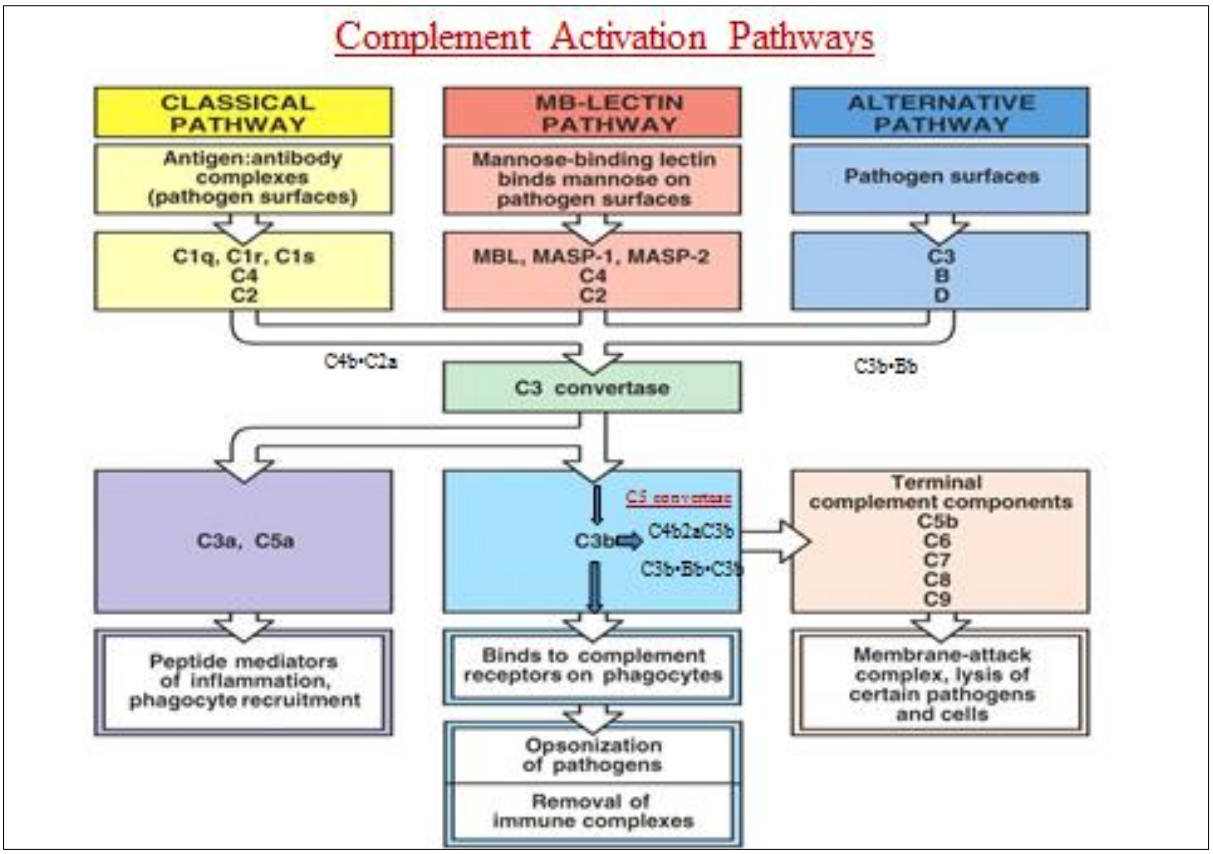

Figure 1.6: Complement activation pathways. The classical pathway is activated by binding of C1q to antibodies bound to pathogens, activating C1s to split C2 and C4 to C2a, C2b, C4a, and C4b. The lectin pathway is initiated by binding of MBL to mannose sugar on pathogen surfaces, which activate MASP-2 to split C2 and C4. Both classical and lectin pathways activation generate C3 convertase (C4b2a). The alternative pathway is activated by C3 and generating C3b. C3b binds to pathogen surfaces and opsonises them for phagocytosis by phagocytic cells. C5 convertase (C4b2aC3b) cleaves C5 which generate C5a and C5b, which initite the assembly terminal complement components, forming the membrane attack complex (MAC). Membrane attack complex lead to lysis of pathogens and cells (Janeway, 2005).

1.9.1 C1q Structure and Receptors

C1q is one of the components of C1 macromolecule complex ($C1r_2$-$C1s_2$) involved in the classical pathway of complement system. The normal concentration of C1q in human serum is around 56-275µg/ml (Dillon *et al*., 2009). The main source for C1q is macrophages, immature dendritic cells, fibroblasts and epithelial cells. C1q is produced in higher concentrations at inflammation sites (Castellano *et al*., 2004). It is composed of six identical globular heads subunits and a long collagen like region (Figure 1.7). C1q has a total of 18 chains to give a molecular weight of 460 kDa. Each sub-unit of C1q consists of three chains A (223 residues), B (226

residues) and C (217 residues). Each chain consists of globular head (135 amino acids), collagen like region (81 amino acids) and short N terminal (3-9 amino acids). Chain A, B and C has molecular weight of 25, 26 and 22 respectively. There is 27% of amino acids similarity between A, B and C chains (Smith *et al.,* 1994). In human, C1q chains genes are located on chromosome 1 at location1 p34.1-1p36.3 (Sellar & Reid, 1992).

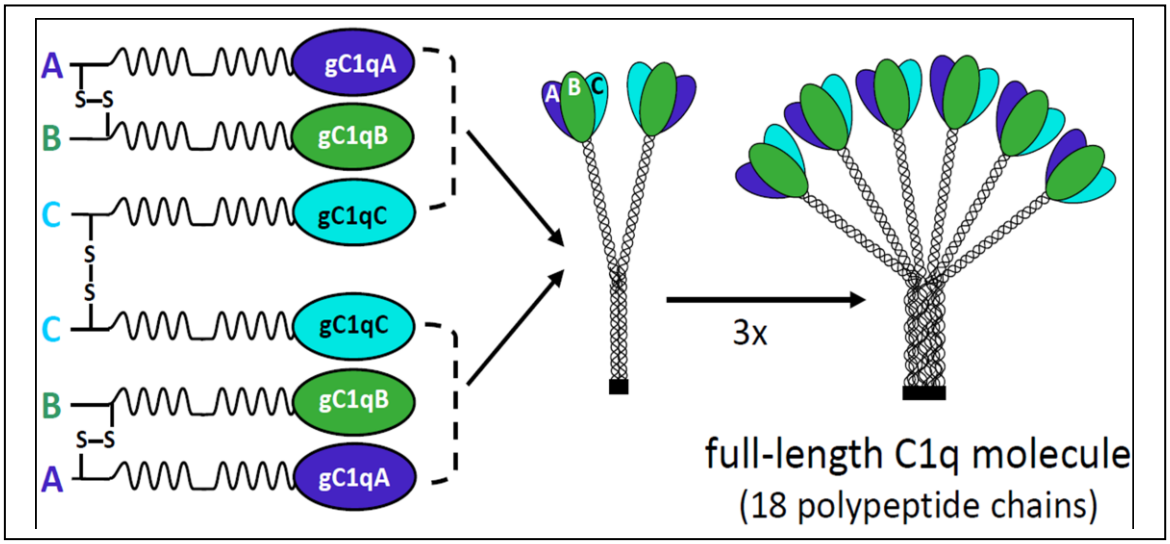

Figure 1.7: C1q structure. C1q is composed of six identical globular heads subunits. Each subunit includes a C-terminal globular region and a N-terminal collagen-like region, with disulfide bonds joining the N-terminal ends of the A and B chains and two C chains. An A-B dimer links the C chain, forming the basic chain subunit. The association of the subunits (A, B and C) together result in a full-length C1q (18 polypeptide chains) with a bouquet shape of six flowers, stalks held together in N terminal region (Frachet et al., 2015). C1q is a basic component of the classical complement pathway. It recognizes antigens bounds to antibodies and initiates activation of the classical complement pathway. C1q also plays an important role in apoptotic cells recognition and clearance.

The globular head of C1q can bind to the pathogen surface and to the immunoglobulins (Murphy, 2012). The globular C1q receptor (gC1qR) (33kDa) is known to bind with C1q globular heads. This receptor is acidic and multifunctional protein (Lim *et al.*, 1996). The gC1q binding site on this receptor is located on 76-93 residues (Ghebrehiwet *et al*., 1996). The collagen like region (CLR) of C1q was shown to bind with complement receptor 1 (CR1) and enhances the uptake of C3b and iC3b opsonized bacteria by macrophages (Medof *et al.,* 1982). CLR also binds to calreticulin–CD91 complex and this binding enhances phagocytosis and the clearance of apoptotic cells by phagocytic cells. Calreticulin is an intracellular

protein, and which binds the CD91 receptor on the cell surface (Vandivier *et al.,* 2002). Table 1.7 below shows receptors on host cells that interact with C1q.

Table 1.7: Receptors for C1q on host cells

Receptors on host cells	Part of C1q involved	Function	Reference
CR1	CLR of C1q	Phagocytosis of C3b and iC3b opsonized bacteria	Medof *et al*., 1982
Calreticulin (CRT) linked to CD91 (intracellular receptor)	CLR of C1q	Clearance of IgG opsonized *Mtb* and clearance of apoptotic cells	Vandivier *et al.,* 2002
C1qRp (CD93)	CLR	Enhances phagocytosis	Steinberger *et al.*, 2002
CRT(intracellular on ER)	globular head	Apoptotic cells clerance	Ogden *et al*., 2001, Kishore et al., 1997
gC1qR (33 kDa)	Globular head	Coagulation	Ghebrehiwet *et al*., 1994
β1 integrin (on fibroblasts & endothelial cells	CLR	Adhesion of mononuclear cells to complement containing immune complex s	Edelson *et al*., 2006

1.9.2 C1q functions through complement activation

The main known function of C1q is to activate the classical pathway of complement system by binding to antibodies bound to pathogens. Pathogens can escape the immune system by developing different mechanisms for down regulating complement activation; they can mimic complement inhibitors such as FH (Carroll *et al.,* 2009). Some pathogens produce proteases to destroy or stop the complement activation such as *Salmonella enterica* and *Porphyromonas gingivalis* (Jagels *et al*., 1996). C1q deficiency is associated with higher susceptibility to infectious diseases including otitis media, pneumonia, and meningitis (Pickering *et al.,* 2008)

M. tuberculosis is adapted to live inside macrophages and it could activate the complement system to increase its uptake by macrophages. C1q has been shown to bind with *M. bovis BCG* (Carroll *et al*., 2009). There are no previous reports about the binding of C1q to *Mtb* or it is effect on mycobacteria. Binding of C1q to BCG suggesting that C1q may be involved in the pathogenesis of tuberculosis as

levels of the C1q expression was seen to be increased in peripheral blood taken from active untreated TB patients (Cai, *et al*., 2014).

1.9.3 The non- complement functions for C1q

C1q has different non-complement functions; such as clearance of apoptotic cells, cell differentiation, aggregation, chemotaxis, adhesion and modulating B cells activity by stimulating IgG secreation by B lymphocytes (Young and Ambrus, 1991).

C1q is involved in pregnancy; C1q deficiency in mice leads to more abortions when compared to normal mice (Agostinis *et al.,* 2010), and during pregnancy, C1q is expressed on decidual epithelial cells (DECs) and not expressed on non-pregnant uterine epithelial cells (Bulla *et al*., 2008).

C1q play role in autoimmune diseases. Deficiency in C1q is associated with inefficient apoptotic cell clearance and this result in a release of auto antigens that lead to autoimmune diseases, such as glomerulonephritis and systemic lupus erythematous (SLE) (Dillon *et al.,* 2009). SLE is associated with decreased clearance of apoptotic cells and increased cytokine (IFN-α , IL-6, IL-8 and TNF-α) production by DCs, and this induced by immune complexes. Moreover, the phenotype of C1q-deficient mice has been shown apoptotic cells accumulation in diseased glomeruli (Walport *et al.*, 1998).

There is also an emerging role for C1q in cancer, C1q expressed by epithelial cells of prostate tissues sustain the activation of WOXI (tumor suppressor), and it inhibits prostate cancer cells proliferation. C1q down-regulation was also shown to enhance prostate cancer formation (Hong *et al*., 2009).

C1q expression increases in Alzheimer's disease, and this is associated with reduction of microglial proliferation (Färber *et al*., 2009), increase deposition of amyloid plaques which causes neurodegeneration and neuroinflammation (Bonifati and Kishore, 2007). C1q activates microglial cells in CNS for digestion of apoptotic neurons, and by suppressing pro-inflammatory cytokines IL-1a, IL-1b, IL-6 and TNF-α production (Fraser *et al.,* 2010). Table 1.8 shows the known non-complement functions for C1q.

Table 1.8: Non-complement functions for C1q

Function of C1q	Reference
Clearance of apoptotic cells, cell differentiation, aggregation and adhesion of erythrocytes	Vandivier et al., 2002, Hosszu et al., 2007, Suba and Csako,1976, Tas et al., 1999
Recruitment and adhesion of platelets during injury and inflammation	Peerschke and Ghebrehiwet, 1998
C1q enhances dendritic cells maturation	Csomor et al., 2007
Increases deposition of circulating ICs and leukocyte recruitment	Stokol et al., 2004
C1q increases IgG production by B cells	Young et al., 1991
C1q may prevent abortion in pregnancy	Agostins et al., 2010, Bulla et al., 2008
C1q protects against prostate cancer by activating tumor suppressor WOXI	Hong et al., 2009
C1q increases amyloid plaques deposition which causes neuroinflammation	Bonifati and Kishore, 2007
Microglial activation and proliferation by binding to apoptotic neurones	Farber et al., 2009, Fraser et al., 2010
C1q enhances migration of neutrophils to the inflammation site	Leigh, E.L, 1998

1.10 Fibronectin structure

Fibronectin (FN) is a large (440kDa) glycoprotein that is found in two forms; a soluble form in plasma, cerebrospinal fluid and amniotic fluid and an insoluble form in extracellular matrix and in the basement membranes (Mosher, 1980). In plasma, it consists of two subunits joined together by a C terminal disulfide bond (Figure 1.8) (Pasula *et al.,* 2002). Each monomer (220 kDa) consists of homologous modules of 40-90 amino acids, classified as type I, II, and III FN repeats (Sharma *et al.,* 1999, Pankov & Yamada, 2002). FN contains 12 types I repeats, 2 type II repeats and 15-17 type III repeats (Pankov & Yamada, 2002). Type I repeats consist of 40 amino-acids and two disulfide bonds; Type II repeats consist of 60 amino acids and two interchain disulfide bonds; Type III repeats consist of 90 amino acids. Though FN protein is the product of one large single gene (around 50 kb for human FN) located on the long arm of chromosome 2 at 2q34, the resulting FN can be found naturally in more than one form. These forms arise as a result of pre-mRNA splicing and various post translational modifications that can produce as many as 20 variants in human FN (Kosmehl *et al.,* 1996). A major type of splicing occurs within the central part of type III repeats (FN III $_{7}$-FN III $_{15}$). Extra domain A (EDA), extra domain B (EDB), and nonhomologous variable (V) region result from alternative splicing of mRNA. Plasma FN usually has less molecular weight than cellular FN. Also, plasma FN usually lacks EDA and EDB sequences, but contains a non-homologous stretch (V0).

In addition to alternative splicing, different posttranslational modifications are responsible to heterogeneity of FN. After protein synthesis, glucose, phosphor, and sulphate can be added to FN (Paul and Hynes, 1984).

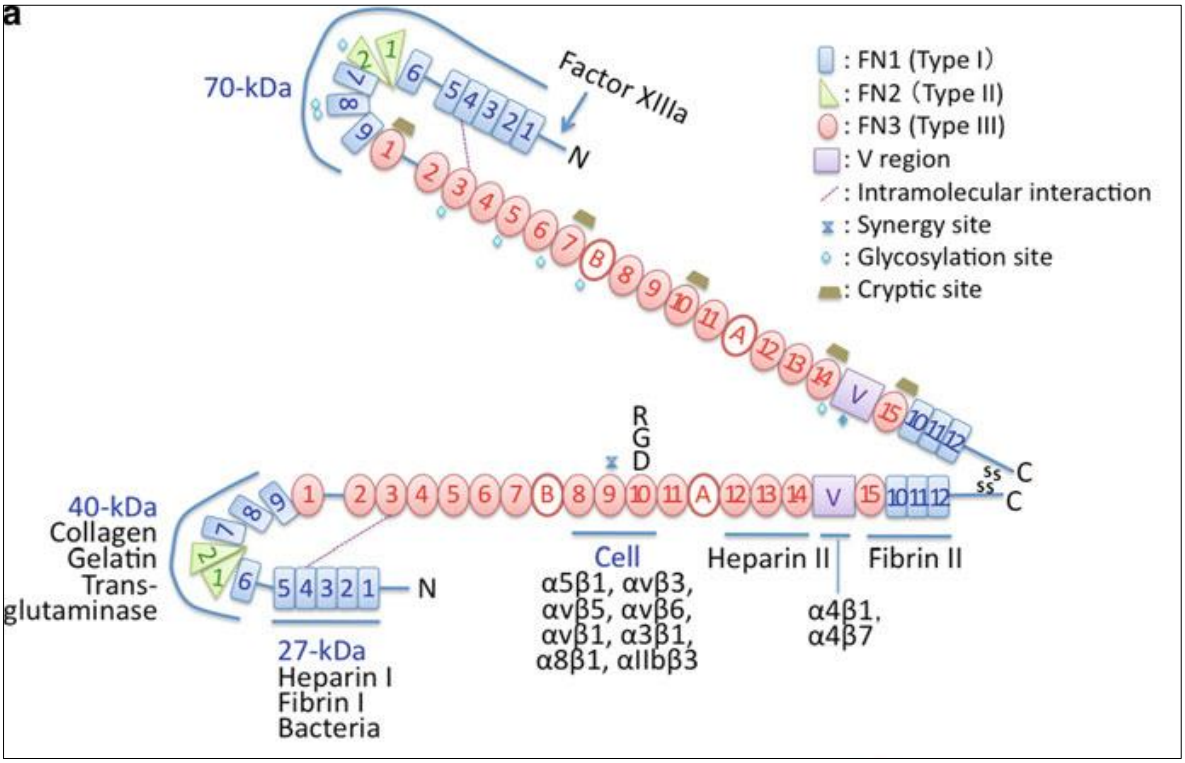

Figure 1.8: Fibronectin structure. This diagram shows the two monomers connected to each other's with carboxyl terminal by a pair of sulfide bonds. 12 type I modules (blue rectangles), 2 type II modules (green triangle), and 15-17 type III modules (red ovals) (Xu & Mosher, 2011).

1.10.1 Fibronectin functions

Fibronectin (FN) is a multifunctional glycoprotein that has a role in cell adhesion, migration, spreading and thrombosis. FN binds to cells via cell surface receptors called integrins. It is involved in the modulation of leukocyte functions (Dobke *et al*., 1983), and it binds fibrin, collagens, and heparin. The function of each domain has been defined by using proteolytic fragments and recombinant DNA technology (Pankov & Yamada, 2002). A tripeptide, Arg-Gly-Asp (RGD) is the major cell binding domain on FN that interacts with integrin receptors and mediates cell adhesion. Mouse embryos which the RGD region was substituted with inactive RGE died at day10 with sever vascular defects (Takahashi *et al*., 2007). FN binds denatured collagen via its collagen binding domain on ^{6}FN1-^{9}FN1 and ^{1}FN2-^{2}FN2 to remove it from blood and tissues (Pankov & Yamada, 2002). FN binds fibrin and

this binding is mediated by Factor XIII. This interaction helps incorporate FN into fibrin clot, stimulate thrombus growth (Cho & Mosher, 2006). FN interacts with heparin sulphate proteoglycans via at least two heparin binding domains. The strongest site localize to ^{12}FN3-^{14}FN3 module in C terminal. The heparin weaker site is localized to ^{1}FN1-^{5}FN1 module in N terminal. Heparin binding domain works with cell binding domain to enhance cell adhesion and spreading. FN can also bind to bacteria via heparin binding domain ^{1}FN1-^{5}FN1 in N terminal. Moreover, FN can be assembled into FN fibrils, and inhibition FN fibril formation causes delay in the embryonic development (Darribere et al., 1990).

Previous studies have shown that FN binds to different bacterial species including *Mycobacterium tuberculosis*, *Mycobacterium avium*, *Staphylococcus aureus, and Streptococcus pyogenes* (Pasula *et al*., 2002, Schorey et al., 1996, Hudson et al., 1999). Binding of *Mtb* to FN facilitates the attachment of *Mtb* to alveolar macrophages and airway epithelial cells (Pasula *et al*., 2002, Hall-Stoodly *et al*., 2006) whilst the binding of *M.avium* with FN facilitates mycobacterial entrance through intestinal epithelial barriers (Schorey *et al*., 1996). The heparin binding domain in COOH terminal of FN plays an essential role in BCG and *Mtb* attachment to FN (Pasula *et al*., 2002). The attachment of BCG to FN is an important step for the treatment of superficial bladder cancer patients; to increase phagocytosis of mycobacteria by epithelial cells and to initiate delayed hypersensitivity to mycobacterial antigens (Ratliff *et al*., 1993).

1.10.2 Fibronectin receptors on mycobacteria

Previous studies have demonstrated the attachment of mycobacterial secreted proteins to FN. These proteins are surface receptors found on several mycobacterial species cell wall, and they are secreted in mycobacterial cultures. One of these identified proteins is 55 kDa from *M. vaccae*. This protein (55kDa) was detected in *M. vaccae* culture supernatant after 3 weeks, and has shown to bind FN (Ratlif *et al*., 1993). Ag85B is another secreted protein of *Mtb* and *M.bovis* that binds FN (Peake *et al.,* 1993). Protein 85B is a member of the secreted protein of the antigen 85 complex (Ag85A, Ag85B, and Ag85C) (Bentley-Hibbert *et al.*, 1999, Peak *et al*., 1993). Protein 85 consists of 3 components with a molecular weight 30-32 kDa. It was demonstrated that 85B protein reacted with the collagen

binding domain (32kDa) of FN (Peak *et al*., 1993). The 32kDa fibronectin attachment protein (FAP) from *M. avium* is one of FN attachment proteins. Addition of recombinant FAP to human respiratory tract inhibited the binding of *M.avium* to the damaged epithelial tissues (Lee *et al*., 2009). Proteins of antigen 85 complex bind to cellular and plasma FN (Bentley-Hibbert *et al*., 1999). Digested fragments of Ag85 complex were shown the minimum binding motif of Ag85, and these six amino acids residues ($_{98}$FEWYYQ$_{103}$) were critical for FN binding (Naito *et al*., 1998).

1.11 THP-1 cells

THP-1 is a human monocytic cell line, used as a model for human macrophages, as they perform the same function of phagocytosis in different pathogens (Tsuchiya *et al*., 1982).

THP-1 cells have become one of most widely used cell lines to investigate the function of monocytes and macrophages. This cell line was derived from the blood of a patient with acute monocytic leukaemia. During culture, the THP-1 cells can maintain these monocytic characteristics for over 14 months. They can produce lysozymes, express FC and C3b receptors, phagocytic and restore the response of T lymphocytes (Tsuchiya, 1982). These cells also express HLA class I (A2, A3, B5) and HLA class II (DRw1, DRw2) (Tsuchiya *et al*., 1980).

In this project THP-1 cells were used without any artificial stimulation such as PMA. THP-1 cells were stimulated naturally with mycobacteria, and performed their functions of phagocytosis, cytokine production, and mycobacterial killing.

1.12 Hypothesis and aims

The main hypothesis of this study is “Surfactant protein-D, C1q and fibronectin have an effect on the growth of *Mtb*”. These proteins are found naturally in the body at the site of *Mtb* infection. SP-D is produced inside the lungs by alveolar type II epithelial cells and Clara cells. C1q is produced at the site of infection by immature dendritic cells, monocyte and macrophages. The concentrations of C1q and FN in plasma are 115 and 300µg/ml respectively, and they leak out from blood vessels to the infection site. It has been shown that FN concentration in the pleura of TB patients is much higher (441µg/ml) as compared to patients with non-specific infections (335µg/ml) (Klockars *et al.,* 1982). Additionally, these proteins have been shown to bind with mycobacteria and host cells. SP-D is known to inhibit the growth of different pathogens, C1q binds with *M. bovis BCG* directly (Carroll *et al*., 2009) and FN binds *Mtb* and BCG directly (Pasula *et al*., 2002). The main aims of this study are:

Aim 1: To investigate the direct effect of rfhSP-D, C1q and fibronectin proteins on the growth of *M. smegmatis* and BCG *in vitro*. This will be performed by incubating mycobacteria in the presence and absence of each protein to investigate whether this protein inhibits mycobacterial growth directly. These proteins could have a direct effect on the growth of mycobacteria.

Aim 2: To investigate the effect of rfhSP-D, C1q and fibronectin proteins on the uptake (phagocytosis) of *M. smegmatis* and *BCG* by THP-1 cells.

For this study, the human monocytic cell line THP-1 will be used as a model for macrophages. It has been shown previously that SP-D increases the uptake of *M.avium,* whilst decreasing the uptake of *Mtb* by macrophages. C1q increases the uptake of BCG through complement activation whereas fibronectin increases the uptake of BCG by endothelial cells in prostate cancer. We hypothesise that these proteins could interact with macrophages and increase or decrease mycobacterial uptake by these cells.

Aim 3: To investigate the effect of rfhSP-D, C1q and fibronectin on the growth of *M. smegmatis* and *BCG* inside THP-1 cells.

The effect of each protein on the growth of mycobacteria inside macrophages will be studied after 24 hours of incubation *in vitro*. This study will show the ability of these proteins to kill mycobacteria inside THP-1 cells after 24 hours.

Aim 4: To investigate the effect of the individual globular heads of C1q (ghA, ghB & ghC) on *M.smegmatis growth* in terms of binding, direct effect, uptake and growth inside THP-1 cells. The results of these experiments will reveal which chain(s) is/are most responsible for the main effect of C1q on mycobacterial growth.

Aim 5: To understand the underlying mechanisms of mycobacterial growth control inside THP-1 cells using rfhSP-D, C1q and fibronectin treated *M.smegmatis* and BCG.

The ability of each self-protein to activate or inactivate human macrophages infected with mycobacteria will be investigated by studying the gene expression and production of different pro-inflammatory and anti-inflammatory cytokines, chemokines and inducible nitric oxide synthase. Macrophages kill bacteria by inducible nitric oxide intermediates. Inducible nitric oxide synthase is responsible for the production of these intermediates. For example, a higher expression level of this enzyme produced by macrophages will be associated with an increased bacterial killing.

Chapter 2 - General Methods and Materials

2.1 Expression of recombinant fragment human surfactant protein- D

Recombinant fragment human SP-D (rfhSP-D) was expressed in *E.coli* strain BL21 (λDE3) pLysS by recombinant DNA technology (Singh *et al*., 2003). Plasmid pUK-D1 containing cDNA for a globular CRD region (residues 236–355), an α-helical coiled-coil neck region (residues 203–235), and eight Gly–X–Y triplets of human SP-D was expressed under bacteriophage T7 promoter (Mahajan *et al*., 2008) (Figure 2.1).

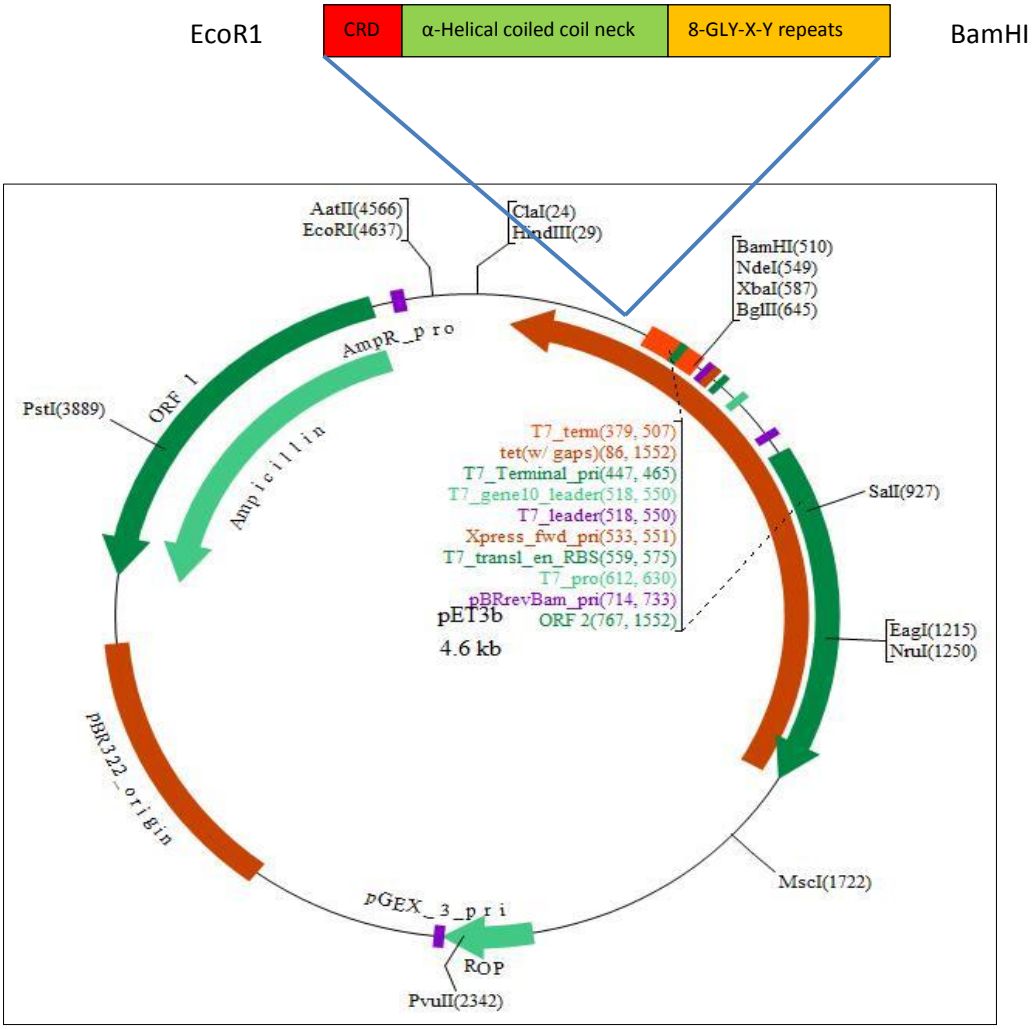

Figure 2.1: Vector map for rfhSP-D expression. Vector pET-3b was used for rfhSP-D expression. SP-D was cloned directly into NdeI/HindIII site in the pET-3b vector. Bam HI, XbaI and BgIII are restriction enzymes that cut DNA at specific sequences and generate short DNA fragments; these are then combined with vector DNA to generate recombinant DNA molecules. The expression involved CRD, α-helical coiled coil neck, and 8 GLY-X-Y repeats from the collagen region.

2.1.1 Competent Cells preparation

Competent cells were prepared using $CaCl_2$ (Dagert and Ehrlich, 1979) in-order to transfect with plasmid PUK-D1 (10-100pg) containing cDNA for the CRD, the neck and 8 Gly-X-Y region of human SP-D gene under bacteriophage T7 promoter.

One colony of BL21 (λDE3) pLysS (Invitrogen) was inoculated in 10 ml of Lauria Broth (LB) media containing 10µl chloramphenicol (50mg/ml dissolved in ethanol) and incubated overnight in the 37^{o}C shaker. Next morning, 0.5 ml of the overnight culture was removed and transferred to a 50 ml falcon tube containing 25 ml of LB medium with 25µl of chloramphenicol. The bacterial culture was incubated at 37^{0}C (200rpm) in the shaker. The optical density (O.D=600nm) was checked after one hour until it reached an O.D value of 0.3-0.4 (Early Log phase). The bacterial culture was then centrifuged at 2000 rpm for 5 minutes. The supernatant was discarded and the cell pellet was re-suspended in 12.5 ml of 0.1M $CaCl_2$ and kept on ice for 1 hour. The cells were then centrifuged for 5 minutes at 2000 rpm. The supernatant was discarded and the cell pellet was re-suspended in 2ml of 0.1M $CaCl_2$. The competent cells were kept on ice ready for transformation.

2.1.2 Transformation of cells

200 µl of the competent cells were transferred into 10 ml falcon tube containing 1-2 µl (10-100pg) of pUK-D1 plasmid for rfhSP-D expression and the tube was placed on ice for 1 hour. The cells were subjected to heat Shock at (42^{o}C) for 90 seconds inside a water bath and placed immediately on ice for 5 minutes. The transformed cells were grown in 800µl LB medium for 45 minutes at 37^{o}C with gentle shaking every 10-15 minutes. Following the incubation, 100µl from the bacterial culture (transformed cells) was spread on an agar plate containing 50µg/ml chloramphenicol and 100µg/ml ampicillin. Presence of chloramphenicol and ampicillin allows the growth of transformed cells only because they contain these two antibiotic resistant genes. The transformed colonies were allowed to grow overnight at 37^{o}C incubator.

2.1.3 Pilot Scale Expression

Four separate colonies from transformed cells were inoculated into 4 separate 20ml culture tubes containing 5 ml LB medium supplemented with the antibiotics (100µg/ml ampicillin and 50µg/ml chloramphenicol). The bacterial cultures were grown for 17 hours inside a 37^{o}C shaker. Next, 250µl of each culture was transferred into 50ml falcon tube containing 10ml LB media supplemented with the antibiotics, and incubated at 37^{o}C shaker for 2 hours. Optical density was measured after 2 hours, and every 10 minutes until the O.D reached a value of 0.6-0.8 at A_{600} (Log phase). 1 ml of un-induced bacterial culture was removed in separate tube, and the remaining culture was induced with 0.4mM IPTG (Sigma-aldrich, cat no. 16758). IPTG is a compound mimics lactose metabolite that initiates transcription of rfhSP-D gene under the control of the lac operon. Both induced and un-induced cultures were incubated inside 37^{o}C shaker for 3 hours. Following the incubation, 1ml of induced culture was removed into an Eppendorf tube and the remaining culture was stored at 4^{o}C. All tubes containing induced and un-induced cultures were centrifuged at 13000 rpm for 15 minutes. The supernatant was discarded and the cell pellet was mixed with 100 µl treatment buffer containing (1.6ml of 1M Tris-CL, 4ml of 10% SDS, 2ml of 100% glycerol, 0.04% Bromophenol blue, 1ml of 2-mercaptoethanol, and 1.4 ml distilled water). The tubes were incubated at 100^{o} C using a heating block for 10 minutes and 20µl was loaded into a 12% SDS gel. The gel was run at 120 volts for 90 minutes and stained with Comassie blue (Bio Rad) (0.025g in 25ml of de-staining solution containing (methanol, acetic acid, and water at ratio 5:1:4) overnight. Following overnight staining the gel was placed in the de-staining solution (methanol, acetic acid, and water at ratio 5:1:4) for 2-3 hours. After observing the gel, the colonies giving the best protein expression were streaked on a LB agar plate supplemented with 100µg/ml ampicillin and 50µg/ml chloramphenicol. The plates were grown at 37^{o}C overnight, and were used for large scale expression of generating rfhSP-D.

2.1.4 Large scale Expression

Large scale expression was carried out after getting positive results from the pilot scale expression. One colony of transformed cells (pUK-D1) was inoculated inside 100ml conical flask containing 12.5ml LB medium supplemented with the

antibiotics (100µg/ml ampicillin and 50µg/ml chloramphenicol) and incubated for 17 hours at 37^{o}C inside a shaker. Following the incubation period the culture was transferred into a conical flask containing 500ml LB with antibiotics and grown at 37^{o}C. The optical density was measured every 2 hours until the O.D reached 0.6-0.8 at A_{600} (Log phase). Bacterial culture was then induced with 0.4mM IPTG (Sigma-aldrich, cat no. 16758) and grown at 37^{o}C shaker for 3 hours. Next, the cells were harvested by centrifugation at 5000rpm for 15 minutes. The supernatant was discarded and the cell pellet was stored at $^{-}$20^{o}C for further processing.

2.1.5 Cell Lysis and Sonication

The cells pellet obtained was resuspended with 50ml cold lysis buffer containing (50mM Tris-HCL, 200mM NaCL, 5mM EDTA, 0.1% Triton X-100, 0.1mM PMSF (Sigma-Aldrich), and 50 µg/ml lysozyme (Sigma-Aldrich)) on ice and left spinning on a magnetic stirrer for 1 hour at 4^{o}C in a cold room. The lysate was then sonicated (Heat Systems Sonicator) for 10-15 cycles, 30 seconds each. The sonicated culture was centrifuged at 8500rpm for 15 minutes and the supernatant was discarded. The cell pellet was stored at $^{-}$20^{o}C.

2.1.6 Dialysis

The sonicated pellet was solubilized in 100ml buffer containing (8M urea, 50mM Tris-HCl, pH 7.5, 100mM NaCl, 10mM 2-Mercaptoethanol (Sigma Aldrich, cat no. M3148), and 0.05% Sodium azide (Sigma Aldrich). The solubilized mixture was then dialyzed against buffer containing 4M, 2M and 1M urea for 2 hours each and 0M urea buffer overnight. The following day, the protein from the dialysis was centrifuged at 8500rpm for 20 minutes to remove any impurities. The supernatant containing rfhSP-D was then dialysed against calcium buffer containing (20mM Tris-HCL PH 7.5, 100Mm NaCl. 10mM $CaCl_2$) for 3 hours to eliminate all urea from the protein. Calcium is important for rfhSP-D binding to Maltose-Agarose.

2.1.7 Protein Purification by Affinity Chromatography

The protein mixture obtained from dialysis was loaded onto a Maltose–Agarose column (Sigma-Aldrich, cat.no. 8896). The column was washed prior to use with 50 ml sterile distilled water, this was followed by 50ml sterile affinity column buffer (50mM Tris-HCL PH 7.5, 100mM NaCl, 5mM $CaCl_2$). The protein mixture was then passed twice through the column, and rfhSP-D was eluted by passing elution buffer (containing 5mM EDTA, 50mM Tris–HCl PH 7.5, 100mM NaCl). 10-15 fractions of purified rfhSP-D were collected into 1ml eppendorf tubes and the protein concentration was measured at 280nm using a DNAwave Spectrophotometer. The presence of rfhSP-D was confirmed by running samples from each protein fraction on a 12% SDS PAGE.

2.1.8 Endotoxin removal from purified proteins

The endotoxin LPS (present in the *E.coli* cell wall) was removed from purified proteins because it is presence could interfere with the experemintal results. LPS is able to bind with TLR4 on the surface of phagocytic cells and induces pro-inflammatory responses (Lu et al., 2008). A polymyxin B column (Sigma-Aldrich) was used to remove lipopolysaccharides from the purified protein. The column was washed prior to use with 50ml of 1% sodium deoxycholate (Thermo Scientific, cat.no. 89904), followed by 50ml pure water. The protein was then loaded onto the column and incubated at 4^oC on a roller shaker for 1 hour. Next, the protein was collected and the concentration was measured using a Nanodrop Spectrophotometer. A sample of LPS free protein was verified by 12% SDS PAGE. The LPS free purified proteins were stored at $^-20^oC$ in 50µl aliquots to be used for experiments.

2.1.9 Endotoxin level measurement in purified proteins

Limulus amebocyte lysate (LAL) is an extract from amoebocytes of horseshoe crab (*Limulus polyphemus*) blood cells. LAL reacts with very low levels of LPS from gram negative bacteria, and causes coagulation. This reaction is the basis of

the LAL test, which is used for quantification of bacterial endotoxins. The Chromogenic Lumulus Amebocyte Lysate (LAL) endotoxin assay kit (Gen Script) was used for detection of endotoxin level in purified proteins after LPS removal. Firstly, Serial dilutions of endotoxin standard were prepared as following: The endotoxin standard provided with the kit was dissolved by adding 2ml of LAL Reagent Water to give 20EU/ml stock; this solution was mixed for 15 minutes by using a vortex. Then, 1EU/ml solution was prepared from 20EU/ml stock solution by adding 50µl stock to 950µl LAL reagent water. Next, serial dilutions were carried out from 1EU/ml solution to get 0.5, 0.25 and 0.125EU/ml standard solutions.

Endotoxin level was measured for each endotoxin standard solution, protein sample and blank as following: 100µl of protein sample and 100µl of each standard solution were placed in separate labelled test tubes. One tube containing 100µl of LAL reagent water was used as blank. Then, 100µl of LAL reagent was added to all tubes, mixed gently and incubated at 37^{o}C for 7 minutes using a heating block. After that, 100µl of substrate solution was added to each tube, mixed and incubated at 37^{o}C for 6 minutes. Following incubation, 500µl of stop solution was added to all tubes and mixed gently, and 500µl of Colour-stabilizer number 2 was added to all tubes and mixed. Then, 500µl of Colour-stabilizer number 3 was added with gentle mixing. Finally, the absorbance was read at 540nm for all tubes. The mean absorbance for the four standards solutions (EU/ml) was plotted and a line of best fit was drawn. The endotoxin concentration of protein sample was measured according to the following equation (0.2618x-0.0012) EU/ml, where x is the mean absorbance. The table below summarize the full testing procedure.

Table 2.1: Preparation of blank and protein samples for endotoxin measurement by LAL assay

	Sample	Blank
Protein or standard	100µl	
LAL Reagent Water		100µl
LAL	100µl	100µl
Mix and incubate at 37^{0}C	7 minutes	7 minutes
Substrate solution	100µl	100µl
Mix and incubate at 37^{0}C	6 minutes	6 minutes
Stop solution	500µl	500µl
Colour-stabilizer number 2	500µl	500µl
Colour-stabilizer number 3	500µl	500µl
Mix and read absorbance at 540nm		

2.2 Expression of MBP fused ghA, ghB, and ghC of C1q protein

The recombinant fusion proteins, MBP-ghA, MBP-ghB, and MBP-ghC were expressed in *E.coli* BL21 (DE3). This *E.coli* strain was transformed with pkBM-A (vector containing ghA linked to MBP), pkBM-B (vector containing ghB linked to MBP), and pkBM-C (vector containing ghC linked to MBP). Plasmid pMAL-c (Figure 2.2), which codes for maltose binding protein (MBP) under the P_{lac} promoter was used for protein expression (New England Biolabs, Beverly, MA). The expression included amino acids sequences: 88-223 of ghA, 90-226 of ghB, and 87-217 of ghC (Kishore *et al*., 2003).

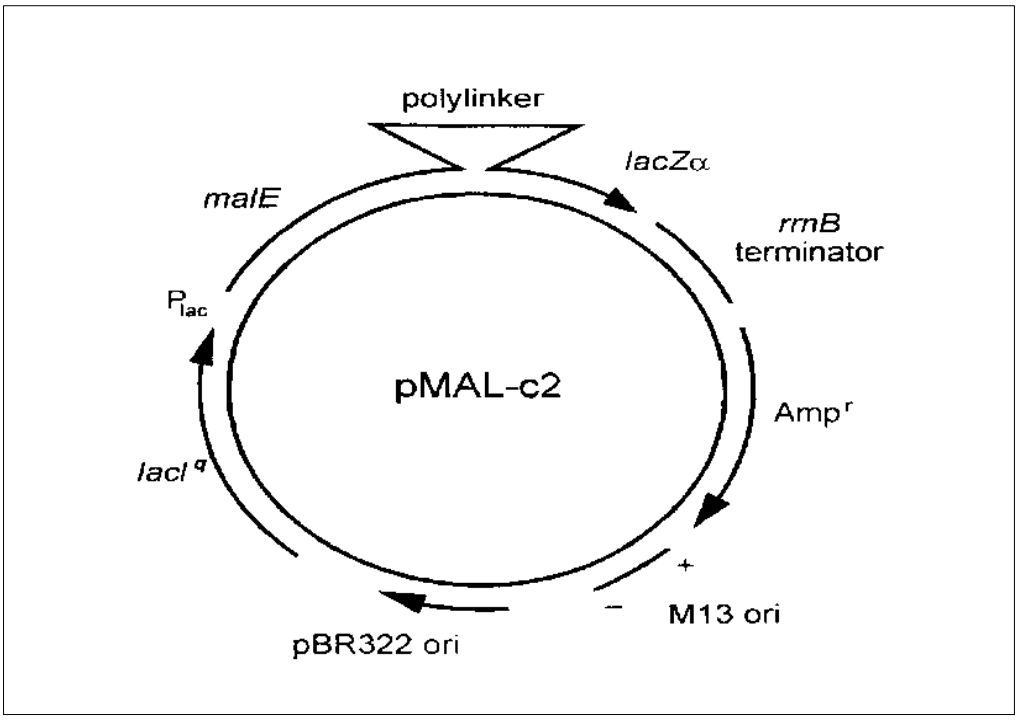

Figure 2.2: Vector map for MBP fused ghA, ghB, and ghC expression. Vector pMAL-c2 which codes for MBP under the Plac promoter was used for proteins expression (Wise and McIntosh, 1998). The ghA, ghB and ghC genes were cloned into a pMAL vector downstream of the malE gene that encodes MBP. The recombinant vectors, containing MBP linked with ghA, ghB, or ghC gene sequences were nominated pKBM-A, pKBM-B, and pKBM-C, respectively. MBP-ghA, -ghB, and –ghC proteins were expressed using *E. coli* BL21 transformed with pKBM-A, pKBM-B, and pKBM-C, respectively (Kishore et al., 2003). The recombinant fused proteins were purified using amylose affinity chromatography.

2.2.1 Large scale expression

The transformed bacterial cells containing MBP-ghA, -ghB, and –ghC were grown in 25ml LB containg 100µg/ml ampicillin overnight at 37^{o}C shaker. The overnight cultures were transferred into a sterile flask containing 1litre of LB with 100µg/ml ampicillin. The flasks were incubated in a 37^{o}C shaker until the cells reached an optical density of 0.6-0.8 at A_{600}. After that 1ml of uninduced culture was removed and the remaining cell culture was induced with 0.4mM isopropyl -D-thiogalactoside (IPTG) (Sigma-aldrich, cat no. 16758). All induced and un-induced cultures were incubated at 37^{o}C shaker for 2.30-3.00 hours. After the incubation period, cultures were centrifuged at 5000rpm for 10 minutes. Samples (100µl)

from induced and un-induced cultures were mixed with 100µl treatment buffer containing β-mercaptoethanol, and heated for 10-15 minutes at 100^{o}C before being loaded onto 12% SDS PAGE gel.

2.2.2 Lysis and Sonication

The cell pellet obtained by large scale was resuspended in 50 ml lysis buffer (20mM Tris-HCl, pH 8.0, 0.5 M NaCl, 0.2% Tween 20, 1 mM EDTA, and 5% v/v glycerol) and incubated at 4°C for 1 hour. 50 µg/ml Lysozyme and 0.1mM PMSF was added before lysis. The cells were then sonicated for 30 seconds with 2 minute gaps for 12 cycles. The lysate was centrifuged at 13,000rpm for 15 minutes and the supernatent collected.

2.2.3 Purification of MBP fused ghA, ghB, and ghC by Affinity Chromatography

The supernatant was diluted 5 folds in buffer I (20mM Tris-HCl, pH 8.0, 100mM NaCl, 0.2% v/v Tween 20, 1 mM EDTA, and 5% v/v glycerol). An amylose resin column was washed with 75ml sterile distilled water, 75ml 0.1% SDS solution and 75ml buffer I. Next the protein supernatent was passed through the column. The column was then washed with 75ml buffer I, followed by 60ml of 1M salt buffer (containing 1M NaCl, 20mM tris-Cl, and 0.5mM EDTA), and 75ml of buffer II (Buffer I without tween 20). Each fusion protein was eluted in 5 ml fractions with 10mM maltose in 100ml buffer II and stored at $^{-}$20^{o}C. The protein concentration was measured at 280nm using DNAwave spectrophotometer. LPS was removed by using a polymyxin B column (section 2.1.8) and endotoxin levels was measured by using LAL assay as described in section 2.1.9.

2.3 Protein characterization techniques

2.3.1 Sodium Dodecyl Sulfate Polyacrylamide Gel Electrophoresis (SDS-PAGE)

The presence of the protein was verified by running samples on a SDS-PAGE following protein purification in order to determine the correct molecular weight. The molecular weight of the desired protein was compared to a protein marker (Bio Rad, cat no. 161-0374). In this technique SDS covers the protein with a negative charge, and the protein migrates towards the anode (positively charged electrodes) in the electrical field. Purified rfhSP-D (20kDa), C1q chains (21-26kDa) and purified MBP fused ghA, ghB, and ghC (60kDa) were characterized by using 12% SDS-PAGE gel whilst fibronectin chains (220kDa) was characterized by using 8% SDS-PAGE.

SDS-PAGE consists of a resolving gel that separates the protein according to its molecular weight and stacking gel on which the sample is loaded. The gel was prepared using the following methodology: Two glass plates were cleaned and inserted into the stand. The resolving gel (Table 2.2) was prepared and immediately poured between the two glass plates. A layer of distilled water was added on top of the gel, and the gel was allowed to polymerize for 30 minutes at room temperature. After polymerization, the water layer was removed and the stacking gel (Table 2.3) was added on the top of resolving gel. The 10 slot comb was inserted immediately in order to form wells and the stacking gel was allowed to polymerize for a further 15 minutes.

Table 2.2: Components of resolving gel for SDS-PAGE

Acylamide percentage	8%	12%
H_2O	2.3ml	1.6ml
Acrylamide/Bis-acrylamide (30%/0.8% w/v)	1.3ml	2ml
1.5M Tris(pH=8.8)	1.3ml	1.3ml
10% (w/v)SDS	0.05ml	0.05ml
10% (w/v) ammonium persulfate (APS)	0.05ml	0.05ml
TEMED	0.003ml	0.002ml

Table 2.3: Components and volume for preparing 1 ml of stacking gel

H_2O	0.68 ml
1 M Tris-HCl, pH 6.8	0.13 ml
10% (w/v) SDS	0.01 ml
Acrylamide/Bis-acrylamide (30%/0.8% w/v)	0.17 ml
10% (w/v) Ammonium persulfate (APS)	0.01 ml
TEMED	0.001 ml

The glass plates containing polymerized gel were placed in a holder with a buffer dam (Bio-Rad). The whole arrangement was placed inside the tank containing 1X running buffer (containing 10ml 10% SDS, 100ml of 10X running buffer and 890ml distilled water) and running buffer was added on the top of the gel. The comb was removed gently and 5µl of protein marker (Bio Rad, cat no. 161-0374) was loaded in the first well. Native and recombinant proteins were diluted in 1:1 v/v ratio in treatment buffer (1.6 ml of 1M Tris-Cl (PH 6.8), 4ml of 10% (w/v) SDS, 2ml glycerol, 0.04% (w/v) Bromophenol blue, 1ml of 2-mercaptoethanol and 1.4ml of distilled water) and they were heated for 10 minutes at 100^{o}C using heating block in order to denature proteins. Diluted proteins (20 µl) were loaded into the wells using a Hamilton syringe. The gel was run at 120 volts for 90 minutes. Following this, the gel was stained with staining solution (50% Methanol, 10%v/v acetic acid, 40% water with 0.1%Comassie blue) overnight on a rocking shaker. The following day, the gel was washed with distilled water and destained using 50% methanol, 10% acetic acid and 40% water for 2 hours. The gel image was captured using Molecular Imager (Bio Rad).

2.3.2 Western blot

A western blot was used to detect the presence of the desired proteins by a specific antibody. In this technique, protein samples were run on a 12% SDS-PAGE for rfhSP-D and 8% for fibronectin as described in section (2.3.1). Next, the gel was soaked in 1X transfer buffer (glycine, tris base, methanol and water, pH 7.5-8) along with fibro pads, 2 pieces of Whatmann filter paper and a nitrocellulose membrane for 10 minutes. The sandwich was prepared in the following order: fibro pad, 2 filter papers, gel, nitrocellulose membrane, 2 filter papers, and fibro pad. Air bubbles between nitrocellulose paper and gel was removed by a roller. The sandwich was inserted inside a western blot cassette and placed inside a holder with electrodes inside a tank containing 1X transfer buffer. An ice pad was fixed near the sandwich arrangement in the tank to prevent overheating. The tank was placed inside a tray filled with ice and the blot was transferred at 320mA for 2 hours. Once the transfer was complete, the nitrocellulose membrane was removed and placed in a petri dish containing 5% non- fat milk (w/v) in PBS overnight to block the membrane.

For rfhSP-D protein, the next morning the membrane was washed 3 times (5 minutes each) with washing buffer (PBS 0.02% Tween 20), then 1:1000 dilution of rabbit anti-human SP-D (in 1% non-fat milk in PBS) was added to the membrane and left for 2 hours at room temperature. The nitrocellulose membrane was then washed 3 times (5 minutes each) with the washing buffer and the membrane was incubated for 1 hour with Protein G (Invitrogen) conjugated with HRP (1:1000 in 1% milk in PBS). The membrane was washed 3 times with washing buffer for 5 minutes each. One OPD tablet and one urea hydrogen peroxide/buffer tablet (Sigma-Fast) were dissolved in 20 ml of water and poured on the membrane. The membrane was incubated with the solution for 2-10 minutes in the dark until sufficient colour developed and the bands became visible.

For fibronectin protein detection, the following morning the nitrocellulose membrane was washed 3 times with the washing buffer 5 minutes each. Later 1:1000 dilution of sheep anti-human fibronectin (AbD) conjugated with HRP suspended in 1% non-fat milk solution in PBS was added to the membrane for 2 hours at room temperature. Next the nitrocellulose paper was washed 3 times

with the washing buffer and Finally DAB solution was added to develop the bands as mentioned above in this section.

2.3.3 Dot blot

A dot blot was used to confirm the presence of human C1q protein. 5µg of C1q and the negative control amyloid P protein were blotted separately on nitrocellulose paper for 2 hours. The membrane was then blocked with 5% non-fat milk in PBS buffer overnight to block the membrane. The next morning, the membrane was washed 4 times for 5 minutes with washing buffer and incubated with 1:1000 of sheep anti-human C1q HRP conjugated (AbD) in 1% non-fat milk in PBS for 1 hour. Following this, the membrane was washed 5 times with the washing buffer. Finally DAB solution was added to detect the protein as mentioned in section 2.3.2.

2.4 Enzyme-Linked Immunosorbent Assay (ELISA)

Enzyme Linked Immunosorbent Assay (ELISA) was used to measure the binding of proteins to mycobacteria or THP-1 cells.

A 96-well ELISA plate (Fisher Scientific) was coated with either $10x10^6$ bacteria or $1x10^5$ THP-1 cells per well in carbonate/bicarbonate buffer, PH 9.6 (prepared by dissolving one capsule in 100ml distilled water) (Sigma-Aldrich, C3041-50CAP) and incubated overnight at 4^oC. The following morning, the plate was washed twice with 200µl of PBS-tween (PBS/0.05% Tween 20) per well. The plate was blocked with 200µl per well of 1% w/v BSA in PBS for 2 hours at room temperature. Next, the contents were discarded and the plate was washed 3 times with 200µl PBS-tween solution. Different concentrations (10, 5, 2.5, 1.25 and 0.6µg/ml) of the desired protein (50µl/well) were added to their specific wells in PBS/0.1% BSA buffer containing 5mM$CaCl_2$. The negative control wells were prepared similarly to test wells with the exception of the protein of interest. The plate was incubated for 2 hours at 37^oC. After the incubation period, the contents

were discarded and wells were washed 5 times with PBS-tween solution. 100µl of the primary antibody conjugated to HRP (1:1000) in PBS was added per well and the plate was incubated for 1 hour at 37^{o}C. After the incubation, contents were discarded and the wells were washed. Substrate TMB (Biolegend) was prepared as recommended by manufacturer, and 100µl was added per well. The ELISA plate was incubated in the dark (1-5 minutes) to allow colour to develop. Next the reaction was stopped by adding 50µl of H_2SO_4. The binding was read at 450nm using an ELISA reader (Bio-RAD, Microplate reader).

When using HRP unconjugated primary antibodies including anti-human SP-D and anti-MBP, an extra step was performed after washing the primary antibody. The secondary probe, Protein G conjugated to HRP (1:5000) in PBS/0.1BSA was added (50µl per well), and the plate was incubated for 45 minutes at room temperature. The plate was repeatedly washed and developed using TMB as mentioned above.

2.5 Immunofluorescence microscopy

2.5.1 Binding of THP-1 cells to proteins by immunofluorescence microscopy

This method was used to examine the binding between proteins and THP-1 cells. 1x10^{6} THP-1 cells were washed and suspended in 200µl PBS-BSA (PBS/0.1% BSA) per each tube. Protein (10µg/ml) was added to THP-1 cells in the presence of 5mM calcium chloride and incubated for 2 hours in a CO_2 incubator at 37°C. Untreated THP-1 cells suspended in PBS/0.1%BSA were used as a negative control. The THP-1 cells were then washed 4 times with 1ml of PBS by centrifugation at 5000 rpm for 5 minutes. The primary antibody (1:200 diluted in PBS containing 0.1% BSA) was added to all tubes and incubated for further 1 hour at room temperature. Next, the cells were washed 4 times. Protein A conjugated to FITC (Sigma) (1:200 diluted in PBS) and Hoechst (1:10000 diluted in PBS) were added to all the tubes. The tubes were incubated for 30 minutes in the dark. The cells were washed 3 times with PBS. The supernatant was discarded and the pellet was suspended in 50µl of Citifluor Glycerol/PBS Solution (PH around 10) (Agar Scientific). Slides were prepared by adding 20µl of the cell

suspension on a clean glass slide and covered with a coverslip. Slides were examined by using Lucia microscope (HF14 Leica DM4000 SOP v2).

2.5.2 Binding of BCG to proteins by immunofluorescence microscopy

This method was used to show the binding between proteins (rfhSP-D, C1q and fibronectin) with BCG. The BCG vial was thawed on ice, mixed and sonicated for 20 minutes. Four eppedorf tubes were taken, each labelled with the names of the proteins given above and a negative control. BCG was added to each tube ($20x10^6$). Respective protein (10µg/ml) was added to their particular tubes with 5mM calcium chloride. Negative control tube contained untreated BCG with calcium chloride (5mM final concentration). All tubes were incubated for 2 hour at 37^oC. The rest of the methodology was carried out as mentioned in section 2.5.1 with the exception of no Hoechst.

2.6 Growing and storing Mycobacteria

M.smegmatis (provided by Dr. Brian Robertson, Imperial collage London) were grown by inoculating one colony in 30 ml Lauria broth (LB) media containing 0.0016% (v/v) glycerol and 0.001% (v/v) Tween 80. *M.smegmatis* liquid culture was incubated at 37^oC shaker for 3 days until the $O.D_{600nm}$ reached 0.9-1.00. Liquid cultures of BCG (Pasteur strain) were grown by inoculating one colony of BCG in 100 ml Middlebrook 7H9 media (Table 2.4) containing 10% (v/v) albumin dextrose catalase (ADC) (Table 2.5). BCG cultures were incubated at 37^oC with continuous mixing using magnetic stirrer (200 rpm) for 2-3 weeks. Once the BCG cultures reached an optical density of $O.D_{600nm}$= 0.9-1.00 they were stored. For storage, 30ml *M.smegmatis* and 50ml of BCG cultures were centrifuged at 3000rpm for 30 minutes. The supernatant was discarded and the pellets were then mixed by vortexing. Bacterial suspension from each tube was mixed with the freezing solution (0.5 ml culture medium (LB or 7H9) and 0.5 ml glycerol). In each freezing vial, 100 µl of this mixture was placed and stored at $^-80^oC$. Around 15 freezing vials each containing 100µl bacteria was prepared from each culture. All vials were stored at $^-80^oC$.

Table 2.4 Preparation of Middlebrook 7H9 liquid medium

component	Per L
Middlebrook 7H9 powder	4.7 g
100% glycerol	2 ml
100% Tween 80	0.5 ml
Distilled water	897.5 ml

Table 2.5 Preparation of Albumin-dextrose-catalase (ADC)

Component	Per L
NaCl	8.5 g
Bovine Serum Albumin fraction	50 g
Dextrose	20 g
Catalase (beef)	30 mg
Distilled water	1 L

2.7 Acid-Fast staining

Acid fast staining was used to identify BCG and *M.smegmatis* and to check for any contamination in the growing mycobacterial cultures before storing. The staining protocol was carried out as following: 1ml of mycobacterial culture (O.D 0.9-1) was centrifuged at 5000 rpm for 5 minutes. The supernatant was discarded and a smear was made from the pellet on a clean slide and left to dry at room temperature. Next, the smear was fixed by passing the slide 3-4 times through the flame. For the staining, the smear was covered with filter paper, and the red colour Carbol Fuschin stain (PRO-LAB, cat. No.PL.7018) was added. The smear covered with filter paper and soaked with Carbol Fuschin was then heated for 5 minutes under the flame in order to enhance dye penetration. The filter paper was never allowed to dry by adding Carbol Fuschin stain during heating. After that, the smear was allowed to cool down, and it was washed in a gentle and indirect stream of tap water until no colour appeared in the effluent. Then, a few drops of (Acid-alcohol) decolorizing solution (PRO-LAB, cat no. PL. 7024) was added to the smear and immediately washed with tap water. The bacterial smear was then flooded with methylene blue counter stain for 20 seconds (PRO-LAB, cat. no. pl.7027). Methylene blue will stain any other contaminant bacteria with blue colour

but not mycobacteria. Then, the smear was washed with tap water. The slide was air dried, and one drop (20µl) of lens emersion oil was added to the smear just before examining bacteria by oil emersion lens (100X) of light microscope. The mycobacteria appeared as red rods due to retention of Carbol Fuschin stain. This is due to fatty acids present in the cell wall, which resist decolorizing solution (Figure 2.3).

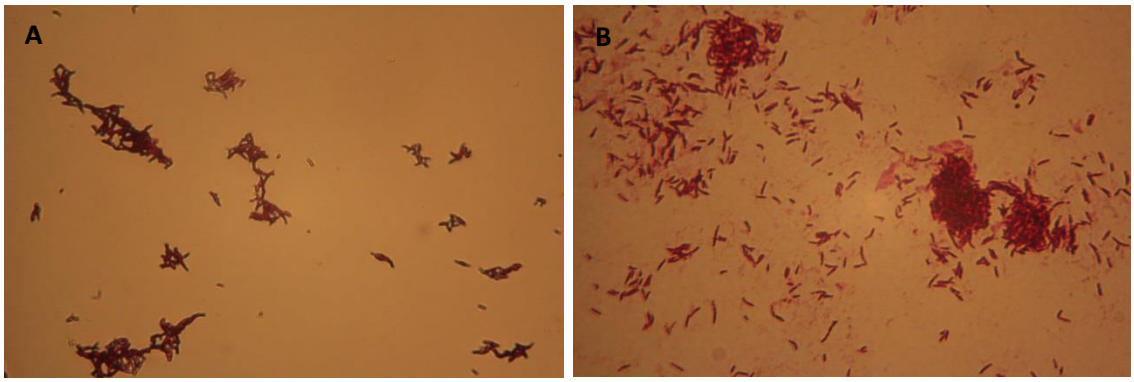

Figure 2.3 Acid fast staining for mycobacteria. A: *M.smegmatis.* B: BCG. Air- dried bacterial smear was stained with Carbol Fuschin for 5 minutes with heating. A few drops of acid/alcohol solution were added for decolorization the bacteria. Counter stain (Methylin blue) was added for 20 seconds. Slide was washed with water and examined using Oil emersion lens (100X). Total magnification was 1000x.

2.8 Counting bacterial colonies

One bacterial vial was taken from -80^{0}C, thawed and sonicated for 20 seconds using CAMLAB, Transsonic T460 Sonicator. Then, serial 10-fold bacterial dilution was prepared as the following (Figure 2.4): 10µl of sonicated and well mixed bacteria was added to 990ml of media (LB for *M.smegmatis* and 7H9 for BCG) to make 1x10^{-2}. This tube was mixed thoroughly with vortexing and immediately 100µl of bacterial suspension was removed and added to another tube containing 900µl media to make 1x10^{-3} dilution. From the later tube, 100µl of bacterial suspension was placed in a tube containing 900µl media to make 1x10^{-4}. The serial dilution was carried out until 1x10^{-8} serial dilution was reached. Tubes containing bacterial dilutions 1x10^{-4}, 1x10^{-5}, 1x10^{-6}, 1x10^{-7} and 1x10^{-8} were used. For bacterial counting, 250µl from each dilution was plated on an agar plates for *M. smegmatis*, and 7H10 media containing 10 % ADC for *BCG*. 3 media plates

were used for each dilution. Plates containing *M. smegmatis* were incubated at 37°C for 72 hours and BCG plates for two to three weeks at 37°C. Finally, grown bacterial colonies were counted by visual inspection. The number of bacteria was calculated using the equation bellow:

$$\text{Number of bacteria per ml} = \frac{\text{Average number of colonies in 3 plates}}{\text{Amount plated (ml) x Dilution factor}}$$

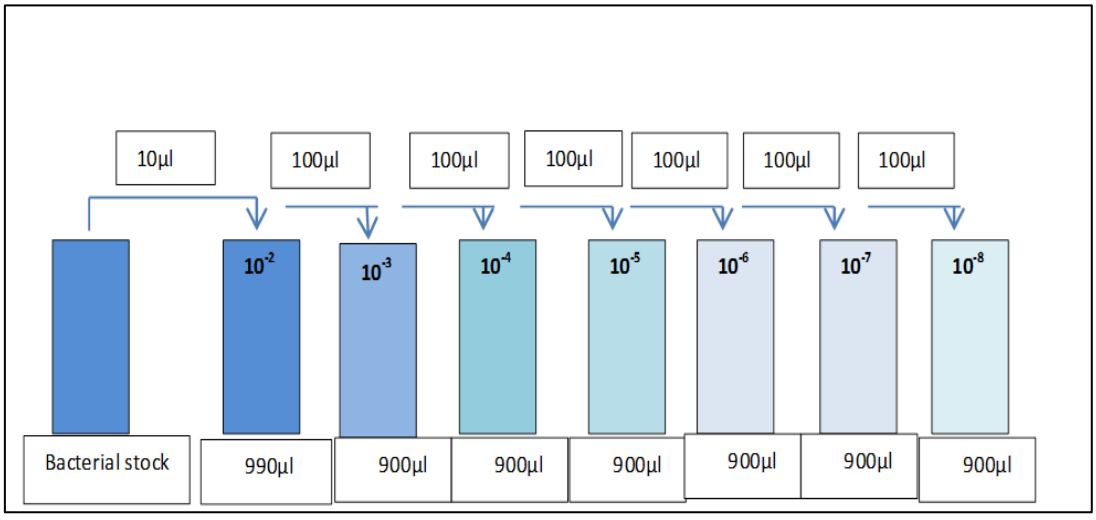

Figure 2.4: Preparation of 10 fold serial dilution of bacteria. 10µl of stored bacterial stock was added to 990µl of media to prepare $1x10^{-2}$ dilution. 100µl was taken from each dilution to make $1x10^{-3}$, $1x10^{-4}$, $1x10^{-5}$, $1x10^{-6}$, $1x10^{-7}$ and$1x10^{-8}$ respectively.

2.9 Agglutination assay

This assay was carried out to examine if our proteins (rfhSP-D, C1q and fibronectin) can agglutinate BCG. In this assay, one vial of frozen BCG stock was thawed on ice and mixed by vortexing. 50µl of BCG stock ($30x10^6$ bacteria per ml) was mixed with 1ml 7H9 media and sonicated for 20 seconds by using CAMLAB, Transsonic T460 sonicator. The sonicated BCG was passed through 8µm filter to remove large clumps. The desired protein was added to BCG at concentration of 10µg/ml in presence of 5mM $CaCl_2$. The total volume of BCG containing protein

with calcium chloride was 1ml. Untreated BCG containing 5mM $CaCl_2$ was used as a negative control. Both proteins treated and untreated BCG tubes were incubated at room temperature for 2 hours. After the incubation, all proteins treated and untreated BCG tubes were centrifuged at 5000rpm for 5 minutes to obtain the bacterial pellet. The supernatant was discarded, and the BCG pellet from each condition was suspended in 50µl of fresh 7H9. Only 20µl was taken by micropipette from each tube to make a smear on clean glass slide. Smears were air dried and stained by acid fast staining (section 2.7). Both proteins treated and untreated stained slides were examined using light microscope at 1000x magnification. For each slide 70 fields were examined for the presence of clumps, and all clumps were counted.

2.10 Thawing, culturing and storing of THP-1 cells

One frozen vial of THP1- cells (ATCC number TIB-202) (containing $5x10^6$ cells) was removed from liquid nitrogen, thawed on ice and transferred quickly into 10ml RPMI media. The cells were washed twice by using 10ml fresh RPMI by centrifugation at 1500 rpm for 10 minutes each. Then, THP-1 cells were counted as following. After washing, the supernatant was discarded and THP-1 cells pellet was suspended in 5ml RPMI. From cell suspension, 20µl was mixed with 20µl of Trypan blue. Then, 10µl of cell mixture was inserted under the coverslip of haemocytometer. Cells were counted using 40x lens of light microscopy. The large 4 squares containing 16 smaller squares were counted. The number of THP-1 cells/ml = Average number of cells in 4 large square X 10^4 X dilution factor (2).

For culturing, the washed THP-1 cells pellet was suspended in 10ml of cRPMI (Table 2.6) in a falcon tube. Then, cells were transferred into a 25ml tissue culture flask and incubated in the CO_2 incubator at 37^oC. The viability of THP-1 cells was checked every two days. Live THP-1 cells appear round and shiny under the light microscope. The growing THP-1 cells were transferred into 75ml culture flask after a week. For storage, washed THP-1 cells pellet was mixed with freezing solution containing (1:1 fetal bovin serum and 2% DMSO in RPMI) on ice. The cells were stored at density of $5x10^6$ cells per ml, and stored at -80^0C for 24 hours before being transferred to liquid nitrogen.

Table 2.6 Components and volume for preparing cRPMI medium

Component	volume	Suppliers and cat. number
RPMI – 1640 medium (1x)	435 ml	Sigma, cat. No: R0883
10% Fetal bovine serum	50 ml	Sigma- Aldrech
2 mM L-glutamine	5 ml	Sigma- Aldrech, cat. No: G7513
100 µg/ml Pen/Strep	5 ml	Sigma- Aldrech, cat. No: D0781
1mM Sodium pyruvate	5 ml	Sigma- Aldrech, cat. No: S8636

2.11 Direct effect of proteins on bacterial growth

One vial of frozen bacteria with known bacterial stock was removed from $^{-}80^{o}$C, thawed on ice and mixed by vortexing. The mycobacteria were sonicated for 20 seconds to remove any clumps. Serial dilutions were carried out (see figure 2.4) by taking 10µl of bacteria in 1ml LB or 1ml 7H9 for BCG. 100µl of bacterial suspension was transferred into another tube containing 900µl of LB or 7H9. This process of a 10 fold serial dilution was repeated until a dilution of $1x10^{-6}$ was reached. Tubes containing $1x10^{-5}$ and $1x10^{-6}$ bacterial dilutions in a total 1ml medium were used for the experiments. The desired proteins were then added to their respective test tubes in presence of 5mM $CaCl_2$. Both test and negative control tubes (containing untreated bacteria with 5mM $CaCl_2$ in their growth medium) were incubated at 37^{o}C for two hours. Following the incubation, tubes were vortexed, and 250µl of bacterial cultures were plated on either LB agar or 7H10 plates supplemented with 10% ADC. For each condition triplicate plates were set up. Agar plates containing *M.smegmatis* were incubated at 37^{o}C for three days, and BCG on 7H10 plates were incubated for 2-3 weeks at 37^{o}C. Bacterial colonies were counted by visual inspection.

2.12 Mycobacterial phagocytic assay

A phagocytic assay was carried out to study the effect of the proteins rfhSP-D, C1q, and FN on the phagocytosis of mycobacteria by THP-1 cells.

Beads preparation

Dynabeads bound to anti-human MHC class I was prepared as following: For each tube containing $0.25x10^{6}$ of THP-1 cells, 1µl (0.5µg) of mouse anti-human MHC class I antibody (W632 against HLA A,B & C, BioLegend, 311402) was mixed with

2.5µl (1x10^6) Dynabeads® Pan Mouse IgG (4x10^8/ml beads, Invitrogen, cat no. 11041). The ratio of THP-1 cells to beads was 1:4. The tube was incubated for at least 1 hour on ice. Next, the beads bound to anti MHC class I were washed twice by 1ml RPMI using a magnet.

Treatment of mycobacteria with protein

Two tubes were used for each phagocytic assay. In each tube, 1.25x10^6 of mycobacteria was suspended in 500µl RPMI containing 5mM final concentration of $CaCl_2$. The desired protein (10µg/ml) was added to the test tubes. Untreated mycobacteria containing 5mM calcium chloride was used as a negative control. Both test and negative control tubes were mixed by vortexing and incubated at 37^{o}C for two hours. Tubes were mixed every 30 minutes.

Infection of THP-1 cells

During the incubation period (above), the THP-1 cells were washed 3 times with RPMI by centrifugation at 1500rpm, 10 minutes each to remove the antibiotics from the media. Next, THP-1 cells were counted and suspended in cRPMI media without antibiotics. Following the incubation period, 0.25x10^6 THP-1 cells suspended in 500µl of complete RPMI (cRPMI) without antibiotics was added to each tube. Both tubes were incubated for one hour at 37^{o}C inside a 5% CO_2 incubator. Figure 2.5 shows BCG phagocytosed by THP-1 cells after an hour incubation at 37^{o}C in a CO_2 incubator. The ratio of THP-1 cells to bacteria used was 1:5.

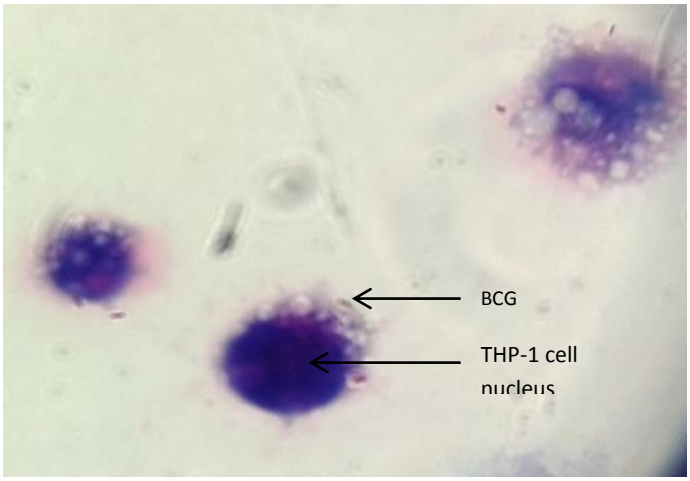

Figure 2.5: Phagocytosis of BCG by THP-1 cells. THP-1 cells were incubated with BCG for 1h at 37^{o}C inside 5% CO_2 incubator. Cell to bacteria ratio was 1:5. After incubation, the cell suspension was centrifuged for 10 minute at 1500rpm to precipitate the THP-1 cells. Supernatant was discarded; 50µl of cells was used to make a thin smear on glass slide. Then, air dried smear was stained by using acid fast staining. This picture shows BCG bacilli (red rod shaped) inside THP-1 cells after one hour incubation in the CO_2 incubator. Arrows show BCG inside and outside the phagosomes. Image was taken at 1000x using light microscope.

Binding of THP-1 cells to magnetic beads

Following the 1 hour incubation of protein treated and untreated mycobacteria with THP-1 cells, 20µl of washed magnetic dynabeads bound with anti-human MHC class1 was added to each tube. The tubes were buried horizontally in ice and left on a shaker for 30 minutes. This resulted in binding of MHC class I on surface of THP-1 cells with anti MHC class I bound to antimouse conjugated magnetic beads (Figure 2.6). Following the incubation period, the THP-1 cells were washed 3 times with 1 ml RPMI by applying the magnet (Figure 2.6). Washing removed extracellular, un phagocytosed mycobacteria from THP-1 cells.

Lysis of THP-1 cells and culturing of phagocytosed mycobacteria

Washed THP-1 cells containing phagocytosed mycobacteria were resuspended in 1ml of 0.1% saponin (Acros, 419231000). The THP-1 cell suspension was mixed for 15 minutes by vortexing to lyse the cells and release any phagocytosed bacteria. Next, a serial 10 fold dilution was carried out for both test and negative control tubes. For each dilution ($1x10^{-1}$, $1x10^{-2}$ and $1x10^{-3}$), 250µl was plated on each plate (Agar or 7H10) in triplicates. Plates containing protein treated and

untreated mycobacteria were incubated at 37^{o}C for 3 days for *M.smegmatis,* and for 2-3 weeks for BCG.

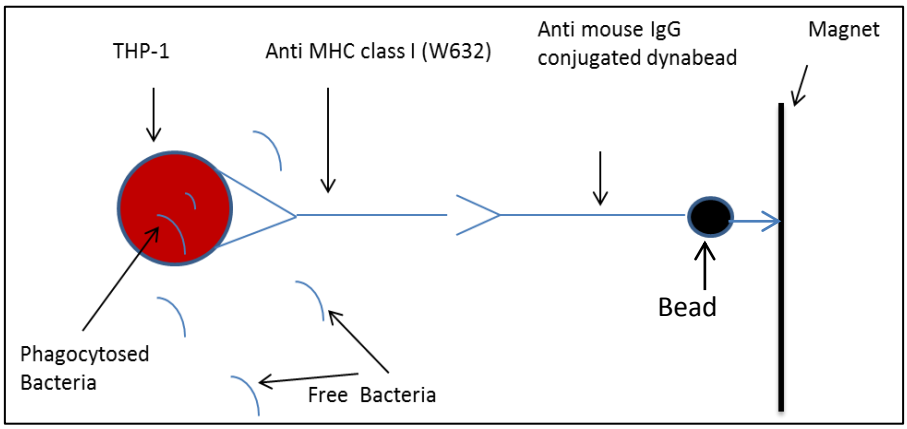

Figure 2.6: Separation of THP-1 cells attached to magnetic beads using magnet. MHC class I on the surface of THP-1 cells bound with anti MHC class I (W632) bound to anti-mouse conjugated magnetic beads.

2.13 Mycobacterial inhibition assay

The experiment described in section 2.12 was performed with the exception of adding 1ml of cRPMI instead of saponin. Both test and negative control tubes were incubated at 37^{o}C inside a CO_2 incubator with 5% CO_2 for 24 hours. The following day, the THP-1 cells were separated from the supernatant using a magnet.

Overnight supernatant was collected in a separate tube. The THP-1 cells were lysed by adding 1ml of 0.1% saponin and mixed for 15 minutes by vortexing. An equal volume of both cell lysate and supernatant were mixed together. Next, 10 fold serial dilutions were performed by taking 100µl of the bacterial solution in 900µl sterile distilled water to give a $1x10^{-1}$ dilution. Two further 10 fold dilutions were carried out to give a $1x10^{-2}$ dilution and a $1x10^{-3}$ dilution. For each dilution ($1x10^{-1}$, $1x10^{-2}$ and $1x10^{-3}$), 250µl was plated on LB Agar for *M.smegmatis* and 7H10 supplemented with 10% ADC for BCG in triplicates. Agar plates containing *M.smegmatis* were incubated at 37^{o}C for 72 hours. 7H10 plates containing BCG were incubated at 37^{o}C for 2-3 weeks.

To show the effect of THP-1 cells pre-treatment with proteins on the uptake and growth of mycobacteria, the same phagocytic and inhibition assays were carried

out as mentioned in section 2.12 and 2.13. Instead of treating mycobacteria with proteins (rfhSP-D, C1q, and fibronectin), THP-1 cells ($0.25x10^6$ cells/tube) in 1ml RPMI were treated with 10µg/ml of each protein in separate tubes for 2 hours at 37^oC in a CO_2 incubator. Next, the tubes were centrifuged at 1500 rpm for 5 minutes. The supernatant was discarded and the pellet was suspended in fresh RPMI and centrifuged for another 5 minutes at 1500 rpm. The THP-1 cells treated and untreated were washed 3 times to remove free unbound proteins. The cells were suspended in 0.5ml of RPMI media and $1.25x10^6$ of mycobacteria suspended in 0.5ml was added to each tube. Both tubes were incubated for 1 hour at 37^oC in a CO_2 incubator. Following the incubation, 20µl of magnetic dynabeads bound with anti-human MHC class1 (see section 2.12) were added to each tube. The tubes were buried horizontally in ice and left on a shaker for 30 minutes. The THP-1 cells attached to magnetic beads were isolated and washed 3 times with RPMI by applying a magnet. For the phagocytic assay, the THP-1 cells were then lysed by adding 1ml of 0.1% saponin and mixied for 15 minutes by vortexing. Following that, a serial 10 fold dilution was carried out. 250µl of lysed THP-1 cells suspension was plated on each media plate. Each dilution ($1x10^{-1}$, $1x10^{-2}$ and $1x10^{-3}$) was plated in triplicates. For the inhibition assay, 1ml cRPMI media without antibiotics was added to each tube containing washed THP-1 cells before an overnight incubation in CO_2 incubator. The rest of the procedure was carried out as mentioned above (section 2.13).

2.14 Determination cytokine expression by qPCR

Quantitative PCR (qPCR) was carried out in order to determine different cytokines expressed by THP-1 cells infected with protein treated and untreated mycobacteria. For these experiments, the inhibition assay mentioned in section 2.13 was carried out with a higher number of THP-1 cells and bacteria. A total number of $10x10^6$ BCG or *M.smegmatis* in 0.5ml RPMI with 5mM $CaCl_2$ (final concentration) was incubated in the presence and absence of 10µg protein for 2 hours at 37^oC. Next, $2x10^6$ THP-1 cells were added to the bacteria and incubated for one hour in a CO_2 incubator at 37^oC. THP-1 cells alone were used as a

negative control. The magnetic beads bound to anti human MHC class 1 were added, (Cells: beads ratio was 1:4) and the tubes were incubated in ice vertically for 30 minutes. Cells pellets were collected using the magnet and washed 3 times using RPMI media. 1ml cRPMI (without antibiotics) was added to each pellet and incubated at 37^{o}C. Cells pellets were collected after 1, 2, 5, 10 and 24 hours by applying the magnet. The cell pellets were stored at $^{-}$20^{o}C before RNA was extracted.

2.14.1 Primer design

The following human primers were designed using the nucleotide BLAST and Primer-BLAST (Table 2.7) (http://blast.ncbi.nlm.nih.gov/BLAT.cgi).

Table 2.7: Primer design

Primer name	Strand	Primer sequence
TNF-α	FWD	5'-AGCCCATGTTGTAGGAAACC-3'
TNF-α	REV	5'-TGAGGTACAGGCCCTCTGAT-3'
TGF-β	FWD	5'-GGACATCAACGGGTTCACTA-3'
TGF-β	REV	5'-CCGGTTCATGCCATGAATGG-3'
IL-1β	FWD	5'-CTCCAGGGACAGGATATGGA-3'
IL-1β	REV	5'-TCTTTCAACACGCAGGACAG-3'
NOS	FWD	5'-ACCATATTCCCCCAGAGGAC-3'
NOS	REV	5'-GAAGAGCTCAGGGTCATTGC-3'
IL-6	FWD	5'-GAAAGCAGCAAAGAGGCACT-3'
IL-6	REV	5'-TTTCACCAGGCAAGTCTCCT-3'
IL-10	FWD	5'-TTACCTGGAGGAGGTGATGC-3'

IL-10	REV	5'-GGCCTTGCTCTTGTTTTCAC-3'
IL-12	FWD	5'-AAGGAGGGGAGGTTCTAAGC-3'
IL-12	REV	5'-AAGAGCCTCTGCTGCTTTTG-3'
18S	FWD	5'-ATGGCCGTTCTTAGTTGGTG-3'
18S	REV	5'-CGCTGAGCCAGTCAGTGTAG-3'

2.14.2 RNA Extraction

RNA was extracted using GenElute reagent (Sigma- Aldrich, cat no. RTN70-1KT). The cell pellets were thawed on ice and mixed by vortex to loosen the cells. 250µl of lysis (1µl of guanidine thiocyanate and 10µl 2-mercaptoethanol) solution was added to release RNA and inactivate RNases. The solution was pipetted thoroughly to remove any clumps. The solution was loaded onto the filtration column to remove cellular fragments and sheer DNA and spun at 15.000rpm for 2 minutes. The filtration column was discarded. Next, 250µl of 70% ethanol was added and mixed by vortexing. The solution was loaded onto the binding column (silica column) and washed once with 500µl of wash solution 1 for 15 seconds at maximum speed following 500µl of wash solution 2 (containing ethanol). Finally, the column was washed with 500µl wash solution 2 for 2 minutes at maximum speed to dry the column. The flow-through was discarded after each wash. The RNA was eluted by adding 50µl of elution solution and centrifugation for 1 minute at maximum speed. Eluted RNA was stored at $^{-}80^{o}$C.

2.14.3 DNase Treatment

A DNase kit (Sigma SLBC 3g35 AMpD) was used to remove any contaminating DNA from RNA preparations. RNA (45µl) was mixed gently with 4.5µl of 10x buffer and 4.5µl of DNase I (Deoxyribonuclease I). The tubes were incubated at room temperature for 15 minutes to digest double and single-stranded DNA into mononucleotides and remove DNA from RNA preparation. The stop solution

(4.5µl) was added and the tubes were heated for 10 minutes at 70^{o}C to inactivate the enzyme DNase. The tubes were kept on ice and RNA concentration was measured using a Nanodrop. This RNA was used directly in complementary DNA synthesis.

2.14.4 Complementary DNA (cDNA) Synthesis

Single-stranded cDNA was synthesized by reverse transcription of total RNA by using a high capacity RNA to DNA kit, (Applied Bio-Systems). The master mix (10µl of 2X RT buffer + 1µl of 20X Enzyme mix containing RNase inhibitor) was prepared for all samples (n+1) in one tube. For each sample, 11µl of master mix was mixed with 9µl of RNA inside q-PCR tube. All samples were kept on ice at all times. Next, the tubes were placed in a thermal cycler (Peq Lab) and the lid was heated to 110^{o}C. The samples were incubated at 37^{o}C for 60 minutes following heating to 95^{o}C for 5 minutes. The tubes were then held at 4^{o}C. The cDNA was used directly for q-PCR experiments or stored at $^{-}$20^{o}C.

2.14.5 Gene expression by using quantitative PCR analysis

Quantitative PCR (q-PCR) was performed in order to detect the gene expression of inducible nitric oxide synthase (iNOS), pro-inflammatory cytokines (TNF-α, IL-1β, IL-6 and IL-12) and anti-inflammatory cytokines (TGF-β, and IL-10).

2.14.5.1 Primer preparation

A primer stock of 100µM for each primer (Table 2.7) was prepared as instructed in the data sheet. A 5µM stock (2.5µl of 100µM stock + 47.5µl of water) was prepared and stored at 20^{o}C to be used for q-PCR.

2.14.5.2 qPCR experiment

The prepared cDNA (section 2.14.4) was used as a templet for quantitative reverse transcription PCR (RT-qPCR) reaction. QPCR was used to study the gene expression of inducible nitric oxide synthase, pro-inflammatory and anti-inflammatory cytokines inside THP-1 cells infected with protein treated and

untreated mycobacteria. Untreated THP-1 cells were used as a negative control. The qPCR experiments were performed as the following:

A qPCR (96 wells) plate was labelled and kept on an ice holder during the experiment. A Master Mix (5µl cyber green (Bio rad, cat no. 172-5124) + 0.15µl of 5µM forward primer + 0.15µl of 5µM reverse primer + 3.7µl ultra-pure water) was prepared (n+1) for each gene separately inside a sterile tube kept on ice. 9µL of the master mix and 1µl of the relevant cDNA sample was added to the desired wells (Figure 2.7) to give a final volume of 10µl per well. Experiments were conducted in triplicates for each sample. Next, the plate was covered with a transparent stick cover and spun at 1500rpm for 1 minute. Finally, the qPCR plate was inserted inside the qPCR machine (Step One Plus, Applied Biosystems) and run for 2 hours using ΔΔCT, SYBR Green with melt curve.

Neg+ TNF-α	Neg+ TNF-α	Neg+ TNF-α	Neg+ TGF-β	Neg+ TGF-β	Neg+ TGF-β	Neg+ iNOS	Neg+ iNOS	Neg+ iNOS	Neg+ 18S	Neg+ 18S	Neg+ 18S
Untreat + TNF-α	Untrea+ TNF-α	Untret+ TNF-α	Untret+ TGF-β	Untreat+ TGF-β	Untreat+ TGF-β	Untreat+ iNOS	Untrat+ iNOS	Untreat+ iNOS	Untreat+ 18S	Untreat+ 18S	Untreat+ 18S
Test+ TNF-α	Test+ TNF-α	Test+ TNF-α	Test+ TGF-β	Test+ TGF-β	Test+ TGF-β	Test+ iNOS	Test+ iNOS	Test+ iNOS	Test+ 18S	Test+ 18S	Test+ 18S
water	water	water	water	water	water	water	water	water	water	water	water
Neg+ IL-1β	Neg+ IL-1β	Neg+ IL-1β	Neg+ IL-6	Neg+ IL-6	Neg+ IL-6	Neg+ IL-10	Neg+ IL-10	Neg+ IL-10	Neg+ IL-12	Neg+ IL-12	Neg+ IL-12
Untreat+ IL-1β	Untreat+ IL-1β	Untreat+ IL-1β	Untreat+ IL-6	Untreat+ IL-6	Untreat+ IL-6	Untreat+ IL-10	Untreat+ IL-10	Untreat+ IL-10	Untreat+ IL-12	Untreat+ IL-12	Untreat+ IL-12
Test+ IL-1β	Test+ IL-1β	Test+ IL-1β	Test+ IL-6	Test+ IL-6	Test+ IL-6	Test+ IL-10	Test+ IL-10	Test+ IL-10	Test+ IL-12	Test+ IL-12	Test+ IL-12
water	water	water	water	water	water	water	water	water	water	water	water

Figure 2.7: The qPCR plate design. Assays were conducted in triplicates. Genes: TNF-α, TGF-β, iNOS, 18S, IL-1β, IL-6, IL-10, and IL-12. Samples: uninfected THP-1 cells (Neg), THP-1 cells infected with untreated *M.smegmatis* or BCG (Untreat) and THP-1 cells infected with protein (rfhSP-D, C1q or fibronectin) treated *M.smegmatis* or BCG (Test). 18S was used as an Endogenous control. Ultra-pure water was added to all empty wells.

2.14.6 qPCR data analysis

Cycle threshold (CT) values were obtained from qPCR experiment were analysed and the relative expression of each cytokine gene was calculated using the Relative Quantification (RQ) value using the equation: $RQ = 2^{-\Delta\Delta Ct}$ for each cytokine target gene. The following equations were used to calculate RQ and the error bars for both THP-1 cells infected with untreated mycobacteria and THP-1 cells infected with protein treated mycobacteria. $\Delta Ct = Ct_{Test} - Ct_{18S}$; $\Delta\Delta Ct = \Delta Ct_{Test} - \Delta Ct_{Calibrator\ (THP\text{-}1)}$; $RQ = 2^{-(\Delta\Delta Ct)}$; $\text{Log } RQ = \text{Log } 2^{-(\Delta\Delta Ct)}$; $\Delta Ct\ SD = \text{square root of } (SD_{Test})^2 + (SD_{18S})^2$; $RQ\ \text{minimum} = 2^{-(\Delta CtSD + \Delta\Delta Ct)}$; $\text{Error bars} = \text{Log}_{RQ} - \text{log}_{RQmin.}$

2.14.7 Multiplex analysis

Multiplex is an immunoassay used to measure multiple proteins within a sample in a single run or cycle. This assay was carried out in order to determine the presence of cytokines and chemokines produced by THP-1 cells infected with C1q treated and untreated BCG after 24 hours incubation. Uninfected THP-1 cells were used as negative control. For these experiments, the inhibition assay mentioned in section 2.13 was carried out. Supernatant collected after 24 hours was used for this analysis. Multiplex assays were carried out at Imperial College, London by my colleague Dr. Kouser. Millipore MULTIPLEX MAP Multiple assay kit (cat.no HCYPOTMAG-60k) was used for this analysis. This assay is based on the Luminex® xMAP® technology which performs an immunoassay on the surface of fluorescent-coded magnetic beads known as MagPlex®-C microspheres. In this assay, colored beads of polystyrene microspheres or magnetic microspheres are produced; each bead is labelled with a specific antibody. Antibodies against different cytokines and chemokines on the surface of magnetic beads can bind and detect cytokines and chemokines in test sample. After that, a biotin conjugated secondary antibody is added. The reaction mixture is then incubated with Streptavidin-PE conjugate to complete proteins detected on the surface of each microsphere. Data obtained by this assay were analysed using Microsoft Excel.

2.15 Neutralization the effect of iNOS, pro-inflammatory cytokines and anti-inflammatory cytokines in THP-1 cells infected with proteins treated mycobacterial

The role of cytokine activity and nitric oxide production inside THP-1 cells infected with either rfhSP-D or C1q treated mycobacteria was investigated by using neutralizing antibodies and a nitric oxide synthase inhibitor (N^G-Methyl-L-arginine acetate). The experiments were carried out as described in the mycobacterial inhibition assay (section 2.13). In these experiments additional tubes containing THP-1 cells infected with protein (rfhSP-D or C1q) treated mycobacteria (*M.smegmatis* or BCG) were prepared, washed and suspended in 1ml of cRPMI media. One specific inhibitor or anti-body was added to its desired tube containing washed THP-1 cells (Figure 2.8). For experiments with rfhSP-D and M.smegmatis the following inhibitor and antibodies were used: 500µM final concentration of N^G-Methyl-L-arginine acetate, 5µl (1mg/ml) of anti TGF-β (R&D Systems, cat no. AB-100-NA) and 10µl of anti TNF-α (BD) (0.5mg/ml). For experiments with C1q with BCG, N^G-Methyl-L-arginine acetate, anti TNF-α and anti TGF-β were added as above and more antibodies were used as following: 10µl (0.5mg/ml) of anti IL-6 (BD), 10µl (0.5mg/ml) of anti IL-10 (BD),10µl (0.5mg/ml) of anti IgG (rabbit) and 10µl (0.5mg/ml) of anti IgG (mouse). An isotypes against IgG (rabbit) and IgG(mouse) were added as a negative controls in this study. All tubes were incubated for 24 hours at 37°C inside CO_2 incubator. Next day, THP-1 cells were separated by magnet. The supernatant was kept inside a clean tube. THP-1 cells were lysed with 1ml of 0.1% saponin and mixed by vortexing for 15 minutes. Next, lysed THP-1 cells were mixed with an equal volume with their supernatant. After that, 10 fold serial dilutions were performed by taking 100µl of the solution in 900µl of sterile distilled water to give $1x10^{-1}$ dilution, as described in sections 2.8 & 2.9. For dilution $1x10^{-1}$, 250µl was spread on LB agar plates and incubated at 37^{o}C for 72 hours for *M.smegmatis.* For BCG, 250µl from each dilution was spread on 7H10 plates supplemented with 10% ADC and incubated at 37^{o}C for 2-3 weeks.

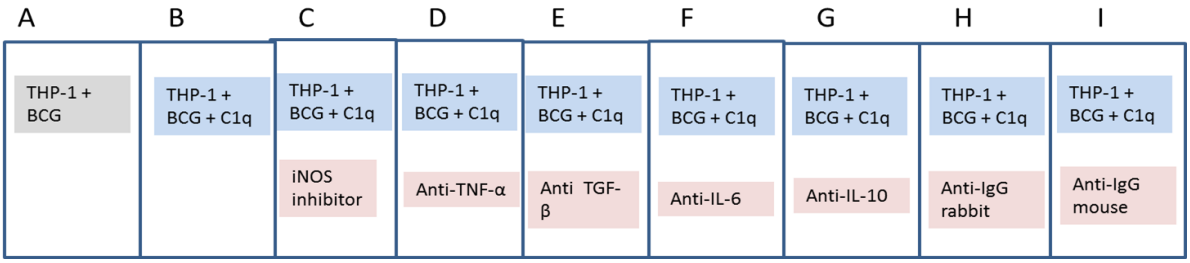

Figure 2.8: Neutralizing experiments design. For each experiment 9 tubes were prepared for inhibition assay. A: THP-1 cells infected with BCG only. B: THP-1 cells infected with C1q treated BCG. C: iNOS inhibitor treated THP-1 cells infected with C1q treated BCG. D: anti-TNF-α treated THP-1 cells infected with C1q treated BCG. E: anti-TGF-β treated THP-1 cells infected with C1q treated BCG. F: anti IL-6 treated THP-1 cells infected with C1q treated BCG. G: anti-IL-10 treated THP-1 cells infected with C1q treated BCG. H: anti IgG (rabbit) treated THP-1 cells infected with C1q treated BCG. I: anti-IgG (mouse) treated THP-1 cells infected with C1q treated BCG.

2.16 Statistical analysis

Statistical analysis was performed using PrismPad-5 software. A paired non parametric test was used to analyse experimental data. The Willcoxon test was used to compare the means of bacterial colonies counted in two sets of data. The Friedman test and Dunn's post-hoc test were used to compare the means of multiple sets of data.

Chapter 3- Interaction of recombinant fragment human SP-D (rfhSP-D) with mycobacteria

3.1 Introduction

Surfactant protein-D (SP-D) is produced naturally inside the lungs by alveolar type II epithelial cells and Clara cells, where *Mtb* infection starts. Normal SP-D concentration in broncho alveolar lavage fluid is around 51µg/ml, and this level increases in pulmonary infections. Furthermore, SP-D is known to play a key role in immune responses to different pathogens. It has been shown to bind oligosaccharides found on the surface of pathogens, and it can agglutinate, neutralize, or oppsonize microorganisms for phagocytosis (Hansen & Holmskov,1998). SP-D is involved in the clearance of bacteria, fungi, apoptotic cells, necrotic cells, and in the determination of inflammation (Kishore *et al*., 2006).

Previous studies showed various aspects of SP-D on phagocytosis of pathogens. It increases the phagocytosis of *Streptococcus pneumonia* and *Mycobacterium avium* (Kuroki *et al*., 2007 and Ariki *et al*., 2011). Moreover, SP-D decreases the growth of *Histoplasma capsulatum*, *Mycoplasma pneumonia, (*Wu *et al*., 2003).

SP-D deficiency is associated with chronic lung inflammation and fibrosis in SP-D knockout mice (Wert *et al.,* 2000). It is most likely that this protein plays an important role in the pathogenesis of tuberculosis. For this study, we used two mycobacterial species; *M.smegmatis* and BCG (Bacillus Calmette-Guérin) as a model for *M. tuberculosis* (*Mtb*). These two mycobacterial species are very similar to *Mtb* genetically. BCG is a live attenuated strain of *M.bovis* and it shares 99.95% gene similarity with *Mtb*. Whilst, *M.smegmatis* shares 95% gene homology and the same cell wall structure as *Mtb* (King, 2003 and Garnier *et al*., 2003).

Human monocytic cell line THP-1 was used in this study as a model for the human macrophage. These cells can phagocytose pathogenes (Tsuchiya *et al.,* 1982), produce lysozymes, express FC and C3b receptors, and express HLA class I and HLA class II (Tsuchiya et al., 1980,1982). THP-1 cells used in this project were stimulated naturally with mycobacteria, and they performed their full function, such as phagocytosis, cytokine production and mycobacterial killing.

The first aim in this study was to express, purify and characterize human recombinant surfactant protein-D (rfhSP-D). This protein was produced using the

E.coli, BL21 (λDE3) pLysS expression system. This system expresses a truncated form of SP-D which lacks the collagen region. The expressed rfhSP-D is composed of CRD, neck, and 8 GLY-X-Y repeats (x and y can be any amino acid). The second aim in this study was to investigate the following roles of rfhSP-D on mycobacteria (*M.smegmatis* and BCG): 1. Direct effect of rfhSP-D on mycobacterial growth. 2. Effect of rfhSP-D on the uptake (phagocytosis) of mycobacteria by THP-1 cells. 3. Effect of rfhSP-D on the growth of mycobacteria inside the THP-1 cells. 4. Understanding the underlying mechanisms of mycobacterial growth inhibition inside the THP1 cells.

3.2 Results

The first objective of the study was to produce and characterize rfhSP-D composed of the CRD region, neck and eight GLY-X-Y repeats.

3.2.1 Production and characterization of rfhSP-D

The rfhSP-D was successfully expressed and purified in this study. The pilot and large scale expression in *E. coli* showed the expected molecular weight of this protein at 20 kDa, this is under reducing conditions of a 12% w/v SDS-PAGE (Figure 3.1 & Figure 3.2). The protein appeared mainly in the pellet after lysis and sonication (Figure 3.3). The rfhSP-D band could be detected after dialysis against 4M, 2M, 1M, 0M urea and calcium buffers (Figure 3.4). After purification by maltose/agarose column, a clear rfhSP-D band can be detected at the correct molecular weight (20kDa) (Figure 3.5). Each lane on the gel represents one eluted protein fraction.

During protein purification sodium azide was used to prevent any microbial contamination. For microbiological studies the protein should be free from sodium azide as it can kills the bacteria in the experiments. Therefore, the protein was dialysed to get rid of this toxic reagent against calcium buffer (without sodium azide). The lipopolysaccharide(LPS) which may be a contaminant during rfhSP-D preparation was also removed. This was done by passing the protein through the polymixin agarose B column (Figure 3.6). The endotoxin level for the purified rfhSP-D measured by LAL assay was 0.32 EU/ml (Figure 3.7), and the accepted endotoxin levels are below 1 EU/mg (Wang et al., 2010). This protein was further characterized by Western blot, where polyclonal anti-SP-D sera from rabbit identified this protein as a clear band at 20kDa position (Figure 3.8).

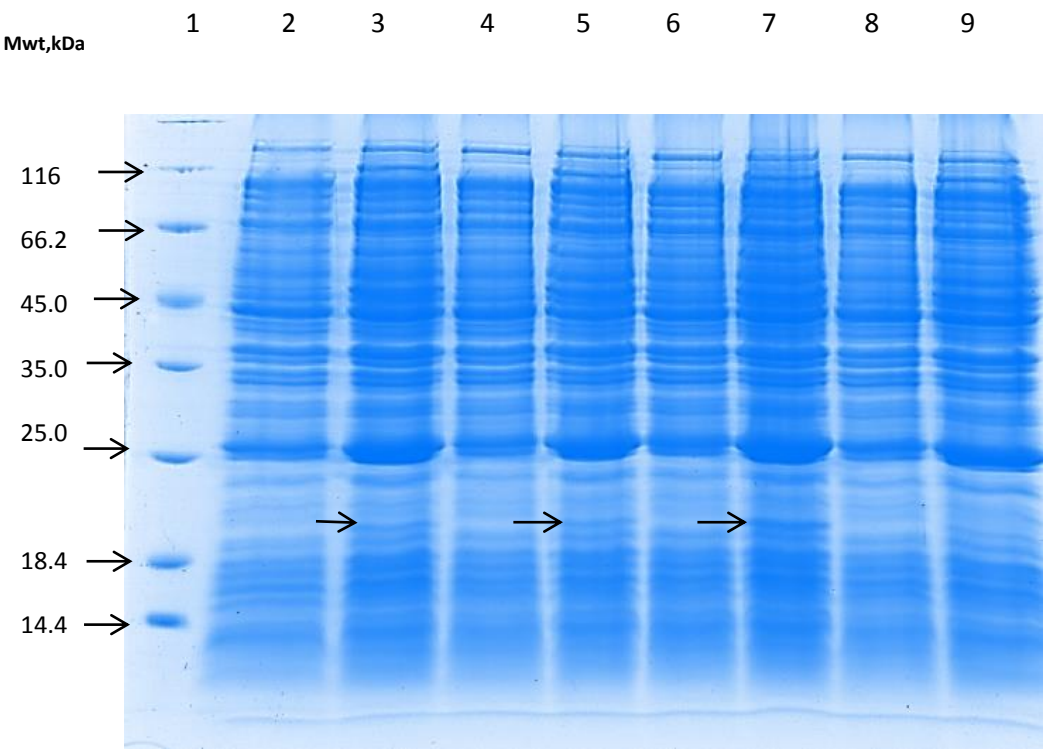

Figure 3.1: Characterization of rfhSP-D on 12% SDS-PAGE produced during pilot scale expression 12% (under reducing conditions). *E. coli* BL21(λDE3)pLysS strain transformed with PUK-D1 plasmid containing cDNA for the CRD, neck and 8Gly-x-y region of human SP-D gene under T7 promoter. Bacterial culture was induced with IPTG for 3 hours. The cell pellet of 100µl of bacterial culture was boiled under reduced conditions and loaded in each lane. Bacterial cultures, grown in parallel but not induced with IPTG were used as an uninduced control. The protein band appears in lane 3, 5 and 7 of the induced cultures at molecular weight 20 KDa. Lane 1 is the protein marker. Lanes 2, 4, 6 and 8 are un-induced cultures; Lanes 3, 5, 7 and 9 are the induced cultures.

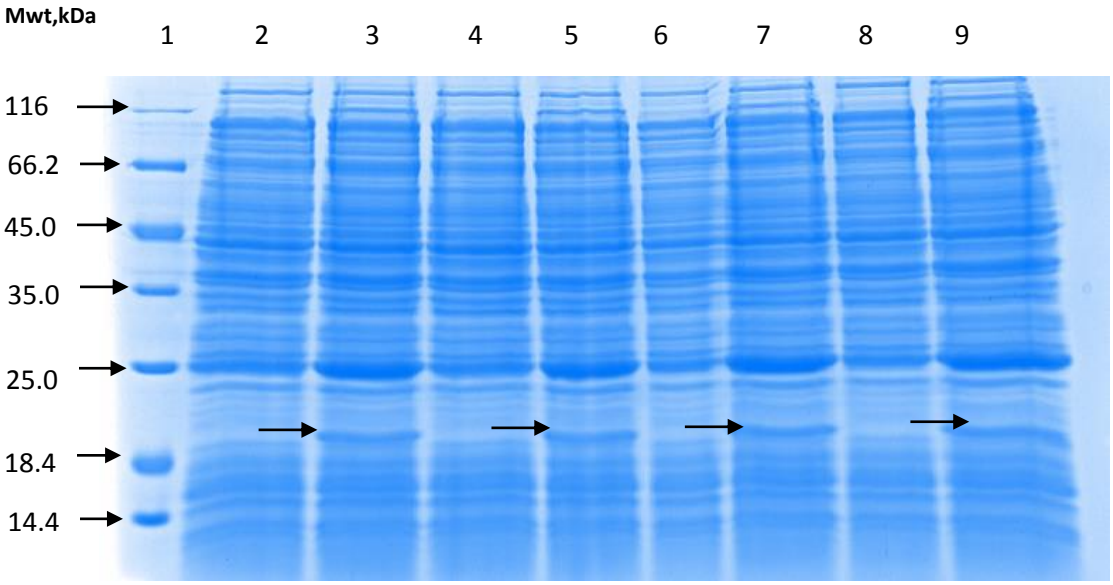

Figure 3.2: Characterization of rfhSP-D on 12% SDS-PAGE produced during large scale expression (under reducing conditions). There is a clear rfhSP-D band at molecular weight 20 kDa in all induced samples (lanes 3, 5, 7 & 9). Lane 1 is Protein marker. Lanes 2, 4, 6 & 8 are un-induced cultures.

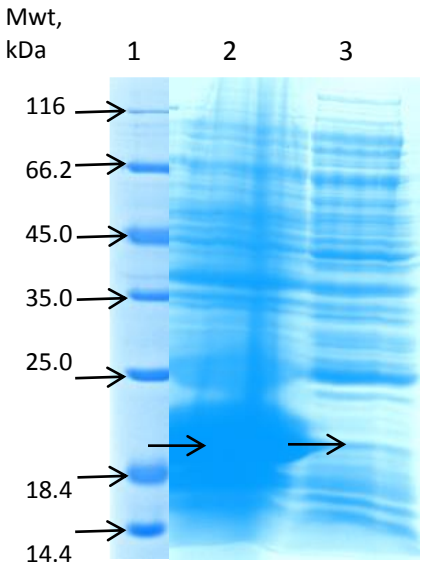

Figure 3.3: SDS-PAGE (12% under reducing conditions) shows pellet and supernatant after lysis and sonication. The cell pellet obtained by large scale was suspended in lysis buffer and incubated at 4^0C for 1 hour. Following incubation, the cell mixture was sonicated for 15 cycles, 30 seconds each. The sonicated cells were spun at 8500rpm for 15 minuters. Samples from both pellet and supernatant were mixed with an equal volume treatment buffere containing β-mercaptoethanol and heated at 100^0C for 10 minutes. Both pellet and supernatant (20µl) were run at 120 volts for 90 minutes. The protein is present mainly in the pellet and expressing very well. Lane 1: protein marker. Lane 2: pellet after sonication. Lane 3: supernatant after sonication.

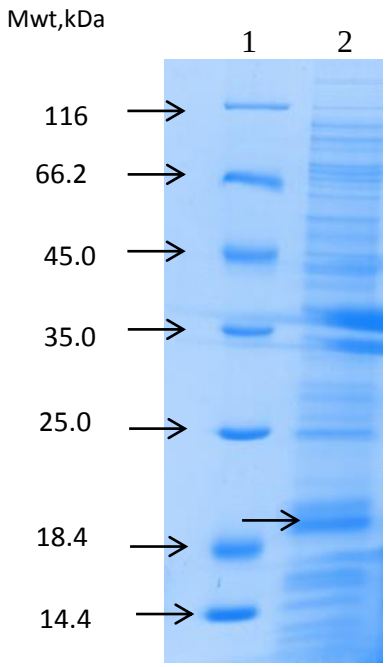

Figure 3.4: SDS-PAGE (12% under reducing conditions) shows rfhSP-D after dialysis. The sonicated pellet was solubilized in 8M urea buffer for one hour in cold room. The solubilized mixture was dialyzed against 4M, 2M and 1M urea buffers for 2 hours each and 0M buffer overnight. The following morning, protein from the dialysis bages was centrifuged at 8500 rpm for 20 minutes. The supernatant containing rfhSP-D was dialysed against calcium buffer for 2 hours. Lane 1: protein marker. Lane 2: the supernatant after dialysis.

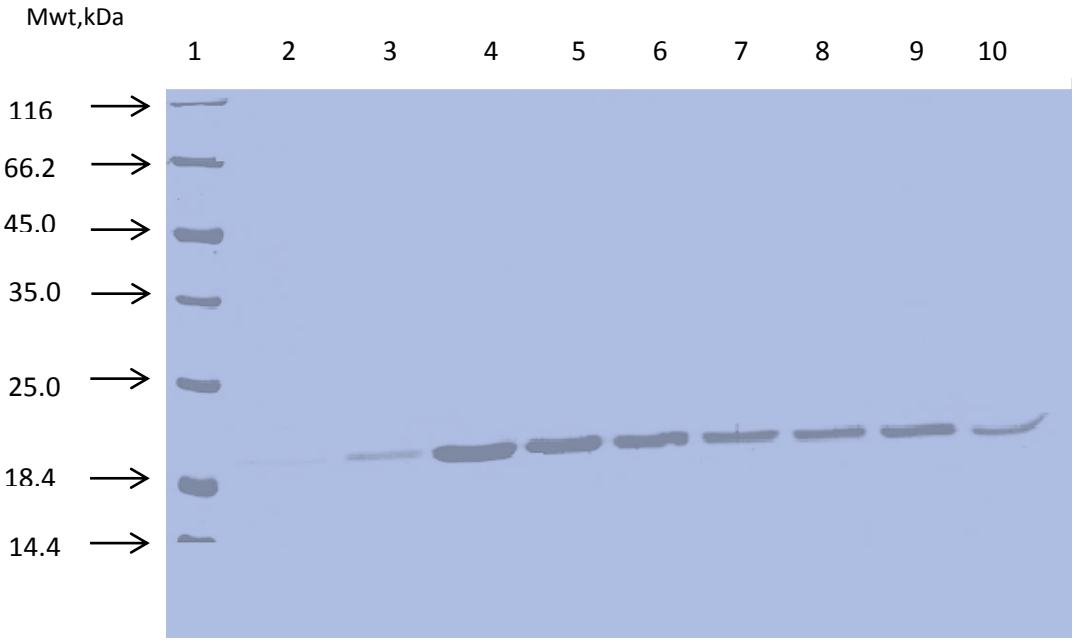

Figure 3.5: SDS-PAGE (12% under reducing conditions) shows purified rfhSP-D fractions. Following dialysis, samples were run through maltose-agarose column and eluted with elution buffere conaining 5mM EDTA. 1ml fractions were collected and run on a 12% SDS-PAGE. The rfhSP-D fractions are migrating at a molecular weight of approximately 20 kDa. Lane 1: Protein marker. Lane 2-10: rfhSP-D fractions. The expression is obvious matching to the 20 kDa marker.

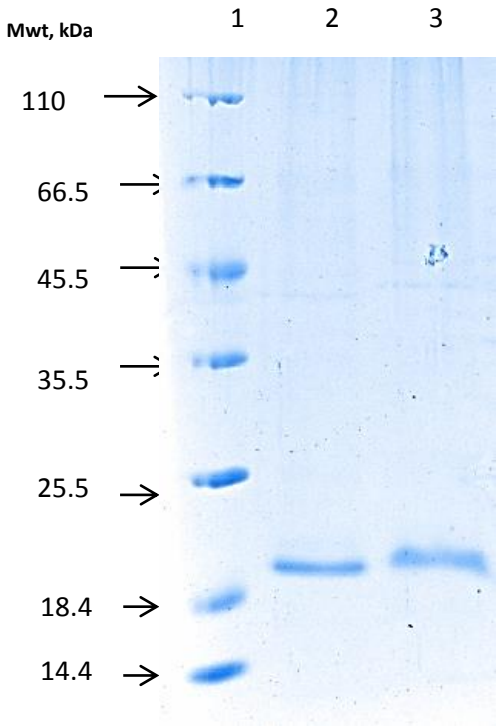

Figure 3.6: SDS-PAGE (12% under reducing conditions) shows the rfhSP-D after lipopolysaccarides removal. The rfhSP-D was loaded into polymyxin column and incubated for one hour at 4°C on a roller shaker. The protein was collected by passing through the column. Lane 1: protein marker. Lane 2: rfhSP-D free from LPS but containing sodium azide. Lane 3: rfhSP-D free from LPS and sodium azide.

3.2.2 Endotoxin level measurement (LAL assay)

The LAL assay was carried out in order to measure the endotoxin level inside rfhSP-D. The endotoxin level was carried out by chromogenic LAL endotoxin assay kit (Genscript). The assay was linear (Figure 3.7). The endotoxin level was calculated by the equation (Y=0.2618X - 0.0012), where X is the optical density (Table 3.1). The endotoxin level for rfhSP-D was 0.32EU/ml. One EU is equal to 100pg of *E. coli* lipopolysaccharide.

Table 3.1: Endotoxin level measurement using LAL assay

	O.D at 540 nm	O.D at 540 nm	O.D at 540 nm	Mean O.D at 540 nm	Δ Absorbance
Blank	0.077	0.077	0.079	0.077667	0
0.125EU/ml	0.187	0.195	0.189	0.190333	0.112667
0.25EU/ml	0.361	0.359	0.402	0.374	0.296333
0.5EU/ml	0.666	0.648	0.661	0.658333	0.580667
1.0EU/ml	1.027	0.933	0.968	0.976	0.898333
rfhSP-D	1.235	1.213	1.243	1.230333	
rfhSP-D	1.258	1.266	1.27	1.264667	

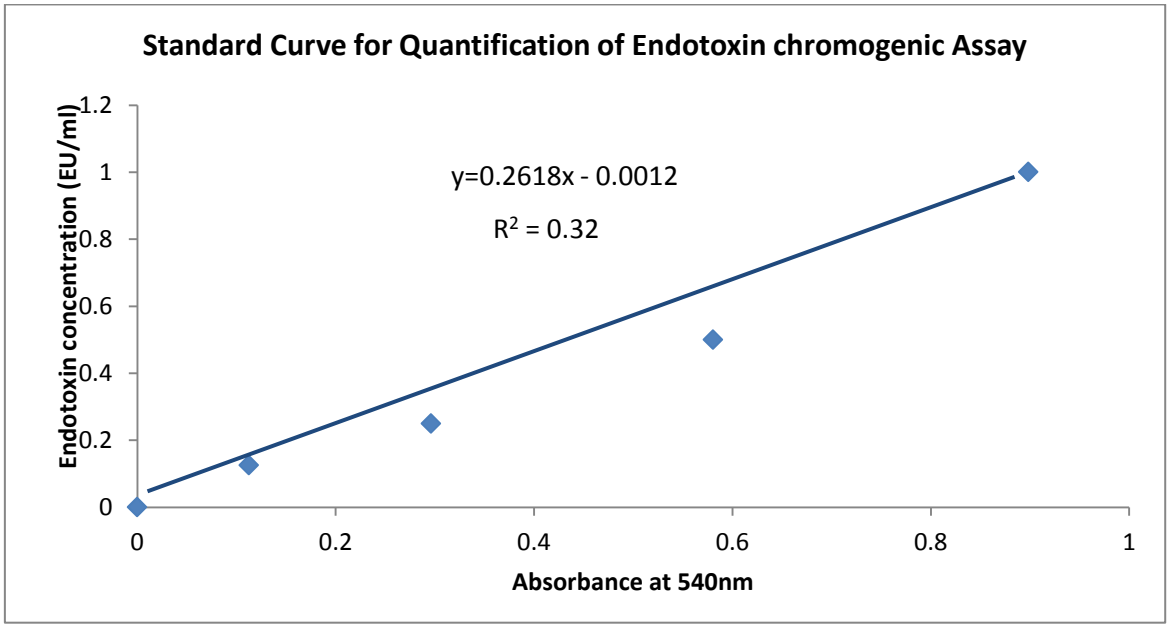

Figure 3.7: LAL assay to detect endotoxin level in rfhSP-D. Each data point represents the optical density for triplicate data from different concentrations of endotoxin solution. The optical density is zero for the blank solution.

3.2.3 Western Blot

In order to confirm that protein purified is rfhSP-D, Western blot was carried out. The result confirmed the binding of polyclonal rabbit anti human SP-D with the purified rfhSP-D (Figure 3.8). There is no binding with the negative control containing different concentrations of amyloid P component. The rfhSP-D bands are visible at molecular weight of 20 kDa.

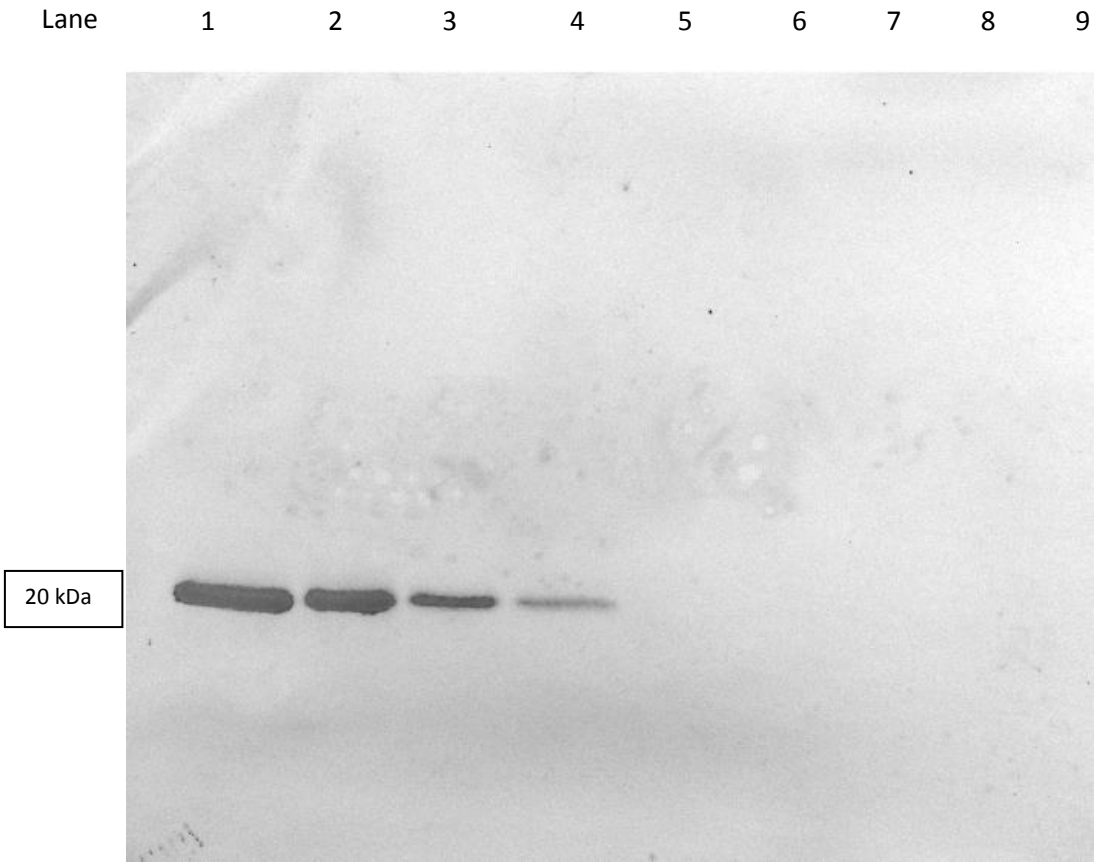

Figure 3.8: Western Blot showing the binding of rfhSP-D with rabbit anti-human SPD. Different concentrations (10, 5, 2.5, 1.25µg) of rfhSP-D and negative control protein amyloid P component were run on a gel and transferred onto a nitrocellulose membrane for 2 hour at 320mA. After that, the membrane was blocked for with 5% non-fat milk powder in PBS overnight. The next morning the membrane was washed 3 times for 5 minutes each with 0.02% Tween 20 in PBS. Rabbit anti-human SP-D (1:1000) was added in 1% non-fat milk in PBS and the membrane was incubated for 2 hours at room temperature. After washing, the membrane was incubated with protein G conjugated with HRP (1:1000) in 1% non fat milk in PBS. The bands were developed using DAB tablets. Lane 1: 10µg rfhSP-D, lane 2: 5µg rfhSP-D, Lane 3: 2.5µg rfhSP-D, Lane 4: 1.25µg rfhSP-D. Lane 5 is empty. Lanes 6, 7, 8, and 9 containing 10 µg, 5 µg, 2.5 µg, and 1.25 µg respectively of amyloid P Component (binding is not detected).

3.2.4 Binding of rfhSP-D with mycobacteria by ELISA

ELISA was used to study the binding of rfhSP-D with antigens on the surface of mycobacteria. Binding was studied by using different concentrations of rfhSP-D to show the optimal binding concentration of protein. The rfhSP-D was shown to bind with *M.smegmatis*, BCG and *Mtb* antigens (PPD) using ELISA and in the presence of 5mM $CaCl_2$. The binding of rfhSP-D with BCG and PPD from *Mtb* was strongest at 10µg/ml. There was also binding of rfhSP-D with *M.smegmatis* but it was weak as compared to rfhSP-D binding with BCG and with PPD from *Mtb* (Figure 3.9).

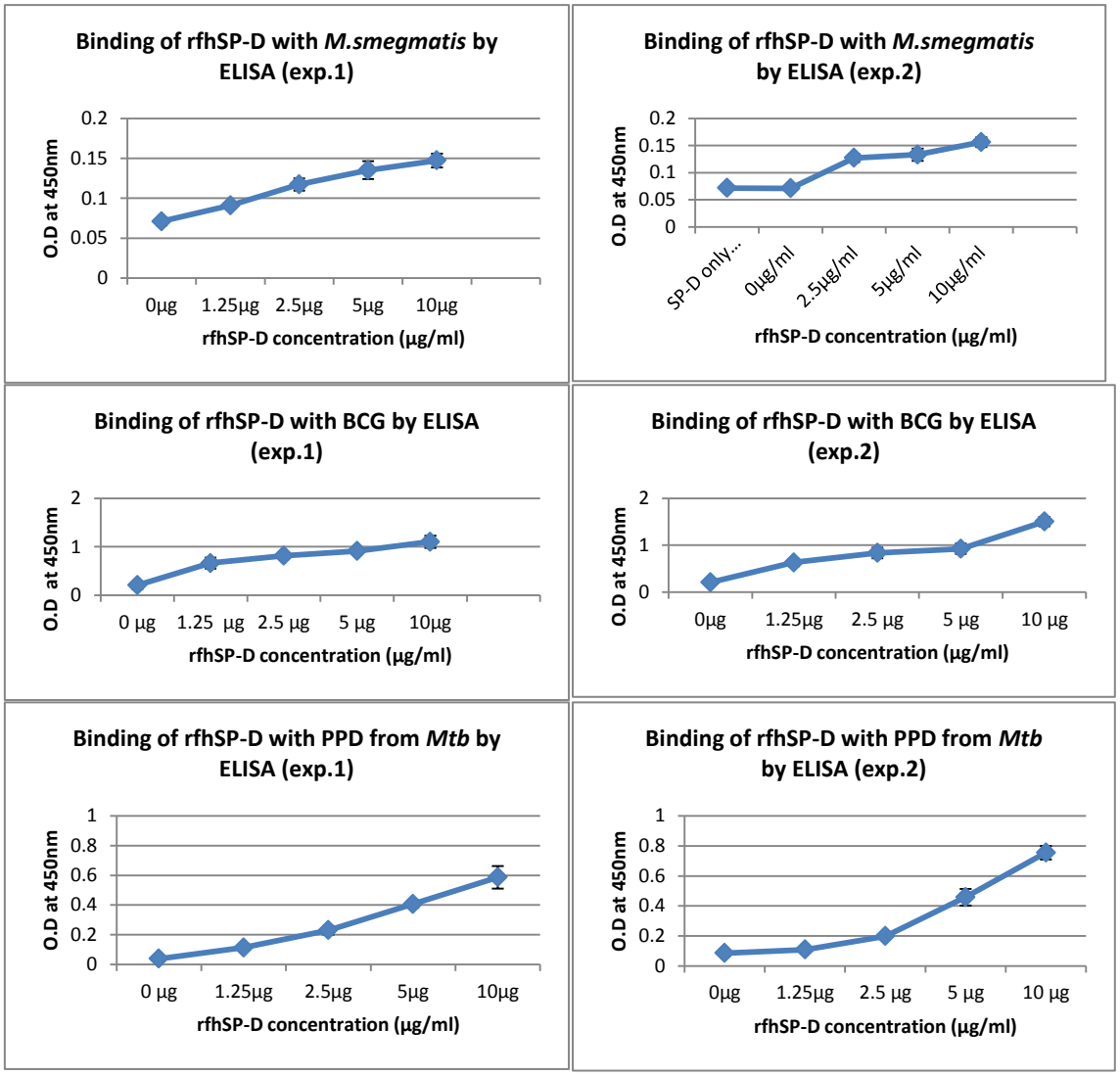

Figure 3.9: Binding of rfhSP-D with mycobacteria by ELISA. The rfhSP-D showed binding with BCG and *Mtb* antigens (PPD) and minimal binding with *M.smegmatis*. Each data point represents average triplicate reading. Error bars represent ±standard deviation. Different concentrations of rfhSP-D were added in the test wells and untreated mycobacteria were used as a negative control. Both negative control and test wells were treated with 5mM $CaCl_2$. A 96-well plate was coated with

$10x10^6$ mycobacteria per well in carbonate/bicarbonate buffer overnight at 4°C. The next morning, the plate was washed and blocked with 1% BSA in PBS for 2 hours at room temperature. Mycobacteria adhered to the wells were treated with different concentrations of rfhSP-D in PBS for 2 hours at 37°C. The wells were washed and treated with 1:1000 of polyclonal rabbit anti-human SP-D in PBS for 1 hour, and with 1:5000 of protein G conjugated to HRP for 45 minutes at 37°C. After washing, substrate TMB was added and incubated for 1-5 minutes in the dark. Finally, the reaction was stopped by adding H_2SO_4, and the plate was read at 450nm.

3.2.5 Binding of rfhSP-D with BCG by immunofluorescence microscopy

Immunofluorescence microscopy was performed to confirm binding of 10μg/ml rfhSP-D to BCG in presence of 5mM $CaCL_2$, as described in the material and methods section (2.5.2). In the image shown in Figure 3.10, the untreated BCG (A & B) is compared with rfhSP-D treated BCG (C & D). It can be seen that there is a binding of rfhSP-D with BCG where BCG has green florescence (D) compared to untreated BCG (B) due to the interaction of mouse anti- rabbit conjugated to FITC with rabbit anti-human SPD.

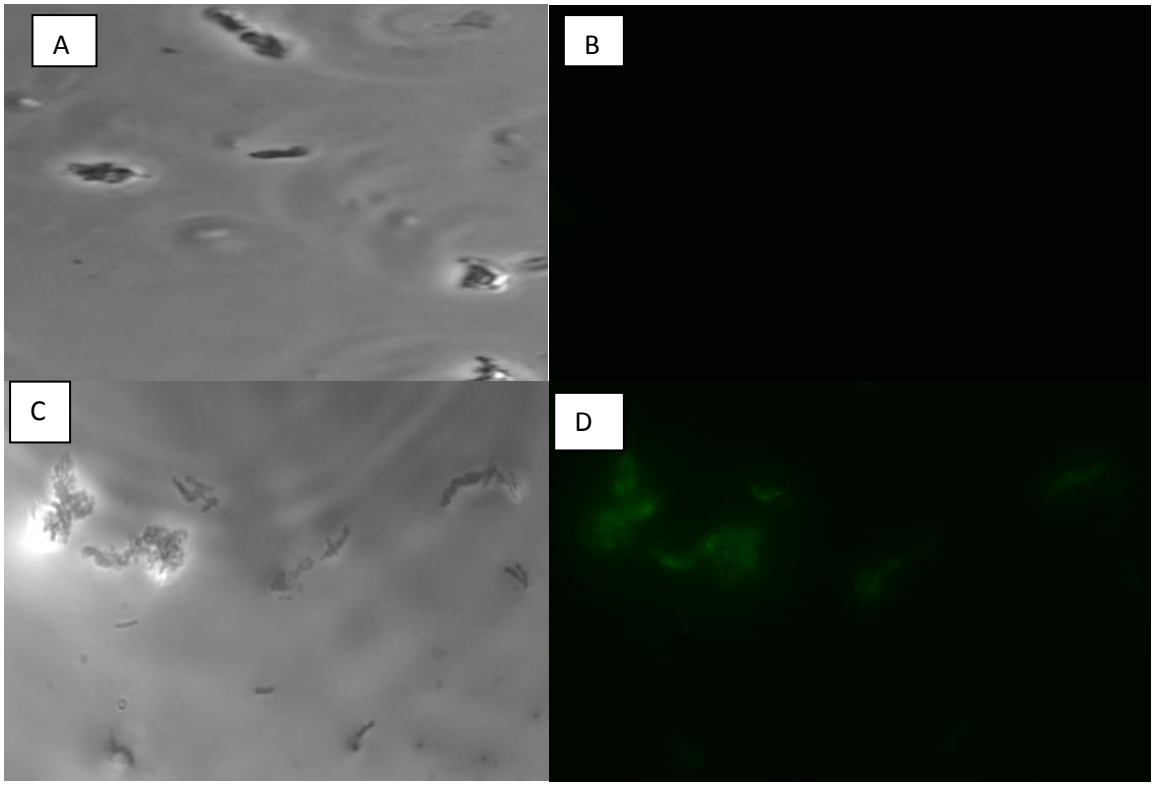

Figure 3.10: Binding of rfhSP-D with BCG by immunofluorescence microscopy. RfhSP-D treated BCG shows binding with rabbit anti human SP-D (D). This antibody was detected by using mouse anti rabbit conjugated to FITC (green fluorescence) (D). Untreated BCG (B) doesn't bind to secondary antibody (no green fluorescence). A: Untreated BCG (Bright field). C: rfhSP-D treated BCG (Bright field).

3.2.6 Effect of sugars on rfhSP-D binding with BCG by ELISA

The interaction between rfhSP-D and different sugars was studied in order to see whether this protein binds with sugars on the mycobacterial cell wall. The rfhSP-D was shown to bind with BCG using ELISA at 10µg/ml. The binding was enhanced in presence of 5mM calcium chloride. Incubation of rfhSP-D with different sugars was shown to decrease rfhSP-D binding with BCG. This suggests that sugars compete with mycobacteria for the same binding site on rfhSP-D, which reduces mycobacterial binding. Moreover, Incubation of rfhSP-D with EDTA was shown to decrease BCG binding to rfhSP-D more than sugars does (Figure 3.11).

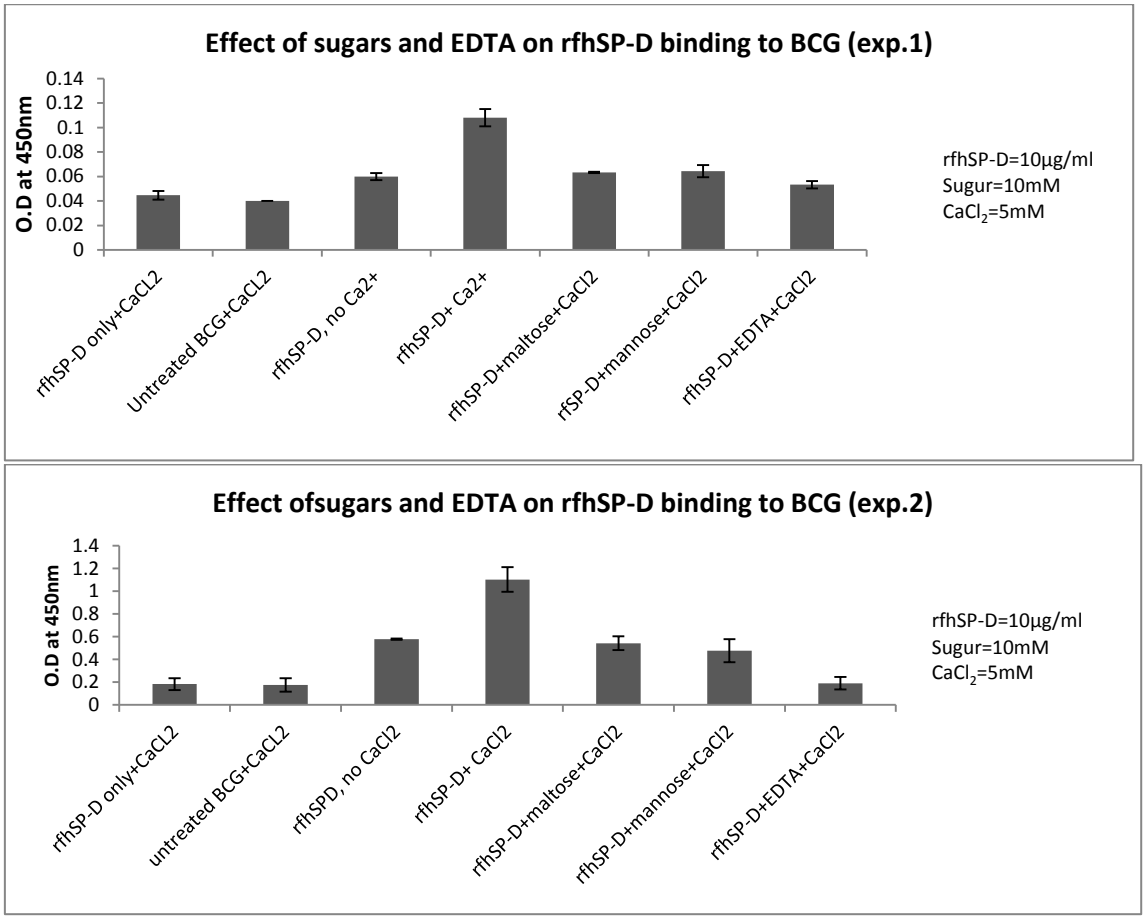

Figure 3.11: Effect of sugars and EDTA on rfhSP-D binding with BCG. ELISA plate wells were coated with $10x10^6$ mycobacteria in carbonate/bicarbonate buffer overnight. After washing and blocking the wells with 0.1%BSA in PBS, 10µg/ml of rfhSP-D previously treated with 10mM of sugar or EDTA was added to the desired wells, and incubated for 2 hours at 37°C. Two negative controls were used, 10µg/ml rfhSP-D only, and untreated mycobacteria. The binding of rfhSP-D to mycobacteria was reduced in the absence of 5mM $CaCl_2$. Binding was assessed by ELISA. Each bar represents the average of triplicate reading. Error bars represent ±standard deviation.

3.2.7 Binding of rfhSP-D with THP-1 cells by ELISA

ELISA was used to show the binding between rfhSP-D and human monocytic cell line THP-1. The rfhSP-D was shown to bind to THP-1 cells, and the binding was enhanced in the presence of 5mM $CaCl_2$. The best binding of rfhSP-D to THP-1 cells was obtained at 10µg/ml. However lower concentrations (1.25, 2.5, and 5µg/ml) of rfhSP-D showed similar binding to THP-1 cell (Figure 3.12).

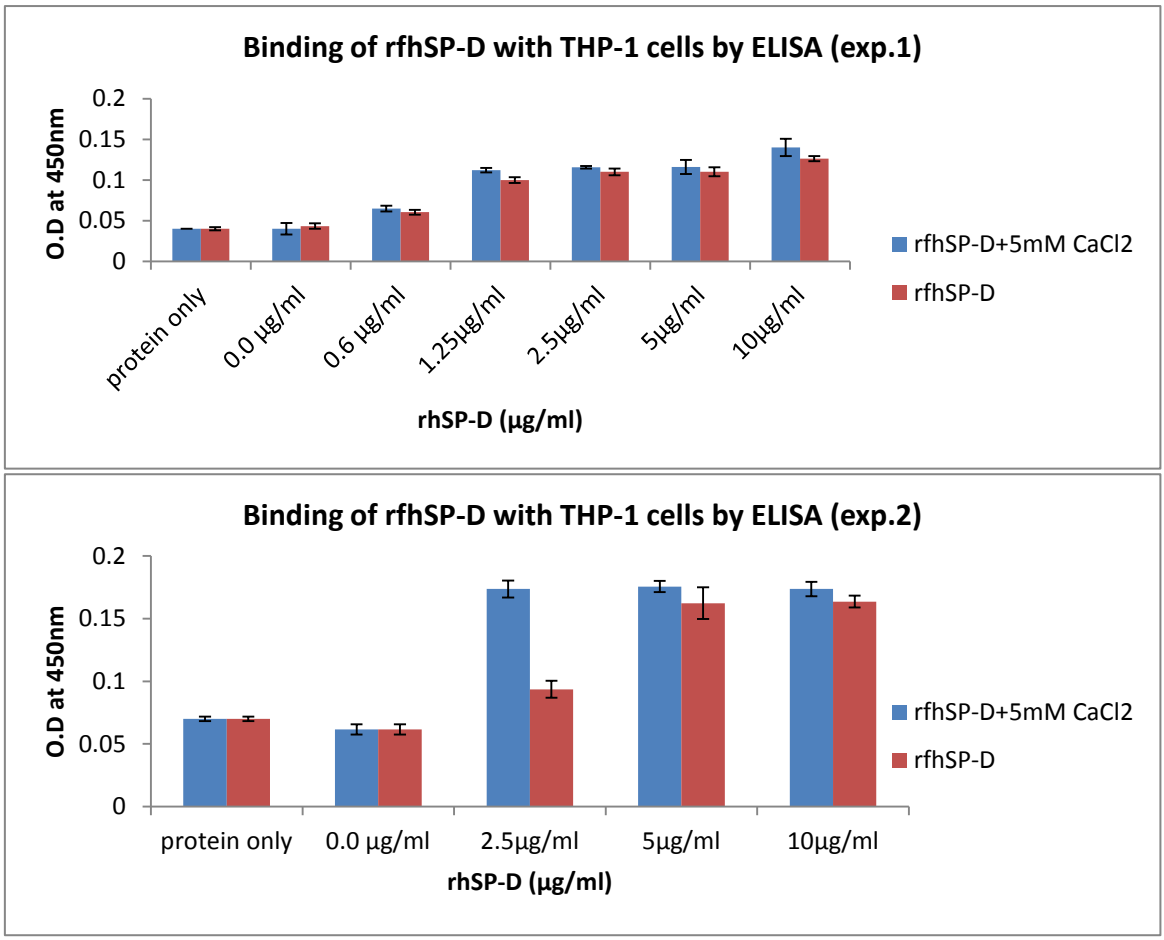

Figure 3.12: Binding of rfhSP-D with THP-1 cells by ELISA. Each bar represents average triplicate readings. Error bars represent ±standard deviation. The negative control wells contain either 10µg/ml protein or mycobacteria only. Test wells contain different concentrations (0, 2.5, 5, 10µg/ml) of rfhSP-D. Both negative control and test wells were treated with 5mM $CaCl_2$. A 96-well plate was coated with $1x10^5$ THP-1 cells per well in carbonate/bicarbonate buffer overnight at 4°C. The next morning, the plate was washed and blocked with 1% BSA in PBS for 2 hours at room temperature. THP-1 cells adhered to the wells were treated with different concentrations of rfhSP-D in PBS for 2 hours at 37°C. The wells were washed and treated with 1:1000 of polyclonal rabbit anti-human SP-D in PBS for 1 hour, and with 1:5000 of protein G conjugated to HRP for 45 minutes at 37°C. After washing, substrate TMB was added and incubated for 1-5 minutes in the dark. The reaction was stopped by adding H_2SO_4, and the plate was read at 450nm.

3.2.8 Binding of rfhSP-D with THP-1 cells by immuneflurscence

Immunofluorescence microscopy was used to show the binding of 10μg/ml rfhSP-D with THP-1 cells in the presence of 5mM $CaCl_2$. Figure 3.13 shows, untreated THP-1 cells (A, B & C) compared with rfhSP-D treated THP-1 cells (D, E & F). The binding can be seen in rfhSP-D treated THP-1 cells, where the THP-1 cells emit green florescence (F) as compared to untreated THP-1 cells (C) without florescence. The green florescence is the result of binding of protein A conjugated to FITC with Rabbit anti human SP-D.

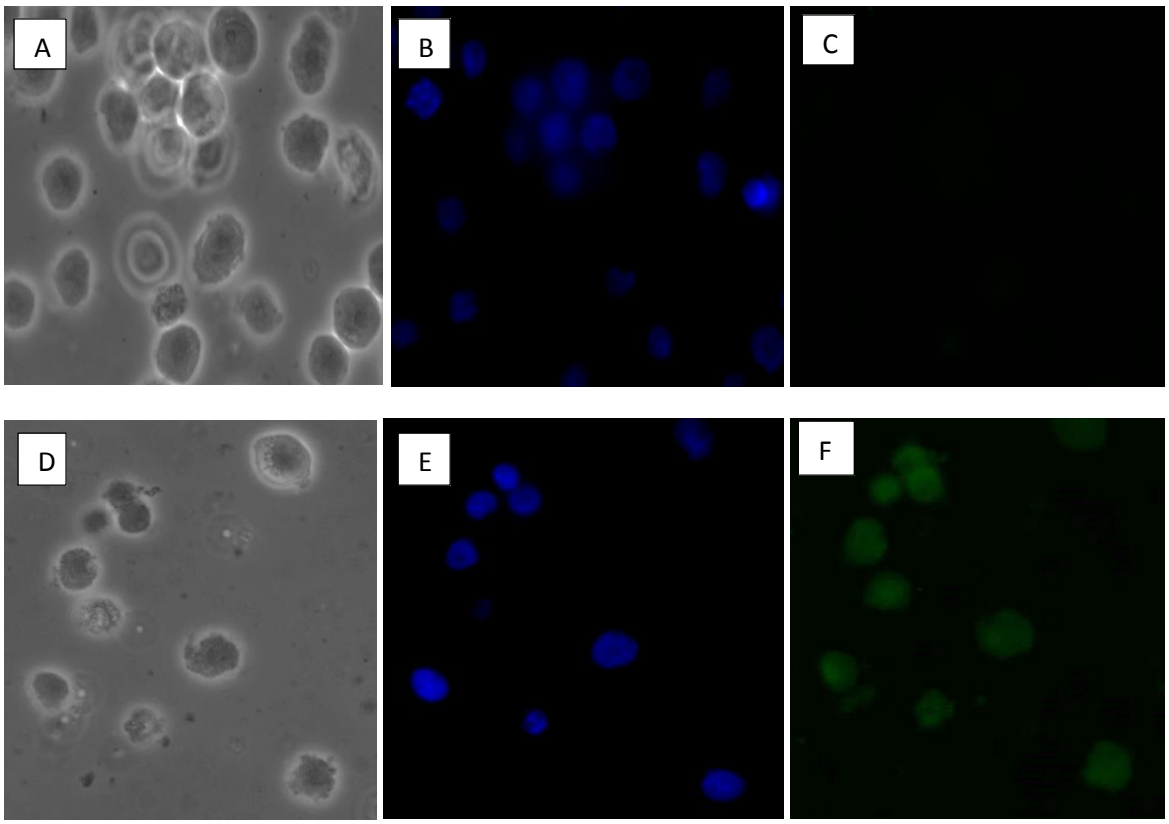

Figure 3.13: Binding of rfhSP-D with THP-1 cells by immunofluorescence microscopy. A: Untreated THP-1 cells (Bright field). B: Untreated THP-1 cells, nuclei stained with Hoechst (blue). C: Untreated THP-1 cells, but treated with anti-SPD and protein A FITC (no binding). D: rfhSP-D treated THP-1 cells (bright field). E: rfhSP-D treated THP-1 cells, nuclei stained with Hoechst (blue). F: rfhSP-D treated THP-1 cells treated with anti human SP-D and protein A FITC (emitting green florescence).

3.2.9 Effect of rfhSP-D on mycobacterial agglutination

This study showed that incubation of 10µg/ml rfhSP-D with BCG in presence of 5mM $CaCl_2$, for 2 hours does not agglutinate BCG. The numbers of small clumps in each slide made from rfhSP-D treated and untreated BCG were very similar and statistically non significant in 3 independent experiments (Figure 3.14).

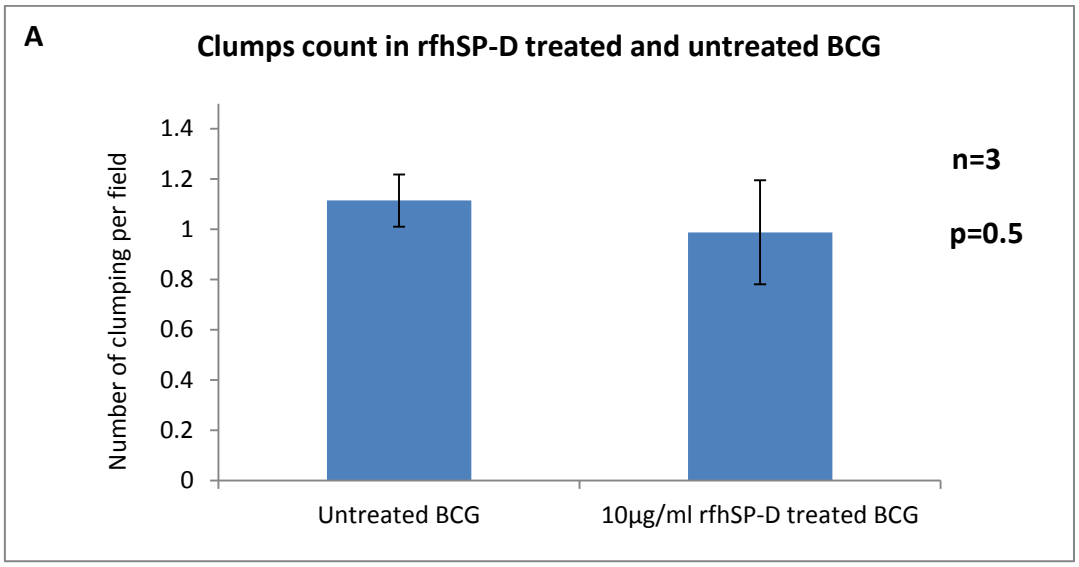

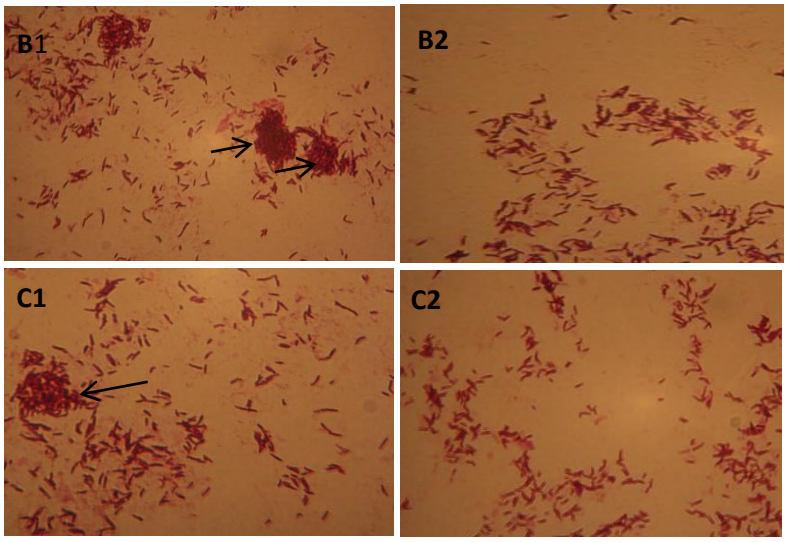

Figure 3.14: Effect of rfhSP-D on BCG agglutination. RfhSP-D does not cause agglutination for BCG. Clumps were counted in 70 different fields for both rfhSP-D treated and untreated BCG slides. A: Each bar represents the average number of small clumps from 3 slides. Error bars represent ±standard error of the mean. B1 & B2: Acid fast staining image for untreated BCG. C1&C2: Acid fast staining for rfhSP-D treated BCG. Arrows are pointing to the small BCG clumps. Pictures were taken at 1000x magnification using light microscopy.

3.2.10 Direct effect of rfhSP-D on mycobacterial growth

3.2.10.1 Direct effect of rfhSP-D on *M.smegmatis* growth

In this study, we demonstrated that rfhSP-D directly inhibited the growth of *M.smegmatis* in presence of 5mM $CaCl_2$, after 2 hours treatment and further culture for 72 hours. Presence of rfhSP-D inhibited the growth of *M.smegmatis* directly by 20%, and the results are statistically significant (p=0.03) (Figure 3-15-A). Six independent experiments were shown the same trend of growth inhibition as compared to untreated *M.smegmatis* (Figure 3.15-B).

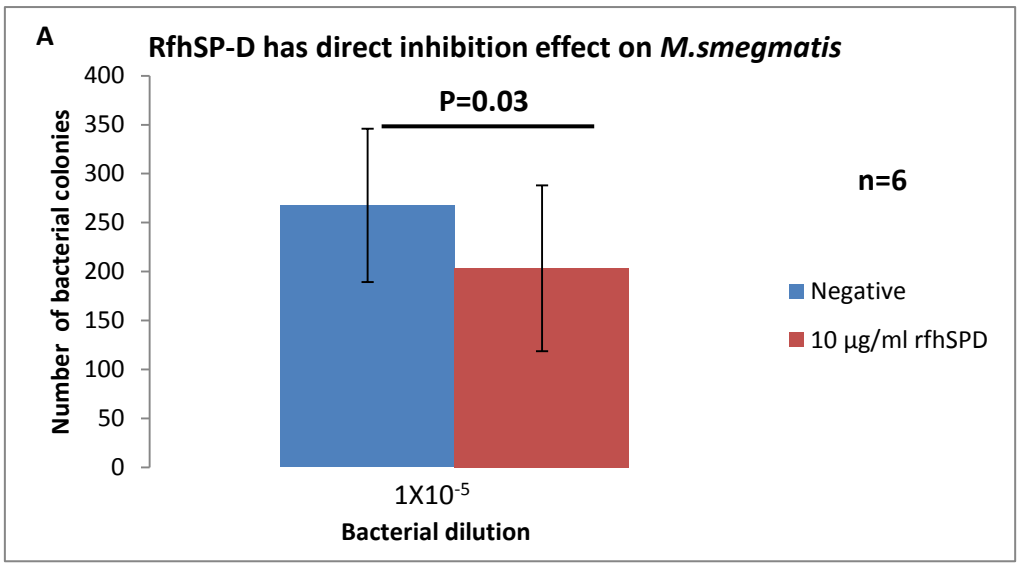

Figure 3.15-A: The direct effect of rfhSP-D on *M. smegmatis* growth. Both rfhSP-D treated and untreated *M.smegmatis* (negative) were incubated for 2 hours at 37°C in presence of 5mM $CaCl_2$. After incubation, 250µl of bacterial cultures were plated on LB agar plates in triplicates and incubated for 3 days at 37°C. The number of bacterial colonies in each plate was counted by visual inspection for each experiment. Each bar represents the average of 6 experiments. P value was calculated using Wilcoxon Signed rank test. Error bars represent ±standard error of the mean. Negative control contains untreated *M.smegmatis.*

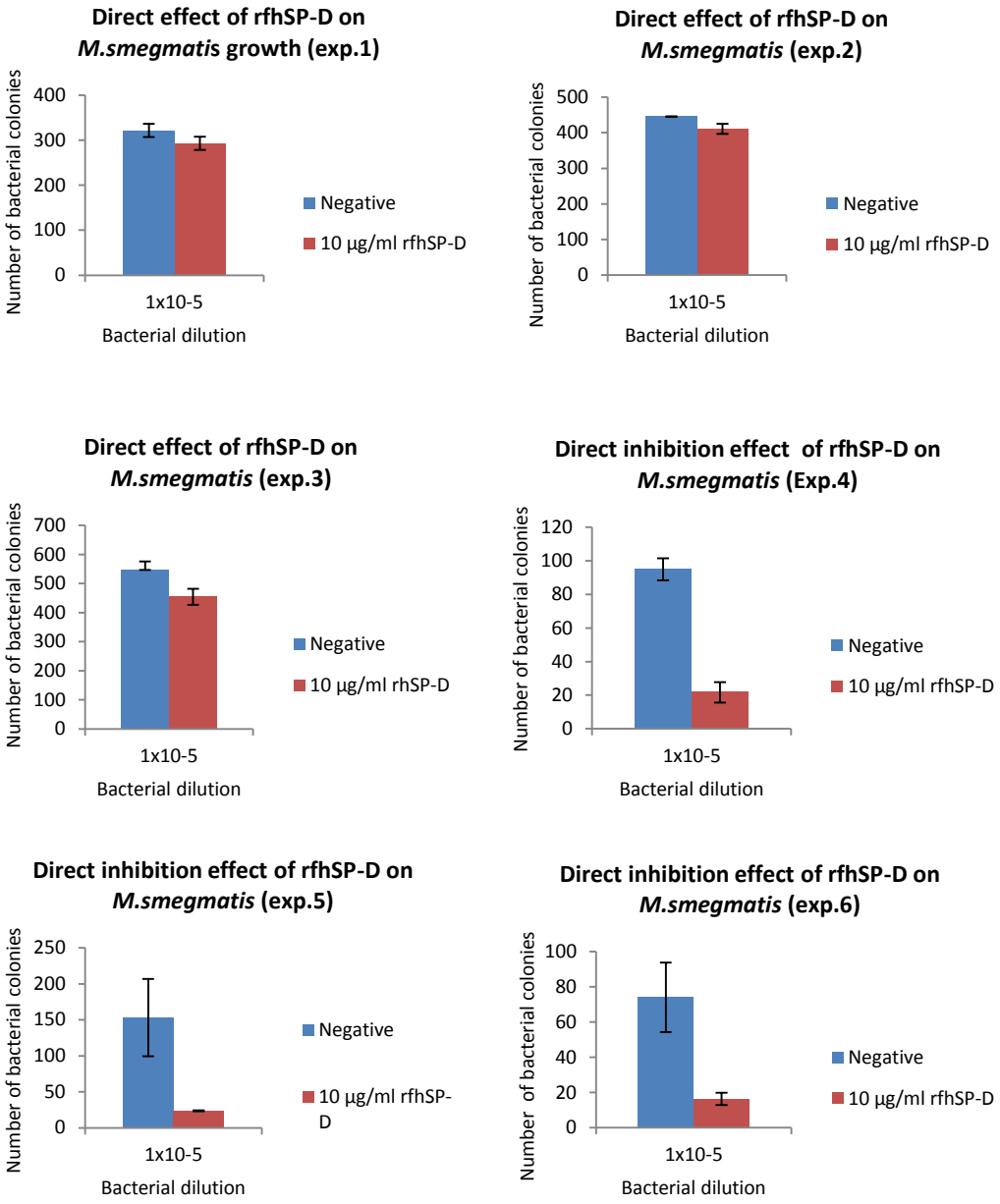

Figure 3.15-B: Direct effect of rfhSP-D on *M. smegmatis* growth in 6 individual experiments. Both rfhSP-D treated and untreated *M.smegmatis* (negative) were incubated for 2 hours at 37°C in presence of 5mM $CaCl_2$. After incubation, 250µl of bacterial cultures were plated on LB agar plates in triplicates and incubated for 3 days at 37°C. The number of colonies in each plate was counted by visual inspection for each experiment. Each histogram represents the average of triplicate data. Error bars represent ±standard deviation.

3.2.10.2 Direct effect of rfhSP-D on BCG growth

Presence of rfhSP-D with 5mM $CaCl_2$ inhibited the growth of BCG directly by 50%, and the direct inhibition effect is statistically significant ($p<0.05$) (Figure 3.16-A). Five independent experiments were carried out and all the experiments showed the same trend of growth inhibition (Figure 3.16-B).

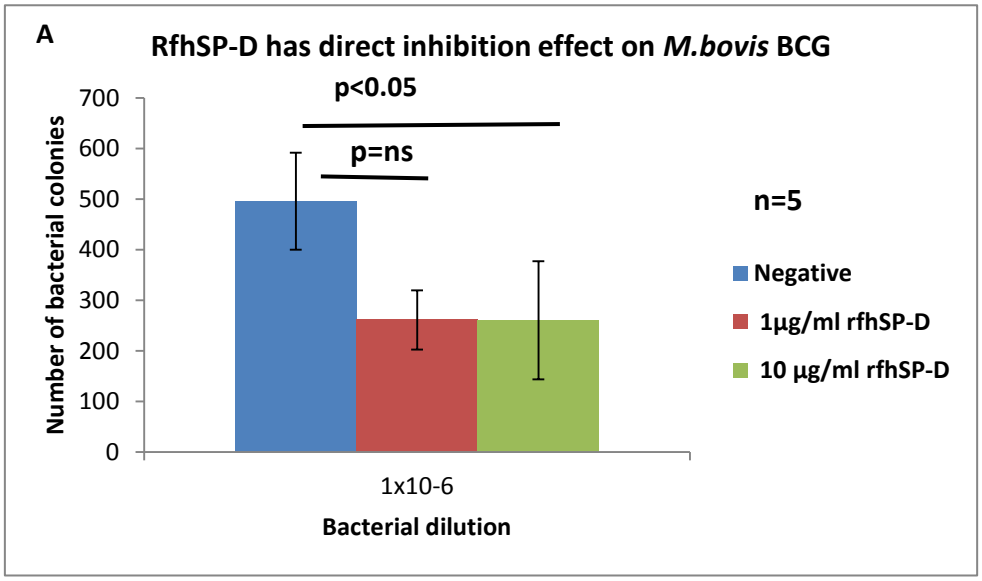

Figure 3.16-A: Direct effect of rfhSP-D on BCG growth. Both rfhSP-D treated and untreated BCG (negative) were incubated for 2 hours at 37°C in presence of 5mM CaCl. Next, 250µl of bacterial cultures were plated on 7H10 plates supplemented with 10% ADC in triplicates. Plates were incubated inside 37°C incubator for 2-3 weeks. The number of colonies in each plate was counted by visual inspection for each experiment. The average of 5 independent experiments is shown here. Each bar represents the average of 5 experiments. Error bars represent ±standard error of the mean. Multiple comparison of the data sets was done using Friedman test (p=0.0085). Individual data were compared with each other using Dunn's post hoc test: Negative vs 1µg/ml rfhSP-D, p=ns (non- significant; Negative vs 10µg/ml rfhSP-D, p<0.05 (signficant). Negative contains untreated BCG.

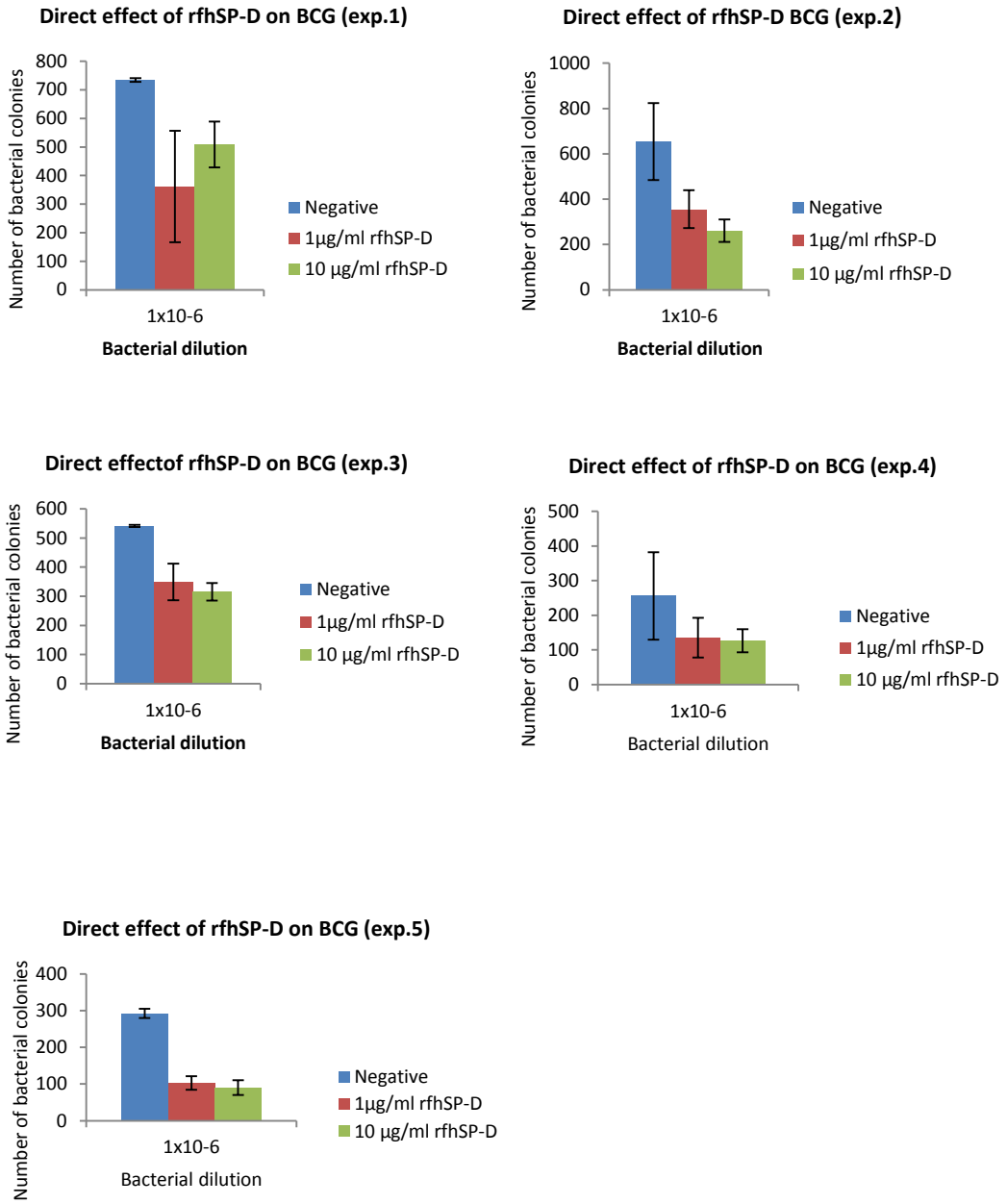

Figure 3.16-B: Direct effect of rfhSP-D on BCG growth (5 individual experiments). Both rfhSP-D treated and untreated BCG (negative) were incubated for 2 hours at 37°C in presence of 5mM $CaCl_2$. After incubation, 250µl of bacterial cultures were plated on 7H10 plates supplemented with 10% ADC in triplicates. Plates were incubated at 37°C for 2-3 weeks. The number of colonies in each plate was counted by visual inspection for each experiment. Each histogram represents the average of triplicate readings. Error bars represent ±standard deviation. Negative contains untreated BCG.

3.2.11 Effect of rfhSP-D on the uptake (phagocytosis) of mycobacteria by THP1 cells

3.2.11.1 Effect of rfhSP-D on the uptake of *M. smegmatis* by THP1 cells

Treatment of mycobacteria with 10μg/ml rfhSP-D in 5mM calcium chloride was shown to decrease mycobacterial uptake by THP-1 cells (Figure 3.17 A,B and C). Seven independent experiments were carried out and all the experiments showed the same trend in decrease the uptake of *M.smegmatis* by THP-1 cells (Figure 3.17-B). There is about 47% reduction in the uptake of rfhSP-D treated *M.smegmatis* by THP-1 cells *as* compared to untreated *M.smegmatis* (negative control), and the results are statistically significant ($p < 0.05$) (Figure 3.17-A).

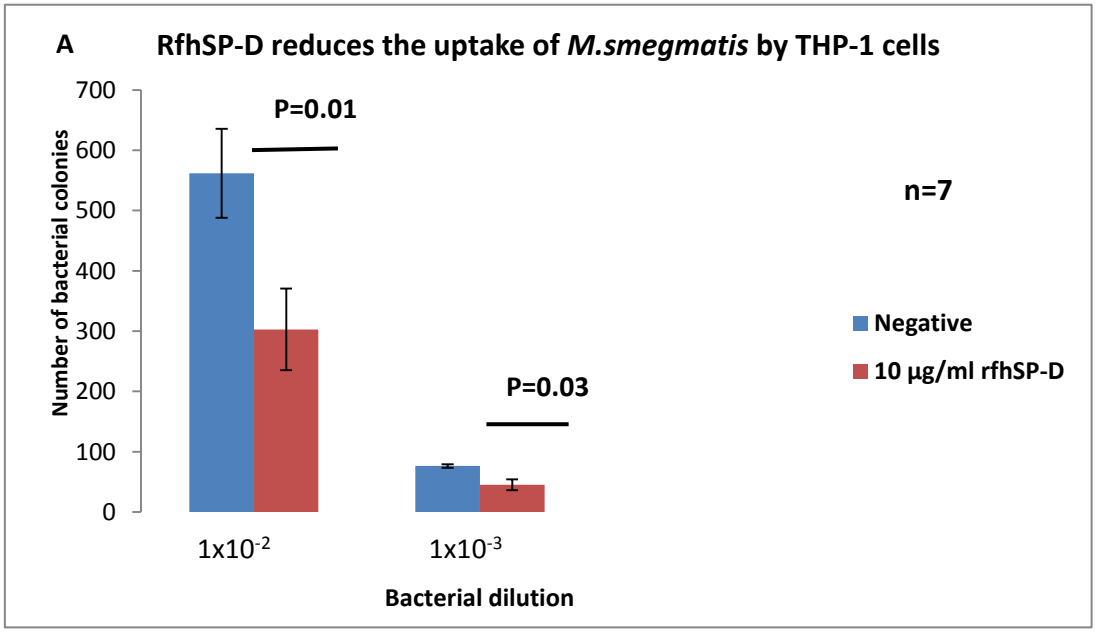

Figure 3.17-A: Effect of rfhSP-D on the uptake of *M.smegmatis* by THP-1 cells. Both rfhSP-D treated and untreated tubes (negative) were incubated for 2 hours at 37°C in presence of $CaCl_2$. After incubation, THP-1 cells were added to mycobacteria in ratio 1:5 (THP-1 cells:*M.smegmatis*), and incubated for 1 hour at 37°C to allow phagocytosis of mycobacteria by THP-1 cells. Following incubation, magnetic beads bound with anti-human MHC class 1 was added to each tube in ratio 1:4 (THP-1: beads) and the tubes were incubated on ice for 30 minutes on a shaker. Next, the THP-1 cells were washed 3 times to remove extracellular bacteria. Washed cells were laysed with 0.1% saponin with vortexed for 15 minutes to release phagocytosed mycobacteria. Error bars represent ±standard error of the mean. P value calculated using Wilcoxon signed rank test. Negative control contains untreated *M.smegmatis*.

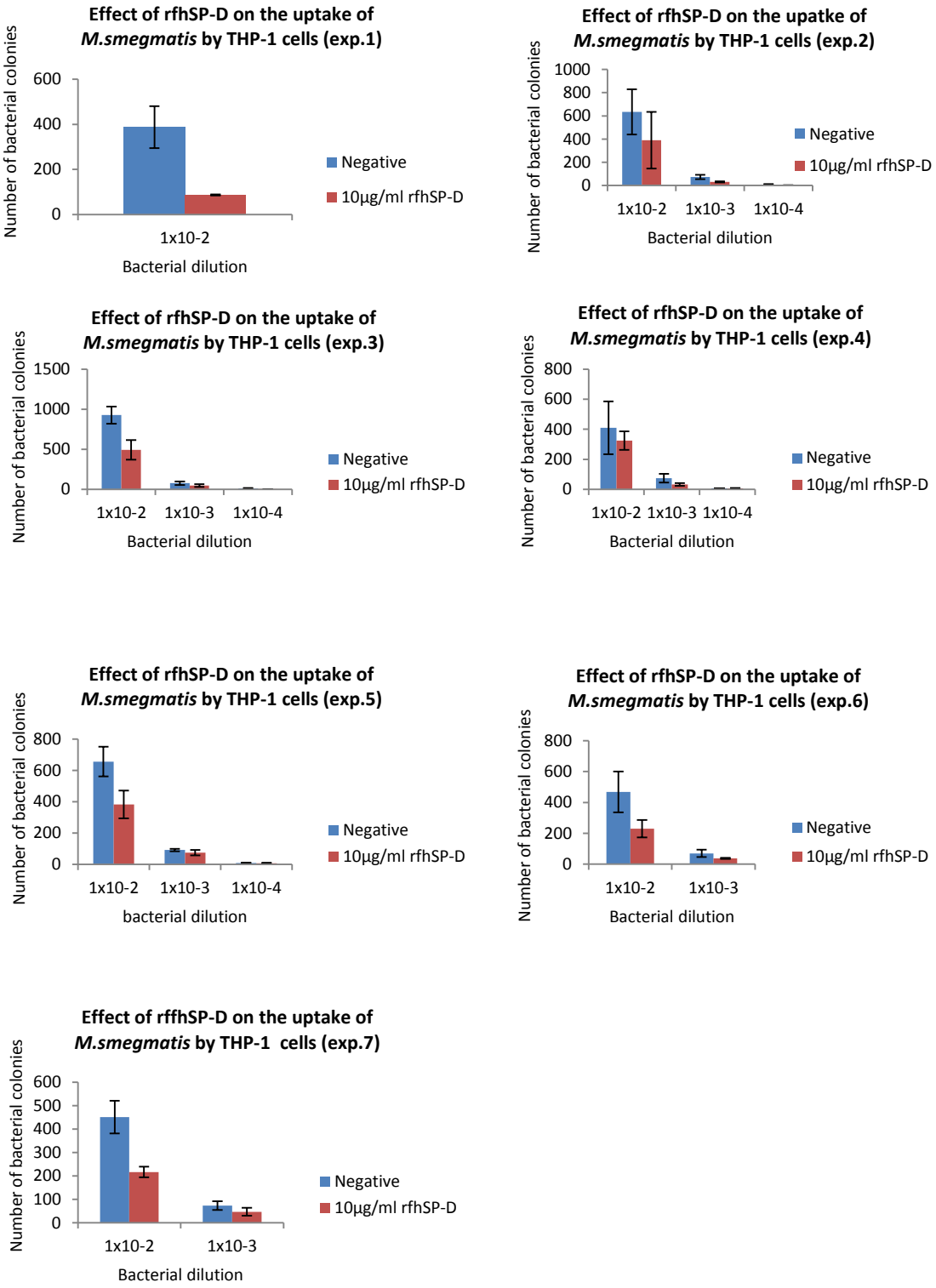

Figure 3.17-B: Effect of rfhSP-D on the uptake of *M.smegmatis* by THP-1 cells (7 individual experiments). The rfhSP-D reduces the uptake of *M.smegmatis* by THP1 cells in each individual experiment. Each histogram represents the average of 3 triplicate data. Error bars represent ±standard deviation. Negative contains untreated *M.smegmatis*.

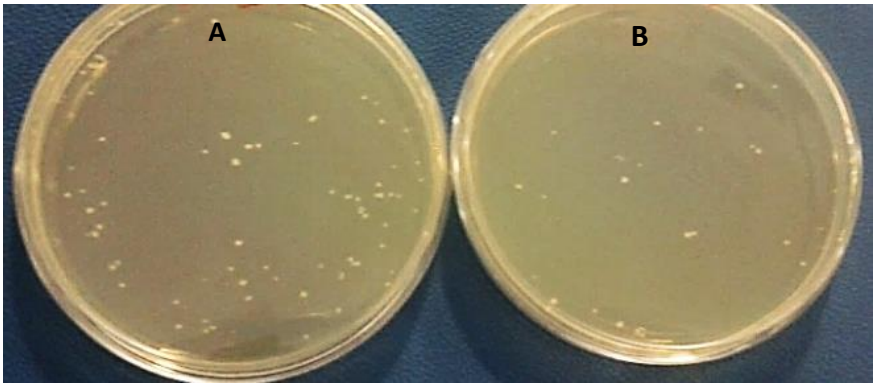

Figure 3.17-C: Effect of rfhSP-D on the uptake of *M.smegmatis.* Colonies were grown on LB agar plates for 3 days at 37°C in triplicates and counted by visual inspection. *M.smegmatis* colonies are white in colour, rough and dry. A: Untreated *M.smegmatis*. B: RfhSP-D treated *M.smegmatis*. RfhSP-D reduces the uptake of *M.*smegmatis by THP-1 cells.

3.2.11.2 Effect of rfhSP-D on the uptake of BCG by THP1 cells

Six independent experiments were carried out. All the experiments showed the same trend in decrease the uptake of BCG by THP-1 cells in presence of rfhSP-D in 5mM calcium chloride (Figure 3.18-B&C). There were 63% reduction in the uptake of BCG by the macrophages treated with rfhSP-D as compared to untreated BCG (Negative). The results are statistically significant (p value < 0.05) (Figure 3.18).

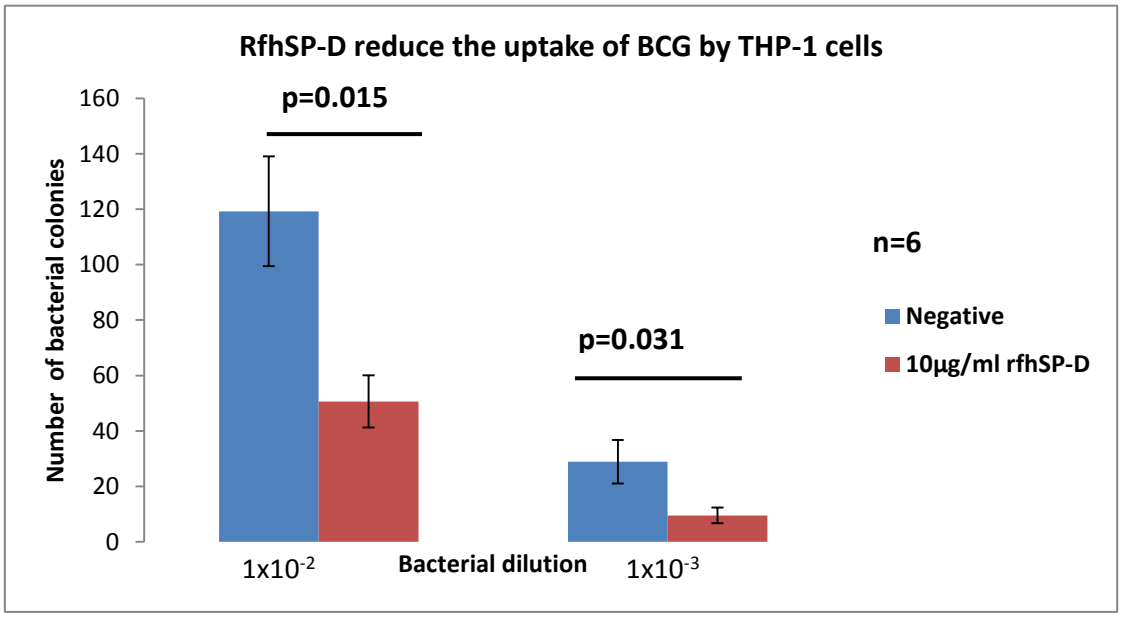

Figure 3.18-A: Effect of rfhSP-D on the uptake of BCG by THP1 cells. The uptake (phagocytosis) of rfhSP-D treated BCG was reduced by THP-1 cells as compared to untreated BCG. Both rfhSP-D treated and untreated tubes (negative) were incubated for 2 hours at 37°C in presence of $CaCl_2$. Following the incubation, THP-1 cells were added to each tube in ratio 1:5 (THP-1 cells:BCG), and incubated for an hour inside at 37°C to allow the uptake of mycobacteria by THP-1 cells. Next, magnetic beads bound with anti-human MHC class 1 were added to THP-1 cells in a ratio of 1:4 (THP-1 cells: beads), and tubes were incubated in ice horizontally for 30 minutes on a shaker. Next, THP-1 cells were washed 3 times to remove extracellular bacteria. Washed cells were lysed with 0.1% saponin by vortexing for 15 minutes to release phagocytosed mycobacteria. Each histogram represents the average of 6 independent experiments. Error bars represent ±standard error of the mean. P value calculated using Wilcoxon signed rank test. Negative control contains untreated BCG.

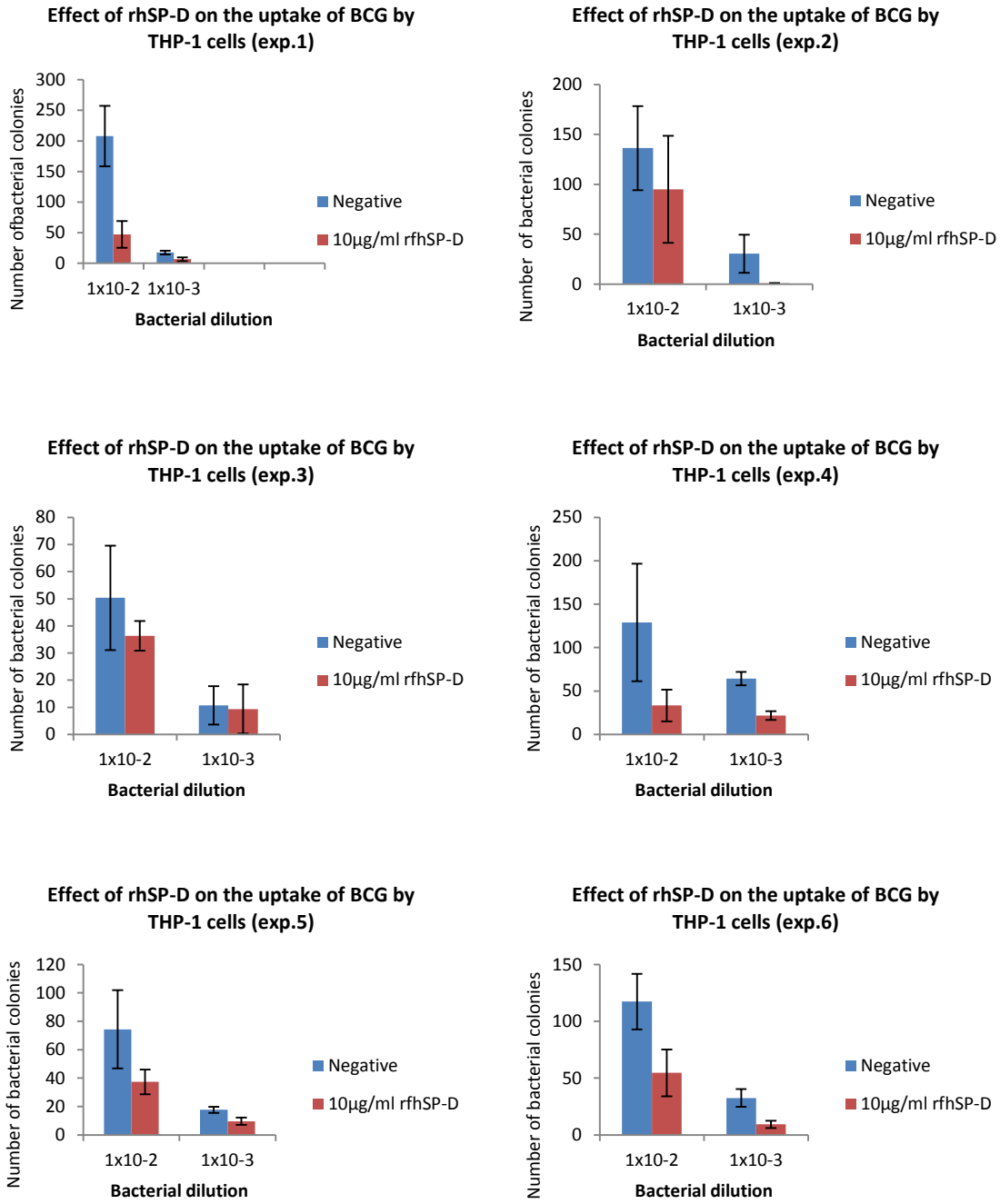

Figure 3.18-B: Effect of rfhSP-D on the uptake of BCG by THP1 cells (6 individual experiments). Each histogram represents the average of 3 triplicate data. Error bars represent ±standard deviation.

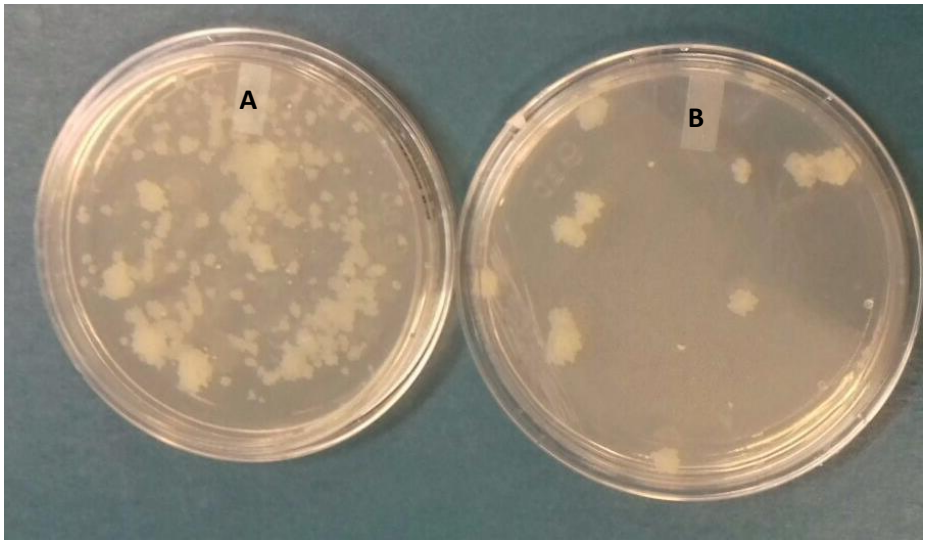

Figure 3.18-C: Effect of rfhSP-D on BCG uptake by THP-1 cells (BCG colonies grown on 7H10 plates) after 3 weeks incubation at 37°C). Plate A: shows the number of untreated BCG colonies uptaken by THP-1 cells in presence of 5mM calcium chloride. Plate B: shows the number of rfhSP-D treated BCG colonies phagocytosed by THP-1 cells in presence of 5mM calcium chloride. The uptake (phagocytosis) of rfhSP-D treated BCG was reduced by THP-1 cells as compared to untreated BCG.

3.2.12 Effect of rfhSP-D on the growth of mycobacteria inside THP1 cells

3.2.12.1 Effect of rfhSP-D on the growth of *M. smegmatis* inside THP1 cells

Treatment of mycobacteria with 10µg/ml rfhSP-D in calcium chloride was shown to inhibit *M.smegmatis* growth inside THP-1 cells (Figure 3.19-A). There was around 33% reduction in *M.smegmatis* growth, and growth inhibition was statistically significant ($p < 0.05$). Six independent experiments were carried out and all the experiments showed the same trend in decreasing rfhSP-D treated *M.smegmatis* growth inside THP-1 cells as compared to untreated *M.smegmatis* (negative control) (Figure 3.19A).

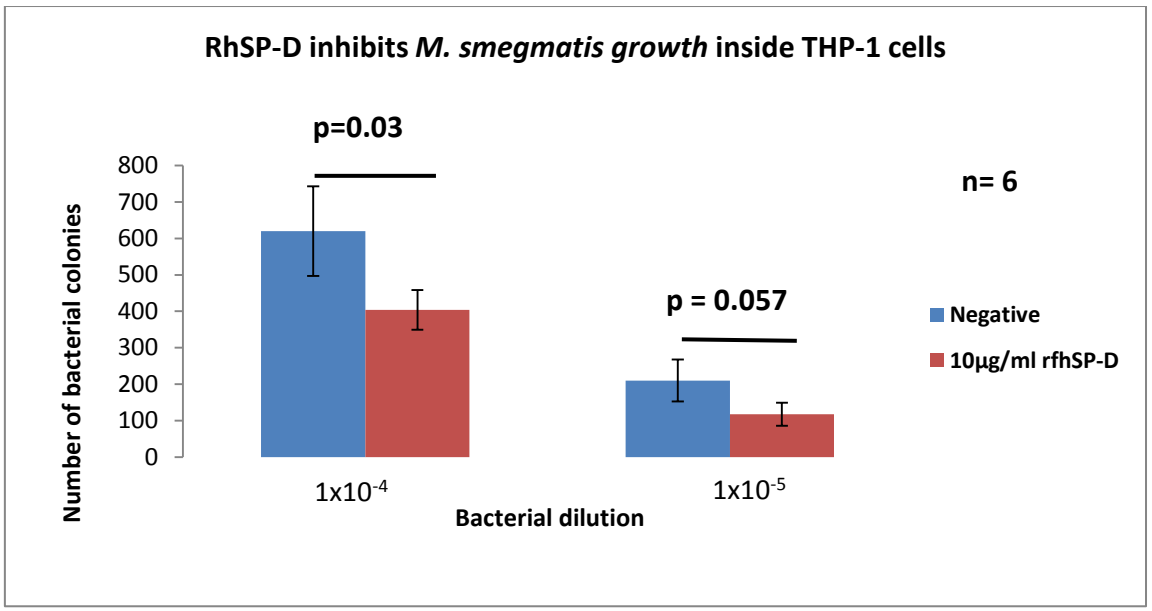

Figure 3.19-A: Effect of rfhSP-D on *M.smegmatis* growth inside THP-1 cells, 24h after phagocytosis. Both rfhSP-D treated and untreated *M.smegmatis* (negative) were incubated for 2 hours at 37°C with 5mM $CaCl_2$. After incubation, THP-1 cells were added to mycobacteria in a 1:5 ratio (THP-1 cells:*M.smegmatis*) and incubated for an hour inside CO_2 incubator at 37^0C. Following incubation, magnetic beads bound with anti-human MHC class 1 were added to each tube in a ratio of 1:4 (THP-1: beads) and the tubes were incubated in ice for 30 minutes on a shaker. Next, the cells were washed 3 times to remove extracellular bacteria. Washed cells were suspended in complete RPMI medium (without antibiotics) and incubated inside a CO_2 incubator for 24 hours. Following incubation, the cells were separated by a magnet and lysed with 0.1% of saponin and vortexing for 15 minutes. Equal volumes of cell lysate and supernatant were mixed together and bacterial dilutions of $1x10^{-4}$ and $1x10^{-5}$ were prepared. For each dilution, 250µl was plated on LB agar in triplicates. Plates were incubated at 37°C for 3 days. Each histogram represents the average of 6 independent experiments. Error bars represent ± standard error of the mean. P value calculated using Wilcoxon signed rank test. Negative control contains untreated *M.smegmatis*.

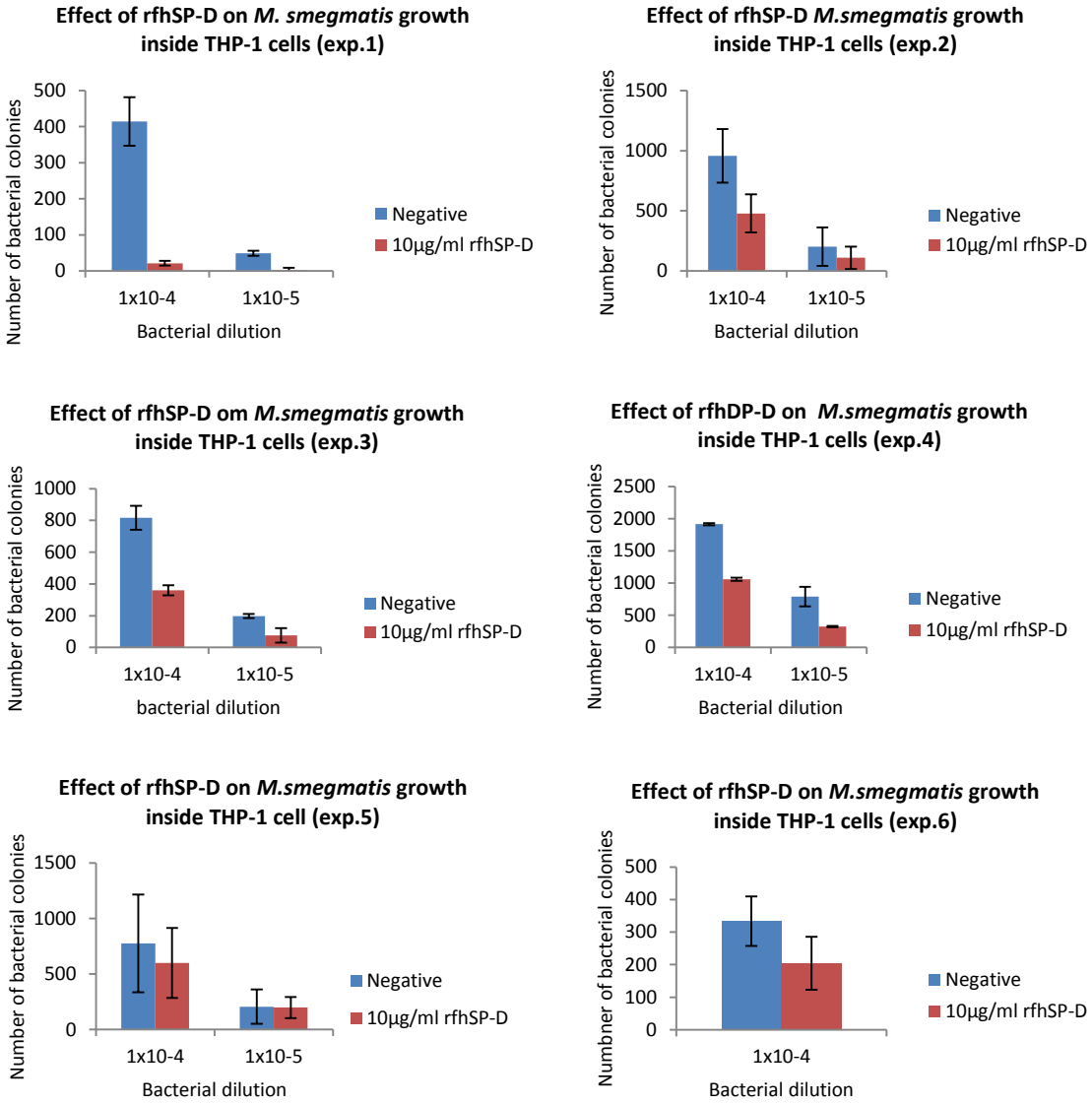

Figure 3.19-B: Effect of rfhSP-D on *M.smegmatis* growth inside THP-1 cells after 24h of phagocytosis (6 individual experiments). The rfhSP-D inhibits the growth of *M.smegmatis* inside THP1 cells in individual experiments. Each histogram represents the average of triplicate readings. Error bars represent ±standard deviation. Negative contains untreated *M.smegmatis*.

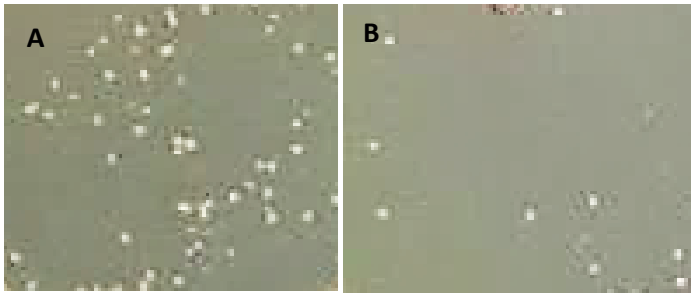

Figure 3.19-C: Effect of rfhSP-D on *M.smegmatis* growth inside the THP-1 cells (Colonies grown for 72 hours on LB agar plates). The picture on the left (A) shows the negative control containing untreated *M.smegmatis*, and the picture on the right (B) shows *M.smegmatis* treated with 10 µg/ml of rfhSP-D. It is clear that bacterial growth inside THP-1 cells is reduced in rfhSP-D treated *M.smegmatis.*

3.2.12.2 Effect of rfhSP-D on the growth of BCG inside THP1 cells

Six independent experiments were carried out to see the effect of rfhSP-D in presence of $CaCl_2$ on BCG growth, and all the experiments showed the same trend in decreasing the growth of BCG inside human THP-1 cells (Figure 3.20-B). There is around 70% reduction in BCG growth and the results were statistically significant, p <0.05 (Figure 3.20-A).

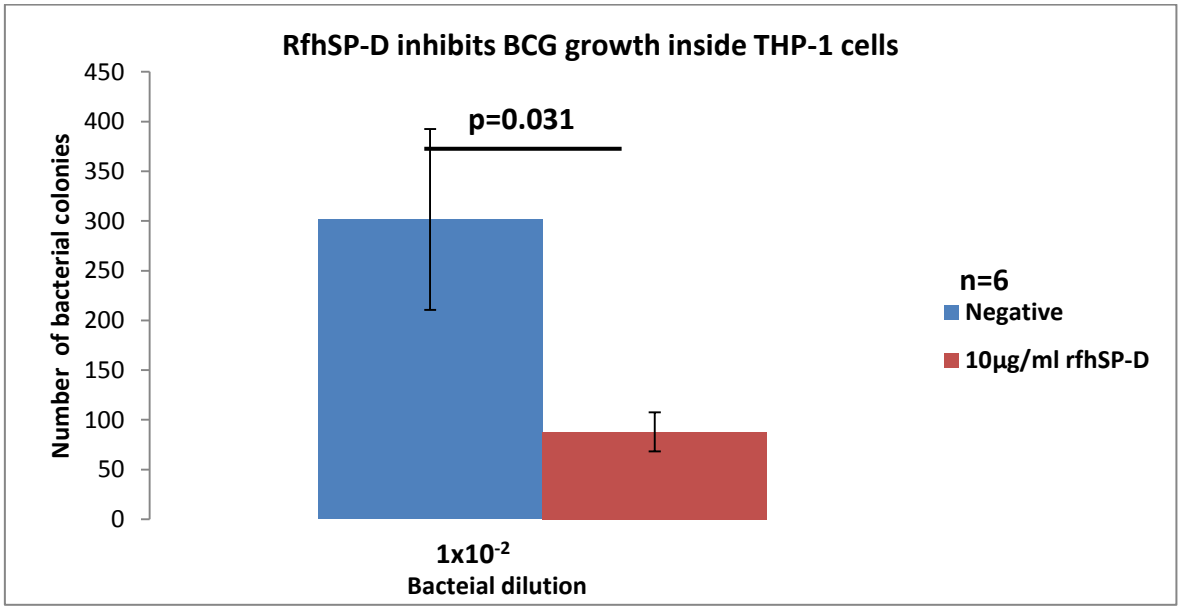

Figure 3.20-A: Effect of rfhSP-D on BCG growth inside THP-1 cells after 24h of phagocytosis. RfhSP-D inhibits BCG growth inside THP1 cells. Both rfhSP-D treated and untreated BCG (negative) were incubated for 2 hours at 37°C with 5mM $CaCl_2$. The cells were added to mycobacteria in a 1:5 ratio (THP-1 cells:BCG) and incubated for one hour inside a CO_2 incubator. Next, magnetic beads bound with anti-human MHC class 1 were added to each tube in a ratio of 1:4 (THP-1: beads), and all tubes were incubated in ice for 30 minutes on a shaker. Following incubation, the cells were washed 3 times using RPMI. Washed cells were suspended in complete RPMI medium (without antibiotics) and incubated inside a CO_2 incubator for 24 hours. The cells were then separated using a magnet and lysed with 0.1% of saponin by vortexing for 15 minutes. Equal volumes of cell lysate and supernatant were mixed together and bacterial dilutions of $1x10^{-4}$ and $1x10^{-5}$ were prepared. For each dilution, 250µl was plated on 7H10 plates supplemented with 10% ADC in triplicates. The plates were incubated at 37°C for 2-3 weeks. Each histogram represents the average of 6 independent experiments**.** Error bars represent ±standard error of the mean. P value calculated using Wilcoxon signed rank test. Negative control contains untreated BCG.

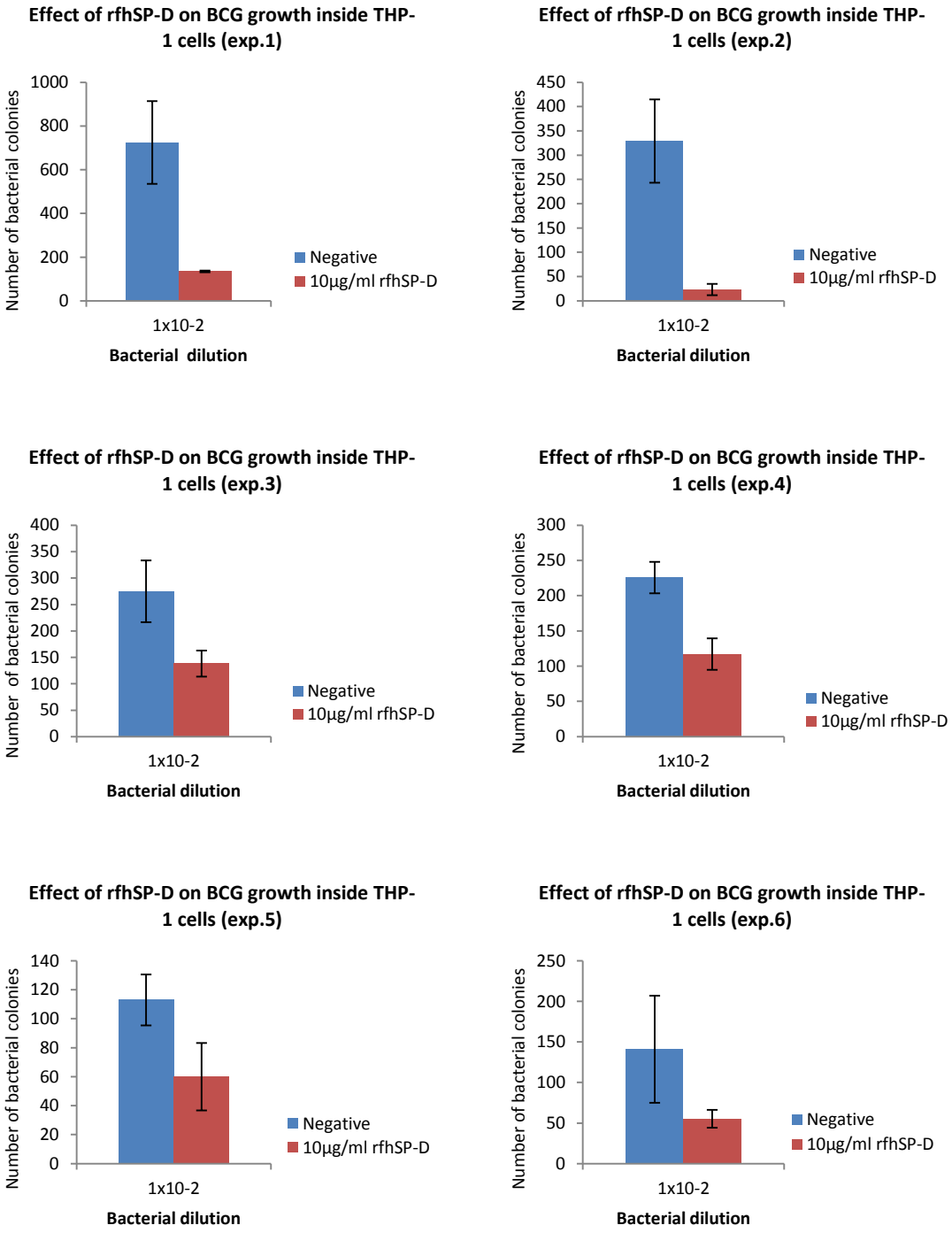

Figure 3.20-B: Effect of rfhSP-D on BCG growth inside THP-1 cells (6 individual experiments). RfhSP-D inhibits the growth of BCG inside THP1 cells in all independent experiment. Each histogram represents the average of triplicate readings**.** Error bars represent ±standard deviation.

3.2.13 Understanding the mechanism of mycobacterial inhibition inside THP1 cells by studying cytokine gene expression profile of THP-1 cells infected with untreated mycobacteria and rfhSP-D treated mycobacteria

A selected group of target genes were used for qPCR analysis where upregulation or down regulation of these genes help in the control of tuberculosis. A qPCR study was carried out to examine the effect of rfhSP-D on the gene expression of inducible nitric oxide synthase, pro-inflammatory cytokines (TNF-α, IL-1β, IL-6, and IL-12) and anti-inflammatory cytokines (TGF-β and IL-10).

3.2.13.1 Gene expression of inducible nitric oxide synthase (iNOS)

This study showed that iNOS expression was slightly enhanced in the presence of rfhSP-D as compared to untreated mycobacteria at 5 and 10 hours only (Figure 3.21). The gene expression of iNOS was studied due to this enzyme being responsible for production of reactive nitrogen intermediates (RNI) through the conversion of L-arginine to citrulline. RNI are very toxic to bacteria, they have been detected in previously *Mtb* infected macrophages (Nicholson et al., 1996). Moreover, it have been shown that the inhibition of iNOS in latent TB human leads to *Mtb* reactivation (Gardam et al., 2003).

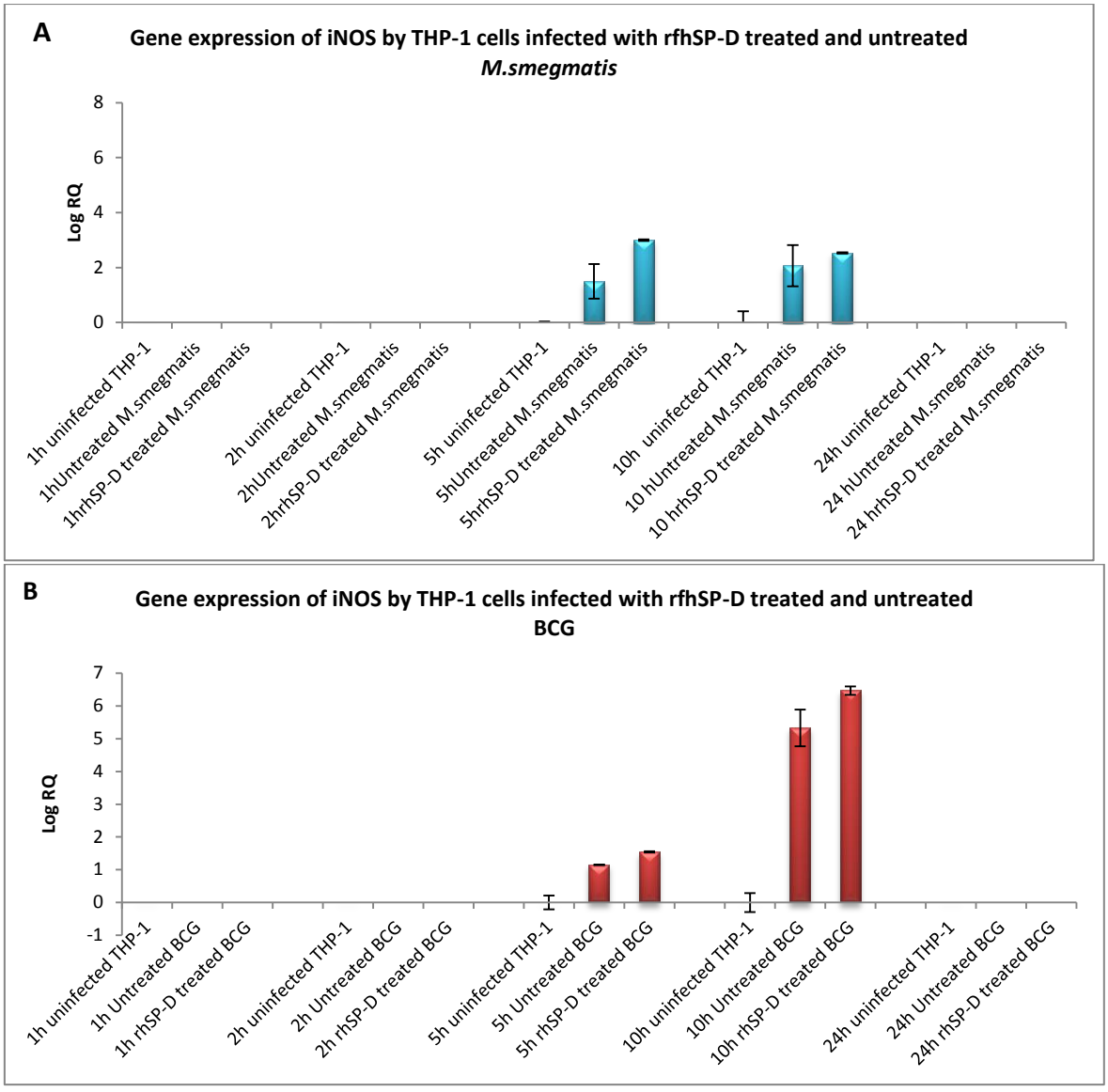

Figure 3.21: Expression of nitric oxide synthase (iNOS) gene by THP-1 cells infected with rfhSP-D treated and untreated *M.smegmatis* (A) and BCG (B). THP-1 cells were incubated for 1, 2, 5, 10 and 24 hours after infection with mycobacteria at 37°C inside a CO_2 incubator. The cell pellet was collected and used for RNA extraction and cDNA synthesis. The expression of the gene was measured using qPCR and data was normalized to 18sRNA expression as control. RQ values were calculated using the formula; $RQ=2^{\Delta\Delta Ct}$. Log RQ values were plotted to show the gene expression. Un-infected THP-1 cells were used as negative control. Each bar represents the average of triplicate readings. Error bars represent ±standard deviation.

3.2.13.2 Gene expression of tumour necrosis factor-α (TNF-α)

The gene expression for TNF-α was studied because it has been shown to regulate the growth of mycobacteria inside granulomas and initiation of adaptive immunity and host protection. Moreover, neutralization of TNF-α in rheumatoid arthritis patients lead to activation of latent TB (Gardam et al., 2003).

TNF-α gene was expressed by THP-1 cells infected with rfhSP-D treated and untreated mycobacteria (Figure 3.22). The gene expression of this cytokine was generally down regulated in the presence of rfhSP-D as compared to untreated mycobacteria.

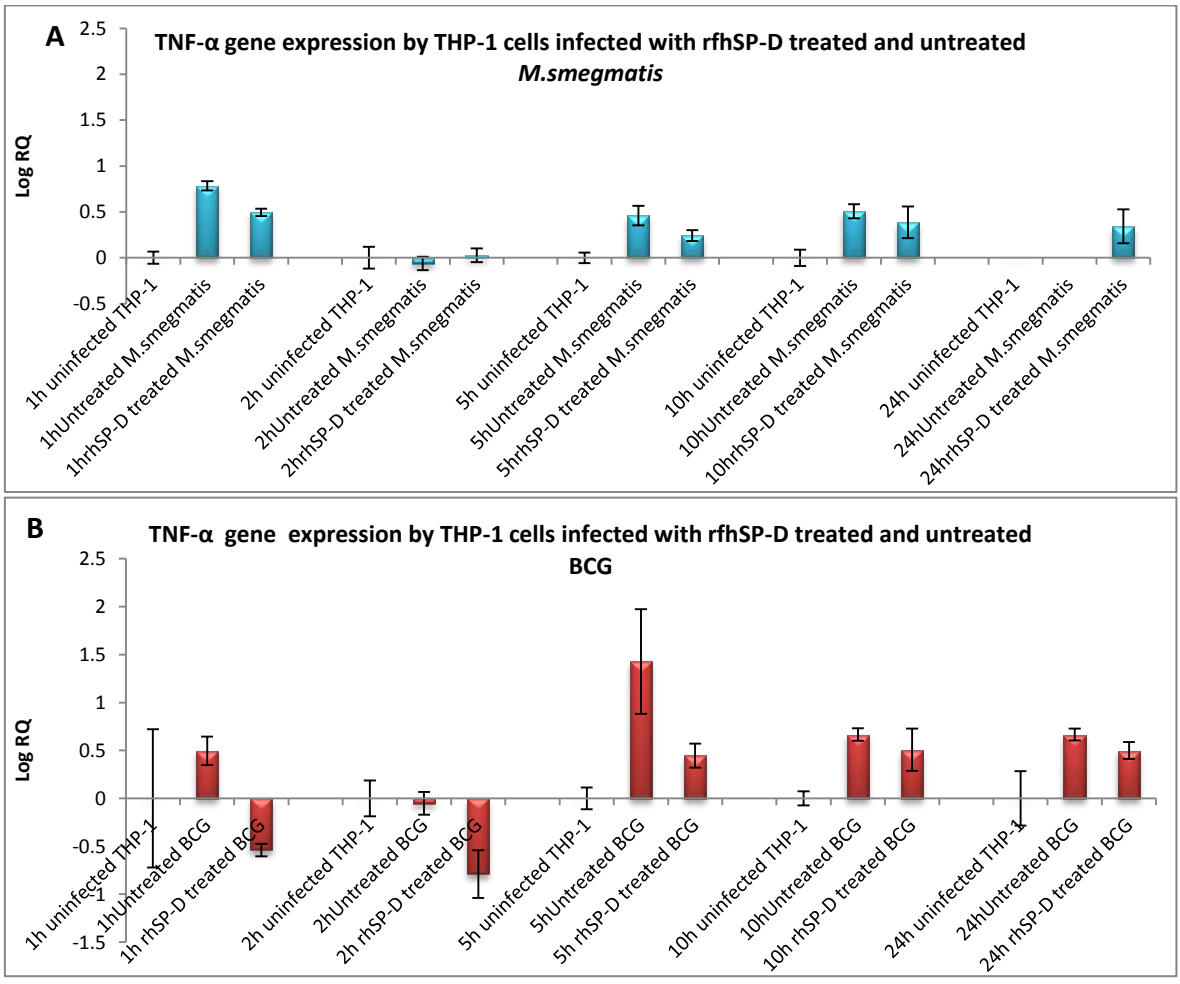

Figure 3.22: Expression of Tumour necrosis factor-α (TNF-α) gene by THP-1 cells infected with rfhSP-D treated and untreated *M.smegmatis* (A) and BCG (B). THP-1 cells were incubated for 1, 2, 5, 10 and 24 hours following infection with mycobacteria at 37°C inside a CO_2 incubator. The cell pellet was collected and used for RNA extraction and cDNA synthesis. The expression of the gene was measured using qPCR and data was normalized to 18sRNA expression as control. RQ values were calculated using the formula; $RQ=2^{-\Delta\Delta Ct}$. Log RQ values were plotted to show the gene expression. Un-infected THP-1 cells were used as negative control. Each bar represents the average of triplicate readings. Error bars represent ±standard deviation.

3.2.13.3 Gene expression of interleukin-1β (IL-1 β)

IL-1β is a pro-inflammatory cytokine expressed inside granulomas. IL-1β receptor deficient mice have shown impaired granuloma formation (Juffermans et al., 2000). IL-1β gene was expressed by both THP-1 cells infected with rfhSP-D treated mycobacteria and untreated mycobacteria. It appears that the expression of IL- β was generally down regulated in rfhSP-D treated mycobacteria as compared to untreated mycobacteria (Figure 3.23).

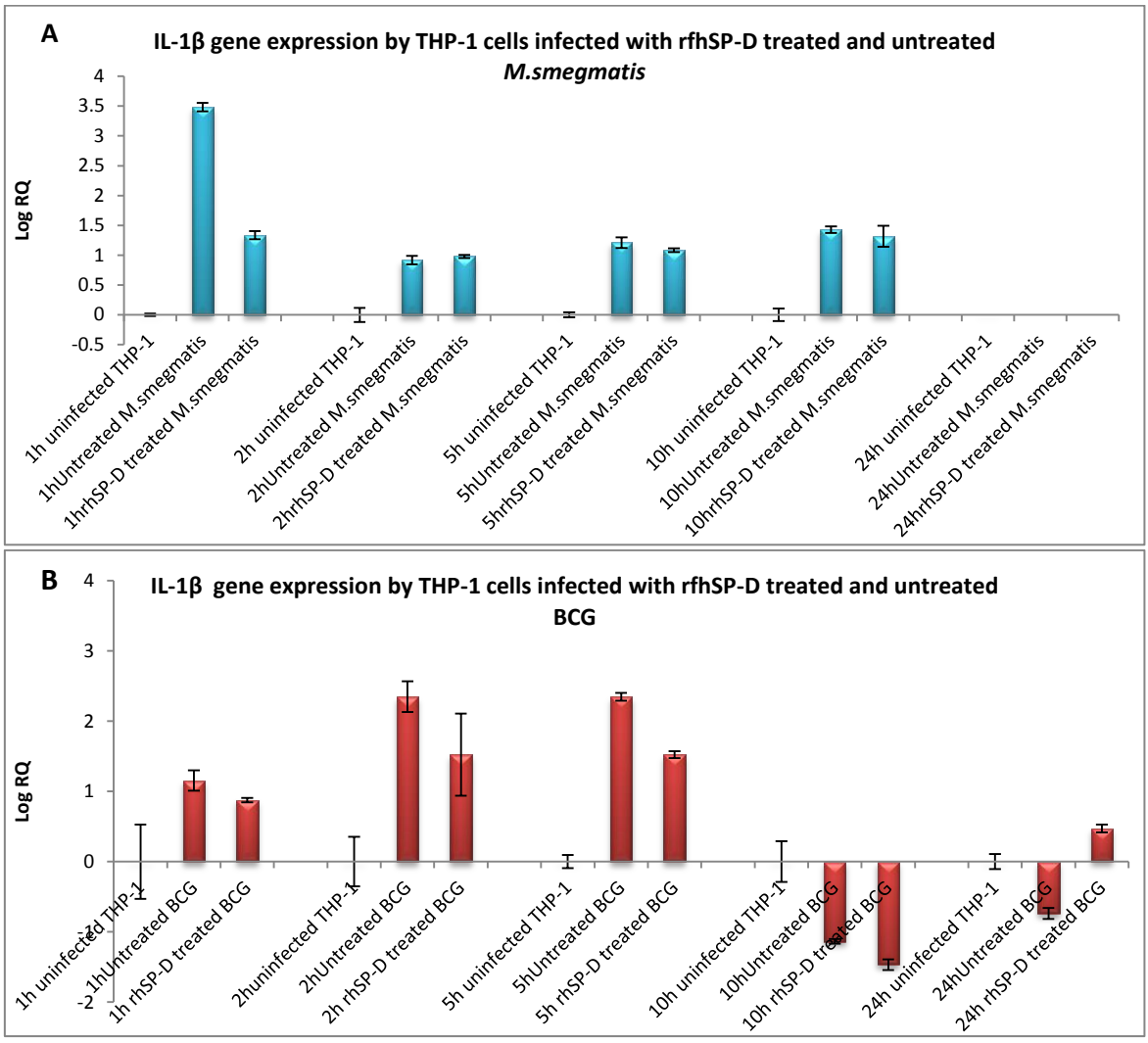

Figure 3.23: Expression of Interleukin 1-β (IL-1β) gene by THP-1 cells infected with rfhSP-D treated and untreated *M.smegmatis* (A) and BCG (B). THP-1 cells were incubated for 1, 2, 5, 10 and 24 hours after infection with mycobacteria at 37°C inside a CO_2 incubator. The cell pellet was collected and used for RNA extraction and cDNA synthesis used in this analysis. The expression of the gene was measured using qPCR and data was normalized to 18sRNA expression as control. RQ values were calculated using the formula; $RQ=2^{-\Delta\Delta Ct}$. Log RQ values were plotted to show the gene expression. Un-infected THP-1 cells were used as negative control. Each bar represents the average of triplicate readings. Error bars represent ±standard deviation.

3.2.13.4 Gene expression of interleukin-6 (IL-6)

IL-6 gene was expressed by both THP-1 cells infected with rfhSP-D treated mycobacteria and untreated mycobacteria. This suggests that rfhSP-D presence does not affect the gene expression of IL-6 cytokine (Figure 3.24). IL-6 plays opposing roles in pathogenesis of tuberculosis. IL-6 deficient mice are more susceptible to *Mtb* infection (Saunders et al., 2000) whereas IL-6 inhibits TNF-α and IL-1β production and facilitates the growth of mycobacteria (Schindler et al., 1990).

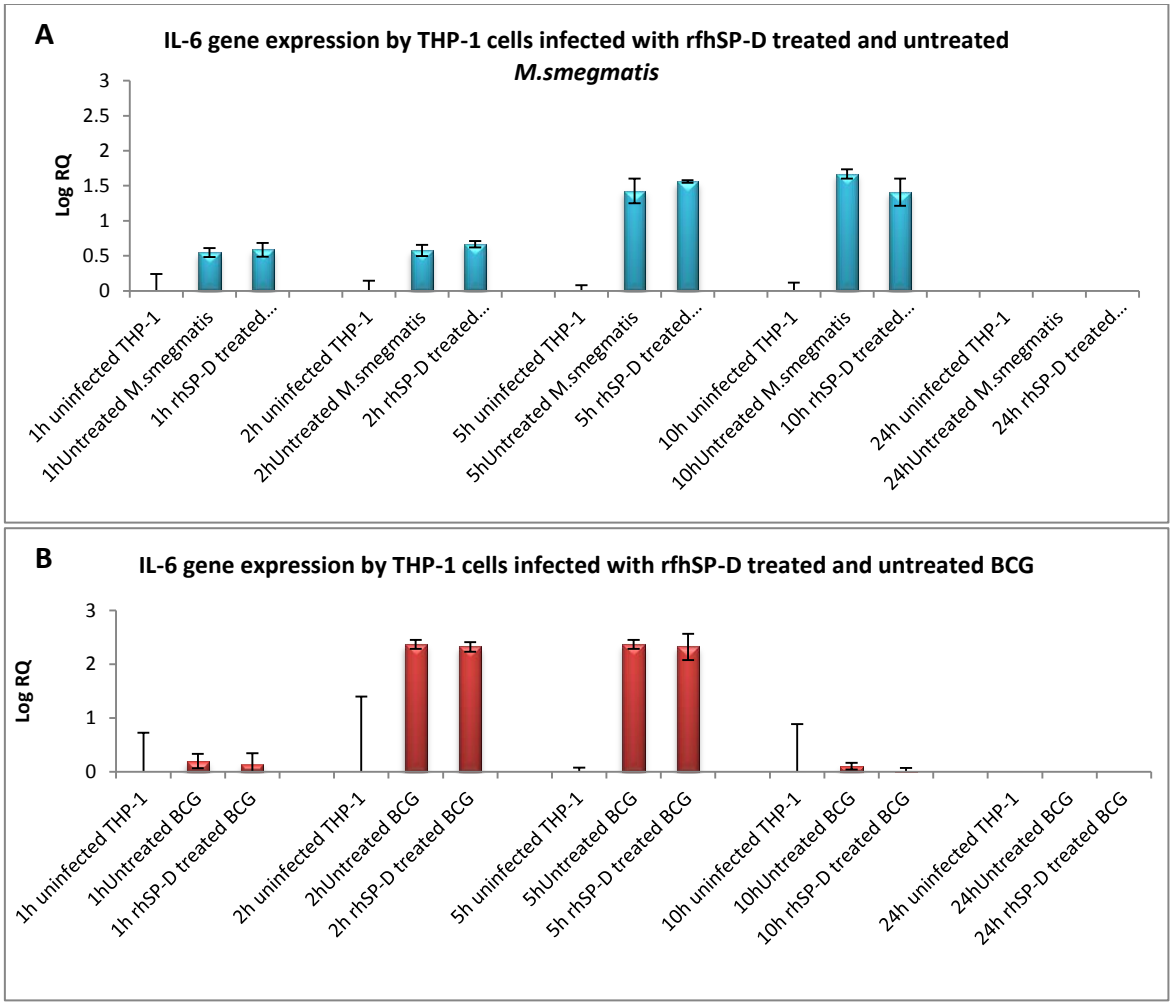

Figure 3.24: Expression of IL-6 gene by THP-1 cells infected with rfhSP-D treated and untreated *M.smegmatis* (A) and BCG (B). THP-1 cells were incubated for 1, 2, 5, 10 and 24 hours after infection with mycobacteria at 37°C inside a CO_2 incubator. The cell pellet was collected and used for RNA extraction and cDNA synthesis. The expression of the gene was measured using qPCR and data was normalized to 18sRNA expression as control. RQ values were calculated using the formula; $RQ=2^{\Delta\Delta Ct}$. Log RQ values were plotted to show the gene expression. Un-infected THP-1 cells were used as negative control. Each bar represents the average of triplicate readings. Error bars represent ±standard deviation.

3.2.13.5 Gene expression of interleukin-12 (IL-12)

IL-12 is pro-inflammatory cytokine that initiates Th1 immunity against tuberculosis. It is expressed inside granulomas of active TB patients. It has been shown that IL-12 supplements leads to *Mtb* killing in infected mice (Flyyn et al., 1995). IL-12 gene was expressed by both THP-1 cells infected with rfhSP-D treated mycobacteria and untreated mycobacteria. The expression of IL-12 is generally higher in THP-1 cells infected with rfhSP-D treated *M.smegmatis* as compared to untreated *M.smegmatis* and uninfectedTHP-1 cells (Figure 3.25-A), but the expression of IL-12 was increased after 24 hours in THP-1 infected with rfhSP-D treated BCG (Figure 3.25-B).

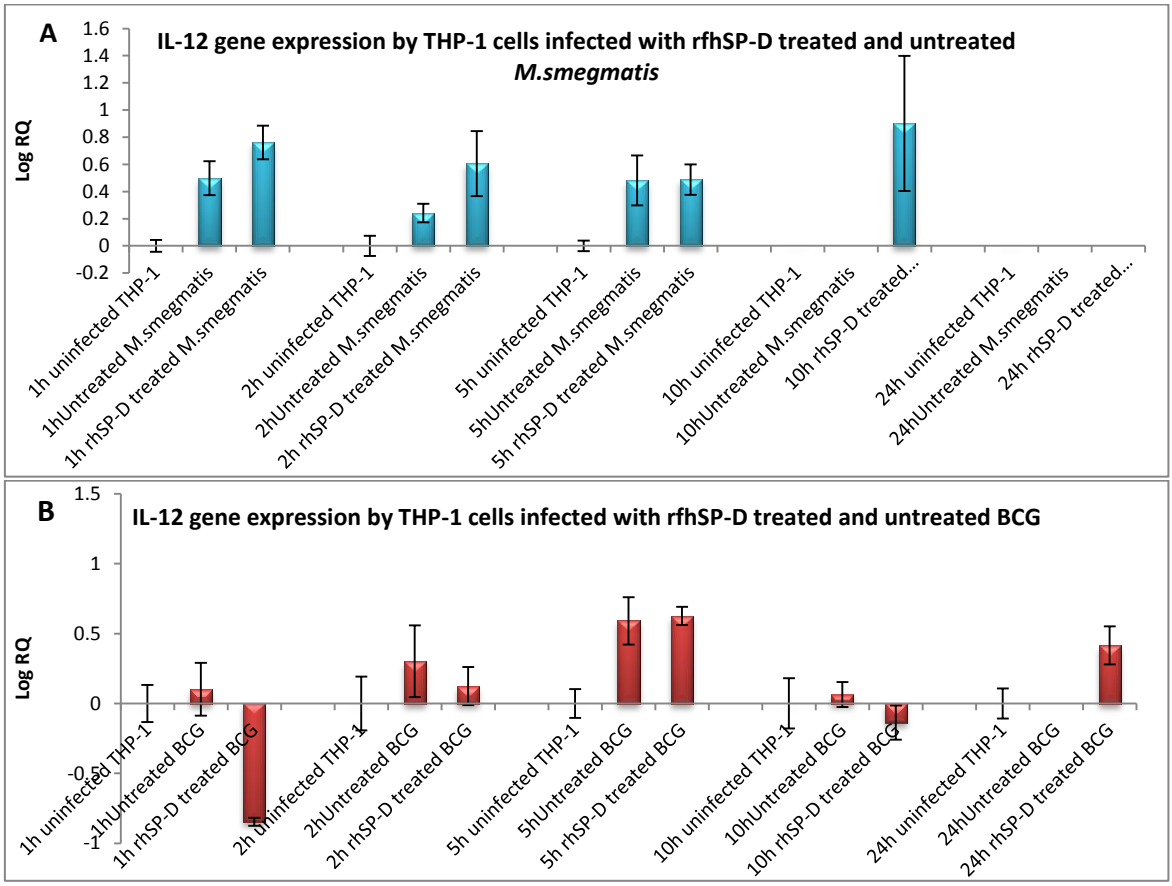

Figure 3.25: Expression of IL-12 gene by THP-1 cells infected with rfhSP-D treated and untreated *M.smegmatis* (A) and BCG (B). THP-1 cells were incubated for 1, 2, 5, 10 and 24 hours after infection with mycobacteria at 37°C inside a CO_2 incubator. The cell pellet was collected and used for RNA extraction and cDNA synthesis used in this analysis. The expression of the gene was measured using qPCR and data was normalized to 18sRNA expression as control. RQ values were calculated using the formula; $RQ=2^{-\Delta\Delta Ct}$. Log RQ values were plotted to show the gene expression. Un-infected THP-1 cells were used as negative control. Each bar represents the average of triplicate readings. Error bars represent ±standard deviation.

3.2.13.6 Gene expression of transforming growth factor-β (TGF-β)

TGF-β is an anti-inflammatory cytokine that opposes the protective immunity in tuberculosis. It is secreted inside the granulomasby infected macrophages and inhibits ROI and RNI production (Ding et al., 1990). Furthermore, it inhibits the phagocytosis of mycobacteria and increases their growth (Toossi et al., 1995).

It appears that TGF-β was expressed in THP-1 cells infected with rfhSP-D treated mycobacteria (after 24 hours in THP-1 cells infected with *M.smegmatis* and after 6 and 10 hours in THP-1 cells infected with BCG). The expression of TGF- β is slightly lower in the presence of rfhSP-D as compared to untreated mycobacteria (Figure 3.26).

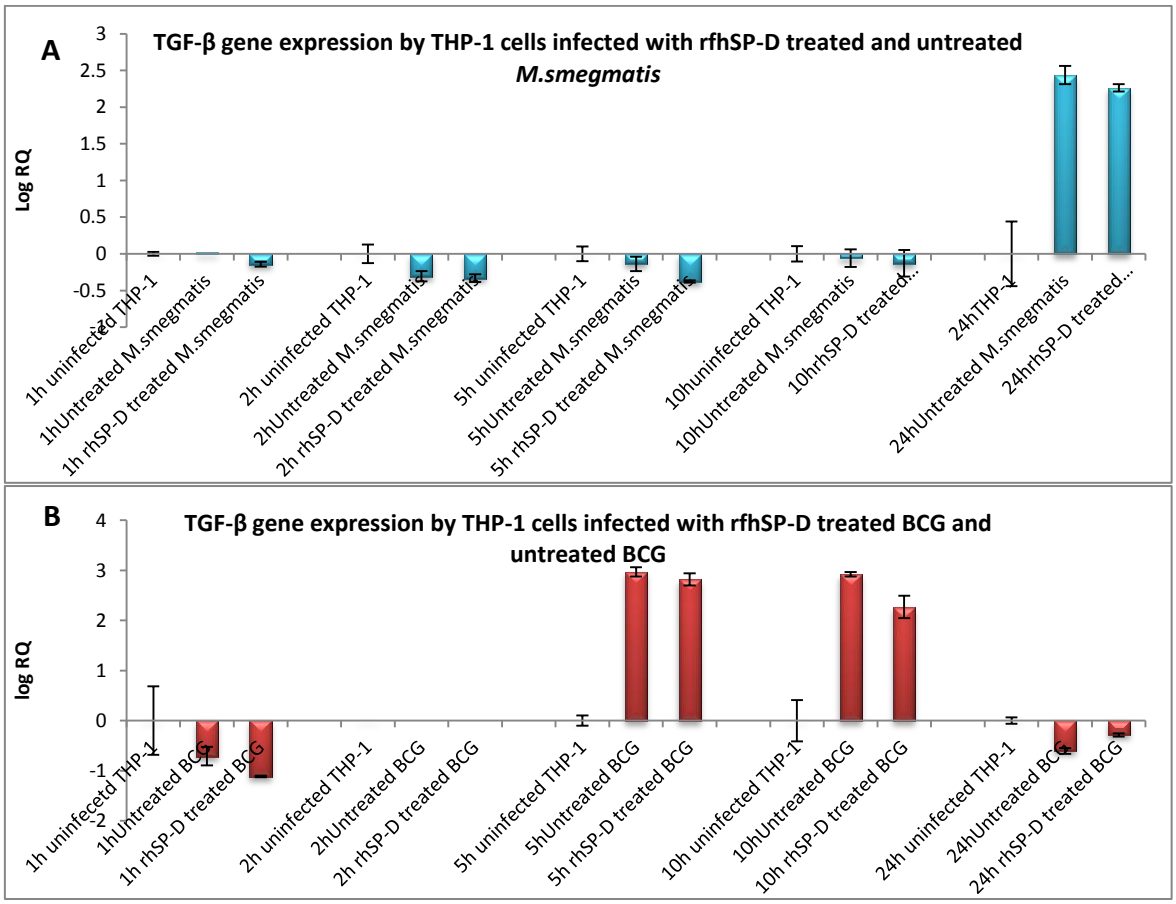

Figure 3.26: Expression of TGF-β gene by THP-1 cells infected with rfhSP-D treated and untreated *M.smegmatis* (A) and BCG (B). THP-1 cells were incubated for 1, 2, 5, 10 and 24 hours after infection with mycobacteria at 37°C inside a CO_2 incubator. The cell pellet was collected and used for RNA extraction and cDNA synthesis used in this analysis. The expression of the gene was measured using qPCR and data was normalized to 18sRNA expression as control. RQ values were calculated using the formula; $RQ=2^{-\Delta\Delta Ct}$. Log RQ values were plotted to show the gene expression. Un-infected THP-1 cells were used as negative control. Each bar represents the average of triplicate readings. Error bars represent ±standard deviation.

3.2.13.7 Expression of interleukin-10 (IL-10)

IL-10 is an anti-inflammatory cytokine that down regulates TNF-α and IL-12 expression inside infected macrophages, which reduces ROI and RNI intermediates production and increases *Mtb* survival (Moore et al., 2001). IL-10 gene was expressed by THP-1 cells infected with rfhSP-D treated *M.smegmatis* and untreated *M.smegmatis* after 1, 2, 5 and 10 hours of incubation (Figure 3.27-A). Also, IL-10 was expressed after 1 hour by THP-1 cells infected with rfhSP-D treated BCG and untreated BCG. This cytokine was increased after 5 hours by THP-1 cells infected with rfhSP-D treated BCG only . It appears that IL-10 gene expression is enhanced in the presence of rfhSP-D (Figure 3.27-B).

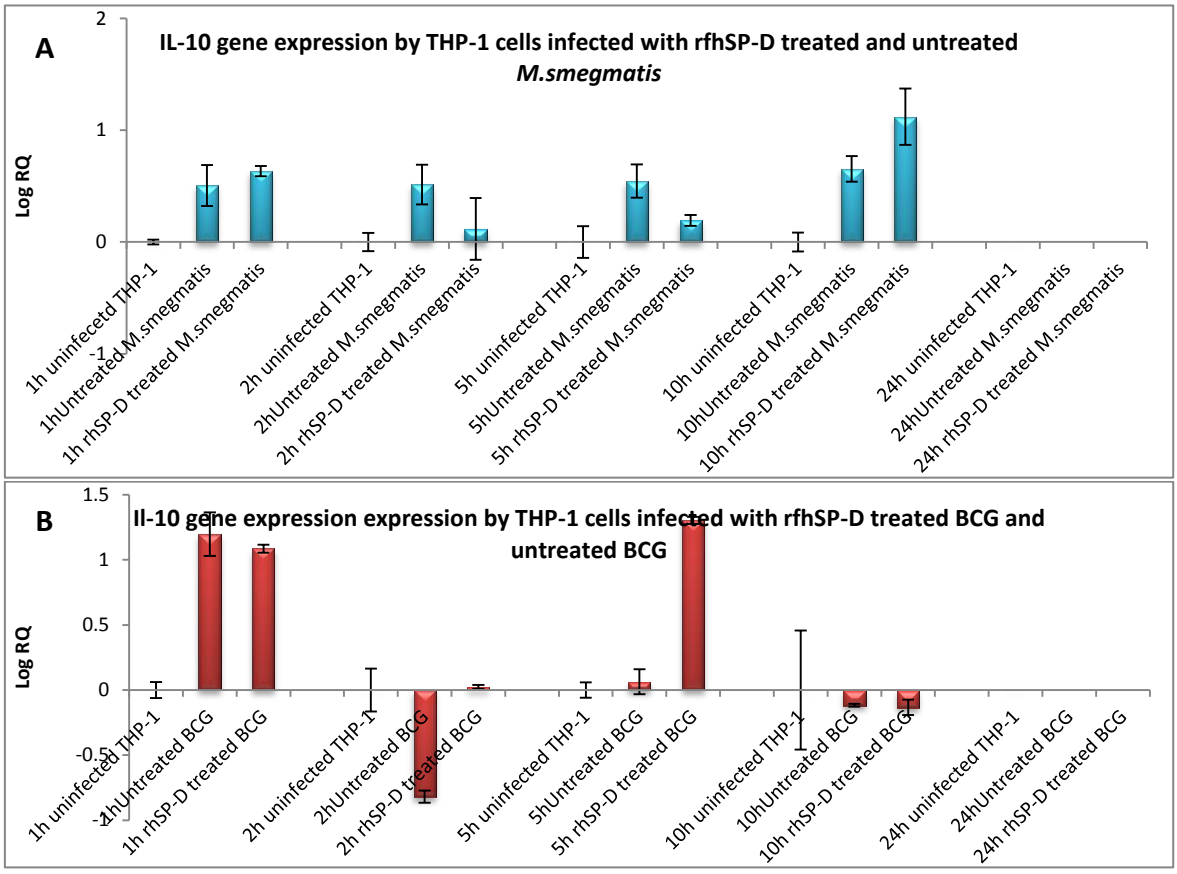

Figure 3.27: Expression of IL-10 gene by THP-1 cells infected with rfhSP-D treated and untreated *M.smegmatis* (A) and BCG (B). THP-1 cells were incubated for 1, 2, 5, 10 and 24 hours after infection with mycobacteria at 37°C inside a CO_2 incubator. The cell pellet was collected and used for RNA extraction and cDNA synthesis used in this analysis. The expression of the gene was measured using qPCR and data was normalized to 18sRNA expression as control. RQ values were calculated using the formula; $RQ=2^{\Delta\Delta Ct}$. Log RQ values were plotted to show the gene expression. Un-infected THP-1 cells were used as negative control. Each bar represents the average of triplicate readings. Error bars represent ±standard deviation.

3.2.14 Effect of neutralization of inducible nitric oxide synthase, TGF-β and TNF-α on the growth of rfhSP-D treated *M. smegmatis* inside THP1 cells

3.2.14.1 Effect of neutralization of inducible nitric oxide synthase on *M.smegmatis* growth inside THP-1 cells

Human macrophages can kill different pathogens by production nitric oxide free radicals. In this study, nitric oxide synthase inhibitor (NG-Methyl-L-arginine acetate) was used in order to inhibit the production of nitric oxide by THP-1 cells. The results showed that nitric oxide synthase inhibitor treatment of THP-1 cells increases the bacterial growth inside THP-1 cells infected with rfhSP-D treated *M.smegmatis* (Figure 3.28- A&B), which means that nitric oxide free radicals were produced by THP-1 cells infected with rfhSP-D treated *M.smegmatis*, and neutralization the effect of nitric oxide synthase which is responsible for nitric oxide free radicals production leads to increased mycobacterial growth *in vitro*.

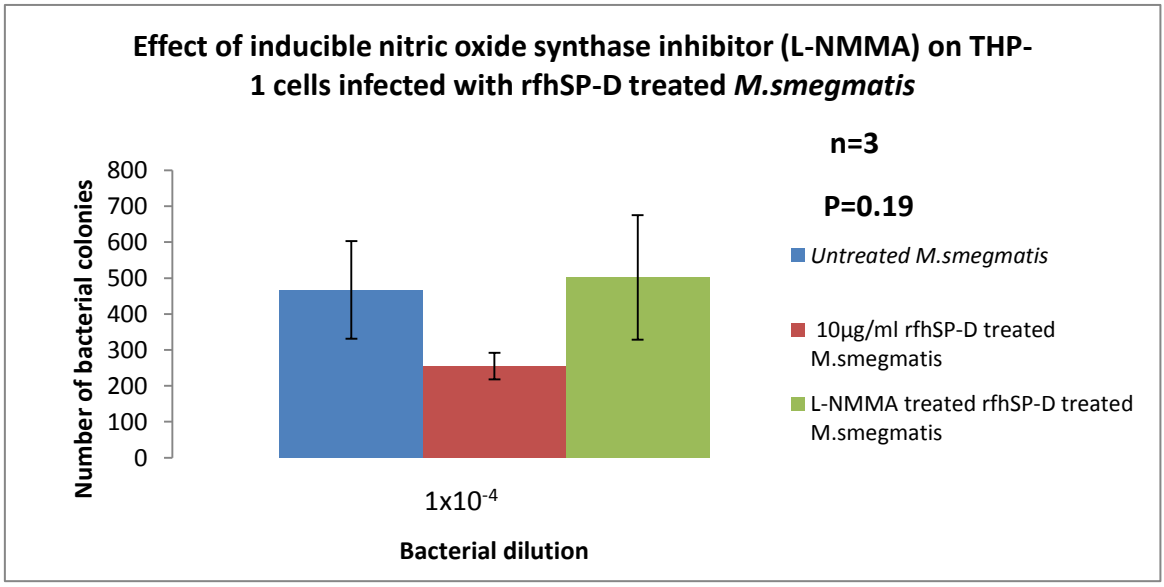

Figure 3.28-A: The effect of inducible nitric oxide synthase inhibitor on THP-1 cells infected with rfhSP-D treated mycobacteria. RfhSP-D treated mycobacteria showed lower numbers of bacterial colonies in comparison with THP-1 cells infected with untreated mycobacteria. The number of bacterial colonies was increased after the addition of nitric oxide synthase inhibitor (L-NMMA) to THP-1 cells infected with rfhSP-D treated *M.smegmatis*. Each histogram represents the average of 3 experiments. Error bars represent ±standard error of the mean. Multiple comparison of the data sets was done using Friedman test (p=0.19).

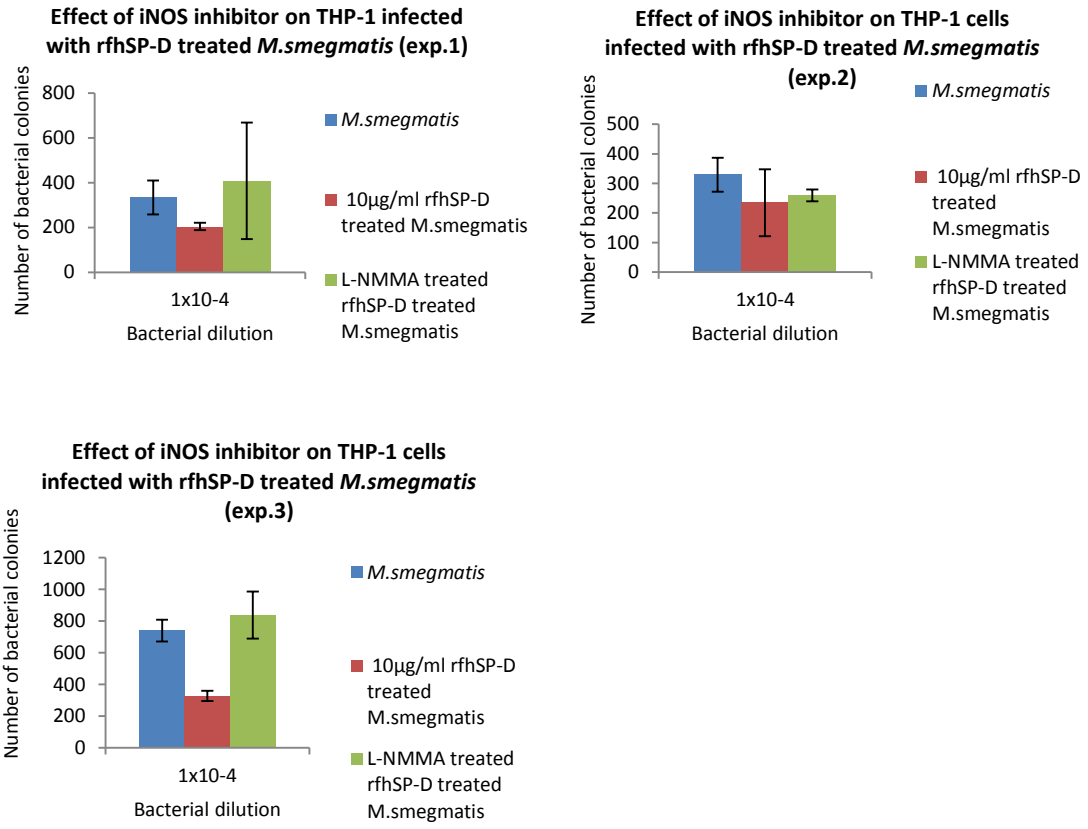

Figure 3.28-B: The effect of inducible nitric oxide synthase inhibitor on THP-1 cells infected with rfhSP-D treated mycobacteria (3 individual experiments). The iNOS inhibitor increases the growth of *M.smegmatis* inside THP1 cells in each individual experiment. Each histogram represents the average of triplicate readings**.** Error bars represent ±standard deviation.

3.2.14.2 Effect of neutralization of TNF-α on *M.smegmatis* growth inside THP-1 cells

The pro-inflammatory cytokine TNF-α, which is produced by macrophages and T cells and also acts in an autocrine fashion on macrophages to stimulate them was also investigated. The result showed that neutralization of the cytokine by anti-TNF-α increases the number of bacterial colonies inside THP-1 cells infected with rfhSP-D treated mycobacteria as compared to THP-1 cells infected with rfhSP-D treated mycobacteria without treatment with anti-TNF antibody (Figure 3.29-A &. 3.29-B). These results confirms that TNF-α is produced by THP-1 cells containing rfhSP-D treated mycobacteria, and neutralization of this cytokines increased mycobacterial growth inside THP-1 cells.

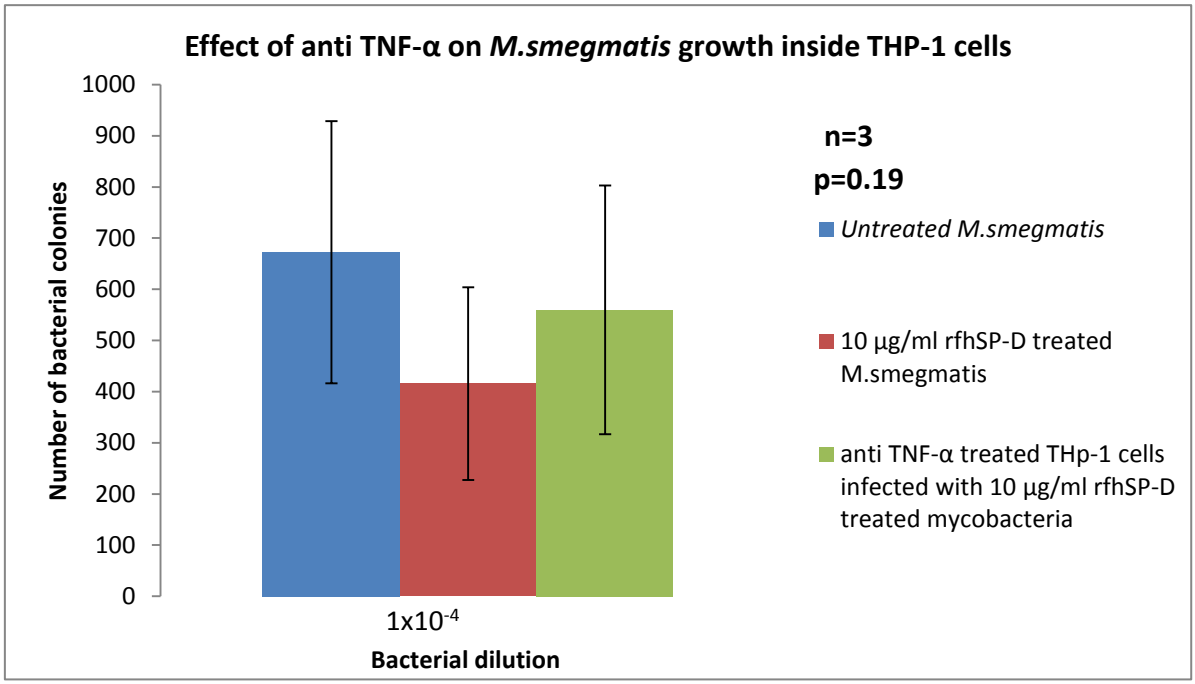

Figure 3.29-A: Effect of anti-TNF-α on THP-1 cells infected with rfhSP-D treated mycobacteria. The number of bacterial colonies was increased after the addition of anti-TNF-α to THP-1 cells infected with rfhSP-D treated *M.smegmatis*. Each histogram represents the average of three separate experiments. The error bars represent ± standard error of the mean. Multiple comparisons of the data sets was done using Friedman test (p=0.19).

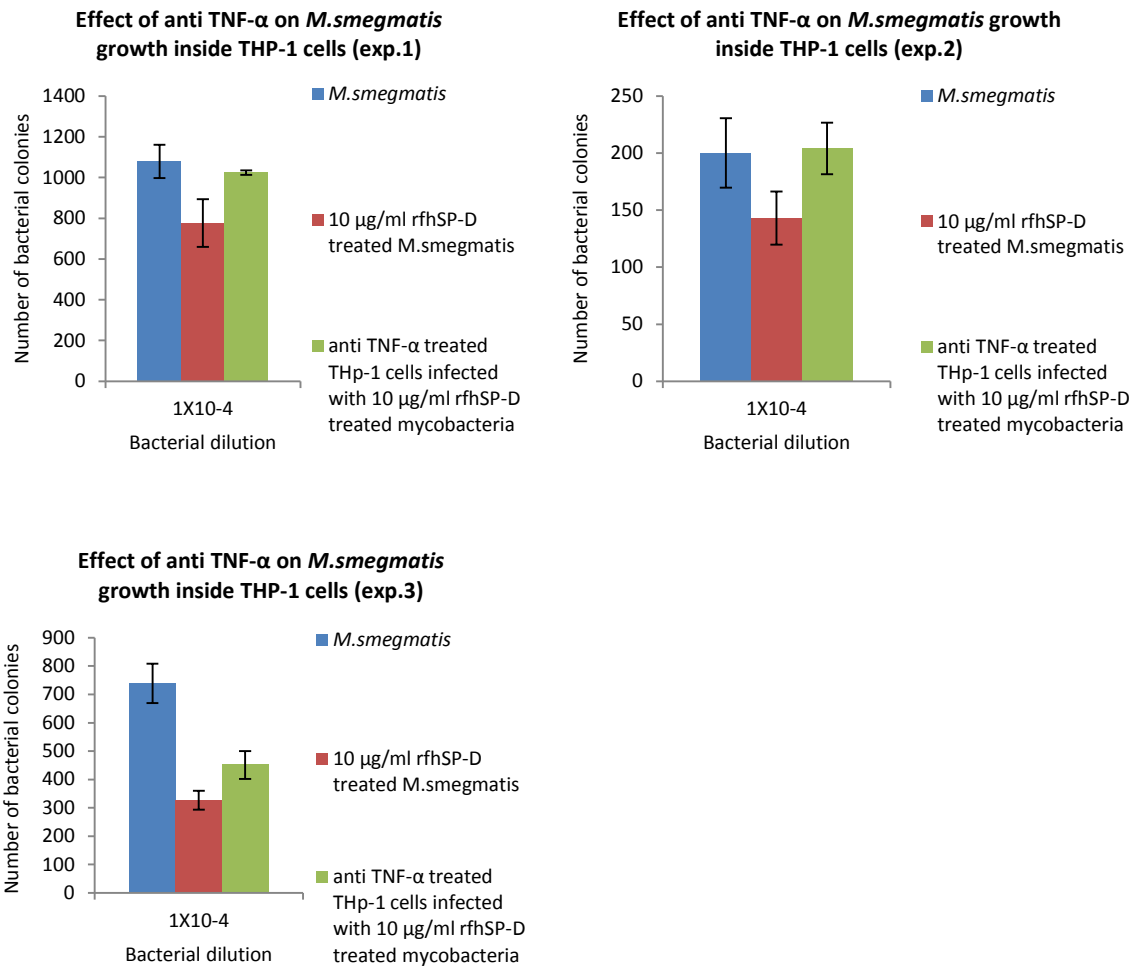

Figure 3.29-B: Effect of anti-TNF-α on THP-1 cells infected with rfhSP-D treated mycobacteria (3 individual experiments). Each histogram represents the average of triplicate readings**.** Error bars represent ±standard deviation.

3.2.14.3 Effect of neutralization TGF-β on *M.smegmatis* growth inside THP-1 cells

The role of immune-suppressive cytokine transforming growth factor beta (TGFβ) produced by macrophages during the infection with mycobacterium was also investigated. The result showed on neutralization of this cytokine the capacity of THP-1 cells to inhibit the *M. smegmatis* was dramatically improved. The result was statistically significant ($p<0.05$) as compared to THP-1 cells infected with untreated *M.smegmatis* (Figure 3.30), and the trend was the same in all the three experiments (Figure 3.30-B).

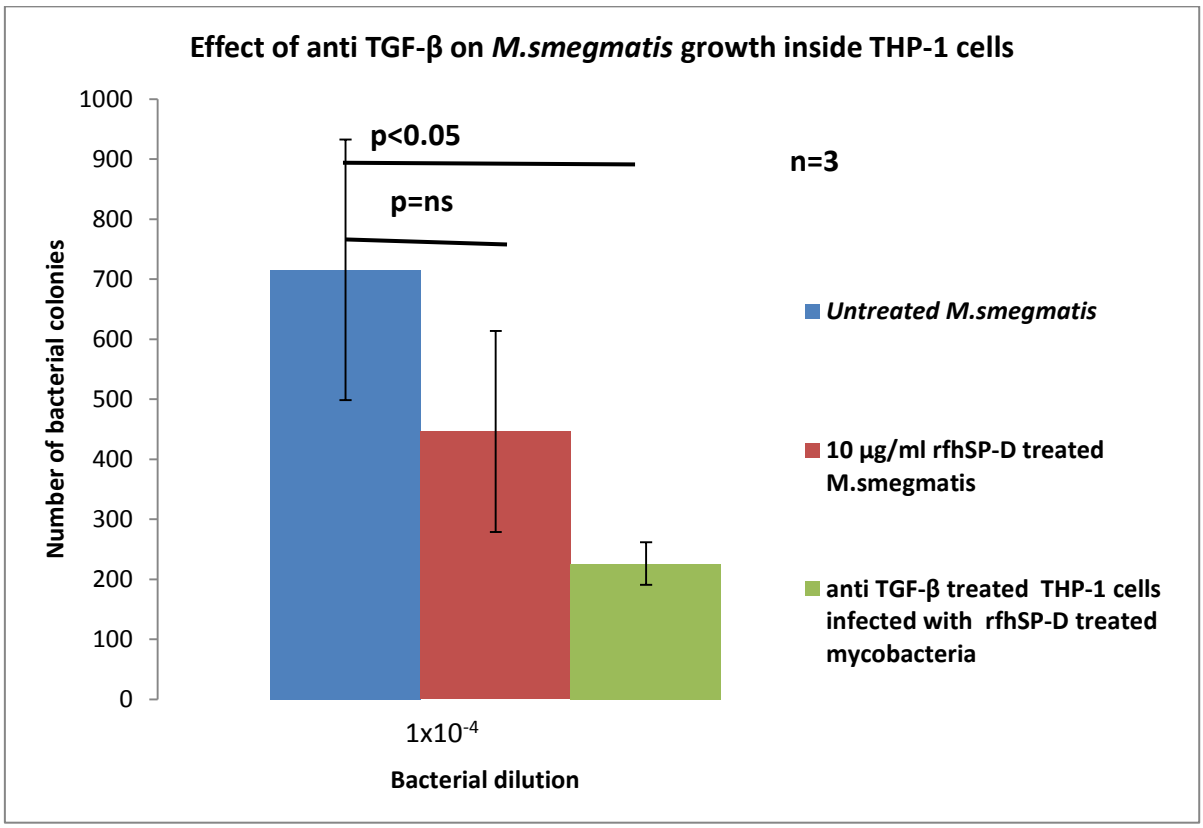

Figure 3.30-A: Effect of neutralizing of TGFβ in THP-1 cells infected with rfhSP-D treated mycobacteria. RfhSP-D treated *M.smegmatis* showed lower number of bacterial colonies in comparison with the untreated mycobacteria. The number of bacterial colonies was decreased dramatically after the addition of anti-TGFβ to THP-1 cells infected with rfhSP-D treated mycobacteria. Each histogram represents average of three experiments. Error bars represent ±standard error of the mean. Multiple comparison of the data sets was done using Friedman test ($p=0.027$). Individual data were compared with each other using Dunn's post hoc test: *M.smegmatis* vs 10µg/ml rfhSP-D, p=ns (non- significant; *M.smegmatis* vs anti-TGF-β treatment, $p<0.05$ (signficant).

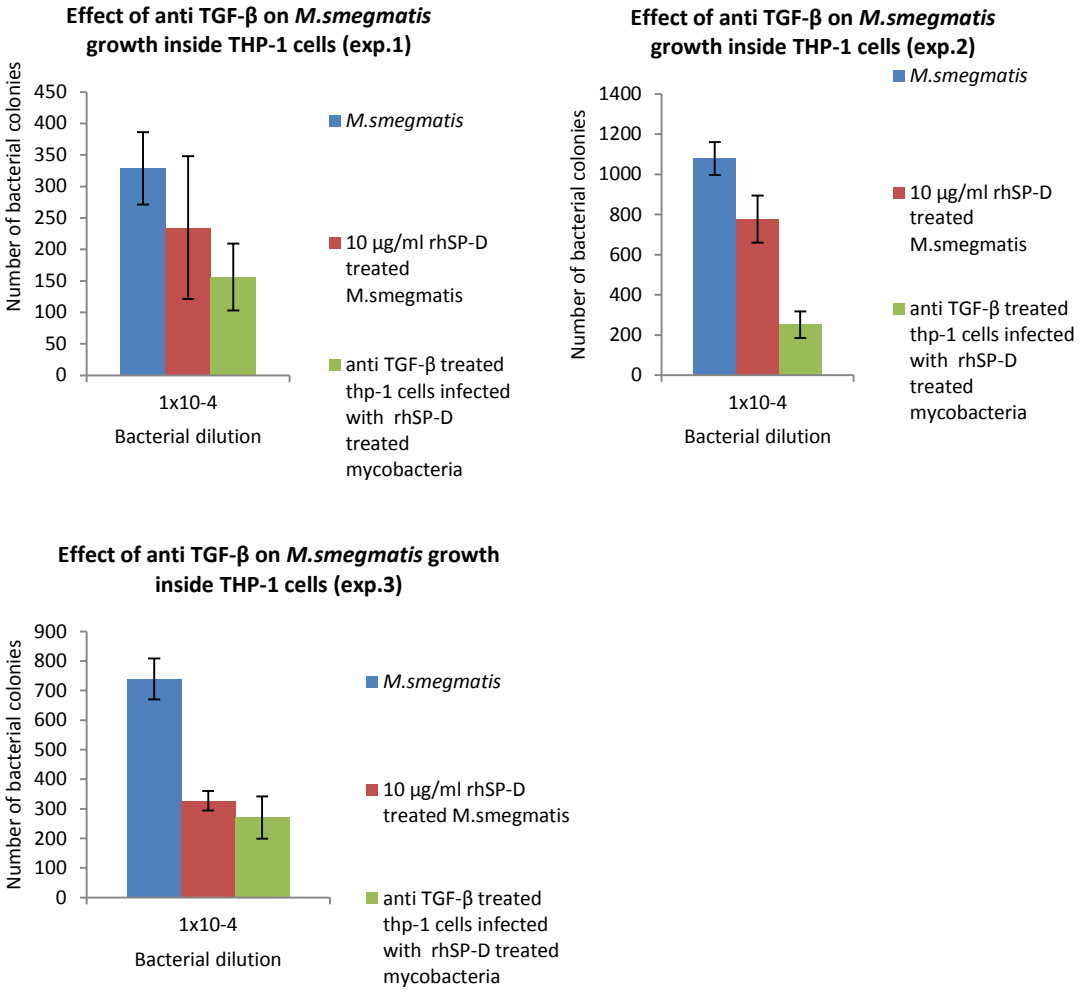

Figure 3-30-B: Effect of neutralizing of TGFβ in THP-1 cells infected with rfhSP-D treated *M.smegmatis* (3 individual experiments). Each histogram represents the average of triplicate readings. Error bars represent ±standard deviation.

3.2.15 Effect of rfhSP-D treated THP-1 cells on phagocytosis of mycobacteria

Pre-treatment of THP-1 cells with 10µg/ml rfhSP-D for 2 hours before the infection with *M.smegmatis*, and removal of unbound rfhSP-D before the infection with mycobacteria has increased mycobacterial uptake (phagocytosis) and growth inside THP-1 cells.

Four independent experiments were carried out and all four experiments showed the same trend in increase the uptake of *M.smegmatis.* The results were also statistically significant (Figure 3.31).

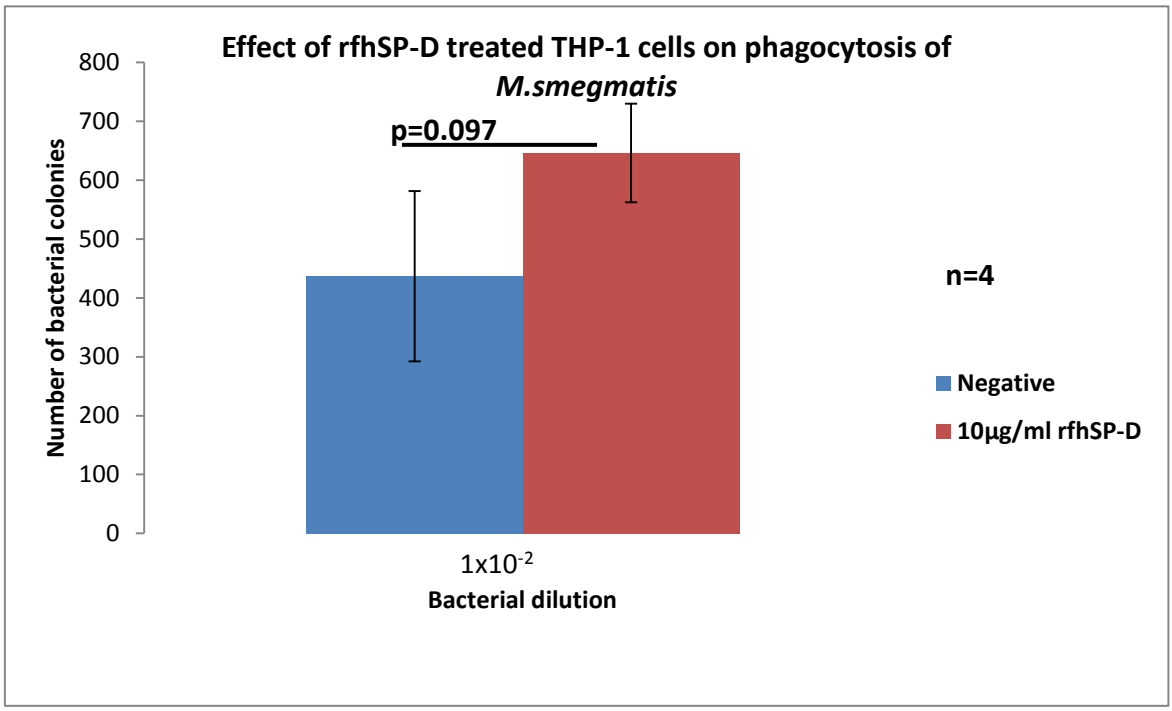

Figure 3.31-A: Effect of rfhSP-D treated THP-1 cells on the uptake of *M.smegmatis*. THP-1 cells were treated with rfhSP-D and 5mM calcium chloride and incubated for 2 hours inside CO_2 incubator. Following incubation, THP-1 cells were washed 3 times from non-bound rfhSP-D by centrifugation at 1500rpm, 10 minutes each. Next, *M.smegmatis* was added to the washed THP-1 cells in ratio 5:1 and incubated for 1 hour at 37°C inside CO_2 incubator. Following incubation, magnetic beads bound with anti-human MHC class 1 was added in ratio 1:4 (THP-1: beads) and the tubes were incubated on ice for 30 minutes on a shaker. Next, the THP-1 cells were washed 3 times to remove extracellular bacteria. Washed cells were laysed with 0.1% saponin with vortexed for 15 minutes to release phagocytosed mycobacteria. Bacterial dilutions were prepared, 250µl bacteria were plated in triplicates on LB agar and incubayed for72 hours at 37°C. The rfhSP-D treated THP1 cells increased the phagocytosis of *M.smegmatis*. Each histogram represents the average of 4 independent experiments. Error bars represent ±standard error of the mean. Statistical test used Wilcoxon Signed rank test. Negative contains untreated *M.smegmatis*.

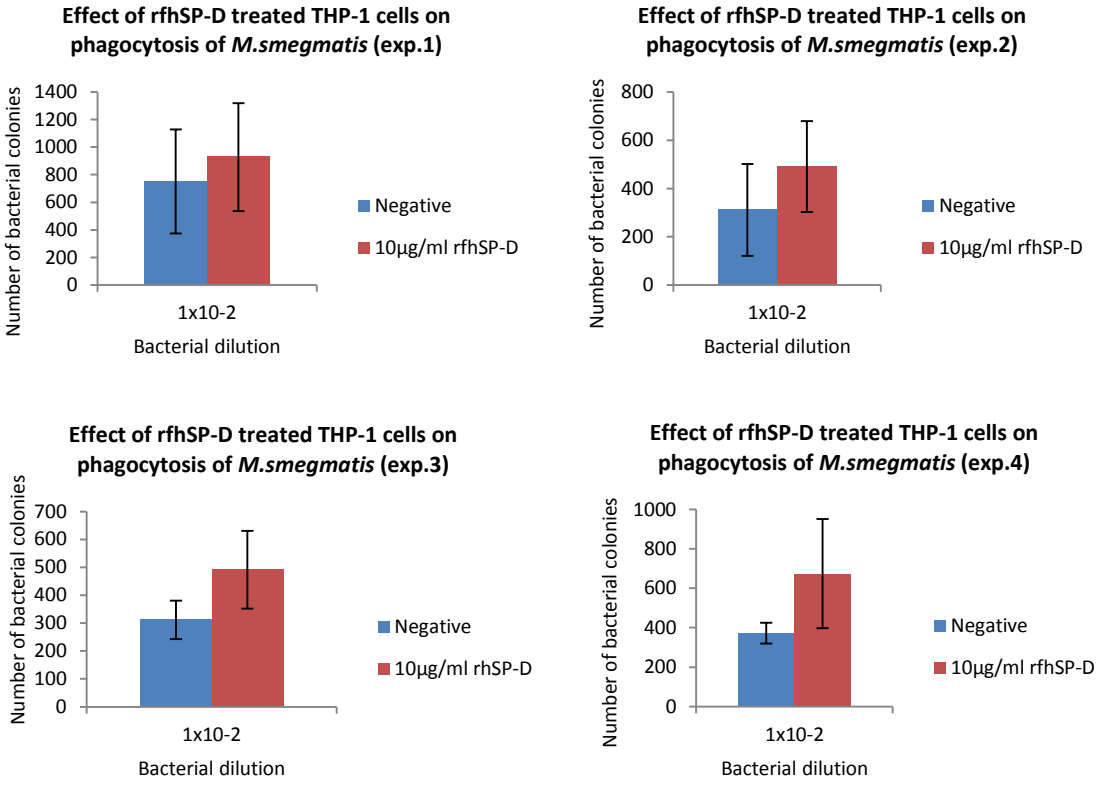

Figure 3-31-B: Effect of rfhSP-D treated THP-1 cells on the uptake of *M.smegmatis* (4 individual experiments). RfhSP-D treated THP1 cells increased *M.smegmatis* uptake by THP-1 cells in each individual experiment. Each histogram represents the average of triplicate readings**.** Error bars represent ±standard deviation. Negative contains untreated *M.smegmatis*.

3.2.16 Effect of rfhSP-D treated THP-1 cells on mycobacterial growth inside THP-1 cells

Pre-treatment of THP-1 cells with rfhSP-D, followed by removal of unbound rfhSP-D by washing prior to infection with mycobacteria, has increased mycobacterial growth inside THP-1 cells (Figure 3.32-A). Three independent experiments showed the same trend of *M.smegmatis* growth increase (Figure 3.32-B).

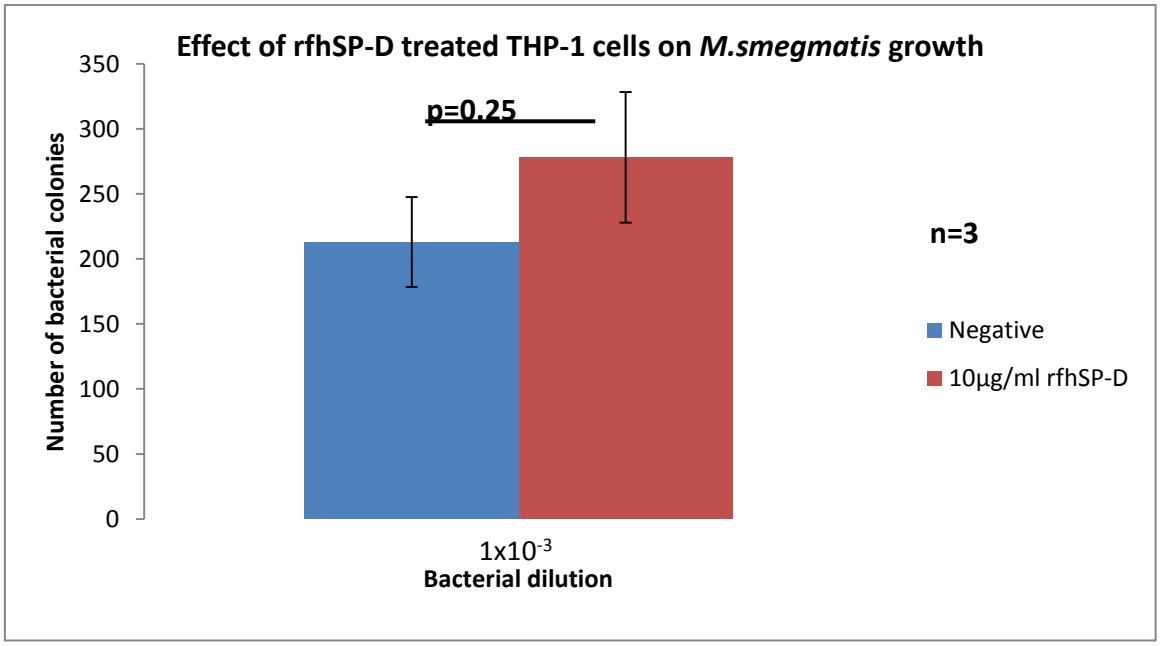

Figure 3.32-A: Effect of rfhSP-D treated THP-1 cells on *M.smegmatis growth inside THP-1 cells.* The rfhSP-D treated THP1 cells have increased *M.smegmatis* growth inside THP-1 cells. In these experiments, THP-1 cells were treated with rfhSP-D in presence of 5mM calcium chloride and incubated for 2 hours inside CO_2 incubator. Following incubation, THP-1 cells were washed 3 times from non-bound rfhSP-D by centrifugation at 1500rpm, 10 minutes each. Next, *M.smegmatis* was added to THP-1 cells in ratio 5:1 (bacteria: THP-1) and incubated for 1 hour at 37°C inside CO_2 incubator. Following incubation, magnetic beads bound with anti-human MHC class 1 was added in ratio 1:4 (THP-1: beads) and the tubes were incubated on ice for 30 minutes on a shaker. Next, the THP-1 cells were washed 3 times to remove the extracellular bacteria. Washed cells were suspended with 1ml of cRPMI without antibiotics and incubated for 24 hours inside CO_2 incubator. Next, the THP-1 cell pellet was separated from the supernatant using magnet. Cell pellet was laysed with 0.1% saponin with vortexed for 15 minutes to release phagocytosed mycobacteria. Eqal volumes from lysed cells and supernatant were mixed. Bacterial dilutions were prepared, 250µl bacteria were plated in triplicates on LB agar and incubayed for72 hours at 37°C. Each histogram represents the average of 3 independent experiments. Error bars represent ±standard error of the mean. Statistical test used was Wilcoxon Signed rank test. Negative contains untreated *M.smegmatis*.

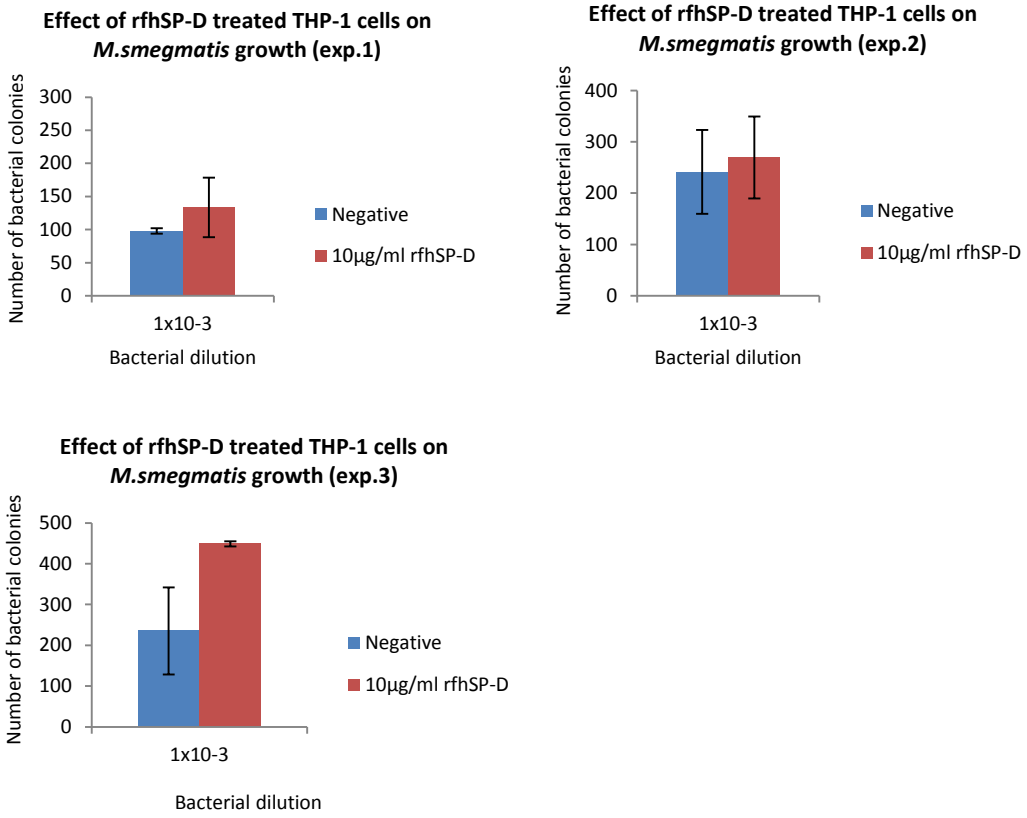

Figure 3.32-B: Effect of rfhSP-D treated THP-1 cells on *M.smegmatis* growth inside THP-1 cells (3 individual experiments). *M.smegmatis* growth increases inside THP-1 cells treated with 10µg/ml rfhSP-D prior to infection with *M.smegmatis*. Each histogram represents the average of triplicate readings**.** Error bars represent ±standard deviation. Negative contains untreated *M.smegmatis*.

3.3 Discussion

In this study, we used rfhSP-D which was produced using the T7 promoter expression system. This rfhSP-D consists of carbohydrates recognition domain (CRD), neck, and 8 GLY-X-Y repeats. Lipopolysaccharide (LPS) which may present as a contaminanet in our proteins preparations was removed using polymyxin-B column. The LPS concentration in rfhSP-D detected using LAL assay was 0.32EU/ml (<1EU/ml), which is generally acceptable in research. Endotoxin level can be measured using other methods; an alternative method is based on toll-like receptor 4 (TLR 4) (Smulders et al., 2012). Moreover, LPS can be detected and determined by ELISA using LPS capture molecules such as antibodies, lectins, or antibiotics (James et al., 1996).

Purified rfhSP-D was characterized by SDS-PAGE and western blot (Figure 3.6 & 3.8) at the expected molecular weight of 20kDa under reducing conditions (heating protein to 100^{o}C for 10 minutes in treatment buffer containing β-mercaptoethanol). Previous studies have been shown that purified recombinant SP-D forms trimers in solution (Leth-Larsen et al., 2005). Furthermore, SP-D purified from amniotic fluid has been shown to run as a trimer on the filtration column (Dodagatta et al., 2014). In this study, trimerization of rfhSP-D has never been tested. Protein trimers can be checked by cross- linking assay (Crouch et al., 2005 and Zhang et al., 2001). Additionally, running the protein on SDS-PAGE under non reducing conditions (without heating and without using β-mercaptoethanol), followed with western blot could confirm that rfhSP-D is a trimer.

The rfhSP-D used in this study has been shown to work in the same way as the full length SP-D (Duvoix, *et al*., 2001, Souji *et al*., 1997). This recombinant protein was produced using *E.coli*, BL21 (DE3) pLysS expression system, as this system yields a good amount of protein. However, *E. coli* cannot perform post translation modifications such as the hydroxylation of proline to hydroxyl proline, which plays a key role in collagen stability. Therefore a truncated version of rfhSP-D without collagen and N-terminal regions was expressed and purified. Although, full length SP-D can be produced in mammalian expression system using Chinese hamster ovary (CHO) or Human embryonic kidney cells 293 (HEK 293 cells), but the

downside is that the yield is very low. The full length SPD can also be purified from Broncho-alveolar lavage samples from alveolar proteinoses patients, but samples are difficult to obtain (Honda *et al*., 1995, Crouch *et al*., 1993).

This study showed that rfhSP-D bound to BCG (Figure 3.9 & Figure 3.10) and to purified protein derivatives from *Mtb* (Figure 3.9). Furthermore, the data showed that rfhSP-D bound minimally to the non-pathogenic strain *M.smegmatis* (Figure 3.9). The slight difference in the cell wall structure between *M.smegmatis* and both BCG and *Mtb* could be responsible for the weak binding of rfhSP-D to *M.smegmatis*. SP-D binds to both LAM and specifically mannose capped LAM (ManLAM) exposed on the surface of *Mtb.* SP-D binds less to *M. smegmatis*, which exposes AraLAM on the surface which does not contain mannose caps (Ferguson *et al*., 1999). This could explain the weak binding between rfhSP-D and *M.smegmatis*.

Since recombinant protein was used, which lacks the collagen region, the binding of this protein was localized to the CRD region. This finding is in an agreement with previous studies, which showed that SP-D binding to *Mtb* occurs via the CRD region, and LAM from the virulent *Mtb* strain is the major binding molecule for SP-D (Ferguson, 1999). It is known that LAM serves as a ligand for mannose receptor which is found on macrophages, these receptors are responsible for facilitating phagocytosis of *Mtb* (Schlesinger, 1990, 1993, 1996). Furthermore, it has been shown that SP-D binds to the mannose caps of *Mtb* LAM and the other carbohydrates present on the surface of *Mtb* (Ferguson, 2002). Moreover, our study showed less binding between rfhSP-D and BCG in presence of sugars which confirm previous finding that this protein has lectin activity (Ferguson *et al*., 1999) (Figure 3.11). It is possible that rfhSP-D binding to LAM and ManLAM may interfere in the uptake of this pathogen by the mannose receptor inside phagocytic cells. This explains our findings which showed that rfhSP-D decreased phagocytosis of both *M. smegmatis* and BCG by THP-1 cells (Figure 3.17 & Figure 3.18).

Previous studies showed that full length SPD can agglutinate mycobacteria (Ferguson, 2002, Kuroki *et al*., 2007). However, the agglutination is not required for mycobacterial phagocytosis by macrophages. Ferguson, 2002, showed that both the agglutinating and non-agglutinating concentrations of SP-D reduced the

uptake and inhibited *Mtb* growth inside phagocytic cells. Also our current study showed that rfhSP-D reduced mycobacterial uptake by THP-1 cells but it does not agglutinate mycobacteria (BCG) (Figure 3.14). So, the lower uptake of rfhSP-D treated mycobacteria by THP-1 cells is not related to agglutination. Full length human SP-D has been shown to causes microscopic agglutination of *Mtb* (Ferguson *et al*., 1999), and it could be possible that collagen region in full length SPD is playing role in bacterial agglutination. It is possible that full length SPD agglutinates the inhaled mycobacteria inside lung alveoli. This mycobacterial agglutination could enhance their clearance by mucus and cilia, before they infect the alveolar macrophages. This could be the first step in prevention of *Mtb* infection inside the lungs.

In this study, direct effect of rfhSP-D on *M. smegmatis* and BCG growth was investigated. The results revealed a trend that rfhSP-D inhibited the growth of both BCG and *M. smegmatis* in all independent experiments. This inhibition effect of rfhSP-D on mycobacteria is statistically significant (Figure 3.15 & 3.16). This direct inhibition of mycobacterium has not been reported before. It is known that SP-D inhibits the growth of Gram negative bacteria (*E.coli*, *Klebsiella pneumonia*, *Enterobacter aerogenes* and *Legionella pneumonia)* by increasing membrane permeability (Wu *et al*., 2003) but not mycobacteria (Ariki, 2011). This suggests that SP-D does not kill mycobacteria by increasing cell membrane permeability. RfhSP-D could kill mycobacteria by interfering with bacterial intracellular signalling pathways, which could affect transcription of genes important for metabolism and survival of mycobacteria. This need to be tested in the future researches.

In this study, treatment of mycobacteria with rfhSP-D for 2 hours prior to THP-1 cells infection was shown to reduce the uptake of rfhSP-D treated mycobacteria by THP-1 cells (Figure 3.17 & 3.18). The reason for mycobacterial reduced uptake could be that 1) rfhSP-D might kill mycobacteria directly. 2) Binding of rfhSP-D to LAM and ManLAM on mycobacterial surface could inhibit mycobacterial binding to mannose receptors on THP-1 cells. The current study also confirms that reduced BCG and *M.smegmatis* uptake was associated with reduced intracellular growth inside human THP-1 cells (Figure 3.19 & 3.20). The reasons for mycobacterial growth inhibition could be: 1) the rfhSP-D killed mycobacteria directly before THP-

1 cells infection, and these killed mycobacteria could not grow inside THP-1 cells. 2) It could be less uptake lead to less mycobacterial growth. 3) Mycobacteria may be killed by nitric oxide components. This study was shown that rfhSP-D increases the expression of nitric oxide synthase (Figure 3.21), which help in mycobacterial killing inside phagocytic cells. 4) rfhSP-D coated mycobacteria increases the fusion between phagosomes containing the mycobacteria and lysosomes (Ferguson, 2006), which enhances their killing. An increased Phagosome-lysosome fusion due to SPD does not require the collagen region, as both full length SPD and rfhSP-D has been shown to increase the fusion of *Mtb* phagosomes with lysosomes inside human macrophages (Ferguson, 2006).

On the other hand, this study was shown that pre-treatment of THP-1 cells with rfhSP-D for 2 hours prior to infection with *M.smegmatis* has increased the uptake of mycobacteria by THP-1 cells (Figure 3.31), and increased mycobacterial growth inside these cells (Figure 3.32). The explanation of these results could be rfhSP-D increased the expression of mannose and scavenger receptors on THP-1 cells, that enhanced mycobacterial uptake. One previous study indicated that direct interaction of SP-D with macrophages increases the localization of scavenger and mannose receptors on macrophage surface (Kuroki *et al*., 2007). Moreover, this increased uptake was associated with increased mycobacterial growth inside THP-1 cells. This could be explained by 1) more mycobacterial uptakes caused more bacterial growth. 2) Untreated mycobacteria maybe inhibited the fusion between phagosomes and lysosomes. 3) Binding of rfhSP-D to signal-inhibitory regulatory protein -α (SIRP-α) receptors on THP-1 cells may inhibited the expression of pro-inflammatory cytokines (Gardai *et al*., 2003). It has been shown that binding of SPD via CRD region to SIRP-α present on the surface of alveolar macrophages suppress NF-kB mediated inflammation (Gupta, G., & Surolia, 2007). In this case, presence of SP-D inside the lung alveoli and around alveolar macrophages prior to mycobacterial infection could help mycobacterial invasion and growth inside the alveolar macrophages. This need to be tested *in vivo* using transgenic mice both over expressing human SP-D and SP-D knocked out mice. Infecting both groups of mice with *Mtb* could reveal its importance in *Mtb* infection.

The underlying mechanisms of rfhSP-D treated mycobacterial growth inhibition inside THP-1 cells were also investigated by using real time PCR (qPCR) and neutralizing antibodies. One of the antimicrobial functions of macrophages is the production of reactive nitrogen intermediate (RNI); these RNI can kill mycobacteria inside macrophages. RNI are generated as intermediate products through the conversion of arginine to L- citrulline by nitric oxide synthase, this enzyme could be produced by macrophages and other cell types. Previous studies have shown that reactive nitrogen radicals were responsible for killing of virulent *Mtb* in mice macrophages, this process required activation of macrophages by TNF-α and IFN-γ (Flesch & Kaufmann, 1991, Greenberg *et al*., 1995).

In this study, qPCR results showed that inducible nitric synthase gene was expressed more in THP-1 cells infected with rfhSP-D treated mycobacteria (*M.smegmatis* & BCG) as compared to untreated mycobacteria (Figure 3.21). Moreover, mycobacterial growth was increased when nitric oxide synthase function was inhibited by adding N^G-monomethyl-L-arginine monoacetate (L-NMMA) to THP-1 cells infected with rfhSP-D treated *M.smegmatis* (Figure 3.28). This study suggests that THP-1 cells are able to produce a nitric oxide component when challenged with rfhSP-D treated *M.smegmatis*. This result is convenient with previous studies. It has been shown that treatment of alveolar macrophages with N^G-monomethyl-L-arginine monoacetate (L-NMMA), increased BCG growth in these cells (Rich *et al*., 1997). *Mycobacterium tuberculosis* stimulates nitric oxide production by human macrophages, and nitric oxide inhibitors inhibited the production of nitric oxide by alveolar macrophages (Rich *et al*., 1997). Similarly Chan *et al*., 1992 reported that virulent *Mycobacterium tuberculosis* was killed by reactive nitrogen intermediates produced by murine macrophages activated by INF-γ, LPS or TNF-α.

In this study, the THP1 cells infected with BCG showed increased gene expression of TNF-α cytokine as compared to uninfected THP1 cells (Figure 3.22). However, the TNF-α gene expression in THP-1 cells infected with rfhSP-D treated BCG was lower as compared to THP1 cell infected with untreated BCG. However, mycobacterial growth was increased when function of TNF-α was inhibited by adding anti-TNF-α to THP-1 cells infected with rfhSP-D treated *M.smegmatis*

(Figure 3.29). This suggests that TNF-α is produced inside THP-1 cells infected with rfhSP-D treated mycobacteria, but rfhSP-D was slightly down regulating gene expression of this cytokine. On the other hand, less mycobacterial uptake by THP-1 cells infected with rfhSP-D treated mycobacteria could be responsible for down regulation of TNF-α gene expression as compared with THP-1 cells infected with untreated mycobacteria. The TNF-α is an important pro-inflammatory cytokine in controlling the mycobacterial infection (Balcewicz-Sablinska *et al*., 1998). However, excess production of this cytokine may lead to pathology (Klausner et al., 1996). Thus a fine balance of this cytokine production needs to be maintained and rfhSP-D may be playing this role. The role of SP-D in dampening the inflammatory response has been reported before (Yamazoe, 2008). The role of TNF-α in the control of mycobacteria inside mice macrophages *in vitro* has been reported before (Denis & Gregg, 1990). However, it was reported that role of human TNF-α in controlling mycobacterial infection by THP1 cell line *in vitro* is not clear (Bekker *et al*., 2001). Here we report that this cytokine does play a role in controlling mycobacterial infection inside these cells. Previous *in vivo* studies also showed the importance of this cytokine in the control of *Mtb* infection, as neutralization of TNF-α or TNF-α knockout mice was unable to control the infection as compared to control mice. Also, the granulomas which are important for the control of *Mtb* infection *in vivo* were abnormal in structure and the number of bacilli was higher in knockout mice as compared to control (Flynn *et al*., 1995). Furthermore, in humans, treatment of Rheumatoid Arthritis patients with anti-TNF-α antibody leads to reactivation of latent tuberculosis (Miller and Ernst, 2009). TNF-α can also induce apoptosis of host cells which is one of the host defence mechanisms against intracellular pathogens to limit their growth inside macrophages (Beulter & Cerami, 1986, Laster *et al*., 1988).

Expression of the pro-inflammatory cytokines IL-1β and IL-6 were also investigated by q-PCR (Figure 3.23 & 3.24). The gene expression of IL-1β and IL-6 was reduced in THP1 cells infected with rfhSP-D treated mycobacteria, but this reduction was not dramatic, suggesting that rfhSP-D have some damping effect on the expression of these pro-inflammatory cytokines. This may have some influence in reducing inflammation induced pathology in tissues. Also, treatment of

mycobacteria with rfhSP-D lead to fewer uptakes by THP-1 cell, and less number of mycobacteria inside THP-1 cells could be responsible for less gene expression of IL-1β and IL-6 in these cells, as compared to THP-1 cells infected with untreated mycobacteria. It is well known that IL-1β is mainly produced by monocytes, macrophages, and DCs at the site of infection, and is involved in host immune response against *Mtb* (Law *et al*., 1996). IL-6 has both pro-inflammatory and anti-inflammatory properties; it is also produced by phagocytic cells early in the infection. IL-6 plays opposing roles in *Mtb* infection; IL-6 deficient mice are more susceptible during early infection with *Mtb* (Saunders *et al*., 2000). On the other hand, it has been shown that IL-6 inhibits TNF-α and IL-1β production and enhances *M.avium* growth *in vitro* (Schindler *et al*., 1990). The pro-inflammatory cytokines IL-1β, TNF-α and IL-6 are also responsible for rising body temperature, which is believed that at higher temperature the bacterial replication is less efficient, whereas the adaptive immune response become more efficient (Murphy, 2012). Dampening the expression of IL-1β, IL-6 and TNF-α by rfhSP-D suggests that rfhSP-D does not enhance strong inflammatory response at the infection site.

The pro-inflammatory cytokine IL-12 gene expression was also investigated (Figure 3.25). The expression of this gene was higher in THP-1 cells infected with rfhSP-D treated as compared to untreated mycobacteria. This suggests that rfhSP-D enhances IL-12 expression. IL-12 is produced upon *Mtb* infection of macrophages (Ladel *et al*., 1997). It plays a key role in host defence against *Mtb*. IL-12 with IL-18 induces INF-Ɣ production and drive Th1 response. IL-12 deficient mice are at high risk for *Mtb* infection, and IL-12 supplement to susceptible mice helped in killing of *Mtb* at the beginning of infection (Flynn *et al*., 1995).

Transforming growth factor-β1 (TGF-β) is produced by macrophages after *Mtb* infection (Aung *et al*., 2005). This cytokine suppresses the activity of macrophages and allows the mycobacterium to grow in these cells. In this study TGF-β was expressed in the THP1 cells infected with untreated BCG and rfhSP-D-treated BCG as compared to uninfected THP1 cells (Figure 3.26). This suggests that BCG enhances the expression of this cytokine in these cells. However, the expression was lower in rfhSP-D treated BCG infected cells as compared to untreated BCG.

This result suggests that rfhSP-D reduces the expression of anti-inflammatory cytokine TGF-β, which is favourable for the host, as it helps in controlling the mycobacterial infection. This is supported by our result that neutralization of TGF-β by anti-TGF-β antibody inhibited the growth *M. smegmatis* in the THP1 cells (Figure 3.30). The mycobacterial component responsible for the production of this cytokine has been identified as lipoarabinomannan (LAM) (Toossi *et al*., 1995). Furthermore, it has been shown that purified protein derivatives from *Mtb* induce the formation of TGF- β1 in human monocytes after 12 and 24 hours (Toossi *et al*., 1995).

The anti-inflammatory cytokine IL-10 gene expression was also studied (Figure 3.27). The expression of this gene was up regulated in the THP1 cells infected with rfhSP-D-treated BCG after 5 hours incubation as compared to untreated BCG and after 10 hours in THP-1 cells infected with rfhSP-D treated *M.smegmatis*. This suggests that IL-10 gene is expressed in presence of rfhSP-D, and this expression could dampen the expression of pro- inflammatory cytokines TNF-α, IL6, and IL-1β.

IL-10 cytokine is produced by macrophages and T cells against *Mtb.* IL-10 disables macrophage function by down regulating the expression of IL-12 and TNF-α (Fujiwara *et al*., 2005), which suppress the production of INF- γ which leads to reduced ROIs and RNIs and inhibits intracellular mycobacterial killing. IL-10 also inhibits phagosome-lysosome fusion, which facilitate the growth of *Mtb* (O'Leary *et al*., 2011). Furthermore, Higgins *et al.,* 2009 demonstrated that the absence of IL-10 during *Mtb* infection in IL-10 depleted mice increased the expression of Th1 type immunity at 60 days of the infection. IL-10 production is helpful in tuberculosis as it plays a central role in reducing of Th1 response and it protects against chronic lung inflammation. It has been suggested that removal of regulatory IL-10 leads to disease progression (Higgins *et al*., 2009).

The inhibition assay performed in this study for both *M.smegmatis* and BCG infected THP-1 cells was incubated for 24 hours. This period of incubation showed the effect of rfhSP-D on mycobacterial killing during 24 hours (1 day). The doubling time for *M.smegmatis* is 2-5 hours, while for BCG is around 24 hours. It will be interesting to increase the incubation period for THP-1 cells infected BCG to 2, 3, 4 and 5 days in order to investigate the effect of this protein on the growth

of phagocytosed BCG. It has been shown previously that THP-1 cells infected with *M.avium* can kill the mycobacteria for up to 5 days (Garcia et al., 2000).

In this study human monocytes THP1 were used naturally and without any stimulation with PMA. We have shown for the first time that THP-1 cells untreated with PMA can behave like macrophages after being infected with mycobacteria. Also, these THP-1 cells were able to uptake and inhibit bacterial growth and to express nitric oxide components, pro-inflammatory and anti- inflammatory cytokines. Studying mycobacterial uptake and growth inside THP-1 cells was done in suspension inside tube to allow THP-1 cells and bacteria to react normally without any external influence.

It is clear that rfhSP-D can bind, directly inhibits mycobacteria, and inhibits their uptake and their growth inside THP-1 cells. Mycobacterial growth could be inhibited by intermediate nitric oxide components, and other mechanisms. Or it could be as simple less uptake resulting in less growth.

Conclusion

In this study, rfhSP-D comprising 8 Gly-X-Y repeats, neck and CRD regions was expressed in *E. coli* and affinity purified. This protein showed weak binding with *M. smegmatis* and a good binding with BCG in ELISA. The binding of rfhSP-D to mycobacteria led to direct inhibition of *M. smegmatis* and BCG growth *in vitro*. Furthermore, the treatment of the mycobacteria with rfhSP-D led to significant inhibition of both mycobacterial uptake and their growth inside THP-1 cell line. This growth inhibition in the rfhSP-D treated mycobacteria appears due to increased expression of inducible nitric oxide synthase, whose inhibition caused a reversal of rfhSP-D induced inhibition of mycobacterial growth. It seems that TNF-α also played a role in both mycobacterial growths inside THP1 cells, as evident by the reversal of the growth inhibition by anti-TNF-α antibody. In contrast, neutralization of TGF-β by anti-TGF-β antibody showed a synergistic effect to that achieved with rfhSP-D treatment, resulting in further inhibition of both mycobacterial growths, suggesting mycobacterial growth enhancing role of this cytokine. Thus, rfhSP-D has the potential to be used in conjunction with anti-TB drugs to treat multi-drug resistant tuberculosis, if these experiments can be validated with *Mtb*.

Chapter 4- Interaction of C1q with mycobacteria

4.1 Introduction

In this study, the effect of C1q on mycobacteria was studied for various reasons; Firstly, C1q concentration in human plasma is relatively high (115μg/ml) and it could leaks from blood to the inflammation site in the lungs. Secondly, C1q is produced locally inside the lungs by macrophages, epithelial cells, immature dendritic cells and fibroblasts. Thirdly, it was shown previously that untreated TB patients express higher C1q in their peripheral blood as compared to individual with latent TB or without infection (Cai et al., 2014). Finally, C1q has been shown previously to bind both BCG (Carroll et al., 2009) and THP-1 cells (Ghebrehiwet et al., 2004 and Song et al., 2016). Presence of C1q in the infection site could play a role in the pathogenesis of TB.

The well-known function of C1q is activating the classical complement pathway through binding to antibodies bound to pathogens. Classical complement pathway activation increases pathogen uptake by host macrophages. The phagocytosed pathogens are killed inside macrophages by inducible nitric oxide components or reactive oxygen species. Various pathogens can stop complement activation by proteases secretion (Carroll et al., 2009) or by interfering with complement components interactions that result in deactivating the C1 complex (Kang *et al.,* 2013). *Mycobacterium tuberculosis* (*Mtb*) is a pathogen that prefers to live inside macrophages. It infects the macrophage and resists the intracellular killing mechanisms. *Mtb* can live and replicate within macrophages for decades without any clinical symptoms. A previous study has shown that *Mtb* can activate both the classical and the alternative pathway of the complement system and increase its uptake by macrophages (Ferguson, 2004). The aims of this study is to investigate the following roles of C1q on mycobacteria:

1. The direct effect of C1q on mycobacterial growth. 2. Effect effect of C1q on the uptake (phagocytosis) of mycobacteria by THP-1 cells. 3. Effect of C1q on the growth of mycobacteria inside the THP-1 cells. 4. Understanding the underlying mechanisms of mycobacterial growth inside the THP1 cells by using qPCR, multiplex and neutralizing antibodies. In this study, both *M.smegmatis* and BCG were used as a model for *Mtb*. THP-1 cells used in this study were stimulated with mycobacteria only.

4.2 Results

4.2.1 Characterization of C1q

The C1q (Merck Milipore) used in this study was characterized by 12% SDS-PAGE and dot blot. The three chains of C1q protein; A, B, and C are clearly visible at the expected molecular weights; 25, 26, and 22 kDa respectively (Figure 4.1). Also, 5µg of C1q was shown to bind with sheep anti-human C1q by dot blot. Whilist the negative control containing 5µg of amyloid P protein was not shown any binding with the same anti-body (Figure 4.2).

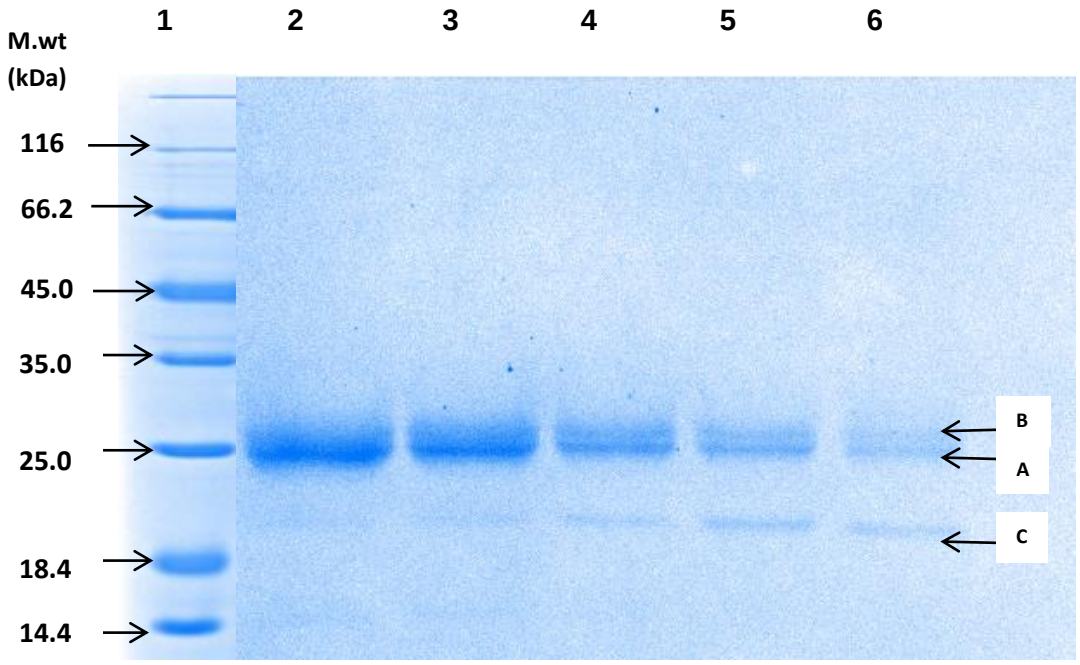

Figure 4.1: Characterization of C1q by 12% SDS-PAGE. The A, B, and C chains of C1q are clearly visible at molecular weight 25, 26, and 22 kDa. Lane 1: protein marker, Lane 2: 5µg C1q, Lane 3: 2.5µg C1q, Lane 4: 1.25µg C1q, Lane 5: 0.6µg C1q, and lane 6: 0.3µg C1q.

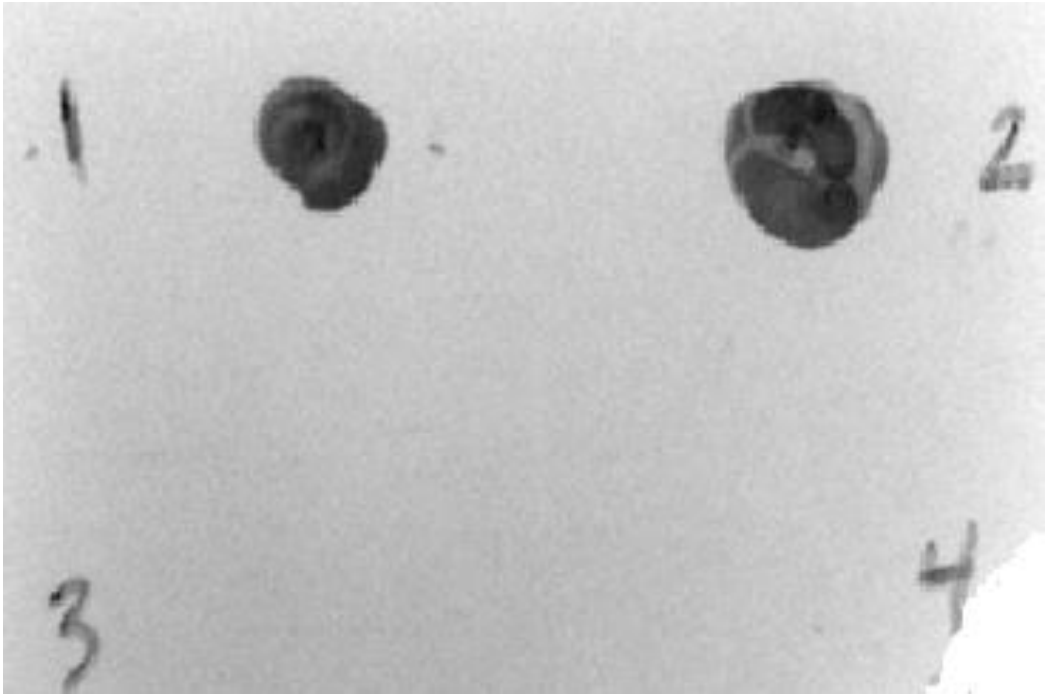

Figure 4.2: Characterization of C1q by dot blot. Image showing the binding of sheep anti-human C1q (HRP conjugated) with adsorbed C1q (5µg) at positions 1 & 2 on nitrocellulose membrane. This antibody did not bind with amyloid P. component (5µg) at positions 3 & 4 on the membrane.

4.2.2 Binding of C1q with Mycobacteria by ELISA

ELISA was used to study the binding of C1q with mycobacteria. The results showed the direct binding of C1q with *M. smegmatis* and BCG in presence of 5mM $CaCl_2$. The binding of C1q with *M.smegmatis* was stronger at 10 µg/ml (Figure 4.3-A&B), and the maximum binding was observed at 5 µg/ml with BCG (Figure 4.3-C&D).

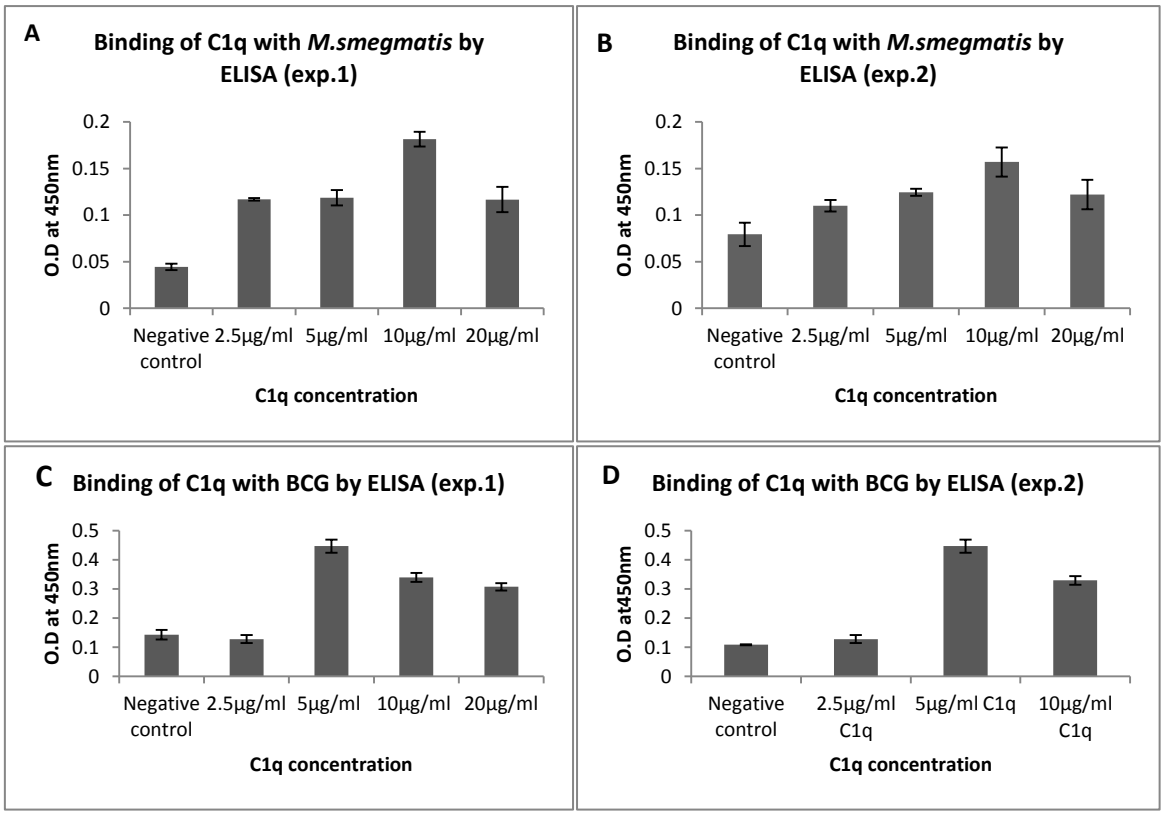

Figure 4.3: Binding of C1q with mycobacteria (*M.smegmatis* and BCG) by ELISA. Each bar represents average of the triplicate readings. Error bars represent ±standard deviation. The negative control contains untreated mycobacteria. Microtitre wells were coated in with $10x10^6$ cell per well of mycobacteria in carbonate buffer and incubated at 4°C overnight. Contents were discarded and wells were blocked for 2 hours with 1% BSA in PBS at 37°C. Following washing with PBS + 0.05% Tween, different concentrations (2.5, 5, 10, 20µg/ml) of C1q and 5mM $CaCl_2$ were added and the plate was incubated for 2 hours at 37°C. Wells were washed and bound protein was detected using polyclonal sheep anti-human C1q (1/1000) in PBS/0.1% BSA. Colour was developed using TMB substrate. The plate was read at a wavelength of 450nm. A).

4.2.3 Binding of C1q with BCG by immunofluorescence microscopy

Immunofluorescence microscopy was used to show the binding of C1q at concentration 5μg/ml with BCG as described in materials and methods section (2.5.2). From the image shown in Figure 4.4, the untreated BCG (A & B) was compared with C1q treated BCG (C & D). It can be seen that there is a binding of C1q with BCG where BCG emits green florescence (D) as compared to untreated BCG (B).

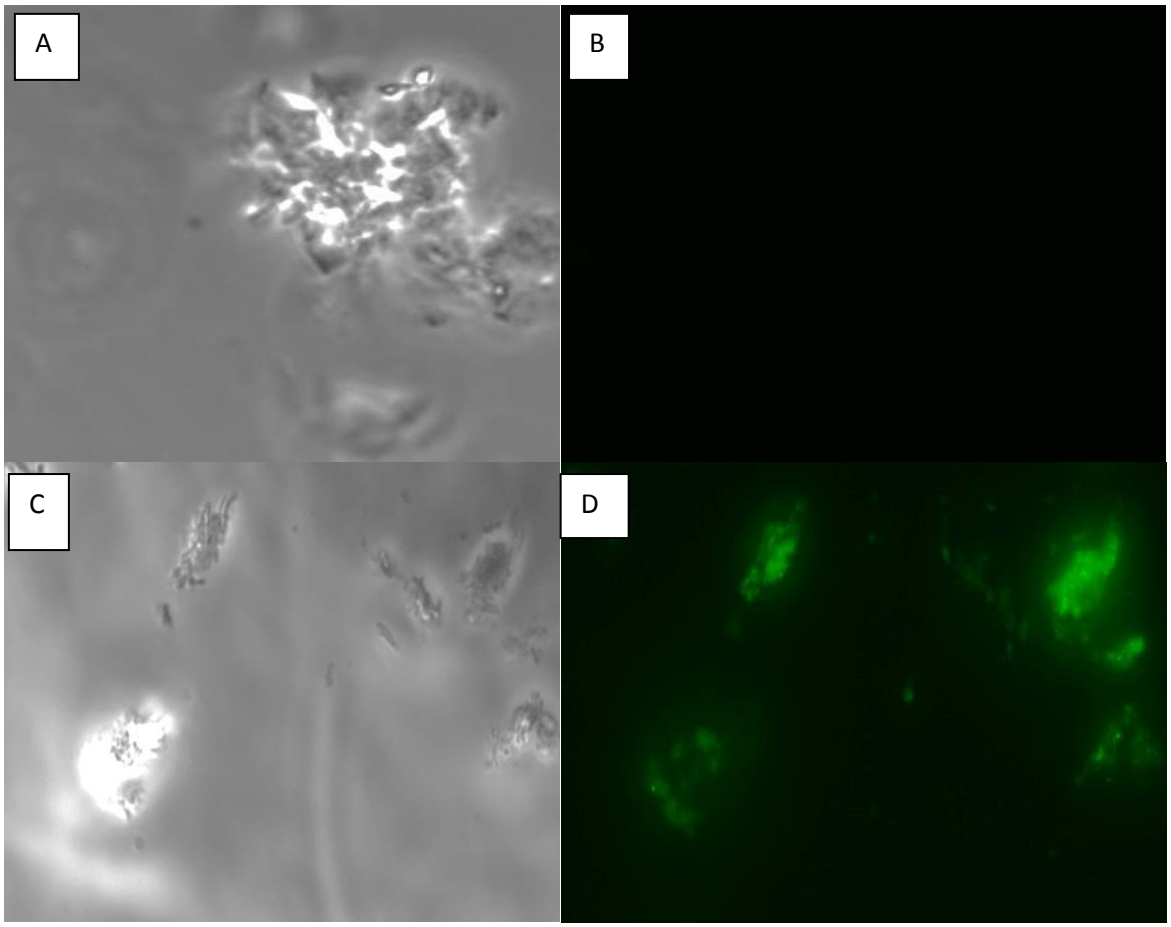

Figure 4.4: Binding of C1q with BCG by immunofluorescence microscopy. A: untreated BCG (bright field). B: untreated BCG (no binding). C: C1q treated BCG (bright field). D: C1q treated BCG (green florescence). All BCG samples were treated with anti-human C1q, followed by treatment with protein A conjugated to FITC.

4.2.4 The effect of sugars on C1q binding with Mycobacteria

The effect of sugars on C1q binding to mycobacteria was studied to show if C1q molecule can bind carbohydrates present on mycobacterial cell wall.

Incubation of C1q with 10mM maltose, mannose or mannan in presence of 5mM $CaCl_2$ slightly decreased C1q binding with mycobacteria suggesting lectin-like activity for C1q protein (Figure 4.5).

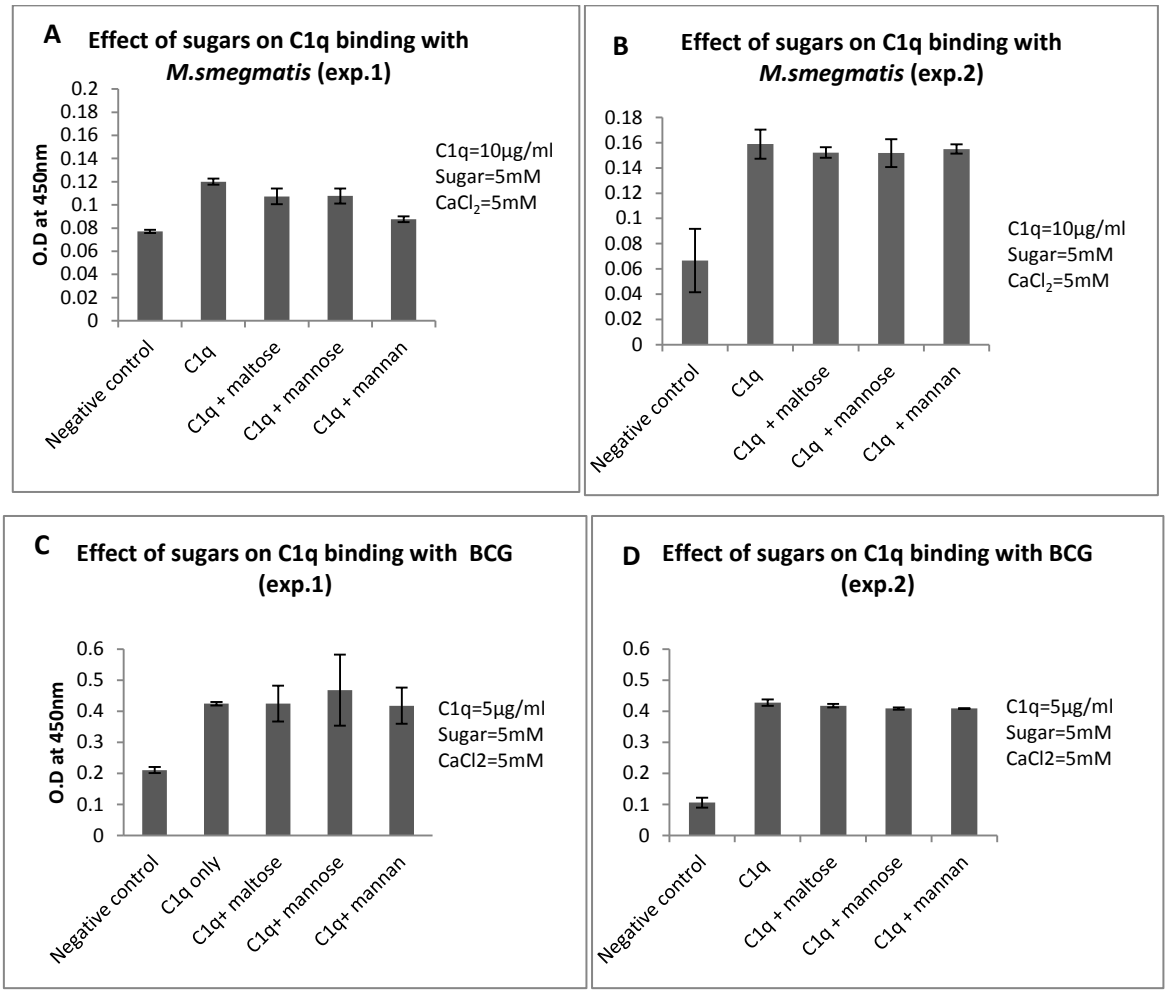

Figure 4.5: Effect of maltose, mannose, and mannan on C1q binding with mycobacteria. A&B: *M.smegmatis.* C&D: BCG. Each bar represents the average of triplicate readings. Error bars represents ±standard deviation. Negative control contains untreated mycobacteria (*M.smegmatis* or BCG). Microtitre wells were coated with $10x10^6$ cell per well of mycobacteria in carbonate buffer and incubated at 4°C overnight. Contents were discarded and wells were blocked for 2 hours with 1% BSA in PBS at 37°C. Following washing with PBS + 0.05% Tween, 10µg/ml untreated C1q treated with 10mM sugar (maltose, mannose or mannan) and in the presence of 5mM $CaCl_2$ were added. The plate was incubated for 2 hours at 37°C. Wells were washed and bound protein was detected using polyclonal sheep anti-human C1q (1/1000) in PBS/0.1% BSA. Colour was developed using TMB substrate. The plate was read at a wavelength of 450nm.

4.2.5 Binding of C1q with THP-1 cells by ELISA

ELISA was carried out to show the binding of different concentrations of C1q to THP-1 cells in presence of 5mM $CaCl_2$. The best binding of C1q to THP-1 cells was observed at 10μg/ml. However lower concentrations (0.6-5μg/ml) of C1q shown to bind to THP-1 cells at a similar level (Figure 4.6).

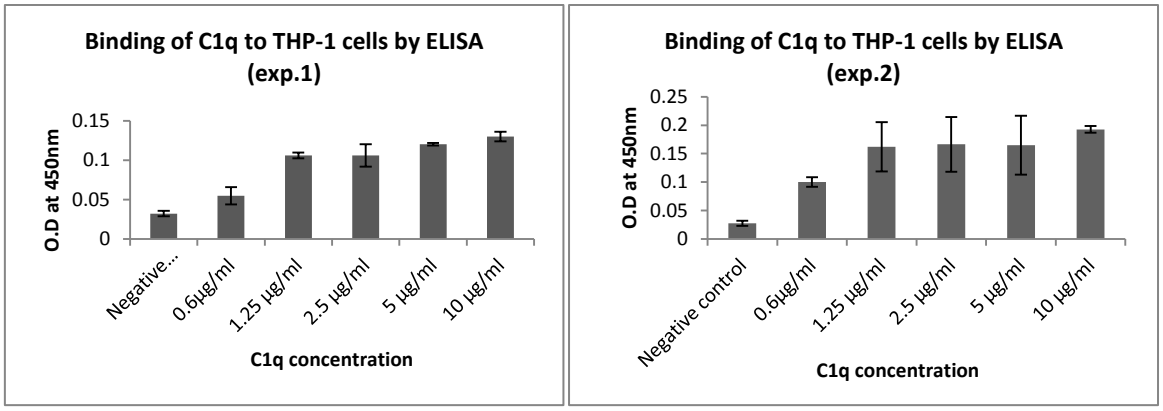

Figure 4.6: Binding of C1q with THP-1 cells by ELISA. Each bar represents average of the triplicate readings. Error bars represent ± standard deviation. Binding was assessed by ELISA using the OPD substrate with signal absorbance measured at 450 nm. Data shown represent one of two independent experiments. The negative control contains untreated THP-1 cells. Microtitre wells were coated with $1x10^5$ THP-1 cell per well in carbonate/bicarbonate buffer and incubated at 4°C overnight. Contents were discarded and wells were blocked for 2 hours with 1% BSA in PBS at 37°C. Following washing with PBS + 0.05% Tween, different concentrations (0.6, 1.2, 2.5, 5, 10, 20μg/ml) of C1q and 5mM $CaCl_2$ were added. The plate was incubated for 2 hours at 37°C. Wells were washed and bound protein was detected using polyclonal sheep anti-human C1q (1/1000) in PBS/0.1% BSA. Colour was developed using TMB substrate. The plate was read at a wavelength of 450nm.

4.2.6 Binding of C1q with THP-1 cells by immunoflurescence microscopy

Immunofluorescence microscopy was used to show the binding of C1q with THP-1 cells. Figure 4.7 shows, untreated THP-1 cells (A, B & C) compared with C1q treated THP-1 cells (D, E & F). The binding can be seen in C1q treated THP-1 cells, where the THP-1 cells emits green florescence (F) as compared to untreated THP-1 cells (C). The green florescence is the result of binding of protein A conjugated to FITC anti-C1q.

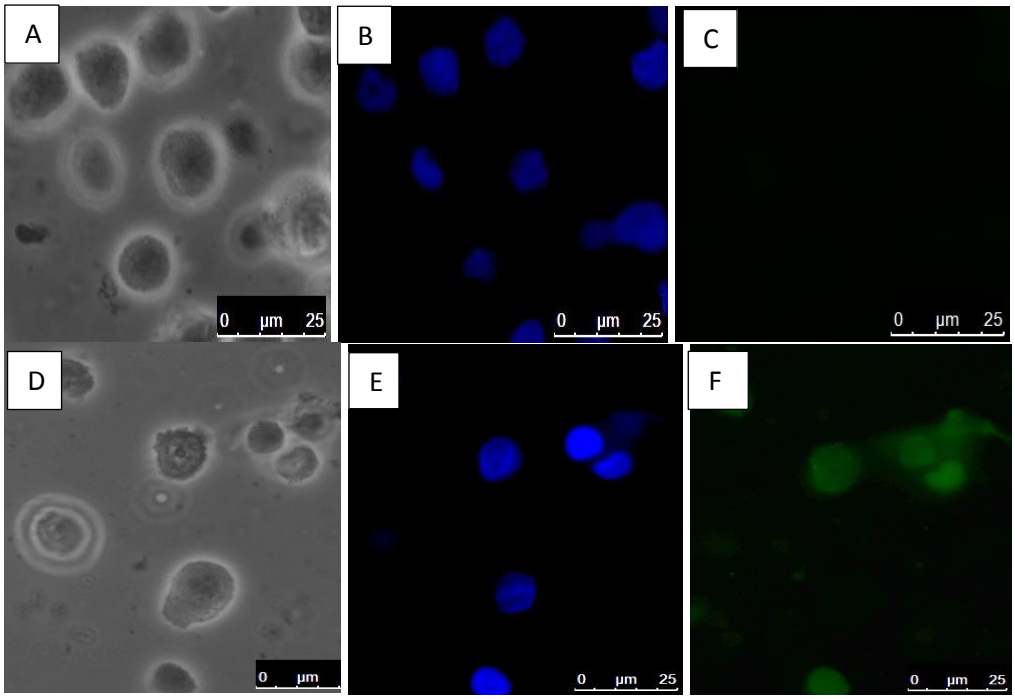

Figure 4.7: Binding of C1q with THP-1 cells by immunofluorescence microscopy. A: Untreated THP-1 cells (Bright field). B: Untreated THP-1 cells, nuclei stained with Hoechst (blue). C: C1q untreated THP-1 cells, but treated with anti-Clq and protein A FITC (no staining). D: C1q treated THP-1 cells (Bright field). E: C1q treated THP-1 cells, nuclei stained with Hoechst (blue). F: C1q treated THP-1 cells treated with anti C1q and protein A FITC (emitting green florescence). These cells were magnified by using picture tools on Microsoft Word.

4.2.7 Effect of C1q on mycobacterial agglutination

Agglutination test was performed to test the ability of C1q protein to clump mycobacteria together. This result showed that C1q does not agglutinate BCG in presence of $CaCl_2$ (Figure. 4.8). The average number of clumps counted in each field (using light microscopy at 1000x final magnification) were very similar for both C1q treated BCG and untreated BCG. All 4 independent experiments showed the same trend.

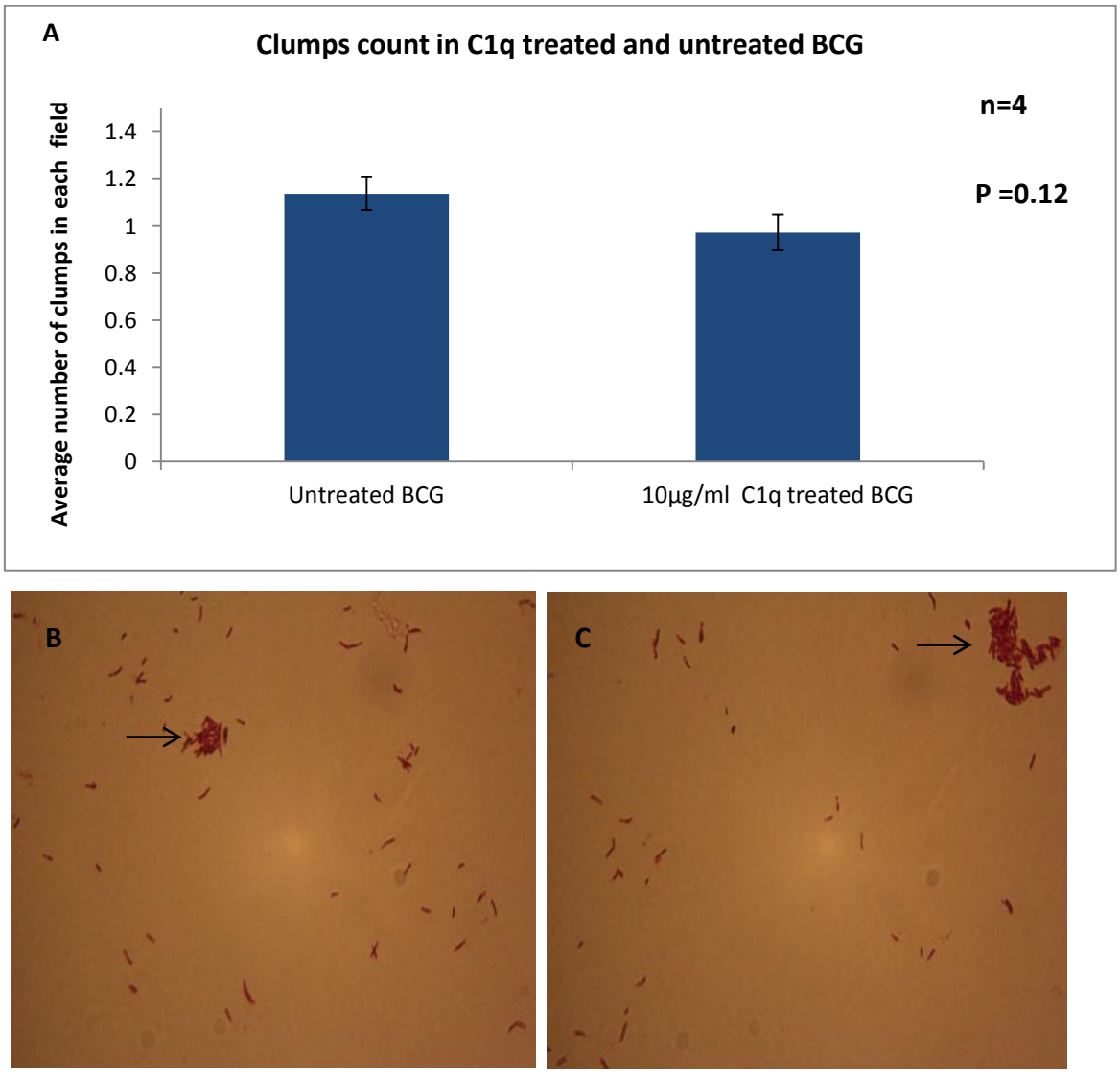

Figure 4.8: A: Effect of C1q on BCG agglutination. Each bar represent the average of small clumps from 4 slides. Error bars represent ±standard error of the mean. Clumps were counted in 70 different fields for each slide for both untreated BCG (B) and C1q treated BCG (C). Images were taken by using light microscopy at 1000x final magnification of Acid fast staining.

4.2.8 Direct effect of C1q on mycobacterial growth.

4.2.8.1 Direct effect of C1q on *M.smegmatis* growth

This study showed that C1q directly inhibited the growth of *M.smegmatis* by 32% and 37% using 1µg/ml and 10µg/ml of C1q respectively. All the 6 independent experiments showed the same trend of growth inhibition in presence of C1q, and the experimental results are statistiacally significant by using 10µg/ml C1q (Figure 4.9-A & 4.9-B).

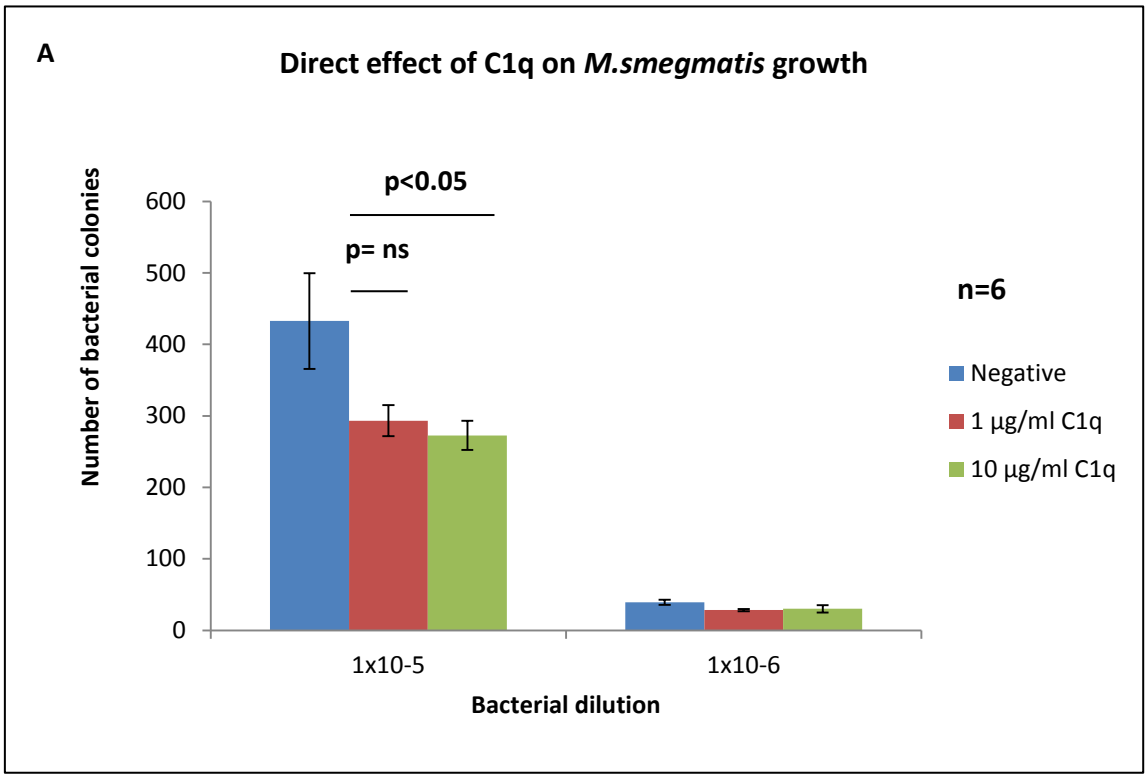

Figure 4.9-A: Direct effect of C1q on *M.smegmatis* growth. *M.smegmatis* was treated with (1 and 10µg/ml) C1q and incubated for 2 hours at 37°C in presence of 5mM $CaCl_2$. Untreated *M.smegmatis* and 5mM $CaCl_2$ were used as negative controls. Following incubation, 250µl of bacterial cultures were plated on LB agar plates in triplicates and incubated for 3 days at 37°C. The number of bacterial colonies in each plate was counted by visual inspection for each experiment. Each bar represents the average of 6 independent experiments. Error bars represents ±standard error of the mean. Multiple comparison of the data sets was done using Friedman test (p=0.005). Individual data were compared with each other using Dunn's post hoc test: Negative vs 1µg/ml vs 1µg/ml C1q, p=non significant; Negative vs 10µg/ml C1q, p<0.05. Negative contains untreated *M.smegmatis*.

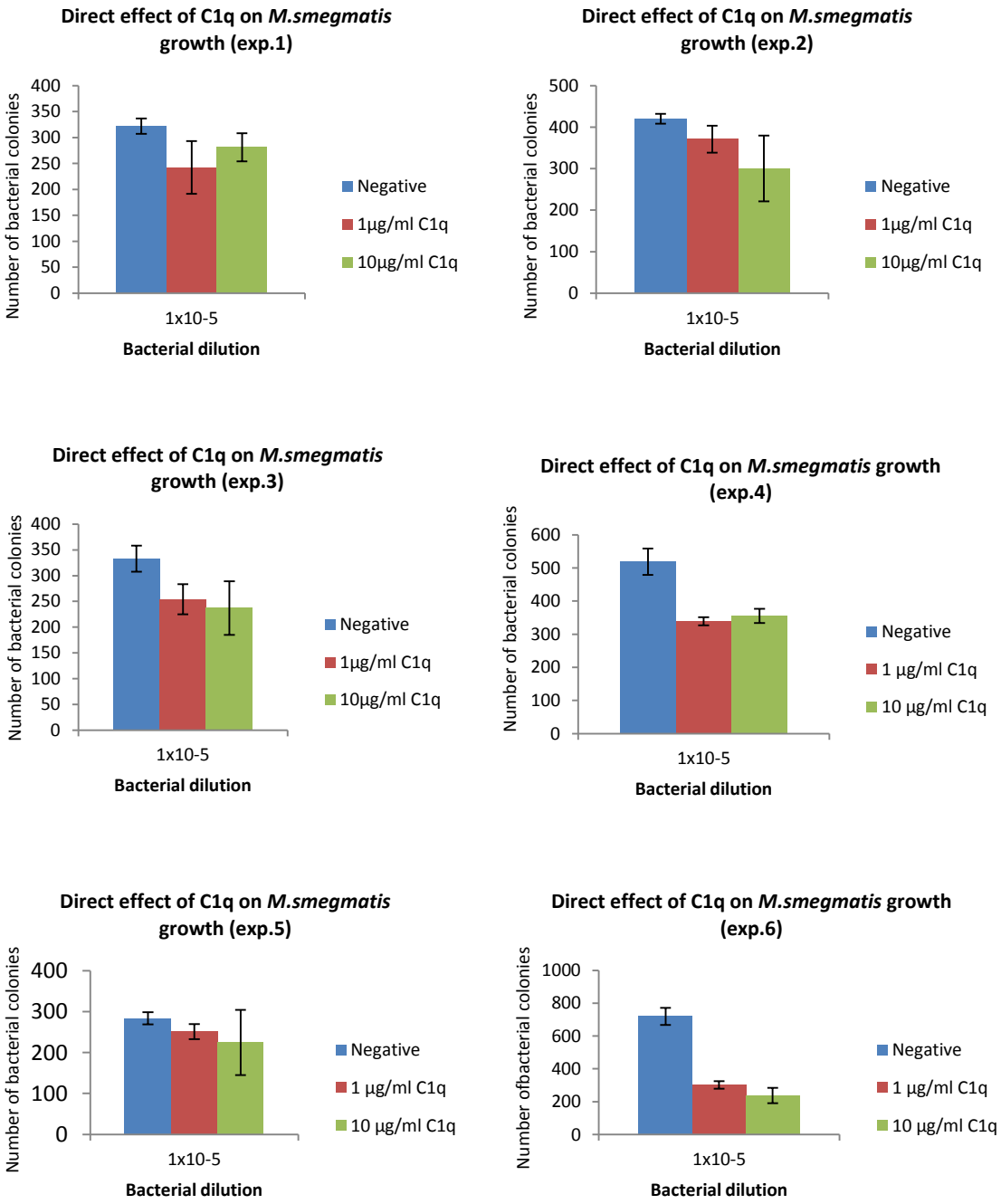

Figure 4.9-B: Direct effect of C1q on *M.smegmatis* growth (6 individual experiments). Each bar represents the average of triplicate data. Error bars represents ±standard deviation.

4.2.8.2 Direct effect of C1q on BCG growth

This study showed that C1q in presence of 5mM $CaCl_2$ inhibited BCG growth by 21% in 3 independent experiments showing the same trend (Figure 4.10A & 4.10B).

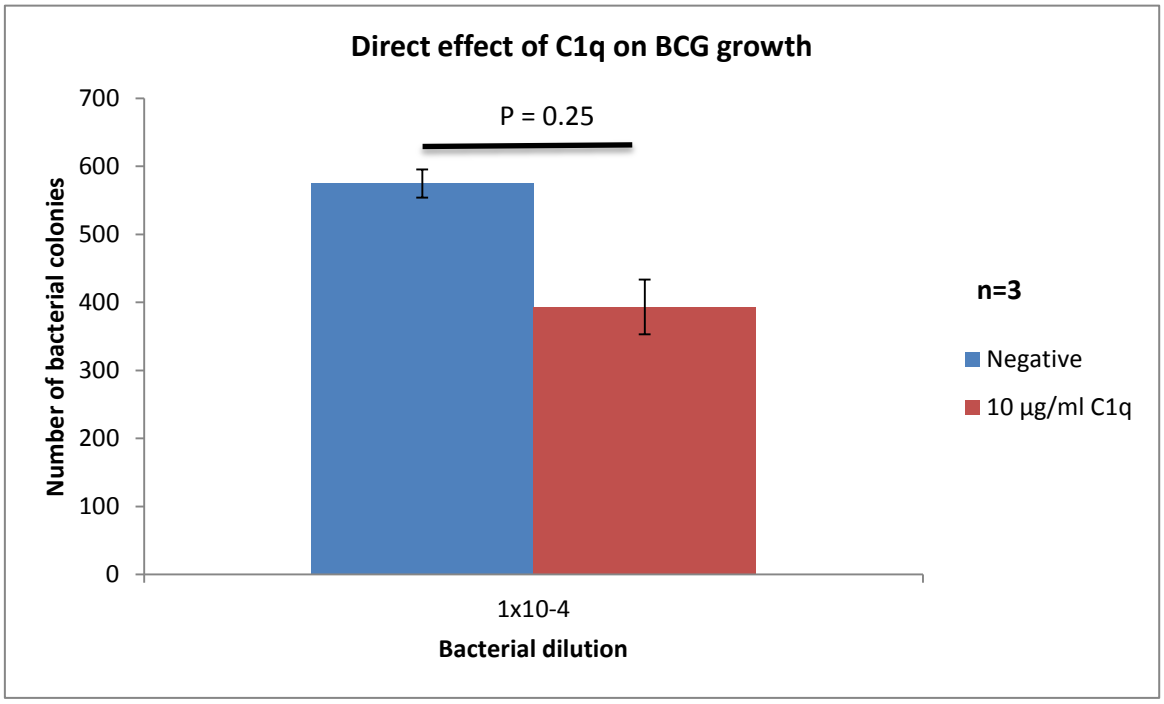

Figure 4.10-A: Direct effect of C1q on BCG growth. Mycobacteria was treated with 10µg/ml C1q and incubated for 2 hours at 37°C in presence of 5mM $CaCl_2$. Negative control contains untreated *M.smegmatis* with 5mM $CaCl_2$. Following incubation, 250µl of bacterial cultures were plated on 7H10 plates supplemented with 10% ADC in triplicates and incubated for 2-3 weeks inside incubator at 37°C. The number of bacterial colonies in each plate was counted by visual inspection. Each bar represents the average of 3 independent experiments. Error bars represent ±standard error of the mean. P value was calculated using Wilcoxon signed rank test. Negative contains untreated BCG.

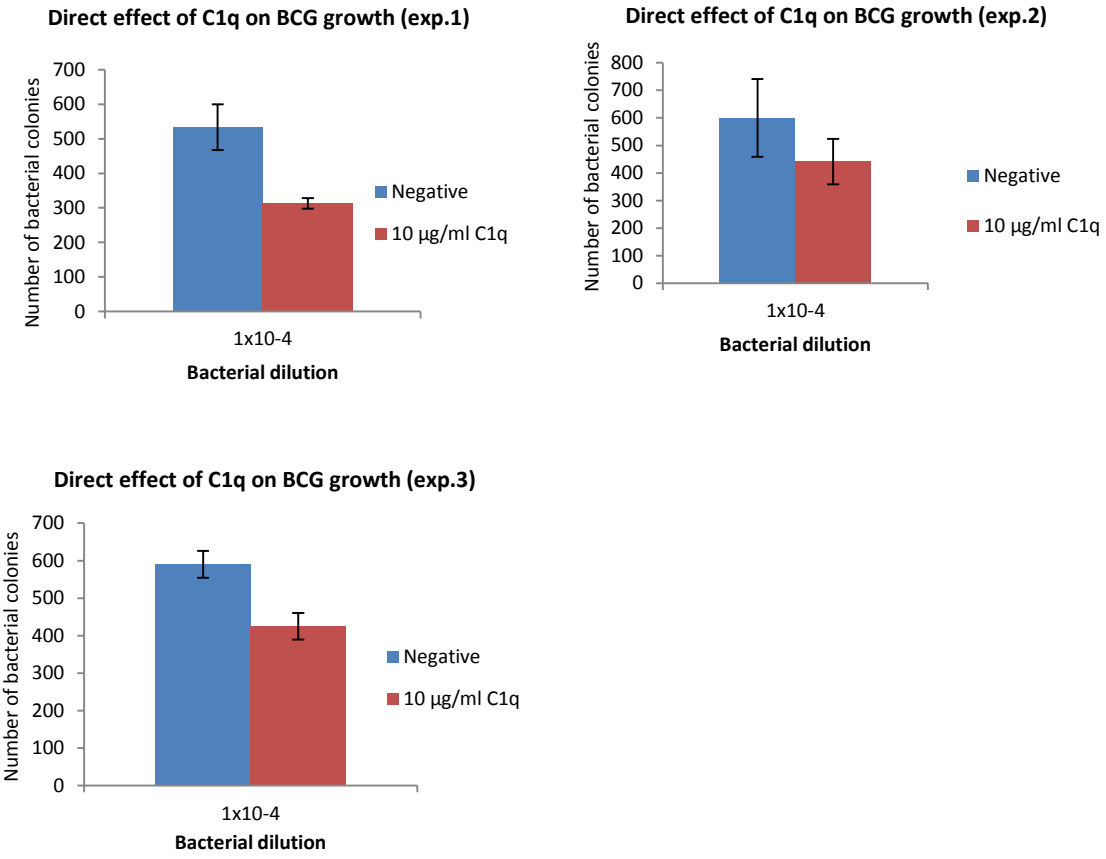

Figure 4.10-B: Direct effect of C1q on BCG growth (3 individual experiments). Each bar represents the average of triplicate data. Error bars represents ±standard deviation. Negative contains untreated BCG.

4.2.9 Effect of C1q on the uptake (phagocytosis) of mycobacteria by THP1 cells

4.2.9.1 Effect of C1q on the uptake of *M.smegmatis* by THP1 cells

Six independent experiments showed 43% an increase in *M.smegmatis* uptake by THP-1 cells infected with C1q treated *M.smegmatis* as compared to THP-1 cells infected with untreated *M.smegmatis* (Negative control), and this increase is statistically significant (p=0.0313) (Figure 4.11-A & 4.11B).

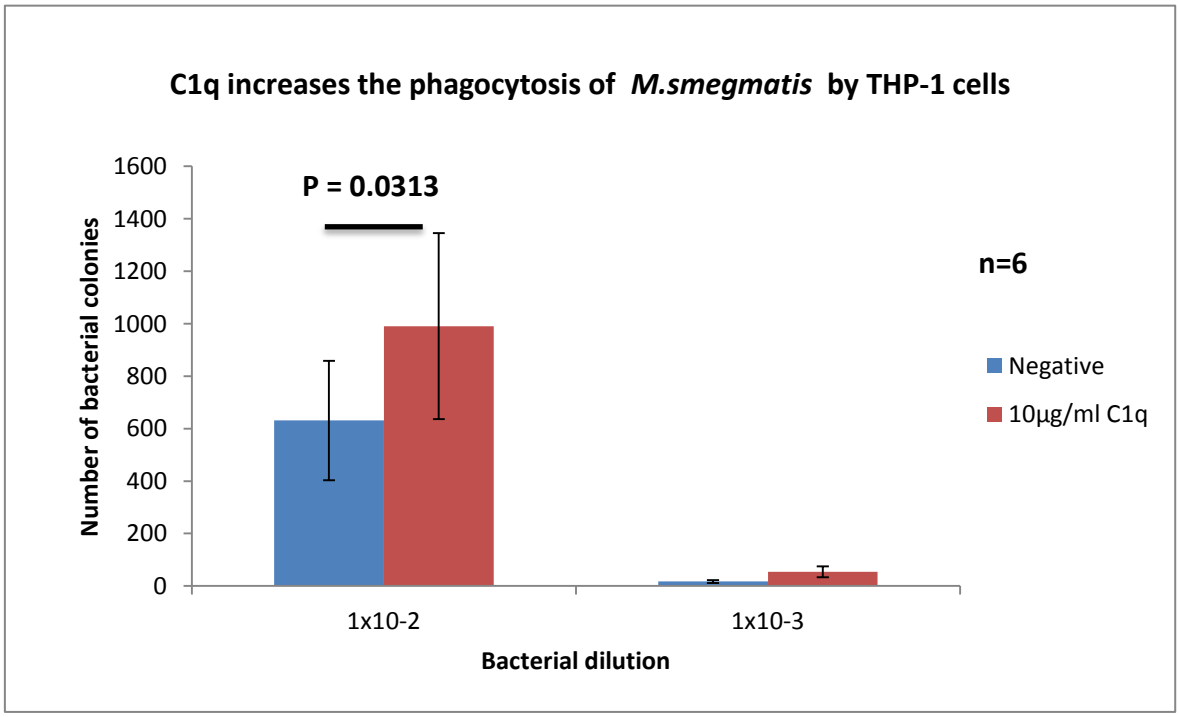

Figure 4.11-A: Effect of C1q on the uptake of *M. smegmatis* by THP1 cells. Each bar represents the average of 6 independent experiments. C1q treated and untreated (negative) mycobacteria were incubated for 2 hours at 37°C in presence of 5mM $CaCl_2$. After incubation, THP-1 cells were added to the mycobacteria in a 1:5 ratio (THP-1 cells:*M.smegmatis*), and incubated for an hour inside CO_2 incubator at 37°C to allow phagocytosis of mycobacteria by THP-1 cells. Following incubation, magnetic beads bound with anti-human MHC class 1 was added to each tube in a 1:4 ratio (THP-1: beads) and tubes were incubated in ice for 30 minutes on a shaker. After that, THP-1 cells were washed 3 times to remove extracellular bacteria. Washed cells were lysed with 0.1% saponin by vortexing for 15 minutes to release phagocytosed mycobacteria. Error bars represent ±standard error of the mean. P value was calculated using Wilcoxon signed rank test. Negative contains untreated *M.smegmatis*.

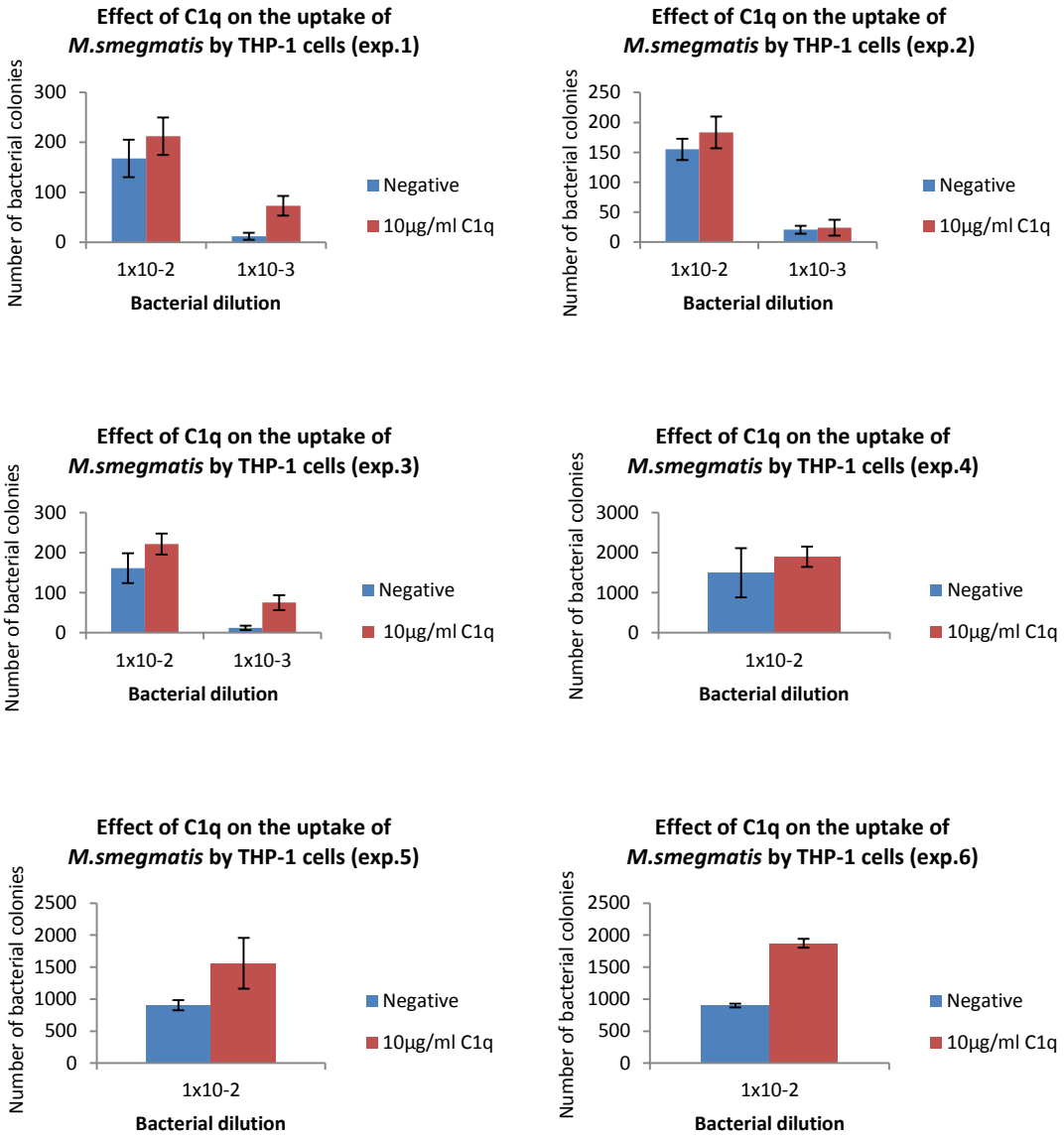

Figure 4.11-B: Effect of C1q on the uptake of *M.smegmatis* by THP1 cells (6 individual experiments). Each bar represents the average of triplicate readings. Error bars represent ±standard deviation. Negative contains untreated *M.smegmatis*.

4.2.9.1 Effect of C1q on the uptake of BCG by THP1 cells

This study showed 50% an increase in BCG uptake by THP-1 cells infected with C1q treated BCG as compared to THP-1 cells infected with untreated BCG. Six independent experiments were shown the same trend of increasing BCG uptake by THP-1 cells (Figure 4.12-A, 4.12-B, & 4.12-C).

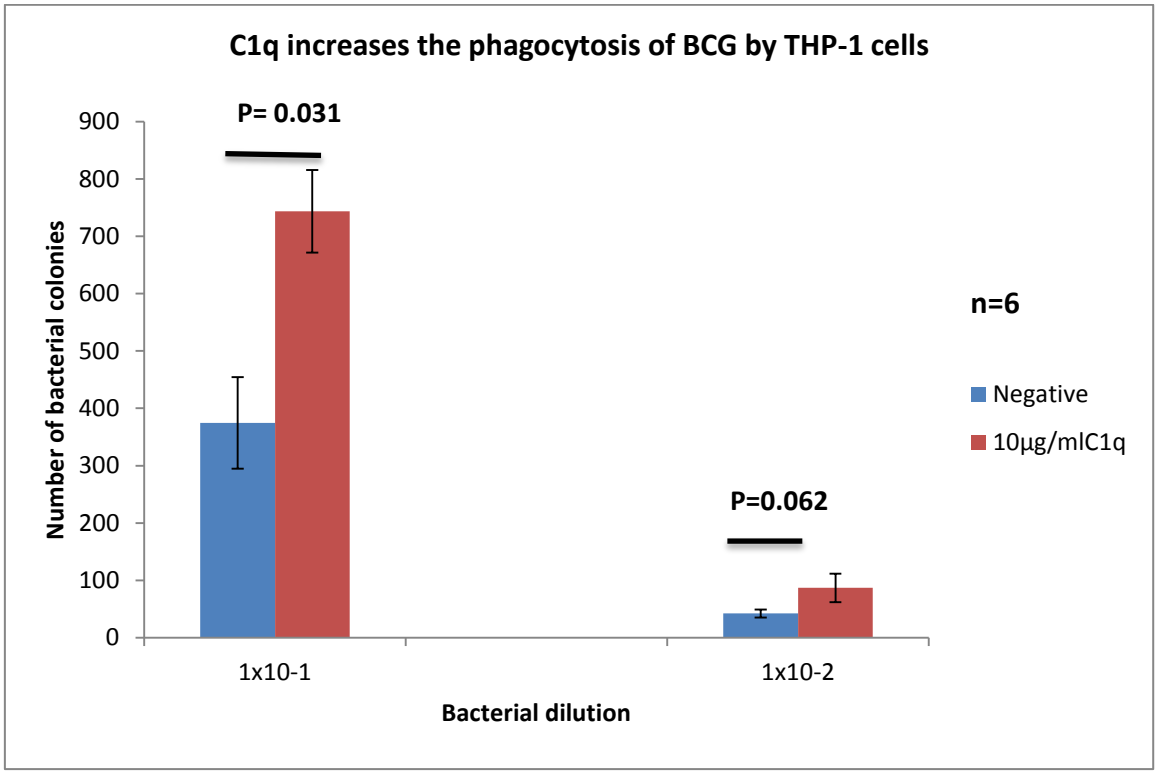

Figure 4.12-A: Effect of C1q on the uptake of BCG by THP-1 cells. The uptake of BCG was increased in C1q treated BCG as compared to untreated BCG. Mycobacteria was incubated in presence and absence of C1q for 2 hours at 37°C. Calcium chloride (5mM) was added to both conditions. Following the incubation, THP-1 cells were added in a 1:5 (THP-1 cells:BCG) ratio and incubated for an hour inside at 37°C. Next, magnetic beads bound with anti-human MHC class 1 were added to the cells in a ratio of 1:4 (THP-1 cells: beads), and incubated on ice horizontally for 30 minutes on a shaker. Next, THP-1 cells were washed 3 times to remove extracellular bacteria. THP-1 cells were lysed using 0.1% saponin by vortexing for 15 minutes. Each bar represents the average 6 independent experiments. Error bars represent ±standard error of the mean. P value was calculated using Wilcoxon Signed rank test. Negative contains untreated BBC.

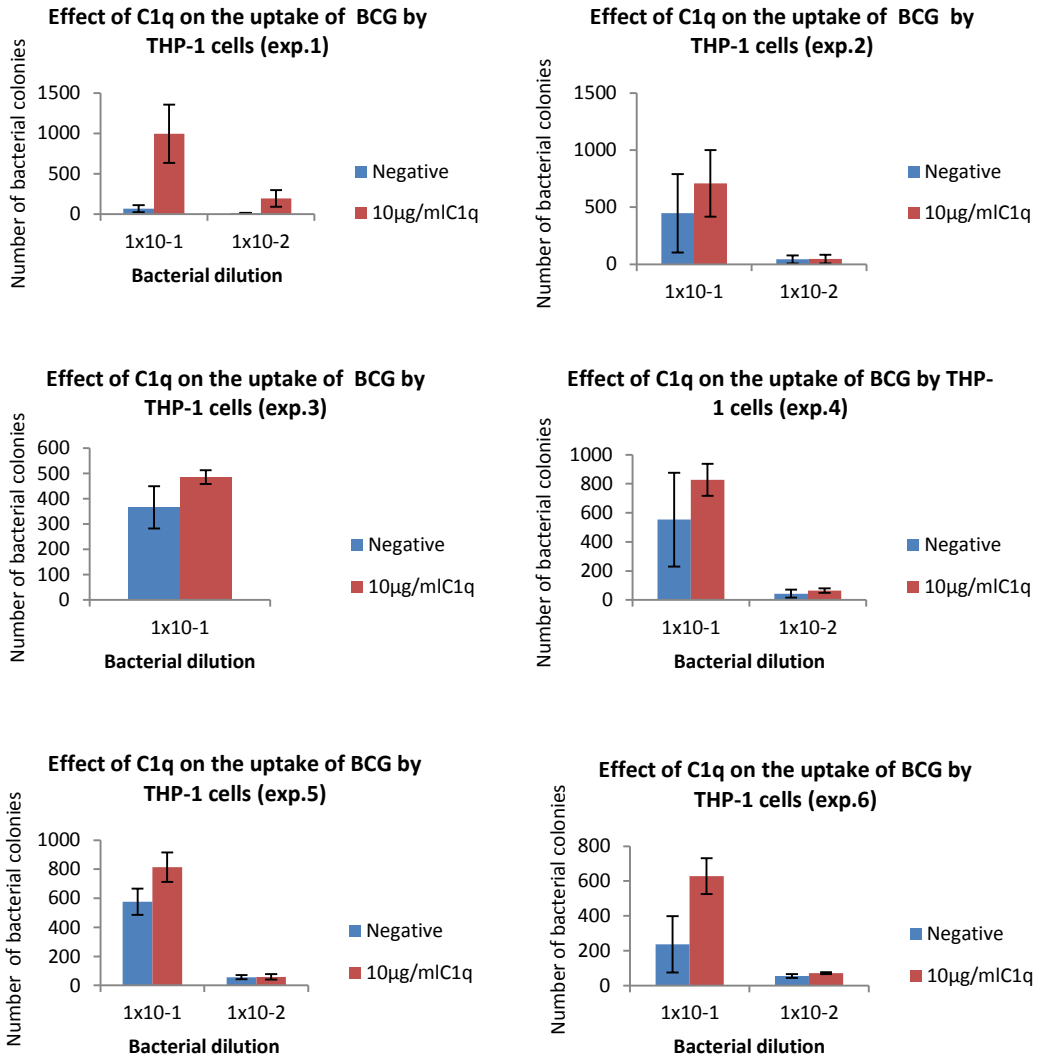

Figure 4.12-B: Effect of C1q on the uptake of BCG by THP-1 cells (6 individual experiments). Each bar represents the average of triplicate readings. Error bars represent ±standard deviation. Negative contains untreated BCG.

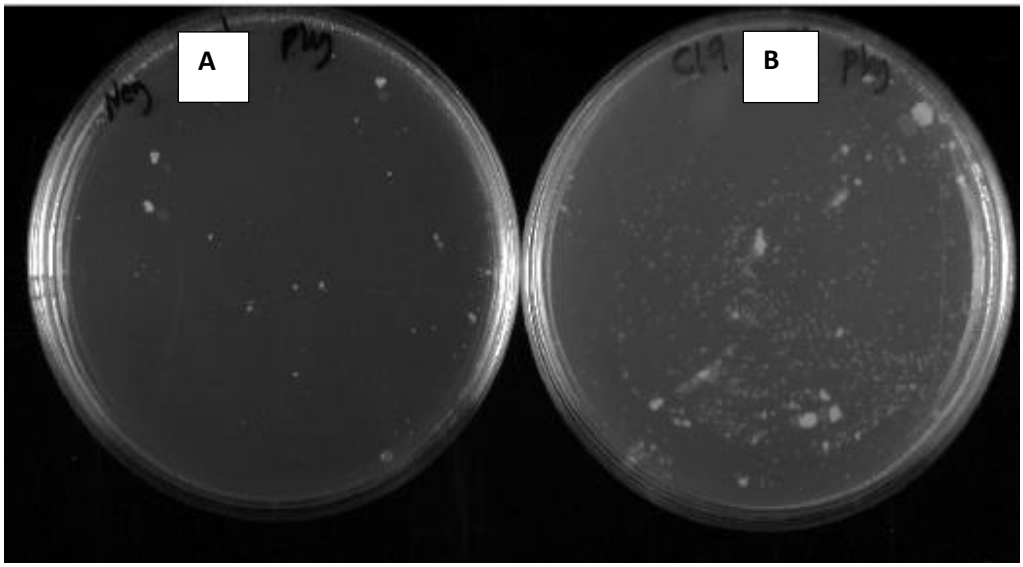

Figure 4.12-C: Effect of C1q on the uptake of BCG by THP-1 cells (BCG colonies on 7H10 plates). The number of C1q treated BCG colonies phagocytosed by THP-1 cells is higher as compared to untreated BCG. Negative control contains untreated BCG. Representative plates for untreated (A) and C1q treated BCG (B) is shown.

4.2.10 Effect of C1q on the growth of mycobacteria inside THP1 cells

4.2.10.1 Effect of C1q on the growth of *M.smegmatis* inside THP1 cells

In this study C1q was shown to increase the growth of *M.smegmatis* by 63% inside THP-1 cells. Six independent experiments have shown the same trend of *M.smegmatis* growth increase (Figure 4.13-B). The experimental results were statistically significant (p=0.03) (Figure 4.13-A).

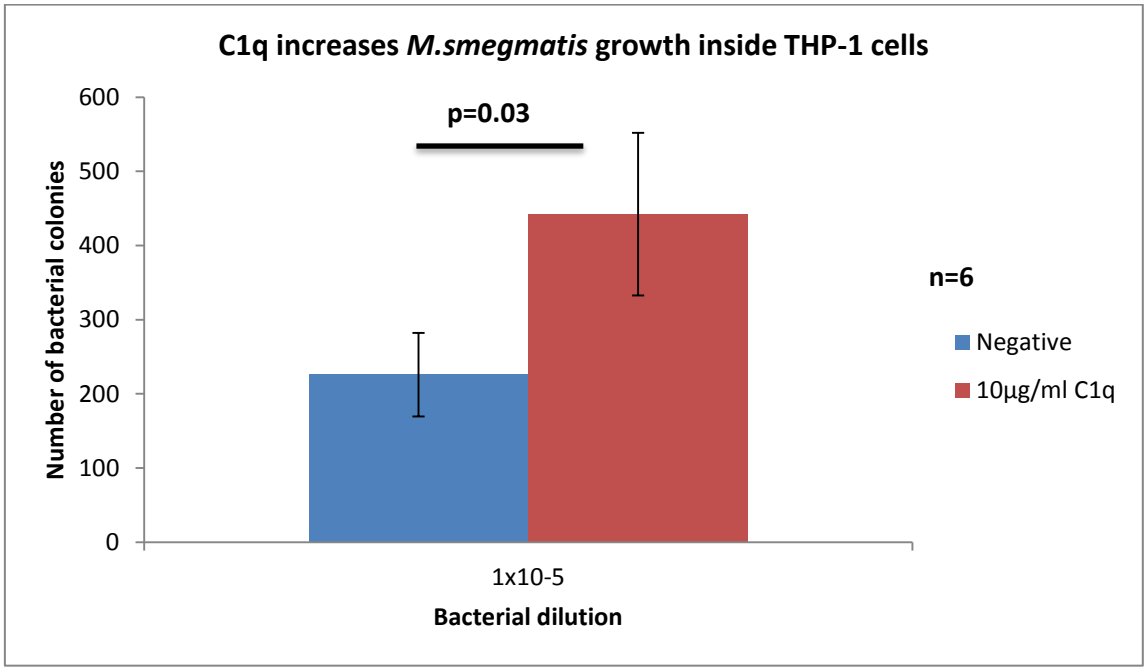

Figure 4.13-A: Effect of C1q on *M.smegmatis* growth inside THP-1 cells. Both C1q treated and untreated *M.smegmatis* (Negative) were incubated at 37°C for 2 hours. 5mM calcium chloride was added to both test and negative control tubes. After incubation, THP-1 cells were added to the mycobacteria in a ratio of 1:5 (THP-1 cells:*M.smegmatis*) and incubated at 37°C for one hour. Following incubation, magnetic beads bound with anti-human MHC class 1 were added to each tube in a ratio of 1:4 (THP-1: beads), and tubes incubated in ice for 30 minutes on a shaker. THP-1 cells were washed and suspended in complete RPMI medium (without antibiotics). Tubes were incubated at 37°C for 24 hours. Following incubation, the cells were separated using a magnet and lysed with 0.1% of saponin by vortexing for 15 minutes. Equal volumes of cell lysate and supernatant were mixed together. 250µl of $1x10^{-4}$ and $1x10^{-5}$ bacterial dilutions were plated on LB agar in triplicates. Plates were incubated at 37°C for 3 days. Each bar represents the average of 6 independent experiments**.** Error bars represent ±standard error of the mean. P value was calculated using Wilcoxon Signed rank test. Negative control contains untreated *M.smegmatis*.

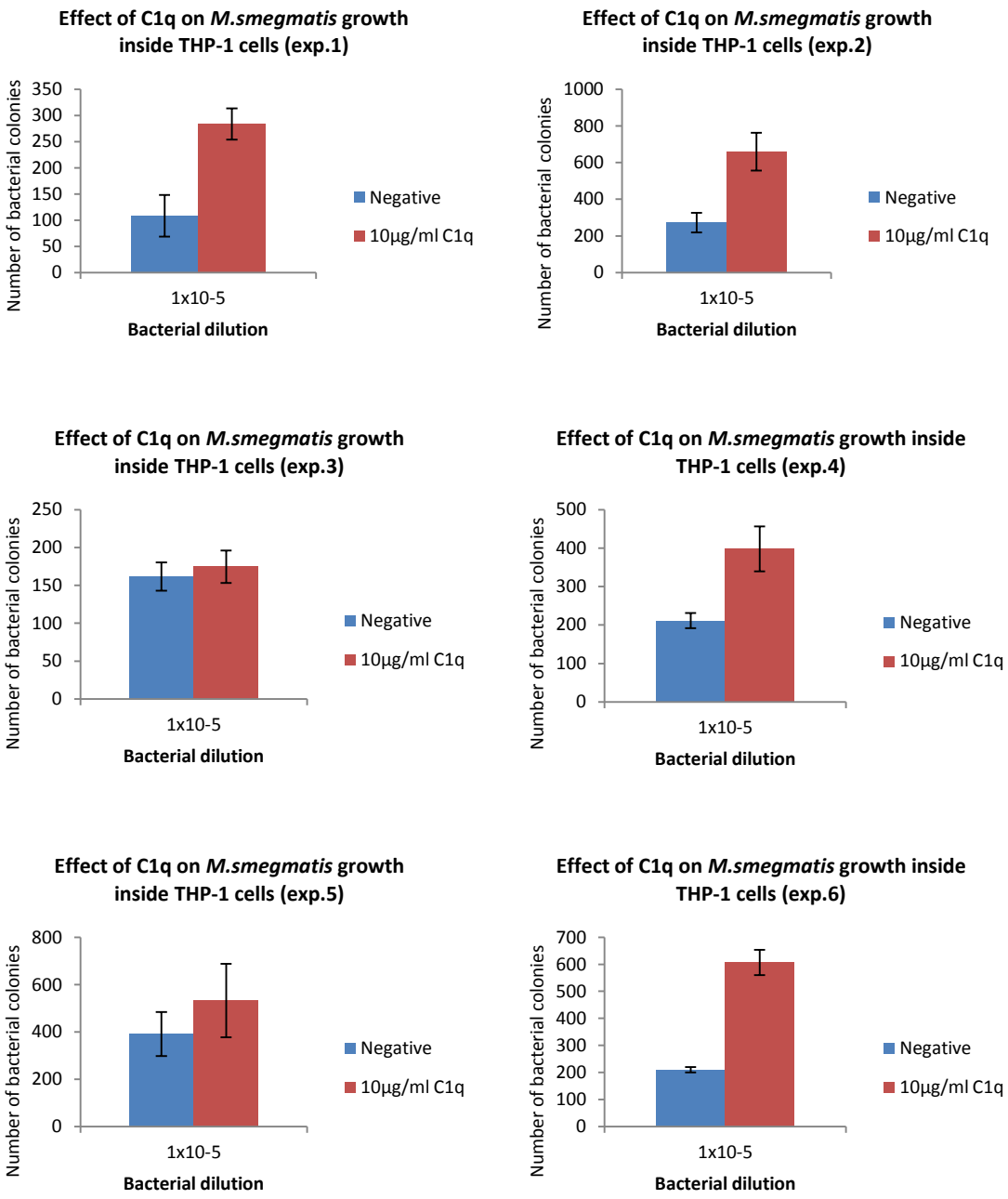

Figure 4.13-B: Effect of C1q on *M.smegmatis* growth inside THP-1 cells (6 individual experiments). Each bar represents the average of triplicate readings. Error bars represent ±standard deviation.

4.2.10.2 Effect of C1q on the growth of BCG inside THP1 cells

C1q was shown to inhibit BCG growth by 70% inside THP-1 cells. All six independent experiments showed the same trend (Figure 4.14-B). Also, the results were statistically significant (p=0.0313) (Figure 4.14-A).

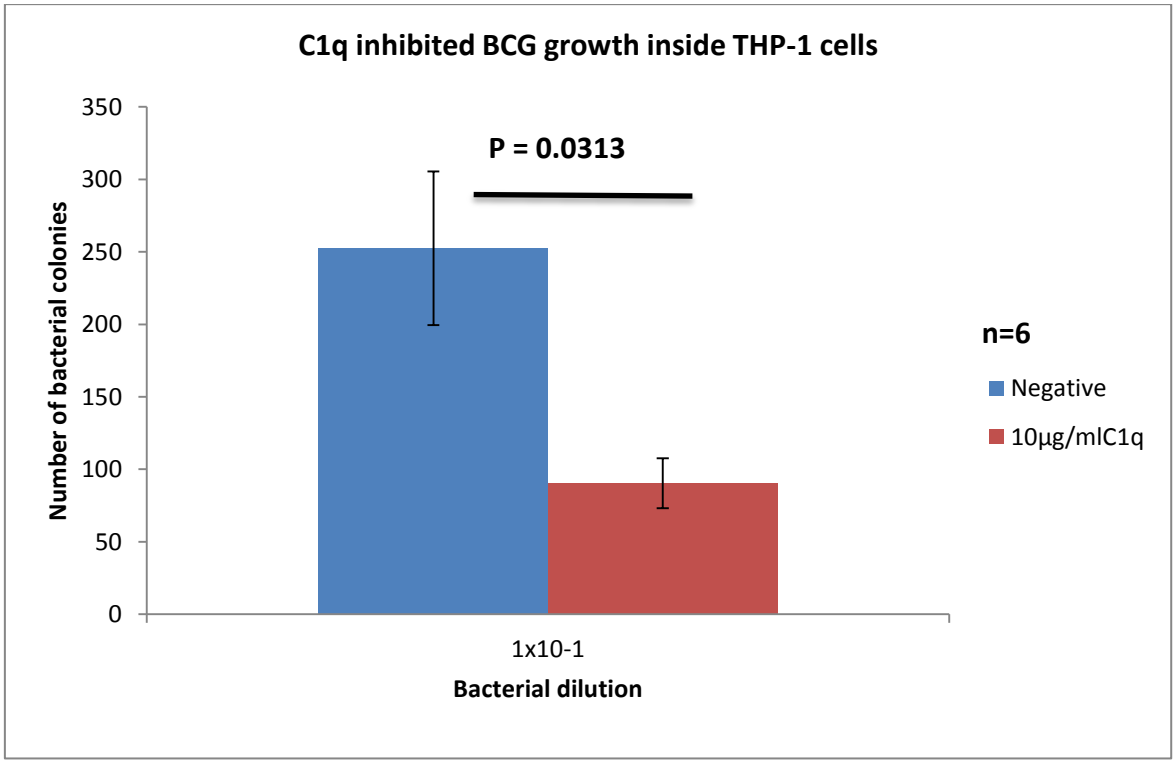

Figure 4.14-A: Effect of C1q on BCG growth inside THP-1 cells. C1q treated and untreated BCG was incubated at 37°C for 2 hours in presence of 5mM $CaCl_2$. After incubation, THP-1 cells were added to the mycobacteria in a 1:5 (THP-1 cells:BCG) ratio and incubated for one hour inside a CO_2 incubator. Next, magnetic beads bound with anti-human MHC class 1 were added to each tube in a ratio of 1:4 (THP-1: beads), and all tubes were incubated in ice for 30 minutes on a shaker. Following incubation, the cells were washed 3 times using RPMI. Washed cells were suspended in complete RPMI medium (without antibiotics) and incubated inside a CO_2 incubator for 24 hours. The next day the cells were separated by the magnet and lysed with 0.1% of saponin by vortexing for 15 minutes. Equal volumes of cell lysate and supernatant were mixed together, and bacterial dilutions of $1x10^{-4}$ and $1x10^{-5}$ were prepared. For each dilution, 250µl was plated on 7H10 plates supplemented with 10% ADC in triplicates. Plates were incubated at 37°C for 2-3 weeks. Each bar represents the average of 6 independent experiments. Error bars represent ±standard error of the mean. P value was calculated using Wilcoxon Signed rank test. Negative contains untreated BCG.

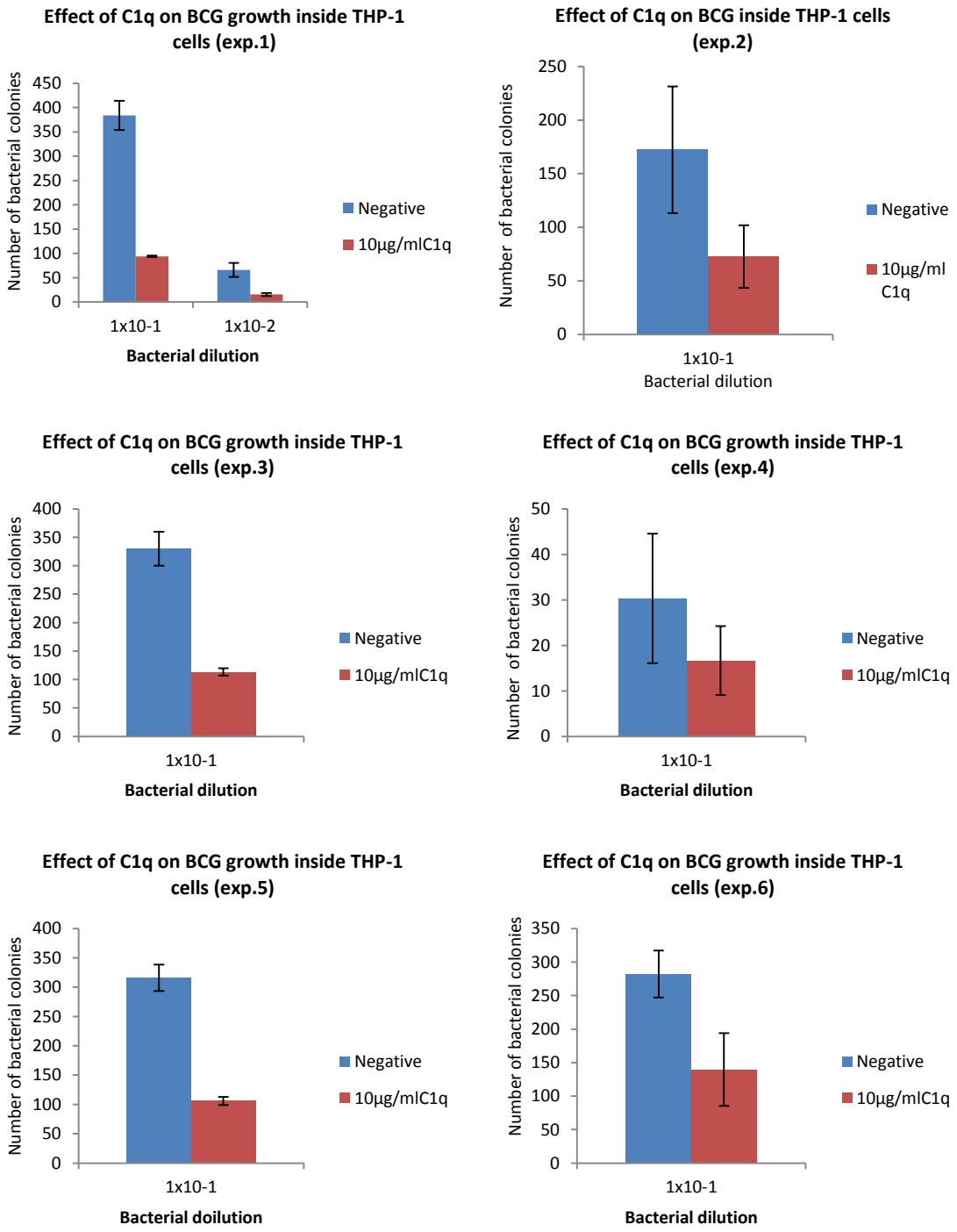

Figure 4.14-B: Effect of C1q on BCG growth inside THP-1 cells (6 individual experiments). Each bar represents the average of triplicate readings. Error bars represent ±standard deviation. Negative contains untreated BCG.

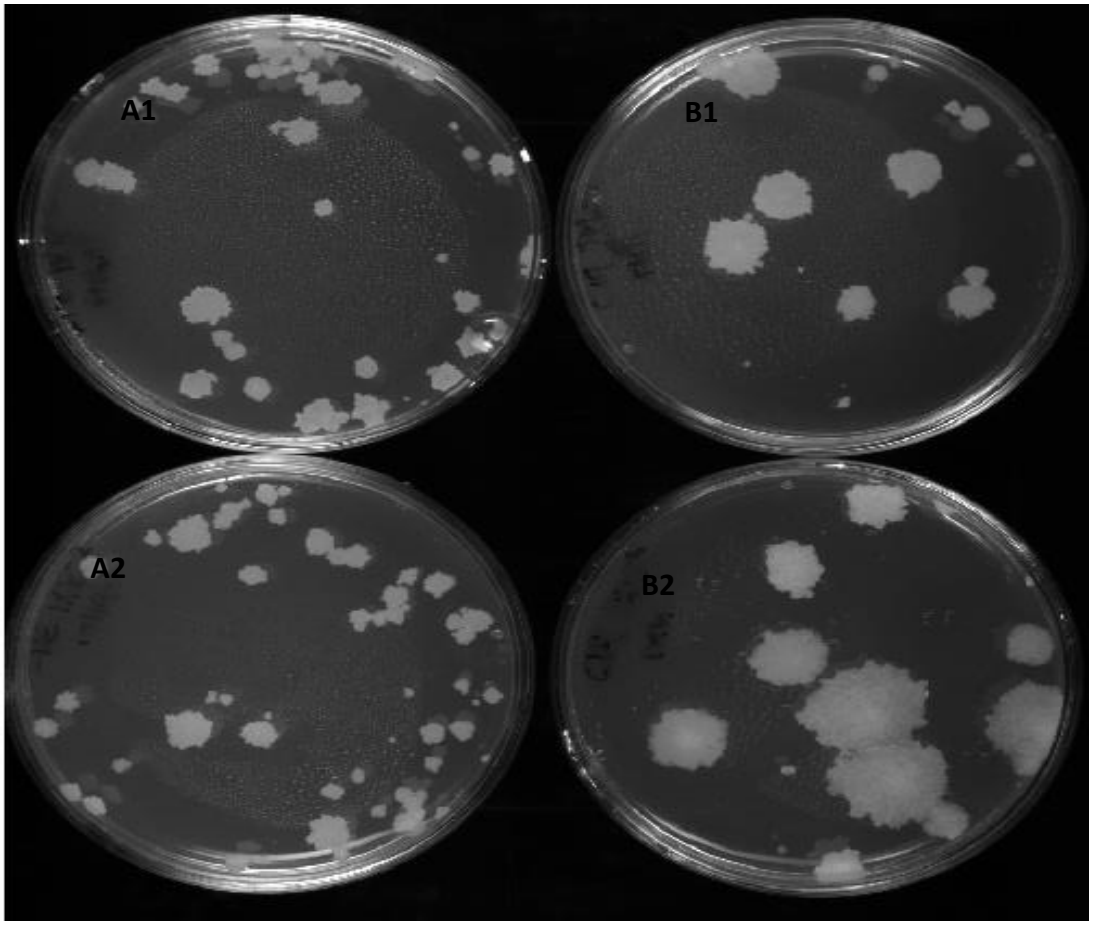

Figure 4.14-C: Effect of C1q on BCG growth inside THP-1 cells (BCG colonies on 7H10 plates). C1q inhibited BCG growth inside THP-1 cells. BCG colonies were allowed to grow in volume for 4-5 weeks. Two representative plates from untreated (A1 & A2) and C1q treated BCG (B1 & B2) are shown.

4.2.11 Understanding the mechanisms of differential mycobacterial (*M.smegmatis* and BCG) growth inside THP-1 cells by studying the expression of cytokine and non-cytokine genes

The q-PCR was used to study the gene expression of inducible nitric oxide synthase (iNOS), pro-inflammatory and anti-inflammatory cytokines inside THP-1 cells infected with C1q treated and untreated mycobacteria (*M.smegmatis* and BCG).

4.2.11.1 The gene expression of inducible nitric oxide synthase (iNOS)

Human macrophages kill different pathogens by producing nitric oxide free radicals. These free radicals are produced through conversion of arginine to

citrulline by inducible nitric oxide synthase. Nitric oxide free radicals have been produced in macrophages infected with *Mtb* (Nicholson et al., 1996), and inhibition of iNOS in latent TB human leads to *Mtb* reactivation (Gardam et al., 2003). The iNOS gene was expressed by THP-1 cells infected with untreated *M.smegmatis* only after 5 and 10 hours of incubation. The iNOS gene was not expressed in THP-1 cells infected with C1q treated *M.smegmatis* (Figure 4.15-A). On the other hand, iNOS gene was expressed after 5 and 10 hours by THP-1 cells infected with both C1q treated and untreated BCG, and the gene expression of iNOS was enhanced in THP-1 cells infected with C1q treated BCG (Figure 4.15-B).

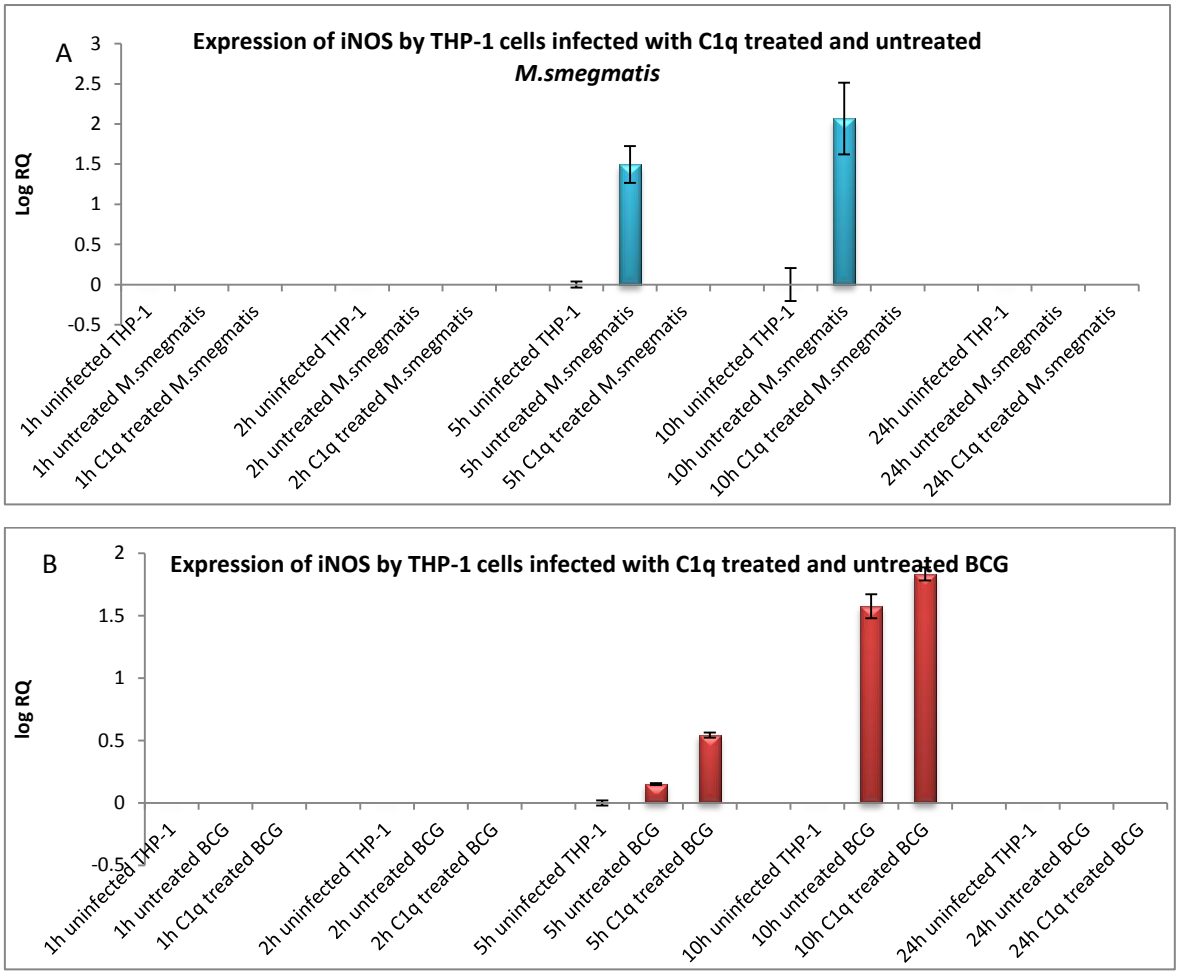

Figure 4.15: Expression of inducible nitric oxide synthase (iNOS) gene by THP-1 cells infected with C1q treated and untreated *M.smegmatis* (A) and BCG (B). THP-1 cells were incubated for 1, 2, 5, 10 and 24 hours after infection with mycobacteria at 37°C inside a CO_2 incubator. The cell pellet was collected and used for RNA extraction and cDNA synthesis used in this analysis. The expression of the gene was measured using qPCR and data was normalized to 18sRNA expression as control. RQ values was calculated using the formula; $RQ=2^{-\Delta\Delta Ct}$. Log RQ values were plotted to show the gene expression. Un-infected THP-1 cells were used as negative control. Each bar represents the average of triplicate readings. Error bars represent ±standard deviation.

4.2.11.2 The gene expression of tumour necrosis factor-α (TNF-α)

TNF-α is pro-inflammatory cytokine. It regulates mycobacterial growth in granulomas and initiates adaptive immunity. Additionally, neutralization of TNF-α in rheumatoid arthritis patients lead to activation of latent TB (Gardam et al., 2003). TNF-α gene was expressed after 1, 5, and 10 hours by THP-1 cells infected with untreated *M.smegmatis*. TNF-α was expressed after 1 hour by THP-1 cells infected with C1q treated *M.smegmatis* and the expression of this cytokine was down-regulated after 2 hours of incubation (Figure 4.16-A). This suggests that C1q down regulate the expression of TNF-α inside THP-1 cells infected with *M.smegmatis*. On the other hand, C1q upregulate the expression of TNF- α inside THP-1 cells infected with C1q treated BCG (Figure 4.16-B).

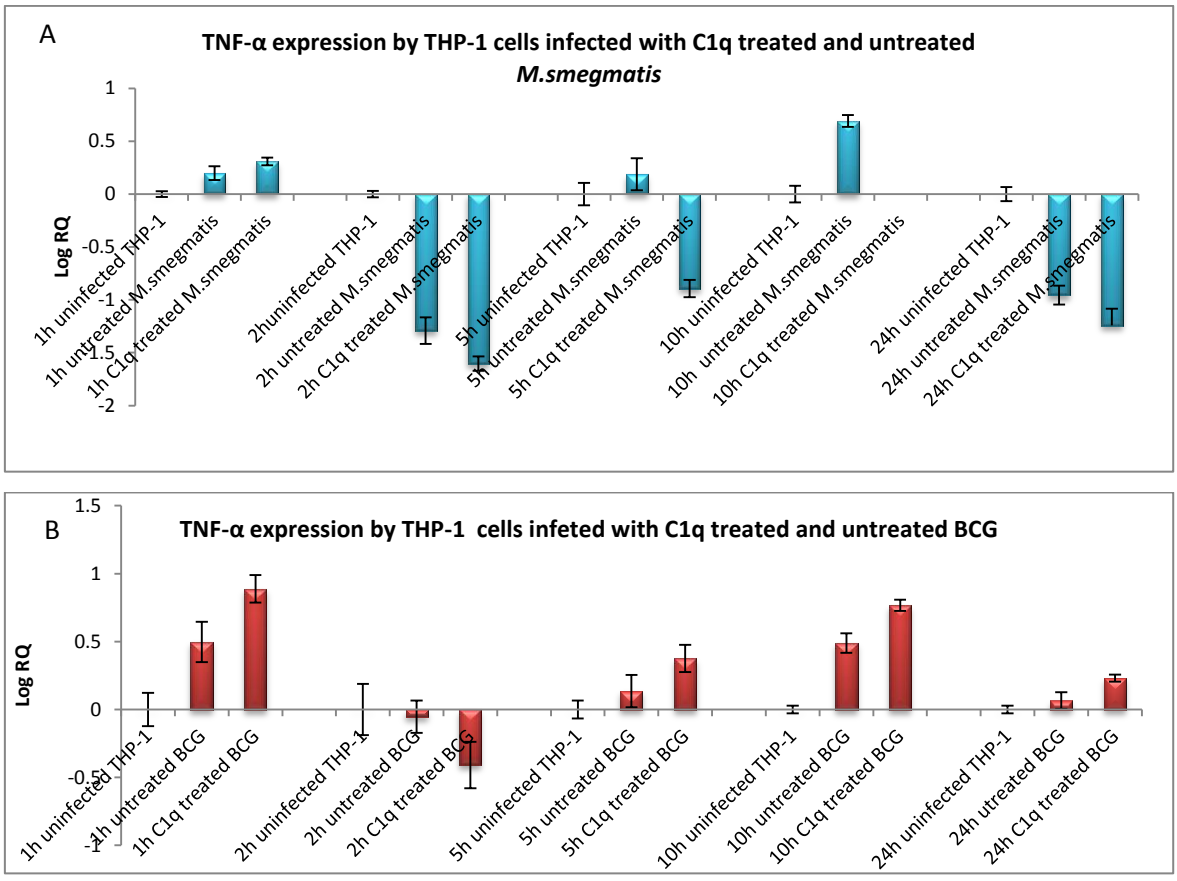

Figure 4.16: Expression of TNF-α gene by THP-1 cells infected with C1q treated and untreated *M.smegmatis* (A) and BCG (B). THP-1 cells were incubated for 1, 2, 5, 10 and 24 hours after infection with mycobacteria at 37°C inside a CO_2 incubator. The cell pellet was collected and used for RNA extraction and cDNA synthesis used in this analysis. The expression of the gene was measured using qPCR and data was normalized to 18sRNA expression as control. RQ values were calculated using the formula; $RQ=2^{-\Delta\Delta Ct}$. Log RQ values were plotted to show the gene expression. Un-infected THP-1 cells were used as negative control. Each bar represents the average of triplicate readings. Error bars represent ±standard deviation.

4.2.11.3 Expression of interleukin-1β (IL-1β)

IL-1β is a protective cytokine against tuberculosis; it is expressed in granulomas by infected macrophages. IL-1β receptor deficient mice have been shown to impair granuloma formation. The pro-inflammatory cytokines IL-1β was expressed after 1, 2, 5, and 10 hours by THP-1 cells infected with untreated *M.smegmatis* only (Figure 4.17-A). Also, IL-1β gene was expressed after 1, 2, 5, 10 and 24 hours in THP-1 cells infected with C1q treated and untreated BCG (Figure 4.17-B) . After 24hours the expression of IL-1 β was up-regulated in THP-1 cells infected with C1q treated BCG only, suggesting late upregulation of this cytokine.

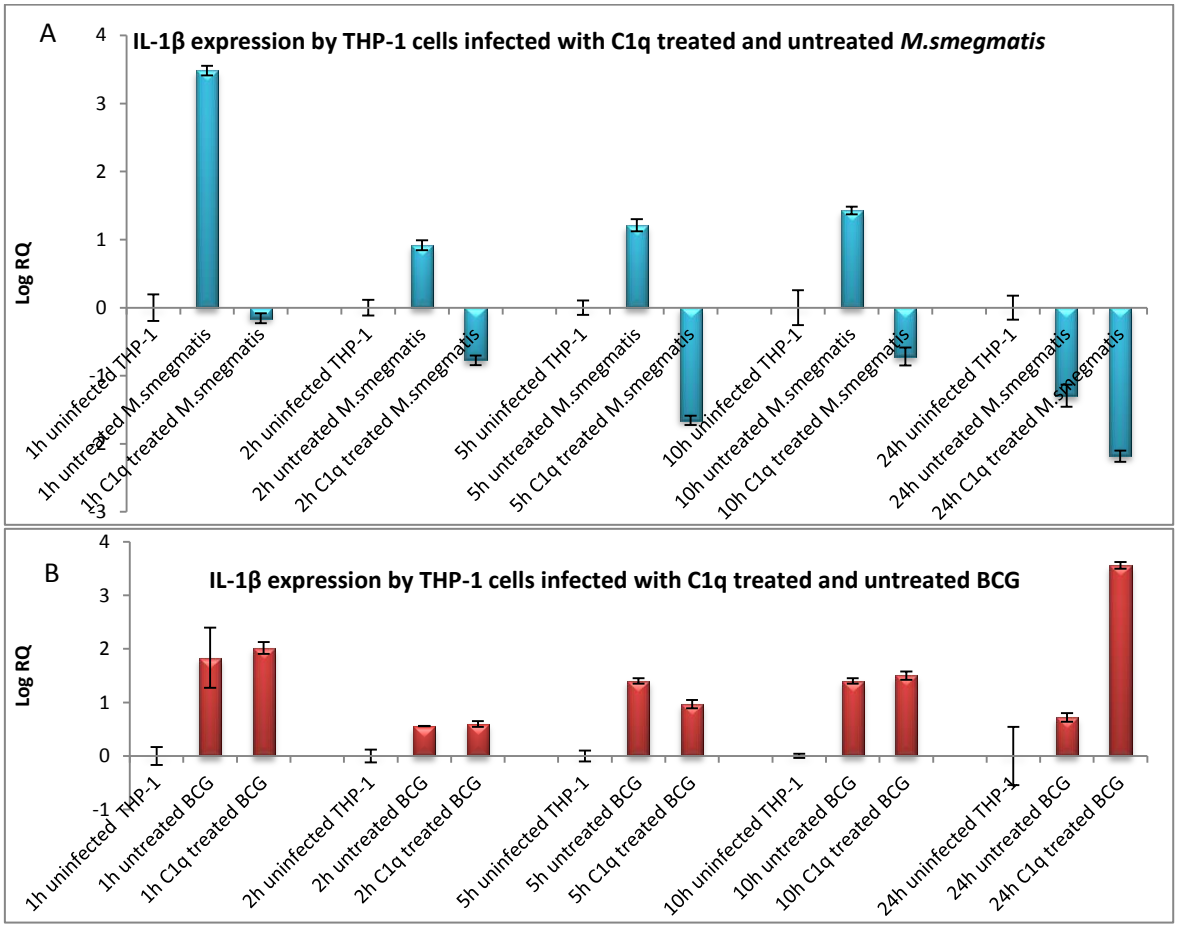

Figure 4.17: Expression of IL-1 β gene by THP-1 cells infected with C1q treated and untreated *M.smegmatis* (A) and BCG (B). THP-1 cells were incubated for 1, 2, 5, 10 and 24 hours after infection with mycobacteria at 37^0C inside CO_2 incubator. The cell pellet was collected and used for RNA extraction and cDNA synthesis used in this analysis. The expression of the gene was measured using qPCR and data was normalized to 18sRNA expression as control. RQ values were calculated using the formula; $RQ=2^{-\Delta\Delta Ct}$. Log RQ values were plotted to show the gene expression. Un-infected THP-1 cells were used as negative control. Each bar represents the average of triplicate readings. Error bars represent ±standard deviation.

4.2.11.4 Expression of interleukin -6 (IL-6)

The role of IL-6 in tuberculosis is still unclear. It plays differing roles in the pathogenesis of tuberculosis. IL-6 inhibits TNF-α and IL-1β production and facilitates mycobacterial growth (Schindler et al., 1990). On the other hand, IL-6 deficient mice have been shown to be more susceptible to *Mtb* infection (Saunders et al., 2000). The pro-inflammatory cytokines IL-6 was expressed after 1, 2, 5, and 10 hours by THP-1 cells infected with untreated *M.smegmatis* only (Figure 2.18-A). While, IL-6 was expressed after 1, 2, 5, 10 and 24 hours by THP-1 cells infected with C1q treated and untreated BCG. After 24hours the expression of IL-6 was increased in THP-1 cells infected with C1q treated BCG only (Figure 2.18-B).

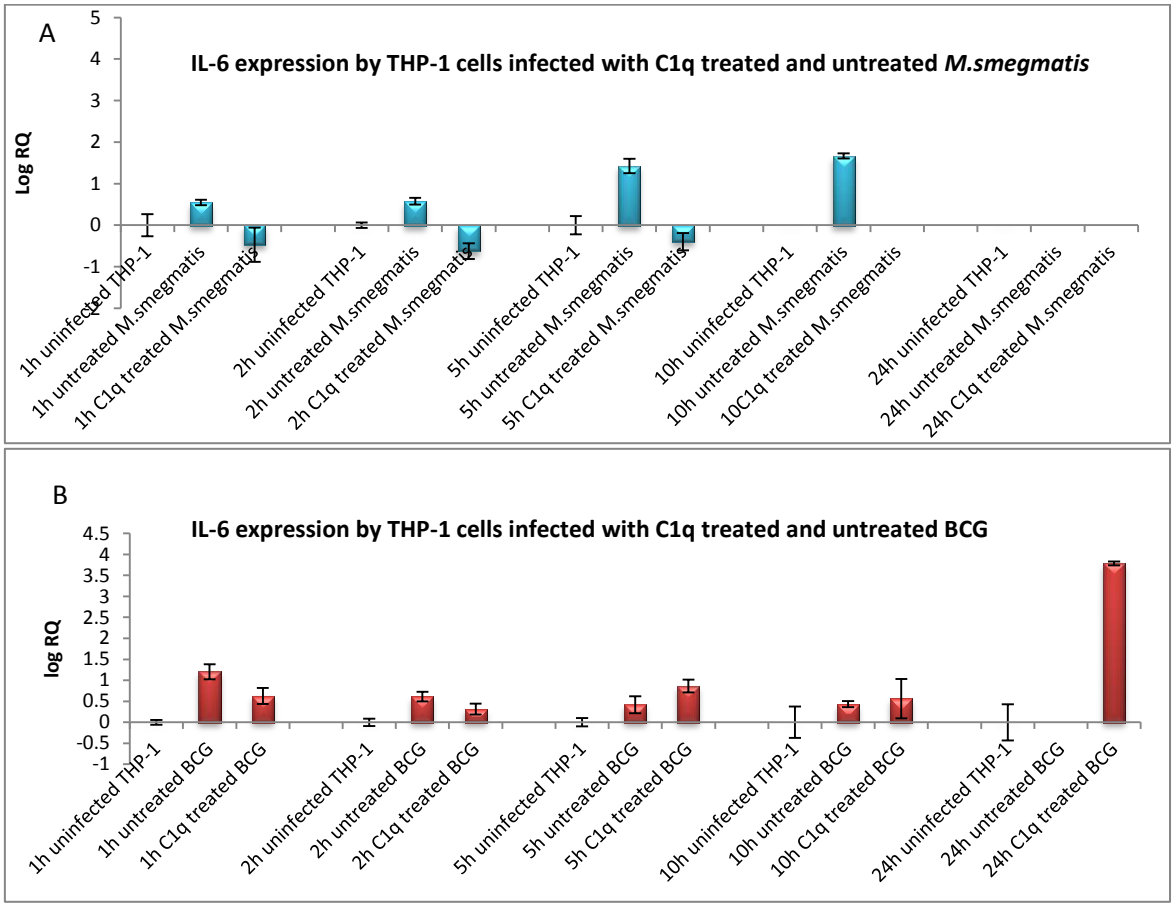

Figure 4.18: Expression of IL-6 gene by THP-1 cells infected with C1q treated BCG and untreated *M.smegmatis* (A) and BCG (B). THP-1 cells were incubated for 1, 2, 5, 10 and 24 hours after infection with mycobacteria at 37°C inside a CO_2 incubator. The cell pellet was collected and used for RNA extraction and cDNA synthesis used in this analysis. The expression of the gene was measured using qPCR and data was normalized to 18sRNA expression as control. RQ values were calculated using the formula; $RQ=2^{\Delta\Delta Ct}$. Log RQ values were plotted to show the gene expression. Un-infected THP-1 cells were used as negative control. Each bar represents the average of triplicate readings. Error bars represent the ±standard deviation.

4.2.11.5 Expression of interleukin-12 (IL-12)

IL-12 is pro-inflammatory cytokine. It has been detected inside granulomas. It initiates Th1 immunity against tuberculosis. Giving IL-12 supplements have been shown to kill *Mtb* in infected mice (Flyyn et al., 1995). The pro-inflammatory cytokines IL-12 was expressed after 1, 2 and 5 hours by THP-1 cells infected with untreated *M.smegmatis* only (Figure 4.19-A), while IL-12 was expressed after 1 hour and up to 5 hours by THP-1 cells infected with C1q treated and untreated BCG. C1q treatment of BCG slightly increased IL-12 expression by THP-1 cells. The expression of this cytokine was down regulated after 10 & 24 hours (Figure 4.19-B).

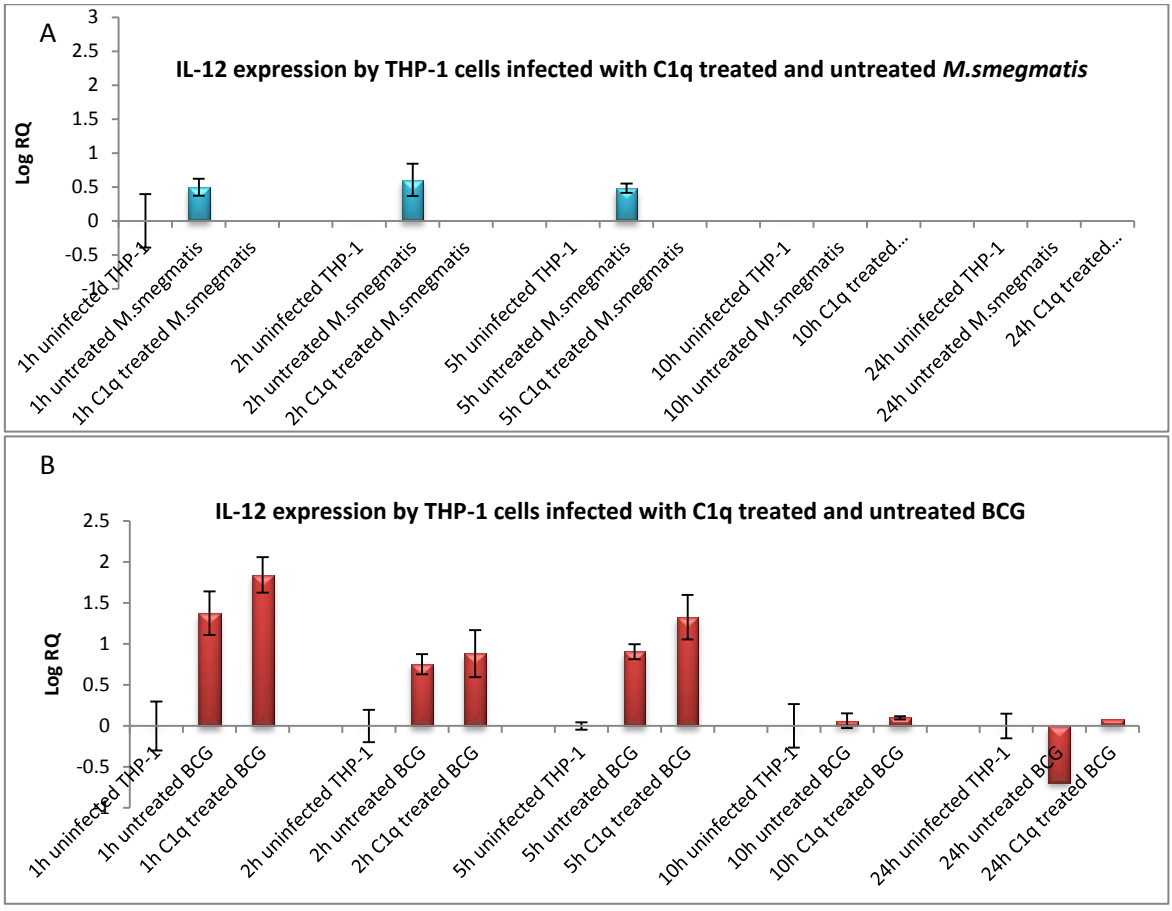

Figure 4.19: Expression of IL-12 gene by THP-1 cells infected with C1q treated BCG and untreated *M.smegmatis* (A) and BCG (B). THP-1 cells were incubated for 1, 2, 5, 10 and 24 hours after infection with mycobacteria at 37°C inside a CO_2 incubator. The cell pellet was collected and used for RNA extraction and cDNA synthesis used in this analysis. The expression of the gene was measured using qPCR and data was normalized to 18sRNA expression as control. RQ values were calculated using the formula; $RQ=2^{-\Delta\Delta Ct}$. Log RQ values were plotted to show the gene expression. Un-infected THP-1 cells were used as negative control. Each bar represents the average of triplicate readings. Error bars represent ±standard deviation.

4.2.11.6 Expression of interleukin (IL-10)

IL-10 is an anti-inflammatory cytokine. It deactivates macrophages and down regulates the expression of IL-12 and TNF-α which lead to a decrease in reactive nitrogen intermediates (RNI) and increases mycobacterial survival.

The anti-inflammatory cytokines IL-10 was expressed after 1, 2, 5, and 10 hours by THP-1 cells infected with untreated *M.smegmatis* only (Figure 4.20-A). On the other hand, Both THP-1 cells infected with C1q treated and untreated BCG expresses IL-10 up to 5 hours of incubation and the expression is higher in C1q treated BCG (Figure 4.20-B).

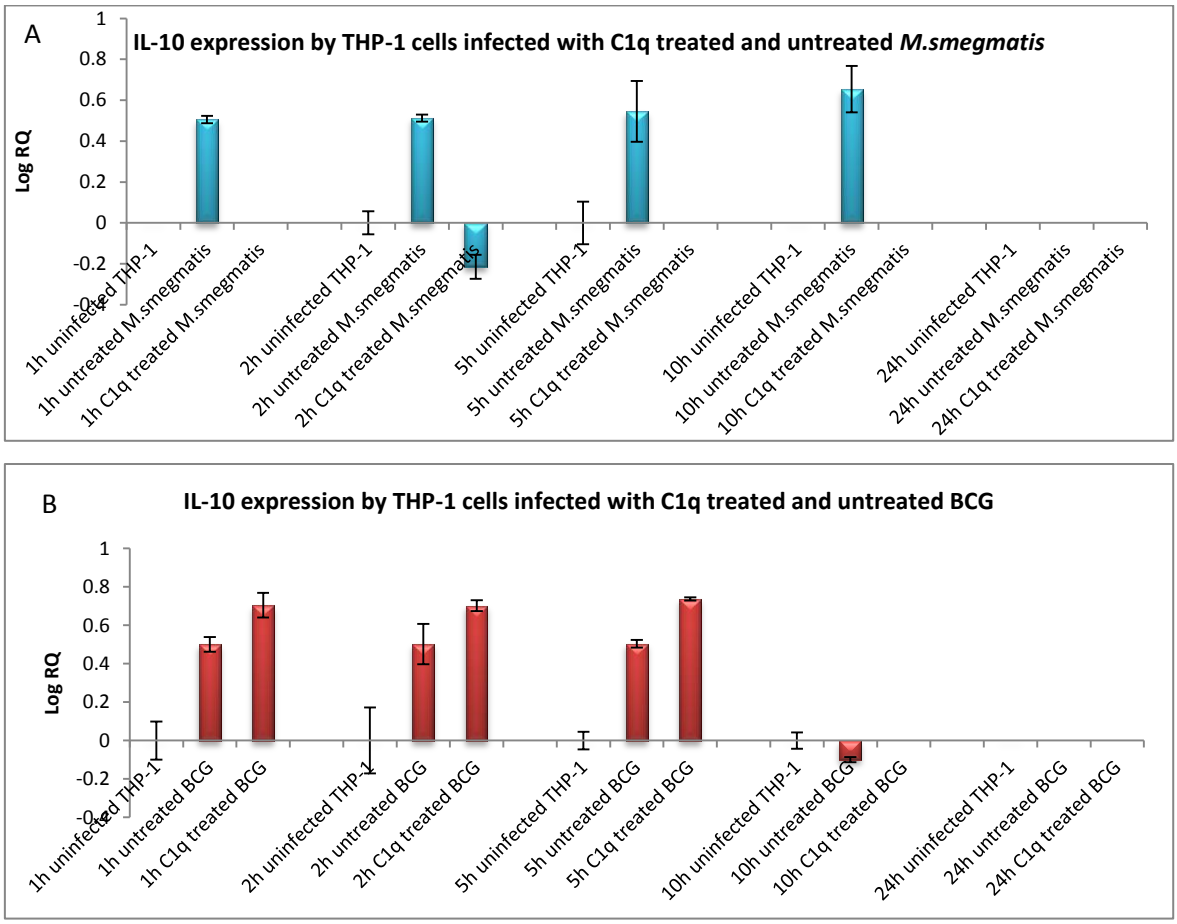

Figure 4.20: Expression of IL-10 gene by THP-1 cells infected with C1q treated *M.smegmatis* (A) and BCG (B). THP-1 cells were incubated for 1, 2, 5, 10 and 24 hours after infection with mycobacteria at 37^0C inside CO_2 incubator. The cell pellet was collected and used for RNA extraction and cDNA synthesis used in this analysis. The expression of the gene was measured using qPCR and data was normalized to 18sRNA expression as control. RQ values were calculated using the formula; $RQ=2^{-\Delta\Delta Ct}$. Log RQ values were plotted to show the gene expression. Un-infected THP-1 cells were used as negative control. Each bar represents the average of triplicate readings. Error bars represent ±standard deviation.

4.2.11.7 Expression of transforming growth factor-β (TGF-β)

TGF-β is an anti-inflammatory cytokine that opposes the protective immunity in tuberculosis. It is expressed by infected macrophages and inhibits ROI and RNI production (Ding et al., 1990). Additionally, it increases mycobacterial growth (Toossi et al., 1995). The anti-inflammatory cytokines TGF-β was expressed after 10 and 24 hours by THP-1 cells infected with untreated *M.smegmatis* only (Figure 4.21-A). On the other hand, TGF-β was expressed after 5 and 10 hours by THP-1 cells infected with both C1q treated and untreated BCG. The expression of this cytokine was higher in THP-1 cells infected with C1q treated BCG as compared to untreated BCG (Figure 4.21-B).

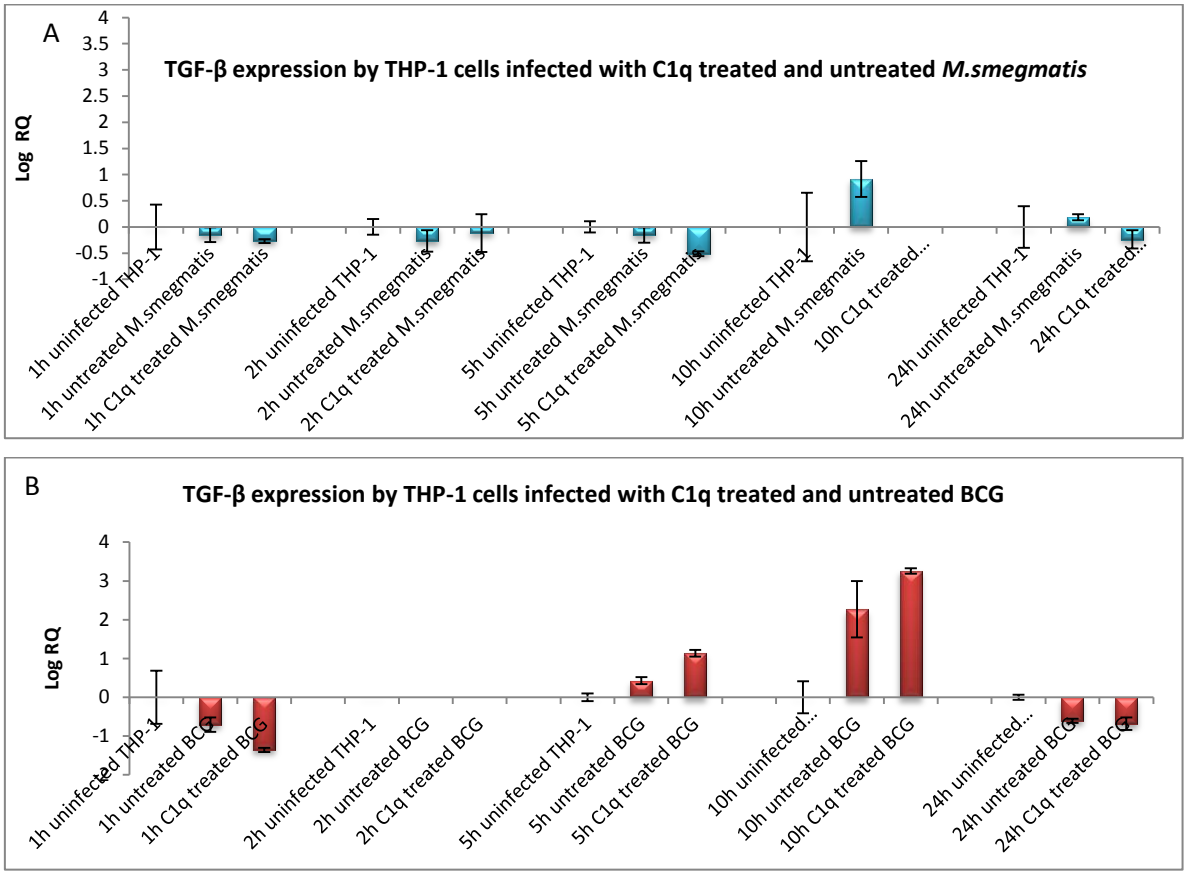

Figure 4.21: Expression of TGF-β gene by THP-1 cells infected with both C1q treated *M.smegmatis* (A) and BCG (B). THP-1 cells were incubated for 1, 2, 5, 10 and 24 hours after infection with mycobacteria at 37°C inside a CO_2 incubator. The cell pellet was collected and used for RNA extraction and cDNA synthesis used in this analysis. The expression of the gene was measured using qPCR and data was normalized to 18sRNA expression as control. RQ values were calculated using the formula; $RQ=2^{-\Delta\Delta Ct}$. Log RQ values were plotted to show the gene expression. Un-infected THP-1 cells were used as negative control. Each bar represents the average of triplicate readings. Error bars represent ±standard deviation.

4.2.12 Neutralising the effect of (inducible nitric oxide synthase, pro-inflammatory and anti-inflammatory cytokines) on BCG growth inside THP-1 cells

4.2.12.1 Neutralising the effect of inducible nitric oxide synthase (iNOS) on BCG growth inside THP1 cells

In this study, THP-1 cells infected with C1q treated BCG showed lower numbers of bacterial colonies in comparison with THP-1 cells infected with untreated BCG (Figure 4.22-A). The number of bacterial colonies was increased after the addition of inducible nitric oxide synthase inhibitor (NG-Methyl-L-arginine acetate) to THP-1 cells infected with C1q treated BCG (Figure 4.22 A & 4.22B).

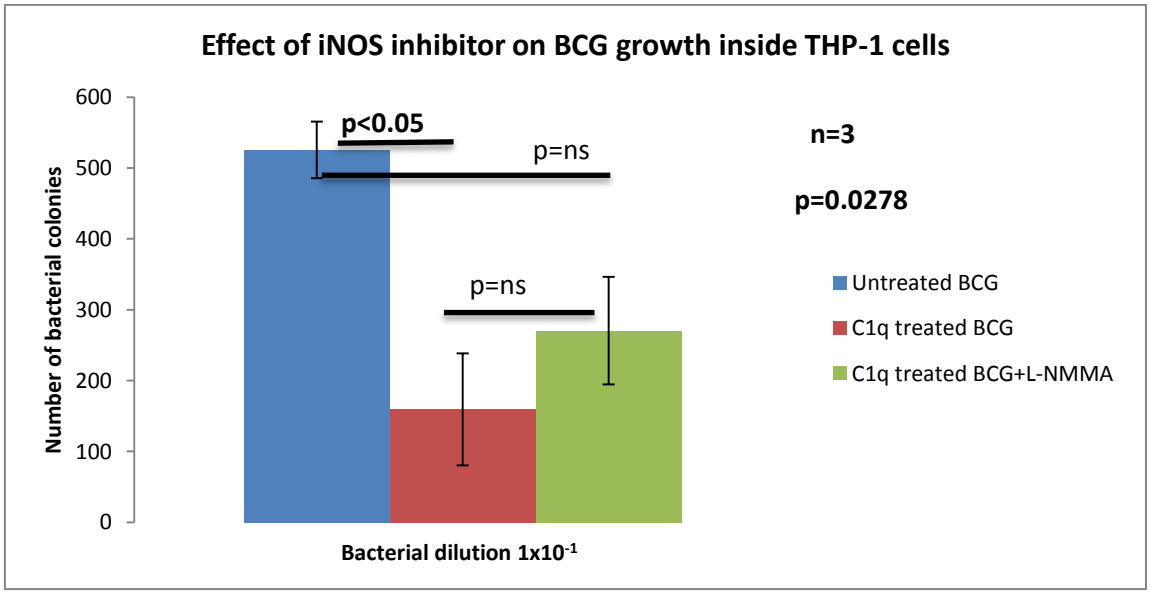

Figure 4.22-A: Effect of iNOS inhibitor on BCG growth inside THP-1 cells. C1q treated BCG showed lower numbers of bacterial colonies in comparison with THP-1 cells infected with untreated BCG. The number of BCG colonies was increased after the addition of iNOS inhibitor to THP-1 cells infected with C1q treated BCG. Each histogram represents average of three experiments. Error bars represent ±standard error of the mean. Multiple comparison of the data sets was done using Friedman test (p=0.0278). Individual data were compared with each other using Dunn's post hoc test: Untreated BCG vs C1q, p<0.05; Untreated BCG vs L-NMMA, p=ns; C1q vs L-NMMA, P=ns (non-significant).

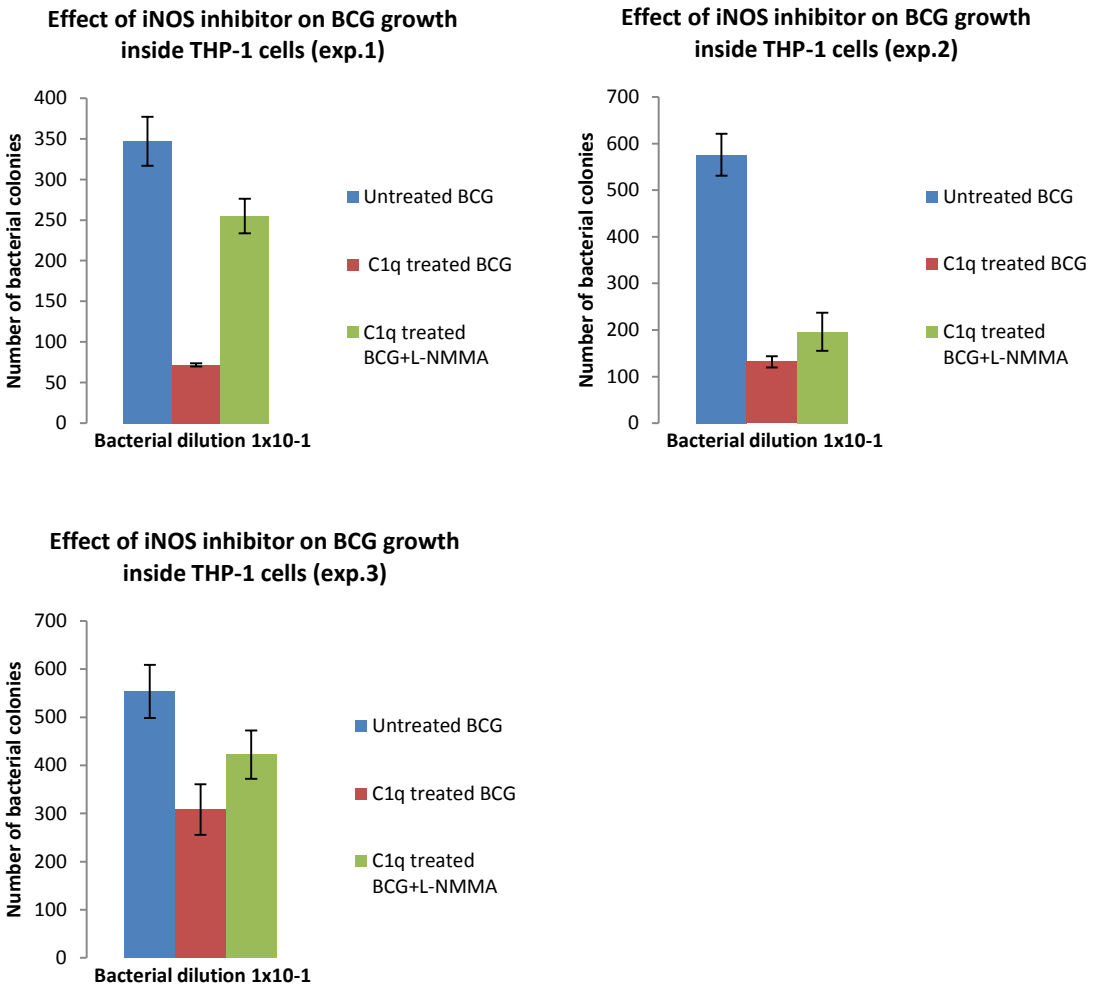

Figure 4.22-B: Effect of neutralising iNOS on C1q treated BCG growth inside THP-1 cells (3 individual experiments). Each bar represents the average of triplicate readings. Error bars represent ±standard.

4.2.12.2 Neutralising the effect of TNF-α on BCG growth inside THP1 cells

In this study, THP-1 cells infected with C1q treated BCG showed lower numbers of bacterial colonies in comparison with THP-1 cells infected with untreated BCG (Figure 4.23-A). The number of bacterial colonies was increased after the addition of mouse anti human TNF-α, to THP-1 cells infected with C1q treated BCG. Anti-immunoglobulin G (IgG) (mouse) was used as a negative control in this study (Figure 4.23).

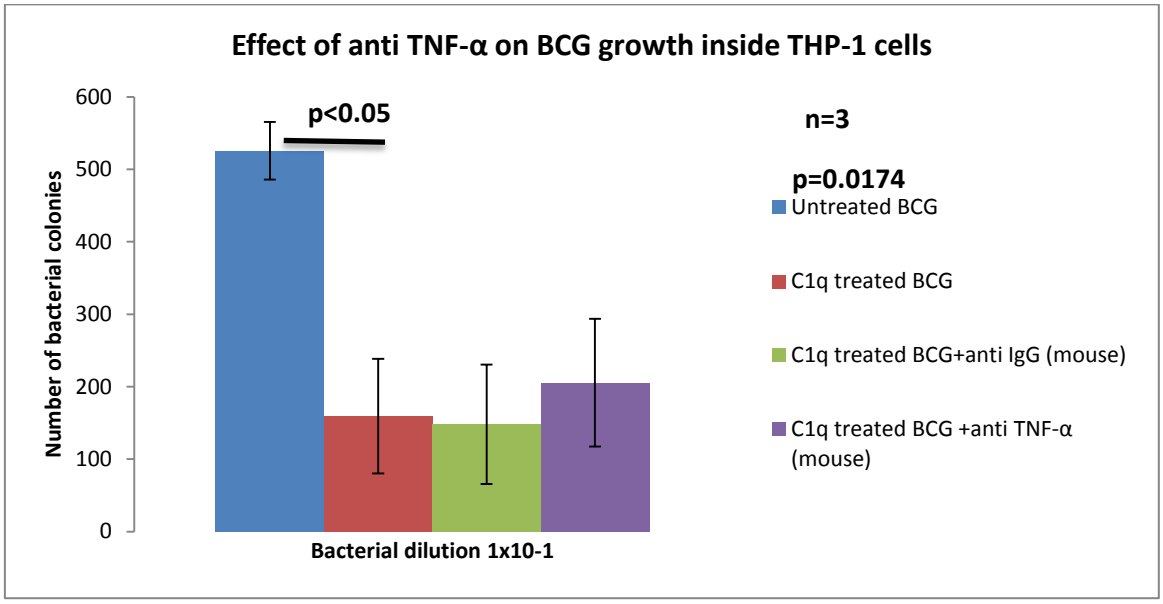

Figure 4.23-A: Effect of anti TNF-α on BCG growth inside THP-1 cells. C1q treated BCG showed lower numbers of bacterial colonies in comparison with THP-1 cells infected with untreated BCG. The number of BCG colonies was increased after the addition of antibody against TNF-α to THP-1 cells infected with C1q treated BCG. Anti IgG (mouse) was used as a negative control in this study. Each histogram represents average of three experiments. Error bars represent ±standard error of the mean. Multiple comparison of the data sets was done using Friedman test (p=0.0174). Individual data were compared with each other using Dunn's post hoc test: Untreated BCG vs C1q, p<0.05 (signficant); Untreated BCG vs C1q treated BCG incubated with anti-IgG from mouse, p=ns; Untreated BCG vs C1q treated BCG incubated with anti-TNF-α, p=ns (non significant).

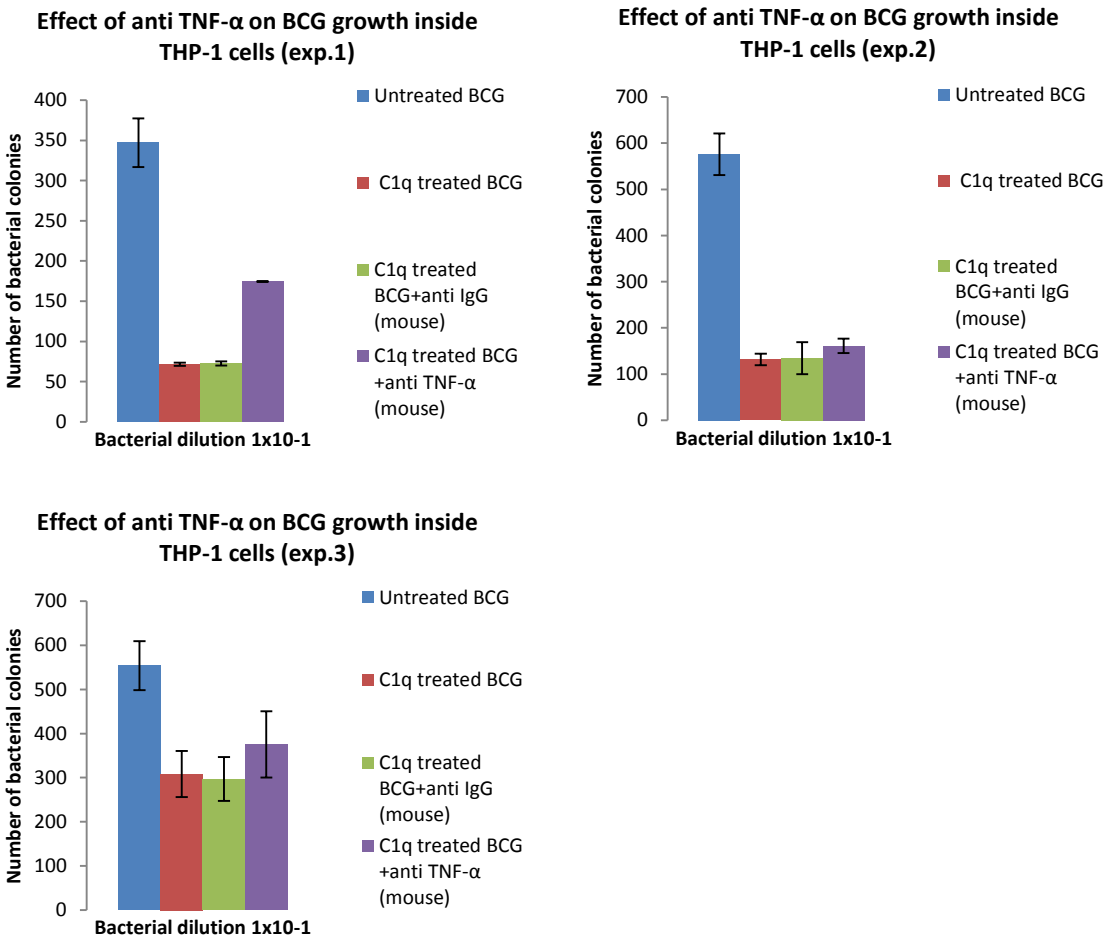

Figure 4.23-B: Effect of neutralising TNF-α on C1q treated BCG growth inside THP-1 cells (3 individual experiments). Each bar represents the average of triplicate readings. Error bars represent ±standard.

4.2.12.3 Neutralising the effect of IL-6 on BCG growth inside THP1 cells

In this study, THP-1 cells infected with 10µg/ml C1q treated BCG showed lower numbers of bacterial colonies in comparison with THP-1 cells infected with untreated BCG (Figure 4.24-A). The number of bacterial colonies was increased after the addition of mouse anti human IL-6, to THP-1 cells infected with C1q treated BCG. Anti-IgG from mouse was used as a negative control in this study (Figure 4.24).

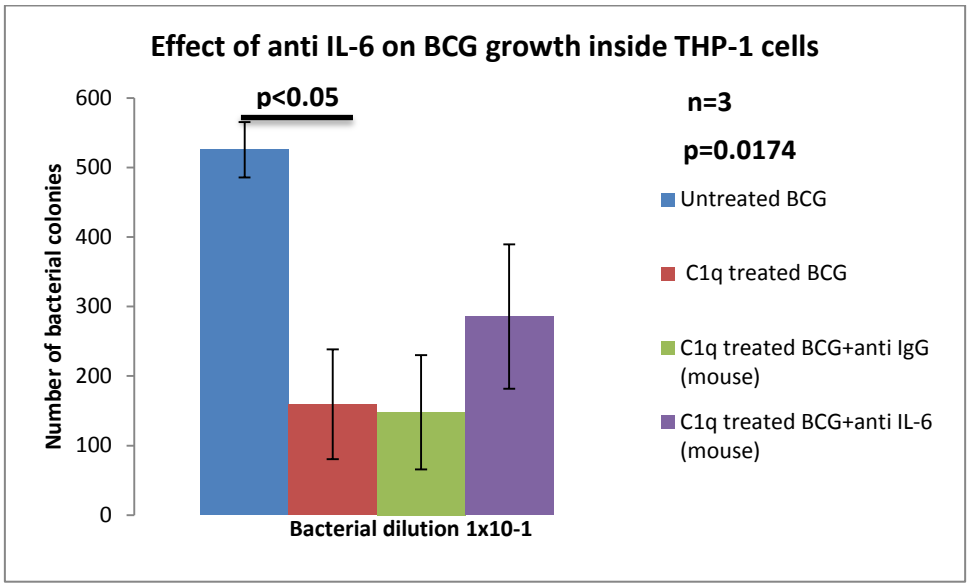

Figure 4.24-A: Effect of anti-IL-6 on BCG growth inside THP-1 cells. The number of BCG colonies decreased after C1q treatment of BCG. The number of colonies was increased after the addition of antibody against IL-6 to THP-1 cells infected with C1q treated BCG. Anti- IgG (mouse) was used as a negative control in this study. Each histogram represents average of three experiments. Error bars represent ±standard error of the mean. Multiple comparison of the data sets was done using Friedman test (p=0.0174). Individual data were compared with each other using Dunn's post hoc test: Negative vs C1q treated BCG, p<0.05 (signficant); Untreated BCG vs C1q treated BCG incubated with anti-IgG from mouse, p=ns; Untreated BCG vs C1q treated BCG incubated with anti-IL-6, p=ns (non significant).

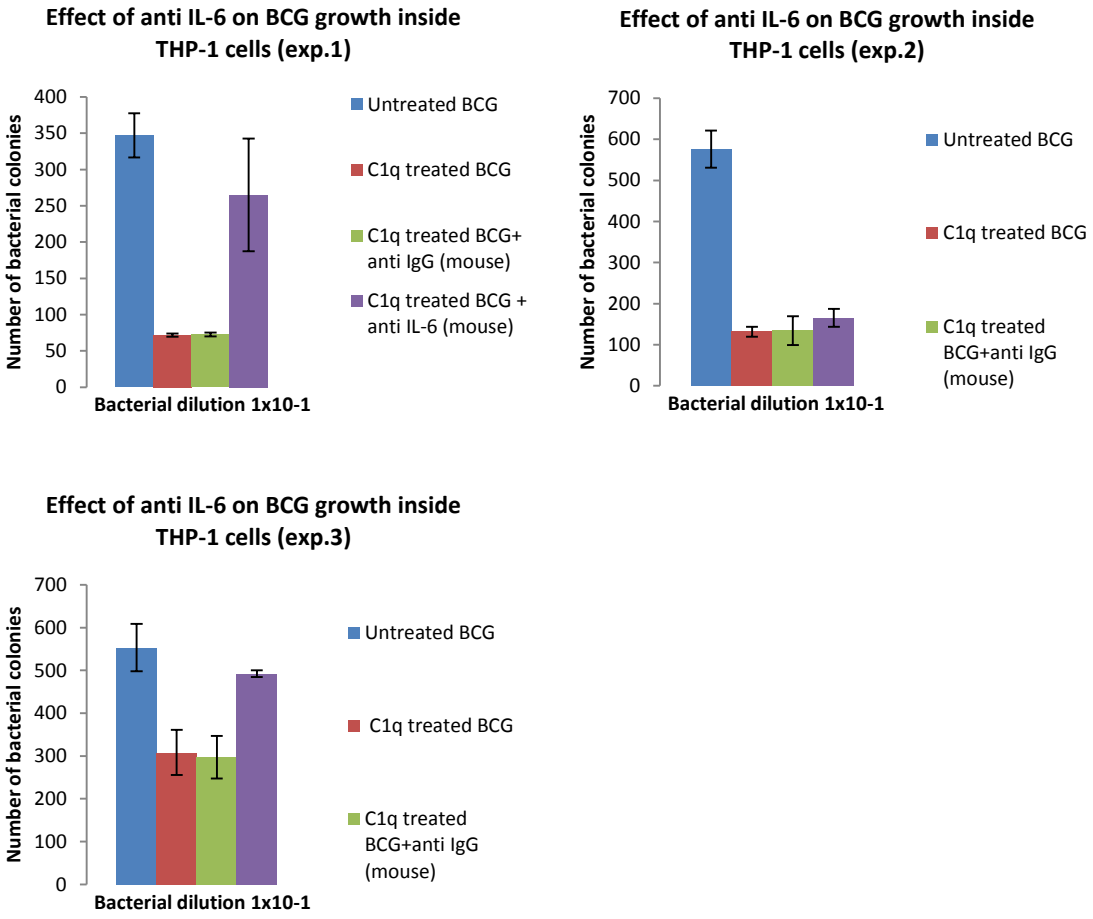

Figure 4.24-B: Effect of neutralising IL-6 on C1q treated BCG growth inside THP-1 cells (3 individual experiments). Each bar represents the average of triplicate readings. Error bars represent ±standard.

4.2.12.4 Neutralising the effect of TGF-β on BCG growth inside THP1 cells

In this study, THP-1 cells infected with 10µg/ml C1q treated BCG showed lower numbers of bacterial colonies in comparison with THP-1 cells infected with untreated BCG (Figure 4.25-A). The number of bacterial colonies was decreased after the addition of Rabbit anti-human TGF-β, to THP-1 cells infected with C1q treated BCG. An anti-IgG from Rabbit was used as a negative control in this study (Figure 4.25).

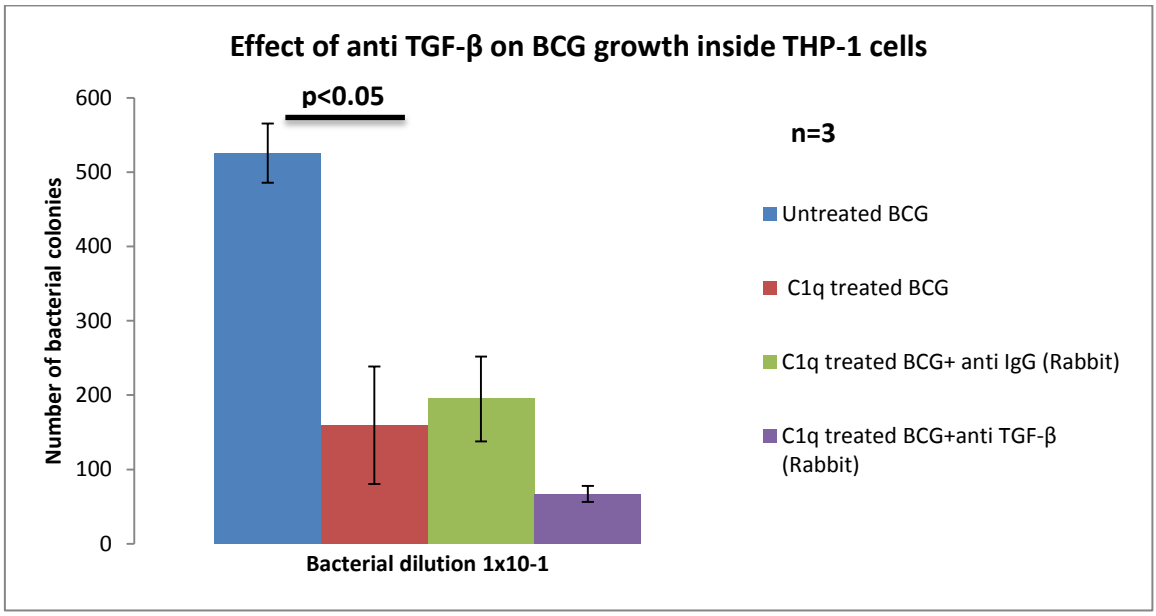

Figure 4.25-A: Effect of anti-TGF-β on BCG growth inside THP-1 cells. The number of BCG colonies was decreased after the addition of antibody against TGF-β to THP-1 cells infected with C1q treated BCG. Anti- IgG from Rabbit was used as a negative control in this study. Each histogram represents average of three experiments. Error bars represent ±standard error of the mean. Multiple comparison of the data sets was done using Friedman test (p=0.0538). Individual data were compared with each other using Dunn's post hoc test: Untreated BCG vs 10µg/ml C1q, p<0.05; Untreated BCG vs C1q treated BCG incubated with anti-IgG from rabbit, p=ns; Untreated BCG vs C1q treated BCG incubated with anti-TGF-β, p=ns (non significant).

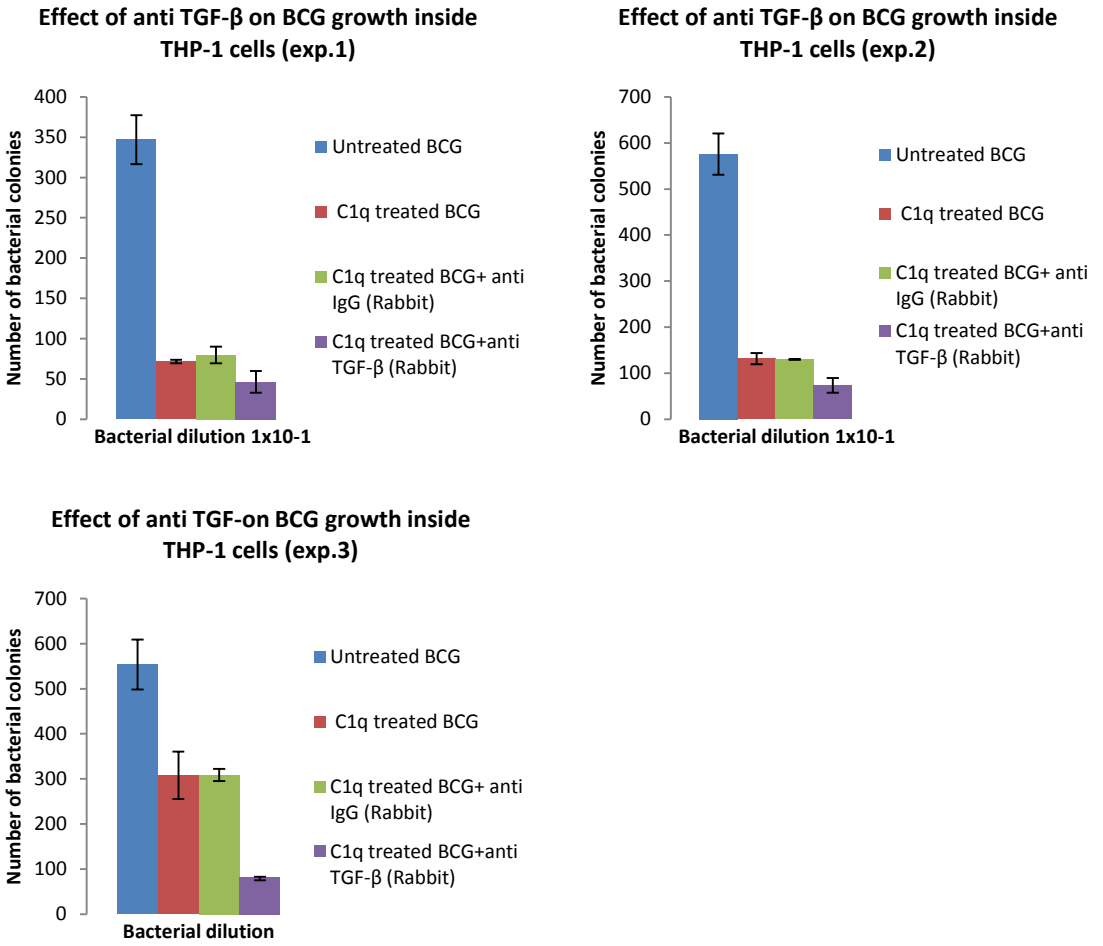

Figure 4.25-B: Effect of neutralising TGF-β on C1q treated BCG growth inside THP-1 cells (3 individual experiments). Each bar represents the average of triplicate readings. Error bars represent ±standard.

4.2.13 Studying cytokines and chemokines production in BCG infected THP-1 cells by Multiplex analysis

Multiplex was used in this study to detect and quantify different cytokines and chemokines produced by THP-1 cells infected with C1q treated and untreated BCG after 24 hours of infection. Different cytokines (IL-1β, IL-6, IL-12 and IL-10) and chemokines (MIP-1α, MIP-1β, MCP-1, GM-CSF, MDC, and GRO) were detected by this analysis.

4.2.13.1 Effect of C1q on pro-inflammatory and anti-inflammatory cytokines production after 24 hours incubation

A group of cytokines (IL-1β, IL-6, IL-12 and IL-10) were produced by THP-1 cells infected with C1q treated BCG. IL-1β and IL-12 are pro-inflammatory cytokines produced by macrophages and they are protective in tuberculosis. Il-6 is pro-inflammatory cytokine produced by macrophages and its role is still unclear in *Mtb* pathogenesis. On the other hand, the anti-inflammatory cytokine IL-10 is also produced by macrophages and is known to increase mycobacterial survival by deactivating macrophages.

Multiplex analysis showed that THP-1 cells infected with C1q treated BCG enhanced the production of pro-inflammatory cytokines and anti-inflammatory cytokine IL-10 as compared to THP-1 cells infected with untreated BCG and uninfected THP-1 cells after 24 hours of incubation. The result shows that C1q enhanced the production of IL-1β in THP-1 cells infected with BCG as compared to untreated BCG and uninfected THP-1 cells (Figure 4.26-A). Also, C1q enhanced the production of IL-6, IL-12 and IL-10 although their production was low (8.5pg/ml & 2pg/ml) (Figure 4.26-B &C).

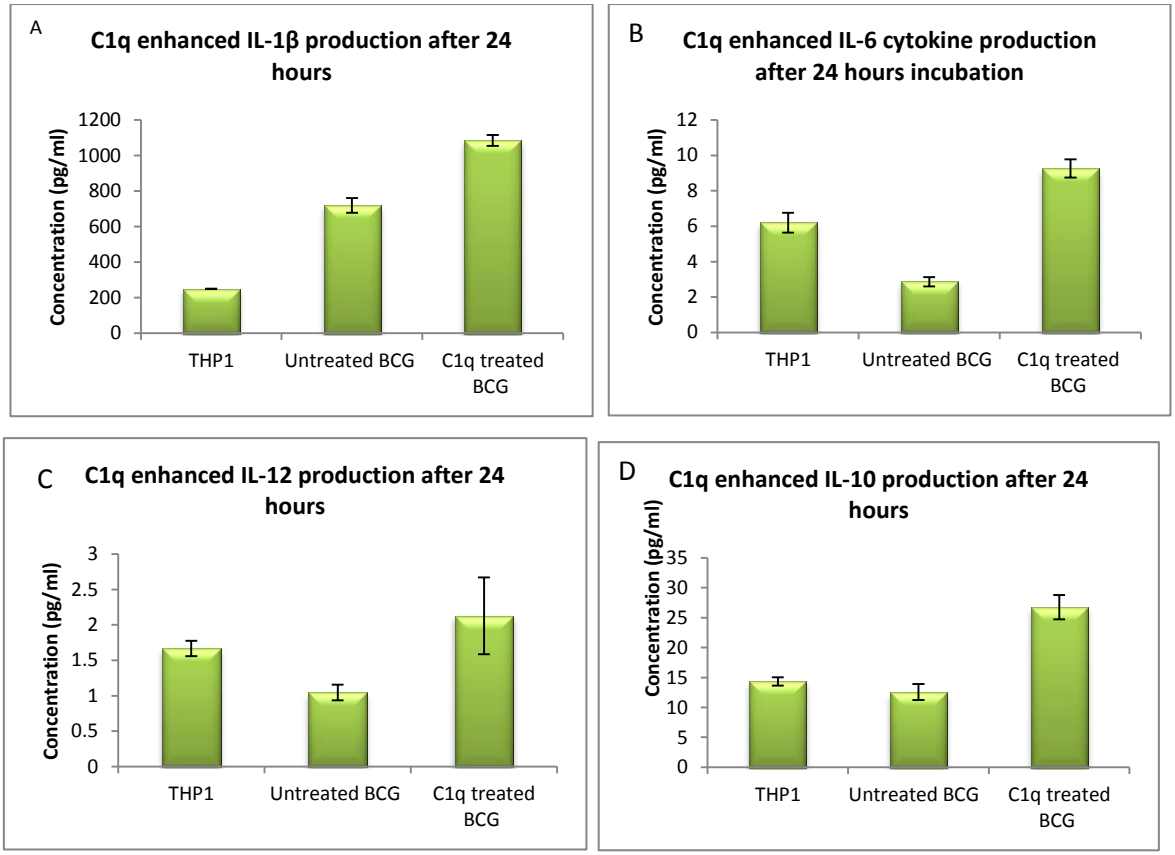

Figure 4.26: Effect of C1q on pro-inflammatory and anti-inflammatory cytokines production. C1q enhanced the production of IL-1β, IL-6, IL-12 and IL-10 inside THP-1 cells as compared to THP-1 cells infected with untreated BCG and uninfected THP-1 cells after 24 hours incubation. THP-1 cells were incubated for 24 hours after infection with mycobacteria at 37°C inside a CO_2 incubator. The supernatant was collected and used for this analysis. The quantity of each protein was measured using multiplex and graphs were plotted using excel. Each bar represents the average of duplicate readings. Error bars represent ±standard deviation.

4.2.13.2 Effect of C1q on chemokine production after 24 hours incubation

Chemokine production was studied using multiplex in order to investigate wheather their production increases in THP-1 cells infected with C1q treated BCG. Chemokines can be produced by monocytes and macrophages. They attract other immune cells such as neutrophils, monocytes, memory T cells, and dendritic cells to the infection site. Cell migration usually causes inflammation and tissue damage.

In this study, THP-1 cells infected with C1q treated BCG has dramatically enhanced the expression of IL-8 as compared to THP-1 cells infected with untreated BCG and uninfected THP-1 cells (4.27-A). Moreover, C1q enhanced the

expression of chemokines (MIP-1α, MIP-1β, MCP-1, GM-CSF, MDC, and GRO) (Figure 4.27) (Function of each chemokine is described in section 1.4.7). This suggests that C1q enhances the attraction of innate immune cells such as neutrophils and macrophages to the site of *Mtb* infection.

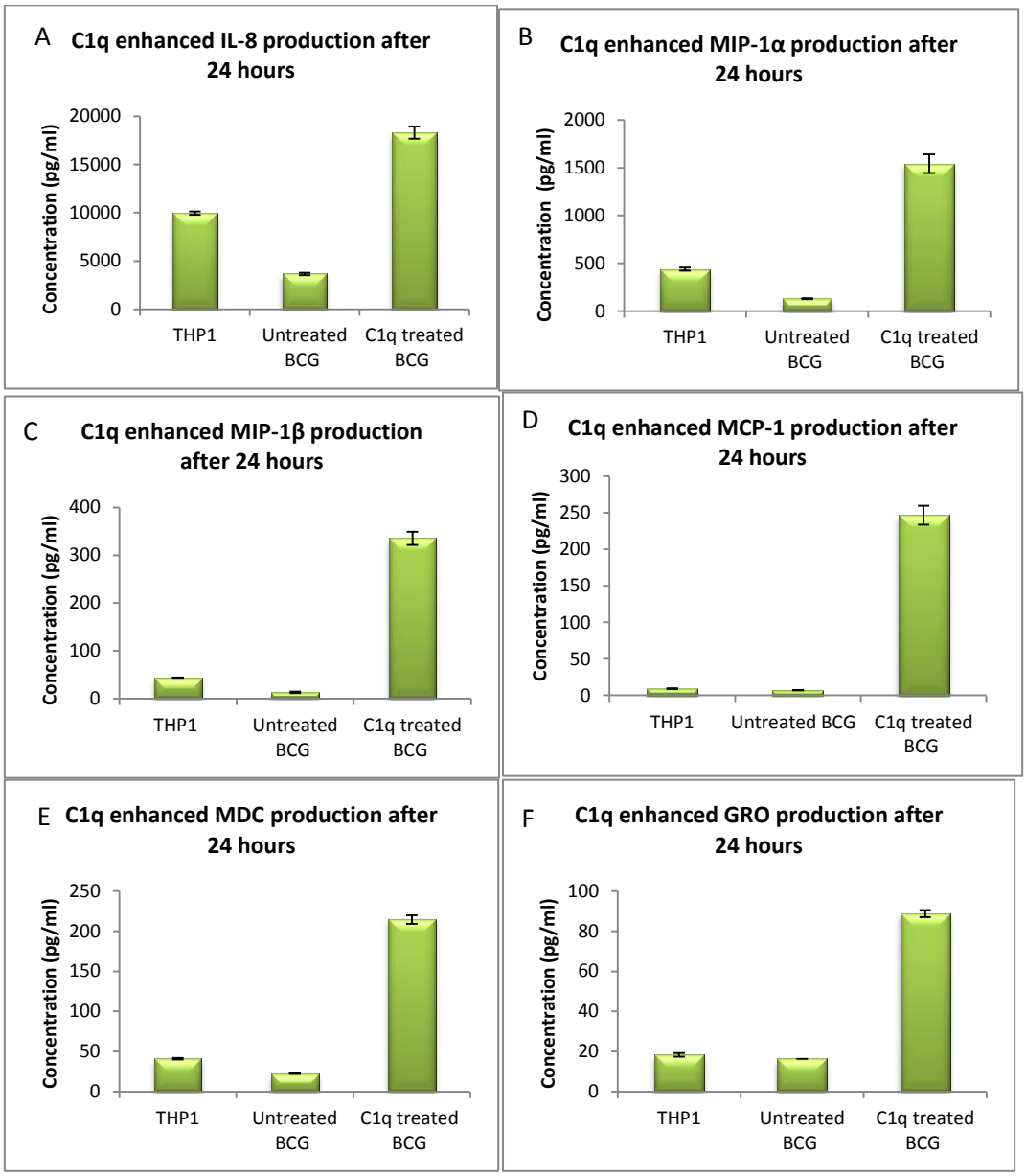

Figure 4.27: Effect of C1q on chemokine production. C1q enhanced the production of chemokine (IL-8, MIP-1α, MIP-1β, MCP-1, MDC and GRO) inside THP-1 cells after 24 hours incubation. THP-1 cells were incubated for 24 hours following infection with mycobacteria at 37°C inside a CO_2 incubator. The supernatant was collected and used for analysis. The quantity of each protein was measured using multiplex and graphs were plotted using excel. Each bar represents the average of duplicate readings. Error bars represent ±standard deviation.

4.2.14 Effect of C1q treated THP-1 cells on the phagocytosis of *M.smegmatis*

In these experiments, THP-1 cells were treated with C1q for 2 hours and washed before being infected with *M.smegmatis*. The result showed that the uptake of *M.smegmatis* by C1q treated THP-1 cells was increased as compared to untreated THP-1 cells (Negative) (Figure 4.28 A, B & C). All the 3 independent experiments have shown the same trend of increasing *M.smegmatis* uptake by C1q treated THP-1 cells (Figure 4.28-B)

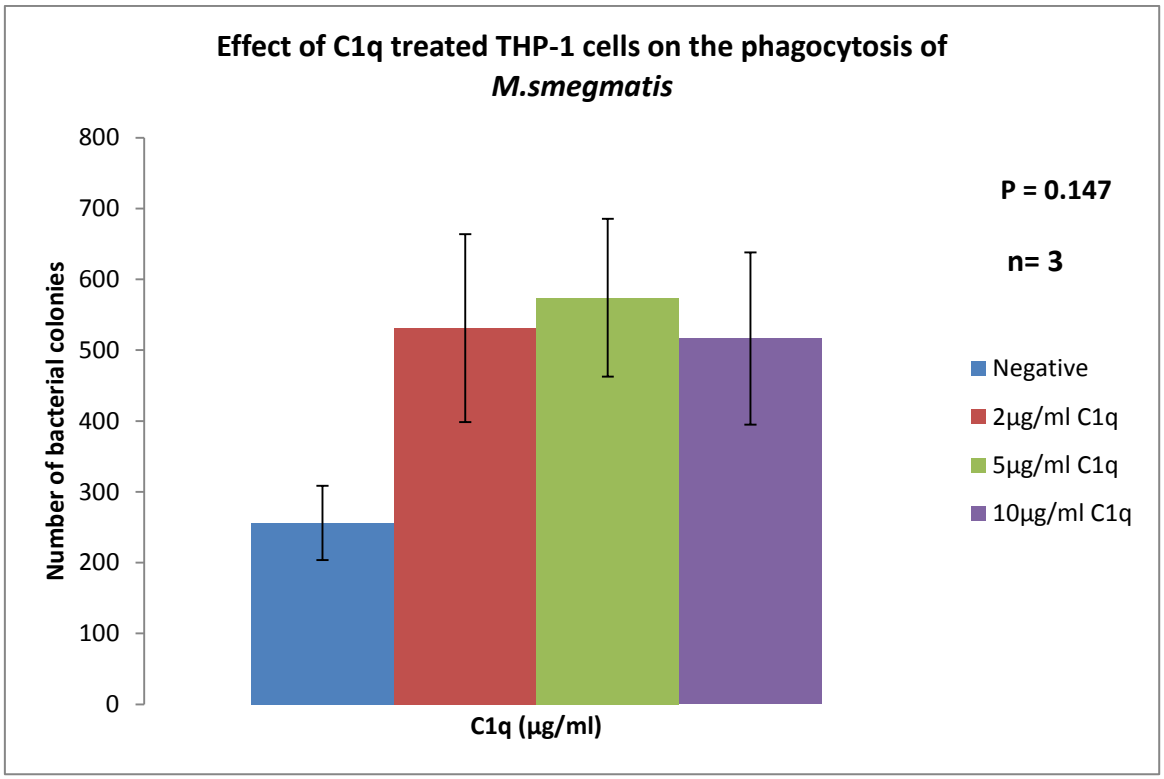

Figure 4.28-A: Effect of C1q treated THP-1 cells on the phagocytosis of *M. smegmatis*. THP-1 cells were treated with 10µg/ml C1q for 2 hours at 37^{o}C in presence of 5mM calcium chloride. Untreated THP-1 cells with calcium were used as a negative control. Following incubation, the cells were washed 3 times by centrifugation at 1500rpm for 10 minutes each. The cells were then infected with *M.smegmatis* in at ratio of 1:5 (THP-1 cell:bacteria), and incubated for 1 hour at 37^{o}C. Following incubation, magnetic beads bound with anti-human MHC class 1 were added to each tube in a 1:4 ratio (THP-1: beads) and the tubes were incubated in ice for 30 minutes on a shaker. Next, the cells were washed 3 times to remove extracellular bacteria. Washed cells were lysed with 0.1% saponin by vortexing for 15 minutes. A bacterial dilution of 1x10^{-1} was prepared and 250µl was plated on LB agar in triplicates. The plates were incubated at 37^{o}C for 72 hours. Each bar represents the average of 3 independent experiments**.** Error bars represent ±standard error of the mean. Multiple comparison of the data sets was done using Friedman test (p=0.147). Negative contains untreated THP-1 cells.

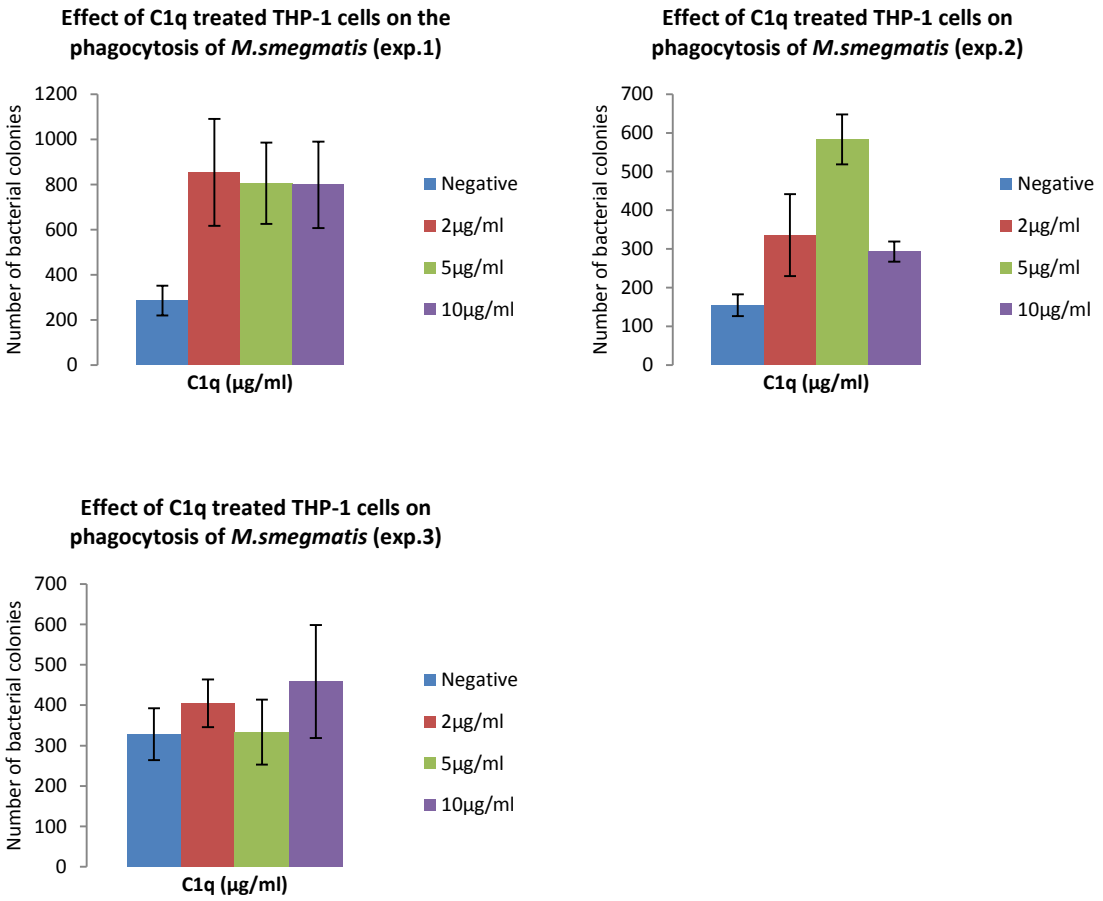

Figure 4.28-B: Effect of C1q treated THP-1 cells on the phagocytosis of *M.smegmatis* (3 individual experiments). Each bar represents the average triplicate readings. Error bars represent ±standard deviation. Negative contains untreated THP-1 cells.

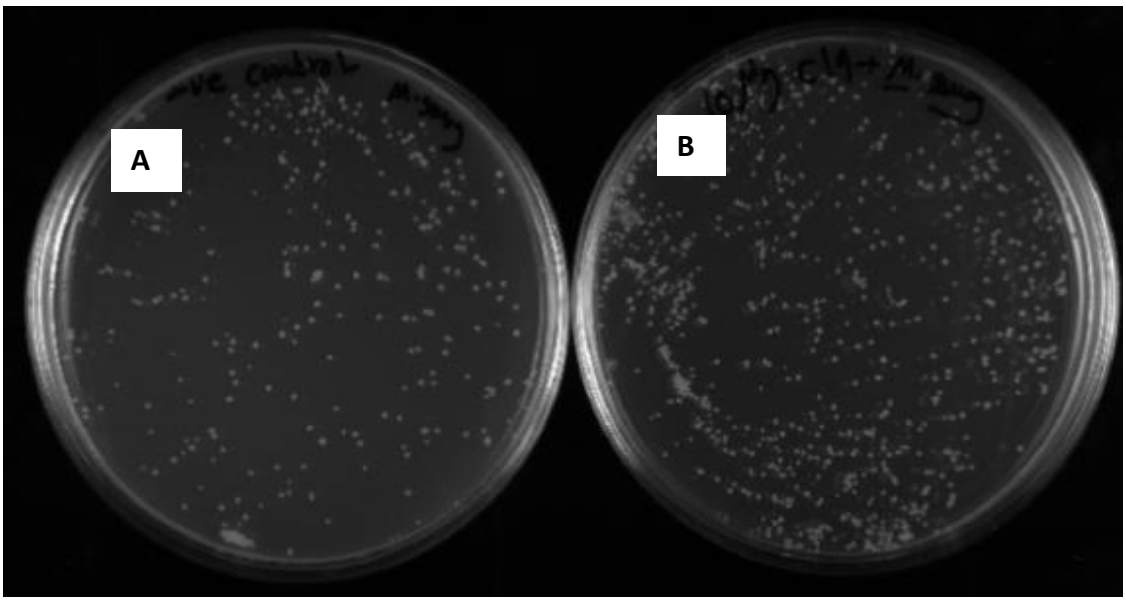

Figure 4.28-C: Effect of C1q treatment of THP-1 cells on the uptake of *M.smegmatis* (colonies on LB agar). THP-1 cells were treated for 2 hours and later washed and infected with *M.smegmatis*. The numbers of *M.smegmatis* colonies are higher in THP-1 cells treated with 5μg/ml and 10μg/ml C1q. One representative plate showing *M.smegmatis* growth for both untreated (A) and C1q treated THP-1 cells (B) are shown here.

4.2.15 Effect of C1q treated THP-1 cells on the growth of *M.smegmatis*

Pre-treatment of THP-1 cells with 10µg/ml C1q before *M.smegmatis* infection have shown to increase growth in 2 out of 3 experiments (Figure 4.29A & 4.29-B).

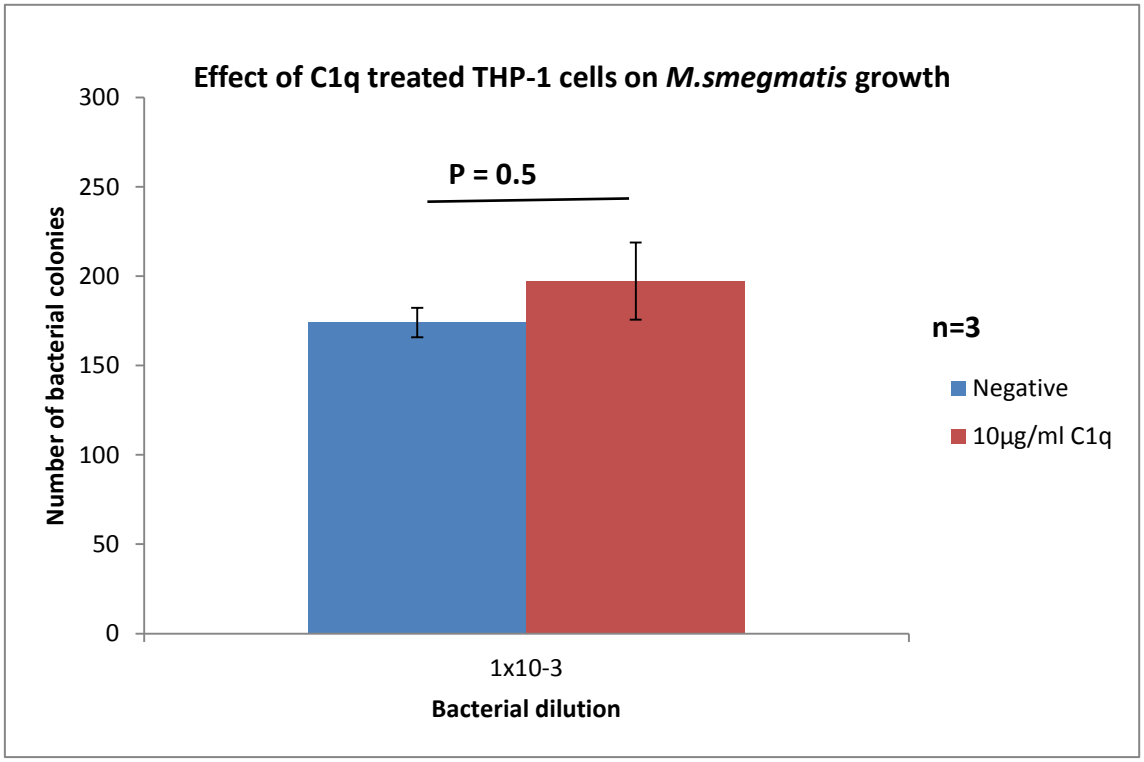

Figure 4.29-A: Effect of C1q treated THP-1 cells on the growth of *M. smegmatis* inside THP-1 cells. THP-1 cells were treated with C1q in presence of 5mM calcium chloride and incubated for 2 hours inside CO_2 incubator. Following incubation, THP-1 cells were washed 3 times from non-bound C1q by centrifugation at 1500rpm, 10 minutes each. Next, *M.smegmatis* was added to THP-1 cells in ratio 5:1 (bacteria: THP-1) and incubated for 1 hour at 37°C inside CO_2 incubator. Following incubation, magnetic beads bound with anti-human MHC class 1 was added in ratio 1:4 (THP-1: beads) and the tubes were incubated on ice for 30 minutes on a shaker. Next, the THP-1 cells were washed 3 times to remove the extracellular bacteria. Washed cells were suspended with 1ml of cRPMI without antibiotics and incubated for 24 hours inside CO_2 incubator. Next, the cell pellet was separated from the supernatant using magnet. Cells pellet was laysed with 0.1% saponin with vortexed for 15 minutes to release phagocytosed mycobacteria. Eual amounts of lysed cells and supernatant were mixed and bacterial dilutions were prepared, 250µl bacteria were plated in triplicates on LB agar and incubayed for 72 hours at 37°C. Each bar represents the average of 3 independent experiments. Error bars represent ±standard deviation. P value was calculated using Willcoxon test. Negative contains untreated THP-1 cells. Negative contains untreated THP-1 cells.

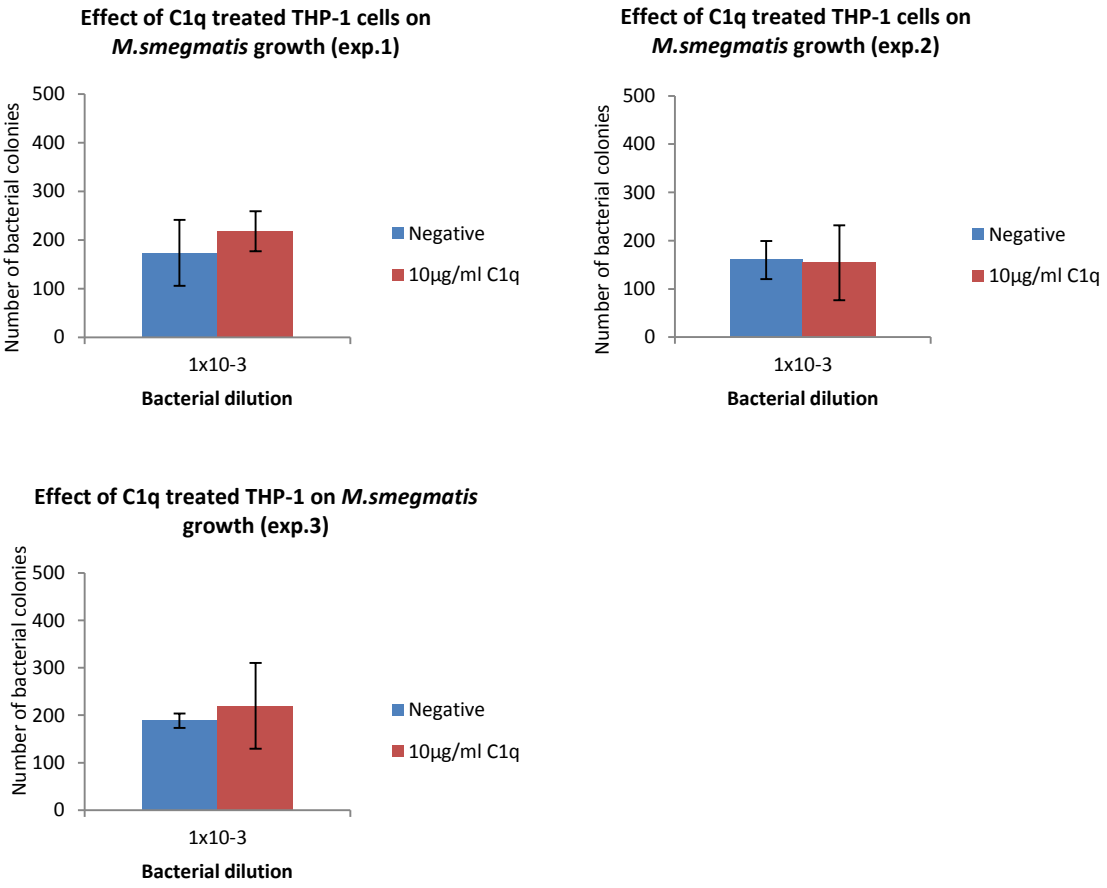

Figure 4.29-B: Effect of C1q treated THP-1 cells on the growth of *M. smegmatis* inside THP-1 cells (3 individual experiments). Each bar represents the average of triplicate readings. Error bars represent standard deviation. Each bar represents the average triplicate readings. Error bars represent ±standard deviation. Negative contains untreated THP-1 cells.

4.3 Discussion

This study showed the ability of C1q to bind directly with mycobacteria (*M.smegmatis* and BCG) in presence of 5mM $CaCl_2$ (Figure 4.3 & 4.4). The binding site of calcium is present at the top of globular head region of C1q (Gaboriaud *et al*., 2003). Calcium ion was shown to link ghA domain with ghB domain. Presence of calcium ion could increase the stability of the heterotrimeric assembly of C1q or it could have other roles (Gaboriaud *et al*., 2003). The direct binding of C1q with BCG has previously been shown by Carroll *et al*., 2009. Our results showed that addition of sugars slightly reduced C1q binding with mycobacteria (Figure 4.5), suggesting this protein has some lectin-like activity, therefore the C1q might be binding to mycobacterium through mannose sugar present on LAM in the mycobacterial cell wall. In addition, it has been shown previously that C1q binds lipids such as lipid A of *E.coli* (Tan *et al.,* 2011), and it could be possible that C1q may be interacting with lipids on mycobacterial cell wall.

C1q showed to bind with human monocytes cell line THP-1 (Figure 4.6 & 4.7). It has been reported that C1q can bind specifically with globular C1q receptor (gC1qR) on cells surface (Pednekar, 2013). Moreover, C1q binds complement receptor-1 (CR1) on phagocytic cells via collagen like region (Klickstein *et al.,* 1997).

In this study, C1q inhibited mycobacterial (*M.smegmatis* and BCG) growth directly by 37% and 21% respectively (Figure 4.9 & Figure 4.10). It has been reported previously that surfactant protein-D inhibits the growth of Gram negative bacteria (*E.coli*, *Klebsiella pneumonia*, *Enterobacter aerogenes* and *Legionella pneumonia)* by increasing membrane permeability (Wu *et al*., 2003). We have also shown that C1q inhibited *E.coli* growth directly by 42.5% (See data in appendix). Therefore, it could be possible that C1q might have inhibited bacterial growth by increasing membrane permeability. This can be tested in future by taking images for mycobacteria treated and untreated with C1q by electron microscopy, and comparing the structure of the cell wall.

This study showed that C1q treatment of mycobacteria (*M.smegmatis* & BCG) enhanced their uptake by THP-1 cells by 43% and 50% respectively (Figure 4.11

& Figure 4.12). It has been reported that *Mtb* and *BCG* can activate both the classical and alternative complement pathway (Furguson, 2004). This results in the formation of C3b or iC3b, which act as opsonins to help in the uptake of the mycobacterium via CR1, CR3 or CR4 receptors on the surface of macrophages (Cywes *et al.* 1996, Ferguson *et al*., 2004, Mueller-Ortiz *et al.,* 2001). CR3 plays an important role as in the absence of this receptor, human monocytes and macrophages showed 70-80% less *Mtb* uptake (Ferguson, 2004). Complement activation begins through the binding of C1q through its globular head region to the Fc portion of an antibody bound to a pathogen. This leads to a conformational change within the C1q collagen-like region that aid in C1r binding and activating the classical complement pathway (Roumenina *et al*., 2008). In this study, heat inactivated serum was used, and therefore, the role of complement activation, and the roles of C3b and iC3b in the uptake by phagocytic cells can be excluded. Since C1q has 6 trimeric subunits, this multi-valency could explain the possibility of C1q binding to both mycobacteria, as well as to phagocytic receptors on THP-1 cells, such as gC1qR and/or CR1. In this way, C1q can crosslink mycobacteria with these receptors, and may aid in the uptake of the mycobacteria inside these cells. In this study, C1q inhibited BCG growth inside THP-1 cells by 70% (Figure 4.14). Results obtained by q-PCR revealed that C1q inhibited BCG growth by enhancing the expression of inducible nitric oxide synthase (iNOS). The expression of iNOS was 73% and 14% higher in THP-1 cells infected with C1q treated BCG as compared to THP-1 cells infected with untreated BCG at 5h and 10h of incubation (Figure 4.15). Furthermore, BCG growth was increased when nitric oxide synthase was inhibited by adding nitric oxide synthase inhibitor (N^G-monomethyle-L-arginine monoacetate) to THP-1 cells infected with C1q treated BCG (Figure 4.22). This suggests that nitric oxide was involved in mycobacterial growth inhibition. It was shown previously that inhibition of iNOS in human leads to latent *Mtb* reactivation (Gardam *et al*., 2003). The gene expression of TNF-α was higher in THP-1 cells infected with C1q treated BCG as compared to untreated BCG (Figure 4.16). Moreover, neutralizing the function of TNF-α showed an increase in BCG growth (Figure 4.23). This suggests that C1q induced TNF-α was involved in the control of mycobacterial infection. It has been shown previously that TNF-α secretion by *Mtb* infected macrophages stimulates the production of

reactive nitrogen intermediates, which has been shown to be involved in control the *Mtb* infection (Chan *et al.,* 1992). Moreover, it has been shown that TNF-α deficient mice are more susceptible to *Mtb* infection (Kaneko *et al*., 1999), and neutralization of TNF-α in latent *Mtb* infection, induce the reactivation of the disease in mice (Mohan *et al*., 2001). In human, it has been shown that *Mtb* infection was reactivated in rheumatoid arthritis patients who received anti-TNF-α antibody treatment (Gardam *et al.,* 2003). The gene expression of IL-1β was higher in THP-1 cells infected with C1q treated BCG as compared to untreated BCG at 24 hours (Figure 4.17). Additionally, Multiplex analysis showed an increase in IL-1β production by THP-1 cells infected with C1q treated BCG after 24 hours of incubation (Figure 4.26-A). The pro-inflammatory cytokine IL-1β was shown to be involved in the host immune response against *Mtb.* It has been shown that the IL-1β receptor deficient mice are more susceptible to *Mtb* infection, and showed impaired granuloma formation (Juffermans *et al*., 2000, Yamada *et al.,* 2000). Our experiments showed the gene expression of pro-inflammatory cytokine IL-6 was enhanced by the THP1 cell infected with C1q treated as compared to untreated BCG (Figure 4.18). The same pattern was seen at protein level for this cytokine using multiplex analysis (Figure 4.26-B). Neutralizing the effect of IL-6 with Anti-IL-6 antibody showed increase in BCG growth in THP1 cells infected with C1q treated BCG (Figure 4.24). This study suggests that IL-6 may be responsible for inhibiting BCG growth inside THP-1 cells. It has been shown previously that IL-6 deficient mice are more susceptible to *Mtb* infection as compared to control mice (Saunders *et al.,* 2000). The gene expression of the pro-inflammatory cytokine IL-12 was also up-regulated in THP-1 cells infected with C1q treated BCG as compared to cells infected with untreated BCG (Figure 2.19). This pattern was also verified at protein level using multiplex analysis which showed higher L-12 production by THP1 cells infected with C1q treated BCG (Figure 4.26-C). The role of IL-12 is better understood in tuberculosis; it plays a role in INF-γ production by T cells and initiates Th1 immunity (Flyyn *et al*., 1995). IL-12 deficient mice were more susceptible to mycobacterial infection (Hossain and Norazmi, 2013).

This study showed that the expression of anti-inflammatory cytokines TGF-β was higher in THP-1 cells infected with C1q treated BCG as compared to untreated

BCG (4.21-B). Neutralizing the effect of TGF-β reduced BCG growth and this growth reduction is statistically significant (Figure 4.25). This finding is in consistence with previous findings where TGF-β was shown to be produced in excess amount at the site of active tuberculosis that inhibited T-cell activation. The same study showed neutralization of TGF-β improved T-cells response to *Mtb* in mice (Toossi and Ellner, 1998).

The gene expression of IL-10 was higher in THP-1 cells infected with C1q treated BCG as compared to untreated BCG (4.20-B). IL-10 is an anti-inflammatory cytokine that deactivates macrophages, down regulate the expression of TNF-α and IL-12, reduce INF- γ production by $CD4^+$ T- cells, decrease reactive nitrogen intermediates (RNIs) and increase *Mtb* survival (Gazzinelli *et al.,* 1992, Moore *et al.*, 2001). *Mtb* infection in IL-10 deficient mice results in reduced bacterial loads in the lung, as well as enhanced IFN-γ response, increased entry of CD4+ T cells to the lung, and enhanced production of chemokines and cytokines (Redford *et al*., 2010). On the other hand, presence of IL-10 & TGF-β could be helpful in reducing tissue damage caused by prolonged inflammation as a result of pro-inflammatory cytokines (Sanjabi *et al.,* 2009).

We demonstrated using multiplex analysis that C1q enhanced production of a number of chemokines by THP-1 cells infected with C1q treated as compared to untreated BCG. These chemokines include: Interleukin-8 (IL-8), Macrophage inflammatory proteins (MIP-1α & MIP-1β), Monocyte chemotactic proteins (MCP-1 & MCP-3), Granulocyte-colony stimulating factor (G-CSF), Macrophage derived chemokine (MDC) and Growth-related oncogene (GRO) (Figure 4.27). Chemkines play a protective role in tuberculosis by recruitment of polymorphonuclear cells (PMNs), monocytes, Th1 and γδ T cells (Ferrero *et al.,* 2003). IL-8 attracts neutrophils to the infection site (Baggiolini *et al.,* 1989). Also, release of MCP-1 and IL-8 was correlated with strong chemotaxis induction towards monocytes and PMNs (Ferrero *et al.,* 2003). MIP-1α & MIP-1β attract monocytes, natural killer cells, neutrophils and T cells to the site of infection (Schall et al., 1993). G-CSF regulates neutrophils survival by inhibition of apoptosis (Hu, B., & Yasui, K., 1997). MDC attracts monocytes and IL-2–activated natural killer cells to the infection site

(Godiska et al., 1997), and GRO attracts neutrophils and monocytes (Nakagawa et al., 1994).

In this study, THP-1 cells were incubated for 24 hours after BCG infection. This period showed the effect of C1q on killing of BCG by THP-1 cells. The doubling time for BCG during infection is around 24 hours (Beste et al., 2005), and it will be interesting to increase the infection period for THP-1 cells infected with BCG to 2, 3, 4 and 5 days in order to investigate the effect of C1q on the growth of BCG inside these cells. It has been shown previously that THP-1 cells infected with *M.avium* can kill mycobacteria up to 5 days of infection (Garcia et al., 2000), and the amount of fraction proteins and nucleolin inside THP-1 cells have not been changed for up to 5 days of infection. Nucleolin is a predominant protein found in growing THP-1 cells.

In contrast to BCG, this study showed that C1q enhanced the growth of *M.smegmatis* inside THP-1 cells by 63% (Figure 4.13). C1q treated *M.smegmatis* down-regulated the gene expression of inducible nitric oxide synthase (iNOS) and pro-inflammatory cytokines (TNF-α, IL-1β, IL-6 & IL-12). The enzyme iNOS is responsible for formation of inducible nitric oxide components. These components are very toxic to bacteria and they kill pathogens by damaging their lipids in cell wall and nucleic acids (MacMicking *et al*., 2003). The down-regulation of the pro-inflammatory cytokines could be responsible for increasing *M.smegmatis* growth inside THP-1 cells, in particular TNF-α. This study suggests that differential expression of these factors may be responsible for differential growth of *M.smegmatis* and BCG inside THP-1 cells.

Pre-treatment of THP-1 with C1q and later removal of C1q by washing, prior to infection with *M.smegmatis* increased the uptake and growth of *M.smegmatis* inside THP-1 cells (Figure 4.28 & 4.29). These results are similar to those obtained with *M.smegmatis* treatment with C1q before THP-1 cell infection (Figure 4.11 & 4.13). Since in the latter experiment C1q is present both as bound form with *M. smegmatis* and free form, which can bind with THP1 cells, it can be concluded from both above experiments that C1q is very likely enhancing the uptake and growth of *M. smegmatis* through its interaction with receptors on THP1 cells. However, the contribution of C1q opsonisation in the uptake cannot be

excluded totally. It is possible that C1q through its globular head interaction with its receptor gC1qR may enhance the uptake of *M. smegmatis*, whereas collagen like region of C1q after interaction with its receptor LAIR may be responsible for increase *M.smegmatis* growth in THP1 cells. LAIR is an inhibitory receptor expressed on hematopoietic cells and it has been suggested that C1q binding with LAIR suppress immune cells activity (Son *et al*., 2012). Furthermore, the interaction of globular heads with gC1qR has been reported before (Pednekar 2016).

Conclusion

In this study a C1q comprising C-terminal (globular head) and collagen like region showed binding with *M. smegmatis* and BCG in ELISA. The binding of C1q to mycobacteria led to direct inhibition of *M. smegmatis* and BCG growth *in vitro*. Moreover, the treatment of the mycobacteria with C1q resulted in significant increase of both mycobacterial uptakes by THP-1 cells. Furthermore, the treatment of the mycobacteria with C1q inhibited BCG growth and enhanced *M.smegmatis* growth inside THP-1 cell line. This BCG growth inhibition in the C1q treated mycobacteria seems due to increased expression of inducible nitric oxide synthase, whose inhibition caused a reversal of C1q induced inhibition of BCG growth. It appears that TNF-α, IL-1β, IL-6 also played a role in BCG growth inhibition inside THP1 cells, as evident by the reversal of the growth inhibition by anti-TNF-α, anti-IL-1β and anti-IL-6 antibodies. In contrast, neutralization of TGF-β by anti-TGF-β antibody showed a synergistic effect to that achieved with C1q treatment, resulting in further inhibition of BCG growth, suggesting mycobacterial growth enhancing role of this cytokine. The enhancement of C1q treated *M.smegmatis* growth inside THP-1 cells appears due to decreased expression of inducible nitric oxide synthase, TNF-α, IL-1β and IL-6.

This study also suggests that C1q has the capability to activate and inactivate macrophages. In presence of BCG, C1q activates macrophages and inhibits BCG growth. In presence of *M.smegmatis*, C1q inactivates macrophages, which enhances mycobacterial growth. BCG is the most related model bacterium for *Mtb.* Such functions of C1q can be further explored to assist in therapeutic beneficiary in the treatment of TB.

Chapter 5- Interaction of MBP fused ghA, ghB and ghC of C1q with mycobacteria

5.1 Introduction

C1q molecule consists of 6A, 6B and 6C chains. Each chain is made up a short N terminal domain, a collagen like middle region (CLR) and C terminal globular head (gC1q). The globular head (gh) of each chain is designated as ghA, ghB & ghC (Kishore *et al* 2003). Data obtained in chapter 4 revealed that C1q has direct inhibitory effect on the growth of *M.smegmatis* and BCG. Moreover, C1q enhanced the uptake of both *M.smegmatis* and BCG by THP-1 cells. In addition, C1q enhanced *M.smegmatis* growth and inhibited BCG growth inside phagocytic cells. It will be interesting to investigate which individual chain is responsible for these effects of C1q on both mycobacteria. It has been shown previously that ghA, ghB and ghC are functionally independent modules (Kishore *et al* 2003). However, there is no information available for their individual interaction with mycobacteria.

Aim of study: To investigate the role of individual globular heads ghA, ghB and ghC on *M.smegmatis* growth directly and through their interaction with phagocytic cells.

Objectives

1. Expression of MBP fused ghA, ghB and ghC of C1q by using the *E.coli* BL21 expression system. The expression includes 88-223 residues of ghA, 90-226 of ghB, and 87-217 of ghC (Kishore *et al*., 2003).
2. Investigating the direct binding between the individual heads (ghA, ghB and ghC) of C1q with *M.smegmatis*, BCG and THP-1 cells.
3. Studying the direct effect of ghA, ghB and ghC on *M.smegmatis* growth.
4. Studying the effect of ghA, ghB and ghC on the uptake of *M.smegmatis* by THP-1 cells.
5. Studying the effect of ghA, ghB and ghC on the growth of *M.smegmatis* inside THP-1 cells.

5.2 Results

5.2.1 Expression and characterization of MBP fused ghA, ghB, and ghC of C1q

The MBP fused ghA, ghB and ghC were successfully expressed as soluble proteins in this study. Clear bands for these globular heads can be detected at the expected molecular weight (~60kDa) after large scale expression (Figure 5.1 and Figure 5.2). These proteins were further purified by passing them through an amylose resin column and endotoxin was removed by passing them through polymyxin B column. The eluted fractions, were further characterized on 12% SDS-PAGE, and as expected the bands showed at around 60kDa (Figure 5.3).

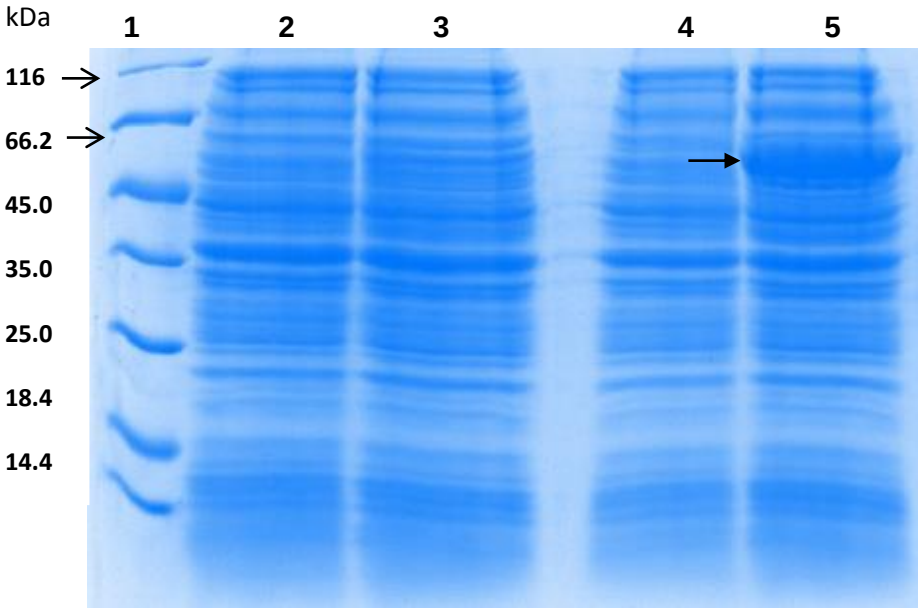

Figure 5.1: Characterization of MBP fused ghB on 12% SDS-PAGE (under reducing conditions) produced during large scale expression. *E. coli* BL21(DE3) strain transformed with vector pkBM-B (containing ghB linked to MBP). Bacterial culture was induced with IPTG for 3 hours. The cell pellet of 100µl of bacterial culture was boiled under reduced conditions and loaded in each lane. Bacterial cultures, grown in parallel but not induced with IPTG were used as an uninduced control. There is a clear MBP-ghB band at molecular weight around 60 kDa in the induced sample (lane 5). Lane 1 is Protein marker. Lanes 2, 3 and 4 are un-induced cultures. The molecular weight of free MBP is 42 kDa.

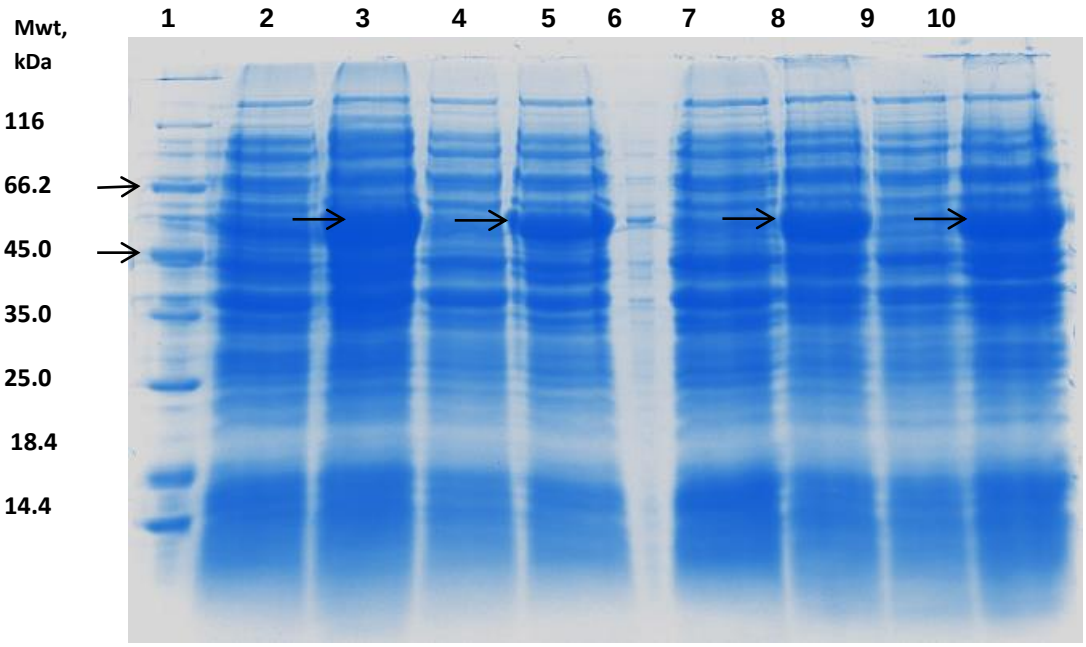

Figure 5.2: Characterization of MBP fused ghA and ghC on 12% SDS-PAGE produced during large scale expression. *E. coli* BL21(DE3) strain transformed with vector pkBM-A (containing ghA linked to MBP) and pkBM-c (vector containing ghC linked to MBP) respectively. Bacterial culture was induced with IPTG for 3 hours. Samples of 100µl of the bacterial culture cell pellet was boiled under reduced conditions and loaded in each lane. Bacterial cultures, grown in parallel but not induced with IPTG were used as an uninduced control. There is a clear band for MBP- ghA and MBP-ghC around molecular weight of 60 kDa in the induced sample. Lane 1 is Protein marker. Lane 2, 4 un- induced MBP-ghA, lane 3, 5 are induced MBP-ghA. Lane 7, 9 are un-induced MBP-ghC, Lane 8, 10 are induced MBP-ghC cultures. Lane 6 empty.

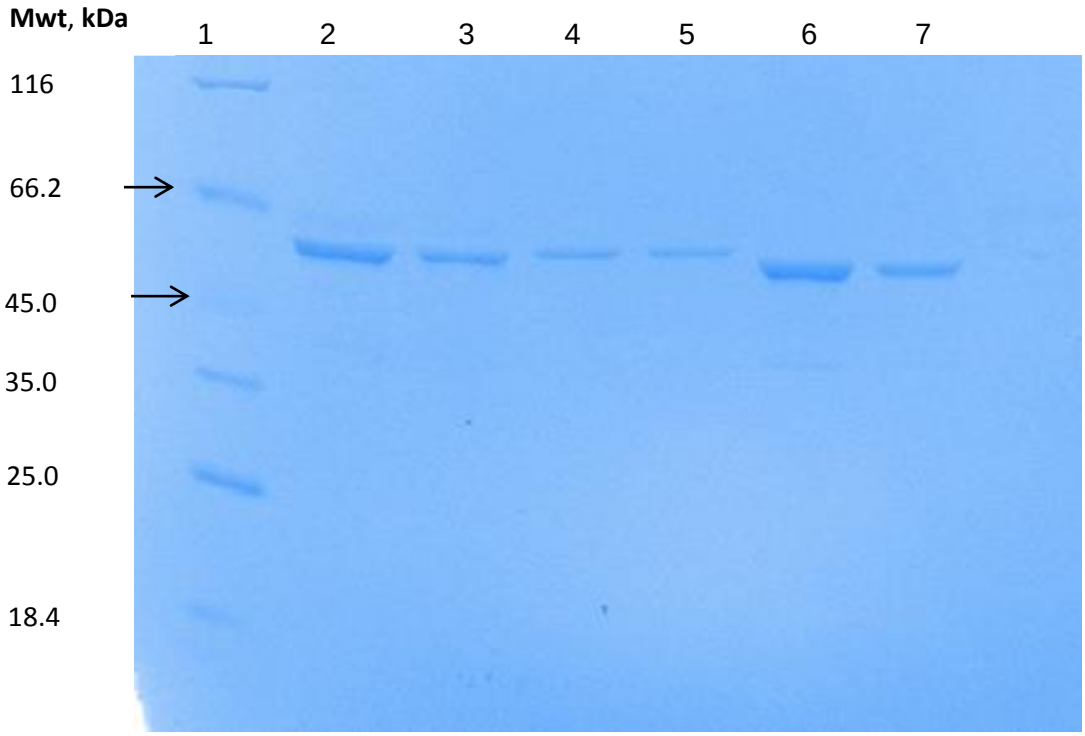

Figure 5.3: SDS-PAGE (12%) shows purified MBP fused ghA, ghB, and ghC protein samples after passing through amylose resin column and polymyxin column. Purified proteins migrated at a molecular weight of approximately 60 kDa. Lane 1: Protein marker. Lanes 2-3: MBP fused ghA fractions. Lanes 4-5: MBP fused ghB fractions. Lanes 6-7: MBP fused ghC fractions.

5.2.2 Endotoxin level measurement for purified MBP fused globular heads ghA, ghB and ghC of C1q protein

The LAL assay was carried out in order to detect the endotoxin level in the expressed proteins. The assay was linear over the range 0.1-1.0EU/ml (Figure 5.4). From the equation, the endotoxin level for MBP fused ghA, ghB and ghC was around 0.3 EU/ml and it was 0.04 EU/ml for MBP (Table 5.1). The amount of endotoxin present in these recombinant proteins estimated to be <0.04 ng/ml (10 EU = 1 ng of endotoxin).

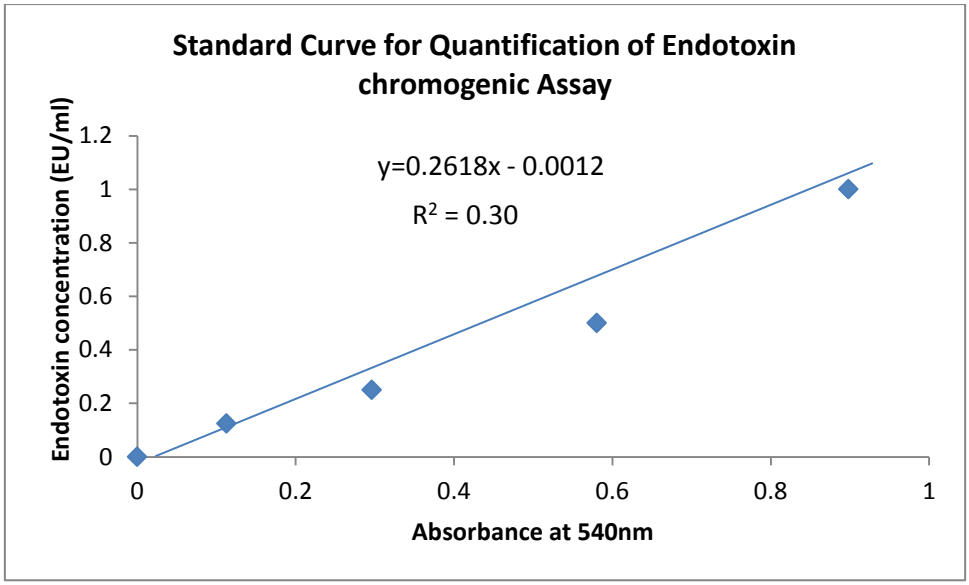

Figure 5.4: Measurement of endotoxin level for MBP fused ghA, ghB, and ghC by LAL assay. Each data point represents triplicate readings for the endotoxin standard solutions. The absorbance for the blank solution was zero.

Table 5.1: Endotoxin level inside purified proteins.

	Average Absorbance at 540nm of triplicate readings	Endotoxin level (EU/ml)
ghA	1.298667	0.338791
ghB	1.278333	0.333468
ghC	1.192667	0.31104
MBP	0.163333	0.041561

5.2.3 Binding of MBP fused ghA, ghB and ghC of C1q with Mycobacteria

The results show the binding of purified MBP fused globular heads A, B and C with mycobacteria using ELISA in the presence of 5mM $CaCl_2$. The binding of MBP fused ghA, ghB, and ghC to mycobacteria is qualitatively similar to native C1q protein. Binding of the recombinant forms of C1q globular heads ghA, ghB and ghC to *M.smegmatis* is weak (Figure 5.5-A & B). The best binding was achieved at 10μg/ml. These globular heads binding with BCG is moderate and the best binding is seen at 5μg/ml for each protein (Figure 5.6-A & B). GhA binds better with *M.smegmatis* while ghC binds better with BCG (Figure 5.5 & 5.6).

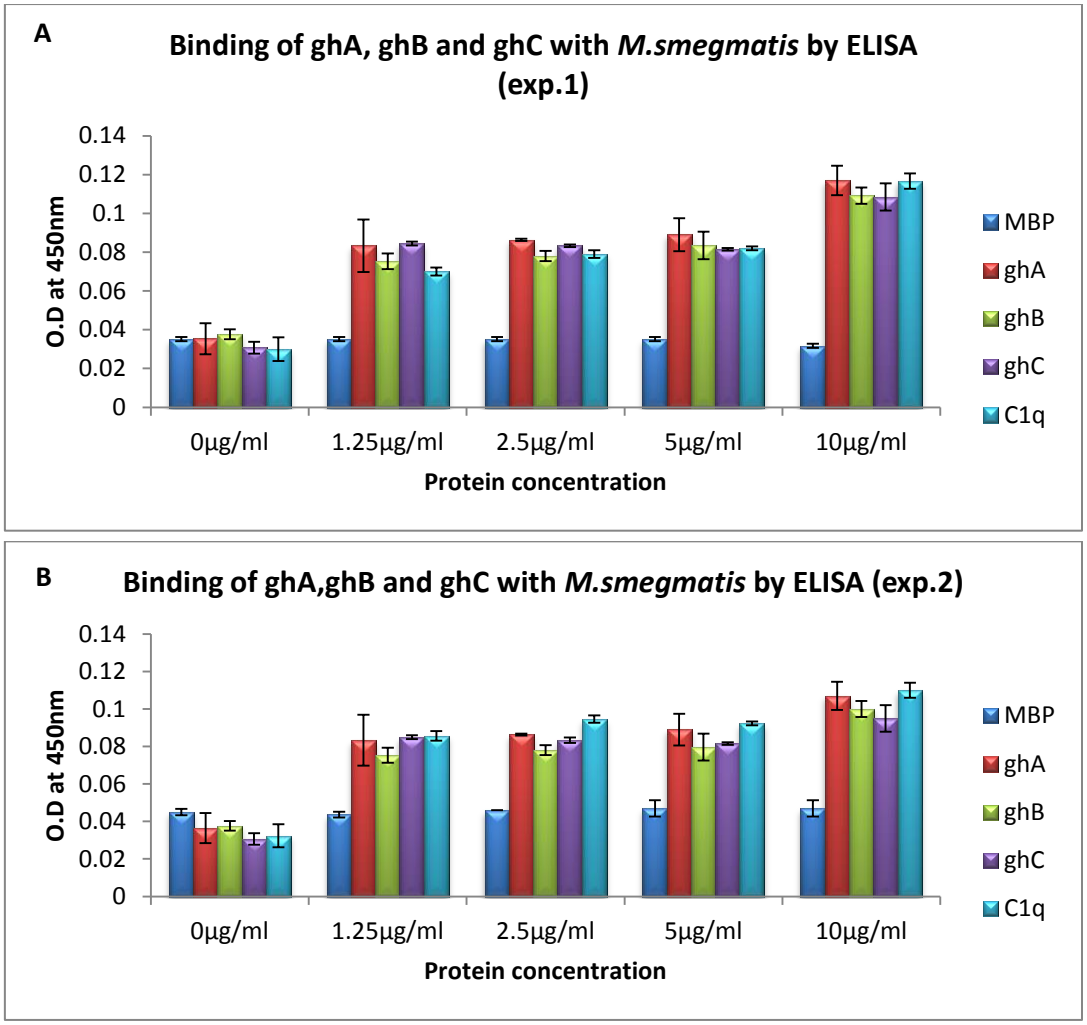

Figure 5.5: Binding of MBP fused ghA, ghB, ghC, and C1q with *M.smegmatis* by ELISA. Each data point represents the average of triplicate readings. Error bars represent ±standard deviation. Two separate experiments have shown here (A & B). Microtitre wells were coated in with $10x10^6$ *M.smegmatis* per well in carbonate buffer and incubated at 4^oC overnight. Contents were discarded and wells were blocked for 2 hours with 1% BSA in PBS at 37°C. Following washing with PBS + 0.05% Tween, different concentrations (1.25, 2.5, 5, 10µg/ml) of C1q, ghA, ghB, ghC and MBP were added to desired wells in triplicates and the plate was incubated for 2 hours at 37°. Negative control wells containing adhered *M.smegmatis* were treated with PBS. 5mM CaCl2 was added to all wells before incubation. Wells were washed and bound protein was detected using anti-human MBP (1:1000) and protein G HRP-conjugated (1:5000) in PBS/0.1% BSA. Colour was developed using TMB substrate. The reaction was stopped using $H2SO_4$. The plate was read at a wavelength of 450nm.

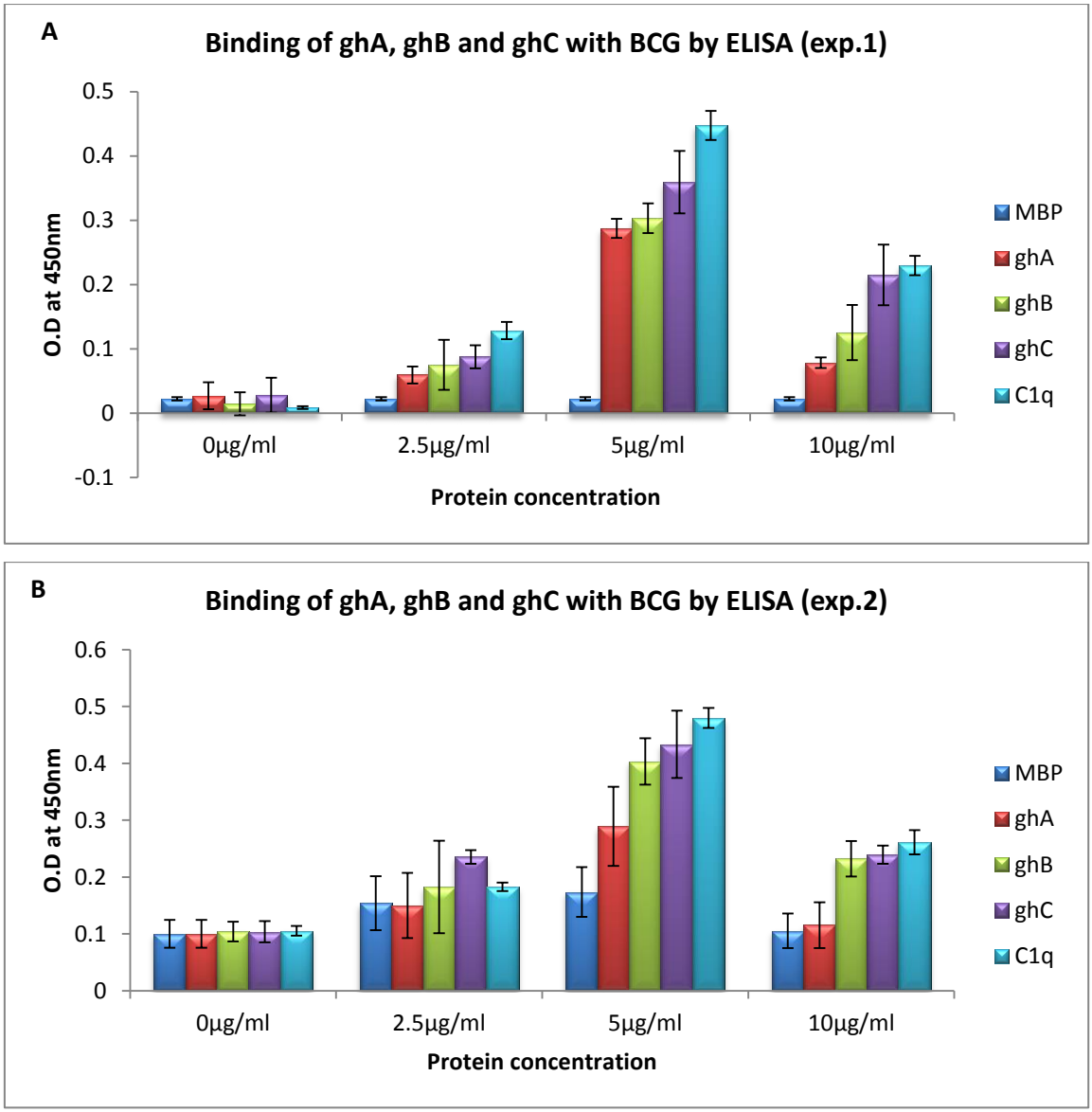

Figure 5.6: Binding of MBP fused ghA, ghB, ghC, and C1q with BCG by ELISA. Each data point represents the average of triplicate readings. Error bars represent ±standard deviation. Two separate experiments have shown here (A & B). Microtitre wells were coated with $10x10^6$ BCG per well in carbonate buffer and incubated at 4^oC overnight. Contents were discarded and wells were blocked for 2 hours with 1% BSA in PBS at 37°C. Following washing with PBS + 0.05% Tween, different concentrations (2.5, 5, 10µg/ml) of C1q, ghA, ghB, ghC and MBP were added to desired wells in triplicates and 5mM $CaCl_2$ was added to all wells. The plate was incubated for 2 hours at 37°C. Negative control wells containing adhered BCG were treated with PBS and calcium only. Wells were washed and bound protein was detected using anti-human MBP (1:1000) and protein G HRP-conjugated (1:5000) in PBS/0.1% BSA. Colour was developed using TMB substrate. The reaction was stopped using H_2SO_4 and the plate was read at a wavelength of 450nm.

5.2.4 Binding of MBP fused ghA, ghB and ghC with THP-1 cells by ELISA

The results show the binding of MBP fused ghA, ghB and ghC in presence of 5mM $CaCl_2$ with THP-1 is very weak. Furthermore, the binding of native C1q protein with THP-1 cells is better than the binding of each globular head separately. MBP protein was used as a negative control in this binding assay (Figure 5.7-A & B).

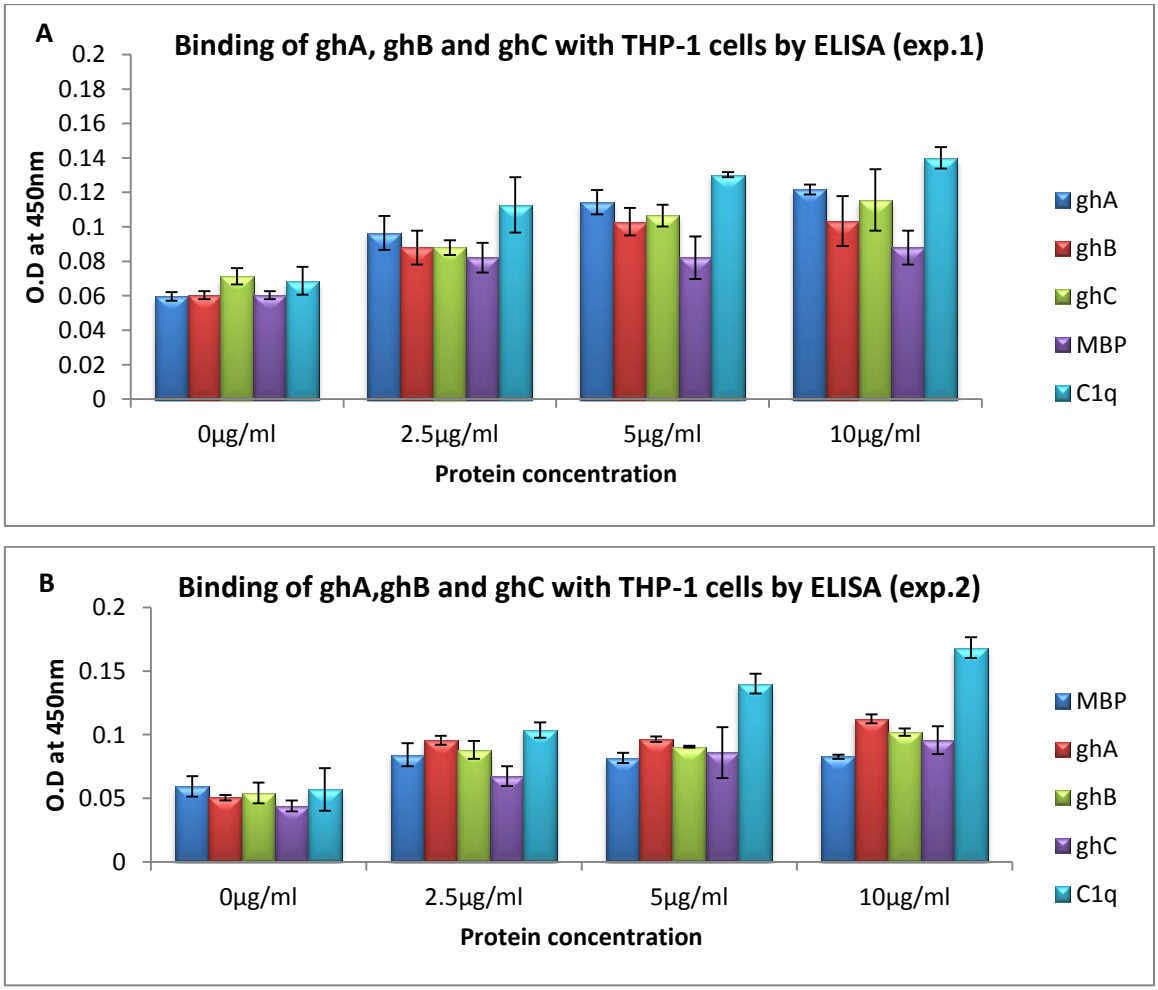

Figure 5.7: Binding of MBP fused ghA, ghB, ghC and C1q with THP-1 cells by ELISA. Each data point represents the average of the triplicate readings. Error bars represent ±standard deviation. Two separate experiments have shown here (A & B). Microtitre wells were coated with $1x10^5$ THP-1 cells per well in carbonate buffer and incubated at 4^oC overnight. Contents were discarded and the wells were blocked for 2 hours with 1% BSA in PBS at 37°C. Following washing with PBS + 0.05% Tween, different concentrations (2.5, 5, 10µg/ml) of C1q, ghA, ghB, ghC and MBP were added to desired wells in triplicates and 5mM $CaCl_2$ was added to all wells. The plate was incubated for 2 hours at 37°C. Negative control wells containing adhered THP-1 cells were treated with PBS and calcium only. Wells were washed and bound protein was detected using anti-human MBP (1:1000) and protein G HRP-conjugated (1:5000) in PBS/0.1% BSA. Colour was developed using TMB substrate. The reaction was stopped using H_2SO_4 and the plate was read at a wavelength of 450nm.

5.2.5 Direct effect of MBP fused ghA, ghB and ghC on *M.smegmatis* growth

Both C1q and each globular head inhibited the growth of *M.smegmatis* in presence of 5mM $CaCl_2$ (Figure 5.8-A).The experimental results show the same trend of inhibition of *M.smegmatis* growth using ghA, ghB and ghC in four independent experiments (Figure 5.8-B).

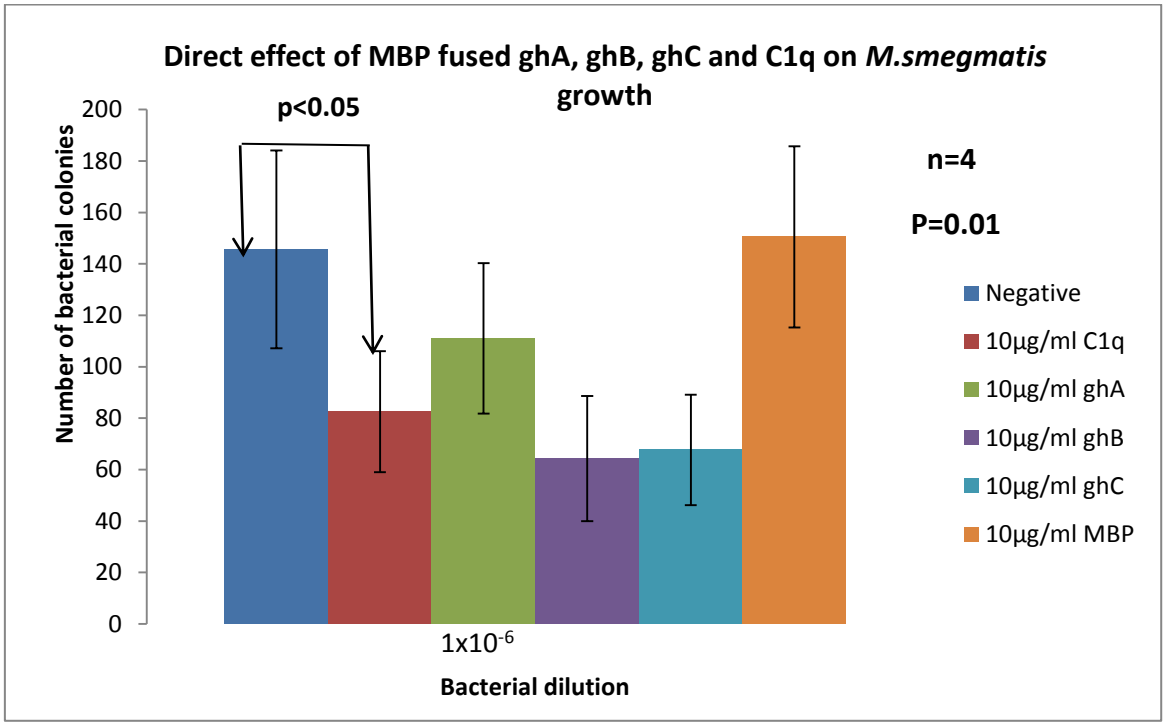

Figure 5.8-A: Direct effect of MBP fused ghA, ghB, and ghC on *M.smegmatis* growth. The MBP fused ghA, ghB, ghC has direct inhibition effect on *M.smegmatis* growth. Globular heads treated mycobacteria have low number of bacterial colonies in comparison with the negative control (untreated *M.smegmatis*). Mycobacteria ($1x10^{-6}$ dilution) were treated with 10µg/ml (C1q, ghA, ghB, ghC, MBP) and incubated for 2 hours at $37^{o}C$ with 5mM $CaCl_2$. Negative control contains untreated *M.smegmatis* with 5mM $CaCl_2$. Following incubation, 250µl of bacterial cultures were plated on agar plates in triplicates and incubated at $37^{o}C$ for 3 days. The number of bacterial colonies in each plate was counted by visual inspection. Each bar represent the average of 4 independent experiments, Error bars represent ±standard error of the mean. Multiple comparison of the data sets was done using Friedman test (p=0.01). Individual data were compared with each other using Dunn's post hoc test: Negative vs C1q treated *M.smegmatis*, p<0.05; Negative vs ghA, p=ns; Negative vs ghB, p=ns; Negative vs ghC, p=ns (non-significant). Negative vs MBP, p=ns. Negative contains untreated *M.smegmatis*.

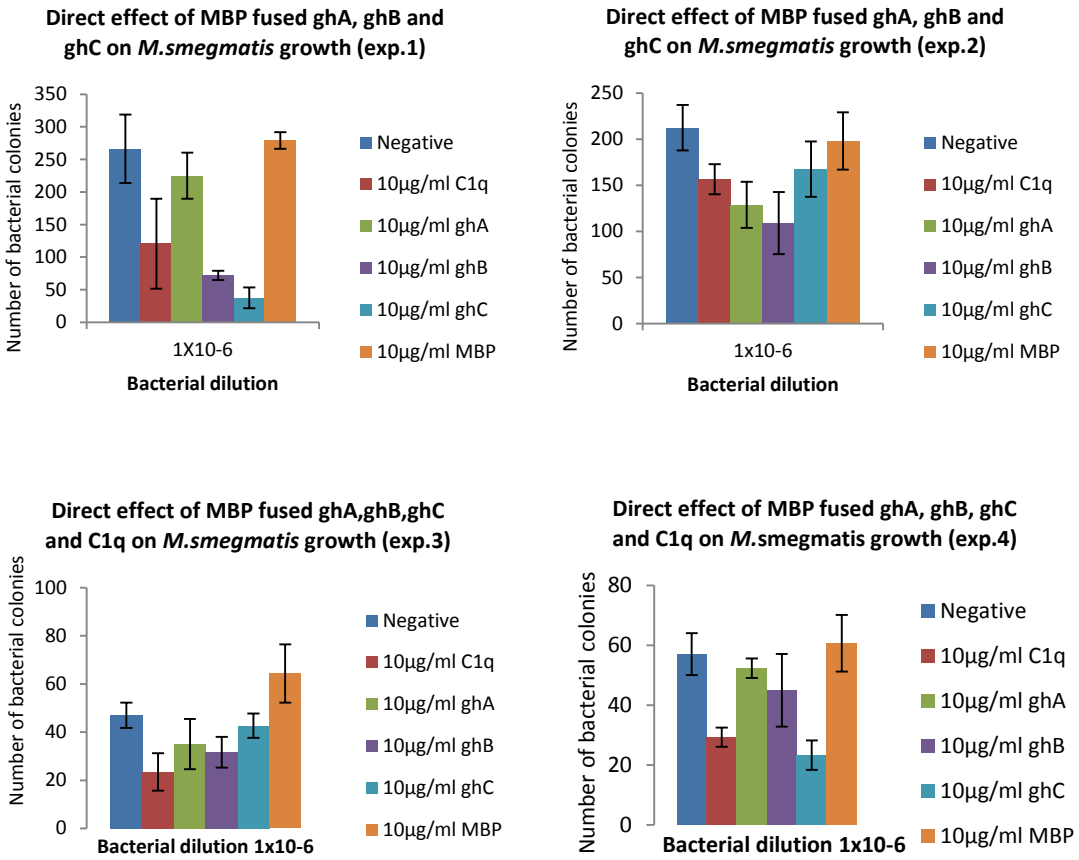

Figure 5.8-B: Direct effect of MBP fused ghA, ghB, and ghC on *M.smegmatis* growth (4 individual experiments). These proteins showed inhibition of *M.smegmatis* growth as compared to MBP treated *M.smegmatis* and negative control containig untreated *M.smegmatis*. Each bar represents the average of triplicate reading, Error bars represent ±standard deviation. Negative contains untreated *M.smegmatis*.

5.2.6 Effect of MBP fused ghA, ghB, ghC on the uptake of *M.smegmatis* by THP-1 cells

The results showed that 10µg/ml of ghA, ghB and ghC in presence of 5mM $CaCl_2$ increased *M.smegmatis* uptake by THP-1 cells. All three independent experiments showed the same trend of increased uptake (Figure 5.9-B). The experimental results were statistically significant (p=0.019). The *M.smegmatis* uptake was 35% higher using the individual globular heads as compared to C1q treated *M.smegmatis*, and the uptake was increased by 56-58% using individual globular heads as compared to negative control containing untreated *M.smegmatis.* On the other hand, MBP inhibited the uptake by 39.5% (Figure 5.9-A).

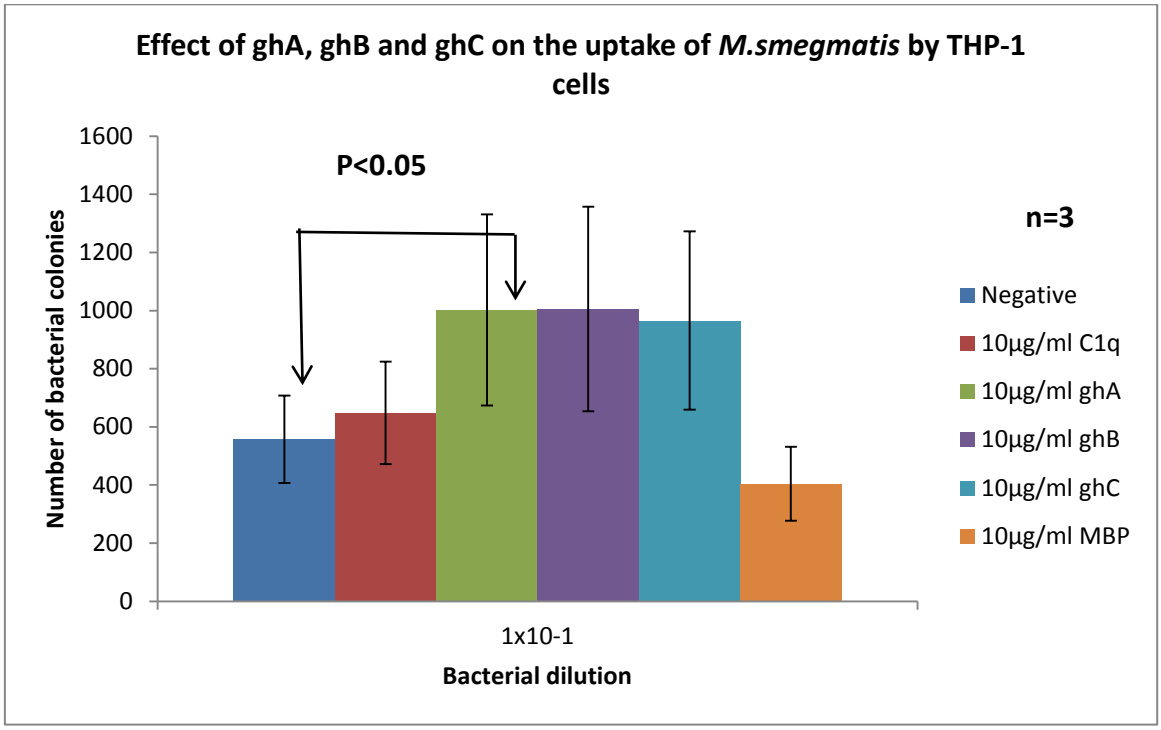

Figure 5.9-A: Effect MBP fused ghA, ghB, and ghC on the uptake of *M.smegmatis* by THP-1 cells. Gloubular heads of C1q ghA, ghB, and ghC increased the uptake of *M.smegmatis* by THP-1 cells. Each bar represent the average of 3 independent experiments, Error bars represent ±standard error of the mean. Multiple comparison of the data sets was done using Friedman test (p=0.019). Individual data were compared with each other using Dunn's post hoc test: Negative vs C1q, p=ns (non-significant); Negative vs ghA, p<0.05; Negative vs ghB, p=ns; Negative vs ghC, p=ns. Negative contains untreated *M.smegmatis*.

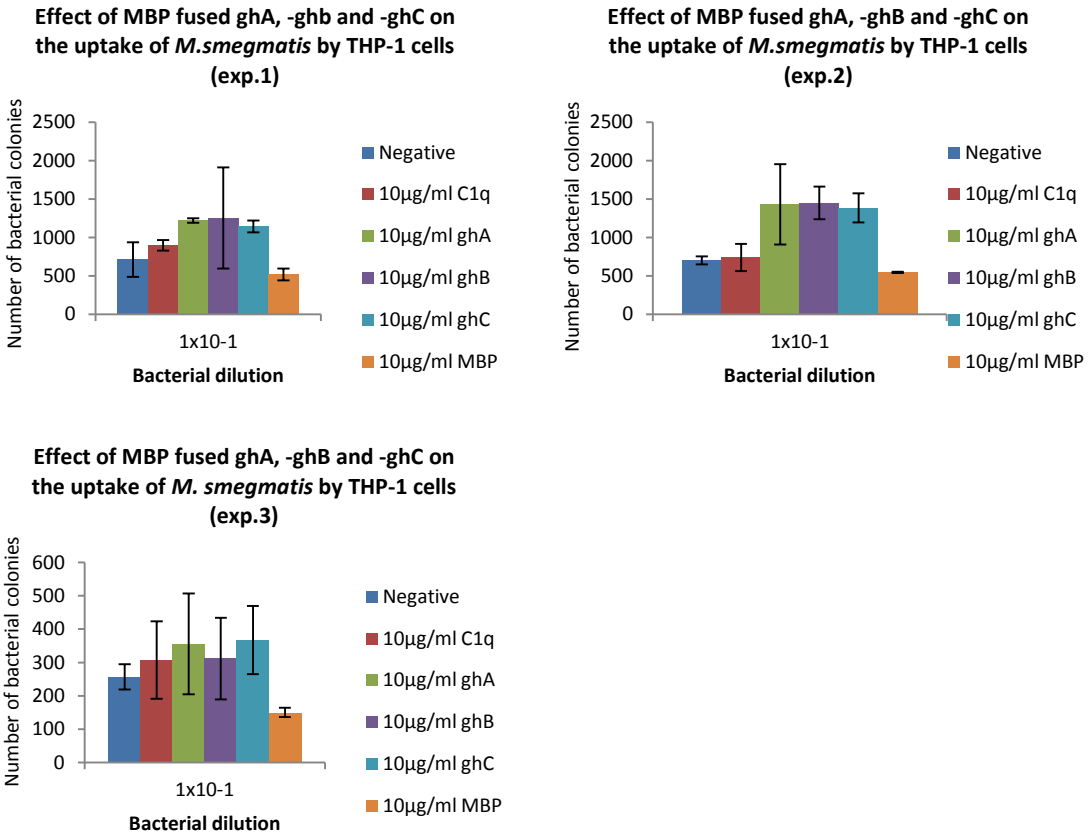

Figure 5.9 -B: Effect of MBP fused ghA, ghB, and ghC on the uptake of *M.smegmatis* by THP-1 cells (3 individual experiments). Each bar represent the average of triplicate reading, Error bars represent ±standard deviation. Negative contains untreated *M.smegmatis*.

5.2.7 Effect of MBP fused ghA, ghB and ghC on *M.smegmatis* growth inside THP-1 cells

The results showed that C1q in presence of 5mM $CaCl_2$ increased *M.smegmatis* growth inside THP-1 cells. Similarly, ghA and MBP increased the growth in presence of calcium chloride. However, this growth increase was less than whole C1q protein (Figure 5.10-A & 5.10-B). On the other hand, ghC inhibited the growth in all 4 independent experiments. Wherase ghB inhibited the growth in 3 out of 4 experiments (Figure 5.10-B). This growth inhibition was more prominent with ghC ($p<0.05$).

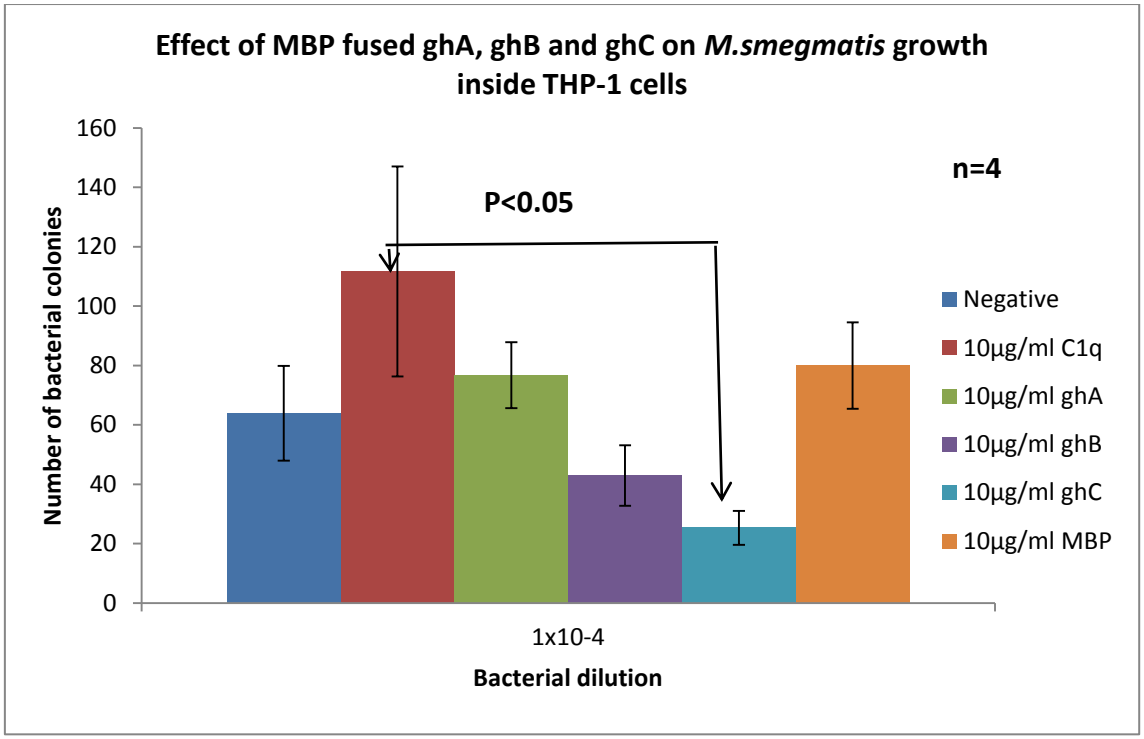

Figure 5.10-A: Effect of MBP fused ghA, ghB, and ghC on *M.smegmatis* growth inside THP-1 cells. Each bar represent the average of 4 independent experiments, Error bars represent ±standard error of the mean. Multiple comparison of the data sets was done using Friedman test (p=0.011). Individual data were compared with each other using Dunn's post hoc test: Negative vs C1q, p=ns; Negative vs ghA, p=ns; Negative vs ghB, p=ns; Negative vs ghC, p=ns; Negative vs MBP, p=ns; C1q vs ghC, p<0.05. Negative control contains untreated *M.smegmatis*.

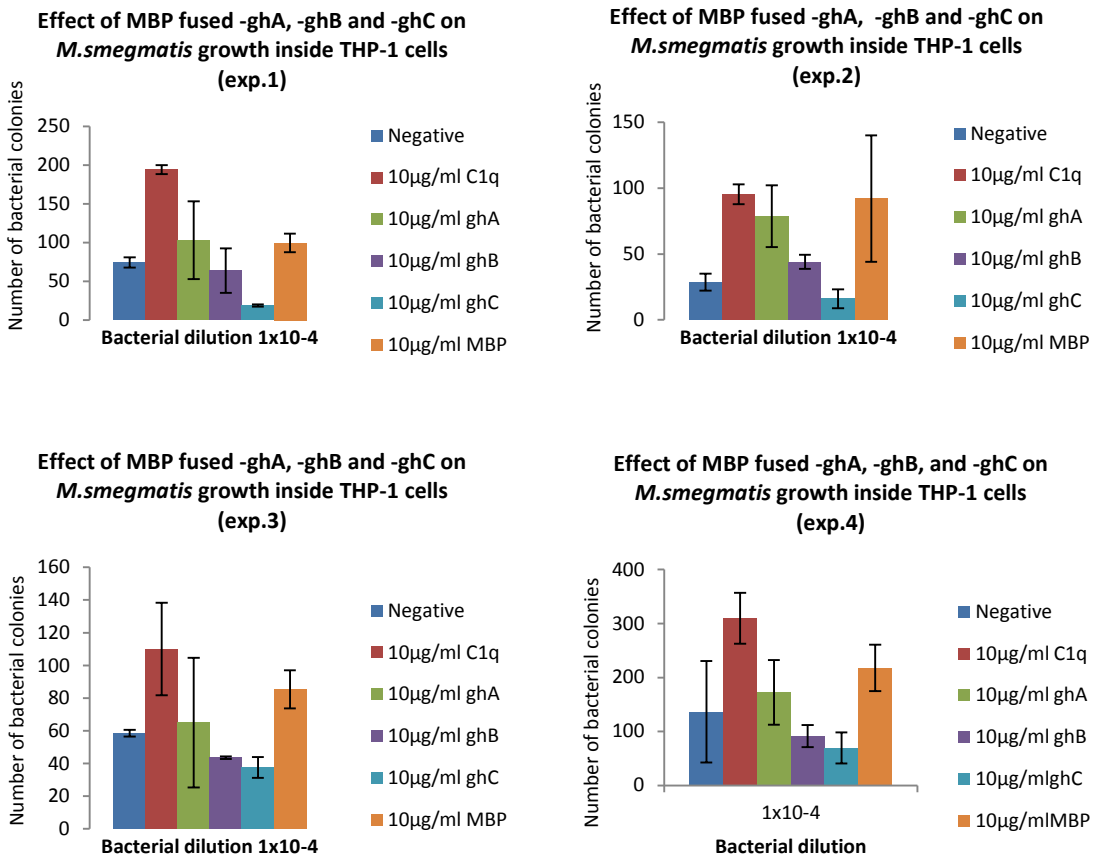

Figure 5.10 -B: Effect of MBP fused ghA, ghB, and ghC on *M.smegmatis* growth inside THP-1 cells (4 individual experiments). Each bar represent the average of triplicate reading, Error bars represent ± standard deviation. Negative control contains untreated *M.smegmatis*.

5.3 Discussion

In this study, recombinant fusion proteins, ghA, ghB, and ghC linked to maltose binding protein (MBP) were expressed and purified. MBP is commonly used in recombinant protein purification. Only MBP fused proteins can bind to Amylose resine during purification, and due to their affinity to maltose sugar, they can be eluted by maltose buffer. Moreover, MBP does not contain any cysteine residues (Lutsenko etal., 1997), and it increases the solubility of recombinant fusion proteins and prevents their aggregation (Sachdev and Chirgwin, 1998).

The Endotoxin was removed from these proteins before their usage, as it can interfere in the experiments by activating macrophages (Martinez *et al*., 2007). The concentration of Endotoxin of these proteins after its removal was less than 1EU/ml, which is generally acceptable in research. These globular heads were produced in order to understand whether these proteins function independently or whether C1q's ability to function is dependent on these globular heads in a joined structure. In this study, all individual globular heads of C1q were shown to bind with mycobacteria (*M.smegmatis* and BCG) in presence of 5mM $CaCl_2$, but native C1q consisting of globular heads (6A, 6B and 6C) and collagen like region bound better to mycobacteria than any of the individual globular heads (ghA, ghB and ghC), and this binding is stronger with BCG than *M.smegmatis* (Figure 5.5 & 5.6). Moreover, it seems that ghA binds better with *M.smegmatis*, whereas ghC domain binds better with BCG. Since these purified globular heads lack the collagen like region, binding of C1q to mycobacteria is localized to globular head region of C1q (gC1q), and it seems collagen like region of C1q is not needed for this binding. This result is in agreement with previous findings, which reported that C1q binds to a range of ligands through its globular domain in the presence of calcium chloride (Ghebrehiwet *et al*, 2002, Nayak *et al*., 2010). C1q binds to various ligands on microorganisms such as lipid A from *E.coli* and porin from *Klebsiella pneumonia* (Tan *et al*., 2011; Albertí *et al*., 1993). It has been shown in the previous chapter that the binding between C1q and mycobacteria was reduced when sugars were added, which suggests that globular head region of C1q could bind sugar such as mannose and may be with lipids on mycobacterial cell wall.

The binding of recombinant proteins (ghA, ghB and ghC) with THP-1 cells was investigated, and the result showed that native C1q molecule binds better to THP-

1 than the individual globular heads (Figure 5.7). C1q has 18 binding sites as compared to a single binding site with the individual globular head (Kishore *et al.*, 2003). This gives flexibility to the C1q molecule to bind its ligand with higher affinity than any individual heads and therefore better binding with THP1 cells. The main receptor on the cell surface identified for the globular head region of C1q (gC1q) is gC1qR (Ghebrehiwet *et al.,* 1994, Pednekar, 2013). This receptor is expressed ubiquitously in various cell types including adherent monocytes, macrophages, dendritic cells and THP1 cells (Pednekar 2016, Ghebrehiwet *et al.,* 2004, Song *et al.,* 2016). The C1q binding site on gC1qR was identified at 76-94 residues (Ghebrehiwet *et al.,* 2002), and this receptor plays an essential role in blood coagulation, infection and inflammation (Ghebrehiwet *et al*., 2002). Furthermore, individual recombinant ghA, ghB, ghC have been shown to bind with gC1qR independently (Pednekar 2016). Since gC1qR is also expressed in THP1 cells (Song *et al*., 2016), it could be that these C1q globular heads may be binding to gC1qR. In our study ghA binds with THP1 cell better than ghB or ghC, which could be due to the primary role of C1q-A chain in the high affinity binding of C1q with C1qR (Ghebrehiwet *et al.,* 2001). Previous studies have shown that individual ghA, ghB, and ghC can interact differentially with aggregated immunoglobulin's IgG and IgM, HIV1 GP41 and β amyloid peptides (Kishore *et al*., 2003, Gadjeva *et al.,* 2008), suggesting each globular head can function independently. Moreover, it was shown that ghA, ghB, and ghC bind to apoptotic Peripheral blood mononuclear cells (PBMCs) (Kishore *et al*., 2003). Furthermore, ghA, ghB, and ghC have been shown to bind acute-phase protein (Pentraxin 3), and binding of C1q via its globular head region to Pentraxin 3 activate the classical complement pathway (Nauta *et al.,* 2003). However, the interaction of individual ghA, ghB and ghC with bacteria is not known.

Although the binding of native C1q molecule to *M. smegmatis* was better than the individual globular heads, both C1q and individual globular heads of C1q (ghA, ghB, and ghC) inhibited *M.smegmatis* growth directly at similar level. This is therefore, first report, showing the anti-microbial role of individual globular head in C1q molecule. It will be interesting to investigate which ligand these globular heads bind on the surface of mycobacteria. Further investigation is now needed to understand underlying mechanism of direct growth inhibition, which may be due to

either direct membrane damaging effect or via intracellular signalling through their receptor on bacterial membrane.

MBP fused ghA, ghB and ghC increased *M.smegmatis* uptake by human THP-1 cells and this effect was 35% higher than whole C1q protein in our study. This could be due to individual globular heads without collagen region may act as better opsonin as compared to whole C1q molecule to facilitate the uptake of *M.smegmatis* in the phagocytic cells. Moreover, using 10μg/ml of one individual head means that the total number of this specific head is 3 times more as compared to number of this individual head in 10μg/ml of C1q. For example, the number of ghA in 10μg/ml of ghA solution is 3 times more as compared to number of ghA heads in 10μg/ml of C1q solution.

In this study, the effect of C1q and each individual globular head on the growth of *M.smegmatis* inside THP-1 cells is variable. Both MBP fused ghC and ghB inhibited *M.smegmatis* growth inside THP-1 cells, whereas MBP fused ghA and whole C1q increased *M.smegmatis* growth in the same cells. The inhibition effect of ghC on *M.smegmatis* growth is more clear and stronger than ghB, and it will be very interesting to show this effect on the growth of *Mtb* in future researches. The differential effects of individual globular heads of C1q on mycobacterial growth may be due to their differential ability to produce nitric oxide, oxygen burst and TNF-α production, which may help in the control of this mycobacterial infection. It has been reported previously that C1q-collagen like domain can bind to LIAR which down regulate the immune cell activation and this may explain an increased *M.smegmatis* growth in monocytic cell line THP1 using whole C1q molecule. It will be interesting to investigate whether ghA can also bind to LIAR and therefore induces negative signal through this receptor, which may explain the increase of *M.smegmatis* growth.

Conclusion

In this study MBP fused ghA, ghB and ghC of C1q molecule were produced in *E.coli* and these proteins were purified. All these globular heads showed binding with *M. smegmatis* and BCG in ELISA. The binding of individual globular heads of C1q to mycobacteria resulted in direct inhibition of *M. smegmatis* growth *in vitro*. Moreover, treatment of *M.smegmatis* with individual globular heads increased their

uptakes by THP-1 cells. Furthermore, whole C1q and ghA treatment increased *M.smegmatis* growth inside THP-1 cells. In contrast, treatment of *M.smegmatis* with ghB and ghC inhibited their growth inside these cells. Since ghB and ghC showed direct growth inhibition as well as indirect growth inhibition (through phagocytic cells) of *M. smegmatis*. These proteins may have potential role in the treatment of Multi-drug resistant tuberculosis, if these findings are reproducible using *Mycobacterium tuberculosis*.

Chapter 6 - Interaction of fibronectin with mycobacteria

6.1 Introduction

Fibronectin (FN) is a glycoprotein present in plasma and connective tissues. FN was selected in this study because it is present in the blood at high concentrations (<300μg/ml) and this protein could leaks from blood to the inflammation site in the lung. Moreover, higher levels of FN have been shown in pleural effusions of TB patients. Previouslly, FN has been shown to bind with BCG, Mtb, Ag85B and FAP. It is most likely this protein could have an effect of mycobacterial growth directly or indirectly. FN has high molecular weight around 440kDa, and composed of two nearly identical polypeptides of molecular weight 220kDa each. FN mainly produced by liver hepatocytes and fibroblasts. FN has a role in cell adhesion, migration and thrombosis (Pankov & Yamada, 2002; Schwarzbauer, 1991), and is also known to play a role in bacterial adhesion to host cells (Schwarz-Linek *et al*., 2004). FN has been shown to bind with bacteria and facilitate their uptake by target cells. Moreover, heparin binding domain in the C-terminal of FN has been shown to bind with *Mtb* (Pasula *et al*., 2002). FN binding to *Mtb* was shown to enhance the attachment of these bacteria to alveolar macrophages. A previous study showed that FN concentration in pleural fluid of TB patients was much higher (441μg/ml) as compared to patients with infections pleural effusion (335μg/ml) (Klockars *et al*., 1982). FN can leak out from blood vessels to the lungs (Vijayan et al., 1995) where *Mtb* infection starts. Moreover, it is produced locally by activated macrophages (Klockars *et al.,* 1982).

It appears that FN can interact with both bacteria and host cells and this could influence the outcome of the infection. In this study we are investigating the direct effect of FN on mycobacterial growth and indirectly through human monocytes THP-1 cells. The aims of this study are:

1. To characterize human FN by SDS-PAGE and Western Blot. 2. To show FN binding with both mycobacteria and THP-1cells.

3. To investigate the direct effect of FN on mycobacterial growth.

4. To study the effect of FN on the uptake of mycobacteria by THP-1 cells.

5. To examine the effect of FN on mycobacterial growth inside THP-1 cells.

6. To understand the underlying mechanisms of mycobacterial growth increase inside THP-1 cells using gene expression by q-PCR.

This line of research will help to determine whether FN is helpful in controlling mycobacterial infection or not.

6.2 Results

6.2.1 Characterization of Fibronectin

The fibronectin (Merck Milipore) used in this study was characterized by 8% SDS-PAGE. The two chains of FN protein are clearly visible at the expected molecular weight of 250 kDa (lanes 2, 3 & 4) (Figure 6.1). Amyloid P component was used as negative control, and it was detected at the expected molecular weight of 25kDa (lanes 7, 8, 9 & 10). Also, this protein was further characterized by western blot where sheep polyclonal anti-human FN identified this protein as clear bands at around 250kDa. The negative control, amyloid P protein was not detected with the same antibody (Figure 6.2).

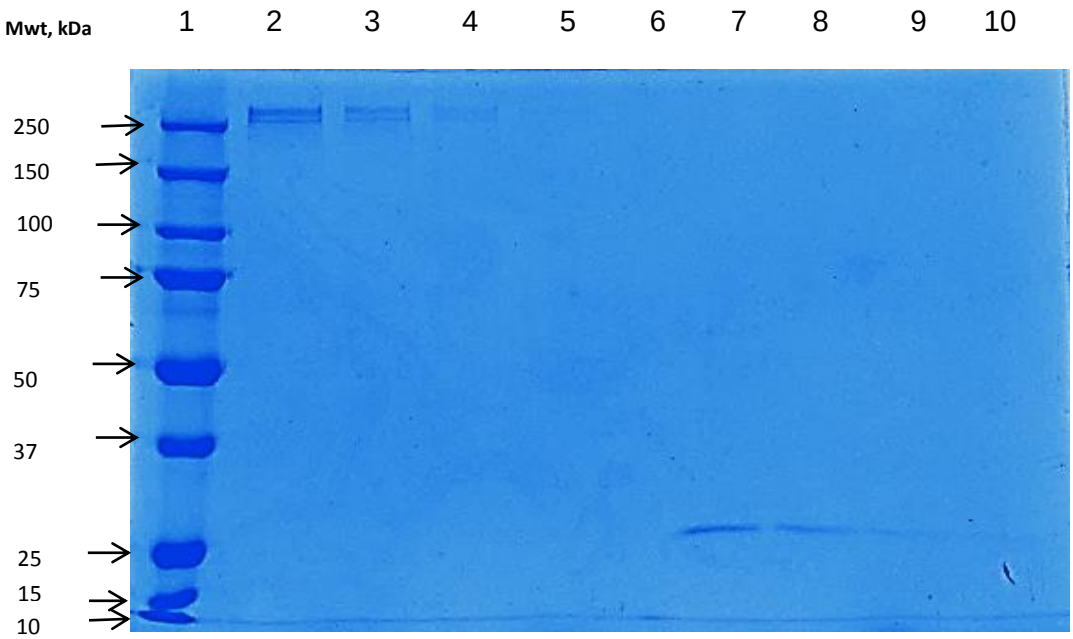

Figure 6.1: Characterization of Fibronectin on 8% SDS-PAGE. Lane 1: Bio-Rad protein marker, lanes 2, 3, 4 and 5 contain 3, 1.5, 0.75 & 0.375µg of FN respectively. Lane 6: Empty, Lanes 7, 8, 9 & 10 contain 3, 1.5, 0.75 & 0.375µg of amyloid P. component (negative control).

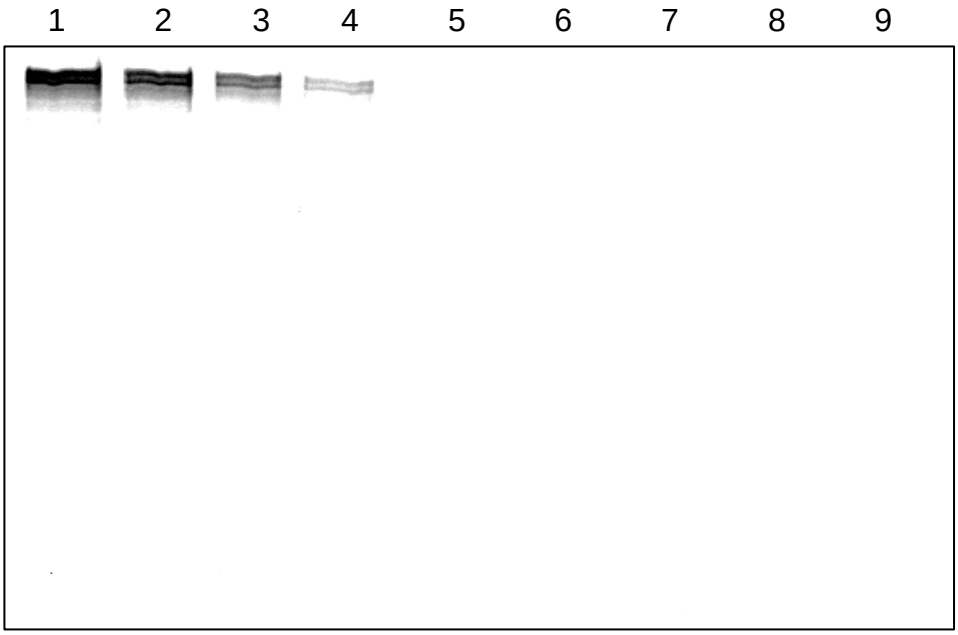

Figure 6.2: Characterization of Fibronectin by Western Blot. FN was detected with sheep anti human FN. Lanes 1, 2, 3, 4 contain 3, 1.5, 0.75 & 0.375µg of FN respectively. Lane 5: Empty. Lanes 6, 7, 8 & 9 contain 3, 1.5, 0.75 & 0.375µg of amyloid P component. FN and the negative control protein amyloid P component (3, 1.5, 0.75 & 0.375µg) were run on a gel and transferred onto nitrocellulose membrane for 2 hours at 320mA. Following this, the membrane was blocked with 5% non-fat milk powder in PBS overnight. The next morning the membrane was washed 3 times for 5 minutes each with 0.02% Tween 20 in PBS. Sheep anti-human fibronectin HRP-conjugated (1:1000) was added in 1% non-fat milk in PBS and the membrane was incubated for 2 hours at room temperature. The bands were developed using DAB tablets.

6.2.2 Binding of Fibronectin with Mycobacteria by ELISA

Fibronectin was shown to bind with *M.smegmatis* and BCG using ELISA. Binding is calcium and dose dependent. The best binding was obtained at 10µg/ml FN (Figure 6.3).

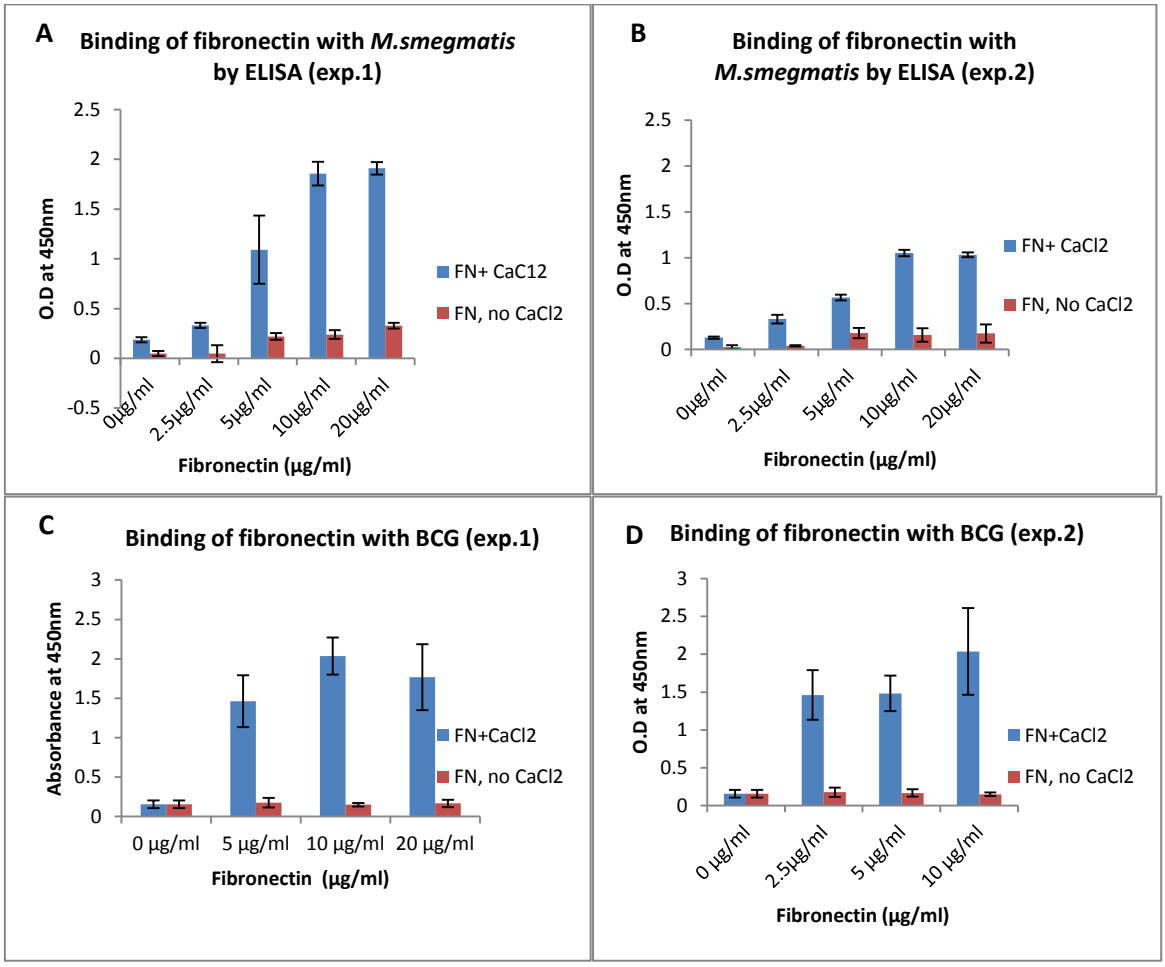

Figure 6.3: Binding of Fibronectin with mycobacteria (*M.smegmatis* and BCG) by ELISA. Binding of FN to *M.smegmatis* is dose dependent in presence of 5mM $CaCl_2$ (A & B). FN binding to BCG is stronger with 10µg/ml in presence of 5mM $CaCl_2$ (C&D). Each bar point represents the average of triplicate readings. Error bars represent ±standard deviation. Microtitre wells were coated with $10x10^6$ mycobacteria per well in carbonate buffer and incubated at 4^oC overnight. The contents were discarded and the wells were blocked for 2 hours with 1% BSA in PBS at 37°C. After washing with PBS + 0.05% Tween, 2.5, 5, 10 and 20µg/ml of FN was added and the plate was incubated for 2 hours at 37°C. The wells were washed and bound protein was detected using anti-human fibronectin conjugated to HRP (1:1000) in 0.1% BSA in PBS. Colour was developed using TMB substrate. The reaction in each well was stopped by adding H_2SO_4. The plate was read at a wavelength of 450nm.

6.2.3 Binding of Fibronectin with BCG by immunofluorescence microscopy

Immunofluorescence microscopy was used to show the binding of FN at concentration 10µg/ml with BCG in presence of 5mM $CaCl_2$. From the image shown in Figure 6.4, the untreated BCG (A & B) is compared with FN treated BCG (C & D). It can be seen that there is a binding of FN with BCG where BCG emitting green florescence (D) as compared to untreated BCG (B). This binding is due to interaction of protein A conjugated to FITC with sheep anti human FN.

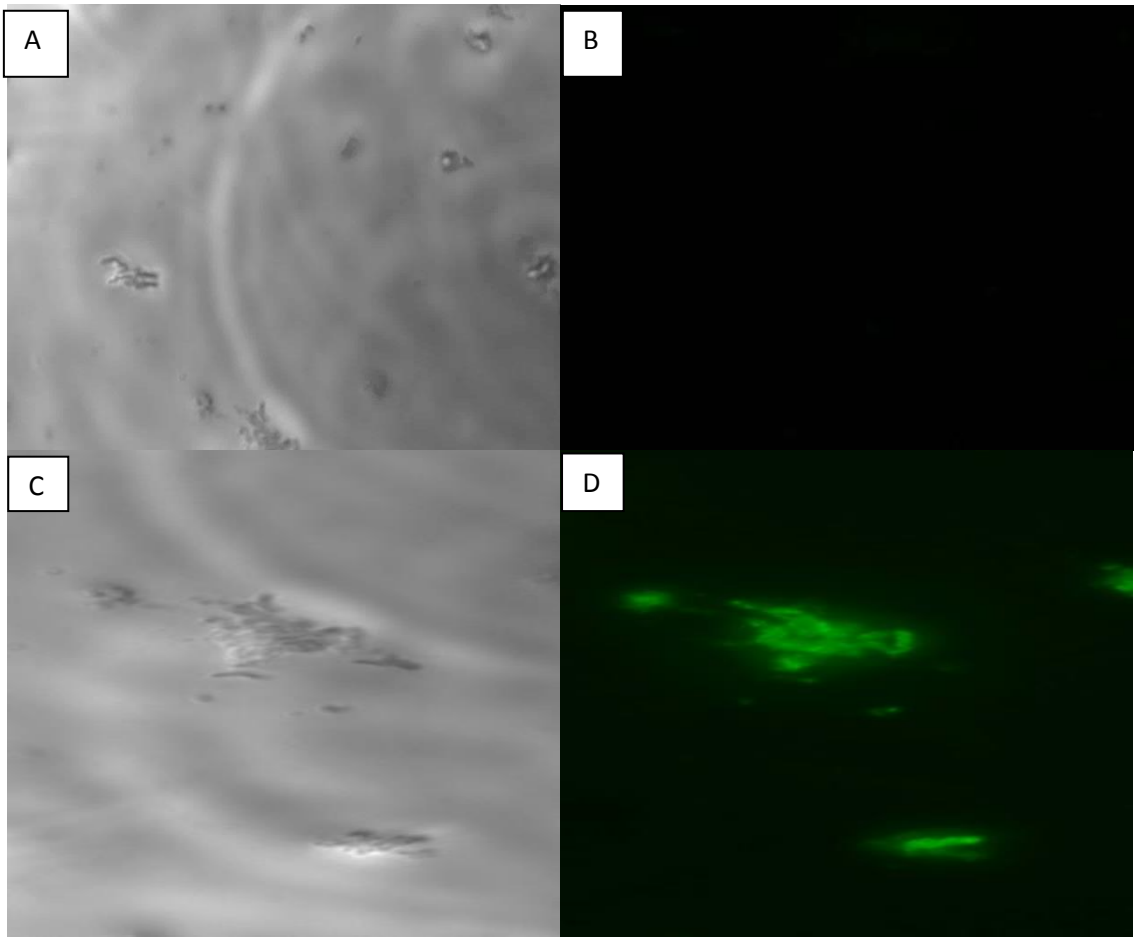

Figure 6.4: Binding of Fibronectin (10µg/ml) with BCG by immunofluorescence microscopy. A: Untreated BCG (bright field). B: Untreated BCG did not show binding with sheep anti human FN (fluorescence field). C: FN treated BCG (Bright field). D: FN treated BCG binding with sheep anti human FN (fluorescence field). All the above BCG samples were treated with sheep anti human FN and protein A conjugated to FITC.

6.2.4 Binding of Fibronectin with THP-1 cells by ELISA

FN was shown to bind with the THP-1 cells using ELISA. The binding was dose dependent upto 10µg/ml FN, but declined at 20µg/ml. Also, the binding is better in presence of 5mM $CaCl_2$ (Figure 6.5).

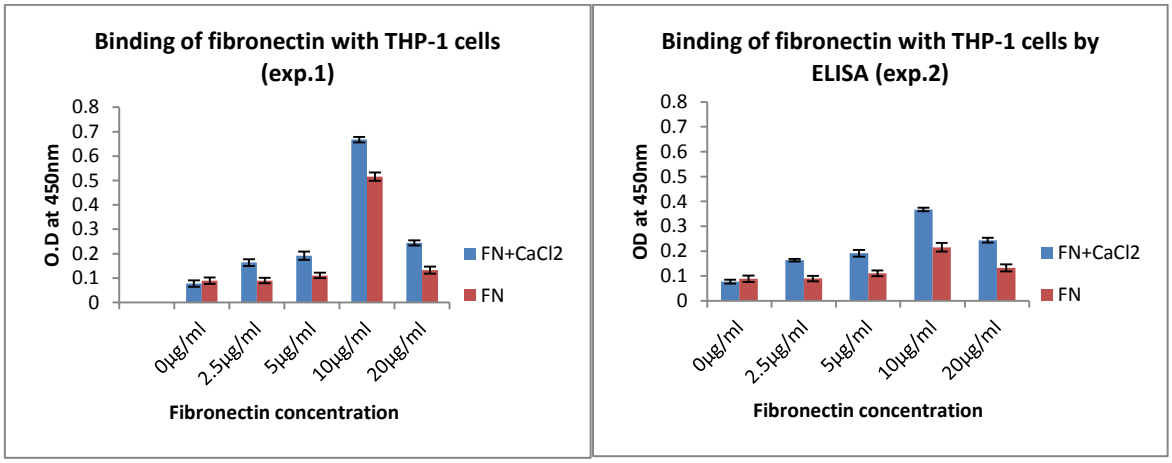

Figure 6.5: Binding of Fibronectin with THP-1 cells by ELISA. Each bar represents the average of triplicate readings. Error bars represent ±standard deviation. ELISA plate wells were coated with $1x10^5$ THP-1 cells per well in carbonate buffer and incubated at 4^oC overnight. The contents were discarded and the wells were blocked for 2 hours with 1% BSA in PBS at 37°C. After washing with PBS + 0.05% Tween, 2.5, 5, 10 and 20µg/ml of FN was added in triplicates. $CaCl_2$ (5mM) was added to all wells and the plate was incubated for 2 hours at 37°C. Wells were washed and bound protein was detected using anti-human fibronectin conjugated to HRP (1:1000) in 0.1% BSA in PBS. Colour was developed using TMB substrate. The reaction in each well was stopped by adding H_2SO_4 and the plate was read at a wavelength of 450nm.

6.2.5 Binding of fibroinectin with THP-1 cells by immunofluorescence microscopy

Immunofluorescence microscopy was used to show the binding of 10µg/ml fibronectin with THP-1 cells in presence of 5mM $CaCl_2$. Figure 6.6 shows, untreated THP-1 cells (A, B & C) compared with fibronectin treated THP-1 cells (D, E & F). The binding can be seen in fibronectin treated THP-1 cells, where the THP-1 cells emit green florescence (F) as compared to untreated THP-1 cells (C) without florescence. The green florescence is the result of binding of protein A conjugated to FITC with sheep anti human FN.

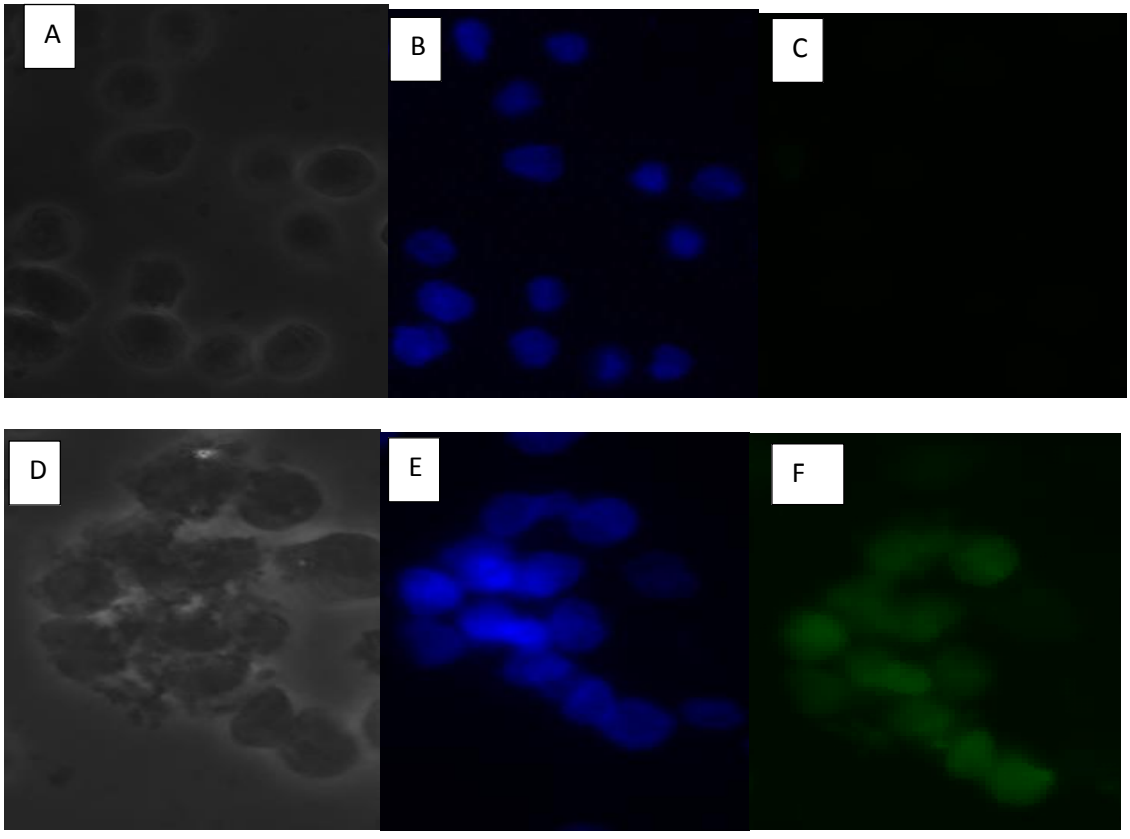

Figure 6.6: Binding of Fibronectin with THP-1 cells by immunofluorescence microscopy. A: Untreated THP-1 cells (Bright field). B: Untreated THP-1 cells, nuclei stained with Hoechst (blue). C: Untreated THP-1 cells, but treated with anti-fibronectin and protein A FITC (no binding). D: Fibronectin treated THP-1 cells (bright field). E: Fibronectin treated THP-1 cells, nuclei stained with Hoechst (blue). F: Fibronectin treated THP-1 cells treated with anti fibronectin and protein A FITC (emitting green florescence).

6.2.6 Effect of fibronectin on mycobacterial agglutination

This study showed that FN does not agglutinate BCG. The average number of BCG clumps per field on slides made from FN treated and untreated BCG were similar and statistically non-significant. A total of 70 fields were examined for each experiment (Figure 6.7).

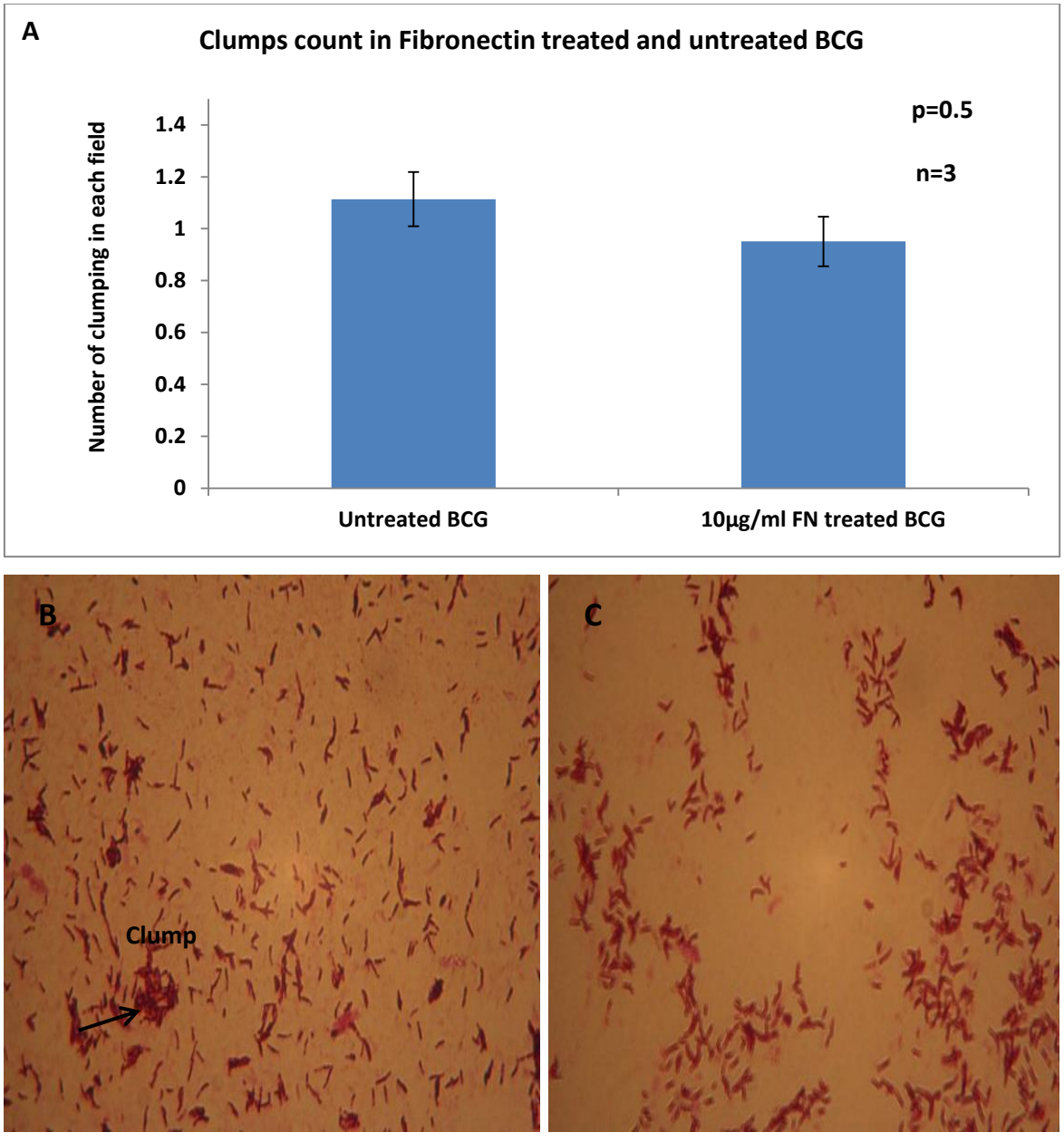

Figure 6.7: Effect of Fibronectin on BCG agglutination. FN doesn't cause agglutination of BCG (A). Each bar represents the average number of small clumps per field on slides from 3 independent experiments. A total of 70 fields were examined for each experiment. Error bars represent ± standard error of the mean. Clumping of BCG after Acid fast staining of FN treated (C) and untreated BCG (B).

6.2.7 Direct effect of Fibronectin on mycobacterial growth

6.2.7.1 Direct effect of Fibronectin on *M.smegmatis* growth

In this study, incubation of *M.smegmatis* with 10µg/ml did not showed consistant trend. FN slightly decreased *M.smegmatis* growth in 2 experiments, increased the growth in 1 experiment and the growth was the same in another experiment (Figure 6.8-B). This growth inhibition was not statistically significant (p=0.125) (Figure 6.8-A). Incubation of *M.smegmatis* with higher concentrations of FN (25 and 50 µg/ml) was shown to increase *M.smegmatis* growth by 34.3% & 22.5% repectively in 3 independent experiments showing the same trend (Figure 6.9-A &B), and the growth increase was statistically significant (p<0.05).

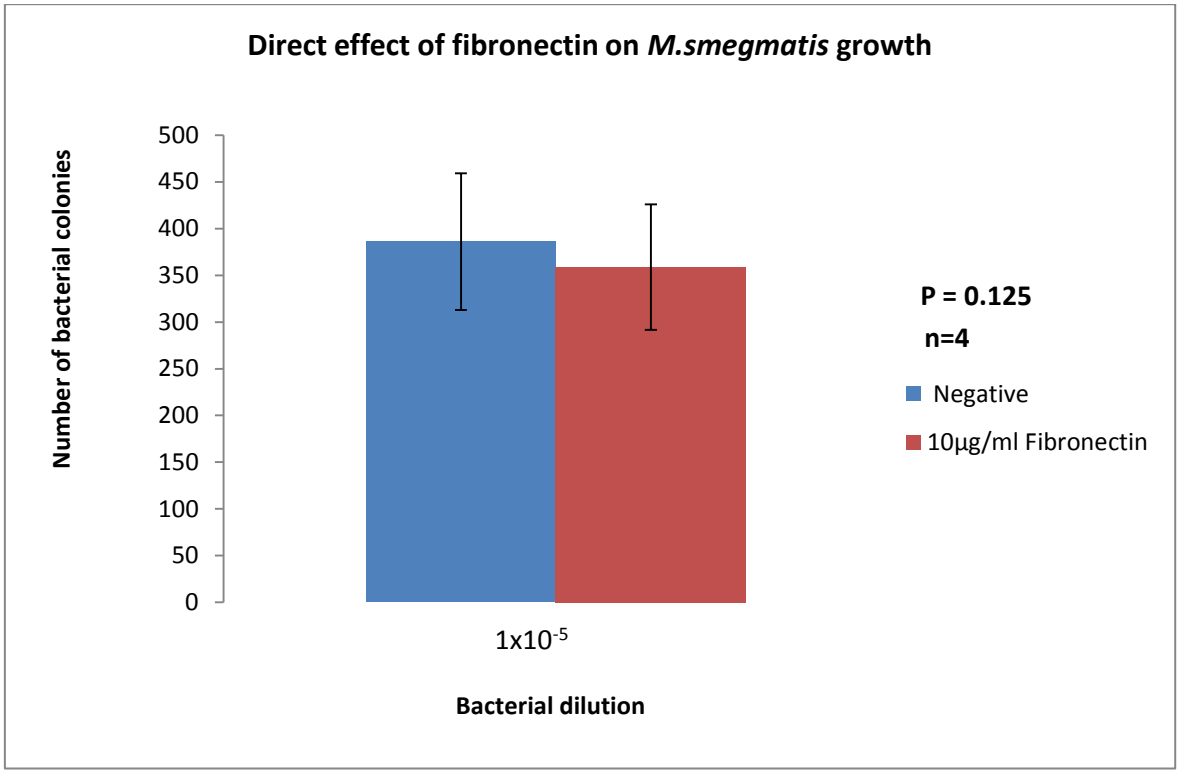

Figure 6.8-A: Direct effect of fibronectin (10µg/ml) on *M.smegmatis* growth. Mycobacteria ($1x10^{-5}$ dilution) were treated with 10µg/ml FN and incubated for 2 hours at 37°C with 5mM $CaCl_2$. Untreated *M.smegmatis* with 5mM $CaCl_2$ was used as a negative control. Following incubation, 250µl of bacterial culture was plated on agar plates in triplicates and incubated at 37°C for 72 hours. The number of bacterial colonies in each plate was counted by visual inspection. Each bar represents the average of four independent experiments. Error bars represent ± standard error of the mean. P value was calculated using Wilcoxon Signed Rank test. Negative contains untreated *M.smegmatis*.

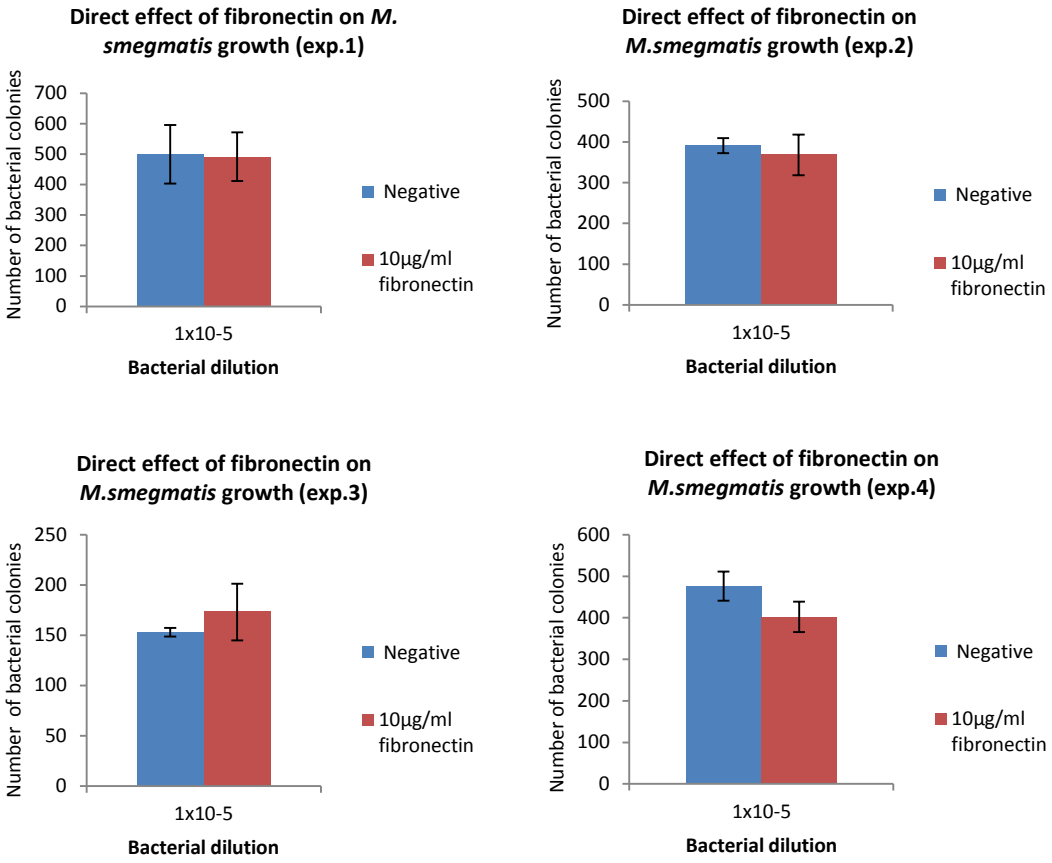

Figure 6.8 -B: Direct effect of Fibronectin (10µg/ml) on *M.smegmatis* growth (4 individual experiments). Each bar represents the average of triplicate data. Error bar represents ± standard deviation. Negative contains untreated *M.smegmatis*.

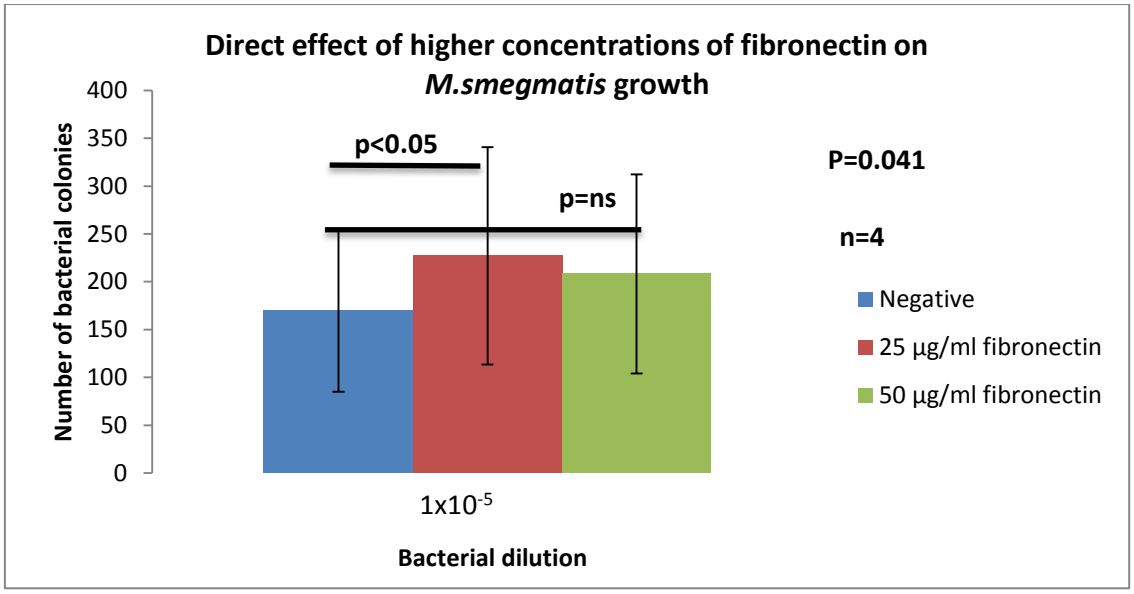

Figure 6.9-A: Direct effect of higher concentrations of Fibronectin on *M.smegmatis* growth. Each bar represents the average of 4 independent experiments. Error bars represent ± standard error of the mean. Multiple comparison of the data sets was done using Friedman test (p=0.041). Individual data were compared with each other using Dunn's post hoc test: Negative vs 25µg/ml FN, P<0.05; Negative vs 50µg/ml FN, P=ns (non-significant). Negative contains untreated *M.smegmatis*.

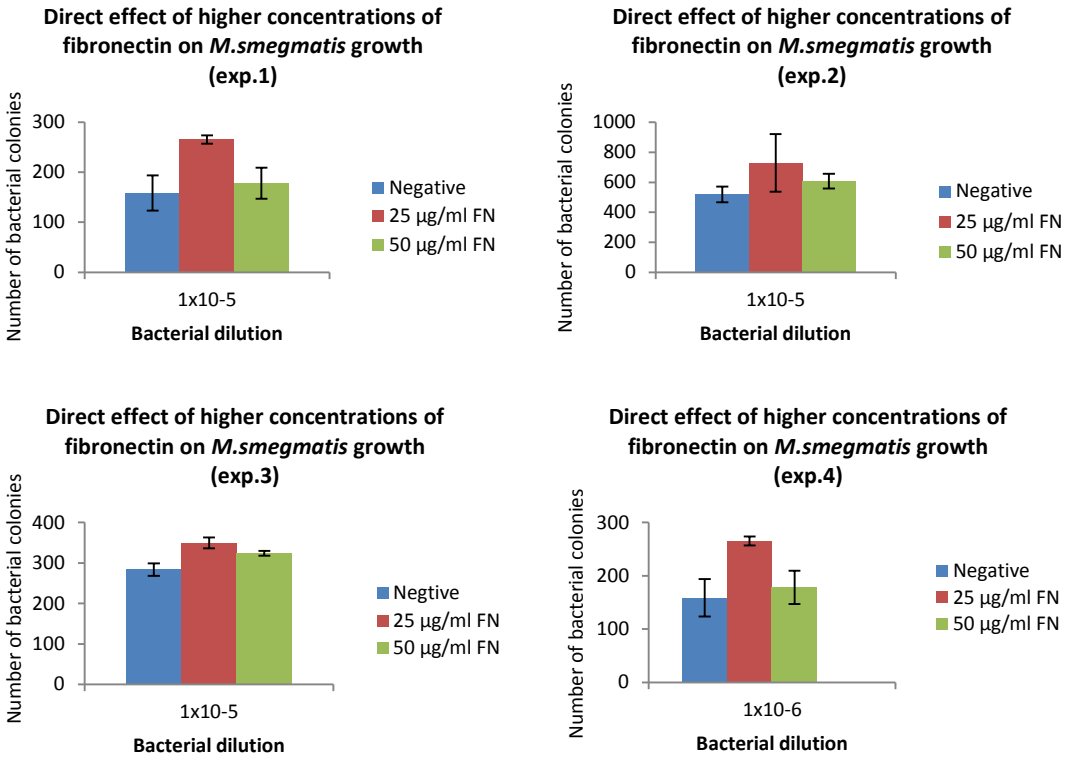

Figure 6.9-B: Direct effect of higher concentrations of Fibronectin on *M.smegmatis* growth in presence of 5mM $CaCl_2$ (4 individual experiments). Each bar represents the average of triplicate data. Error bars represents ±standard deviation. Negative contains untreated *M.smegmatis*.

6.2.7.2 Direct effect of Fibronectin on BCG growth

The presence of 10µg/ml FN was shown to increase BCG growth in 6 independent experiments by 14.5%. The growth increase was statistically significant ($p<0.05$) (Figure 6.10-A). All the experiments showed same trend of increase growth (Figure 6.10-B).

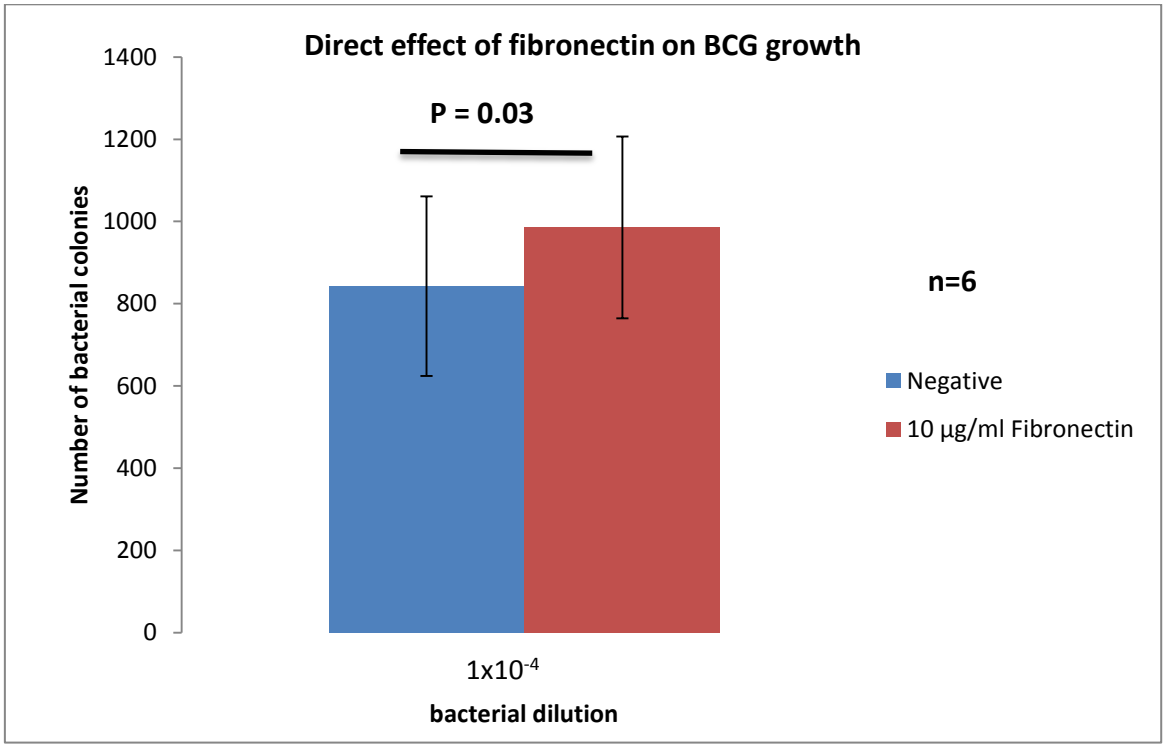

Figure 6.10-A: Direct effect of fibronectin on BCG growth. FN slightly increased BCG growth *in vitro*. A dilution of $1x10^{-4}$ BCG was treated with 10µg/ml FN and incubated for 2 hours at 37°C with 5mM $CaCl_2$. Untreated BCG with 5mM $CaCl_2$ was used as a negative control. Following incubation, 250µl of bacterial culture was plated on 7H10 plates containing 10% ADC and incubated at 37°C for 72 hours. The number of bacterial colonies was counted by visual inspection. Each bar represents the average of six independent experiments. Error bars represent ±standard error of the mean. P value was calculated using Wilcoxon Signed Rank test. Negative contains untreated BCG. Negative contains untreated BCG.

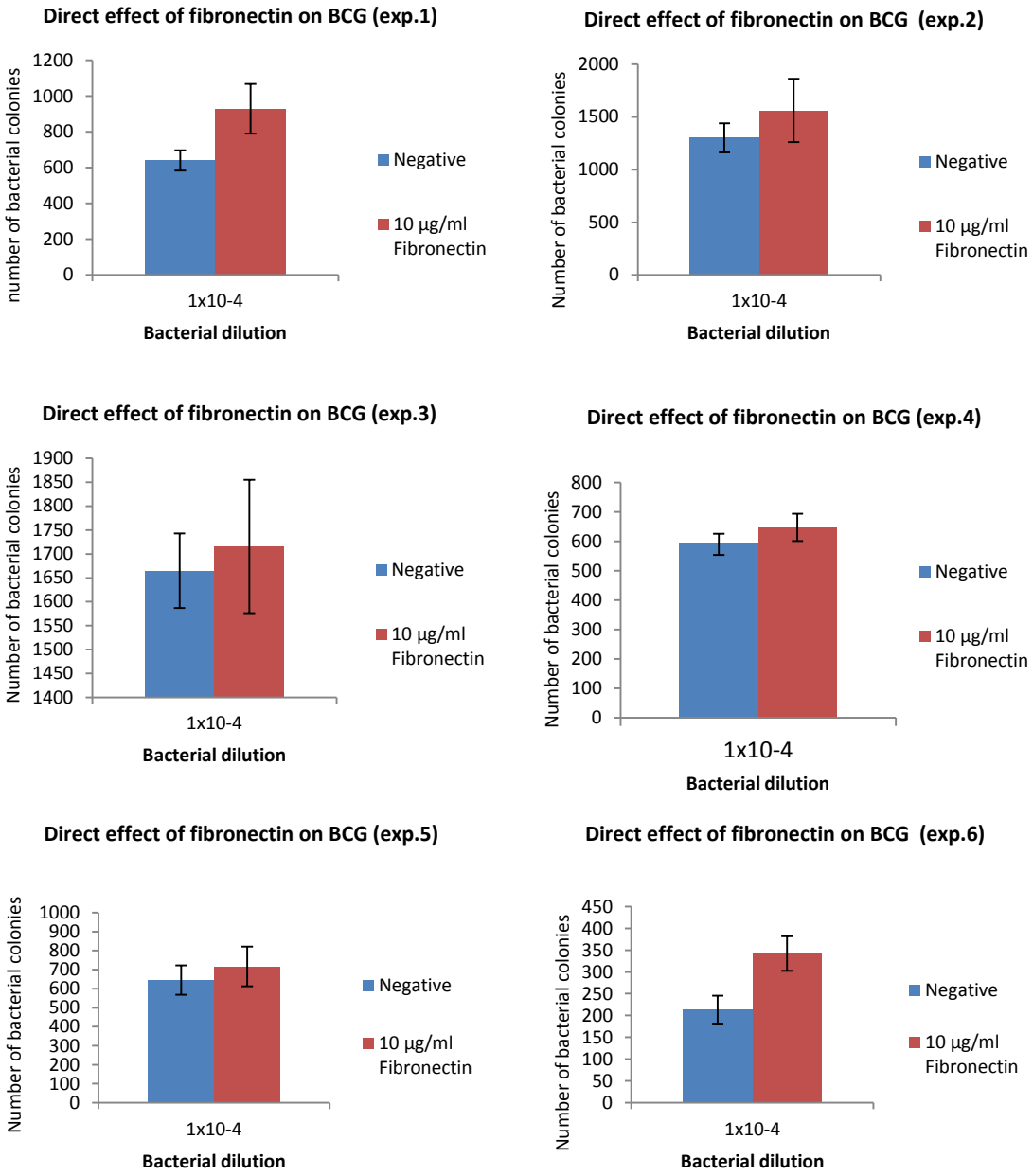

Figure 6.10-B: Direct effect of Fibronectin on BCG growth (6 individual experiments). FN directly increased BCG growth. Each bar represents the average of triplicate data. Error bar represents ±standard deviation. Negative contains untreated BCG. Negative contains untreated BCG.

6.2.8 Effect of Fibronectin on the uptake (phagocytosis) of mycobacteria by THP-1 cells

6.2.8.1 Effect of Fibronectin on the uptake of *M.smegmatis* by THP-1 cells

FN was shown to increase the uptake of *M.smegmatis* by THP-1 cells in presence of 5mM $CaCl_2$. All the 3 independent experiments showed the same trend (Figure 6.11-B). There was about 51% increase in the uptake of *M.smegmatis* by THP-1 cells infected with FN treated as compared to untreated *M.smegmatis,* and this result was statistically significant (p=0.03) (Figure 6.11-A).

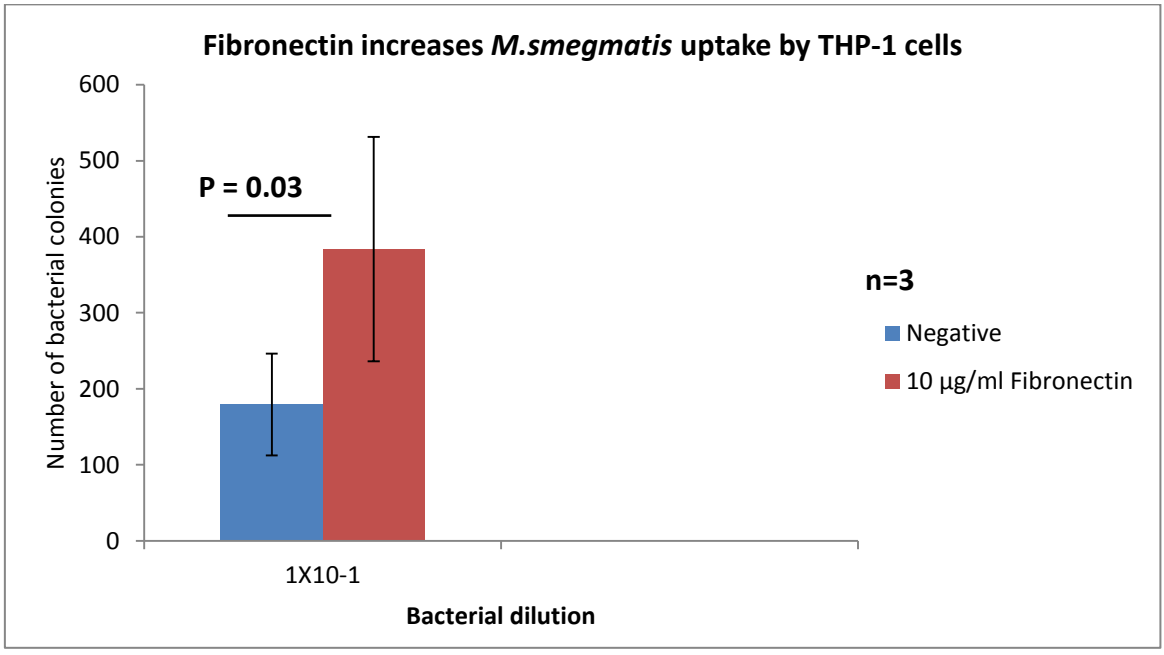

Figure 6.11-A: Effect of Fibronectin on the uptake of *M.smegmatis* by THP-1 cells. Both FN treated and untreated tubes (negative) were incubated for 2 hours at 37°C in presence of $CaCl_2$. After incubation, THP-1 cells were added to mycobacteria in ratio 1:5 (THP-1 cells:*M.smegmatis*), and incubated for 1 hour at 37°C to allow phagocytosis of mycobacteria by THP-1 cells. Following incubation, magnetic beads bound with anti-human MHC class 1 was added to each tube in ratio 1:4 (THP-1: beads) and the tubes were incubated on ice for 30 minutes on a shaker. Next, the THP-1 cells were washed 3 times to remove extracellular bacteria. Washed cells were laysed with 0.1% saponin with vortexed for 15 minutes to release phagocytosed mycobacteria. Each bar represents the average of three independent experiments. Error bars represent ± standard error of the mean. P value calculated using Wilcoxon signed rank test. Negative contains untreated *M. smegmatis*.

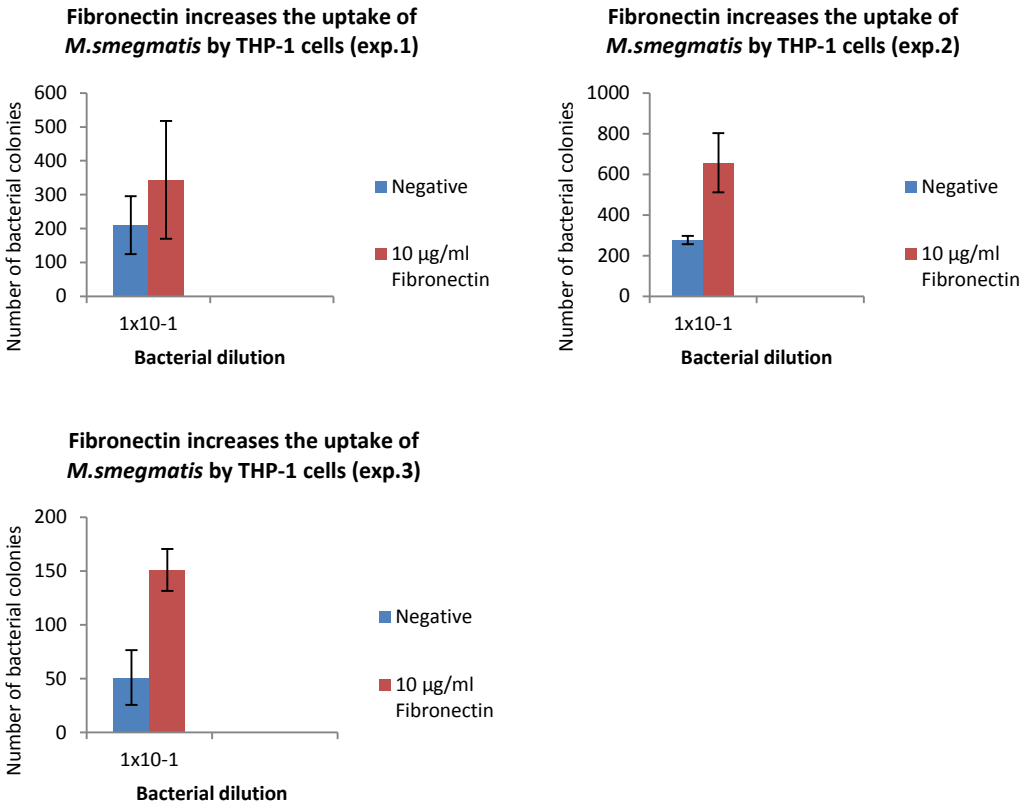

Figure 6.11-B: Effect of Fibronectin on the uptake of *M.smegmatis* by THP-1 cells (3 individual experiments). Each bar represents the average of triplicate data. Error bars represent ± standard deviation. Negative contains untreated *M.smegmatis*.

6.2.8.2 Effect of Fibronectin on the uptake of BCG by THP-1 cells

FN was shown to increase the uptake of BCG in presenceof 5mM $CaCl_2$ by THP-1 cells by 35% in six independent experiments. All the independent experiments showed the same trend in increase the uptake (Figure 6.12-B), and the results were also statistically significant ($p<0.05$) (Figure 6.12-A).

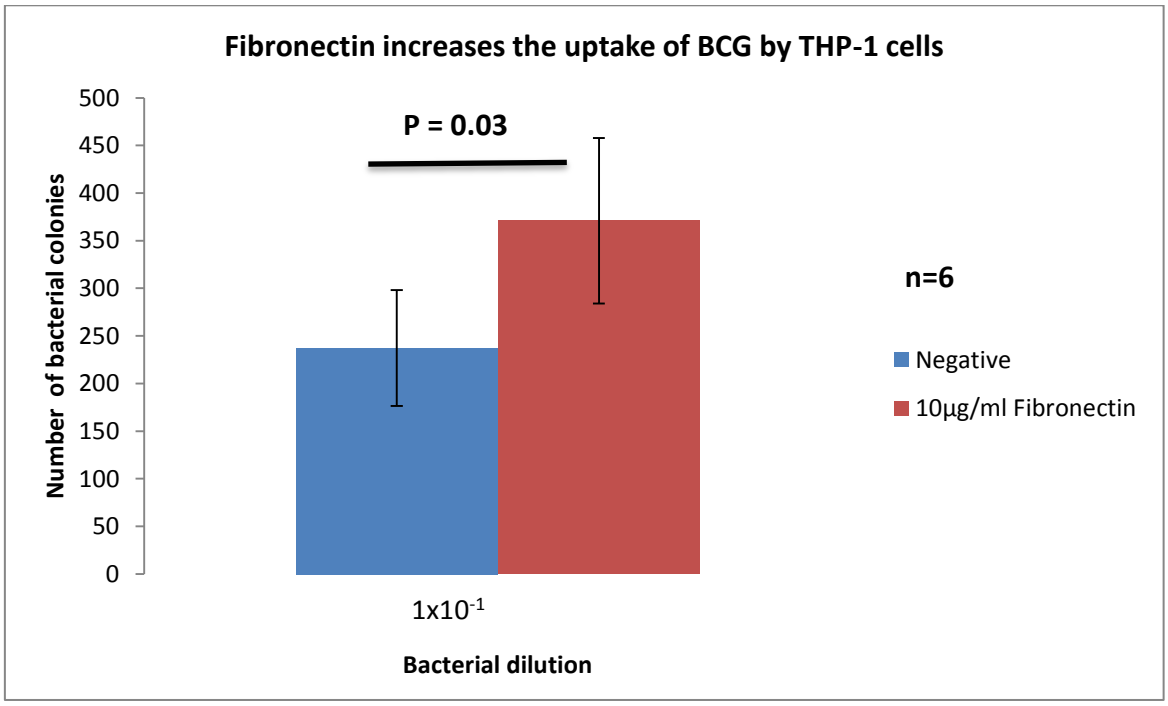

Figure 6.12-A: Effect of Fibronectin on the uptake of BCG by THP-1 cells. The uptake of BCG THP-1cells was enhanced with FN. Both FN treated and untreated BCG was incubated for 2 hours at 37°C in presence of $CaCl_2$. Following the incubation, THP-1 cells were added to each tube in ratio 1:5 (THP-1 cells:BCG), and incubated for an hour inside at 37°C to allow the uptake of BCG by THP-1 cells. Next, magnetic beads bound with anti-human MHC class 1 were added to THP-1 cells in a ratio of 1:4 (THP-1 cells: beads), and tubes were incubated in ice horizontally for 30 minutes on a shaker. Next, THP-1 cells were washed 3 times to remove extracellular bacteria. Washed cells were lysed with 0.1% saponin by vortexing for 15 minutes to release phagocytosed mycobacteria. Each bar represents the average of six independent experiments. Error bars represent ± standard error of the mean. P value calculated using Wilcoxon signed rank test. Negative contains untreated BCG.

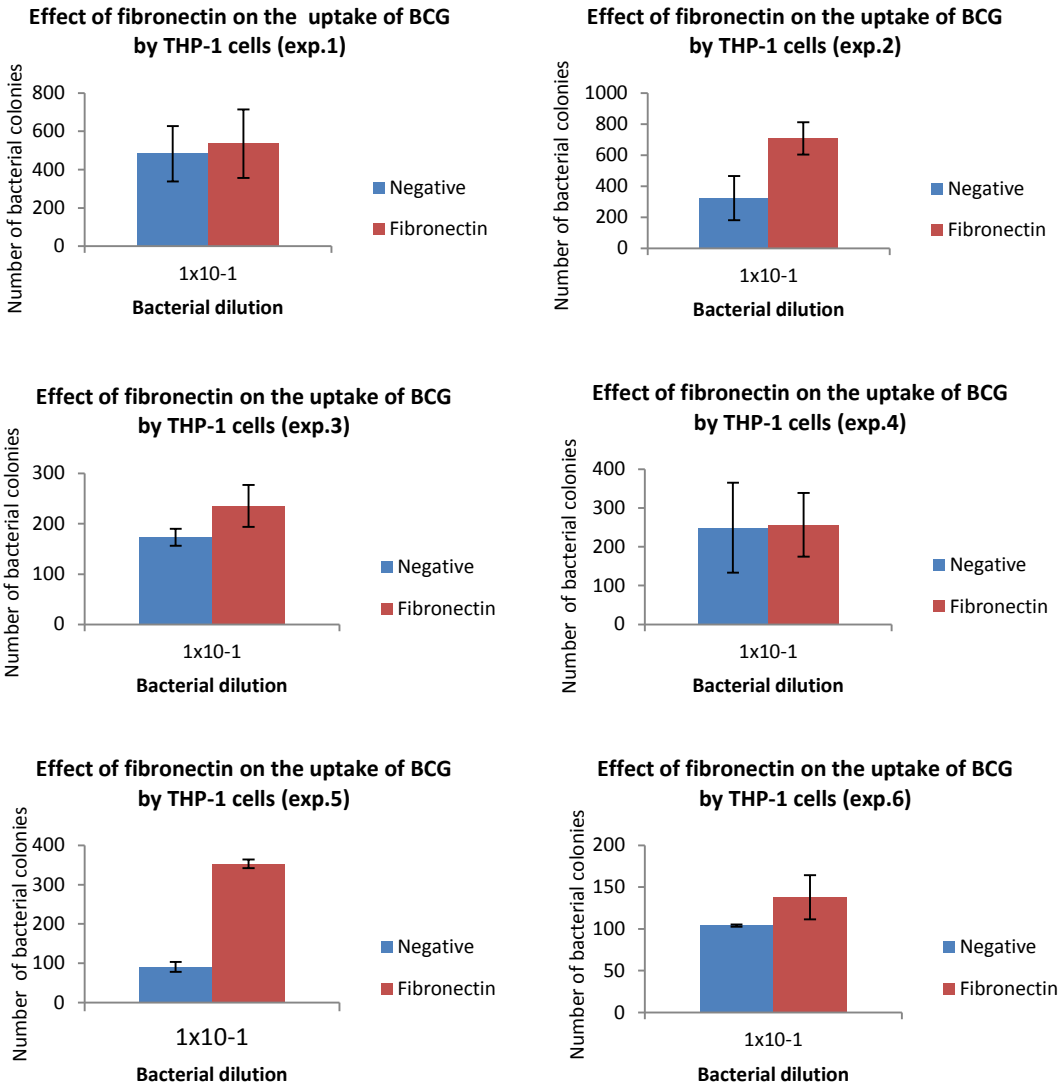

Figure 6.12-B: Effect of 10µg/ml Fibronectin on the uptake of BCG by THP-1 cells (6 individual experiments). Each bar represents the average of triplicate data. Error bars represent ± standard deviation. Negative contains untreated BCG.

6.2.9 Effect of fibronectin on the growth of mycobacteria inside THP-1 cells

6.2.9.1 Effect of Fibronectin on the growth of *M.smegmatis* inside THP-1 cells

Fibronectin was shown to increase *M.smegmatis* growth by 38.5% inside THP-1 cells. All the six independent experiments (Figure 6.13-B) showed the same trend of increased growth inside THP-1 cells infected with FN treated *M.smegmatis* as compared with THP-1 cells infected with untreated *M.smegmatis*, and the experimental result was also statistically significant (p=0.03) (Figure 6.13-A).

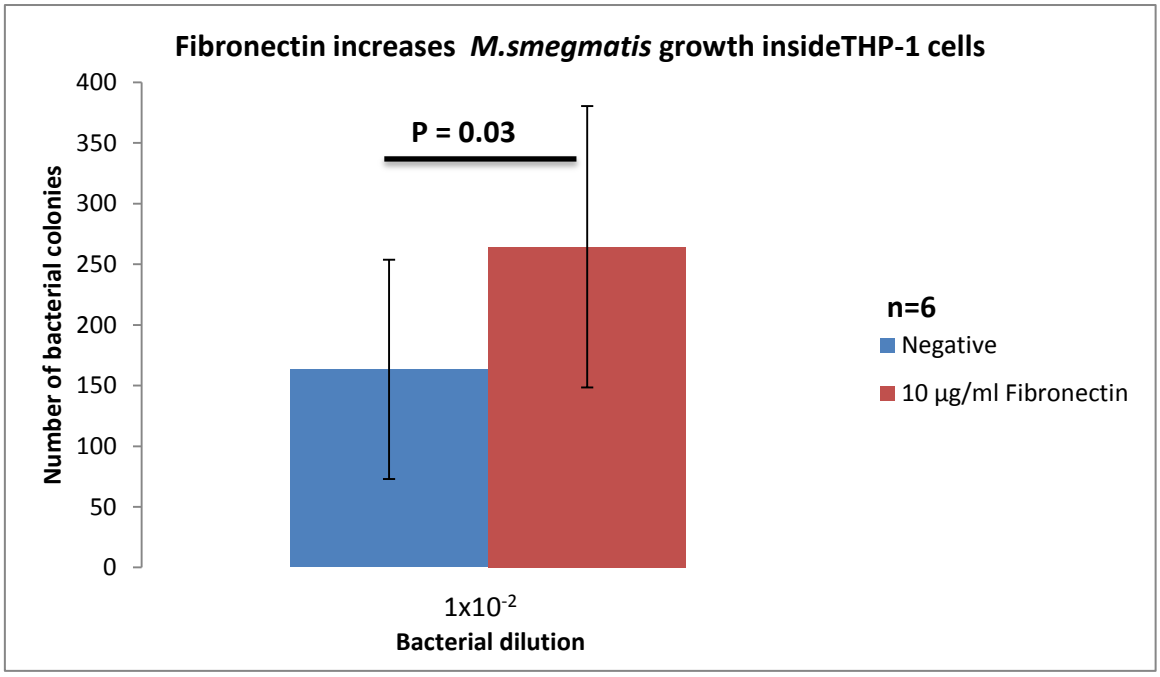

Figure 6.13-A: Effect of Fibronectin on *M.smegmatis* growth inside THP-1 cells. FN treated and untreated *M.smegmatis* were incubated for 2 hours at 37°C with 5mM $CaCl_2$. Following incubation, THP-1 cells were added to mycobacteria in a 1:5 ratio (THP-1 cells:*M.smegmatis*) and incubated for an hour inside CO_2 incubator at 37^0C. After incubation, magnetic beads bound with anti-human MHC class 1 were added to each tube in a ratio of 1:4 (THP-1: beads) and the tubes were incubated in ice for 30 minutes on a shaker. Next, the cells were washed 3 times to remove extracellular bacteria. Washed cells were suspended in complete RPMI medium (without antibiotics) and incubated inside a CO_2 incubator for 24 hours. Following incubation, the cells were separated by a magnet and lysed with 0.1% of saponin and vortexing for 15 minutes. Equal volumes of cell lysate and supernatant were mixed together and bacterial dilution of $1x10^{-2}$ was prepared. 250µl of bacteria was plated on LB agar in triplicates. Plates were incubated at 37°C for 3 days. Each bar represents the average of 6 independent experiments. Error bars represent ±standard error of the mean. P value was calculated by using Wilcoxon Signed rank test. Negative contains untreated *M.smegmatis*.

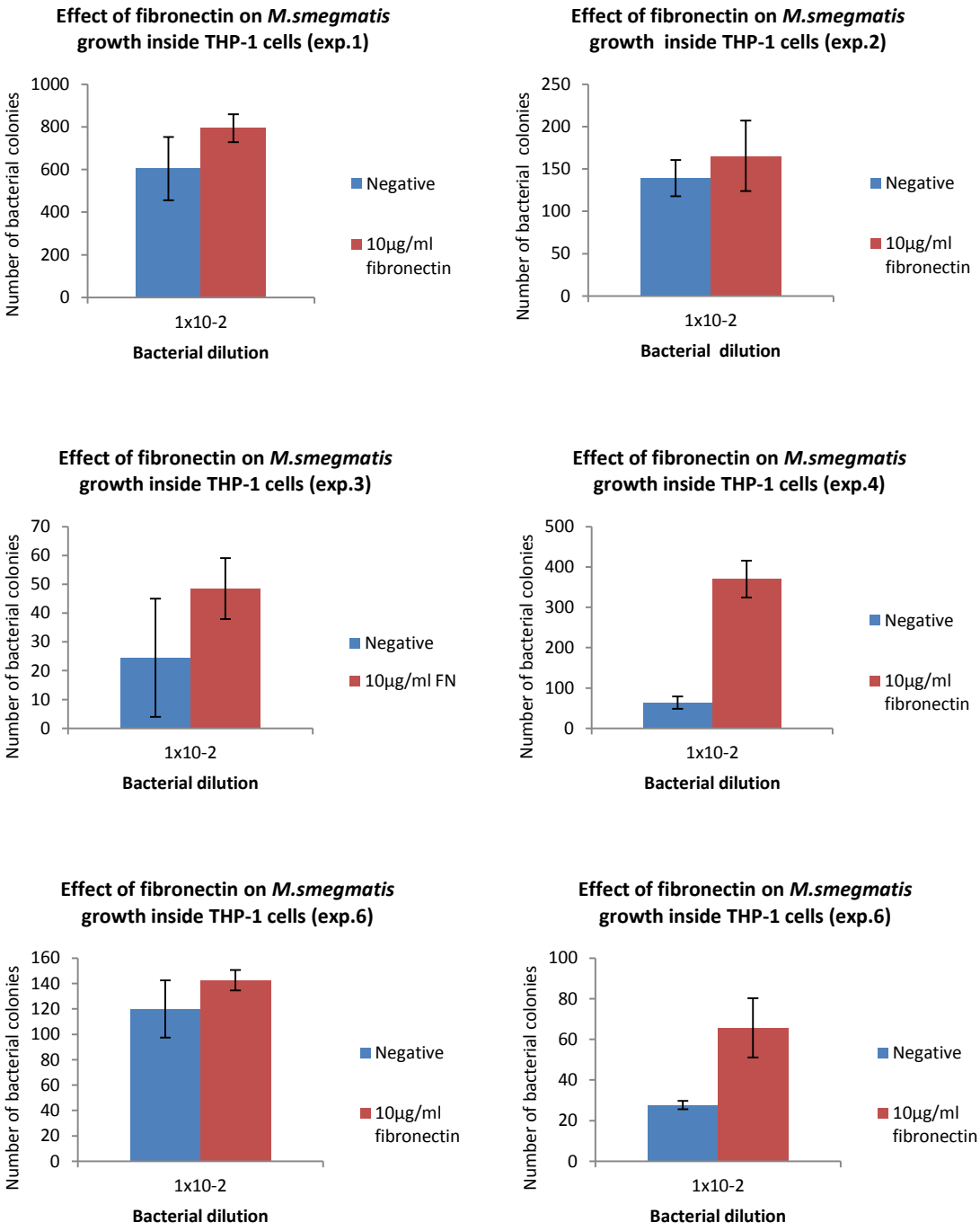

Figure 6.13-B: Effect of Fibronectin on *M.smegmatis* growth inside THP-1 cells (6 individual experiments). Each bar represents the average of triplicate data. Error bar represents ±standard deviation.

6.2.9.2 Effect of Fibronectin on the growth of BCG inside THP-1 cells

Fibronectin was shown to increase BCG growth inside THP-1 cells by 50%. Six independent experiments (Figure 6.14-B) showed the same trend of BCG growth increase inside THP-1 cells infected with FN treated BCG as compared with THP-1 cells infected with untreated mycobacteria, and the results were statistically significant ($p<0.05$) (Figure 6.14-A).

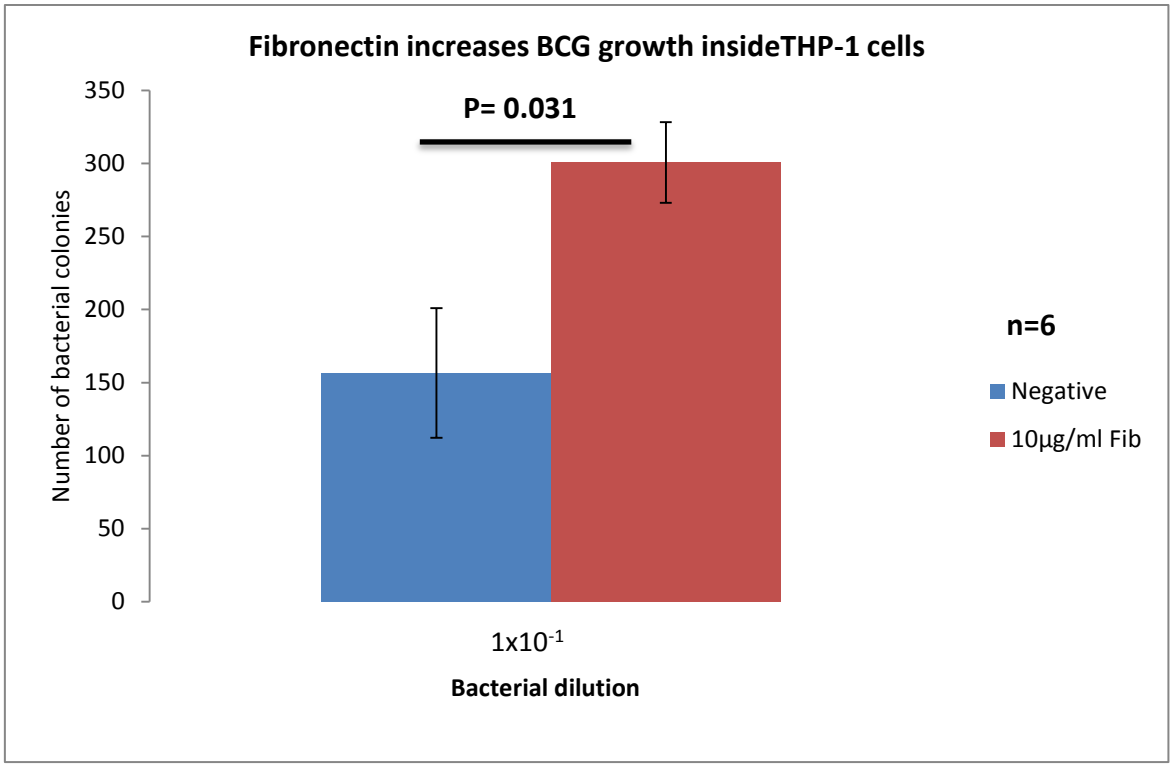

Figure 6.14-A: Effect of Fibronectin on the growth of BCG inside THP-1 cells. FN enhanced BCG growth inside THP-1 cells. Both FN treated and untreated BCG (negative) were incubated for 2 hours at 37°C with 5mM $CaCl_2$. THP-1 cells were added to mycobacteria in a 1:5 ratio (THP-1 cells:BCG) and incubated for one hour inside a CO_2 incubator. Next, magnetic beads bound with anti-human MHC class 1 were added to each tube in a ratio of 1:4 (THP-1: beads). Tubes were incubated in ice for 30 minutes on a shaker. Following incubation, the cells were washed 3 times using RPMI. Cells were suspended in 1ml complete RPMI medium (without antibiotics) and incubated inside a CO_2 incubator for 24 hours. The cells were then separated using a magnet and lysed with 0.1% of saponin by vortexing for 15 minutes. Equal volumes of cell lysate and supernatant were mixed together and bacterial dilution of $1x10^{-1}$ was prepared and 250µl was plated on 7H10 plates supplemented with 10% ADC in triplicates. The plates were incubated at 37°C for 2-3 weeks. Each bar represents the average of six independent experiments. Error bars represent ±standard error of the mean. P value calculated using Wilcoxon signed rank test. Negative contains untreated BCG.

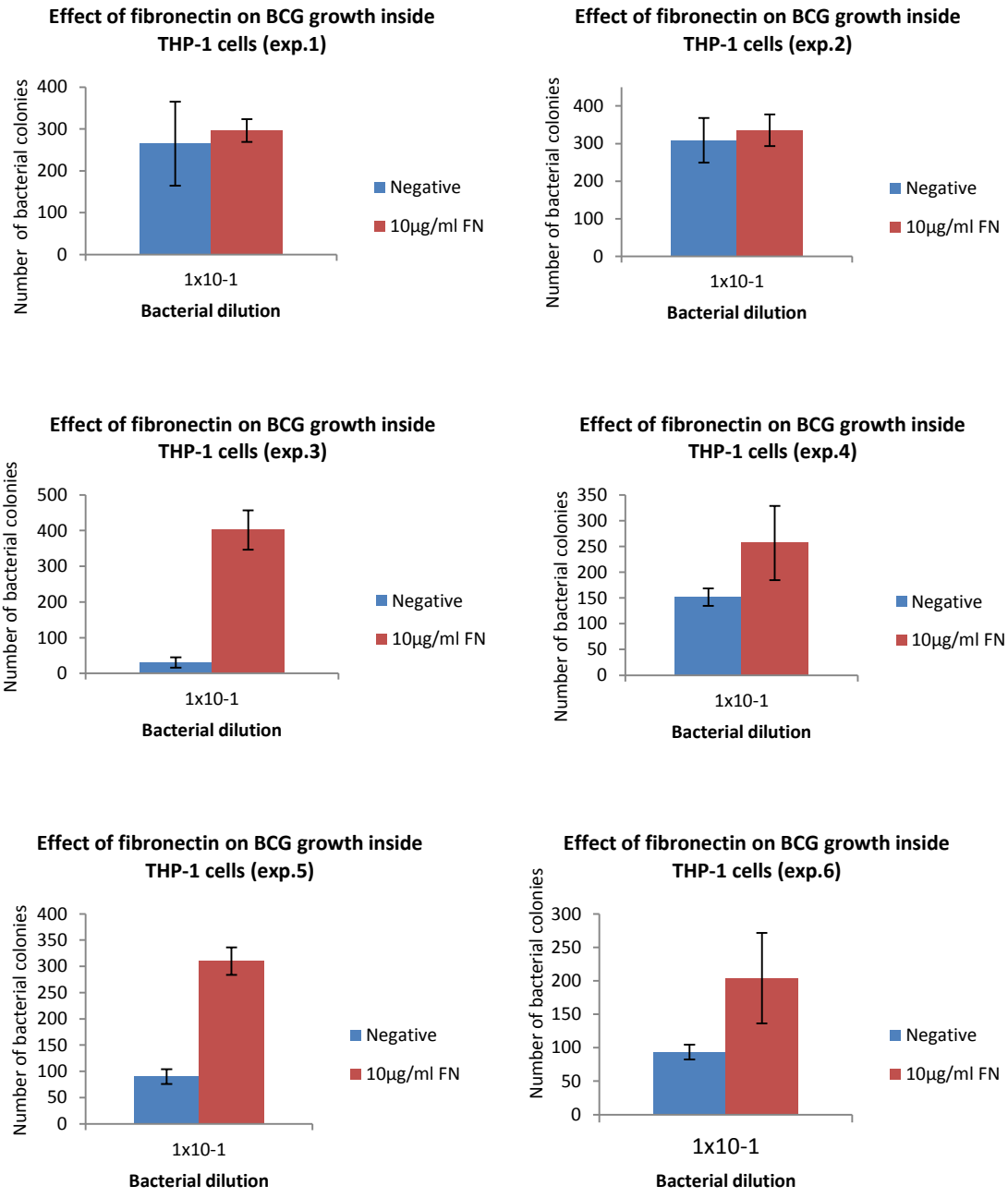

Figure 6.14-B: Effect of Fibronectin on BCG growth inside THP-1 cells (6 individual experiments). Each bar represents the average of triplicate data. Error bars represent ±standard deviation. Negative contains untreated BCG.

6.2.10 Underlying mechanisms of mycobacterial growth enhancement inside THP-1 cells infected with fibronectin treated and untreated mycobacteria

The gene expressions of inducible nitric oxide synthase, pro-inflammatory and anti-inflammatory cytokines were studied by using q-PCR.

6.2.10.1 Expression of inducible nitric oxide synthase (iNOS)

This enzyme (iNOS) is responsible for production of reactive nitrogen intermediates (RNI), which kills mycobacteria inside infected macrophages. RNI have been detected in previously *Mtb* infected macrophages and inhibition of iNOS in latent TB human leads to *Mtb* reactivation (Gardam et al., 2003). This study showed that iNOS was expressed by THP-1 cells infected with un treated *M.smegmatis* (Figure 6.15-A) and BCG (Figure 6.15-B) at 5 and 10 hours. This enzyme (iNOS) was not detected in THP-1 cells infected with FN treated mycobacteria (*M.smegmatis* and BCG).

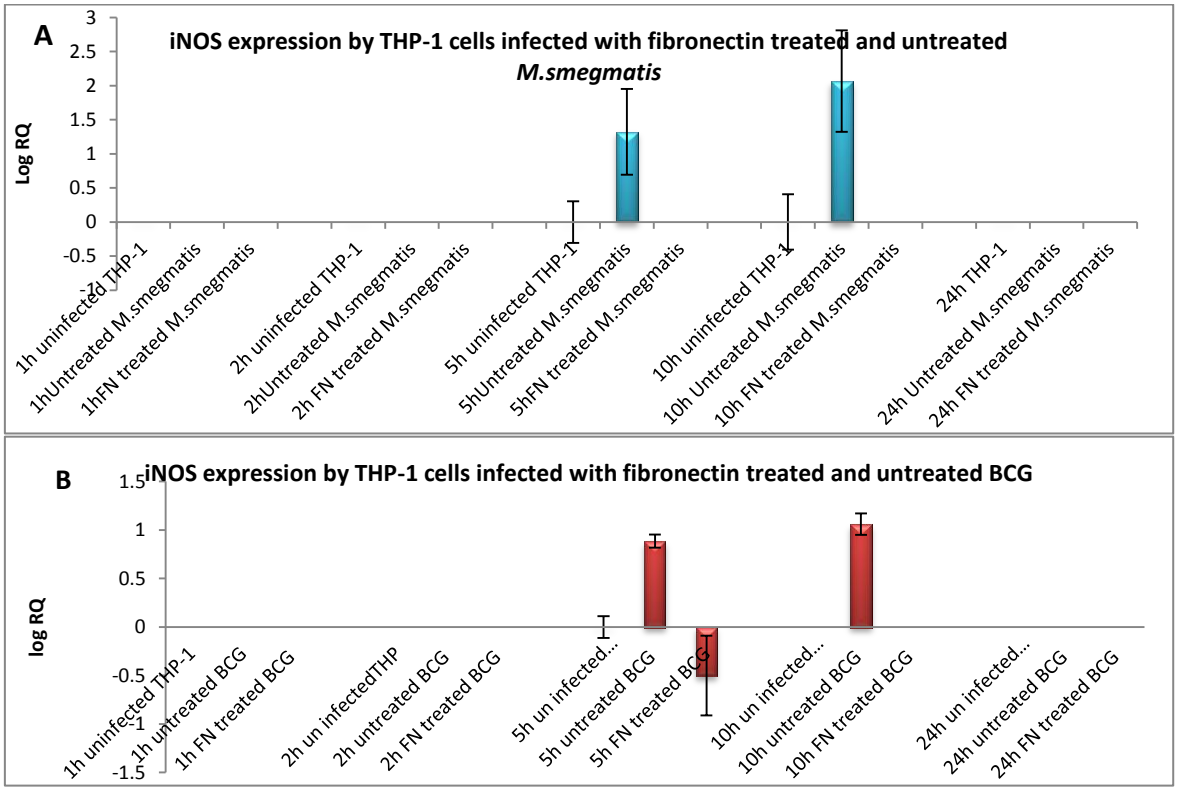

Figure 6.15: Expression of iNOS gene by THP-1 cells infected with fibronectin treated and untreated mycobacteria. **A:** *M.smegmatis.* **B:** BCG. THP-1 cells were incubated for 1, 2, 5, 10 and 24 hours after infection with mycobacteria at 37^{o}C inside a CO_2 incubator. Data was normalized to 18sRNA expression as control. RQ values were calculated using the formula; RQ=$2^{\Delta\Delta Ct}$. Log RQ values were plotted to show the gene expression. Un-infected THP-1 cells were used as negative

control. Each bar represents the average triplicate readings. Error bars represent ±standard deviation.

6.2.10.2 Expression of tumour necrosis factor-α (TNF-α) gene

The gene expression for TNF-α was studied because it regulates the growth of mycobacteria inside granulomas. Moreover, it initiates adaptive immunity against tuberculosis. TNF-α was expressed by THP-1 cells infected with FN treated and untreated mycobacteria (Figure 6.16). Treatment of FN showed downregulation of the expression of this cytokine at 5, 10 & 24 hours for both *M.smegmatis* and BCG (Figure 6.16- A & B).

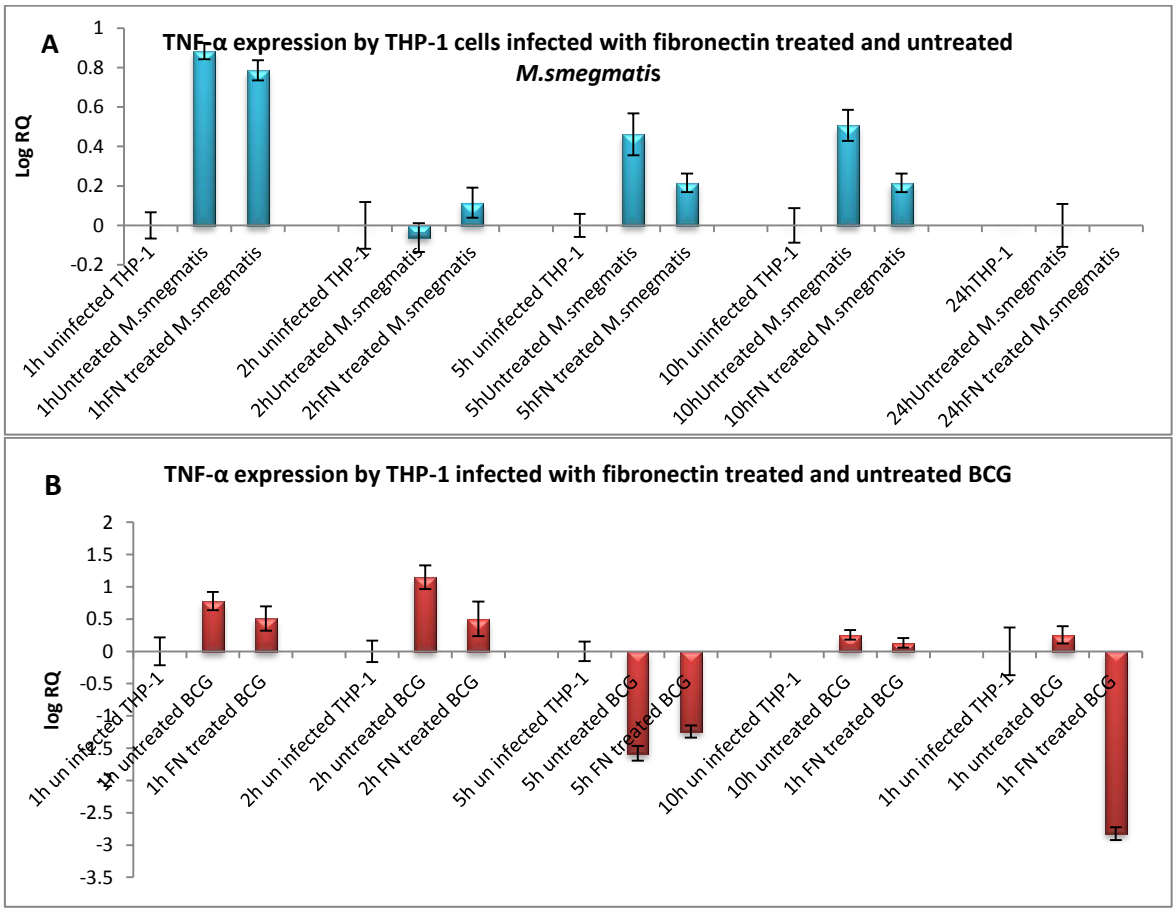

Figure 6.16: TNF-α gene expression by THP-1 cells infected with fibronectin treated and untreated mycobacteria. **A:** *M.smegmatis.* **B**: BCG. THP-1 cells were incubated for 1, 2, 5, 10 and 24 hours after infection with mycobacteria at 37°C inside a CO_2 incubator. The cell pellet was collected and used for RNA extraction and cDNA synthesis used in this analysis. The expression of the gene was measured using qPCR and data was normalized to 18sRNA expression as control. RQ values were calculated using the formula; $RQ=2^{\Delta\Delta Ct}$. Log RQ values were plotted to show the gene expression. Each bar represents the average of triplicate readings. Un-infected THP-1 cells were used as negative control. Error bars represent ±standard deviation.

6.2.10.3 Expression of Interleukin 1β (IL-1β) gene

IL-1β is a pro-inflammatory cytokine expressed inside granulomas. It is protective against tuberculosis. IL-1β receptor deficient mice showed impaired granuloma formation. This cytokine was expressed by THP-1 cells infected with fibronectin treated mycobacteria (*M.smegmatis* and BCG) and untreated mycobacteria at one hour and up to 10 hours. It appears that the expression of IL-1β is less in THP-1 cells infected with fibronectin treated BCG compared to untreated BCG (Figure 6.17).

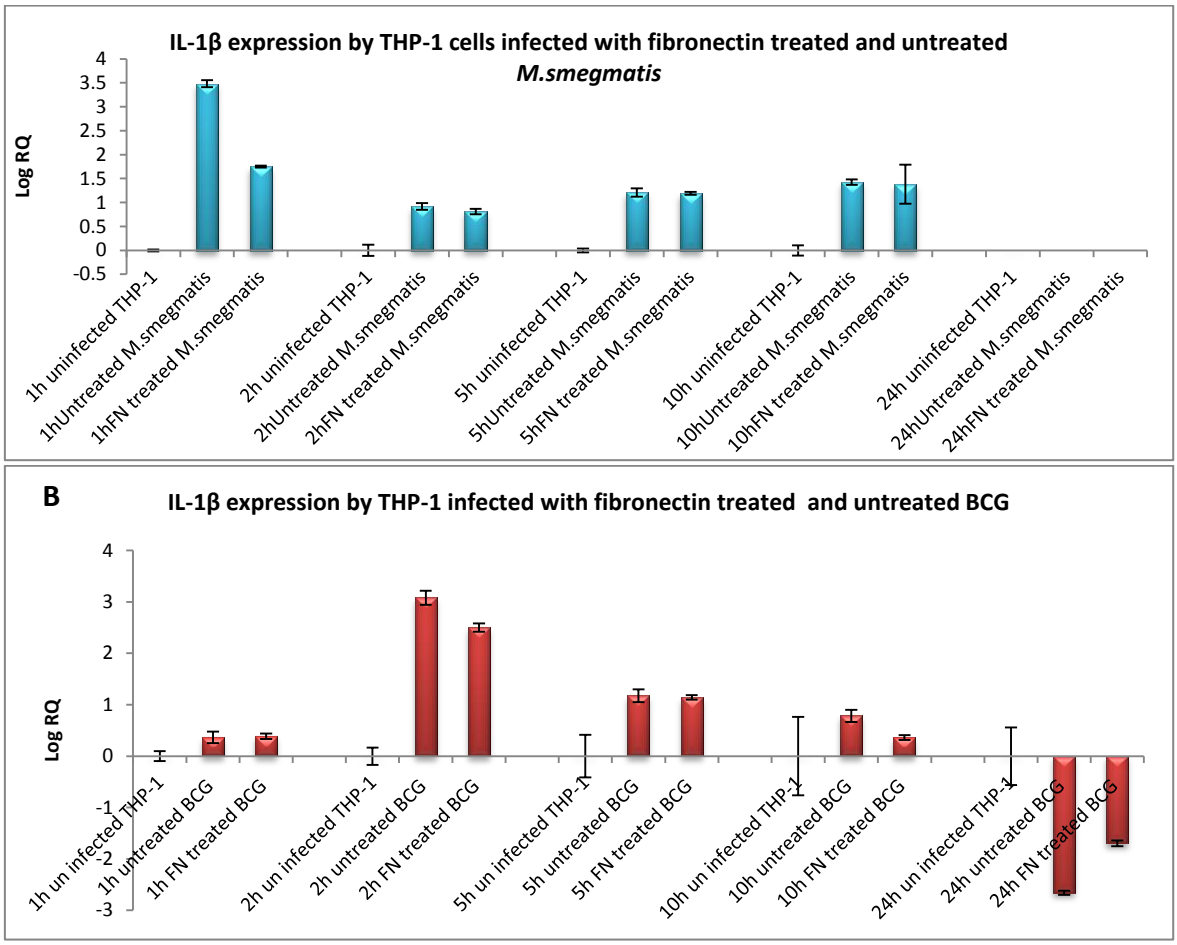

Figure 6.17: IL-1β gene expression by THP-1 cells infected with fibronectin treated and untreated mycobacteria. **A**: *M.smegmatis.* **B***:* BCG. THP-1 cells were incubated for 1, 2, 5, 10 and 24 hours after infection with mycobacteria at 37°C inside a CO_2 incubator. The cell pellet was collected and used for RNA extraction and cDNA synthesis used in this analysis. The expression of the gene was measured using qPCR and data was normalized to 18sRNA expression as control. RQ values were calculated using the formula; $RQ=2^{\Delta\Delta Ct}$. Log RQ values were plotted to show the gene expression. Un-infected THP-1 cells were used as negative control. Each bar represents the average of triplicate readings. Error bars represent ±standard deviation.

6.2.10.4 Expression of interleukin- 6 (IL-6) gene

IL-6 is pro-inflammatory cytokine that plays opposing roles in pathogenesis of tuberculosis. IL-6 has been shown to inhibit TNF-α and IL-1β production by macrophages, as well as facilitating the growth of mycobacteria (Schindler et al., 1990). The pro-inflammatory cytokines IL-16 was expressed by THP-1 cells infected with FN treated mycobacteria (*M.smegmatis* & BCG) and untreated mycobacteria after one hour and up to 10 hours of incubation. It appears that the expression of IL-6 is increased in THP-1 cells infected with FN treated *M.smegmatis* while it was similar in THP-1 cells infected with FN treated and untreated BCG (Figure 6.18 A &B).

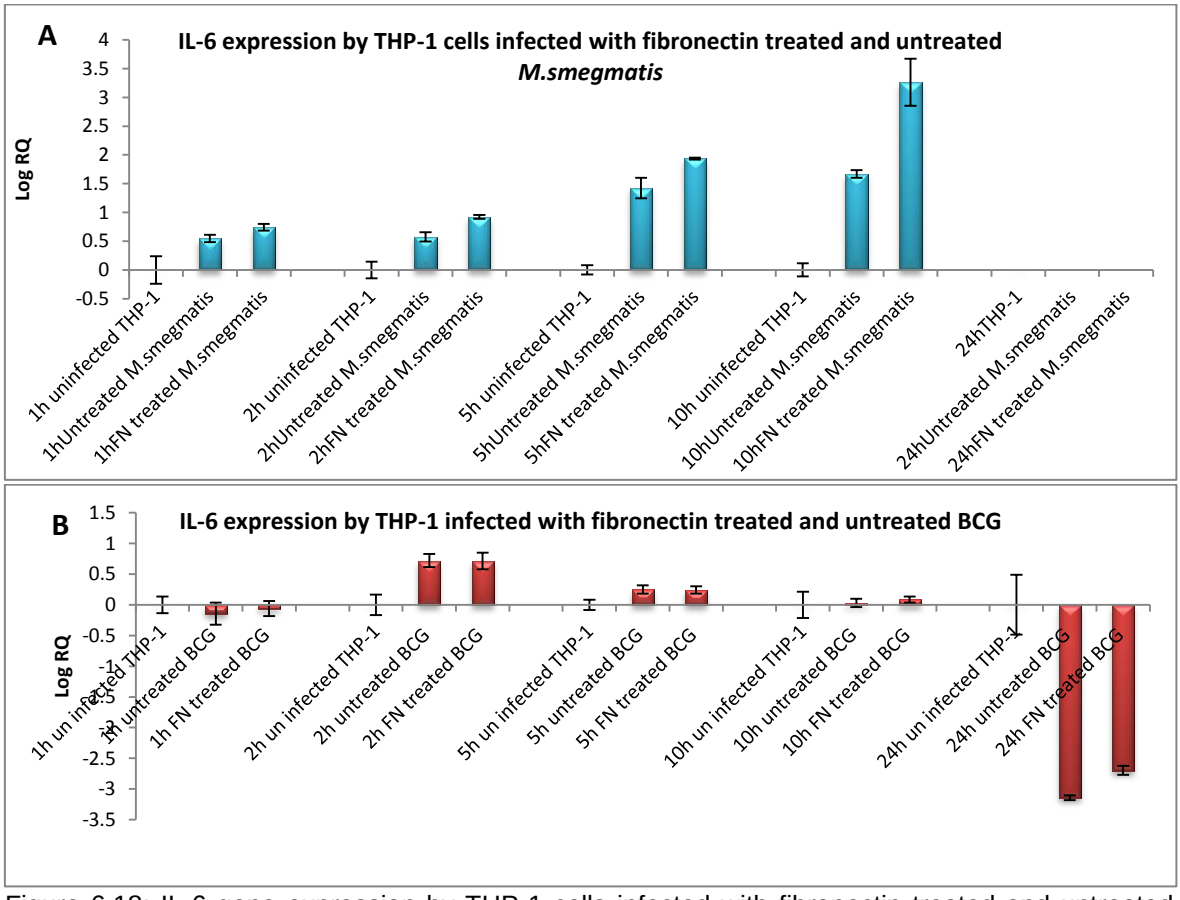

Figure 6.18: IL-6 gene expression by THP-1 cells infected with fibronectin treated and untreated mycobacteria. **A**: *M.smegmatis.* **B***:* BCG. THP-1 cells were incubated for 1, 2, 5, 10 and 24 hours after infection with mycobacteria at 37°C inside a CO_2 incubator. The cell pellet was collected and used for RNA extraction and cDNA synthesis used in this analysis. The expression of the gene was measured using qPCR and data was normalized to 18sRNA expression as control. RQ values were calculated using the formula; $RQ=2^{\Delta\Delta Ct}$. Log RQ values were plotted to show the gene expression. Un-infected THP-1 cells were used as negative control. Each bar represents the average of triplicate readings. Error bars represent ±standard deviation.

6.2.10.5 Expression of interleukin- 12 (IL-12)

IL-12 is pro-inflammatory cytokine and is protective in tuberculosis; it that initiates Th1 immunity and INF-Ɣ production by CD4 T-cells. It is expressed inside granulomas of active TB patients. It has been shown that IL-12 supplements leads to *Mtb* killing in infected mice (Flyyn et al., 1995). The pro-inflammatory cytokine IL-12 was expressed by THP-1 cells infected with FN treated and untreated mycobacteria (*M.smegmatis* and BCG). IL-12 gene expression was down-regulated by THP-1 cells infected with FN treated mycobacteria as compare to untreated mycobacteria (Figure 6.19-A & B).

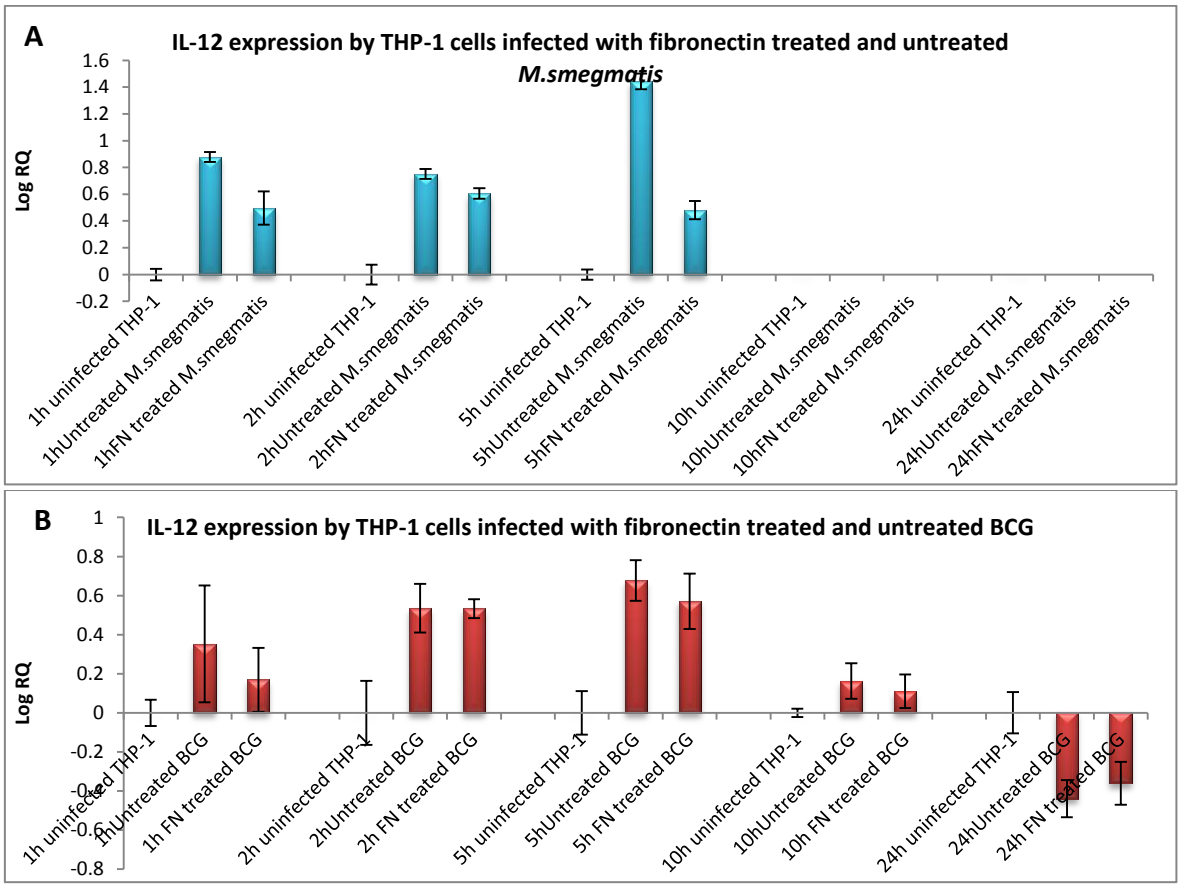

Figure 6.19: IL-12 gene expression by THP-1 cells infected with fibronectin treated and untreated mycobacteria. **A**: *M.smegmatis*. **B***:* BCG. THP-1 cells were incubated for 1, 2, 5, 10 and 24 hours after infection with mycobacteria at 37°C inside a CO_2 incubator. The cell pellet was collected and used for RNA extraction and cDNA synthesis used in this analysis. The expression of the gene was measured using qPCR and data was normalized to 18sRNA expression as control. RQ values were calculated using the formula; $RQ=2^{\Delta\Delta Ct}$. Log RQ values were plotted to show the gene expression. Un-infected THP-1 cells were used as negative control. Each bar represents the average of triplicate readings. Error bars represent ±standard deviation.

6.2.10.6 Expression of transforming growth factor β (TGF-β)

TGF-β is anti-inflammatory cytokine that is secreated inside the granulomas. TGF-β deactivate macrophages by inhibiting RNI production and increasing the growth of mycobacteria. TGF-β gene expression was upregulated at 10 and 24 hours by THP-1 cells infected with FN treated *M.smegmatis* as compared to untreated *M.smegmatis* (Figure 6.20-A). While, the gene expression for TGF-β was less by THP-1 cells infected with FN treated BCG as compared to untreated BCG at 5 & 10 hours (Figure 6.20-B).

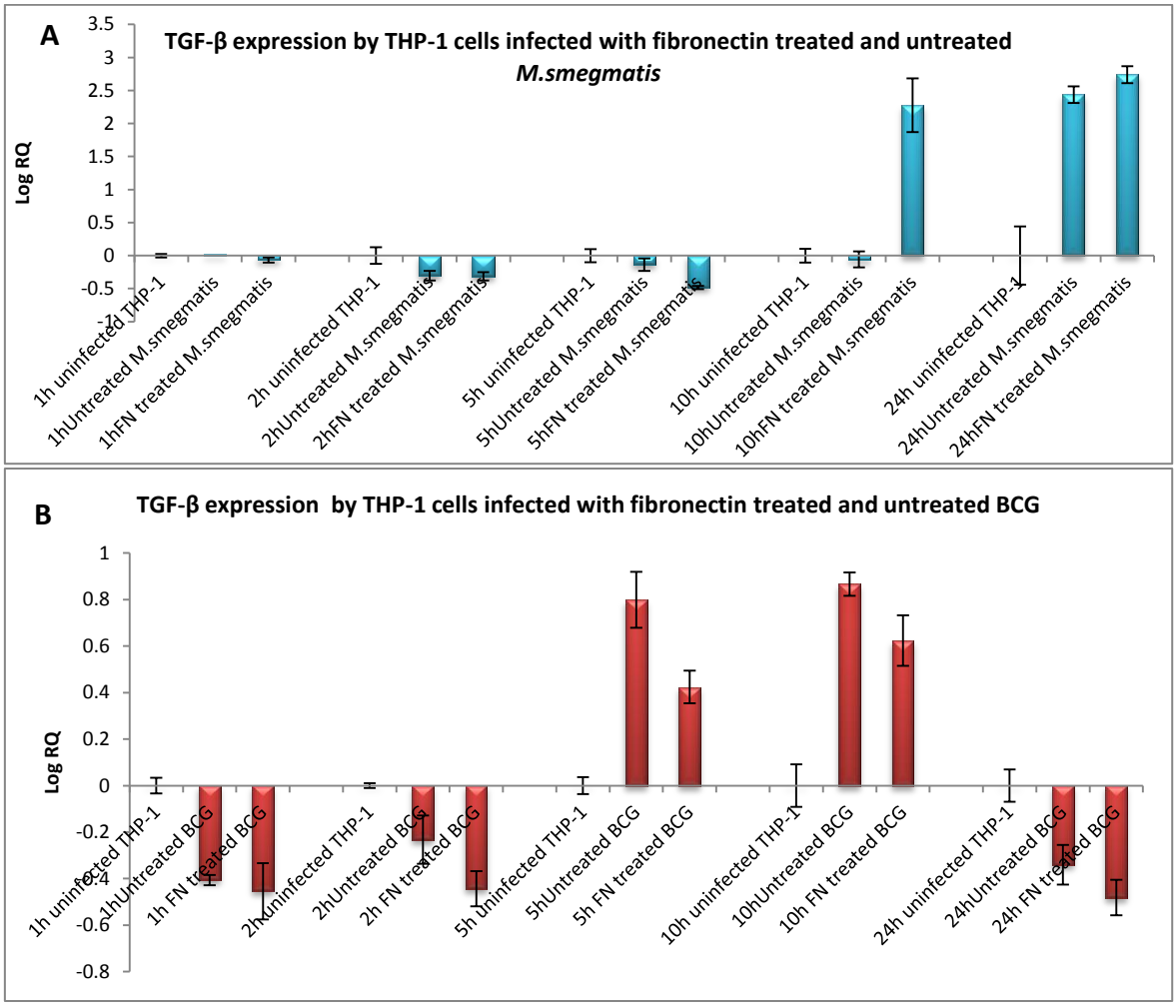

Figure 6.20: TGF-β gene expression by THP-1 cells infected with fibronectin treated and untreated mycobacteria. A: *M.smegmatis. B:* BCG. THP-1 cells were incubated for 1, 2, 5, 10 and 24 hours after infection with mycobacteria at 37°C inside a CO_2 incubator. The cell pellet was collected and used for RNA extraction and cDNA synthesis used in this analysis. The expression of the gene was measured using qPCR and data was normalized to 18sRNA expression as control. RQ values were calculated using the formula; $RQ=2^{\Delta\Delta Ct}$. Log RQ values were plotted to show the gene expression. Un-infected THP-1 cells were used as negative control. Each bar represents the average triplicate readings. Error bars represent ±standard deviation.

6.2.10.7 Expression of interleukin 10 (IL-10)

IL-10 is an anti-inflammatory cytokine that deactivates macrophages by down regulating the expression of IL-12 and TNF-α, which leads to a decrease reactive nitrogen intermediates (RNI) and increases mycobacterial survival. The gene expression of IL-10 was up regulated by THP-1 cells infected with FN *M.smegmatis* after 1, 2, and 10 hours as compared to untreated *M.smegmatis* (Figure 6.21-A). IL-10 was expressed more than 2 log folds higher at one hour of incubation by THP-1 cells infected with FN treated and untreated BCG as coimpared to THP-1 cells without infection (Fig.6.21-B), but this expression was almost undetcted at at later time points.

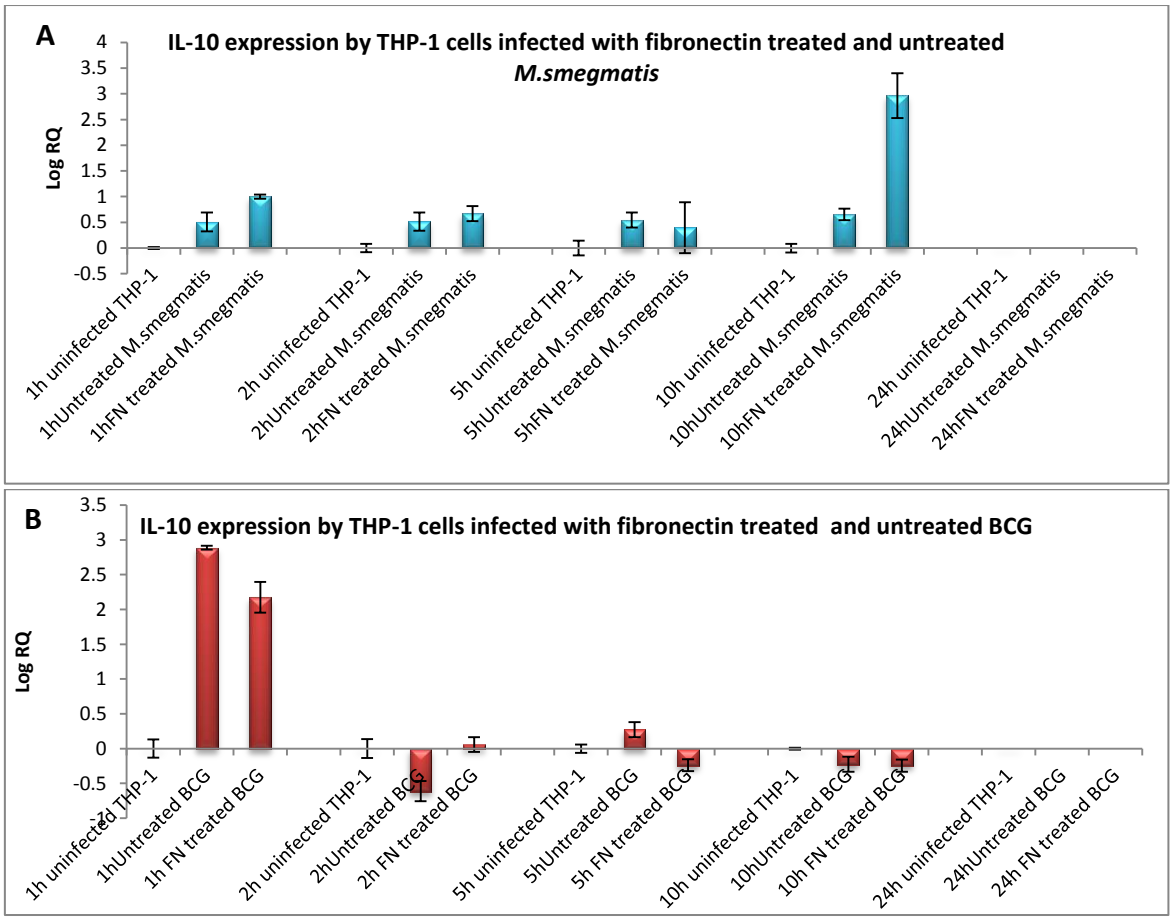

Figure 6.21: IL-10 gene expression by THP-1 cells infected with fibronectin treated and untreated mycobacteria. **A**: *M.smegmatis*. **B***:* BCG. THP-1 cells were incubated for 1, 2, 5, 10 and 24 hours following infection with mycobacteria at 37°C inside a CO_2 incubator. The cell pellet was collected and used for RNA extraction and cDNA synthesis used in this analysis. The expression of the gene was measured using qPCR and data was normalized to 18sRNA expression as control. RQ values were calculated using the formula; $RQ=2^{\Delta\Delta Ct}$. Log RQ values were plotted to show the gene expression. Un-infected THP-1 cells were used as negative control. Each bar represents the average triplicate readings. Error bars represent ±standard deviation.

6.3 Discussion

Fibronectin (FN) is large glycoprotein that is found in two forms; a soluble form in plasma, cerebrospinal fluid and amniotic fluid and an insoluble form in extracellular matrix and in the basement membranes. FN found in blood at concentrations between 300 and 400 µg/ml (Mosher, 2006). Higher levels of FN have been shown in the TB pleural effusions (441µg/ml) as compared to other infectious pleural effusions (335µg/ml) (Klockars *et al.,* 1982). This protein also leaks out from blood vessels during inflammation, where it is may interact with pathogens and phagocytic cells during infection. The effect of this interactions was investigated in this study using BCG and *M. smegmatis* as models for *Mtb*.

This study showed the ability of FN to bind directly with *M.smegmatis* and BCG in presence of 5mM $CaCl_2$ which facilitate its binding (Figure 6.3 & 6.4). It has been shown previously that FN binds directly to *Mtb* and BCG through its heparin binding domain in the C-terminal region (Pasula *et al*., 2002). Fibronectin also binds to Antigen 85-complex secreted by BCG & *Mtb* (Naito *et al*., 1998; Abou-Zeid *et al*., 1988). This complex consists of Ag85A, Ag85B, and Ag85C proteins. Ag85B binds FN to its collagen binding domain, and the minimum binding motif of Ag85B was found to be 6 amino acids ($_{98}$FEWYYQ$_{103}$), which are critical for this binding (Naito *et al*., 1998). The Fibrinectin also binds with a number of other pathogens such as *Ecoli* (Visai *et al*., 1991), *Staphylococcus aureus* (Kuusela, 1978) and *Streptococcus pyogenes* (Schwarz-Linek *et al*., 2004). FN attachment protein (FAP) (55kDa) is another receptor on BCG cell wall that binds FN (Ratliff *et al.,* 1993). This protein is also expressed on a number of other mycobacteria such as *M. tuberculosis, Mycobacterium leprae, Mycobacterium vaccae, M. bovis (BCG), M. kansasii* and *M. smegmatis* (Schorey *et al.,* 1995, 1996). Moreover, the binding site for FAP on mycobacteria has been identified as the N-terminal heparin binding domain (Zhao *et al*., 1999).

This study showed that FN binds THP-1 cells, and this binding was increased when 5mM of calcium chloride was added (Figure 6.5). This effect of calcium chloride on FN binding with phagocytic cells has not been shown previously. It

could be possible that presence of $CaCl_2$ may play a role such as changing the conformation of FN structure for better binding. The role of $CaCl_2$ in the binding of other self proteins; C1q and SP-D with their ligand has been shown previously (Gaboriaud *et al*., 2003; Ferguson et al., 2002). It has been shown that differentiated THP-1 cells express αMβ2 integrins which bind with FN (Faull *et al.,* 1994). Furthermore, FN III domain with repeats 8, 9 and 10 (Figure 1.9) have been identified as cell binding site (Xu & Mosher, 2011), which may be responsible for binding of this protein with THP-1 cells.

In this study, 10µg/ml FN enhanced BCG growth directly, whilst the same concentration did not show clear trend on *M.smegmatis* growth. Furthermore, higher concentrations of FN (25 and 50µg/ml) enhanced *M.smegmatis* growth (Figure 6.9). Although, the binding between FN with mycobacterium and certain Gram positive bacteria was reported previously but, there is very little known about the direct effect of FN on bacterial growth in general and no information for mycobacterial growth in special. This is therefore; first report shows that this protein enhances the growth of both *M. smegmatis* and BCG. If this result is reproducible for *Mtb*, then, this protein is not helpful in the control of *Mt*b at the site of infection. It will be very interesting to investigate the mechanisms involved in the growth enhancement.

The effect of FN on agglutination of BCG was also studied, which showed no effect on agglutination. Full length SP-D has been shown to agglutinate *Mtb*, but it did not affect the uptake of the pathogen by phagocytic cells (Ferguson *et al*., 2002). Furtheromore, FN has been shown to bind and aggregates *S. aureus*, which may play a role in bacterial colonization and later infection of epithelial cells (Vercellotti *et al.,* 1985). However, in this study FN at 10µg/ml did not cause agglutination of BCG as compared to untreated BCG.

This study showed FN treatment of *M.smegmatis* and BCG enhanced their uptake by THP-1 cells by 51 % and 35% respectively (Figure 6.11 & 6.12). It has been shown that binding of FN to bacteria causes conformational changes in FN structure which influence their uptake by macrophages (House-Pompeo *et al*.,

1996). FN bind to both bacteria and macrophages (Brown, 1986), and this binding could cross link mycobacteria (*M.smegmatis* or BCG) with THP-1 cells, which could be responsible for increasing mycobacterial uptake by phagocytic cells. Alternatively, FN may be acting as opsonin to mask the negative charge on bacterial cell membrane and this allow better interaction with phagocytic cells. Our findings are in agreement with previous reports, where FN is used to enhance BCG attachment and uptake by epithelial cells in prostate cancer treatment (Ratliff *et al.,* 1993). Moreover, these results are also similar to one previous work on *M. leprea,* where the uptake of *M. leprea* was reduced in FN depleted serum (Schlesinger and Horwitz, 1988).

In our study, increased *M.smegmatis* and BCG uptake by THP-1 cells was associated with increased growth in these cells. This could be simply due to increased uptake and therefore increased growth. The mechanisms of mycobacterial growth enhancement inside THP-1 cells were also investigated by using q-PCR. Data obtained showed that inducible nitric oxide synthase (iNOS) gene expression was down regulated by THP-1 cells infected with FN treated mycobacteria (*M.smegmatis* & BCG) as compared to untreated mycobacteria. It has been shown previously that *Mtb* infection stimulates nitric oxide production by human macrophages (Rich *et al.,* 1997). However, we showed that FN treatment of mycobacteria reduced the expression of iNOS by THP1 cells which may be responsible for increase in the mycobacterial growth.

The gene expression of TNF-α was also down-regulated by THP-1 cells infected with FN treated as compared to untreated *M.smegmatis* and BCG in our experiments. TNF-α is pro-inflammatory cytokine that regulates mycobacterial growth inside the granulomas and stimulates reactive nitrogen intermediates production by the infected macrophages (Chan *et al.,* 1992). Down-regulation the gene expression of this cytokine could explain the growth increase of both *M.smegmatis* and BCG.

The IL-1β gene expression was down-regulated by THP-1 cells infected with FN treated BCG as compared to untreated BCG in our study. IL-1β is a pro-inflammatory cytokine involved in the immune response against tuberculosis (Law

et al., 1996). IL-1β receptor deficient mice were more susceptible to *Mtb* infection, and they showed impaired granuloma formation (Juffermans *et al*., 2000, Yamada *et al*., 2000). In this study, less gene of expression IL-1β gene could have contributed for more mycobacterial growth inside THP-1 cells.

The gene expression of IL-6 was up-regulated by THP-1 cells infected with FN treated as compared to untreated *M.smegmatis* in our experiments. Whereas, the expression of this cytokine was similar in both THP-1 cells infected with FN treated and untreated BCG. The role of IL-6 is still unclear in mycobacterial infection. IL-6 has both pro-inflammatory and anti-inflammatory properties (Scheller *et al.,* 2011). IL-6 inhibits TNF-α & IL-1β production (Schindler *et al.,* 1990). On the other hand, IL-6 deficient mice have shown to be more susceptible to *Mtb* infection (Saunders *et al.*, 2000). It could be possible that the increase of IL-6 gene expression reduced the expression of both TNF-α & IL-1β and as a result *M.smegmatis* growth was increased inside THP-1 cells infected with FN treated *M.smegmatis*.

This study showed that IL-12 was expressed in both *M.smegmatis* and BCG infected THP-1 cells (Figure 6.19). In addition, the gene expression of IL-12 was generally lower in THP-1 cells infected with FN treated as compared to untreated *M.smegmatis* and BCG. It has been shown previously that bone marrow-derived macrophages infected with BCG, produced IL-12 early after the infection (Flesch *et al.,*1995). The same study showed that IL-12 production depends on IFN-gamma and TNF-α, where blocking TNF-α with the anti-TNF-α antibody inhibited IL-12 production in BCG infected macrophages (Flesch *et al.,*1995). Our results are in consistence with previous findings where the gene expression of IL-12 cytokine could be related to down-regulation of the gene expression of both TNF-α and IL-1β cytokines (Figure 6.16 & 6.17). IL-12 cytokine drives Th1 response by inducing INF-Ɣ production by T-cells, and it is important cytokine in the control of mycobacterial infection (Flyyn *et al.,* 1995). Our study suggests that THP-1 cells infected with FN treated mycobacteria reduced the expression of this cytokine.
In our study TGF-β gene was expressed at 10 and 24 hours by THP-1 cells infected with FN treated *M.smegmatis.* TGF-β down regulate pro-inflammatory cytokine release (Ruscetti *et al.,* 1993), inhibits reactive oxygen and nitrogen

species production (Ding *et al*., 1990), which increase mycobacterial growth inside macrophages (Toossi *et al.,* 1995). In contrast, TGF-β expression at 24 hours could help in protecting tissues from inflammation caused by pro-inflammatory cytokines *in vivo.*

The IL-10 gene was expressed at all time points up to 10 hours in both treated and untreated *M. smegmatis* infected THP1 cells in our study. At 10 hours, the expression was 2.5 fold higher in FN treated as compared untrested *M. smegmatis*. Whereas for BCG infected THP1 cells, it was expressed at 1 hour, but not detected at later time points. This differential IL-10 gene expression may be due to some variation in the cell wall composition (Ferguson *et al.,* 1999), IL-10 is anti-inflammatory cytokine that weakens macrophage function, inhibits phagosome maturation and *Mtb* antigen presentation in the infected cells (Rojas *et al*., 1999, O'Leary *et al*., 2011, Murray *et al*., 1997). This is could contribute for more *M.smegmatis* growth inside THP-1 cells. In contrast, IL-10 could be helpful in protecting tissues from inflammation.

This study provides information about the role of FN in establishing mycobacterial infection, through its effect by increasing: mycobacterial growth, uptake & growth in phagocytic cells and also through modulating of cytokine production.

Conclusion

In this study the anti-mycobacterial function of Fibronectin was investigated. This protein was shown to bind with *M. smegmatis* and BCG in ELISA. The binding of FN to *M. smegmatis* and BCG increased their growth *in vitro*. Moreover, the treatment of the mycobacteria with FN enhanced their uptakes by THP-1 cells. Furthermore, the treatment of the mycobacteria with FN increased *M.smegmatis* and BCG growth inside THP-1 cells. This mycobacterial growth increase was associated with down-regulation of the expression of inducible nitric oxide synthase, pro-inflammatory cytokines particularly TNF-α and IL-1β, which may be responsible for increasing mycobacterial growth inside the phagocytic cells *in vitro*. This study points out the negative effect of FN in the control of mycobacterial infection.

Chapter 7- Conclusions and future perspectives

7.1 Conclusions and future perspectives

In this study, host-proteins (SP-D, C1q & Fibronectin) that are known to bind with mycobacterium were selected in order to investigate their effect on mycobacterial growth. This was carried out using two non-pathogenic mycobacterial species, *M.smegmatis* & *M. Bovis BCG*, which share 95.95% and 99.95% gene homology with *Mtb,* respectively.

SP-D is produced inside the lungs by alveolar type II epithelial cells and Clara cells. Normal SP-D concentration in broncho alveolar lavage fluid is around 51µg/ml. This concentration increases in pulmonary infections and decreases in cigarette smokers and cystic fibrosis. In this study, a recombinant fragment of human SP-D containing neck and carbohydrate recognition domain (CRD) was found to bind mycobacteria and this interaction inhibited its growth. Although not investigated here, it is likely that SP-D causes increased membrane permeability, and therefore, increased death, as has been reported for Gram-negative bacterial growth inhibition (Wu *et al.,* 2003). Alternatively, this inhibition could be through intracellular signalling, which may affect the transcription of genes important for metabolism of the bacteria, and hence, its survival. RfhSP-D also inhibited mycobacterial uptake and growth inside the phagocytic cell THP-1. This may be due to binding of rfhSP-D to LAM and Man-LAM on mycobacterial cell wall. This interaction may interfere with the binding of these molecules with mannose receptor on phagocytic cells, and thus, inhibiting phagocytosis of mycobacteria by these cells. This decreased phagocytosis may lead to decrease growth inside the cells. If these finding are reproducible by using *Mtb*, then this protein has the potential to be used as an adjuvant in treating multi-drug-resistant (MDR) TB. This can be done by delivering this protein through inhaler at the site of infection in the lower respiratory tract. This is supported by the fact that cigarette smokers, which have low SP-D level inside their lungs, are more susceptible to *Mtb* infection (Winkler *et al*., 2011). Proteins can be delivered by the inhalers, it has been reported that using insulin inhaler was well tolerated, and no serious side effects have been reported (Pfützner et al., 2002). This hypothesis needs testing in the animal model using transgenic mice by over-expressing human SP-D in the alveolar epithelium of lung and challenging these mice with *Mtb.* SP-D knock out

mice challenged with *Mtb* may also provide some clue into the role of SP-D in the control of *Mtb* infection *in vivo*. Since SP-D is present in the alveoli of the lungs where *Mtb* induced granulomas are also formed, it will be very interesting to study its role in the formation and stabilization of granuloma structure.

The inhibition assays performed in this study for both *M.smegmatis* and BCG infected THP-1 cells were incubated for 24 hours. This period of incubation showed the effect of proteins on killing of the phagocytosed mycobacteria during 24 hours (1 day). The doubling time for BCG during infection is around 24 hours (Beste et al., 2005), and it will be interesting to increase the incubation period for THP-1 cells infected BCG to 2, 3, 4 and 5 days in order to investigate the effect of the soluble proteins on the growth of BCG. It has been shown previously that THP-1 cells infected with *M.avium* can kill the mycobacteria for up to 5 days (Garcia et al., 2000), and the amount of fration proteins and nucleolin inside THP-1 cells have not changed up to 5 days of infection.

C1q, the first sub-component of the complement protein C1 complex activates the classical complement pathway. Normal concentration of C1q in plasma is around 115µg/ml. Moreover, it is produced at the site by infection by immature dendritic cells, monocyte and macrophages. C1q also leaks out from plasma at the infection site. Higher expression level of blood C1q was reported in untreated TB patients as compared to individuals with latent TB and without TB infection (Cai *et al.,* 2014). It has been shown previously that C1q binding to *Mtb* activated the classical complement pathway and increased *Mtb* uptake by macrophages (Ferguson, 2004). In this study, C1q showed binding to both mycobacteria (*M.smegmatis* and BCG) and THP-1 cells. The domain of C1q binding to mycobacteria can be localized to the globular head region. C1q inhibited mycobacterial growth as well as increased their uptake by THP-1 cells. Moreover, C1q inhibited BCG growth inside THP-1 cells by enhancing the expression of iNOS, TNF-α, and IL-1β. However, it enhanced *M.smegmatis* growth inside these cells by down-regulating the expression of iNOS, TNF-α, and IL-1β. This may have been achieved by simultaneous interaction of C1q and mycobacterial components with their receptors on phagocytic cells. The difference in the lipid component of *M. smegmatis* and BCG has been reported before, which may have impacted upon this differential effect of C1q (Ferguson *et al.,* 1999).

In this study, recombinant forms of individual globular head modules (ghA, ghB and ghC) of C1q were produced. These individual globular heads inhibited *M.smegmatis* growth directly and increased its uptake by THP-1 cells. The ghA module increased *M.smegmatis* growth inside THP-1 cells, whilst, ghB and ghC inhibited bacterial growth inside these cells. It has been suggested that these globular heads are structurally and functionally independent modules. The difference in the functional activities of these globular heads with respect to their binding with aggregated IgG and IgM, HIV gp41 peptide, β-amyloid peptide and HTLV gp21 peptide has been reported before (Kishore *et al.,* 2003).

The effect of individual globular heads of C1q needs to be confirmed with *Mtb.* The inhibition of mycobacterial growth using globular head C (ghC) of C1q showed a more drastic effect than ghA and ghB. The effect of ghC was stronger than ghB, and it will be interesting to concentrate on this particular globular head of C1q in future studies using *Mtb*. If ghC inhibited *Mtb* growth inside macrophages, then this globular head may have potential to be used as a part of adjuvant therapy for MDR TB.

Identification of receptors for C1q and individual globular head of C1q on *Mtb* will help in understanding the underlying mechanism of growth inhibition. This can be achieved by passing the membrane fraction of bacterial through C1q affinity column and eluting C1q ligand. The eluted fractions can then be characterized by Mass spectrometry and SDS-PAGE. The N terminal sequencing of this protein will also provide useful information in identifying this protein ligand from bacterial protein data base.

C1q knockout mice are available and are used to study autoimmune disease such as Systemic Lupus Erythematosus. This model can be used to study the role of C1q *in vivo* in the control of *Mtb* infection. Since C1q is expressed in granuloma, its contribution in the formation and maintenance can be studied using this model.

The third host-protein examined in this study was Fibronectin (FN). This protein is found normally in plasma at the concentration of 300µg/ml. It is also present in tissues and it leaks out of plasma at the site of infection. It has been shown that

FN concentration in the pleura of TB patients is much higher (441µg/ml) as compared to patients with non-specific infections ((335µg/ml) (Klockars *et al.,* 1982). This suggests that FN may play a role in *Mtb* infection. Our results indicated a negative effect of FN on controlling mycobacterial infection. It appears that mycobacteria use FN to enhance their attachment to phagocytic cells, and thus, increase their uptake and growth inside these cells. The growth increase could be due to the down-regulation of nitric oxide and pro-inflammatory cytokines TNF-α and IL-1β expression by THP-1 cells, which play important role in controlling *Mtb* infection.

Inhibiting the attachment of FN to *Mtb* in the lungs could be useful in prevention *Mtb* infection and disease progression. Moreover, FN could help the dissemination of *Mtb* infection because it is found in plasma as well as in basement membranes. Injecting fibronectin attachment protein (FAP) in *Mtb* infection site could be helpful in preventing dissemination of *Mtb* via the blood to other organs. FAP can compete with *Mtb* on the same binding site on fibronectin, which result in inhibiting *Mtb* attachment to FN and hence to host cells.

FN interacts with mycobacterial antigen 85 complex (Ag85A, Ag85B & Ag85C). Members of this complex are highly immunogenic and possess mycolyltransferase activity that helps in the synthesis of glycolipid of mycobacterial cell wall. Antigen 85 complex is mainly present in the culture supernatant as well as in the outer envelope of the mycobacteria. It is possible that fibronectin after interacting with Ag85B on the bacteria may stabilize this enzyme, enhance its activity, and thus increase the growth of BCG.

Overall, this study has discovered novel anti-mycobacterial functions of SP-D and C1q and that of Fibronectin, as a mycobacterial infection facilitator.

Chapter 8- References

- Abbas, A.K. and Lichtman, A.H., 2006. Basic Immunology. Saunders Elsevier. China. Updated edition, 2007.

- Abou-Zeid, C.H.R.I.S.T.I.A.N.E., Ratliff, T.L., Wiker, H.G., Harboe, M., Bennedsen, J. and Rook, G.A., 1988. Characterization of fibronectin-binding antigens released by Mycobacterium tuberculosis and Mycobacterium bovis BCG. Infection and immunity, 56(12), pp.3046-3051.

- Agarwal, S., Nguyen, D.T., Lew, J.D., Teeter, L.D., Yamal, J.M., Restrepo, B.I., Brown, E.L., Dorman, S.E. and Graviss, E.A., 2016. Differential positive TSPOT assay responses to ESAT-6 and CFP-10 in health care workers. Tuberculosis, 101, pp.S83-S91.

- Agostinis, C., Bulla, R., Tripodo, C., Gismondi, A., Stabile, H., Bossi, F., Guarnotta, C., Garlanda, C., De Seta, F., Spessotto, P. and Santoni, A., 2010. An alternative role of C1q in cell migration and tissue remodeling: contribution to trophoblast invasion and placental development. The Journal of Immunology, 185(7), pp.4420-4429.

- Alastair Innes J. (2016) Davidson's Essentials of Medicine, Churchill Livingstone. Second edition. Elsevier. ISBN: 978-0-7020-5592-8. 880p.

- Alberti, S., Marqués, G., Camprubi, S., Merino, S., Tomás, J.M., Vivanco, F. and Benedi, V.J., 1993. C1q binding and activation of the complement classical pathway by Klebsiella pneumoniae outer membrane proteins. Infection and immunity, 61(3), pp.852-860.

- Ariki, S., Kojima, T., Gasa, S., Saito, A., Nishitani, C., Takahashi, M., Shimizu, T., Kurimura, Y., Sawada, N., Fujii, N. and Kuroki, Y., 2011. Pulmonary collectins play distinct roles in host defense against Mycobacterium avium. The Journal of Immunology, 187(5), pp.2586-2594.

- Armstrong, J.A. and Hart, P.A., 1975. Phagosome-lysosome interactions in cultured macrophages infected with virulent tubercle bacilli. Reversal of the usual nonfusion pattern and observations on bacterial survival. The Journal of experimental medicine, 142(1), pp.1-16.

- Aung, H., Wu, M., Johnson, J.L., Hirsch, C.S. and Toossi, Z., 2005. Bioactivation of latent transforming growth factor β1 by Mycobacterium tuberculosis in human mononuclear phagocytes. Scandinavian journal of immunology, 61(6), pp.558-565.

- Baggiolini, M., Walz, A. and Kunkel, S.L., 1989. Neutrophil-activating peptide-1/interleukin 8, a novel cytokine that activates neutrophils. Journal of Clinical Investigation, 84(4), p.1045.

- Bai, W., Liu, H., Ji, Q., Zhou, Y., Liang, L., Zheng, R., Chen, J., Liu, Z., Yang, H., Zhang, P. and Kaufmann, S.H., 2014. TLR3 regulates

mycobacterial RNA-induced IL-10 production through the PI3K/AKT signaling pathway. Cellular signalling, 26(5), pp.942-950.

- Balcewicz-Sablinska, M.K., Keane, J., Kornfeld, H. and Remold, H.G., 1998. Pathogenic Mycobacterium tuberculosis evades apoptosis of host macrophages by release of TNF-R2, resulting in inactivation of TNF-α. The journal of Immunology, 161(5), pp.2636-2641.

- Behr, M.A. and Small, P.M., 1999. A historical and molecular phylogeny of BCG strains. Vaccine, 17(7), pp.915-922.

- Bekierkunst, A., 1966. Nicotinamide-adenine dinucleotide in tubercle bacilli exposed to isoniazid. Science, 152(3721), pp.525-526.

- Bekker, L.G., Freeman, S., Murray, P.J., Ryffel, B. and Kaplan, G., 2001. TNF-α controls intracellular mycobacterial growth by both inducible nitric oxide synthase-dependent and inducible nitric oxide synthase-independent pathways. The Journal of Immunology, 166(11), pp.6728-6734.

- Bemer, P., Palicova, F., Rüsch-Gerdes, S., Drugeon, H.B. and Pfyffer, G.E., 2002. Multicenter evaluation of fully automated BACTEC Mycobacteria Growth Indicator Tube 960 system for susceptibility testing of Mycobacterium tuberculosis. Journal of clinical microbiology, 40(1), pp.150-154.

- Bentley-Hibbert, S.I., Quan, X., Newman, T., Huygen, K. and Godfrey, H.P., 1999. Pathophysiology of antigen 85 in patients with active tuberculosis: antigen 85 circulates as complexes with fibronectin and immunoglobulin G. Infection and immunity, 67(2), pp.581-588.

- Beste, D.J.V., Peters, J., Hooper, T., Avignone-Rossa, C., Bushell, M.E. and McFadden, J., 2005. Compiling a molecular inventory for Mycobacterium bovis BCG at two growth rates: evidence for growth rate-mediated regulation of ribosome biosynthesis and lipid metabolism. Journal of bacteriology, 187(5), pp.1677-1684.

- Beutler, B. and Cerami, A., 1986. Cachectin and tumour necrosis factor as two sides of the same biological coin. Nature, 320, pp.584-588.

- Black, G.F., Weir, R.E., Floyd, S., Bliss, L., Warndorff, D.K., Crampin, A.C., Ngwira, B., Sichali, L., Nazareth, B., Blackwell, J.M. and Branson, K., 2002. BCG-induced increase in interferon-gamma response to mycobacterial antigens and efficacy of BCG vaccination in Malawi and the UK: two randomised controlled studies. The Lancet, 359(9315), pp.1393-1401.

- Bonifati, D.M. and Kishore, U., 2007. Role of complement in neurodegeneration and neuroinflammation. Molecular immunology, 44(5), pp.999-1010.

- Brandt, L., Cunha, J.F., Olsen, A.W., Chilima, B., Hirsch, P., Appelberg, R. and Andersen, P., 2002. Failure of the Mycobacterium bovis BCG vaccine: some species of environmental mycobacteria block multiplication of BCG and induction of protective immunity to tuberculosis. Infection and immunity, 70(2), pp.672-678.

- Brennan, P.J., Rooney, S.A. and Winder, F.G., 1970. The lipids of Mycobacterium tuberculosis BCG: Fractionation, composition, turnover and the effects of isoniazid. Irish Journal of Medical Science (1968-1970), 3(8), pp.371-390.

- Brinker, K.G., Martin, E., Borron, P., Mostaghel, E., Doyle, C., Harding, C.V. and Wright, J.R., 2001. Surfactant protein D enhances bacterial antigen presentation by bone marrow-derived dendritic cells. American Journal of Physiology-Lung Cellular and Molecular Physiology, 281(6), pp.L1453-L1463.

- Brinkmann, V. and Zychlinsky, A., 2012. Neutrophil extracellular traps: is immunity the second function of chromatin?. The Journal of cell biology, 198(5), pp.773-783.

- Brosch, R., Gordon, S.V., Marmiesse, M., Brodin, P., Buchrieser, C., Eiglmeier, K., Garnier, T., Gutierrez, C., Hewinson, G., Kremer, K. and Parsons, L.M., 2002. A new evolutionary scenario for the Mycobacterium tuberculosis complex. Proceedings of the national academy of Sciences, 99(6), pp.3684-3689.

- Brown, E.J., 1986. The role of extracellular matrix proteins in the control of phagocytosis. Journal of leukocyte biology, 39(5), pp.579-591.

- Bulla, R., Agostinis, C., Bossi, F., Rizzi, L., Debeus, A., Tripodo, C., Radillo, O., De Seta, F., Ghebrehiwet, B. and Tedesco, F., 2008. Decidual endothelial cells express surface-bound C1q as a molecular bridge between endovascular trophoblast and decidual endothelium. Molecular immunology, 45(9), pp.2629-2640.

- Bulut, Y., Michelsen, K.S., Hayrapetian, L., Naiki, Y., Spallek, R., Singh, M. and Arditi, M., 2005. Mycobacterium tuberculosis heat shock proteins use diverse Toll-like receptor pathways to activate pro-inflammatory signals. Journal of Biological Chemistry, 280(22), pp.20961-20967.

- Caceres, N.E., Harris, N.B., Wellehan, J.F., Feng, Z., Kapur, V. and Barletta, R.G., 1997. Overexpression of the D-alanine racemase gene confers resistance to D-cycloserine in Mycobacterium smegmatis. Journal of bacteriology, 179(16), pp.5046-5055.

- Cai, Y., Yang, Q., Tang, Y., Zhang, M., Liu, H., Zhang, G., Deng, Q., Huang, J., Gao, Z., Zhou, B. and Feng, C.G., 2014. Increased complement C1q level marks active disease in human tuberculosis. PloS one, 9(3), p.e92340.

- Carroll, M.V., Lack, N., Sim, E., Krarup, A. and Sim, R.B., 2009. Multiple routes of complement activation by Mycobacterium bovis BCG. Molecular immunology, 46(16), pp.3367-3378.

- Castellano, G., Woltman, A.M., Nauta, A.J., Roos, A., Trouw, L.A., Seelen, M.A., Schena, F.P., Daha, M.R. and van Kooten, C., 2004. Maturation of dendritic cells abrogates C1q production in vivo and in vitro. Blood, 103(10), pp.3813-3820.

- Chambers, M.A., Gavier-Widén, D. and Hewinson, R.G., 2004. Antibody bound to the surface antigen MPB83 of Mycobacterium bovis enhances survival against high dose and low dose challenge. FEMS Immunology & Medical Microbiology, 41(2), pp.93-100.

- Chan, J., Xing, Y., Magliozzo, R.S. and Bloom, B.R., 1992. Killing of virulent Mycobacterium tuberculosis by reactive nitrogen intermediates produced by activated murine macrophages. The Journal of experimental medicine, 175(4), pp.1111-1122.

- Chan, J., Mehta, S., Bharrhan, S., Chen, Y., Achkar, J.M., Casadevall, A. and Flynn, J., 2014, December. The role of B cells and humoral immunity in Mycobacterium tuberculosis infection. In Seminars in immunology (Vol. 26, No. 6, pp. 588-600). Academic Press.

- Chen, M. and Wang, J., 2002. Initiator caspases in apoptosis signaling pathways. Apoptosis, 7(4), pp.313-319.

- Chensue, S.W., Warmington, K., Ruth, J., Lincoln, P., Kuo, M.C. and Kunkel, S.L., 1994. Cytokine responses during mycobacterial and schistosomal antigen-induced pulmonary granuloma formation. Production of Th1 and Th2 cytokines and relative contribution of tumor necrosis factor. The American journal of pathology, 145(5), p.1105.

- Chiba, H., Pattanajitvilai, S., Evans, A.J., Harbeck, R.J. and Voelker, D.R., 2002. Human surfactant protein D (SP-D) binds Mycoplasma pneumoniae by high affinity interactions with lipids. Journal of Biological Chemistry, 277(23), pp.20379-20385.

- Cho, J. and Mosher, D.F., 2006. Role of fibronectin assembly in platelet thrombus formation. Journal of Thrombosis and Haemostasis, 4(7), pp.1461-1469.

- Chroneos, Z.C., Sever-Chroneos, Z. and Shepherd, V.L., 2009. Pulmonary surfactant: an immunological perspective. Cellular Physiology and Biochemistry, 25(1), pp.13-26.

- Cohen, J., Hughes, E.J., Day, C.L., de Kock, M., Geldenhuys, H., Gelderbloem, S., Hawkridge, A., Hussey, G.D., Mahomed, H., Makhethe, L. and Tameris, M., 2013. Induction and Regulation of T Cell Immunity by the Novel TB Vaccine M72/AS01 in South African Adults.

- Cooper, A.M., Roberts, A.D., Rhoades, E.R., Callahan, J.E., Getzy, D.M. and Orme, I.M., 1995. The role of interleukin-12 in acquired immunity to Mycobacterium tuberculosis infection. Immunology, 84(3), p.423.

- Cooper, A.M., Kipnis, A., Turner, J., Magram, J., Ferrante, J. and Orme, I.M., 2002. Mice lacking bioactive IL-12 can generate protective, antigen-specific cellular responses to mycobacterial infection only if the IL-12 p40 subunit is present. The Journal of Immunology, 168(3), pp.1322-1327.

- Cosma, C.L., Sherman, D.R. and Ramakrishnan, L., 2003. The secret lives of the pathogenic mycobacteria. Annual Reviews in Microbiology, 57(1), pp.641-676.

- Csomor, E., Bajtay, Z., Sándor, N., Kristóf, K., Arlaud, G.J., Thiel, S. and Erdei, A., 2007. Complement protein C1q induces maturation of human dendritic cells. Molecular immunology, 44(13), pp.3389-3397.

- Crouch, E., Persson, A. and Chang, D., 1993. Accumulation of surfactant protein D in human pulmonary alveolar proteinosis. The American journal of pathology, 142(1), p.241.

- Crouch, E., Hartshorn, K. and Ofek, I., 2000. Collectins and pulmonary innate immunity. Immunological reviews, 173(1), pp.52-65.

- Crouch, E., Tu, Y., Briner, D., McDonald, B., Smith, K., Holmskov, U. and Hartshorn, K., 2005. Ligand specificity of human surfactant protein D expression of a mutant trimeric collectin that shows enhanced interactions with influenza a virus. Journal of Biological Chemistry, 280(17), pp.17046-17056.

- Cruz, A., Fraga, A.G., Fountain, J.J., Rangel-Moreno, J., Torrado, E., Saraiva, M., Pereira, D.R., Randall, T.D., Pedrosa, J., Cooper, A.M. and Castro, A.G., 2010. Pathological role of interleukin 17 in mice subjected to repeated BCG vaccination after infection with Mycobacterium tuberculosis. The Journal of experimental medicine, 207(8), pp.1609-1616.

- Cynamon, M.H. and Palmer, G.S., 1983. In vitro activity of amoxicillin in combination with clavulanic acid against Mycobacterium tuberculosis. Antimicrobial agents and chemotherapy, 24(3), pp.429-431.

- Cywes, C., Godenir, N.L., Hoppe, H.C., Scholle, R.R., Steyn, L.M., Kirsch, R.E. and Ehlers, M.R., 1996. Nonopsonic binding of Mycobacterium tuberculosis to human complement receptor type 3 expressed in Chinese hamster ovary cells. Infection and immunity, 64(12), pp.5373-5383.

- Daffe, M. and Etienne, G., 1999. The capsule of Mycobacterium tuberculosis and its implications for pathogenicity. Tubercle and lung disease, 79(3), pp.153-169.

- Dagert, M. and Ehrlich, S.D., 1979. Prolonged incubation in calcium chloride improves the competence of Escherichia coli cells. Gene, 6(1), pp.23-28.

- Dahl, M., Juvonen, P.O., Holmskov, U. and Husby, S., 2005. Surfactant protein D in newborn infants: factors influencing surfactant protein D levels in umbilical cord blood and capillary blood. Pediatric research, 58(5), pp.908-912.

- Darribère, T., Guida, K., Larjava, H., Johnson, K.E., Yamada, K.M., Thiery, J.P. and Boucaut, J.C., 1990. In vivo analyses of integrin beta 1 subunit function in fibronectin matrix assembly. The Journal of cell biology, 110(5), pp.1813-1823.

- Denis, M. and Gregg, E.O., 1990. Recombinant tumour necrosis factor-alpha decreases whereas recombinant interleukin-6 increases growth of a virulent strain of Mycobacterium avium in human macrophages. Immunology, 71(1), p.139.

- Deshmane, S.L., Kremlev, S., Amini, S. and Sawaya, B.E., 2009. Monocyte chemoattractant protein-1 (MCP-1): an overview. Journal of interferon & cytokine research, 29(6), pp.313-326.

- Dhiman, R., Indramohan, M., Barnes, P.F., Nayak, R.C., Paidipally, P., Rao, L.V.M. and Vankayalapati, R., 2009. IL-22 produced by human NK cells inhibits growth of Mycobacterium tuberculosis by enhancing phagolysosomal fusion. The Journal of Immunology, 183(10), pp.6639-6645.

- Diaz-Silvestre, H., Espinosa-Cueto, P., Sanchez-Gonzalez, A., Esparza-Ceron, M.A., Pereira-Suarez, A.L., Bernal-Fernandez, G., Espitia, C. and Mancilla, R., 2005. The 19-kDa antigen of Mycobacterium tuberculosis is a major adhesin that binds the mannose receptor of THP-1 monocytic cells and promotes phagocytosis of mycobacteria. Microbial pathogenesis, 39(3), pp.97-107.

- Dillon, S.P., D'Souza, A., Kurien, B.T. and Scofield, R.H., 2009. Systemic lupus erythematosus and C1q: A quantitative ELISA for determining C1q levels in serum. Biotechnology journal, 4(8), pp.1210-1214.

- Ding, A., Nathan, C.F., Graycar, J., Derynck, R.I.K., Stuehr, D.J. and Srimal, S., 1990. Macrophage deactivating factor and transforming growth factors-beta 1-beta 2 and-beta 3 inhibit induction of macrophage nitrogen oxide synthesis by IFN-gamma. The Journal of Immunology, 145(3), pp.940-944.

- Dobke, M.K., Pearson, G., Roberts, C., Germany, B., Heck, E., Masters, B.S.S. and Baxter, C.R., 1983. Effect of circulating fibronectin on stimulation of leukocyte oxygen consumption and serum opsonizing function in burned patients. Journal of Trauma and Acute Care Surgery, 23(10), pp.882-890.

- Dodagatta-Marri, E., Qaseem, A.S., Karbani, N., Tsolaki, A.G., Waters, P., Madan, T. and Kishore, U., 2014. Purification of surfactant protein D (SP-D) from pooled amniotic fluid and bronchoalveolar lavage. The Complement System: Methods and Protocols, pp.273-290.

- Dorhoi, A., Nouailles, G., Jörg, S., Hagens, K., Heinemann, E., Pradl, L., Oberbeck-Müller, D., Duque-Correa, M.A., Reece, S.T., Ruland, J. and Brosch, R., 2012. Activation of the NLRP3 inflammasome by Mycobacterium tuberculosis is uncoupled from susceptibility to active tuberculosis. European journal of immunology, 42(2), pp.374-384.

- Dorman, S.E. and Holland, S.M., 2000. Interferon-γ and interleukin-12 pathway defects and human disease. Cytokine & growth factor reviews, 11(4), pp.321-333.

- Dulphy, N., Herrmann, J.L., Nigou, J., Réa, D., Boissel, N., Puzo, G., Charron, D., Lagrange, P.H. and Toubert, A., 2007. Intermediate maturation of Mycobacterium tuberculosis LAM-activated human dendritic cells. Cellular microbiology, 9(6), pp.1412-1425.

- Dunkelberger, J.R. and Song, W.C., 2010. Role and mechanism of action of complement in regulating T cell immunity. Molecular immunology, 47(13), pp.2176-2186.

- Duvoix, A., Mackay, R.M., Henderson, N., McGreal, E., Postle, A., Reid, K. and Clark, H., 2011. Physiological concentration of calcium inhibits elastase-induced cleavage of a functional recombinant fragment of surfactant protein D. Immunobiology, 216(1), pp.72-79.

- Dye, C., 2006. Global epidemiology of tuberculosis. The Lancet, 367(9514), pp.938-940.

- Edelson, B.T., Stricker, T.P., Li, Z., Dickeson, S.K., Shepherd, V.L., Santoro, S.A. and Zutter, M.M., 2006. Novel collectin/C1q receptor mediates mast cell activation and innate immunity. Blood, 107(1), pp.143-150.

- Eisner, M.D., Parsons, P., Matthay, M.A., Ware, L. and Greene, K., 2003. Plasma surfactant protein levels and clinical outcomes in patients with acute lung injury. Thorax, 58(11), pp.983-988.

- Färber, K., Cheung, G., Mitchell, D., Wallis, R., Weihe, E., Schwaeble, W. and Kettenmann, H., 2009. C1q, the recognition subcomponent of the classical pathway of complement, drives microglial activation. Journal of neuroscience research, 87(3), pp.644-652.

- Faull, R.J., Kovach, N.L., Harlan, J.M. and Ginsberg, M.H., 1994. Stimulation of integrin-mediated adhesion of T lymphocytes and monocytes: two mechanisms with divergent biological consequences. Journal of Experimental Medicine, 179(4), pp.1307-1316.

- Feng, C.G., Bean, A.G., Hooi, H., Briscoe, H. and Britton, W.J., 1999. Increase in gamma interferon-secreting CD8+, as well as CD4+, T cells in lungs following aerosol infection with Mycobacterium tuberculosis. Infection and immunity, 67(7), pp.3242-3247.

- Ferguson, J.S., Voelker, D.R., McCormack, F.X. and Schlesinger, L.S., 1999. Surfactant protein D binds to Mycobacterium tuberculosis Bacilli and Lipoarabinomannan via carbohydrate-lectin interactions resulting in reduced phagocytosis of the bacteria by macrophages1. The Journal of immunology, 163(1), pp.312-321.

- Ferguson, J.S., Voelker, D.R., Ufnar, J.A., Dawson, A.J. and Schlesinger, L.S., 2002. Surfactant protein D inhibition of human macrophage uptake of Mycobacterium tuberculosis is independent of bacterial agglutination. The Journal of Immunology, 168(3), pp.1309-1314.

- Ferguson, J.S., Weis, J.J., Martin, J.L. and Schlesinger, L.S., 2004. Complement protein C3 binding to Mycobacterium tuberculosis is initiated by the classical pathway in human bronchoalveolar lavage fluid. Infection and immunity, 72(5), pp.2564-2573.

- Ferguson, J.S., Martin, J.L., Azad, A.K., McCarthy, T.R., Kang, P.B., Voelker, D.R., Crouch, E.C. and Schlesinger, L.S., 2006. Surfactant protein D increases fusion of Mycobacterium tuberculosis-containing phagosomes with lysosomes in human macrophages. Infection and immunity, 74(12), pp.7005-7009.

- Ferrero, E., Biswas, P., Vettoretto, K., Ferrarini, M., Uguccioni, M., Piali, L., Leone, B.E., Moser, B., Rugarli, C. and Pardi, R., 2003. Macrophages exposed to Mycobacterium tuberculosis release chemokines able to recruit

selected leucocyte subpopulations: focus on γδ cells. Immunology, 108(3), pp.365-374.

- Flesch, I.N.G.E. and Kaufmann, S.H., 1987. Mycobacterial growth inhibition by interferon-gamma-activated bone marrow macrophages and differential susceptibility among strains of Mycobacterium tuberculosis. The Journal of Immunology, 138(12), pp.4408-4413

- Flesch, I.E. and Kaufmann, S.H., 1991. Mechanisms involved in mycobacterial growth inhibition by gamma interferon-activated bone marrow macrophages: role of reactive nitrogen intermediates. Infection and immunity, 59(9), pp.3213-3218.

- Flesch, I.E., Hess, J.H., Huang, S., Aguet, M., Rothe, J., Bluethmann, H. and Kaufmann, S.H., 1995. Early interleukin 12 production by macrophages in response to mycobacterial infection depends on interferon gamma and tumor necrosis factor alpha. Journal of Experimental Medicine, 181(5), pp.1615-1621.

- Flynn, J.L., Chan, J., Triebold, K.J., Dalton, D.K., Stewart, T.A. and Bloom, B.R., 1993. An essential role for interferon gamma in resistance to Mycobacterium tuberculosis infection. The Journal of experimental medicine, 178(6), pp.2249-2254.

- Flynn, J.L., Goldstein, M.M., Chan, J., Triebold, K.J., Pfeffer, K., Lowenstein, C.J., Schrelber, R., Mak, T.W. and Bloom, B.R., 1995. Tumor necrosis factor-α is required in the protective immune response against Mycobacterium tuberculosis in mice. Immunity, 2(6), pp.561-572

- Forbes, L.R. and Haczku, A., 2010. SP-D and regulation of the pulmonary innate immune system in allergic airway changes. Clinical & Experimental Allergy, 40(4), pp.547-562.

- Frachet, P., Tacnet-Delorme, P., Gaboriaud, C. and Thielens, N.M., 2015. Role of C1q in efferocytosis and self-tolerance—links with autoimmunity. In Autoimmunity-Pathogenesis, Clinical Aspects and Therapy of Specific Autoimmune Diseases. InTech.

- Francis, K., Van Beek, J., Canova, C., Neal, J.W. and Gasque, P., 2003. Innate immunity and brain inflammation: the key role of complement. Expert reviews in molecular medicine, 5(15), pp.1-19.

- Fraser DA, Pisalyaput K and Tenner AJ. 2010. C1q enhances microglial clearance of apoptotic neurons and neuronal blebs, and modulates subsequent inflammatory cytokine production.
J Neurochem, 112, pp.733–743.

- Frick M. The Tuberculosis Vaccines Pipeline: A New Path to the Same Destination? London, UK: HIV i-Base/Treatment Action Group, 2015.

- Frieden et al., 2003: Frieden TR, Sterling TR, Munsiff SS, Watt CJ, Dye C Tuberculosis. Lancet. 2003; 362(9387): 887 - 899.

- Fujiwara, N. and Kobayashi, K., 2005. Macrophages in inflammation. Current Drug Targets-Inflammation & Allergy, 4(3), pp.281-286.

- Gaboriaud, C., Juanhuix, J., Gruez, A., Lacroix, M., Darnault, C., Pignol, D., Verger, D., Fontecilla-Camps, J.C. and Arlaud, G.J., 2003. The crystal structure of the globular head of complement protein C1q provides a basis for its versatile recognition properties. Journal of Biological Chemistry, 278(47), pp.46974-46982.

- Gadjeva, M.G., Rouseva, M.M., Zlatarova, A.S., Reid, K.B., Kishore, U. and Kojouharova, M.S., 2008. Interaction of human C1q with IgG and IgM: revisited. Biochemistry, 47(49), pp.13093-13102.

- Gallegos, A.M., Van Heijst, J.W., Samstein, M., Su, X., Pamer, E.G. and Glickman, M.S., 2011. A gamma interferon independent mechanism of CD4 T cell mediated control of M. tuberculosis infection in vivo. PLoS Pathog, 7(5), p.e1002052.

- Gangadharam, P.R., J., F. M. Harold, and W. B. Schaefer. 1963. Selective inhibition of nucleic acid synthesis in Myco-bacterium tuberculosis by isoniazid. Nature (London), 198, pp.712-714.

- Ganguly N, Siddiqui I, Sharma P. Role of M. tuberculosis RD-1 region encoded secretory proteins in protective response and virulence. 2008. Tuberculosis (Edinb), 88(6), pp. 510–517.

- Gardai, S.J., Xiao, Y.Q., Dickinson, M., Nick, J.A., Voelker, D.R., Greene, K.E. and Henson, P.M., 2003. By binding SIRPα or calreticulin/CD91, lung collectins act as dual function surveillance molecules to suppress or enhance inflammation. Cell, 115(1), pp.13-23.

- Gardam, M.A., Keystone, E.C., Menzies, R., Manners, S., Skamene, E., Long, R. and Vinh, D.C., 2003. Anti-tumour necrosis factor agents and tuberculosis risk: mechanisms of action and clinical management. The Lancet infectious diseases, 3(3), pp.148-155.
- Garnier, T., Eiglmeier, K., Camus, J.C., Medina, N., Mansoor, H., Pryor, M., Duthoy, S., Grondin, S., Lacroix, C., Monsempe, C. and Simon, S., 2003. The complete genome sequence of Mycobacterium bovis. Proceedings of the National Academy of Sciences, 100(13), pp.7877-7882.

- Garcia, R.C., Banfi, E. and Pittis, M.G., 2000. Infection of Macrophage-Like THP-1 Cells withMycobacterium avium Results in a Decrease in Their

Ability to Phosphorylate Nucleolin. Infection and immunity, 68(6), pp.3121-3128.

- Gazzinelli, R.T., Oswald, I.P., James, S.L. and Sher, A.L.A.N., 1992. IL-10 inhibits parasite killing and nitrogen oxide production by IFN-gamma-activated macrophages. The Journal of Immunology, 148(6), pp.1792-1796.

- Geginat, G., Schenk, S., Skoberne, M., Goebel, W. and Hof, H., 2001. A novel approach of direct ex vivo epitope mapping identifies dominant and subdominant CD4 and CD8 T cell epitopes from Listeria monocytogenes. The Journal of Immunology, 166(3), pp.1877-1884.

- Geijtenbeek, T.B., van Vliet, S.J., Koppel, E.A., Sanchez-Hernandez, M., Vandenbroucke-Grauls, C.M., Appelmelk, B. and van Kooyk, Y., 2003. Mycobacteria target DC-SIGN to suppress dendritic cell function. The Journal of experimental medicine, 197(1), pp.7-17.

- Geissmann, F., Jung, S. and Littman, D.R., 2003. Blood monocytes consist of two principal subsets with distinct migratory properties. Immunity, 19(1), pp.71-82.

- Geldmacher, C., Zumla, A. and Hoelscher, M., 2012. Interaction between HIV and Mycobacterium tuberculosis: HIV-1-induced CD4 T-cell depletion and the development of active tuberculosis. Current Opinion in HIV and AIDS, 7(3), pp.268-274.

- Geunes-Boyer, S., Beers, M.F., Perfect, J.R., Heitman, J. and Wright, J.R., 2012. Surfactant protein D facilitates Cryptococcus neoformans infection. Infection and immunity, 80(7), pp.2444-2453.

- Ghebrehiwet, B., Lim, B.L., Peerschke, E.I., Willis, A.C. and Reid, K.B., 1994. Isolation, cDNA cloning, and overexpression of a 33-kD cell surface glycoprotein that binds to the globular" heads" of C1q. The Journal of experimental medicine, 179(6), pp.1809-1821.

- GHEBREHIWET, B., LU, P.D., ZHANG, W., LIM, B.L., EGGLETON, P., LEIGH, L.E., REID, K.B. and PEERSCHKE, E.I., 1996. Identification of Functional Domains on gClQ-R, a Cell Surface Protein That Binds to the Globular" Heads" of C1Q, Using Monoclonal Antibodies and Synthetic Peptides. Hybridoma, 15(5), pp.333-342.

- Ghebrehiwet, B., Lim, B.L., Kumar, R., Feng, X. and Peerschke, E.I., 2001. gC1q-R/p33, a member of a new class of multifunctional and multicompartmental cellular proteins, is involved in inflammation and infection. Immunological reviews, 180(1), pp.65-77.

- Ghebrehiwet, B., Jesty, J. and Peerschke, E.I., 2002. gC1q-R/p33: structure-function predictions from the crystal structure. Immunobiology, 205(4-5), pp.421-432.

- Ghebrehiwet, B. and Peerschke, E.I., 2004. cC1q-R (calreticulin) and gC1q-R/p33: ubiquitously expressed multi-ligand binding cellular proteins involved in inflammation and infection. Molecular immunology, 41(2), pp.173-183.

- Giannoni, E., Sawa, T., Allen, L., Wiener-Kronish, J. and Hawgood, S., 2006. Surfactant proteins A and D enhance pulmonary clearance of Pseudomonas aeruginosa. American journal of respiratory cell and molecular biology, 34(6), pp.704-710.

- Gideon, H.P. and Flynn, J.L., 2011. Latent tuberculosis: what the host "sees". Immunologic research, 50(2-3), pp.202-212.

- Gillard, P., Yang, P.C., Danilovits, M., Su, W.J., Cheng, S.L., Pehme, L., Bollaerts, A., Jongert, E., Moris, P., Ofori-Anyinam, O. and Demoitié, M.A., 2016. Safety and immunogenicity of the M72/AS01 E candidate tuberculosis vaccine in adults with tuberculosis: A phase II randomised study. Tuberculosis, 100, pp.118-127.

- Gler, M.T., Skripconoka, V., Sanchez-Garavito, E., Xiao, H., Cabrera-Rivero, J.L., Vargas-Vasquez, D.E., Gao, M., Awad, M., Park, S.K., Shim, T.S. and Suh, G.Y., 2012. Delamanid for multidrug-resistant pulmonary tuberculosis. New England Journal of Medicine, 366(23), pp.2151-2160.

- Godiska, R., Chantry, D., Raport, C.J., Sozzani, S., Allavena, P., Leviten, D., Mantovani, A. and Gray, P.W., 1997. Human macrophage–derived chemokine (MDC), a novel chemoattractant for monocytes, monocyte-derived dendritic cells, and natural killer cells. The Journal of experimental medicine, 185(9), pp.1595-1604.

- Greenberg, S.S., Xie, J., Kolls, J., Mason, C. and Didier, P., 1995. Rapid induction of mRNA for nitric oxide synthase II in rat alveolar macrophages by intratracheal administration of Mycobacterium tuberculosis and Mycobacterium avium. Experimental Biology and Medicine, 209(1), pp.46-53.

- Gudjónsdóttir, M.J., Kötz, K., Nielsen, R.S., Wilmar, P., Olausson, S., Wallmyr, D. and Trollfors, B., 2016. Relation between BCG vaccine scar and an interferon-gamma release assay in immigrant children with "positive" tuberculin skin test (≥ 10 mm). BMC Infectious Diseases, 16(1), p.540.

- Gupta, G. and Surolia, A., 2007. Collectins: sentinels of innate immunity. Bioessays, 29(5), pp.452-464.

- Gupta, A., Kaul, A., Tsolaki, A.G., Kishore, U. and Bhakta, S., 2012. Mycobacterium tuberculosis: immune evasion, latency and reactivation. Immunobiology, 217(3), pp.363-374.

- Hall-Stoodley, L., Watts, G., Crowther, J.E., Balagopal, A., Torrelles, J.B., Robison-Cox, J., Bargatze, R.F., Harmsen, A.G., Crouch, E.C. and Schlesinger, L.S., 2006. Mycobacterium tuberculosis binding to human surfactant proteins A and D, fibronectin, and small airway epithelial cells under shear conditions. Infection and immunity, 74(6), pp.3587-3596.

- Hansen, S. and Holmskov, U., 1998. Structural aspects of collectins and receptors for collectins. Immunobiology, 199(2), pp.165-189.

- Happel, K.I., Dubin, P.J., Zheng, M., Ghilardi, N., Lockhart, C., Quinton, L.J., Odden, A.R., Shellito, J.E., Bagby, G.J., Nelson, S. and Kolls, J.K., 2005. Divergent roles of IL-23 and IL-12 in host defense against Klebsiella pneumoniae. The Journal of experimental medicine, 202(6), pp.761-769.

- Haribabu, B., Zhelev, D.V., Pridgen, B.C., Richardson, R.M., Ali, H. and Snyderman, R., 1999. Chemoattractant Receptors Activate Distinct Pathways for Chemotaxis and Secretion ROLE OF G-PROTEIN USAGE. Journal of Biological Chemistry, 274(52), pp.37087-37092.

- Hartshorn, K.L., Crouch, E.C., White, M.R., Eggleton, P., Tauber, A.I., Chang, D. and Sastry, K., 1994. Evidence for a protective role of pulmonary surfactant protein D (SP-D) against influenza A viruses. Journal of Clinical Investigation, 94(1), p.311.

- Hartshorn, K.L., White, M.R., Voelker, D.R., Coburn, J., Zaner, K. and Crouch, E.C., 2000. Mechanism of binding of surfactant protein D to influenza A viruses: importance of binding to haemagglutinin to antiviral activity. Biochemical Journal, 351(2), pp.449-458.

- Hemmi, H., Takeuchi, O., Kawai, T., Kaisho, T., Sato, S., Sanjo, H., Matsumoto, M., Hoshino, K., Wagner, H., Takeda, K. and Akira, S., 2000. A Toll-like receptor recognizes bacterial DNA. Nature, 408(6813), pp.740-745.

- Herbst, S., Schaible, U.E. and Schneider, B.E., 2011. Interferon gamma activated macrophages kill mycobacteria by nitric oxide induced apoptosis. PloS one, 6(5), p.e19105.

- Hernandez-Pando, R., Orozcoe, H., Sampieri, A., Pavon, L., Velasquillo, C., Larriva-Sahd, J., Alcocer, J.M. and Madrid, M.V., 1996. Correlation between the kinetics of Th1, Th2 cells and pathology in a murine model of experimental pulmonary tuberculosis. Immunology, 89(1), p.26.

- Higgins, D.M., Sanchez-Campillo, J., Rosas-Taraco, A.G., Lee, E.J., Orme, I.M. and Gonzalez-Juarrero, M., 2009. Lack of IL-10 alters inflammatory

and immune responses during pulmonary Mycobacterium tuberculosis infection. Tuberculosis, 89(2), pp.149-157.

- Hmama, Z., Gabathuler, R., Jefferies, W.A., de Jong, G. and Reiner, N.E., 1998. Attenuation of HLA-DR expression by mononuclear phagocytes infected with Mycobacterium tuberculosis is related to intracellular sequestration of immature class II heterodimers. The Journal of Immunology, 161(9), pp.4882-4893.

- Honda, Y., Kuroki, Y., Matsuura, E., Nagae, H., Takahashi, H., Akino, T. and Abe, S., 1995. Pulmonary surfactant protein D in sera and bronchoalveolar lavage fluids. American journal of respiratory and critical care medicine, 152(6), pp.1860-1866.

- Hong, Q., Sze, C.I., Lin, S.R., Lee, M.H., He, R.Y., Schultz, L., Chang, J.Y., Chen, S.J., Boackle, R.J., Hsu, L.J. and Chang, N.S., 2009. Complement C1q activates tumor suppressor WWOX to induce apoptosis in prostate cancer cells. PLoS One, 4(6), p.e5755.

- Hossain, M.M. and Norazmi, M.N., 2013. Pattern recognition receptors and cytokines in Mycobacterium tuberculosis infection—the double-edged sword?. BioMed research international.

- Hosszu, K.K., Santiago-Schwarz, F., Peerschke, E.I. and Ghebrehiwet, B., 2010. Evidence that a C1q/C1qR system regulates monocyte-derived dendritic cell differentiation at the interface of innate and acquired immunity. Innate immunity, 16(2), pp.115-127.

- Houben, E.N., Nguyen, L. and Pieters, J., 2006. Interaction of pathogenic mycobacteria with the host immune system. Current opinion in microbiology, 9(1), pp.76-85.

- House-Pompeo, K., Xu, Y., Joh, D., Speziale, P. and Höök, M., 1996. Conformational changes in the fibronectin binding MSCRAMMs are induced by ligand binding. Journal of Biological Chemistry, 271(3), pp.1379-1384.

- Hu, B. and Yasui, K., 1997. Effects of colony-stimulating factors (CSFs) on neutrophil apoptosis: possible roles at inflammation site. International journal of hematology, 66(2), pp.179-188.

- Hudson, M.C., Ramp, W.K. and Frankenburg, K.P., 1999. Staphylococcus aureus adhesion to bone matrix and bone-associated biomaterials. FEMS microbiology letters, 173(2), pp.279-284.

- Hugonnet, J.E. and Blanchard, J.S., 2007. Irreversible inhibition of the Mycobacterium tuberculosis β-lactamase by clavulanate. Biochemistry, 46(43), pp.11998-12004.

- Hugonnet, J.E., Tremblay, L.W., Boshoff, H.I., Barry, C.E. and Blanchard, J.S., 2009. Meropenem-clavulanate is effective against extensively drug-resistant Mycobacterium tuberculosis. Science, 323(5918), pp.1215-1218.

- Idoko, O.T., Owolabi, O.A., Owiafe, P.K., Moris, P., Odutola, A., Bollaerts, A., Ogundare, E., Jongert, E., Demoitié, M.A., Ofori-Anyinam, O. and Ota, M.O., 2014. Safety and immunogenicity of the M72/AS01 candidate tuberculosis vaccine when given as a booster to BCG in Gambian infants: an open-label randomized controlled trial. Tuberculosis, 94(6), pp.564-578.

- Jagels, M.A., Ember, J.A., Travis, J., Potempa, J., Pike, R. and Hugli, T.E., 1996. Cleavage of the Human C5A Receptor by Protienases Derived from Porphyromonas Gingivalis. In Intracellular Protein Catabolism (pp. 155-164). Springer US.

- James, E.A., Schmeltzer, K. and Ligler, F.S., 1996. Detection of endotoxin using an evanescent wave fiber-optic biosensor. Applied biochemistry and biotechnology, 60(3), pp.189-202.

- Janeway, C., Travers, P., Walport, M. 2005. Immunobiology. 2005. Garland Science Publishing. New York, NY.

- Janeway Jr, C.A., Travers, P. and Walport, M., 2012. Immunobiology. 8th Editio. New York: Garland Science.

- Janssen, W.J., McPhillips, K.A., Dickinson, M.G., Linderman, D.J., Morimoto, K., Xiao, Y.Q., Oldham, K.M., Vandivier, R.W., Henson, P.M. and Gardai, S.J., 2008. Surfactant proteins A and D suppress alveolar macrophage phagocytosis via interaction with SIRPα. American journal of respiratory and critical care medicine, 178(2), pp.158-167.

- Jindani, A., Aber, V.R., Edwards, E.A. and Mitchison, D.A., 1980. The Early Bactericidal Activity of Drugs in Patients with Pulmonary Tuberculosis 1, 2. American Review of Respiratory Disease, 121(6), pp.939-949.

- Johnston, B. and Butcher, E.C., 2002, April. Chemokines in rapid leukocyte adhesion triggering and migration. In Seminars in immunology (Vol. 14, No. 2, pp. 83-92). Academic Press.

- Juffermans, N.P., Florquin, S., Camoglio, L., Verbon, A., Kolk, A.H., Speelman, P., Van Deventer, S.J. and Van der Poll, T., 2000. Interleukin-1 signaling is essential for host defense during murine pulmonary tuberculosis. Journal of Infectious Diseases, 182(3), pp.902-908.

- Junqueira-Kipnis, A.P., Kipnis, A., Jamieson, A., Juarrero, M.G., Diefenbach, A., Raulet, D.H., Turner, J. and Orme, I.M., 2003. NK cells respond to pulmonary infection with Mycobacterium tuberculosis, but play a

minimal role in protection. The Journal of Immunology, 171(11), pp.6039-6045.

- Kahan, F.M., Kropp, H., Sundelof, J.G. and Birnbaum, J., 1983. Thienamycin: development of imipenem-cilastatin. Journal of Antimicrobial Chemotherapy, 12(suppl D), pp.1-35.

- Kaneko, H., Yamada, H., Mizuno, S., Udagawa, T., Kazumi, Y., Sekikawa, K. and Sugawara, I., 1999. Role of tumor necrosis factor-alpha in Mycobacterium-induced granuloma formation in tumor necrosis factor-alpha-deficient mice. Laboratory investigation; a journal of technical methods and pathology, 79(4), pp.379-386.

- Kang, P.B., Azad, A.K., Torrelles, J.B., Kaufman, T.M., Beharka, A., Tibesar, E., DesJardin, L.E. and Schlesinger, L.S., 2005. The human macrophage mannose receptor directs Mycobacterium tuberculosis lipoarabinomannan-mediated phagosome biogenesis. The Journal of experimental medicine, 202(7), pp.987-999.

- Kang, M., Ko, Y.P., Liang, X., Ross, C.L., Liu, Q., Murray, B.E. and Höök, M., 2013. Collagen-binding microbial surface components recognizing adhesive matrix molecule (MSCRAMM) of Gram-positive bacteria inhibit complement activation via the classical pathway. Journal of Biological Chemistry, 288(28), pp.20520-20531.

- Karthik, K., Kesavan, M., Tamilmahan, P., Saravanan, M. and Dashprakash, M., 2013. Neutrophils in tuberculosis: will code be unlocked?. Veterinary World, 6(2), pp.118-121.

- Kaufmann, S.H., Weiner, J. and von Reyn, C.F., 2017. Novel approaches to tuberculosis vaccine development. International Journal of Infectious Diseases, 56, pp.263-267.

- Khan, E. A.,Starke J.R., 1995. Diagnosis of tuberculosis in children, increased need for better methods. Emerg. Infect. Dis., 1 (4), pp. 115–123.

- Khanna, K.V., Choi, C.S., Gekker, G., Peterson, P.K. and Molitor, T.W., 1996. Differential infection of porcine alveolar macrophage subpopulations by nonopsonized Mycobacterium bovis involves CD14 receptors. Journal of leukocyte biology, 60(2), pp.214-220.

- King, G.M., 2003. Uptake of Carbon Monoxide and Hydrogen at Environmentally Relevant Concentrations by Mycobacteria†. Applied and environmental microbiology, 69(12), pp.7266-7272.

- Kishore, U., Sontheimer, R.D., Sastry, K.N., Zappi, E.G., Hughes, G.R.V., Khamashta, M.A., Reid, K.B.M. and Eggleton, P., 1997. The systemic lupus erythematosus (SLE) disease autoantigen—calreticulin can inhibit C1q

association with immune complexes. Clinical & Experimental Immunology, 108(2), pp.181-190.

- Kishore, U., Madan, T., Sarma, P.U., Singh, M., Urban, B.C. and Reid, K.B., 2002-A. Protective roles of pulmonary surfactant proteins, SP-A and SP-D, against lung allergy and infection caused by Aspergillus fumigatus. Immunobiology, 205(4-5), pp.610-618.

- Kishore, U., Kojouharova, M.S. and Reid, K.B., 2002-B. Recent progress in the understanding of the structure-function relationships of the globular head regions of C1q. Immunobiology, 205(4), pp.355-364.

- Kishore, U., Gupta, S.K., Perdikoulis, M.V., Kojouharova, M.S., Urban, B.C. and Reid, K.B., 2003. Modular organization of the carboxyl-terminal, globular head region of human C1q A, B, and C chains. The Journal of Immunology, 171(2), pp.812-820.

- Kishore, U., Greenhough, T.J., Waters, P., Shrive, A.K., Ghai, R., Kamran, M.F., Bernal, A.L., Reid, K.B., Madan, T. and Chakraborty, T., 2006. Surfactant proteins SP-A and SP-D: structure, function and receptors. Molecular immunology, 43(9), pp.1293-1315.

- Klausner, J.D., Makonkawkeyoon, S., Akarasewi, P., Nakata, K., Kasinrerk, W., Corral, L., Dewar, R.L., Lane, H.C., Freedman, V.H. and Kaplan, G., 1996. The effect of thalidomide on the pathogenesis of human immunodeficiency virus type 1 and M. tuberculosis infection. JAIDS Journal of Acquired Immune Deficiency Syndromes, 11(3), pp.247-257.

- Kleinnijenhuis, J., Joosten, L.A., van de Veerdonk, F.L., Savage, N., van Crevel, R., Kullberg, B.J., van der Ven, A., Ottenhoff, T.H., Dinarello, C.A., van der Meer, J.W. and Netea, M.G., 2009. Transcriptional and inflammasome-mediated pathways for the induction of IL-1β production by Mycobacterium tuberculosis. European journal of immunology, 39(7), pp.1914-1922.
- Kleinnijenhuis, J., Oosting, M., Joosten, L.A., Netea, M.G. and Van Crevel, R., 2011. Innate immune recognition of Mycobacterium tuberculosis. Clinical and Developmental Immunology, 2011.

- Klickstein, L.B., Barbashov, S.F., Liu, T., Jack, R.M. and Nicholson-Weller, A., 1997. Complement receptor type 1 (CR1, CD35) is a receptor for C1q. Immunity, 7(3), pp.345-355.

- Klockars, M., Pettersson, T., Vartio, T., Riska, H. and Vaheri, A., 1982. Fibronectin in exudative pleural effusions. Journal of clinical pathology, 35(7), pp.723-727.

- Kojouharova, M.S., Gadjeva, M.G., Tsacheva, I.G., Zlatarova, A., Roumenina, L.T., Tchorbadjieva, M.I., Atanasov, B.P., Waters, P., Urban, B.C., Sim, R.B. and Reid, K.B., 2004. Mutational analyses of the recombinant globular regions of human C1q A, B, and C chains suggest an essential role for arginine and histidine residues in the C1q-IgG interaction. The Journal of Immunology, 172(7), pp.4351-4358.

- Kolyva, A.S. and Karakousis, P.C., 2012. Old and new TB drugs: Mechanisms of action and resistance. INTECH Open Access Publisher.

- Korn, T., Oukka, M., Kuchroo, V. and Bettelli, E., 2007, December. Th17 cells: effector T cells with inflammatory properties. In Seminars in immunology (Vol. 19, No. 6, pp. 362-371). Academic Press.

- Kosmehl, H., Berndt, A. and Katenkamp, D., 1996. Molecular variants of fibronectin and laminin: structure, physiological occurrence and histopathological aspects. Virchows Archiv, 429(6), pp.311-322.

- Kozakiewicz, L., Phuah, J., Flynn, J. and Chan, J., 2013. The role of B cells and humoral immunity in Mycobacterium tuberculosis infection. In The New Paradigm of Immunity to Tuberculosis (pp. 225-250). Springer New York.

- Krutzik, S.R. and Modlin, R.L., 2004, February. The role of Toll-like receptors in combating mycobacteria. In Seminars in immunology (Vol. 16, No. 1, pp. 35-41). Academic Press.

- Kudo, K., Sano, H., Takahashi, H., Kuronuma, K., Yokota, S.I., Fujii, N., Shimada, K.I., Yano, I., Kumazawa, Y., Voelker, D.R. and Abe, S., 2004. Pulmonary collectins enhance phagocytosis of Mycobacterium avium through increased activity of mannose receptor. The Journal of Immunology, 172(12), pp.7592-7602.

- Kumar, P., Arora, K., Lloyd, J.R., Lee, I.Y., Nair, V., Fischer, E., Boshoff, H.I. and Barry, C.E., 2012. Meropenem inhibits D, D-carboxypeptidase activity in Mycobacterium tuberculosis. Molecular microbiology, 86(2), pp.367-381.

- Kuroki, Y., Takahashi, H., Chiba, H. and Akino, T., 1998. Surfactant proteins A and D: disease markers. Biochimica et Biophysica Acta (BBA)-Molecular Basis of Disease, 1408(2), pp.334-345.

- Kuroki, Y., Takahashi, M. and Nishitani, C., 2007. Pulmonary collectins in innate immunity of the lung. Cellular microbiology, 9(8), pp.1871-1879.

- Kuusela P., 1978. Fibronectin binds to Staphylococcus aureus. Nature 276: 718–720.

- Ladel, C.H., Szalay, G., Riedel, D. and Kaufmann, S.H., 1997. Interleukin-12 secretion by Mycobacterium tuberculosis-infected macrophages. Infection and immunity, 65(5), pp.1936-1938.

- Laster, S.M., Wood, J.G. and Gooding, L.R., 1988. Tumor necrosis factor can induce both apoptic and necrotic forms of cell lysis. The Journal of Immunology, 141(8), pp.2629-2634.

- Lathigra, R., Zhang, Y., Hill, M., Garcia, M.J., Jackett, P.S. and Ivanyi, J., 1996. Lack of production of the 19-kDa glycolipoprotein in certain strains of Mycobacterium tuberculosis. Research in microbiology, 147(4), pp.237-249.

- Law, K., Weiden, M., Harkin, T., Tchou-Wong, K., Chi, C. and Rom, W.N., 1996. Increased release of interleukin-1 beta, interleukin-6, and tumor necrosis factor-alpha by bronchoalveolar cells lavaged from involved sites in pulmonary tuberculosis. American journal of respiratory and critical care medicine, 153(2), pp.799-804.

- Lee, J., Hartman, M. and Kornfeld, H., 2009. Macrophage apoptosis in tuberculosis. Yonsei medical journal, 50(1), pp.1-11.

- Leigh, E. L., Ghebrehiwet, B., Pereta, P. T., Bird, N. I., Strong,P., Kishore, U., Reid, B.K. and Eggleton, P., 1998. C1q-mediated chemotaxis by human neutrophils: involvement of gClqR and G-protein signalling mechanisms. Biochemical Journal, 330(1), pp.247-254.

- Leroux-Roels, I., Forgus, S., De Boever, F., Clement, F., Demoitié, M.A., Mettens, P., Moris, P., Ledent, E., Leroux-Roels, G., Ofori-Anyinam, O. and M72 Study Group, 2013. Improved CD4+ T cell responses to Mycobacterium tuberculosis in PPD-negative adults by M72/AS01 as compared to the M72/AS02 and Mtb72F/AS02 tuberculosis candidate vaccine formulations: a randomized trial. Vaccine, 31(17), pp.2196-2206.

- Leth-Larsen, R., Garred, P., Jensenius, H., Meschi, J., Hartshorn, K., Madsen, J., Tornoe, I., Madsen, H.O., Sørensen, G., Crouch, E. and Holmskov, U., 2005. A common polymorphism in the SFTPD gene influences assembly, function, and concentration of surfactant protein D. The Journal of Immunology, 174(3), pp.1532-1538.

- Leth-Larsen, R., Floridon, C., Nielsen, O. and Holmskov, U., 2004. Surfactant protein D in the female genital tract. Molecular human reproduction, 10(3), pp.149-154.

- Lim, B.L., Wang, J.Y., Holmskov, U., Hoppe, H.J. and Reid, K.B., 1994. Expression of the carbohydrate recognition domain of lung surfactant protein D and demonstration of its binding to lipopolysaccharides of gram-

negative bacteria. Biochemical and biophysical research communications, 202(3), pp.1674-1680.

- Lim, B.L., Reid, K.B., Ghebrehiwet, B., Peerschke, E.I., Leigh, L.A. and Preissner, K.T., 1996. The Binding Protein for Globular Heads of Complement C1q, gC1qR FUNCTIONAL EXPRESSION AND CHARACTERIZATION AS A NOVEL VITRONECTIN BINDING FACTOR. Journal of Biological Chemistry, 271(43), pp.26739-26744.

- Liu, P.T., Stenger, S., Li, H., Wenzel, L., Tan, B.H., Krutzik, S.R., Ochoa, M.T., Schauber, J., Wu, K., Meinken, C. and Kamen, D.L., 2006. Toll-like receptor triggering of a vitamin D-mediated human antimicrobial response. Science, 311(5768), pp.1770-1773.

- Lönnroth, K. and Raviglione, M., 2008, October. Global epidemiology of tuberculosis: prospects for control. In Seminars in respiratory and critical care Medicine (Vol. 29, No. 05, pp. 481-491). © Thieme Medical Publishers.

- Lowrie DB, Silva CL. 2000. Enhancement of immunocompetence in tuberculosis by DNA vaccination. Vaccine. 18(16):1712–1716.

- Lu, Y.C., Yeh, W.C. and Ohashi, P.S., 2008. LPS/TLR4 signal transduction pathway. Cytokine, 42(2), pp.145-151.

- Luo Y, Lu S, Guo S. 2000. Immunotherapeutic effect of Mycobacterium vaccae on multi-drug resistant pulmonary tuberculosis. Zhonghua Jie He He Hu Xi Za Zhi Feb;23 (2):85-8.

- Lutsenko, S., Petrukhin, K., Cooper, M.J., Gilliam, C.T. and Kaplan, J.H., 1997. N-terminal domains of human copper-transporting adenosine triphosphatases (the Wilson's and Menkes disease proteins) bind copper selectively in vivo and in vitro with stoichiometry of one copper per metal-binding repeat. Journal of Biological Chemistry, 272(30), pp.18939-18944.

- Lyons, M.J., Yoshimura, T. and McMurray, D.N., 2002. Mycobacterium bovis BCG vaccination augments interleukin-8 mRNA expression and protein production in guinea pig alveolar macrophages infected with Mycobacterium tuberculosis. Infection and immunity, 70(10), pp.5471-5478.

- MacMicking, J.D., Taylor, G.A. and McKinney, J.D., 2003. Immune control of tuberculosis by IFN-γ-inducible LRG-47. Science, 302(5645), pp.654-659.

- Madan, T., Kishore, U., Shah, A., Eggleton, P., Strong, P., Wang, J.Y., Aggrawal, S.S., Sarma, P.U. and Reid, K.B.M., 1997. Lung surfactant proteins A and D can inhibit specific IgE binding to the allergens of

Aspergillus fumigatus and block allergen-induced histamine release from human basophils. Clinical & Experimental Immunology, 110(2), pp.241-249.

- Madsen, J., Kliem, A., Tornøe, I., Skjødt, K., Koch, C. and Holmskov, U., 2000. Localization of lung surfactant protein D on mucosal surfaces in human tissues. The Journal of Immunology, 164(11), pp.5866-5870.

- Maglione, P.J. and Chan, J., 2009. How B cells shape the immune response against Mycobacterium tuberculosis. European journal of immunology, 39(3), pp.676-686.

- Mahajan, L., Madan, T., Kamal, N., Singh, V.K., Sim, R.B., Telang, S.D., Ramchand, C.N., Waters, P., Kishore, U. and Sarma, P.U., 2008. Recombinant surfactant protein-D selectively increases apoptosis in eosinophils of allergic asthmatics and enhances uptake of apoptotic eosinophils by macrophages. International immunology, 20(8), pp.993-1007.

- Malhotra, R., Willis, A.C., Bernal, A.L., Thiel, S. and Sim, R.B., 1994. Mannan-binding protein levels in human amniotic fluid during gestation and its interaction with collectin receptor from amnion cells. Immunology, 82(3), p.439.

- Mantovani, A., Gray, P.A., Van Damme, J. and Sozzani, S., 2000. Macrophage-derived chemokine (MDC). Journal of leukocyte biology, 68(3), pp.400-404.

- Marlowe, E.M., Novak-Weekley, S.M., Cumpio, J., Sharp, S.E., Momeny, M.A., Babst, A., Carlson, J.S., Kawamura, M. and Pandori, M., 2011. Evaluation of the Cepheid Xpert MTB/RIF assay for direct detection of Mycobacterium tuberculosis complex in respiratory specimens. Journal of clinical microbiology, 49(4), pp.1621-1623.

- Martinez, F.O., Sica, A., Mantovani, A. and Locati, M., 2007. Macrophage activation and polarization. Frontiers in bioscience: a journal and virtual library, 13, pp.453-461.

- Matsumoto, M., Hashizume, H., Tomishige, T., Kawasaki, M., Tsubouchi, H., Sasaki, H., Shimokawa, Y. and Komatsu, M., 2006. OPC-67683, a nitro-dihydro-imidazooxazole derivative with promising action against tuberculosis in vitro and in mice. PLoS Med, 3(11), p.e466.

- Matsumiya, M., Satti, I., Chomka, A., Harris, S.A., Stockdale, L., Meyer, J., Fletcher, H.A. and McShane, H., 2015. Gene expression and cytokine profile correlate with mycobacterial growth in a human BCG challenge model. Journal of Infectious Diseases, 211(9), pp.1499-1509.

- McNerney, R., Maeurer, M., Abubakar, I., Marais, B., Mchugh, T.D., Ford, N., Weyer, K., Lawn, S., Grobusch, M.P., Memish, Z. and Squire, S.B.,

2012. Tuberculosis diagnostics and biomarkers: needs, challenges, recent advances, and opportunities. Journal of Infectious Diseases, p.jir860.

- Medof, M.E., Iida, K.Y.O.K.O., Mold, C.A.R.O.L.Y.N. and Nussenzweig, V., 1982. Unique role of the complement receptor CR1 in the degradation of C3b associated with immune complexes. The Journal of experimental medicine, 156(6), pp.1739-1754.

- Mikusová, K., Slayden, R.A., Besra, G.S. and Brennan, P.J., 1995. Biogenesis of the mycobacterial cell wall and the site of action of ethambutol. Antimicrobial agents and chemotherapy, 39(11), pp.2484-2489.

- Miller, E.A. and Ernst, J.D., 2009. Anti-TNF immunotherapy and tuberculosis reactivation: another mechanism revealed. The Journal of clinical investigation, 119(5), pp.1079-1082.

- Mitchison, D.A., 1985. The action of antituberculosis drugs in short-course chemotherapy. Tubercle, 66(3), pp.219-225.

- Mohan, V.P., Scanga, C.A., Yu, K., Scott, H.M., Tanaka, K.E., Tsang, E., Tsai, M.C., Flynn, J.L. and Chan, J., 2001. Effects of tumor necrosis factor alpha on host immune response in chronic persistent tuberculosis: possible role for limiting pathology. Infection and immunity, 69(3), pp.1847-1855.

- Montoya, J., Solon, J.A., Cunanan, S.R.C., Acosta, L., Bollaerts, A., Moris, P., Janssens, M., Jongert, E., Demoitié, M.A., Mettens, P. and Gatchalian, S., 2013. A randomized, controlled dose-finding phase II study of the M72/AS01 candidate tuberculosis vaccine in healthy PPD-positive adults. Journal of clinical immunology, 33(8), pp.1360-1375.

- Moore, K.W., de Waal Malefyt, R., Coffman, R.L. and O'Garra, A., 2001. Interleukin-10 and the interleukin-10 receptor. Annual review of immunology, 19(1), pp.683-765.

- Moré, J.M., Voelker, D.R., Silveira, L.J., Edwards, M.G., Chan, E.D. and Bowler, R.P., 2010. Smoking reduces surfactant protein D and phospholipids in patients with and without chronic obstructive pulmonary disease. BMC pulmonary medicine, 10(1), p.1.

- Morlock, G.P., Metchock, B., Sikes, D., Crawford, J.T. and Cooksey, R.C., 2003. ethA, inhA, and katG loci of ethionamide-resistant clinical Mycobacterium tuberculosis isolates. Antimicrobial agents and chemotherapy, 47(12), pp.3799-3805.

- Mosher, D.F., 2006. Plasma Fibronectin Concentration.

- Mosher, D.F., 1980. Fibronectin. Progress in hemostasis and thrombosis, 5, p.111.

- Mueller-Ortiz, S.L., Wanger, A.R. and Norris, S.J., 2001. Mycobacterial protein HbhA binds human complement component C3. Infection and immunity, 69(12), pp.7501-7511.

- Mueller, P. and Pieters, J., 2006. Modulation of macrophage antimicrobial mechanisms by pathogenic mycobacteria. Immunobiology, 211(6), pp.549-556.

- Munder, M., Mallo, M., Eichmann, K. and Modolell, M., 2001. Direct stimulation of macrophages by IL-12 and IL-18—a bridge built on solid ground. Immunology letters, 75(2), pp.159-160.

- Murray, P.J., Wang, L., Onufryk, C., Tepper, R.I. and Young, R.A., 1997. T cell-derived IL-10 antagonizes macrophage function in mycobacterial infection. The Journal of Immunology, 158(1), pp.315-321.

- Murphy, K., Travers, P. and Walport, M., 2012. The generation of lymphocyte antigen receptors. Janeway's Immunobiology 8th Edition. New York: Garland Science, pp.5-1.

- Naito, M., Ohara, N., Matsumoto, S. and Yamada, T., 1998. The novel fibronectin-binding motif and key residues of mycobacteria. Journal of Biological Chemistry, 273(5), pp.2905-2909.

- Nakagawa, H., Komorita, N., Shibata, F., Ikesue, A., Konishi, K., Fujioka, M. and Kato, H., 1994. Identification of cytokine-induced neutrophil chemoattractants (CINC), rat GRO/CINC-2α and CINC-2 β, produced by granulation tissue in culture: purification, complete amino acid sequences and characterization. Biochemical Journal, 301(2), pp.545-550.

- Nauta, A.J., Bottazzi, B., Mantovani, A., Salvatori, G., Kishore, U., Schwaeble, W.J., Gingras, A.R., Tzima, S., Vivanco, F., Egido, J. and Tijsma, O., 2003. Biochemical and functional characterization of the interaction between pentraxin 3 and C1q. European journal of immunology, 33(2), pp.465-473.

- Nayak, A., Ferluga, J., Tsolaki, A.G. and Kishore, U., 2010. The non-classical functions of the classical complement pathway recognition subcomponent C1q. Immunology letters, 131(2), pp.139-150.

- Nayak, A., Dodagatta-Marri, E., Tsolaki, A.G. and Kishore, U., 2012-A. An insight into the diverse roles of surfactant proteins, SP-A and SP-D in innate and adaptive immunity. Frontiers in immunology, 3, p.131.

- Nayak, A., Pednekar, L., Reid, K.B. and Kishore, U., 2012. Complement and non-complement activating functions of C1q: a prototypical innate immune molecule. Innate immunity, 18(2), pp.350-363.

- Nicholson, S., da G Bonecini-Almeida, M., e Silva, J.L., Nathan, C., Xie, Q.W., Mumford, R., Weidner, J.R., Calaycay, J., Geng, J., Boechat, N. and Linhares, C., 1996. Inducible nitric oxide synthase in pulmonary alveolar macrophages from patients with tuberculosis. The Journal of experimental medicine, 183(5), pp.2293-2302.

- Noss, E.H., Harding, C.V. and Boom, W.H., 2000. Mycobacterium tuberculosis inhibits MHC class II antigen processing in murine bone marrow macrophages. Cellular immunology, 201(1), pp.63-74.

- Noss, E.H., Pai, R.K., Sellati, T.J., Radolf, J.D., Belisle, J., Golenbock, D.T., Boom, W.H. and Harding, C.V., 2001. Toll-like receptor 2-dependent inhibition of macrophage class II MHC expression and antigen processing by 19-kDa lipoprotein of Mycobacterium tuberculosis. The Journal of Immunology, 167(2), pp.910-918.

- Oberley, R.E., Goss, K.L., Ault, K.A., Crouch, E.C. and Snyder, J.M., 2004. Surfactant protein D is present in the human female reproductive tract and inhibits Chlamydia trachomatis infection. Molecular human reproduction, 10(12), pp.861-870.

- Oddo, M., Renno, T., Attinger, A., Bakker, T., MacDonald, H.R. and Meylan, P.R., 1998. Fas ligand-induced apoptosis of infected human macrophages reduces the viability of intracellular Mycobacterium tuberculosis. The Journal of Immunology, 160(11), pp.5448-5454.

- Ogden, C.A., Hoffmann, P.R., Bratton, D., Ghebrehiwet, B., Fadok, V.A. and Henson, P.M., 2001. C1q and mannose binding lectin engagement of cell surface calreticulin and CD91 initiates macropinocytosis and uptake of apoptotic cells. The Journal of experimental medicine, 194(6), pp.781-796.

- Ohya, M., Nishitani, C., Sano, H., Yamada, C., Mitsuzawa, H., Shimizu, T., Saito, T., Smith, K., Crouch, E. and Kuroki, Y., 2006. Human pulmonary surfactant protein D binds the extracellular domains of Toll-like receptors 2 and 4 through the carbohydrate recognition domain by a mechanism different from its binding to phosphatidylinositol and lipopolysaccharide. Biochemistry, 45(28), pp.8657-8664.

- O'Leary, S., O'Sullivan, M.P. and Keane, J., 2011. IL-10 blocks phagosome maturation in Mycobacterium tuberculosis–infected human macrophages. American journal of respiratory cell and molecular biology, 45(1), pp.172-180.

- O'Shea, M.K. and McShane, H., 2016. A review of clinical models for the evaluation of human TB vaccines. Human vaccines & immunotherapeutics, 12(5), pp.1177-1187.

- Oswald, I.P., Dozois, C.M., Petit, J.F. and Lemaire, G., 1997. Interleukin-12 synthesis is a required step in trehalose dimycolate-induced activation of mouse peritoneal macrophages. Infection and immunity, 65(4), pp.1364-1369.

- Pai, R.K., Convery, M., Hamilton, T.A., Boom, W.H. and Harding, C.V., 2003. Inhibition of IFN-γ-induced class II transactivator expression by a 19-kDa lipoprotein from Mycobacterium tuberculosis: a potential mechanism for immune evasion. The Journal of Immunology, 171(1), pp.175-184.

- Pai, R.K., Pennini, M.E., Tobian, A.A., Canaday, D.H., Boom, W.H. and Harding, C.V., 2004. Prolonged toll-like receptor signaling by Mycobacterium tuberculosis and its 19-kilodalton lipoprotein inhibits gamma interferon-induced regulation of selected genes in macrophages. Infection and immunity, 72(11), pp.6603-6614.

- Palaniyar, N., Clark, H., Nadesalingam, J., Hawgood, S. and Reid, K., 2003. Surfactant protein D binds genomic DNA and apoptotic cells, and enhances their clearance, in vivo. Annals of the New York Academy of Sciences, 1010(1), pp.471-475.

- Pankov, R. and Yamada, K.M., 2002. Fibronectin at a glance. Journal of cell science, 115(20), pp.3861-3863.

- Pasula, R., Wisniowski, P. and Martin II, W.J., 2002. Fibronectin facilitates Mycobacterium tuberculosis attachment to murine alveolar macrophages. Infection and immunity, 70(3), pp.1287-1292.

- Pathan, A.A., Minassian, A.M., Sander, C.R., Rowland, R., Porter, D.W., Poulton, I.D., Hill, A.V., Fletcher, H.A. and McShane, H., 2012. Effect of vaccine dose on the safety and immunogenicity of a candidate TB vaccine, MVA85A, in BCG vaccinated UK adults. Vaccine, 30(38), pp.5616-5624.

- Paul, J.I. and Hynes, R.O., 1984. Multiple fibronectin subunits and their post-translational modifications. Journal of Biological Chemistry, 259(21), pp.13477-13487.

- Peake, P., Gooley, A. and Britton, W.J., 1993. Mechanism of interaction of the 85B secreted protein of Mycobacterium bovis with fibronectin. Infection and immunity, 61(11), pp.4828-4834.

- Pednekar, L., 2013. Understanding cellular and molecular interactions of gC1qR, a receptor for the globular domain of complement protein C1q (Doctoral dissertation, Brunel University).

- Pednekar, L., Pandit, H., Paudyal, B., Kaur, A., Al-Mozaini, M.A., Kouser, L., Ghebrehiwet, B., Mitchell, D.A., Madan, T. and Kishore, U., 2016. complement Protein c1q interacts with Dc-sign via its globular Domain and Thus May interfere with hiV-1 Transmission. Frontiers in Immunology, 7.

- Peerschke, E.I. and Ghebrehiwet, B., 1998. Platelet receptors for the complement component C1q: implications for hemostasis and thrombosis. Immunobiology, 199(2), pp.239-249.

- Pennini, M.E., Pai, R.K., Schultz, D.C., Boom, W.H. and Harding, C.V., 2006. Mycobacterium tuberculosis 19-kDa lipoprotein inhibits IFN-γ-induced chromatin remodeling of MHC2TA by TLR2 and MAPK signaling. The Journal of Immunology, 176(7), pp.4323-4330.

- Penn-Nicholson, A., Geldenhuys, H., Burny, W., van der Most, R., Day, C.L., Jongert, E., Moris, P., Hatherill, M., Ofori-Anyinam, O. and Hanekom, W., 2015. Bollaerts A, Demoitie MA, Kany Luabeya AK, De Ruymaeker E, Tameris M, Lapierre D, Scriba TJ. Safety and immunogenicity of candidate vaccine M72/AS01E in adolescents in a TB endemic setting. Vaccine, 33, pp.4025-34.

- Pfützner, A., Mann, A.E. and Steiner, S.S., 2002. Technosphere™/Insulin—a new approach for effective delivery of human insulin via the pulmonary route. Diabetes technology & therapeutics, 4(5), pp.589-594.

- Pickering, M.C., Macor, P., Fish, J., Durigutto, P., Bossi, F., Petry, F., Botto, M. and Tedesco, F., 2008. Complement C1q and C8β deficiency in an individual with recurrent bacterial meningitis and adult-onset systemic lupus erythematosus-like illness. Rheumatology, 47(10), pp.1588-1589.

- Pieters, J., 2001. Evasion of host cell defense mechanisms by pathogenic bacteria. Current opinion in immunology, 13(1), pp.37-44.

- Powrie, F., Menon, S. and Coffman, R.L., 1993. Interleukin-4 and interleukin-10 synergize to inhibit cell-mediated immunity in vivo. European journal of immunology, 23(11), pp.3043-3049.

- Prezzemolo, T., Guggino, G., La Manna, M.P., Di Liberto, D., Dieli, F. and Caccamo, N., 2014. Functional signatures of human CD4 and CD8T cell responses to Mycobacterium tuberculosis. Significance of antigen and epitope specificity in tuberculosis, p.33.

- Qaseem, A.S., Sonar, S., Mahajan, L., Madan, T., Sorensen, G.L., Shamji, M.H. and Kishore, U., 2013. Linking surfactant protein SP-D and IL-13: implications in asthma and allergy. Molecular immunology, 54(1), pp.98-107.

- Quesniaux, V.J., Nicolle, D.M., Torres, D., Kremer, L., Guérardel, Y., Nigou, J., Puzo, G., Erard, F. and Ryffel, B., 2004. Toll-like receptor 2 (TLR2)-dependent-positive and TLR2-independent-negative regulation of proinflammatory cytokines by mycobacterial lipomannans. The Journal of Immunology, 172(7), pp.4425-4434.

- Ramos-Kichik, V., Mondragón-Flores, R., Mondragón-Castelán, M., Gonzalez-Pozos, S., Muñiz-Hernandez, S., Rojas-Espinosa, O., Chacón-Salinas, R., Estrada-Parra, S. and Estrada-García, I., 2009. Neutrophil extracellular traps are induced by Mycobacterium tuberculosis. Tuberculosis, 89(1), pp.29-37.

- Ratliff, T.L., McCarthy, R., Telle, W.B. and Brown, E.J., 1993. Purification of a mycobacterial adhesin for fibronectin. Infection and immunity, 61(5), pp.1889-1894.

- Raynaud, C., Lanéelle, M.A., Senaratne, R.H., Draper, P., Lanéelle, G. and Daffé, M., 1999. Mechanisms of pyrazinamide resistance in mycobacteria: importance of lack of uptake in addition to lack of pyrazinamidase activity. Microbiology, 145(6), pp.1359-1367.

- Redford, P.S., Boonstra, A., Read, S., Pitt, J., Graham, C., Stavropoulos, E., Bancroft, G.J. and O'Garra, A., 2010. Enhanced protection to Mycobacterium tuberculosis infection in IL-10-deficient mice is accompanied by early and enhanced Th1 responses in the lung. European journal of immunology, 40(8), pp.2200-2210.

- Rich, E.A., Torres, M., Sada, E., Finegan, C.K., Hamilton, B.D. and Toossi, Z., 1997. Mycobacterium tuberculosis (MTB)-stimulated production of nitric oxide by human alveolar macrophages and relationship of nitric oxide production to growth inhibition of MTB. Tubercle and Lung Disease, 78(5), pp.247-255.

- Rieder, H.L., Arnadottir, T., Trebucq, A. and Enarson, D.A., 2001. Tuberculosis treatment: dangerous regimens?. International Journal of Tuberculosis and Lung Disease, 5(1), pp.1-3.

- Ritz N, Hanekom WA, Robins-Browne R, et al. 2008. Influence of BCG vaccine strain on the immune response and protection against tuberculosis. FEMS Microbiol Rev., 32(5), pp. 821–841.

- Robitzek, E.H. and Selikoff, I.J., 1952. Hydrazine Derivatives of Isonicotinic Acid (Rimifon, Mar-silid) in the Treatment oi Active Progressive Caseous-Pneumonic Tuberculosis. A Prelimin-ary Report. American Review of Tuberculosis and Pulmonary Diseases, 65(4), pp.402-28.

- Rojas, M., Olivier, M., Gros, P., Barrera, L.F. and García, L.F., 1999. TNF-α and IL-10 modulate the induction of apoptosis by virulent Mycobacterium

tuberculosis in murine macrophages. The Journal of Immunology, 162(10), pp.6122-6131.

- Rojas, R.E., Balaji, K.N., Subramanian, A. and Boom, W.H., 1999. Regulation of human CD4+ αβ T-cell-receptor-positive (TCR+) and γδ TCR+ T-cell responses to Mycobacterium tuberculosis by interleukin-10 and transforming growth factor β. Infection and immunity, 67(12), pp.6461-6472.

- Roumenina, L.T., Popov, K.T., Bureeva, S.V., Kojouharova, M., Gadjeva, M., Rabheru, S., Thakrar, R., Kaplun, A. and Kishore, U., 2008. Interaction of the globular domain of human C1q with Salmonella typhimurium lipopolysaccharide. Biochimica et Biophysica Acta (BBA)-Proteins and Proteomics, 1784(9), pp.1271-1276.

- Rose, C.E., Sung, S.S.J. and Fu, S.M., 2003. Significant involvement of CCL2 (MCP-1) in inflammatory disorders of the lung. Microcirculation, 10(3-4), pp.273-288.

Ruhwald, M., Bjerregaard-Andersen, M., Rabna, P., Eugen-Olsen, J. and Ravn, P., 2009. IP-10, MCP-1, MCP-2, MCP-3, and IL-1RA hold promise as biomarkers for infection with M. tuberculosis in a whole blood based T-cell assay. BMC research notes, 2(1), p.19.

- Ruscetti, Francis, et al. 1993. "Pleiotropic Effects of Transforming Growth Factor-β on Cells of the Immune System." Annals of the New York Academy of Sciences 685.1: 488-500.

- Russell, D.G., 2005. Mycobacterium tuberculosis: The indigestible microbe. In Tuberculosis and the Tubercle Bacillus (pp. 427-436). American Society of Microbiology.

- Ryll, R., Kumazawa, Y. and Yano, I., 2001. Immunological Properties of Trehalose Dimycolate (Cord Factor) and Other Mycotic Acid-Containing Glycolipids–-A Review. Microbiology and immunology, 45(12), pp.801-811.

- Sachdev, D. and Chirgwin, J.M., 1998. Solubility of proteins isolated from inclusion bodies is enhanced by fusion to maltose-binding protein or thioredoxin. Protein expression and purification, 12(1), pp.122-132.

- Sakamoto, K., 2012. The pathology of Mycobacterium tuberculosis infection. Veterinary Pathology Online, 49(3), pp.423-439.

- Sánchez, A., Espinosa, P., García, T. and Mancilla, R., 2012. The 19 kDa Mycobacterium tuberculosis lipoprotein (LpqH) induces macrophage apoptosis through extrinsic and intrinsic pathways: a role for the

mitochondrial apoptosis-inducing factor. Clinical and Developmental Immunology, 2012.

- Sandor, F., Latz, E., Re, F., Mandell, L., Repik, G., Golenbock, D.T., Espevik, T., Kurt-Jones, E.A. and Finberg, R.W., 2003. Importance of extra- and intracellular domains of TLR1 and TLR2 in NFκB signaling. The Journal of cell biology, 162(6), pp.1099-1110.

- Sanjabi, S., Zenewicz, L.A., Kamanaka, M. and Flavell, R.A., 2009. Anti-inflammatory and pro-inflammatory roles of TGF-β, IL-10, and IL-22 in immunity and autoimmunity. Current opinion in pharmacology, 9(4), pp.447-453.

- Sano, H., Chiba, H., Iwaki, D., Sohma, H., Voelker, D.R. and Kuroki, Y., 2000. Surfactant proteins A and D bind CD14 by different mechanisms. Journal of Biological Chemistry, 275(29), pp.22442-22451.

- Saunders, B.M., Frank, A.A., Orme, I.M. and Cooper, A.M., 2000. Interleukin-6 Induces Early Gamma Interferon Production in the Infected Lung but Is Not Required for Generation of Specific Immunity to Mycobacterium tuberculosisInfection. Infection and immunity, 68(6), pp.3322-3326.

- Saunders, B.M., Frank, A.A., Orme, I.M. and Cooper, A.M., 2002. CD4 is required for the development of a protective granulomatous response to pulmonary tuberculosis. Cellular immunology, 216(1), pp.65-72.

- Schall, T.J., Bacon, K., Camp, R.D., Kaspari, J.W. and Goeddel, D.V., 1993. Human macrophage inflammatory protein alpha (MIP-1 alpha) and MIP-1 beta chemokines attract distinct populations of lymphocytes. The Journal of experimental medicine, 177(6), pp.1821-1826.

- Schäfer, G., Guler, R., Murray, G., Brombacher, F. and Brown, G.D., 2009. The role of scavenger receptor B1 in infection with Mycobacterium tuberculosis in a murine model. PloS one, 4(12), p.e8448.

- Schaible, U.E., Winau, F., Sieling, P.A., Fischer, K., Collins, H.L., Hagens, K., Modlin, R.L., Brinkmann, V. and Kaufmann, S.H., 2003. Apoptosis facilitates antigen presentation to T lymphocytes through MHC-I and CD1 in tuberculosis. Nature medicine, 9(8), pp.1039-1046.

- Schelenz, S., Malhotra, R., Sim, R.B., Holmskov, U. and Bancroft, G.J., 1995. Binding of host collectins to the pathogenic yeast Cryptococcus neoformans: human surfactant protein D acts as an agglutinin for acapsular yeast cells. Infection and immunity, 63(9), pp.3360-3366.

- Scheller, J., Chalaris, A., Schmidt-Arras, D. and Rose-John, S., 2011. The pro-and anti-inflammatory properties of the cytokine interleukin-6.

Biochimica et Biophysica Acta (BBA)-Molecular Cell Research, 1813(5), pp.878-888.

- Schindler, R., Mancilla, J., Endres, S., Ghorbani, R., Clark, S.C. and Dinarello, C.A., 1990. Correlations and interactions in the production of interleukin-6 (IL-6), IL-1, and tumor necrosis factor (TNF) in human blood mononuclear cells: IL-6 suppresses IL-1 and TNF. Blood, 75(1), pp.40-47.

- Schneider, A., Krüger, C., Steigleder, T., Weber, D., Pitzer, C., Laage, R., Aronowski, J., Maurer, M.H., Gassler, N., Mier, W. and Hasselblatt, M., 2005. The hematopoietic factor G-CSF is a neuronal ligand that counteracts programmed cell death and drives neurogenesis. The Journal of clinical investigation, 115(8), pp.2083-2098.

- Schneider, B.E., Korbel, D., Hagens, K., Koch, M., Raupach, B., Enders, J., Kaufmann, S.H., Mittrücker, H.W. and Schaible, U.E., 2010. A role for IL-18 in protective immunity against Mycobacterium tuberculosis. European journal of immunology, 40(2), pp.396-405.

- Schlesinger, L.S. and Horwitz, M.A., 1988, April. Phagocytosis of leprosy bacilli by human-monocytes is mediated by complement receptors CR-1 and CR3. In CLINICAL RESEARCH (Vol. 36, No. 3, pp. A582-A582). 6900 GROVE RD, THOROFARE, NJ 08086: SLACK INC.

- Schlesinger, L.S., Bellinger-Kawahara, C.G., Payne, N.R. and Horwitz, M.A., 1990. Phagocytosis of Mycobacterium tuberculosis is mediated by human monocyte complement receptors and complement component C3. The Journal of Immunology, 144(7), pp.2771-2780.

- Schlesinger, L.S., 1993. Macrophage phagocytosis of virulent but not attenuated strains of Mycobacterium tuberculosis is mediated by mannose receptors in addition to complement receptors. The Journal of Immunology, 150(7), pp.2920-2930.

- Schlesinger, L.S., Kaufman, T.M., Iyer, S., Hull, S.R. and Marchiando, L.K., 1996. Differences in mannose receptor-mediated uptake of lipoarabinomannan from virulent and attenuated strains of Mycobacterium tuberculosis by human macrophages. The Journal of Immunology, 157(10), pp.4568-4575.

- Schorey JS, Li Q, McCourt DW, Bong-Mastek M, Clark-Curtiss JE, Ratliff TL & Brown EJ., 1995. A Mycobacterium leprae gene encoding a fibronectin binding protein is used for efficient invasion of epithelial cells and Schwann cells. Infect Immun 63: 2652–2657.

- Schorey, J.S., Holsti, M.A., Ratliff, T.L., Allen, P.M. and Brown, E.J., 1996. Characterization of the fibronectin-attachment protein of Mycobacterium

avium reveals a fibronectin-binding motif conserved among mycobacteria. Molecular microbiology, 21(2), pp.321-329.

- Schwarzbauer, J.E., 1991. Identification of the fibronectin sequences required for assembly of a fibrillar matrix. The Journal of Cell Biology, 113(6), pp.1463-1473.

- Schwarz-Linek U, Hook M & Potts JR., 2004. The molecular basis of fibronectin-mediated bacterial adherence to host cells. Mol Microbiol 52: 631–641.

- Segovia-Juarez, J.L., Ganguli, S. and Kirschner, D., 2004. Identifying control mechanisms of granuloma formation during M. tuberculosis infection using an agent-based model. Journal of theoretical biology, 231(3), pp.357-376.

- Sellar, G.C., Cockburn, D. and Reid, K.B., 1992. Localization of the gene cluster encoding the A, B, and C chains of human C1q to 1p34. 1–1p36. 3. Immunogenetics, 35(3), pp.214-216.

- Shaler, C.R., Horvath, C., Lai, R. and Xing, Z., 2012. Understanding delayed T-cell priming, lung recruitment, and airway luminal T-cell responses in host defense against pulmonary tuberculosis. Clinical and Developmental Immunology, 2012.

- Shams, H., Wizel, B., Lakey, D.L., Samten, B., Vankayalapati, R., Valdivia, R.H., Kitchens, R.L., Griffith, D.E. and Barnes, P.F., 2003. The CD14 receptor does not mediate entry of Mycobacterium tuberculosis into human mononuclear phagocytes. FEMS Immunology & Medical Microbiology, 36(1-2), pp.63-69.

- Sharma, A., Askari, J.A., Humphries, M.J., Jones, E.Y. and Stuart, D.I., 1999. Crystal structure of a heparin-and integrin-binding segment of human fibronectin. The EMBO Journal, 18(6), pp.1468-1479.

- Silva Miranda, M., Breiman, A., Allain, S., Deknuydt, F. and Altare, F., 2012. The tuberculous granuloma: an unsuccessful host defence mechanism providing a safety shelter for the bacteria?. Clinical and Developmental Immunology, 2012.

- Singh, M., Madan, T., Waters, P., Parida, S.K., Sarma, P.U. and Kishore, U., 2003. Protective effects of a recombinant fragment of human surfactant protein D in a murine model of pulmonary hypersensitivity induced by dust mite allergens. Immunology letters, 86(3), pp.299-307.

- Sly, L.M., Hingley-Wilson, S.M., Reiner, N.E. and McMaster, W.R., 2003. Survival of Mycobacterium tuberculosis in host macrophages involves resistance to apoptosis dependent upon induction of antiapoptotic Bcl-2 family member Mcl-1. The Journal of Immunology, 170(1), pp.430-437.

- Smith, K.F., Haris, P.I., Chapman, D., Reid, K.B.M. and Perkins, S.J., 1994. β-Sheet secondary structure of the trimeric globular domain of C1q of complement and collagen types VIII and X by Fourier-transform infrared spectroscopy and averaged structure predictions. Biochemical Journal, 301(1), pp.249-256.

- Smith, D.F., Galkina, E., Ley, K. and Huo, Y., 2005. GRO family chemokines are specialized for monocyte arrest from flow. American Journal of Physiology-Heart and Circulatory Physiology, 289(5), pp.H1976-H1984.

- Smulders, S., Kaiser, J.P., Zuin, S., Van Landuyt, K.L., Golanski, L., Vanoirbeek, J., Wick, P. and Hoet, P.H., 2012. Contamination of nanoparticles by endotoxin: evaluation of different test methods. Particle and fibre toxicology, 9(1), p.41.

- Son, M., Santiago-Schwarz, F., Al-Abed, Y. and Diamond, B., 2012. C1q limits dendritic cell differentiation and activation by engaging LAIR-1. Proceedings of the National Academy of Sciences, 109(46), pp.E3160-E3167.

- Song, X., Yao, Z., Yang, J., Zhang, Z., Deng, Y., Li, M., Ma, C., Yang, L., Gao, X., Li, W. and Liu, J., 2016. HCV core protein binds to gC1qR to induce A20 expression and inhibit cytokine production through MAPKs and NF-κB signaling pathways. Oncotarget, 7(23), p.33796.

- Souji, E.D.A., SUZUKI, Y., KAWAI, T., OHTANI, K., Tetsuo, K.A.S.E., FUJINAGA, Y., SAKAMOTO, T., KURIMURA, T. and WAKAMIYA, N., 1997. Structure of a truncated human surfactant protein D is less effective in agglutinating bacteria than the native structure and fails to inhibit haemagglutination by influenza A virus. Biochemical Journal, 323(2), pp.393-399.

- Spira, A., Carroll, J.D., Liu, G., Aziz, Z., Shah, V., Kornfeld, H. and Keane, J., 2003. Apoptosis genes in human alveolar macrophages infected with virulent or attenuated Mycobacterium tuberculosis: a pivotal role for tumor necrosis factor. American journal of respiratory cell and molecular biology, 29(5), pp.545-551.

- Stanley, S.A., Raghavan, S., Hwang, W.W. and Cox, J.S., 2003. Acute infection and macrophage subversion by Mycobacterium tuberculosis require a specialized secretion system. Proceedings of the National Academy of Sciences, 100(22), pp.13001-13006.

- Steinberger, P., Szekeres, A., Wille, S., Stöckl, J., Selenko, N., Prager, E., Staffler, G., Madic, O., Stockinger, H. and Knapp, W., 2002. Identification of human CD93 as the phagocytic C1q receptor (C1qRp) by expression cloning. Journal of leukocyte biology, 71(1), pp.133-140.

- Stokol, T., O'Donnell, P., Xiao, L., Knight, S., Stavrakis, G., Botto, M., von Andrian, U.H. and Mayadas, T.N., 2004. C1q governs deposition of circulating immune complexes and leukocyte Fcγ receptors mediate subsequent neutrophil recruitment. Journal of Experimental Medicine, 200(7), pp.835-846.

- Strohmeier, G.R. and Fenton, M.J., 1999. Roles of lipoarabinomannan in the pathogenesis of tuberculosis. Microbes and infection, 1(9), pp.709-717.

- Suba, E.A. and Csako, G., 1976. C1q (C1) receptor on human platelets: inhibition of collagen-induced platelet aggregation by C1q (C1) molecules. The Journal of Immunology, 117(1), pp.304-309.

- Sugawara, I., Yamada, H., Kaneko, H., Mizuno, S., Takeda, K. and Akira, S., 1999. Role of interleukin-18 (IL-18) in mycobacterial infection in IL-18-gene-disrupted mice. Infection and Immunity, 67(5), pp.2585-2589.

- Sundaramurthy, V. and Pieters, J., 2007. Interactions of pathogenic mycobacteria with host macrophages. Microbes and infection, 9(14), pp.1671-1679.

- Tailleux, L., Schwartz, O., Herrmann, J.L., Pivert, E., Jackson, M., Amara, A., Legres, L., Dreher, D., Nicod, L.P., Gluckman, J.C. and Lagrange, P.H., 2003. DC-SIGN is the major Mycobacterium tuberculosis receptor on human dendritic cells. The Journal of experimental medicine, 197(1), pp.121-127.

- Takahashi, S., Leiss, M., Moser, M., Ohashi, T., Kitao, T., Heckmann, D., Pfeifer, A., Kessler, H., Takagi, J., Erickson, H.P. and Fässler, R., 2007. The RGD motif in fibronectin is essential for development but dispensable for fibril assembly. The Journal of cell biology, 178(1), pp.167-178.

- Takayama, K., Schnoes, H.K., Armstrong, E.L. and Boyle, R.W., 1975. Site of inhibitory action of isoniazid in the synthesis of mycolic acids in Mycobacterium tuberculosis. Journal of lipid research, 16(4), pp.308-317.

- Takimoto, H., Maruyama, H., Shimada, K.I., Yakabe, R., Yano, I. and Kumazawa, Y., 2006. Interferon-γ independent formation of pulmonary granuloma in mice by injections with trehalose dimycolate (cord factor), lipoarabinomannan and phosphatidylinositol mannosides isolated from Mycobacterium tuberculosis. Clinical & Experimental Immunology, 144(1), pp.134-141.

- Tameris, M.D., Hatherill, M., Landry, B.S., Scriba, T.J., Snowden, M.A., Lockhart, S., Shea, J.E., McClain, J.B., Hussey, G.D., Hanekom, W.A. and Mahomed, H., 2013. Safety and efficacy of MVA85A, a new tuberculosis

vaccine, in infants previously vaccinated with BCG: a randomised, placebo-controlled phase 2b trial. The Lancet, 381(9871), pp.1021-1028.

- Tan, L.A., Yang, A.C., Kishore, U. and Sim, R.B., 2011. Interactions of complement proteins C1q and factor H with lipid A and Escherichia coli: further evidence that factor H regulates the classical complement pathway. Protein & cell, 2(4), pp.320-332.

- Tas, S.W., Klickstein, L.B., Barbashov, S.F. and Nicholson-Weller, A., 1999. C1q and C4b bind simultaneously to CR1 and additively support erythrocyte adhesion. The Journal of Immunology, 163(9), pp.5056-5063.

- Telenti, A., Imboden, P., Marchesi, F., Matter, L., Schopfer, K., Bodmer, T., Lowrie, D., Colston, M.J. and Cole, S., 1993. Detection of rifampicin-resistance mutations in Mycobacterium tuberculosis. The Lancet, 341(8846), pp.647-651.

- Thacher, E.G., Cavassini, M., Audran, R., Thierry, A.C., Bollaerts, A., Cohen, J., Demoitié, M.A., Ejigu, D., Mettens, P., Moris, P. and Ofori-Anyinam, O., 2014. Safety and immunogenicity of the M72/AS01 candidate tuberculosis vaccine in HIV-infected adults on combination antiretroviral therapy: a phase I/II, randomized trial. Aids, 28(12), pp.1769-1781.

- Toossi, Z. and Ellner, J.J., 1998. The role of TGFβ in the pathogenesis of human tuberculosis. Clinical immunology and immunopathology, 87(2), pp.107-114.

- Toossi, Z., Gogate, P., Shiratsuchi, H., Young, T. and Ellner, J.J., 1995. Enhanced production of TGF-beta by blood monocytes from patients with active tuberculosis and presence of TGF-beta in tuberculous granulomatous lung lesions. The journal of Immunology, 154(1), pp.465-473.

- Toossi, Z., Young, T.G., Averill, L.E., Hamilton, B.D., Shiratsuchi, H. and Ellner, J.J., 1995. Induction of transforming growth factor beta 1 by purified protein derivative of Mycobacterium tuberculosis. Infection and immunity, 63(1), pp.224-228.

- Torrado, E. and Cooper, A.M., 2010. IL-17 and Th17 cells in tuberculosis. Cytokine & growth factor reviews, 21(6), pp.455-462.

- Tsuchiya, S., Yamabe, M., Yamaguchi, Y., Kobayashi, Y., Konno, T. and Tada, K., 1980. Establishment and characterization of a human acute monocytic leukemia cell line (THP-1). International journal of cancer, 26(2), pp.171-176.

- Tsuchiya, S., Kobayashi, Y., Goto, Y., Okumura, H., Nakae, S., Konno, T. and Tada, K., 1982. Induction of maturation in cultured human monocytic leukemia cells by a phorbol diester. Cancer research, 42(4), pp.1530-1536.

- Tufariello, J.M., Chan, J. and Flynn, J.L., 2003. Latent tuberculosis: mechanisms of host and bacillus that contribute to persistent infection. The Lancet infectious diseases, 3(9), pp.578-590.

- Urdahl, K.B., Shafiani, S. and Ernst, J.D., 2011. Initiation and regulation of T-cell responses in tuberculosis. Mucosal immunology, 4(3), pp.288-293.

- Van de Veerdonk, F.L., Teirlinck, A.C., Kleinnijenhuis, J., Kullberg, B.J., van Crevel, R., van der Meer, J.W., Joosten, L.A. and Netea, M.G., 2010. Mycobacterium tuberculosis induces IL-17A responses through TLR4 and dectin-1 and is critically dependent on endogenous IL-1. Journal of leukocyte biology, 88(2), pp.227-232.

- Van de Wetering, J.K., Van Eijk, M., Van Golde, L.M., Hartung, T., Van Strijp, J.A. and Batenburg, J.J., 2001. Characteristics of surfactant protein A and D binding to lipoteichoic acid and peptidoglycan, 2 major cell wall components of gram-positive bacteria. Journal of Infectious Diseases, 184(9), pp.1143-1151.

- Vandivier, R.W., Ogden, C.A., Fadok, V.A., Hoffmann, P.R., Brown, K.K., Botto, M., Walport, M.J., Fisher, J.H., Henson, P.M. and Greene, K.E., 2002. Role of surfactant proteins A, D, and C1q in the clearance of apoptotic cells in vivo and in vitro: calreticulin and CD91 as a common collectin receptor complex. The Journal of Immunology, 169(7), pp.3978-3986.

- Vankayalapati, R. and Barnes, P.F., 2009. Innate and adaptive immune responses to human Mycobacterium tuberculosis infection. Tuberculosis, 89, pp.S77-S80.

- Van Zyl-Smit, R.N., Lehloenya, R.J., Meldau, R. and Dheda, K., 2016. Impact of correcting the lymphocyte count to improve the sensitivity of TB antigen-specific peripheral blood-based quantitative T cell assays (T-SPOT.® TB and QFT-GIT). Journal of thoracic disease, 8(3), p.482.

- Velasco-Velázquez, M.A., Barrera, D., González-Arenas, A., Rosales, C. and Agramonte-Hevia, J., 2003. Macrophage—Mycobacterium tuberculosis interactions: role of complement receptor 3. Microbial pathogenesis, 35(3), pp.125-131.

- Vercellotti, G.M., McCarthy, J.B., Lindholm, P., Peterson, P.K., Jacob, H.S. and Furcht, L.T., 1985. Extracellular matrix proteins (fibronectin, laminin, and type IV collagen) bind and aggregate bacteria. The American journal of pathology, 120(1), p.13.

- Vijayan, V.K., Sankaran, K., Sharma, S.K. and Misra, N.P., 1995. Chronic lung inflammation in victims of toxic gas leak at Bhopal. Respiratory medicine, 89(2), pp.105-111.

- Visai L, Bozzini S, Petersen TE, Speziale L & Speziale P., 1991. Binding sites in fibronectin for an enterotoxigenic strains of E. coli B3242289c. FEBS Lett 290: 111–114.

- Wade, M.M. and Zhang, Y., 2004. Mechanisms of drug resistance in Mycobacterium tuberculosis. Frontiers in bioscience: a journal and virtual library, 9, pp.975-994.

- Walport, M.J., Davies, K.A. and Botto, M., 1998. C1q and systemic lupus erythematosus. Immunobiology, 199(2), pp.265-285.

- Wert, S.E., Yoshida, M., LeVine, A.M., Ikegami, M., Jones, T., Ross, G.F., Fisher, J.H., Korfhagen, T.R. and Whitsett, J.A., 2000. Increased metalloproteinase activity, oxidant production, and emphysema in surfactant protein D gene-inactivated mice. Proceedings of the National Academy of Sciences, 97(11), pp.5972-5977.

- Weyer, K., 2005. Multidrug-resistant tuberculosis: main topic. CME: Your SA Journal of CPD, 23(2), pp.74-84.

- Wiekowski, M.T., Leach, M.W., Evans, E.W., Sullivan, L., Chen, S.C., Vassileva, G., Bazan, J.F., Gorman, D.M., Kastelein, R.A., Narula, S. and Lira, S.A., 2001. Ubiquitous transgenic expression of the IL-23 subunit p19 induces multiorgan inflammation, runting, infertility, and premature death. The Journal of Immunology, 166(12), pp.7563-7570.

- Winkler, C., Hüper, K., Wedekind, A.C., Rochlitzer, S., Hartwig, C., Müller, M., Braun, A., Krug, N., Hohlfeld, J.M. and Erpenbeck, V.J., 2010. Surfactant protein D modulates pulmonary clearance of pollen starch granules. Experimental lung research, 36(9), pp.522-530.

- Winkler, C., Atochina-Vasserman, E.N., Holz, O., Beers, M.F., Erpenbeck, V.J., Krug, N., Roepcke, S., Lauer, G., Elmlinger, M. and Hohlfeld, J.M., 2011. Comprehensive characterisation of pulmonary and serum surfactant protein D in COPD. Respiratory research, 12(1), p.1.

- Wise, K.S. and McIntosh, M.A., The Curators of the University of Missouri, 1998. DNA sequences coding for mycoplasma hyopneumoniae surface antigens, corresponding proteins and use in vaccines and diagnostic procedures. U.S. Patent 5,788,962.

- Wojciechowski, W., DeSanctis, J., Skamene, E. and Radzioch, D., 1999. Attenuation of MHC class II expression in macrophages infected with Mycobacterium bovis bacillus Calmette-Guerin involves class II

transactivator and depends on the Nramp1 gene. The Journal of Immunology, 163(5), pp.2688-2696.

- Wolf, A.J., Desvignes, L., Linas, B., Banaiee, N., Tamura, T., Takatsu, K. and Ernst, J.D., 2008. Initiation of the adaptive immune response to Mycobacterium tuberculosis depends on antigen production in the local lymph node, not the lungs. The Journal of experimental medicine, 205(1), pp.105-115.

- Wong, D., Bach, H., Sun, J., Hmama, Z. and Av-Gay, Y., 2011. Mycobacterium tuberculosis protein tyrosine phosphatase (PtpA) excludes host vacuolar-H+–ATPase to inhibit phagosome acidification. Proceedings of the National Academy of Sciences, 108(48), pp.19371-19376.
- World Health Organization, 2016. Global tuberculosis report 2016.

- World Health Organization, 1999. What is DOTS?: A guide to understanding the WHO-recommended TB Control Strategy Known as DOTS.

- Worley, M.V. and Estrada, S.J., 2014. Bedaquiline: A Novel Antitubercular Agent for the Treatment of Multidrug-Resistant Tuberculosis. Pharmacotherapy: The Journal of Human Pharmacology and Drug Therapy, 34(11), pp.1187-1197.

- Worthley, D.L., Johnson, D.F., Eisen, D.P., Dean, M.M., Heatley, S.L., Tung, J.P., Scott, J., Padbury, R.T., Harley, H.A., Bardy, P.G. and Angus, P.W., 2009. Donor mannose-binding lectin deficiency increases the likelihood of clinically significant infection after liver transplantation. Clinical Infectious Diseases, 48(4), pp.410-417.
- Wu, H., Kuzmenko, A., Wan, S., Schaffer, L., Weiss, A., Fisher, J.H., Kim, K.S. and McCormack, F.X., 2003. Surfactant proteins A and D inhibit the growth of Gram-negative bacteria by increasing membrane permeability. The Journal of clinical investigation, 111(10), pp.1589-1602.
- Xu, J. and Mosher, D., 2011. Fibronectin and other adhesive glycoproteins. In The extracellular matrix: an overview (pp. 41-75). Springer Berlin Heidelberg.
- Yamada, H., Mizumo, S., Horai, R., Iwakura, Y. and Sugawara, I., 2000. Protective Role of Interleukin-1 in Mycobacterial Infection in IL-1 &agr;/&bgr; Double-Knockout Mice. Laboratory investigation, 80(5), pp.759-767.
- Yamazoe, M., Nishitani, C., Takahashi, M., Katoh, T., Ariki, S., Shimizu, T., Mitsuzawa, H., Sawada, K., Voelker, D.R., Takahashi, H. and Kuroki, Y., 2008. Pulmonary surfactant protein D inhibits lipopolysaccharide (LPS)-induced inflammatory cell responses by altering LPS binding to its receptors. Journal of Biological Chemistry, 283(51), pp.35878-35888.
- Yang, C.T., Cambier, C.J., Davis, J.M., Hall, C.J., Crosier, P.S. and Ramakrishnan, L., 2012. Neutrophils exert protection in the early

tuberculous granuloma by oxidative killing of mycobacteria phagocytosed from infected macrophages. Cell host & microbe, 12(3), pp.301-312.

- Yang, G.Y., Taboada, S. and Liao, J., 2009. Induced nitric oxide synthase as a major player in the oncogenic transformation of inflamed tissue. Inflammation and Cancer: Methods and Protocols: Volume 2: Molecular Analysis and Pathways, pp.119-156.
- Yano, T., Kassovska-Bratinova, S., Teh, J.S., Winkler, J., Sullivan, K., Isaacs, A., Schechter, N.M. and Rubin, H., 2011. Reduction of clofazimine by mycobacterial Type 2 NADH: Quinone oxidoreductase a pathway for the generation of bactericidal levels of reactive oxygen species. Journal of Biological Chemistry, 286(12), pp.10276-10287.
- Yeager, R.L., Munroe, W.G.C. and Dessau, F.I., 1952. Pyrazinamide (aldinamide) in the treatment of pulmonary tuberculosis. American Review of Tuberculosis and Pulmonary Diseases, 65(5), pp.523-46.
- Young, S.L., Murphy, M., Zhu, X.W., Harnden, P., O'Donnell, M.A., James, K., Patel, P.M., Selby, P.J. and Jackson, A.M., 2004. Cytokine-modified Mycobacterium smegmatis as a novel anticancer immunotherapy. International journal of cancer, 112(4), pp.653-660.
- Young Jr KR, Ambrus Jr JL,. 1991. Malbran A, Fauci AS, Tenner AJ. Complement subcomponent C1q stimulates Ig production by human B lymphocytes. J Immunol, 146:3356–64.
- Zhao W, Schorey JS, Groger R, Allen PM, Brown EJ & Ratliff TL., 1999. Characterization of the fibronectin binding motif for a unique mycobacterial fibronectin attachment protein, FAP. J Biol Chem 274: 4521–4526.
- Zhang, M., Gately, M.K., Wang, E., Gong, J., Wolf, S.F., Lu, S., Modlin, R.L. and Barnes, P.F., 1994. Interleukin 12 at the site of disease in tuberculosis. Journal of Clinical Investigation, 93(4), p.1733.
- Zhang, M., Lin, Y., Iyer, D.V., Gong, J., Abrams, J.S. and Barnes, P.F., 1995. T-cell cytokine responses in human infection with Mycobacterium tuberculosis. Infection and immunity, 63(8), pp.3231-3234.
- Zhang, Y., Doerfler, M., Lee, T.C., Guillemin, B. and Rom, W.N., 1993. Mechanisms of stimulation of interleukin-1 beta and tumor necrosis factor-alpha by Mycobacterium tuberculosis components. Journal of Clinical Investigation, 91(5), p.2076.
- Zhang, P., McAlinden, A., Li, S., Schumacher, T., Wang, H., Hu, S., Sandell, L. and Crouch, E., 2001. The amino-terminal heptad repeats of the coiled-coil neck domain of pulmonary surfactant protein d are necessary for the assembly of trimeric subunits and dodecamers. Journal of Biological Chemistry, 276(23), pp.19862-19870.
- Zhang, Y., 2005. The magic bullets and tuberculosis drug targets. Annu. Rev. Pharmacol. Toxicol., 45, pp.529-564.

Appendix - Interaction of C1q with *E.coli*

1. Binding of C1q with *E.coli* by ELISA

C1q binds with *E.coli* in in presence of 5mM $CaCl_2$. The binding is dose dependent. The best binding was obtained at 20μg/ml (Figure A1).

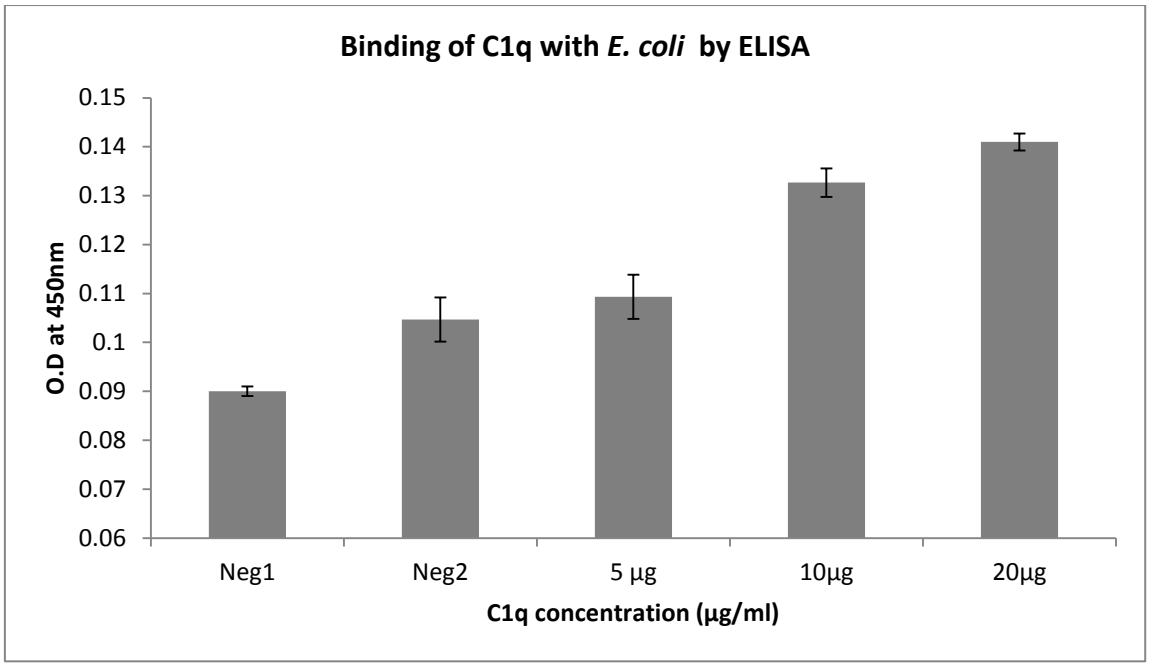

Figure A1: Binding of C1q with *E.coli* by ELISA. Each bar represents the average of triplicate readings. Error bars represent ±standard deviation. Neg1: 10μg/ml C1q without bacteria. Neg2: untreated bacteria. Data shown represents one of two independent experiments.

2. Direct effect of C1q on *E.coli* growth

In this study,we demonstrated that C1q directly inhibited the growth of *E.coli* by 42.5% after 2 hours treatment and further culturing for 24 hours. In all the three independent experiments, there was a trend in *E.coli* growth reduction in presence of C1q (Figure 3). However, the result did not reach statistiacal significance using Wilcoxon signed rank test (Figure A2).

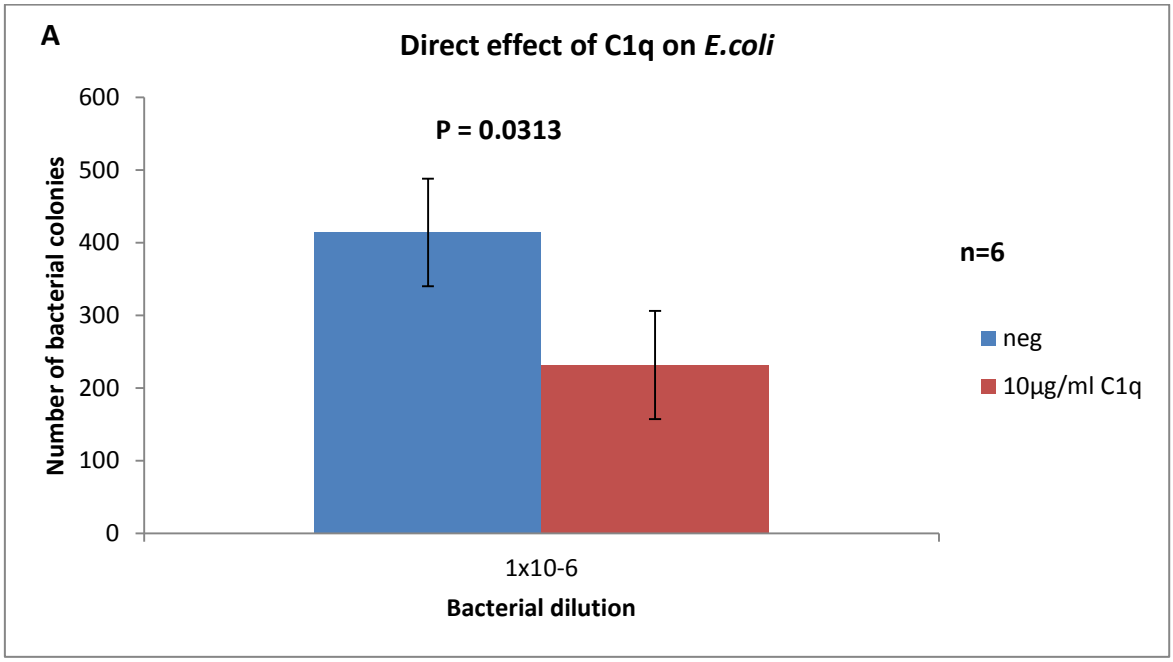

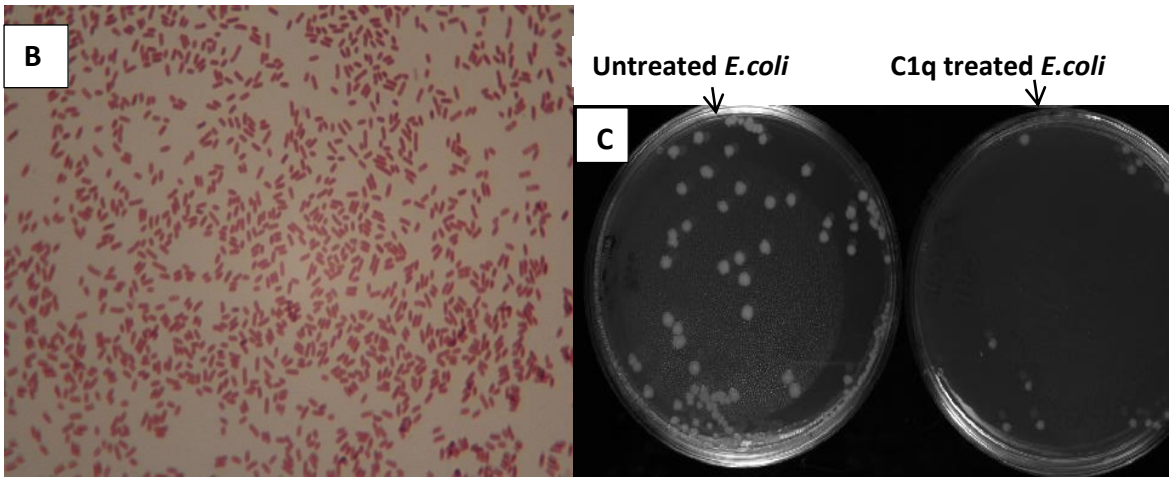

Figure A2: Effect of C1q on *E.coli* growth. Each bar represents the average of six independent experiments. Error bars represents ±standard error of the mean. P was calculated using Wilcoxon signed rank test. B: Gram staining image for *E.coli* was taken by using 1000x total magnification. C: The number of *E.coli* colonies on LB agar is less after C1q treatment.

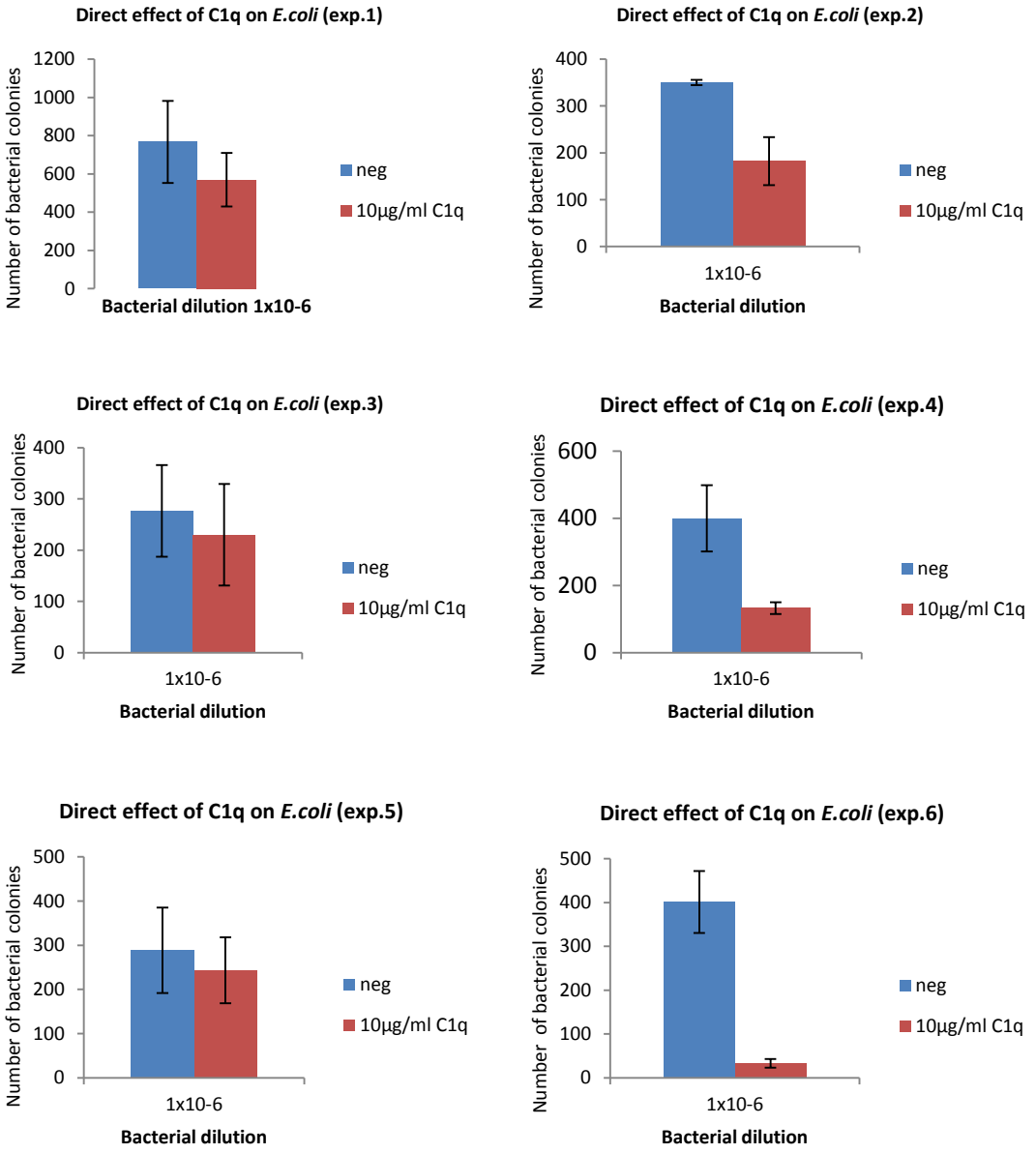

Figure A3: Direct effect of C1q on *E.coli* growth (6 individual experiments). Each bar represents the average of 3 triplicate data. Error bars represents the standard deviation.